Phytochemical and Biological Evaluation of Some Selected Plants from Vitaceae, Dipterocarpaceae, Moraceae and Celastraceae Family

THESIS SUBMITTED TO
THE UNIVERSITY OF KERALA
FOR THE AWARD OF THE DEGREE OF
DOCTOR OF PHILOSOPHY
IN CHEMISTRY
UNDER THE FACULTY OF SCIENCE

BY
SASIKUMAR P.

ORGANIC CHEMISTRY SECTION
CHEMICAL SCIENCES AND TECHNOLOGY DIVISION
CSIR–NATIONAL INSTITUTE FOR INTERDISCIPLINARY SCIENCE AND TECHNOLOGY (CSIR–NIIST)
THIRUVANANTHAPURAM-695 019, KERALA

2018

Dedicated to my beloved Wife & parents....

DECLARATION

I hereby declare that the Ph.D. thesis entitled "**Phytochemical and Biological Evaluation of Some Selected Plants from Vitaceae, Dipterocarpaceae, Moraceae and Celastraceae Family**" is an independent work carried out by me and it has not been submitted anywhere else for any other degree, diploma or title.

Sasikumar P.

Thiruvananthapuram
November, 2018

NATIONAL INSTITUTE FOR INTERDISCIPLINARY SCIENCE & TECHNOLOGY
Council of Scientific & Industrial Research
GOVERNMENT OF INDIA
Trivandrum-695 019, India

Dr. K. V. Radhakrishnan
Organic Chemistry Section
Chemical Sciences and Technology Division

Telephone: 91-471-2515420
Fax: 91-471-2491712

CERTIFICATE

*This is to certify that the work embodied in the thesis entitled "**Phytochemical and Biological Evaluation of Some Selected Plants from Vitaceae, Dipterocarpaceae, Moraceae and Celastraceae Family**" has been carried out by **Mr. Sasikumar P.** under my supervision and guidance at the Organic Chemistry Section of National Institute for Interdisciplinary Science and Technology (CSIR), Trivandrum and the same has not been submitted elsewhere for any other degree.*

K. V. Radhakrishnan
(Thesis Supervisor)

Trivandrum

November, 2018

Email: radhu2005@gmail.com

ACKNOWLEDGEMENTS

It is with great respect and immense pleasure that I express my deep sense of gratitude to my mentor and research supervisor ***Dr. K. V. Radhakrishnan*** *for his constant encouragement and intellectual inspiration during the course of my doctoral studies.*

I am grateful to Dr. A. Ajayaghosh, Dr. Suresh Das and Dr. Gangan Prathap, present and former Directors, National Institute for Interdisciplinary Science and Technology, for providing all the laboratory facilities to carry out this work.

My sincere thanks are also due to

- *Dr. G. Vijay Nair for his inspiration and constructive criticism*
- *Dr. R. Luxmi Varma, and Dr. K. R. Gopidas present and former Head, Chemical Sciences and Technology Division for their support.*
- *Dr. Mangalam S. Nair, Dr. Kaustabh Kumar Maiti and Dr. L. Ravishankar, Dr. B. S. Sasidhar., Dr. Sunil Varghese and Dr. Jubi John, Dr. Ganesh Chandra Nandi Scientists, Organic Chemistry Section for their support and suggestions.*
- *Dr. P. Nisha and Dr. P. Jayamurthy (Agro Processing and Natural Product Division) for antidiabetic studies.*
- *Dr. R. V. Omkumar (Molecular Neurobiology Division, RGCB, Trivandrum) for neurobiological studies.*
- *Dr. N. AnilKumar and Mr. V. V. Sivan (MSSRF Wayanad), Dr. Mathew Dan (TBGRI Palode), Dr. Sheeba Veluthoor (CoreValleys Herbal Technologies) and Dr. Pradeepkumar (University of Calicut) for plant collection and deposition.*
- *Dr. Sunil Varughese (NIIST), Mr. Alex Andrews (IISER-TVM) and Dr. E. Suresh (CSMCRI Bhavnagar) for single crystal X-ray analysis.*
- *Dr. I. G. Shibi (S. N. College Chempazhanthy), Dr. T. K. Manojkumar (IIITM, TVM) for molecular docking studies.*
- *Ms. Sarathna P, Ms. Aswathy M, Mrs. Prabha B, Mr. Rohith K. R and Mr. Jaise Kurian for their assistance in conducting some of the experiments reported in this thesis.*
- *Ms. R. Reshmitha, Mrs. K. Lekshmy, Dr. S. Sini (NIIST) and Mr. Mantosh Kumar (RGCB) for their help in conducting biological assays.*

- *Mrs. S. Viji and Ms. Athira for HRMS and elemental analysis, Mrs. Saumini Mathew, Mr. P. Saran, Mr. S. Syam and Mr. Rakesh Gokul for recording NMR spectra.*
- *Dr. S. Sarath Chand, Dr. P. Preethanuj, Dr. Ajesh Vijayan, Ms. Greeshma Gopalan, Ms. P. Sreedevi, Dr. K. R. Ajish, Dr. P. Praveen, Dr. B. P. Dhanya, Dr. P. S. Aparna, Dr. P. V. Santhini, Dr. T. V. Baiju, Dr. S. Saranya, Dr. M. Shimi, Dr. R. J. Maya, Mrs. Athira Krishna, Dr. Sajin Francis, Dr. S. R. Dhanya for their help and cooperation during various stages of my doctoral studies.*
- *Mr. K. Jagadeesh, Mr. K. K. Rajeev, Mr. A. J. Jayakrishnan, Mr. Thejus and Mr. Srikandan Nair for their love, care, help and support and also for making my stay at Trivandrum a very pleasant and memorable one.*
- *My Juniors; Ms. S. Neethu, Mrs. Meenu, Ms. P. R. Nitha, Mr. Madhukrishnan, Mrs. F. Sulfeena, Ms. S. Santhi, Ms. K. T. Ashitha, Mrs. Renjitha, Mr. Vishnu, Mrs. Biji, Ms. Raji, Mr. Praveen Valmeeki, Mr. Basavaraja, Mr. Mohan for their care, support and friendship during my stay at NIIST.*
- *All my teachers from NSS College and CMS College who bestowed their knowledge upon me and for encouraging me to take up a career in chemistry.*
- *Dr. Roji. J. Kunnath for his guidance, help and encouragement in qualifying the CSIR-UGC-NET exam.*
- *All my friends at NIIST*
- *UGC and DST, New Delhi for financial assistance*

Words are inadequate to express my feelings for my parents, brother, friends and teachers for all the encouragement and support throughout my career.

The successful completion of dissertation would have been practically impossible without the support, encouragement and unconditional love from my wife Anna Thara Jacob.

Above all, I bow before the Almighty for all his blessings

Sasikumar P.

CONTENTS

List of Tables

List of Figures

List of schemes

ABBREVIATIONS

A_0	: Absorbance of control
A_S	: Absorbance of sample
AC	: *Artocarpus camansi*
AD	: Alzheimer's disease
AL	: *Artocarpus lakoocha*
AI	: *Ampelocissus indica*
AMPK	: Adenosine Monophosphate-Activated Protein Kinase
brs	: Broad singlet
BSA	: Bovine serum albumin
CC	: Column chromatography
CCDC	: The Cambridge Crystallographic Data Centre
CD	: Circular Dichroism
$CDCl_3$	: Deuterated chloroform
CD_3COCD_3	: Deuterated acetone
$CD3SOCD_3$	: Deuterated dimethyl sulfoxide
CH_3CN	: Acetonitrile
cm	: Centimetre
CoA	: Coenzyme A
COSY	: Correlation spectroscopy
CP	: *Celastrus paniculatus*
°C	: Degree Celsius
α-CaMKII	: $Ca2^+$/calmodulin-dependent protein kinase II
d	: Doublet
dd	: Doublet of doublet
DCM	: Dichloromethane
DEPT	: Distortionless enhancement by polarization transfer
DM	: Diabetes mellitus
DMSO	: Dimethyl sulphoxide

DMEM : Dulbecco's Modified Eagle's Medium

D2O : Deuterated water

DNA : Deoxyribonucleic acid

DPPH : 1,1'-diphenyl-2-picrylhydrazyl

$DPPH^{\bullet}$: 1,1'-diphenyl-2-picrylhydrazyl radical

EDTA : Ethylenediaminetetraacetic acid

EGTA : Ethylene glycol-bis(β-aminoethyl ether)-N,N,N′,N′-tetraacetic acid

ESI : Electrospray ionization

EI : Electron impact ionization

EtOAc : Ethyl acetate

FACS : Fluorescence Activated Cell Sorting

FAME : Fatty acid methyl esterification

FDA : Food and Drug Administration

FBS : Fetal Bovine Serum

FITC : Fluorescein isothiocyanate

Fr. : Fractions

Fr.A : Acetone fractions

Fr.E : Ethanol fractions

Fr.H : Hexane fractions

g : Gram

GAE : Gallic acid equivalent

GC-MS : Gas Chromatography Mass Spectrometry

GLUT-4 : Glucose Transporter Type 4

h : Hour

HBSS : Hanks' Balanced Salt solution

HEK : Human embryonic kidney

HIV : Human immunodeficiency virus

HMBC : Heteronuclear multiple bond correlation

HMQC : Heteronuclear multiple-quantum correlation

HP : *Hopea ponga*

HPLC : High performance liquid chromatography

HRMS : High-resolution mass spectrometry

HTS : High throughput screening

Hz : Hertz

IC_{50} : Concentration required for 50 % inhibition

IDF : International Diabetic Federation

IR : Infrared

J : Coupling constant

kg : Kilogram

L : Litre

M : Molar

m : Multiplet

M^+ : Molecular ion

MeOH : Methanol

mg : Milligram

MHz : Mega Hertz

mL : Millilitre

mM : Millimolar

mmol : Millimoles

m.p. : Melting point

MTT : 3-(4,5-Dimethylthiazal-2-yl)-2,5-diphenyl terazolium bromide

2-NBDG : 2-[N-(7-nitrobenz-2-oxa-1,3-diaxol-4-yl)amino]-2-deoxyglucose

nM : Nanomolar

NMDAR : N-methyl-D-aspartate receptors

NMR : Nuclear Magnetic Resonance

NOESY : Nuclear overhauser effect spectroscopy

NP : Natural Product

ORTEP : Oak ridge thermal ellipsoid plot

p : para

PBS : Phosphate-buffered saline

PD : Parkinson's disease

PDB : Protein Data Bank

ppm : Parts per million

PI3-K : Phosphoinositide 3-kinase

QE : Quercetin equivalent

RNA : Ribonucleic acid

ROS : Reactive Oxygen Species

r.t. : Room temperature

s : Singlet

SD : Standard deviation

STS : Stilbene synthase enzyme

t : Triplet

TCA : Trichloro acetic acid

TLC : Thin layer chromatography

TMS : Tetramethylsilane

UV : Ultraviolet

VI : *Vateria indica*

WHO : World Health Organization

α : Alpha

β : Beta

γ : Gamma

δ : Delta

λ_{max} : The wavelength at which absorbance is maximum

μg : Microgram

μL : Microlitre

μM : Micromolar

υ_{max} : Maximum frequency

μg : Microgram

PREFACE

Natural products offer a rich source for novel therapeutic agents with enormous structural diversity. About 34 % of all the drugs approved by FDA in the past three decades are based on natural products. However, discovery of these biologically important scaffolds is much more challenging, certainly will attract much devotion in the future.

Medicinal plants based traditional systems of medicines are playing an important role in providing health care to a large section of population, especially in developing countries. India has the unique distinction of having six recognized systems of medicine in this category *viz* Ayurveda, Siddha, Unani, Yoga, Naturopathy and Homoeopathy. All the above systems in India are mainly based on herbal drugs. Many valuable medicinal plants of India are being lost at a shocking rate by the rapid depletion of forests, impairing the availability of raw drugs which leads to a critical phase in herbal medicines. Keeping the traditional knowledge in mind, we would like to apply our modern science by isolating each and every phytomolecules from the selected medicinal plants and use the modern biotechnological tools to assess their effectiveness in antidiabetic studies towards finding new drug molecules and formulations. The investigations along this line form the focal theme of this thesis entitled **"Phytochemical and Biological Evaluation of Some Selected Plants from Vitaceae, Dipterocarpaceae, Moraceae and Celastraceae Family".**

The thesis is divided into six chapters. **Chapter 1** gives a brief introduction to the role of natural products in modern drug discovery process. Even though it is impossible to furnish a comprehensive review on natural products and their classification in drug discovery, an attempt has been made to exemplify the importance of NPs and their classification in a brief manner. Special emphasis was given to diabetes mellitus and plant-derived antidiabetic drugs.

Phytochemical investigation on the rare species *Ampelocissus indica* (L.) belonging to Vitaceae family is the subject matter of **Chapter 2**. The extract level antioxidant and antidiabetic activity of *A. indica* rhizome is also presented in this chapter.

Chapter 3 of the thesis is divided into two parts. First part deals with the isolation and characterization of bioactives from the stem bark of *Vateria indica* (L.) belonging to

Dipterocarpaceae family. In the second part, the structural and antidiabetic activity comparison of (+) and (-)-hopeaphenol is discussed.

In **Chapter 4**, isolation and characterization of resveratrol oligomers from the stem bark of *Hopea ponga* (Dennst.) Mabb. and their antidiabetic effect by modulation of digestive enzymes, protein glycation and glucose uptake in L6 myocytes are explained.

The family Moraceae is gaining lots of research attention in the recent times for its nutritional and health benefits. They are also very good sources of antioxidants and other biologically active compounds. In this category, the plants from *Artocarpus* genus always bear a decorative position. *Artocarpus*, has been used as food and for traditional folk medicines in South-East Asia, Indonesia, Western part of Java and India. Owing to the great biological significance of the genus *Artocarpus*, detailed phytochemical investigations of stem bark of *Artocarpus camansi* Blanco and *Artocarpus lakoocha* Roxb. were undertaken and is described in **fifth chapter**. In addition, the antidiabetic activity of the different extracts and isolated compounds are also explained in this chapter.

Celastrus paniculatus Willd. is a medicinally important woody liana of Celastraceae family indigenous to Western Ghats of India mainly in the deciduous forests and is one of the least explored species in this family. In this regard, we carried out a detailed phytochemical evaluation of seeds of *C. paniculatus* and we could successfully isolate and characterise a number of molecules and have described our observations in the first part of **chapter six**. *C. paniculatus* is one of the most extensively used medicinal plants in the Ayurvedic system of medicine for memory enhancing. Hence, we screened the N-methyl-D-aspartate receptors (NMDARs) inhibitory activity of all the isolated compounds and have described it in the second part. In addition, the antidiabetic activity of the different extracts and isolated compounds were also screened and is discussed in this chapter.

It may be mentioned that each chapter of the thesis is presented as an independent unit and therefore the structural formulae, schemes and figures are numbered chapter wise.

A summary of the work is given towards the end of the thesis.

CHAPTER 1

Natural products: An overview with special emphasis on diabetes mellitus

1.1. Introduction

Natural products (NPs), are chemical compounds or substances produced by living organisms that usually possess distinctive pharmacological effects. Many well-known drugs listed in the current pharmacopoeia have their origin in nature. Natural products chemistry kindled with the isolation of morphine, a plant derived alkaloid from opium poppy in 1803 by Serturner. Almost 50 % of the drugs approved since 1994 are based on NPs, but the interest in natural product based drug discovery have terminated or significantly scaled down during the last few decades due to the intricacies of NP structures, inadequacy of raw materials and the difficulties in obtaining the patent [McChesney *et al*., **2007**]. Another prominent factor which led to the decline in the pace of NPs research in many of the pharmaceutical industries was the rapid growth of other modern drug discovery processes such as advanced synthetic chemistry, combinatorial chemistry, molecular modelling and high-throughput screening which were expected to lead to many new drugs [Rishton, **2008**].

Despite these problems, NPs still manage to provide their fair share in gifting new chemical entities with lead potential and are the source of most successful drug candidates [Butler, **2004**; Newman and Cragg, **2012**]. Major source of these NP drugs were plants followed by microorganisms. Some of the FDA approved purely natural product drugs are shown below (Figure 1.1).

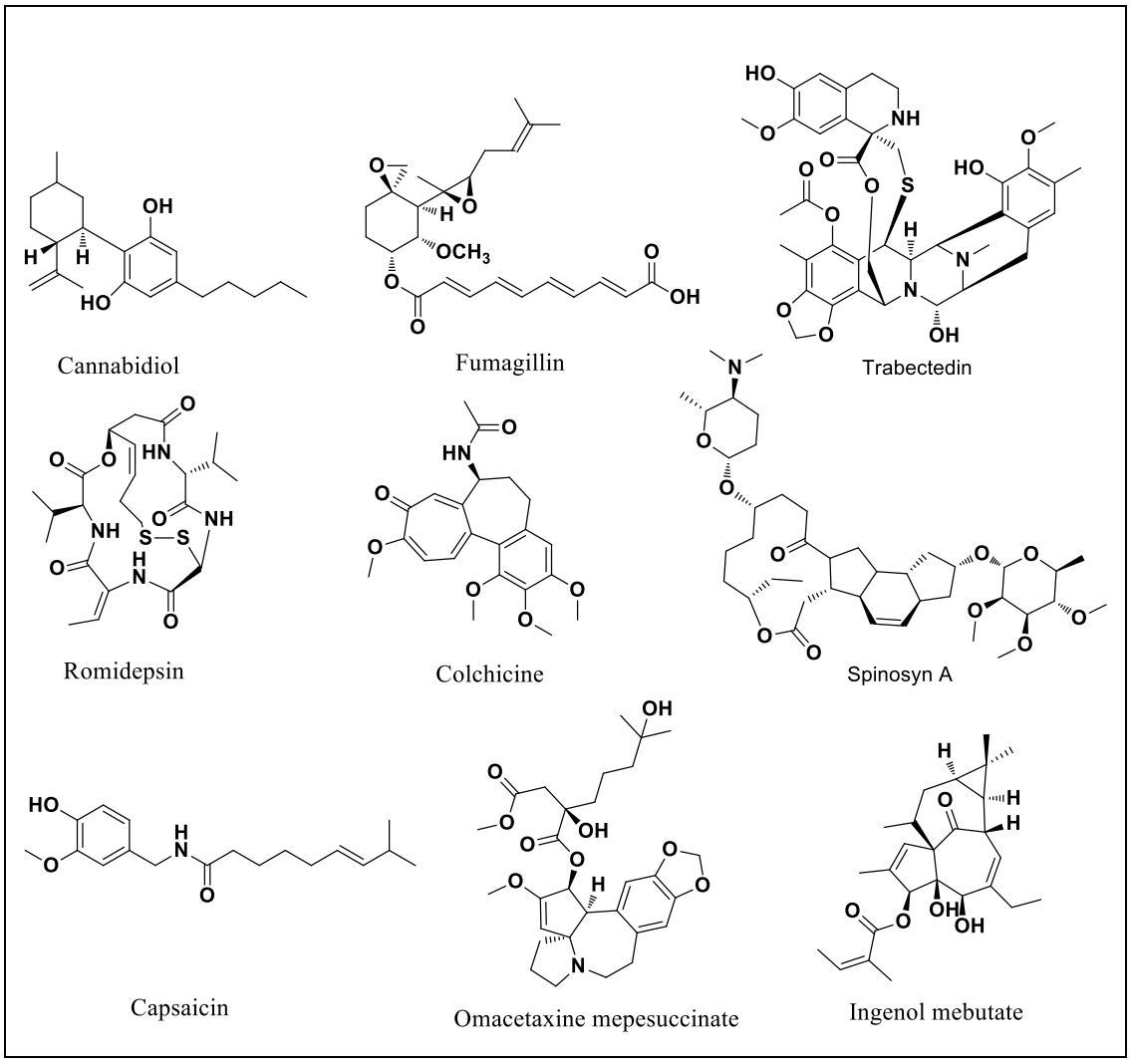

Figure 1.1: FDA approved unmodified NPs drugs

From a total of 1562 new drugs approved in between 1981-2014, only 27 % were found to be purely synthetic drugs. Around 6 % drugs were vaccines and 21 % were NP mimics and synthetic drugs inspired/mimicked from NPs. Approximately 42 % drugs were either NPs or NPs derived compounds [Newman and Cragg, **2016**]. It is to be noted that among all these drugs, 67 were unmodified natural products (Figure 1.2).

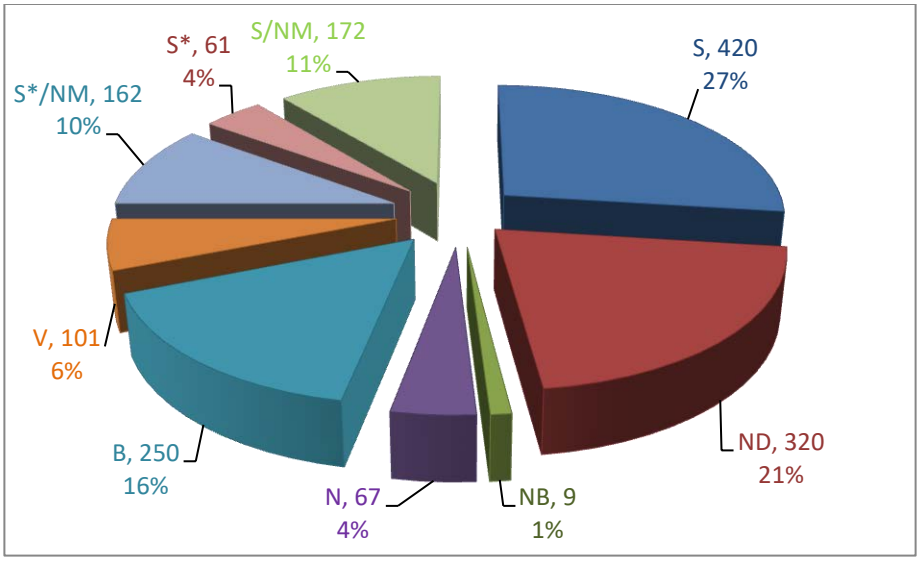

Figure 1.2: FDA approved drugs in 1981-2014; S-Purely synthetic drug, ND-Natural product derivative, NB-Botanical drug (defined mixture), N-Unmodified natural product, B-Biological macromolecule, V-Vaccine, S*/NM-synthetic compounds with natural product pharmacophore showing competitive inhibition of the natural product substrate, S*-Synthetic drug (NP pharmacophore), S/NM-Mimic of natural product.

1.2. Western Ghats of India

Western Ghats or Sahyadri is one of the eight "hottest hotspots" of biological diversity in the world, covering an area of 180000 km^2 with varied flora, fauna and landscapes. Western Ghats that runs parallel to the western coast of the Indian peninsula, and it starts near the border of southern tip of Gujarat and extending from Satpura Range and runs approximately 1,600 km (990 mi) through the states of Maharashtra, Goa, Karnataka, Kerala and Tamil Nadu ending at the southern tip of India, Kanyakumari (Figure 1.3) [Samant *et al.,* **1996**]. In Western Ghats region, only one-third is under natural vegetation and has over 7402 species of flowering plants, 1814 species of non-flowering plants, 140 mammal species, 510 bird species, 6000 insects species, 180 amphibian species and 290 fish species; it is likely that many undiscovered species live in the Western Ghats [Nayar *et al.,* **2014**; Myers *et al.,* **2000**; Dahanukar *et al.,* **2004**].

The rare endemic and endangered plant species are abundant in this region and many of the regions are over exploited due to improper management such as, harvesting, shifting,

grazing, cultivation and uprooting of plant species. Hence, there is an urgent need to propagate and conserve each and every species in the Western Ghats.

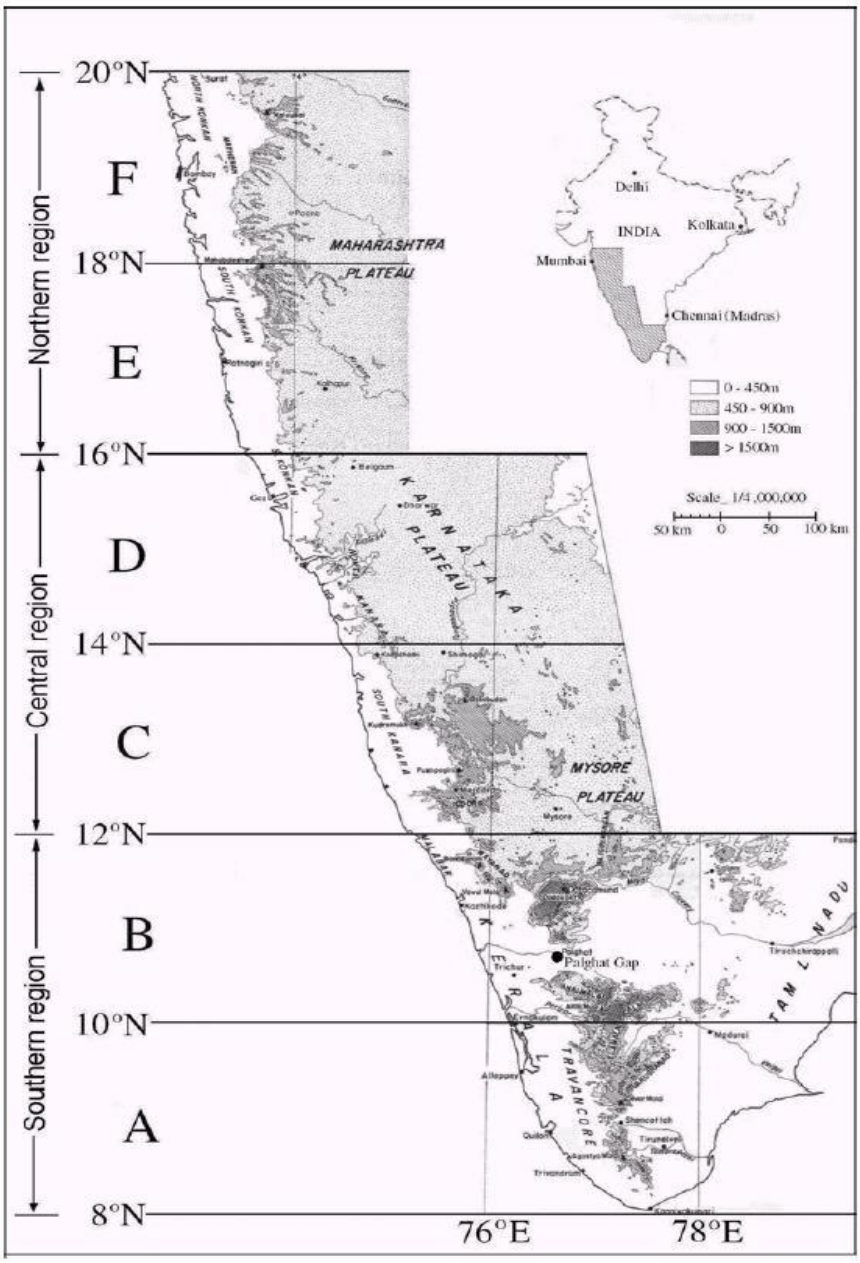

Figure 1.3: Major physiographical units of the Western Ghats

(Adopted from Samant *et al*., **1996]**

.

1.3. Classification of Natural Products

There is no rigid structure for categorizing natural products based on their vast diversity in structure, function and biosynthesis. The first classification in natural products is function based *viz*., as primary metabolites and secondary metabolites. Further classification is carried out by a systematic structure oriented organizing principle. Though classification of natural products is fairly common knowledge, it has been incorporated in this introduction as to use it as a platform for showcasing the diversity, excitement and beauty of natural products in a pictorial way.

A primary metabolite is directly involved in normal growth, development or reproduction of all living organisms. It normally performs physiological functions in the organisms. Examples of primary metabolites include energy rich molecules such as sucrose and starch, structural components such as cellulose, informational molecules such as DNA (deoxyribonucleic acid) and RNA (ribonucleic acid), and pigments such as chlorophyll. In addition to having essential roles in plant growth and development, some primary metabolites are precursors for the synthesis of secondary metabolites.

Secondary metabolites are not directly involved in the normal growth, development or reproduction of an organism or a plant. They often play a vital role in plant defence against herbivory and other interspecies defences. These chemicals are structurally diverse and have been identified in several major classes such as terpenoids, alkaloids, phenyl propanoids, flavonoids and glycosides. Among the various approaches developed so far, the two important and widely accepted ways of classification are; (i) classification based on source/origin and (ii) classification based on chemical structure [Alexander *et al*., **2003**].

1.3.1. Classification based on source/origin

Based on the source or origin, NPs can be categorized into the following groups.

- Plant derived NPs
- Microbial derived NPs
- Marine derived NPs
- Animal derived NPs

1.3.1.1. Plant derived natural products

Plants are a rich source of complex and structurally diverse chemical compounds known as phytochemicals. They have evolved and adapted over millions of years to withstand insects, bacteria, fungi and weather to produce unique structurally diverse secondary metabolites. According to the World Health Organization (WHO), 80 % of people still rely on plant-based traditional medicines for primary healthcare and 80 % of 122 plant-derived drugs were related to their original ethnopharmacological purpose [WHO News 2002]. Hence, modern drug design and discovery cannot ignore the significant contribution extended by the plant based natural entities. Many of such NPs were found beneficial as drugs for the treatment of various fatal diseases.

Plant derived compounds have been used as powerful pharmaceuticals throughout the course of human history. For example, opium poppy (*Papaver somniferum*) has been used since neolithic times. Opium, the dried latex of unripe capsules of *P. somniferum*, contains more than 80 isoquinoline type alkaloids. The main alkaloids in opium are morphine [McCurdy and Scully, **2005**]. A non-steroidal anti-inflammatory drug aspirin, synthesized by acetylation of salicyclic acid from the bark of willow tree, was discovered in nineteenth century. The potent chemotherapy agent paclitaxel (Taxol®), used in the treatment of advanced breast cancer, was discovered from *Taxus brevifolia* in the mid-twentieth century [Altmann and Gertsch, **2007**]. *Artemisia annua*, which has been used for centuries in traditional Chinese medicine to treat fevers including malaria and artemisinin was isolated as the active principle in the late 1970s [Osbourn and Lanzotti, **2007**]. In 1950s, vincristine and vinblastine; alkaloids isolated from *Catharanthus roseus*, by Canadian scientists Robert Noble and Charles Beer have proven to be effective against childhood leukaemia, breast cancer, Hodgkin's disease and choriocarcinoma [Cragg and Newman **2005**]. The structures of a few drugs of plant origin are shown in figure 1.4.

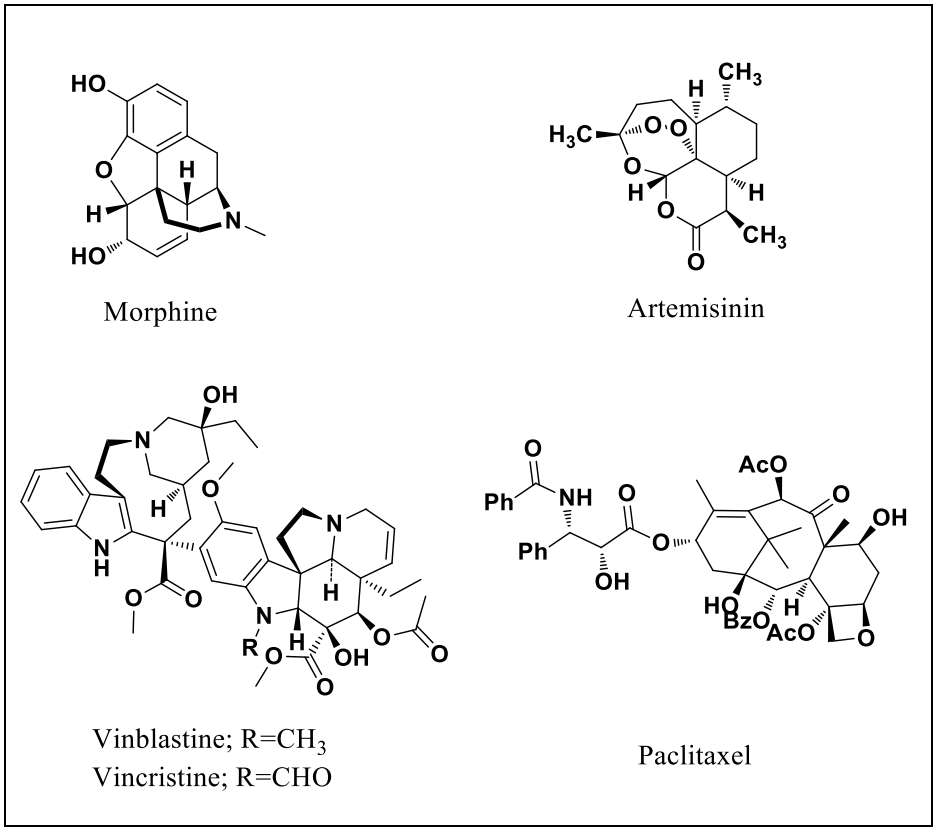

Figure 1.4: Structures of some plant-derived NP drugs

1.3.1.2. Microbial derived natural products

The interest of microbial derived natural products was kindled by the discovery of penicillin from fungus *Penicillium chrysogenum* by Alexander Fleming in 1928. Wide varieties of microorganisms including bacteria and fungi have contributed a significant number of lead molecules to drug discovery and its development. After the success of penicillin, a large number of marine and terrestrial microorganisms have been studied and screened for new drug candidates. Among them, majority of the drugs developed from microorganisms are used as anti-microbial agents belonging to different classes *viz*., *β*-lactams, amino-glycosides, and polyketides [Butler and Cooper, **2011**]. However, a few of these molecules possess other medicinal applications also. For example lovastatin and cyclosporine were used for cholesterol lowering and suppressing the immune response after the transplantation surgeries [Chin *et al*., **2006**]. Some of the microbial world derived natural products are given in figure 1.5.

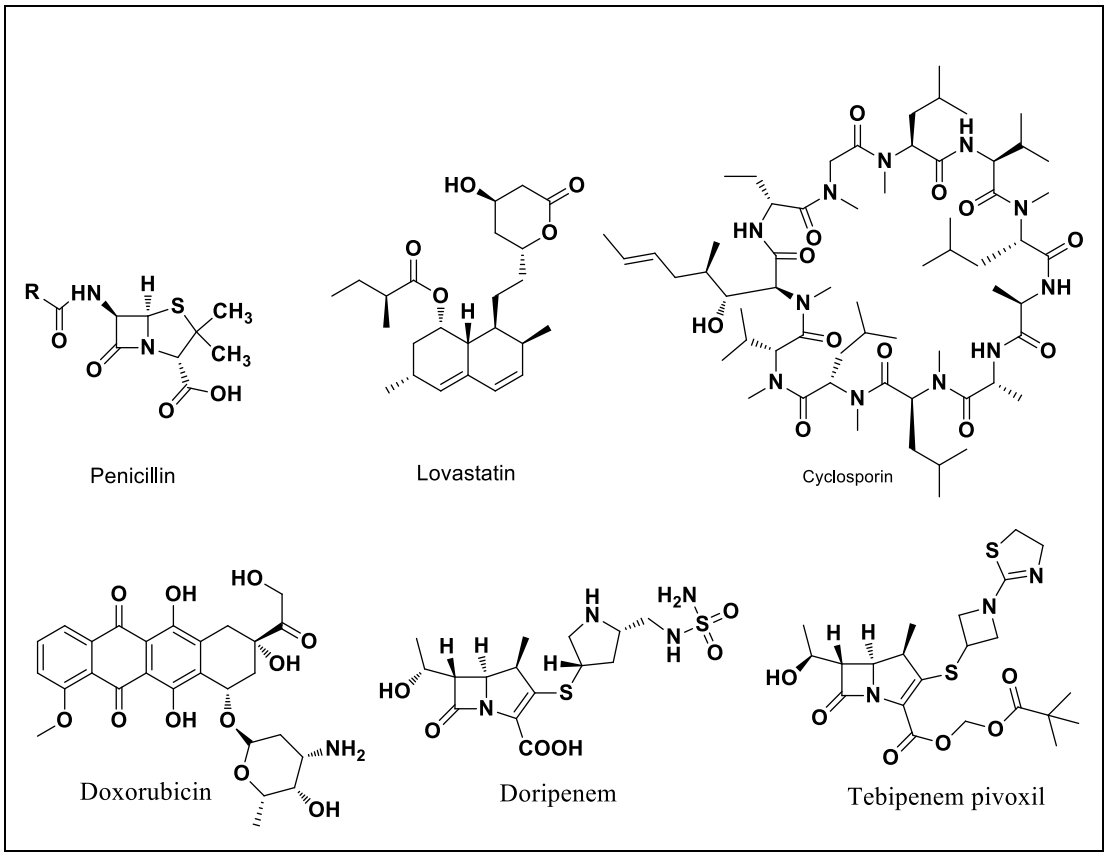

Figure 1.5: Microbial derived NPs

1.3.1.3. Marine derived natural products

The sea contains large number of untapped sources of molecules with promising biological activities due to the extensive varieties of marine species. They cover more than 70 % of earth's surface and are the interminable reservoir of structurally unique natural products. The census shows that over 6000 potentially new species are available in the sea. It points to the fact that the marine world represents a largely unexploited reservoir of many unknown bioactive natural compounds, which in turn needs to be evaluated for their potential medicinal applications [Haefner, **2003**]. In past few years several compounds from marine organisms were reported to have antiviral, antibacterial, anticancer, antifungal, antiprotozoal, immunosuppressive, anti-inflammatory, neuroprotective and antifouling activities.

In 1950s the first two compounds spongouridine and spongothymidine from marine sources were isolated from Carribean sponge (*Cryptotheca crypta*). These nucleotides showed prominent anti-viral and anti-cancer potential. Discodermolide, isolated from the

marine sponge *Discodermia dissoluta*, which has a similar mode of action to that of paclitaxel and it also exhibits better water solubility as compared to paclitaxel. Some of the marine world derived natural products are given in figure 1.6.

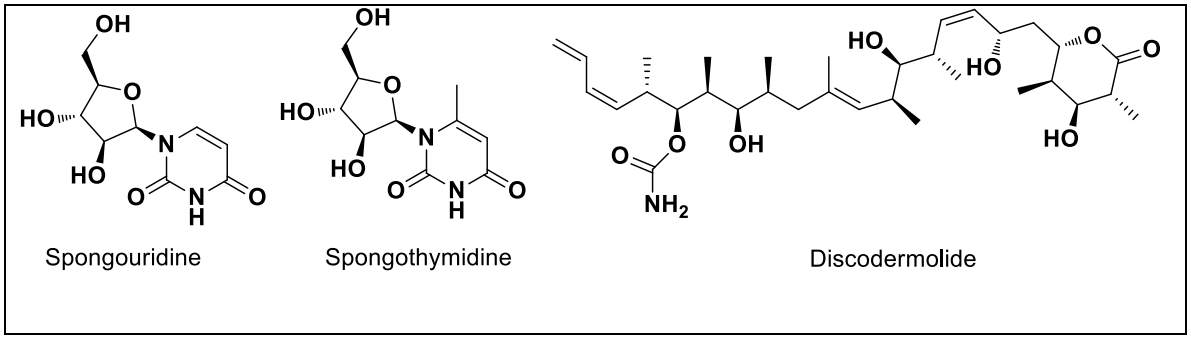

Figure 1.6: Marine derived NPs

1.3.1.4. Animal derived natural products

Animals are also good sources for bioactive compounds that can be used as drugs. An analysis and evaluation of the scientific aspects of drug discovery from animal origin should provide some enlightenment on the future of this drug source. Most of the major categorizations of drug candidate substances known to be produced by the various animal classifications are still under active investigation today. In Indian Ayurvedic medicinal system, about 15–20 % of the formulations contain animal products. A number of medicines (including tablets, capsules, injections, creams, mixtures and vaccines) contain animal products or are animal derived. For example, gelatine (used in making capsule shells) is a partially hydrolysed collagen which is usually bovine (beef) or porcine (pig) in origin and is one of many types of stabilisers added to pharmaceutical products such as vaccines. Heparin, an injectable anticoagulant, was first isolated from canine liver cells and is pharmaceutically prepared from porcine or bovine sources. Venomous organisms such as snakes, scorpions, spiders, caterpillars and frogs have also got much attention. For instance, cilazapril and captopril, two effective drugs against hypertension were developed from a natural product called teprotide isolated from a Brazilian viper (Figure 1.7).

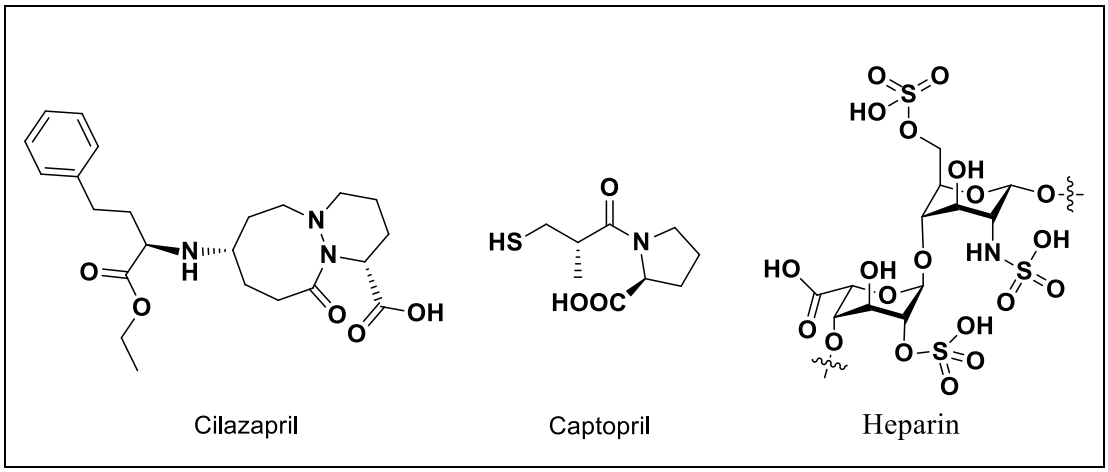

Figure 1.7: Animal derived NPs

1.3.2. Classification based on chemical structure

Natural products show wide variety in their chemical structures. Some contain heteroatoms, some others possess several chiral centres, cyclic structures, higher number of H-bond donors and H-bond acceptors, and some have large polar surface area. Secondary metabolites often possess fascinating pharmacological properties, and therefore their characterization is very important. The terpenes or terpenoids that are present in plants constitute the largest class of secondary metabolites. Most of the bioactives belonging to this class are insoluble in water. The list given below shows major classes of natural products based on their chemical structure.

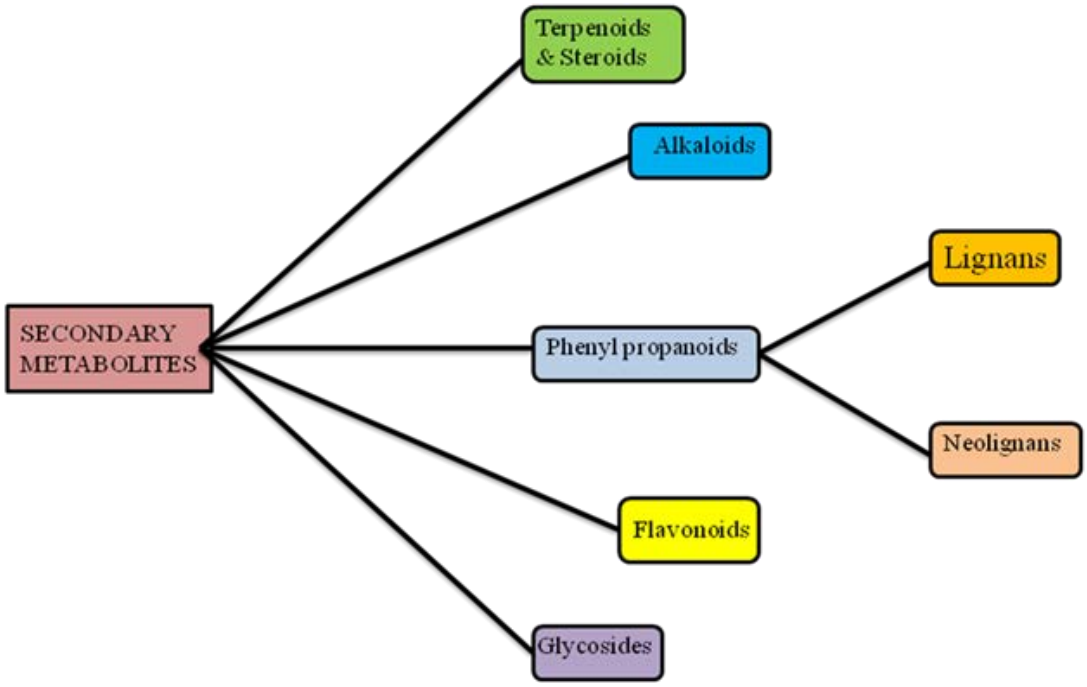

Figure 1.8: Classification of secondary metabolites

Among the various classes of compounds, a detailed account of terpeniods, alkaloids, flavonoids and glycosides are given in the following sections.

1.3.2.1. Terpenoids

Terpenoids or isoprenoids, are the major class of natural products present in plants and comprise more than 40,000 diverse structures. They are originated from a five-carbon monomer called isoprene unit. According to the number of isoprene units, they can be classified into hemiterpenes (5-carbon), monoterpenes (10-carbon), sesquiterpenes (15-carbon), diterpenes (20-carbon), triterpenes (30-carbon), tetraterpenes (40-carbon) and polyterpenes. Terpenoids like menthol, citral, camphor etc., are used extensively in flavourings and perfumery. The odour of a freshly crushed mint leaf, orange peels, lemon grass and similar plant odours are due to the presence of volatile mono and sesquiterpenes present in them. Terpenoids also play a vital role in traditional herbal medicines and are under investigation for their anti-bacterial, anti-neoplastic, and other pharmaceutical functions. Structures of different terpenoids are given in Figure 1.9 [Mcgarvey *et al*., **1995].**

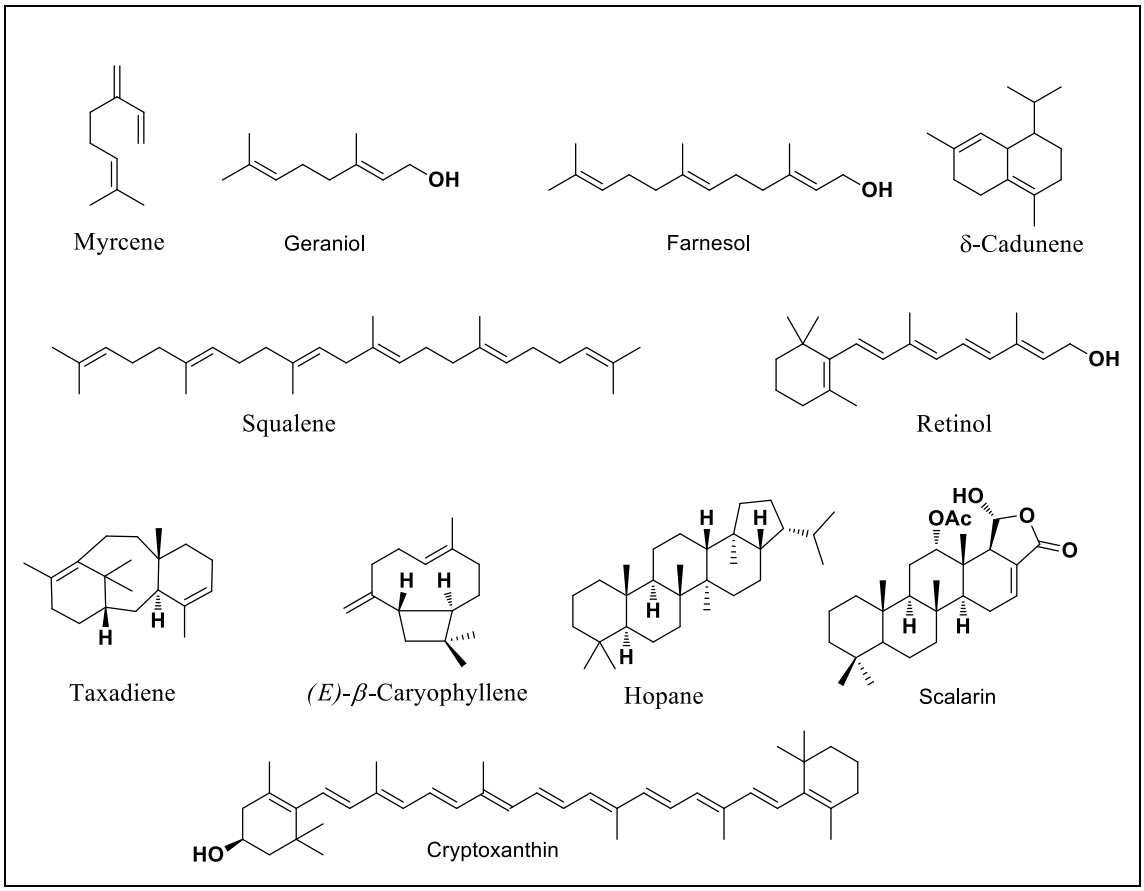

Figure 1.9: Structures of different terpenoids

1.3.2.2. Alkaloids

Alkaloids are nitrogen containing naturally occurring chemical compounds biosynthesized from amino acids. Alkaloids are produced by a large variety of organisms including fungi, bacteria, plants, and animals. Usually alkaloids can be purified by acid-base extraction from crude extracts of these organisms. Several alkaloids have provided lead structures for the synthesis of novel drug molecules. Some of the well-known alkaloids include morphine, strychnine, reserpine, coniine, quinine, ephedrine, and nicotine. Morphine was the first alkaloid isolated in 1803 by Friedrich Serturner, which is generally believed to be the first ever isolation of a natural plant alkaloid in the history. Examples of some important alkaloids and their biological importance are: cocaine-local anaesthetic and stimulant, psilocin-psychedelic, nicotine and caffeine-stimulants, morphine-analgesic, berberine-antibacterial, vincristine-anticancer, reserpine-antihypertension, galantamine-cholinomimetic, atropine-anticholinergic agent, vincamine-

vasodilator, quinidine-antiarrhythmic, ephedrine-antiasthma therapeutic, and quinine-antimalarial [Wall *et al*.,**1966**; Govindachari *et al*., **1972**; Efferth *et al*., **2007**]. Structures of some very interesting and important alkaloids are listed in the Figure 1.10.

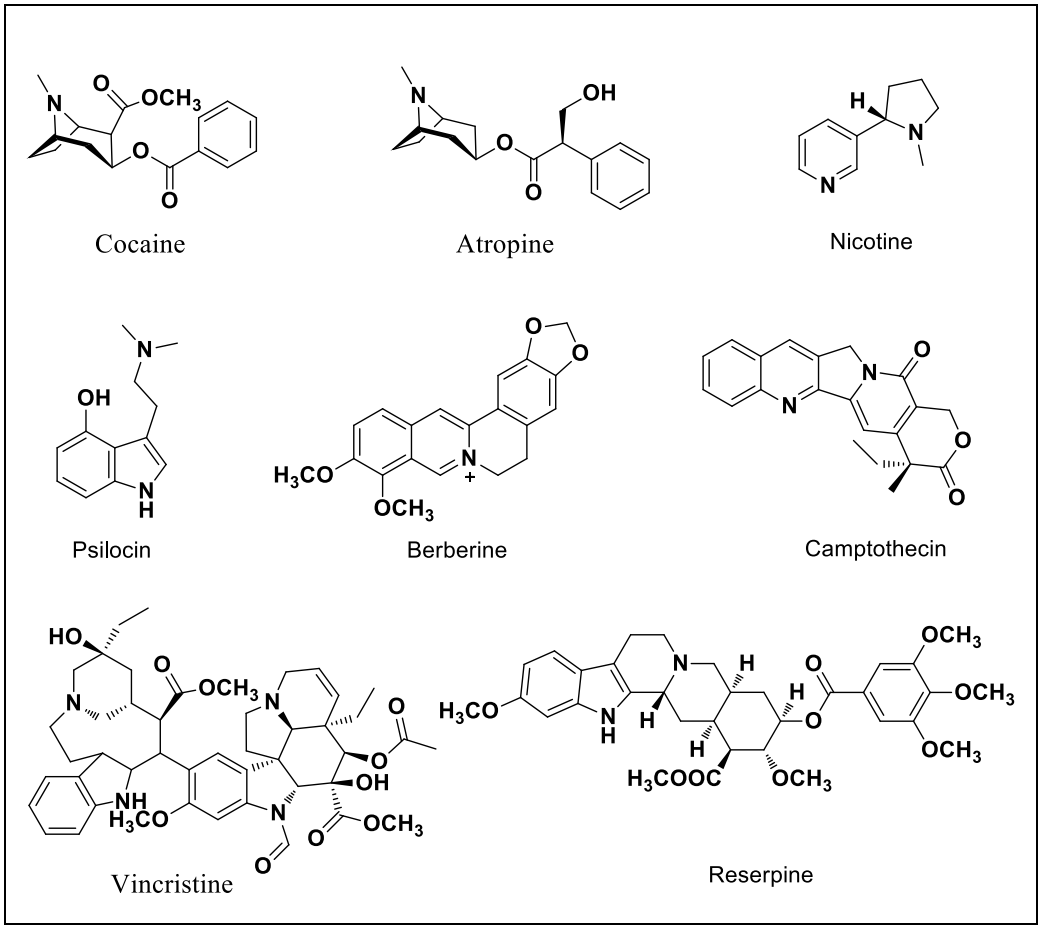

Figure 1.10: Structures of different alkaloids

1.3.2.3. Flavonoids

Flavonoids are a group of more than 6000 polyphenolic compounds. These compounds possess a common phenylbenzopyrone structure. They occur mostly in glycosylated form and are often accumulated in the vacuole. The key intermediates in flavonoid biosynthesis are chalcones which serve as precursors of all other subgroups. The basic structure with the numbering system is shown in Figure 1.11.

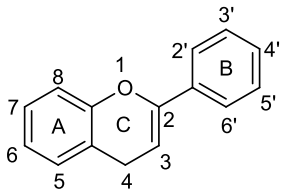

Figure 1.11: Basic structure of flavonoids

There are different ways for classifying flavonoids such as (i) according to their biosynthetic origin, (ii) according to whether the central heterocyclic ring is unsaturated or not, (iii) according to their molecular size etc. The most common way is according to the variation of the heterocyclic C ring. From the flavonoid basic structure, a heterocyclic pyrone C ring can be derivatised in to the flavones, flavonols, flavanones and isoflavones where as a pyran C ring produces the flavonols and anthocyanins [Graf *et al.*, **2005**]. The basic structures of each sub class are shown in figure 1.12.

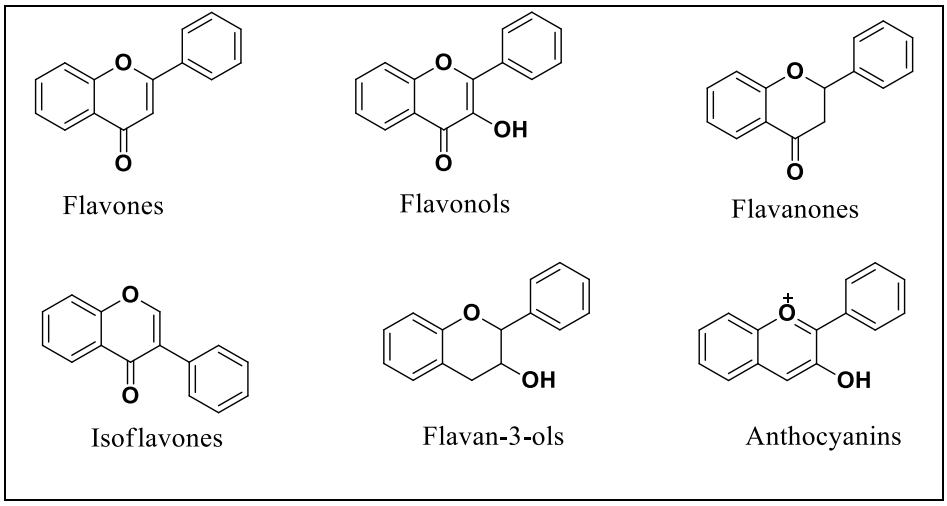

Figure 1.12: Diverse classes of flavonoids

Flavonoids are a part of the human diet, and it is recommended that dietary intake has beneficial health effects due to their antioxidant and radical-scavenging activities. Fruits and vegetables are very good sources of flavonoids. Orange juice contains, antioxidant and anticancer polymethoxylated flavones such as scutellarein, tangeretin, nobiletin and sinensetin, which are found exclusively in citrus species. Proanthocyanidins are the major flavonoids present in apples (*Malus domestica*) and pears (*Pyrus communis*) [Santos-buelga *et al*., **2000**]. Tea, coffee, cocoa, wine and beer are the other significant dietary sources of

flavonoids. The water-soluble thearubigins are the major phenolic compounds of black tea. (+)-Catechin, (-)-epicatechin and oligomeric procyanidins ranging from dimers to decamers are the major polyphenols in fresh coffee beans. Soya bean is one of the richest source of isoflavones such as daidzein, genistein and their β-glycoside conjugates [Coward *et al.,* **1993**]. Among them, genistein is an important anticancer isoflavone that inhibits DNA topoisomerase and tyrosine protein kinase [Akiyama *et al*., **1987**]. Grape (Vitaceae family) is one of the richest source of flavonoids. The most common class of flavonoid found in grapes are anthocyanins and polymeric proanthocyanidins which showed antitumor activity [Bomser *et al*., **1999**]. From the vast data on flavonoids, structure of few interesting flavonoids are shown in Figure 1.13.

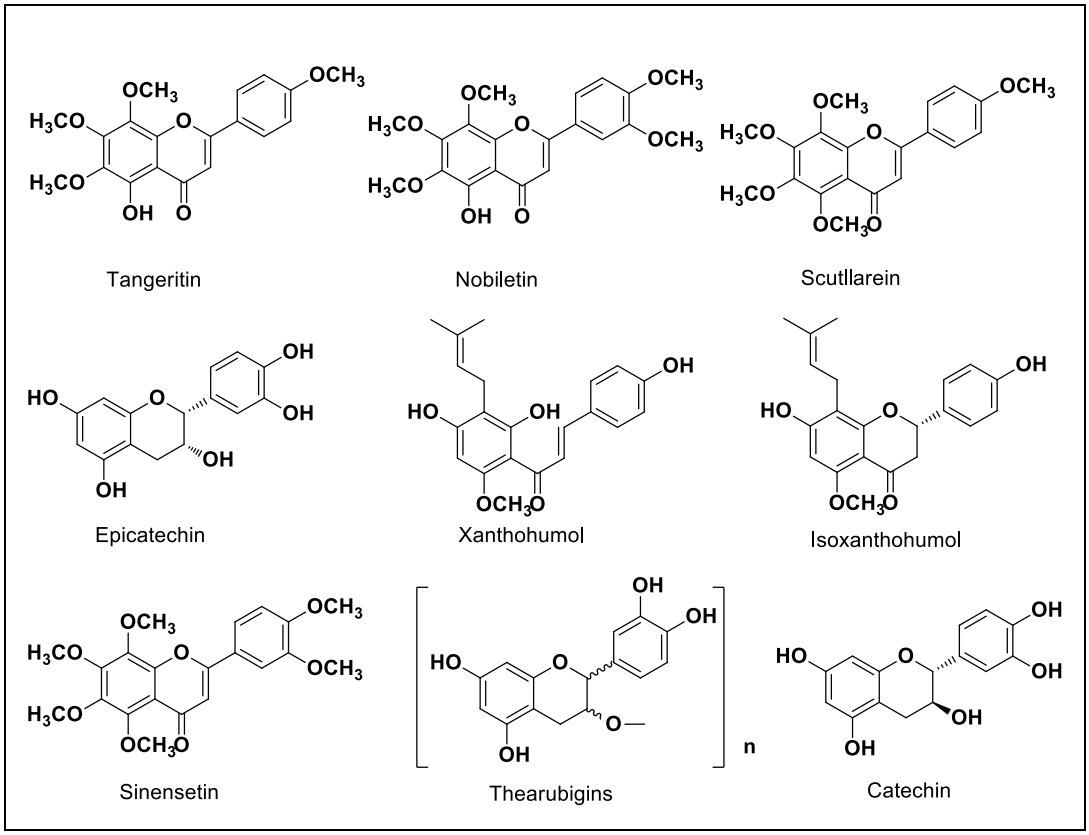

Figure 1.13: Structures of different flavonoids

1.3.2.4. Glycosides

A glycoside is a molecule in which sugar unit is bound to a non-sugar molecule *via* glycosidic bond. These are organic natural compounds mainly present in plants and animals, which upon hydrolysis give one or more glycone/s and aglycone. Depending up on the nature of glycosidic linkage, glycosides can be categorized as *O*-glycosides, *S*-glycosides

(thioglycoside), *N*-glycosides (glycosylamine) and *C*-glycosides. Few glycoside drugs or pharmaceutically important glycosides are given in Figure 1.14. Based on the historical importance, salicin, a *β*-*O*-glycoside, an anti-inflammatory agent isolated from willow bark (*Salix alba*). Frangulin B is a 6-*O*-(D-apiofuranosyl)-1,6,8-trihydroxy-3-methylanthraquinone isolated from *Rhamnus frangula*, which inhibits selectively collagen-induced aggregation and ATP release in rabbit platelets [Wagner *et al*., **1972**].

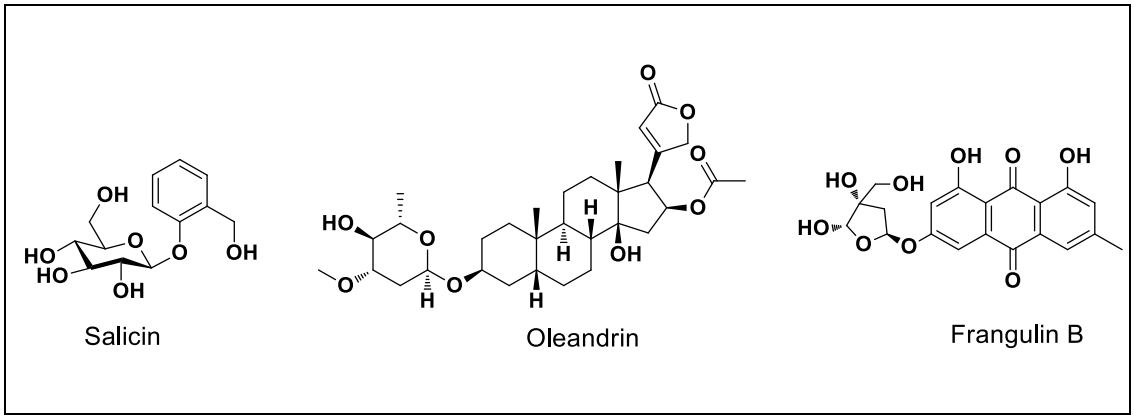

Figure 1.14: Some pharmaceutically important glycosides

1.4. Biosynthetic pathways and precursors for the major classes of secondary metabolites

The common biosynthetic pathways of secondary metabolites include shikimate pathway, acetate-polyketide pathway, pyruvate pathway etc. and are given in Scheme1.1. The major primary precursors are derived from protein (amino acids), carbohydrate (sugars) and lipid (fatty acid) metabolism. The shikimate pathway provides the precursors for benzoic acid derivatives and phenylpropanoid compounds in plants. Shikimate is biosynthesized from D-erythrose-4-phosphate and phosphoenolpyruvate, two metabolites derived from the pentose phosphate cycle and glycolysis, respectively. Shikimate is further converted to chorismate by addition of a C3 unit from phosphoenolpyruvate; and chorismate serves as the precursor of the aromatic amino acids L-phenylalanine, L-tyrosine, and L-tryptophan. The biosynthetic pathway of aromatic amino acids is one of the major sources of compounds such as flavonoids, phenols and some alkaloids. Acetyl-CoA is a central metabolite formed by glycolysis and also via the *β*-oxidation of fatty acids, and is used in the tricarboxylic acid cycle for the synthesis of organic acids, which act as the precursors of secondary metabolites.

In addition, acetyl-CoA is involved in the synthesis of terpenes, which form a distinct class of metabolites. The general chemical reactions involved in these include oxidations, hydroxylations, reductions, methylations, acylations, prenylations and glycosylations [Gutzeit *et al*., **2014**].

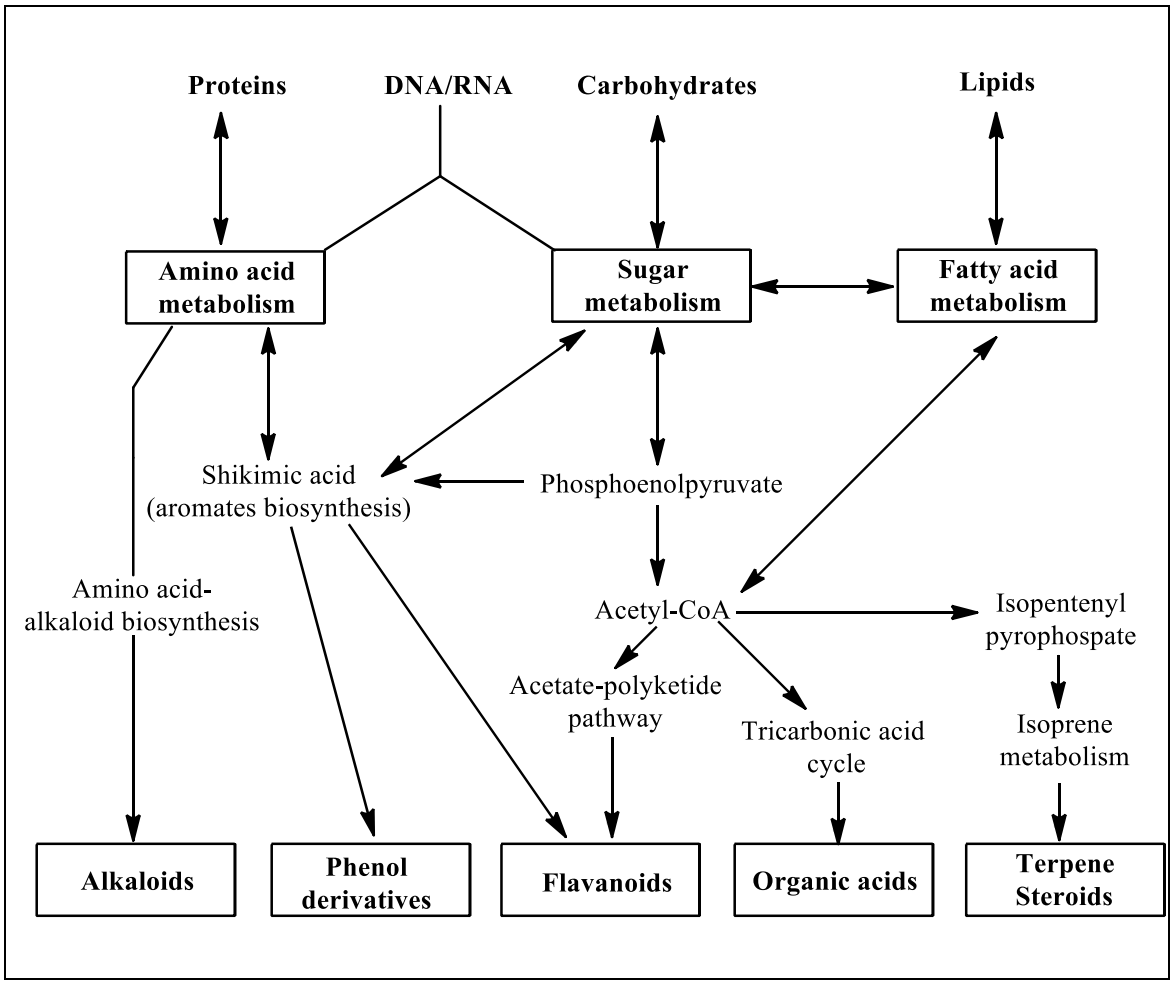

Scheme 1.1: General scheme of biosynthetic pathways and precursors for the major classes of secondary metabolites.

1.5. Diabetes mellitus-An overview

Diabetes mellitus (DM), is one of the lifestyle diseases characterized by polyuria. This is a chronic syndrome of impaired carbohydrate, protein and fat metabolism. These abnormalities will lead to chronic hyperglycemia and result in insufficient secretion of insulin or target-tissue insulin resistance. Complications of diabetes mellitus include

cardiovascular, nephropathy or neuropathy and retinopathy diseases [Alberti *et al*., **1998**; Paik *et al*., **1982**]. Polyuria, polydipsia, weight loss, sometimes with polyphagia, and blurred vision are some of the symptoms of marked hyperglycemia. Patients with diabetes are more susceptible to atherosclerotic cardiovascular, peripheral arterial and cerebrovascular disease [American Diabetes Association, **2010**].

1.5.1. Classification of diabetes

1.5.1.1. Type 1 diabetes

Type 1 diabetes occurs due to the auto immune destruction of beta cell that leads to absolute insulin deficiency. It is also known as insulin-dependent diabetes or juvenile-onset diabetes. Prevalence of Type 1 diabetes usually accounts for 10-20 % of total reported cases of diabetes [American Diabetes Association, 2004]. An individual with Type 1 diabetes may be metabolically regular before the disease is clinically manifest, but the process of beta–cell destruction can be identified [Alberti *et al*., **1998**].

The major symptoms of Type I diabetes includes-abnormal thirst and dry mouth, tiredness, frequent urination, hunger, weight loss and blurred vision.

1.5.1.2. Type II diabetes

Type 2 diabetes or non-insulin dependent diabetes mellitus is the most common form of diabetes which is characterized by disorders of insulin action, a defect in glucose uptake in muscle, a disruption of the secretory function of adipocytes, dysfunction of the pancreatic beta cells, and an impaired insulin action in the liver. Genetic and environmental factors are the main causes of type II diabetes.

Symptoms of Type II diabetes includes-excessive thirst, frequent urination, blurred vision and weight loss. The comparison of Type I and Type II diabetes mellitus has been tabulated in Table 1.1.

Table 1.1: Comparison of Type I and Type II diabetes mellitus

Features	**Type I**	**Type II**
Clinical	Onset <20 years Normal weight Decreased blood insulin Anti-islet cell antibodies	Onset >30 years Obesity Normal or increased blood insulin No anti-islet cell antibodies
Genetics	Ketoacidosis common Human leukocyte antigen (HLA)-D linked	Ketoacidosis rare No HLA association
Pathogenesis	Autoimmunity, immunopathologic mechanisms Severe insulin deficiency	Insulin resistance Relative insulin deficiency
Nutritional status at the time of onset	Frequently under nourished	Obesity usually present
Prevalence	10-20 % of diagnosed diabetes	80-90 % of diagnosed diabetes
Genetic predisposition	Moderate	Very strong
Defect or deficiency	β cells are destroyed, eliminating the production of insulin	Inability of β cells to produce insulin

1.5.2. Diabetes prevalence

Diabetes and its complications forms one of the major causes of death worldwide. Type II diabetes is the most prevalent form of diabetes and has increased alongside cultural and societal changes. According to International Diabetic Federation (IDF), in 2015, 215.2 million men and 199.5 million women had been affected with diabetes. This is expected to increase by 328.4 million men and 313.3 million women by 2040. Among the top ten

countries with the number of people with diabetes, India holds second place with 69.2 million suffering from diabetes (IDF 2015) and is expected to increase to 123.5 million in 2040. Kerala is known as diabetes capital of India, as prevalence of diabetes is high as 14.6 % (Figure 1.15), which is double the national average [Unnikrishnan *et al*., **2016**].

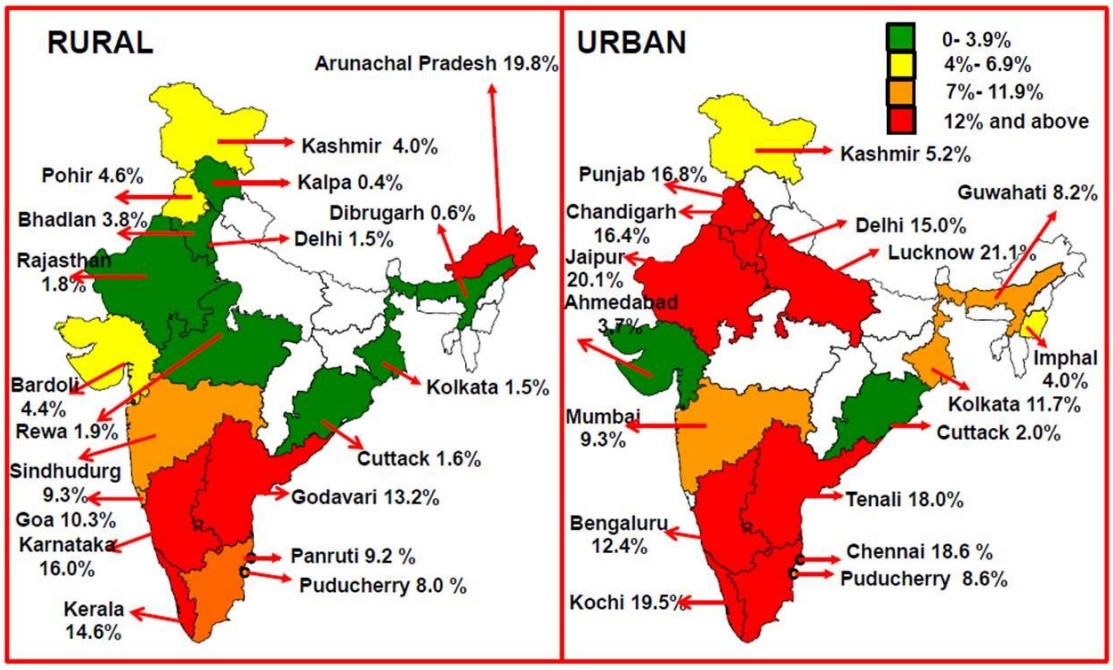

Figure 1.15: Diabetic prevalence in India
(Adopted from Unnikrishnan *et al*., **2016]**

1.5.3. Antidiabetic drugs and their associated side effects

Several drugs are used for the treatment of Type II diabetes, and they differ in the way they function in the body to reduce blood glucose. Similar to all synthetic drugs, diabetic medications also been reported for their side effects. Some diabetic drugs include common side effects such as nausea or an upset stomach. Continuous use of some other drugs can lead to hypoglycemia, back pain etc. Common adverse side effects observed due to the use of some antidiabetic drugs are shown in Table 1.2 [Pandeya *et al*., **2010**].

Table 1.2: Drugs used for the treatment of Type II diabetes and its side effects

Type of drug	**Brand/Generic Name**	**Side effects**
Sulfonylureas	Glimepiride, Glipizide, Glyburide	Skin rash, irritability, upset stomach
Biguanides	Glucophage, Metformin, Glucophage XR	Bloating, gas, diarrhoea, loss of appetite
Thiazolidinediones	Pioglitazone	Low blood glucose
α-glucosidase inhibitors	Acarbose	Upset stomach, abdominal pain, diarrhoea, gas
Meglitinides	Prandin, Starlix, Nateglinide	Back pain, joint pain, cough, a stuffy nose, and diarrhoea. Cause constipation and feelings of numbness, dizziness
Dipeptidyl peptidase 4 inhibitors	Januvia, Onglyza	Head ache, skin rash, gastrointestinal disturbances

1.5.4. Antidiabetic drugs from plants

From the beginning of human civilization, herbs have been used for the treatment of different diseases. According to WHO, Traditional Medicine (TM) refers to health practices, approaches, knowledge, and belief involving plant, animal and mineral based medicine, spiritual therapies, manual techniques and exercises applied singularly or in combination to treat, diagnose and prevent illness or well-being plant-based healthcare [Zhang *et al*., **2004**]. Galegine (isoamylene guanidine) was isolated from the plant *Galega officinalis* (French lilac, goat's rue; Fabaceae family) which is known as a folk medicine in Europe, for the treatment of diabetes. The compound galegine was also found to lower the blood glucose level and served as a model for the synthesis of metformin.

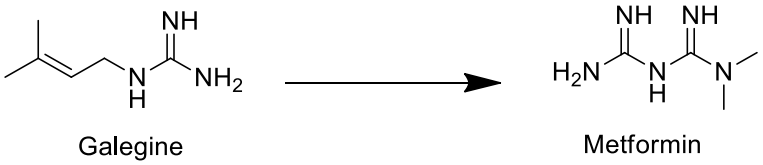

Studies in the late 1800s indicated that *G. officinalis* was rich in guanidine and in 1918 guanidine was shown to possess antidiabetic activity in animals [Watanabe, **1918**]. In 1929, several glucose-lowering biguanides were synthesised, including metformin (dimethylbiguanide). The important biguanides, phenformin and buformin (Figure. 1.16) were more potent than metformin. But in 1970s these biguanides discontinued in most countries in association with lactic acidosis [Nattrass *et al*., **1978**].

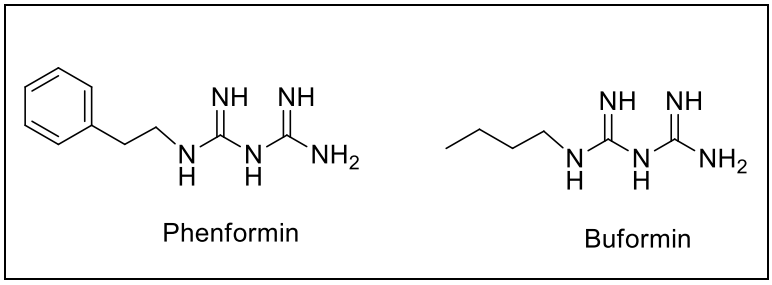

Figure 1.16: Structures of important biguanides

In 1835, French chemists isolated phlorizin (Figure 1.16) (dihydrochalcone glycoside) isolated from the bark of apple tree (*Malus domestica*) belonging to Rocaseae family. Phlorizin lowers glucose plasma levels and improves insulin resistance levels through inhibition of sodium glucose co-transporters (SGLT-2) [Ehrenkranz *et al*., 2005]. However, the compound was halted from becoming a drug, due to the drawbacks such as poor intestinal absorption and inactivation by lactase-phlorizin hydrolase [Butler, **2008**]. Two new innovative phlorizin analogues *viz*., empagliflozin and canagliflozin (Figure. 1.17) got FDA approval in 2013 and 2014 respectively for the treatment of type II diabetes.

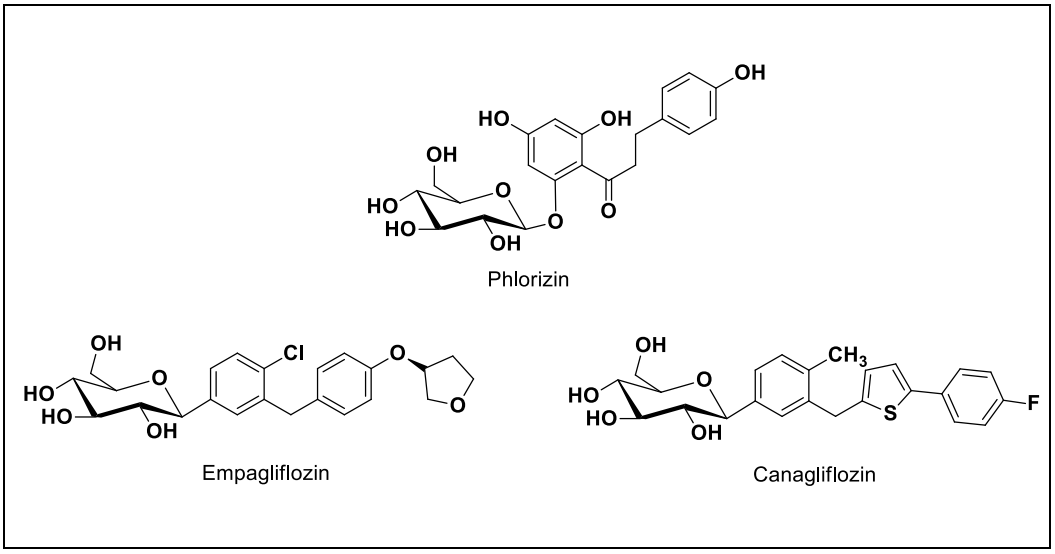

Figure 1.17: Structures of some antidiabetic drugs

1.6. Conclusion and Present Work

From the preceding discussion is clear that the pivotal role of natural products and their analogues in modern drug discovery. There is always an urgent need for finding new chemical entities as leads for future drug discovery and development. Bioprospecting of medicinal plants, which are used in various traditional systems of medicine have provided many effective drugs with unique mechanism of action. Drugs such as artemisinin, quinine, metformin etc., were all established based on the knowledge retrieved from traditional medicine. India is considered as the "Botanical Garden of World" with approximately 45,000 plant species, of which several thousand of them have been found to be of medicinal use. It has been estimated that only 10-20 % of species of plants have been systematically investigated for their bioactive compounds. Ayurveda, the traditional system of medicine practiced in India has been the basis of many modern drugs and has the potential to provide numerous other molecules with lead potential.

Considering the renewed attention in medicinal plants and traditional systems of medicine, we have focused our efforts on the phytochemical evaluation and antidiabetic evaluation of selected medicinal plants during this Ph.D. programme.

Chapter 1 gives a brief introduction to the role of natural products in modern drug discovery process, an attempt has been made to demonstrate the importance of NPs and their

classification in a brief manner. Special emphasis was given to plant-derived drugs, giving focus on antidiabetic agents developed from terrestrial plants.

Phytochemical investigation on the rare species *Ampelocissus indica* (L.) belonging to Vitaceae family is the subject matter of chapter 2. The extract level antioxidant and antidiabetic activity of *A. indica* rhizome is also presented in this chapter.

Chapter 3 of the thesis is divided into two parts. First part deals with the isolation and characterization of bioactives from the stem bark of *Vateria indica* (L.) belonging to Dipterocarpaceae family. In the second part, the structural and antidiabetic activity comparison of (+) and (-)-hopeaphenol is discussed.

Isolation and characterization of resveratrol oligomers from the stem bark of *Hopea ponga* (Dennst.) Mabb. and their antidiabetic effect by modulation of digestive enzymes, protein glycation and glucose uptake in L6 myocytes are explained in fourth chapter.

The family Moraceae is gaining lots of research attention in the recent times for its nutritional and health benefits. They are also very good sources of antioxidants and other biologically active compounds. In this category, the plants from *Artocarpus* genus always bear a decorative position. *Artocarpus*, has been used as food and for traditional folk medicines in South-East Asia, Indonesia, Western part of Java and India. Owing to the great biological significance of the genus Artocarpus, detailed phytochemical investigations of stem bark of *Artocarpus camansi* Blanco and *Artocarpus lakoocha* Roxb. were undertaken and is discussed in fifth chapter. In addition, the antidiabetic activity of the different extracts and isolated compounds are also explained in this chapter.

Celastrus paniculatus Willd. is a medicinally important woody liana of Celastraceae family indigenous to Western Ghats of India, mainly in the deciduous forests and is one of the least explored species in this family. In this regard, we carried out a detailed phytochemical evaluation of seeds of *C. paniculatus* and we could successfully isolate and characterise a number of molecules and have described our observations in the first part of chapter six. *C. paniculatus* is one of the most extensively used medicinal plants in the Ayurvedic system of medicine for memory enhancing. Hence, we screened the N-methyl-D-aspartate receptors (NMDARs) inhibitory activity of all the isolated compounds and have described it in the second part. In addition, the antidiabetic activity of the different extracts and isolated compounds were also screened and is discussed in this chapter.

CHAPTER 2

Phytochemical investigation on *Ampelocissus indica* (L.)

2.1. Introduction

As described in the introduction chapter, there is a renewed interest in the exploration of medicinal plants used in traditional systems of medicine since they have the higher chance of comprising novel bio-active phytochemicals in them. One such family of plants which enjoys great reputation in traditional systems of medicine all over the world is Vitaceae. The name Vitaceae is derived from the genus *Vitis*, and it sometime appears as Vitidaceae. Vitaceae is a family of dicotyledonous flowering plants, which comprises of approximately 14 genera and 910 species including the grapevine and Virginia creeper. The common genera namely; *Acareosperma, Ampelocissus, Ampelopsis, Cayratia, Cissus, Clematicissus, Cyphostemma, Muscadinia, Nothocissus, Parthenocissus, Pterisanthes, Rhoicissus, Tetrastigma* and *Vitis* are mainly found in temperate regions [Riviere *et al*., **2012**].

The Vitaceae (grape) family is one of the most commonly studied group of stilbenoid containing plants. Plants belonging to Vitaceae are a rich source of important biologically active molecules, and since many of them find extensive application in traditional systems of medicine, they have been well explored for their phytochemistry and pharmacology. Among the genera, *Ampelopsis, Cayratia, Cissus, Cyphostemma, Muscadinia, Parthenocissus, Rhoicissus,* and *Vitis* are the most important sources of stilbenoids. Of these studies, the majority of work was performed on the economically important *Vitis* species [Pawlus *et al*., **2012**]. Within this family, the resveratrol derivatives predominate, with multiple patterns of oligomerization and glycosylation. Stilbenes are widely considered phytoalexins in Vitaceae family for their role in plant resistance to fungal pathogens.

In addition to being a plant's defence system, stilbenoids are also of special interest for their potentially valuable health effects. These compounds have demonstrated a wide-range of biological and pharmacological activities such as antitumoral [Bai *et al*., **2010**], anti-atherogenic [Ramprasath and Jones **2010**], anti-inflammatory [Zhang *et al*., **2010**], anti-viral

[Nguyen *et al*., **2011**] and neuroprotective effects [Gonzalez-Sarrias *et al*., **2017**]. Some reviews on biological activitiy of the well-studied stilbene, resveratrol, including its potential neuroprotective activities have recently been published [Rege *et al*., **2014**; Gonzalez-Sarrias *et al*., **2017**].

2.1.1. Chemotaxonomy of Vitaceae

The systematic and phylogenetic connection of Vitaceae to other families is currently being debated. According to phylogenetic studies, Vitaceae is noticed as being closely related to Leeaceae in the isolated order Vitales [Soejima *et al*., **2006**]. Some specialists of these families exclude the genus *Leea* from Vitaceae and treat it as a monospecific genus within the family Leeaceae.

Currently, the phylogeny of Vitaceae is a dynamic area of investigation [Soejima *et al*., **2006**]. Recently, three noncoding intergenic spacers have been employed to construct the plastid phylogeny of Vitaceae. It is well established that *Cayratia, Tetrastigma*, and *Cyphostemma* are closely related and form a clade. Within this clade, Cyphostemma and Tetrastigma are each monophyletic, whereas *Cayratia* is paraphyletic [Soejima *et al*., **2006,** Riviere *et al*., **2012**]. *Ampelopsis* is grouped with *Rhoicissus* and one *Cissus* species, *Cissus striata*, with the remaining *Cissus* species being their own clade. *Vitis, Ampelocissus, Nothocissus* and *Pterisanthes* are grouped into a clade; however, *Vitis*, by its monophyly, forms a subclade. This large clade *Vitis*, *Ampelocissus*, *Nothocissus* and *Pterisanthes* is sister to a *Parthenocissus* and *Yua* clade.

The chemotaxonomy of stilbenoid chemistry to phylogenetic research has not been studied. However, this is currently difficult since only a fraction of plants from about half of the Vitaceae genera have been investigated for their stilbenoid content. Furthermore, since many of the same compounds are produced by the different genera, but in different proportions, differences may be seen more in the relative concentrations of compounds rather than compounds identified in the plant. Without chemical profiling of species, the use of stilbenoid chemistry for phylogenetic purposes is very difficult. Only the comparison and chemical profiling of plant species would provide the information necessary for the chemotaxonomy of Vitaceae, also the similarities and differences in stilbenoid profile between species and genera may be highly useful in phylogenetic and taxonomic studies.

2.1.2. Resveratrol monomer

Stilbenoids exist as both monomers and increasingly complex oligomers. The monomeric stilbene aglycone skeleton comprises of two aromatic rings joined by an ethylene bridge, of which, the *trans* isomer (*E*) is the most stable configuration (Figure 2.1). In 1940, resveratrol ((*E*)-5-(4-hydroxystyryl) benzene-1,3-diol) was identified in the roots of a Japanese plant called white hellebore (*Veratrum grandiflorum* O. Loes) by Takaoka. The vast majority of naturally occurring stilbenes contain several phenolic functionalities. They can be prenylated or geranylated in some species and are often glycosylated. Stilbene monomers reported from Vitaceae family are shown in (Figure 2.1). [Buiarelli *et al*., **2007**, Larronde *et al*., **2005**, Langcake *et al*., **1979,** Pawlus *et al*., **2012**].

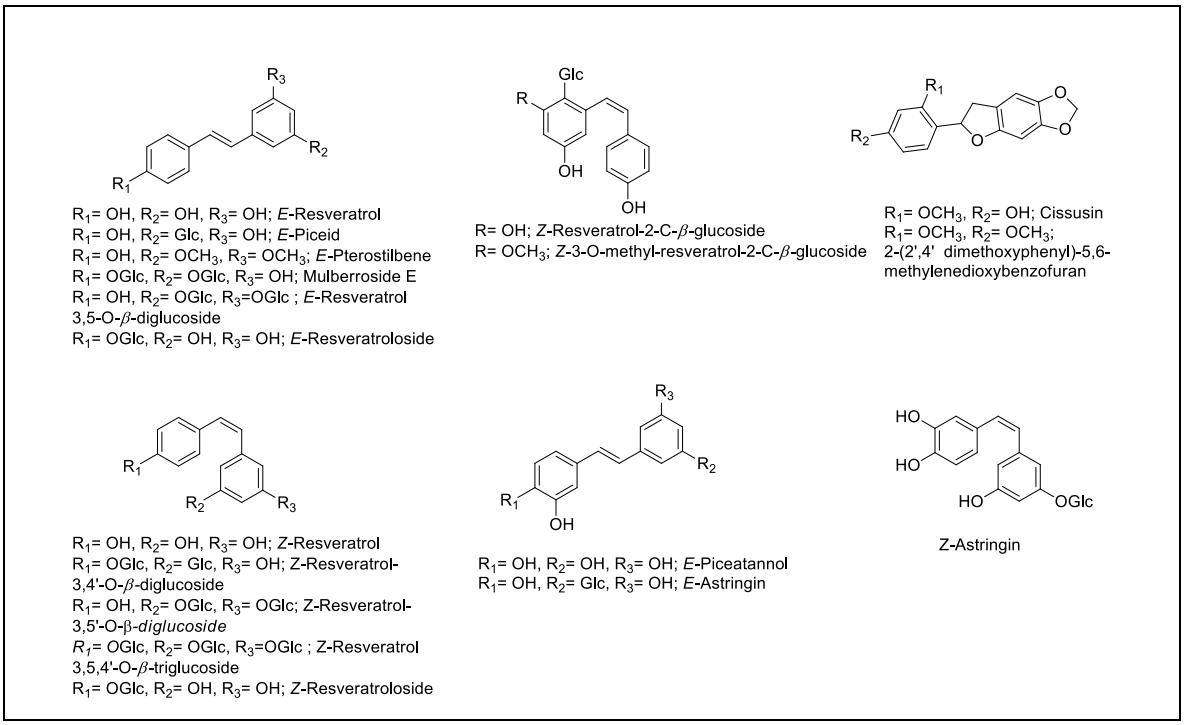

Figure 2.1: Structure of resveratrol monomers isolated from Vitaceae family

2.1.3. Biosynthetic pathway of resveratrol

Resveratrol biosynthesis occurs *via* phenylalanine pathway. The biosynthesis of resveratrol starts by the coupling of *p*-coumaric acid to CoA by the 4CL enzyme. Subsequently, coumaroyl-CoA is converted into resveratrol by sequential addition of three

malonyl-CoA units in presence of *stilbene synthase enzyme (STS)* with the release of carbon dioxide [Mohidul Hasan *et al*., **2017**] (Figure 2.2).

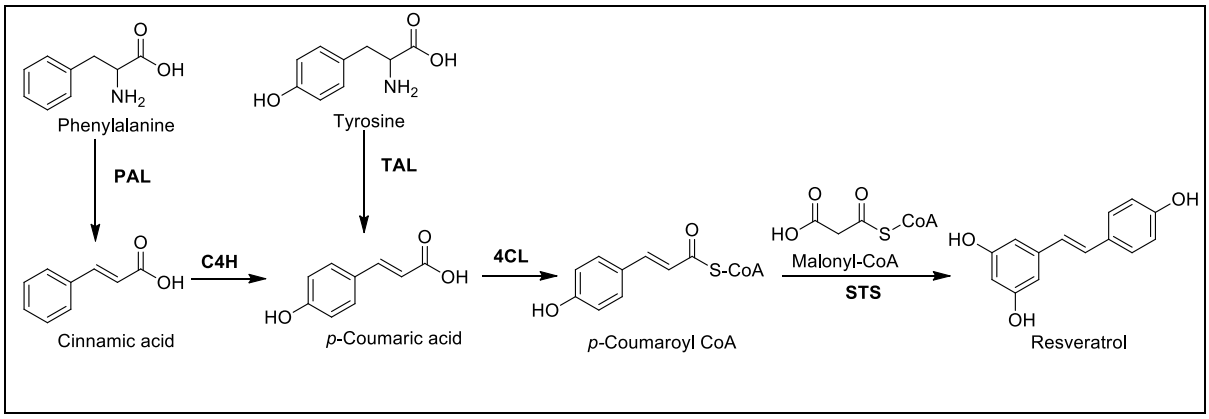

Figure 2.2: Biosynthetic pathway of resveratrol

2.1.4. Resveratrol dimers

Within Vitaceae, the 2,3-dihydrobenzofuran ring system, represented by the resveratrol dimer, (+)-*ε*-viniferin is commonly found. In fact, (+)-*ε*-viniferin, is a major constituent of Vitis species and is assumed to be an important intermediate in the synthesis of other oligomers. Another group of oligomers that commonly occur in Vitaceae are the compounds with non-oxygen-containing ring systems typified by the indanes, such as parthenocissin, viniferether and pallidol [Khan *et al*., **1986**]. These indane type stilbenes have been found in Vitis, and are only found in the most well characterized species, *V. vinifera* and *V. amurensis* [Mattivi *et al*., **2011**, Oshima and Ueno **1993,** Riviere *et al*., **2012**]. Some of the resveratrol dimers isolated from Vitaceae are shown in (Figure 2.3).

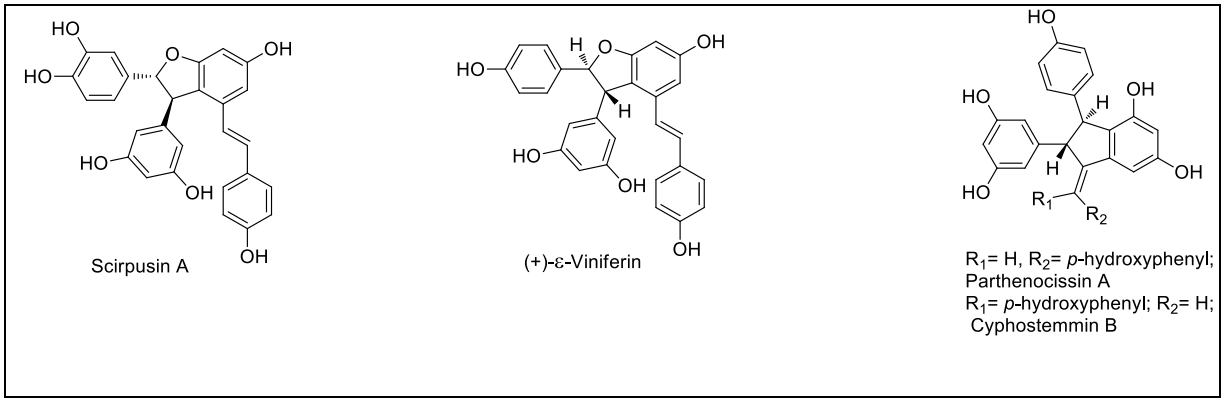

Figure 2.3: Resveratrol dimers isolated from Vitaceae

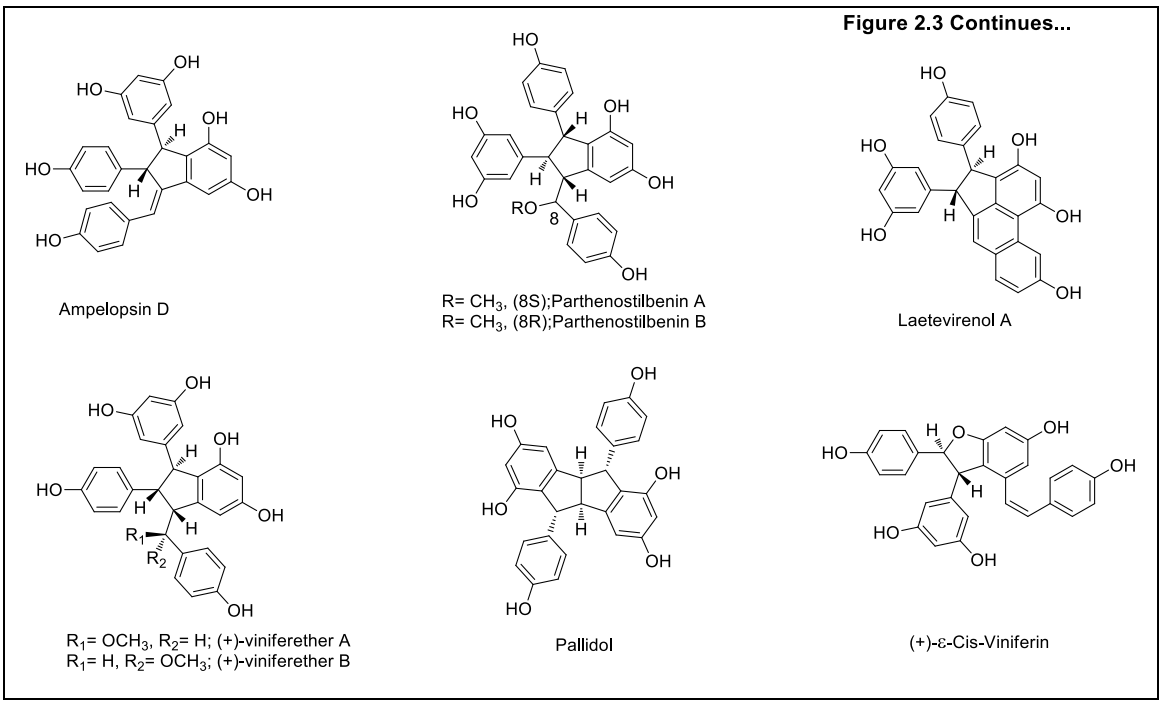

2.1.5. Resveratrol trimers

There are 18 resveratrol trimers reported in Vitaceae family (Figure 2.4). Six of these trimers have been reported from the different parts of *V. vinifera.* The majority of benzofuran type trimers are also reported from *Ampelopsis* species. The remaining known trimers except *α*-viniferin and gnetin E are only found in in *Vitis* and *Ampelopsis* species [Mattivi *et al*., **2011,** Riviere *et al*., **2012**]**.**

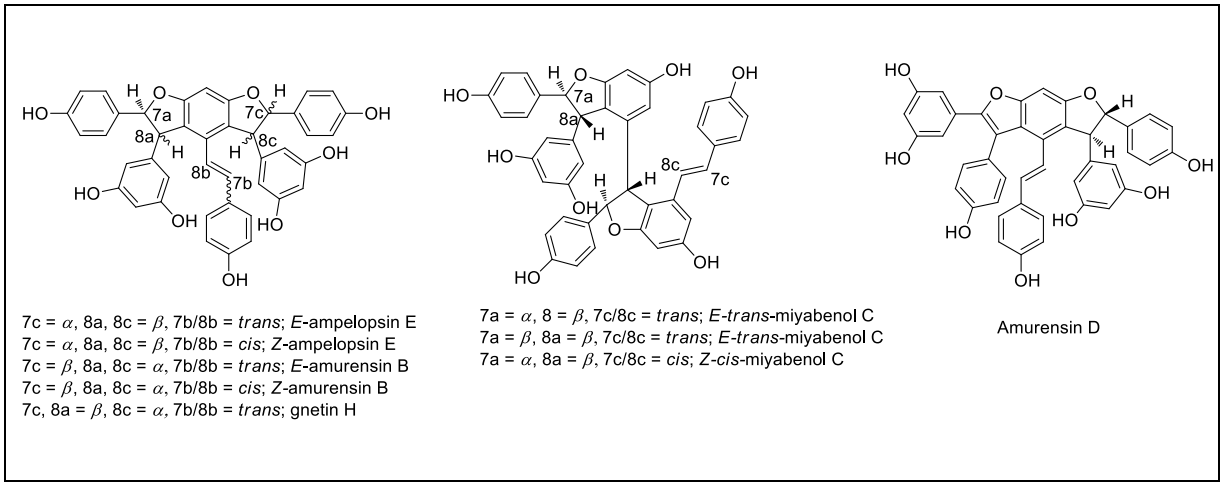

Figure 2.4: Resveratrol trimers isolated from Vitaceae

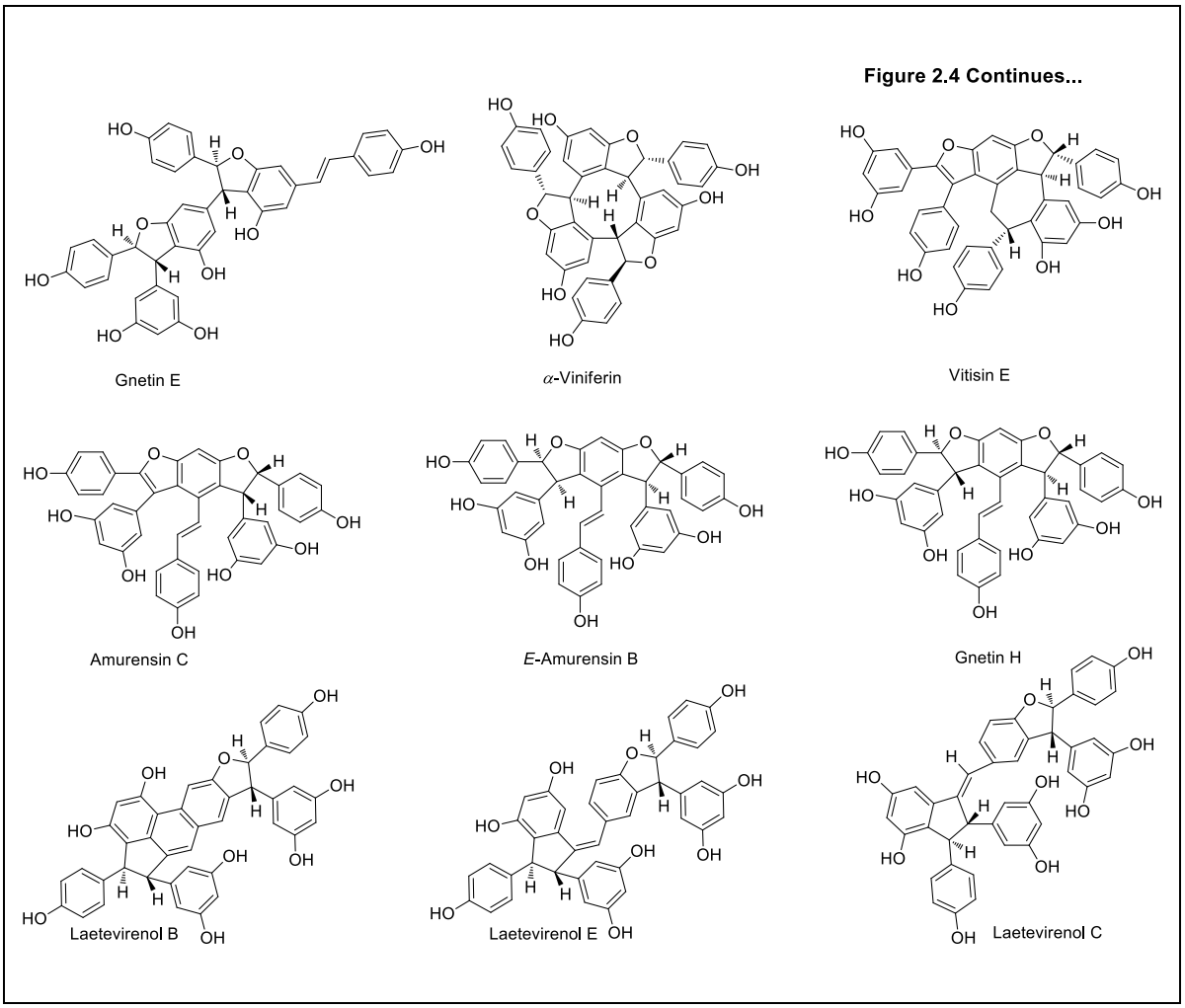

2.1.6. Resveratrol tetramers

There are total of 26 known tetramers, including tetramer breakdown product (-)-viniferal. The majority of stilbene tetramers are only reported from *V. vinifera* species. Some of the reported stilbene tetramers from the genus Vitus are shown in Figure 2.5 [Huang *et al*., **2001**, He *et al*., **2008,** Riviere *et al*., **2012**].

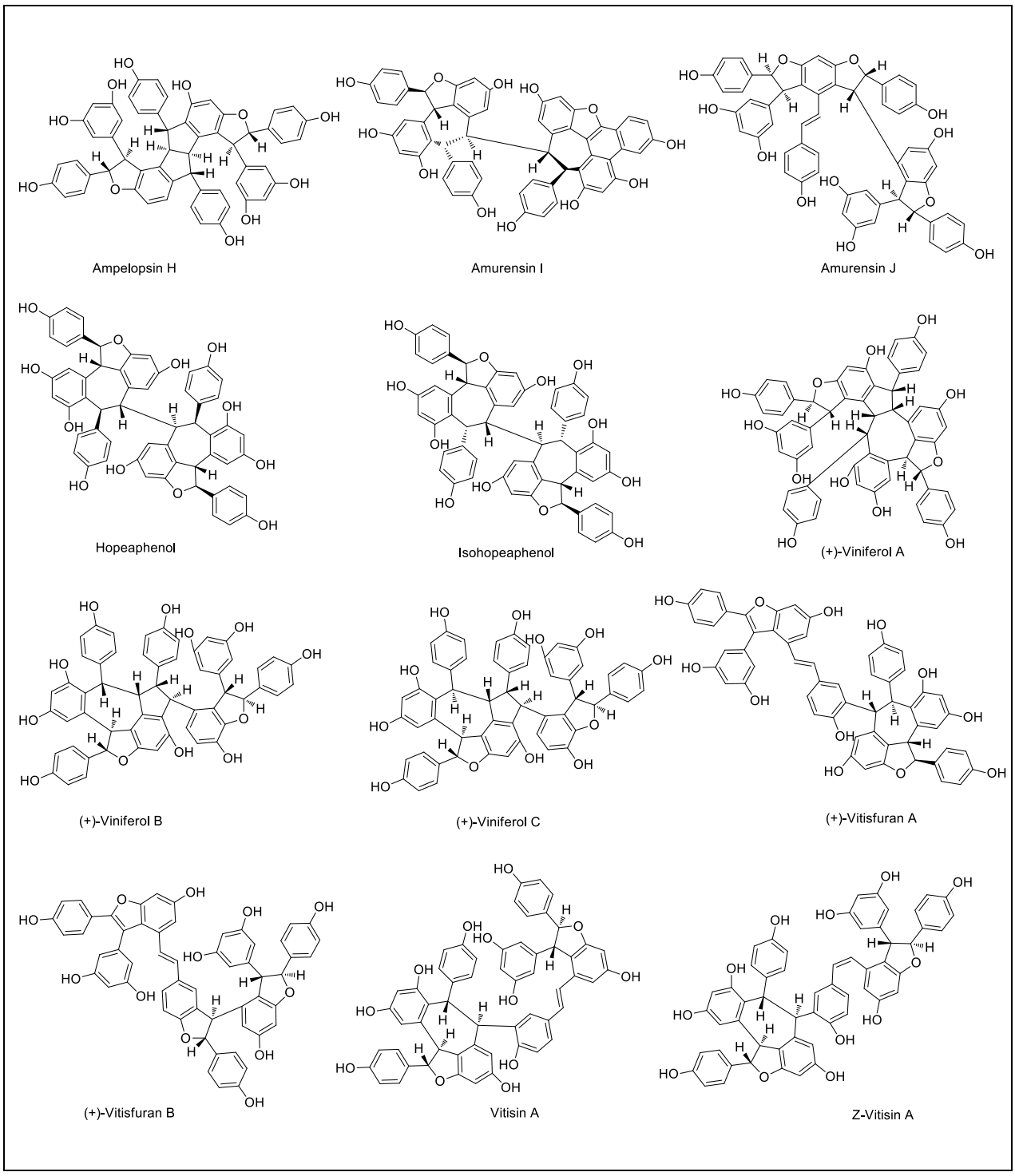

Figure 2.5: Resveratrol tetramer isolated from Vitaceae

2.1.7. An Overview of *Ampelocissus*

The genus *Ampelocissus*, belonging to Vitaceae family is one of the least explored genus of the family, and it consists of nearly 100 species of evergreen herbaceous or woody, polygamo-dioecious flowering plants with tendrils. Fruits are grape-like berries having 1-4 seeds mainly distributed in tropical Africa, Central America, Asia and Indian subcontinent [Riviere *et al*., **2012**]. The name and distribution of important plant species belonging to the genus *Ampelocissus* are given in Table 2.1.

Table 2.1: *Ampelocissus* species and their distribution

SI. No	***Ampelocissus* species**	**Distribution**
1	*A. abyssinica*	Southeast Ethiopia
2	*A. acetosa*	New Guinea, Western Australia
3	*A. aculeata*	Indonesia
4	*A. africana*	Southern Africa
5	*A. amentacea*	Fiji
6	*A. angolensis*	Southern Africa
7	*A. arachnoidea*	Indonesia
8	*A. araneosa*	India
9	*A. ascendiflora*	Malaysia
10	*A. barbata*	India
11	*A. birii*	India
12	*A. bombycina*	Cameroon
13	*A. borneensis*	Malaysia
14	*A. botryostachys*	Philippines
15	*A. capillaris*	Malaysia
16	*A. celebica*	Indonesia
17	*A. changensis*	Thailand
18	*A. cinnamomea*	Malaysia
19	*A. complanata*	Malaysia
20	*A. concinna*	Angola
21	*A. costaricensis*	Costa Rica
22	*A. debilis*	Malaysia
23	*A. dissecta*	Angola
24	*A. divaricata*	Thailand
25	*A. dolichobotrys*	Philippines
26	*A. edulis*	Congo
27	*A. elephantina*	Mauritius
28	*A. erdvendbergiana*	Mexico
29	*A. erdwendbergiana*	Mexico
30	*A. erdwendbergii*	Mexico
31	*A. filipes*	Malaysia
32	*A. floccosa*	Malaysia

Table 2.1 contd…

33	*A. frutescens*	Australia
34	*A. gardineri*	Australia
35	*A. gracilipes*	Liberia
36	*A. gracilis*	Singapore
37	*A. harmandii*	Lao people's democratic republic
38	*A. helferi*	India
39	*A. humulifolia*	Vietnam
40	*A. imperialis*	Indonesia
41	***A. indica***	India, Sri Lanka
42	*A. javalensis*	Costa Rica
43	*A. latifolia*	India
44	*A. leonensis*	Nigeria
45	*A. macrocirrha*	Cameroon
46	*A. madulidii*	Philippines
47	*A. martini*	Vietnam, Hong Kong
48	*A. mesoamericana*	Central America
49	*A. muelleriana*	Papua New Guinea
50	*A. multifoliola*	Philippines
51	*A. multiloba*	Tropical Africa
52	*A. multistriata*	Senegal, Tanzania
53	*A. nitida*	Malaysia
54	*A. obtusata*	Angola
55	*A. Obtusata subsp.*	Congo
56	*A. ochracea*	Indonesia
57	*A. pauciflora*	Philippines
58	*A. pedicellata*	Malaysia
59	*A. polythyrsa*	India, Malaysia
60	*A. pterisanthella*	Malaysia
61	*A. robinsonii*	Jamaica
62	*A. rubiginosa*	Indonesia
63	*A. rubriflora*	Vietnam
64	*A. rugosa*	India, Nepal
65	*A. rupicola*	Thailand
66	*A. sapinii*	Congo
67	*A. sarcocephala*	Congo
68	*A. schimperiana*	Angola
69	*A. sikkimensis*	India
70	*A. thyrsiflora*	Malaysia, Indonesia
71	*A. tomentosa*	India
72	*A. trichoclada*	Philippines
73	*A. verschuerenii*	Congo
74	*A. wightiana*	India

Of the above, none of the species of *Ampelocissus* have been studied for their phytochemical and pharmacological evaluation.

2.1.8. *Ampelocissus indica*

Description: *Ampelocissus indica* is a climbing shrub with young parts covered with brown colored wool. Stems are hollow and cylindrical. Leaves are alternate, simple, sometimes rarely shallowly 3-lobed, broadly egg-shaped or sub-orbicular 10-25 x 8-20 cm and leaf stalks up to 10 cm long. Flowers are bisexual, stalkless, minute, about 2 mm across with brownish red colour. Berries are globose or ovoid-oblong, about 2 cm long, smooth, juicy, sweet and purple in colour when it's ripe. Seeds are 3-angled, smooth, straw colored.

Distribution: Global; Peninsular India and Sri Lanka. National; Western Ghats in Kerala, Tamil Nadu, Karnataka and Maharashtra. Regional; In Kerala (reported from the hills of Thiruvananthapuram, Thrissur and Calicut districts). In Tamil Nadu (present in the hill tracts of Nilgiri and Tirunelveli districts).

Figure 2.6: Picture of *Ampelocissus indica* plant, leaves, fruit and rhizome

2.1.9. Scientific classification

Scientific classification of *Ampelocissus indica* is shown below (Table 2.2). *Ampelocissus indica* belongs to the family Vitaceae and this family is commonly known as grape family.

Table 2.2: Scientific classification of *Ampelocissus indica*

Kingdom	**Plantae**
Phylum	***Tracheophyta***
Sub class	**Vitoideae**
Order	***Vitales***
Family	**Vitaceae – *grape family***
Genus	***Ampelocissus***
Species	***Ampelocissus indica***

2.2. Aim and scope of the present work

Ampelocissus indica, commonly known as Chemparavalli or Semparavalli is belonging to the family Vitaceae. Juice of the rhizome is diuretic, aperient and a blood purifier. Roots are used to cure eye troubles and ulcers. Now the plant is delineated as one of the critically endangered species in the red list of International Union for Conservation of Nature (IUCN Red list-August 2010), needs an urgent attention for conservation. Therefore it is timely and relevant to carry out the phytochemical investigation of *A. indica.* So, as part of this Ph.D. program, a detailed study of *A. indica* rhizome and fruits was undertaken. Detailed investigation of the rhizome of the plant has been carried for identifying its stilbenoid constituents. Evaluation of chemical indices of two different extracts of *A. indica* rhizomes, preliminary *in vitro* antioxidant and antidiabetic potentials of the extracts was carried out. Detailed investigation of the fruits of the plant was undertaken carried for identifying its phytomolecules, and results of our investigation are discussed in the following section.

2.3. Extraction and biological activities of *Ampelocissus indica* rhizome

2.3.1. Plant material and extraction

The rhizomes of *Ampelocissus indica* (L.) were collected from Calicut district of Kerala during the month of January in 2014. The plant material was authenticated by the taxonomist of University of Calicut and a voucher specimen (Voucher no. 6781) was deposited in the herbarium repository of the institute. This was thoroughly cleaned and dried in a hot air oven maintained at 50 ^{o}C for three days. Approximately 750 g of the powdered material was then subjected to repeated extraction three times with hexane (2.5 L x 48 h) at room temperature. Thin layer chromatography indicated that the extraction was complete after six days. The total extract was then concentrated under reduced pressure using a Heidolph rotary evaporator. This yielded about 2.25 g of crude hexane extract (H). The above mentioned extraction procedures were repeated using acetone (A), ethanol (E) and water (W). Acetone extract yielded about 45 g, methanol extract yielded about 40 g and finally we got 25 g of water extract (after lyophilisation). These extracts were analyzed for their antioxidant and antidiabetic activities.

2.3.2. Extract level antioxidant and antidiabetic activities

2.3.2.1. Total Phenolic Content

Plants are considered as a variable source of natural products for maintaining human health. Many investigations have proved that most of the biological activities exhibited by these plants are due to the phenolic components present in them. Different solvent fractions of *Ampelocissus indica* (AI) were analysed for its phenolic content. The results showed that the acetone and methanol fractions of AI are rich in phenolic content (133.02 and 119.04 mg GAE/g dry weight). The results are shown in the Table 2.3.

2.3.2.2. DPPH radical scavenging assay

DPPH radical scavenging activity is one of the most widely used method for screening the antioxidant activity of plant extract. Among different fractions of AI, the highest DPPH radical scavenging activity was observed in acetone extract (IC_{50} 25.46 µg/mL). Whereas the methanol extract showed significant DPPH radical scavenging activity with IC_{50} 41.45 µg/mL. Results are shown in Table 2.3. The results can be correlated to higher phenolic content of respective fractions for its scavenging activity.

2.3.2.3. α-Amylase and α-glucosidase inhibition assay

Diabetes mellitus, is a chronic disorder associated with the metabolism of carbohydrate, protein and fat owing to absolute or corresponding deficiency of insulin. Therefore a therapeutic approach to treat diabetes is to decrease postprandial hyperglycemia. This can be attained by the inhibition of carbohydrate hydrolyzing enzymes like *α*-amylase and *α*-glucosidase. In the present scenario, there is an increasing demand for natural inhibitors from plant sources, due to the side effects exhibited by the synthetic drugs. The results from our study showed that the acetone fraction of AI effectively inhibits the *α*-amylase enzyme (IC_{50} 100.44 ± 0.762 µg/mL), which is less active when compared to the standard acarbose (5.69 ± 0.119 µg/mL) (Figure 2.7). All the fractions of AI, except hexane fraction, inhibited *α*-glucosidase enzyme. The acetone fraction have demonstrated highest activity (IC_{50} 23.20 ± 0.690 µg/mL), which is better than the standard acarbose used (IC_{50} 45.29 ± 0.128 µg/mL) (Figure 2.8). The results are shown in Table 2.3.

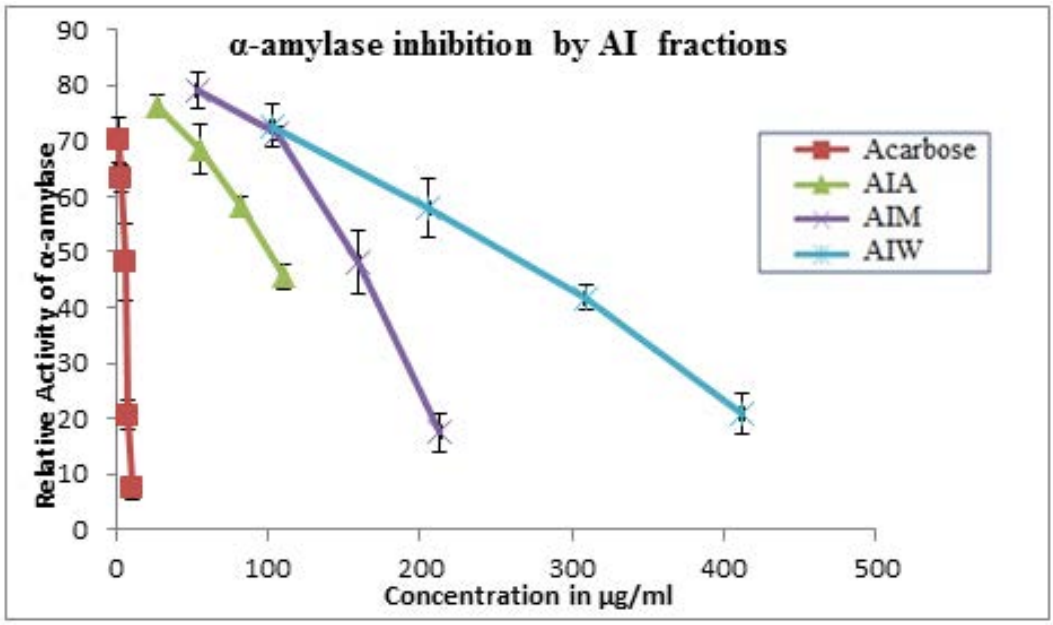

Figure 2.7: *α*-Amylase inhibitory activity of different extracts of *A. indica* rhizome

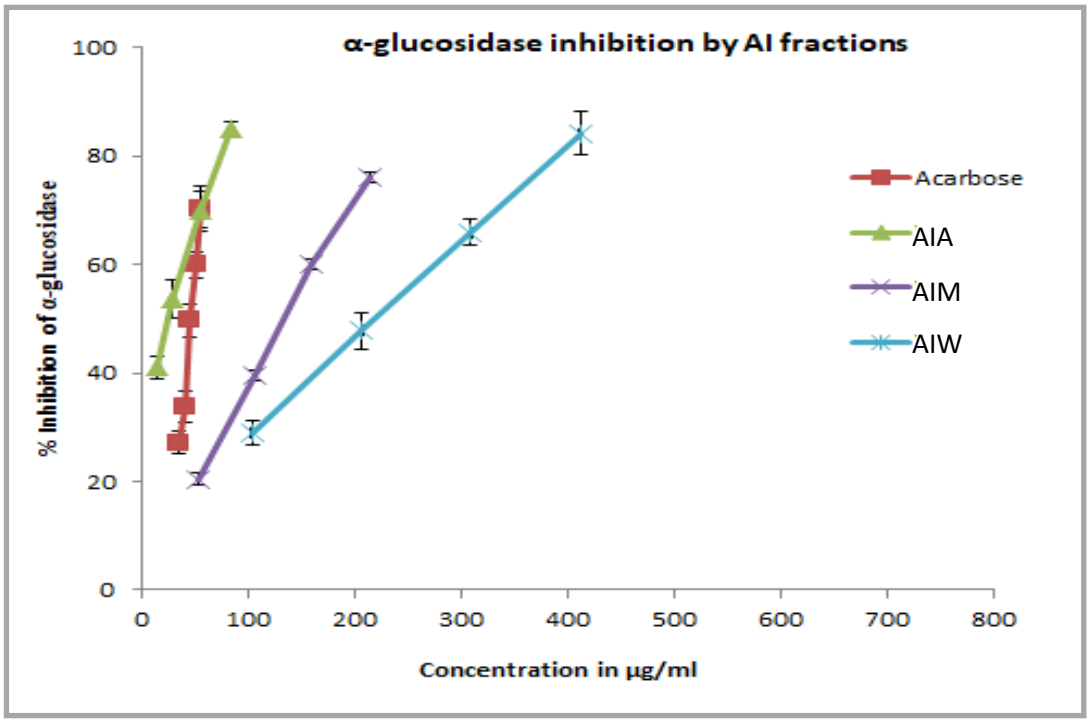

Figure 2.8: α-Glucosidase inhibitory activity of different extracts of *A. indica* rhizome

2.3.2.4. Antiglycation assay

The higher level of glucose in the blood increases the nonenzymatic glycation of proteins which leads to the formation of advanced glycated end products. These advanced glycated end products play key role in many diabetic complications. Therefore, there is an increasing demand for plant extracts or compounds which inhibits glycation. The results from our study depict that the acetone fraction of AI possesses good antiglycation activity (161.71 µg/mL) compared to other extracts. Ascorbic acid is used as the standard (28.11 µg/mL). The results are shown in Figure 2.9 and the values are shown in Table 2.3.

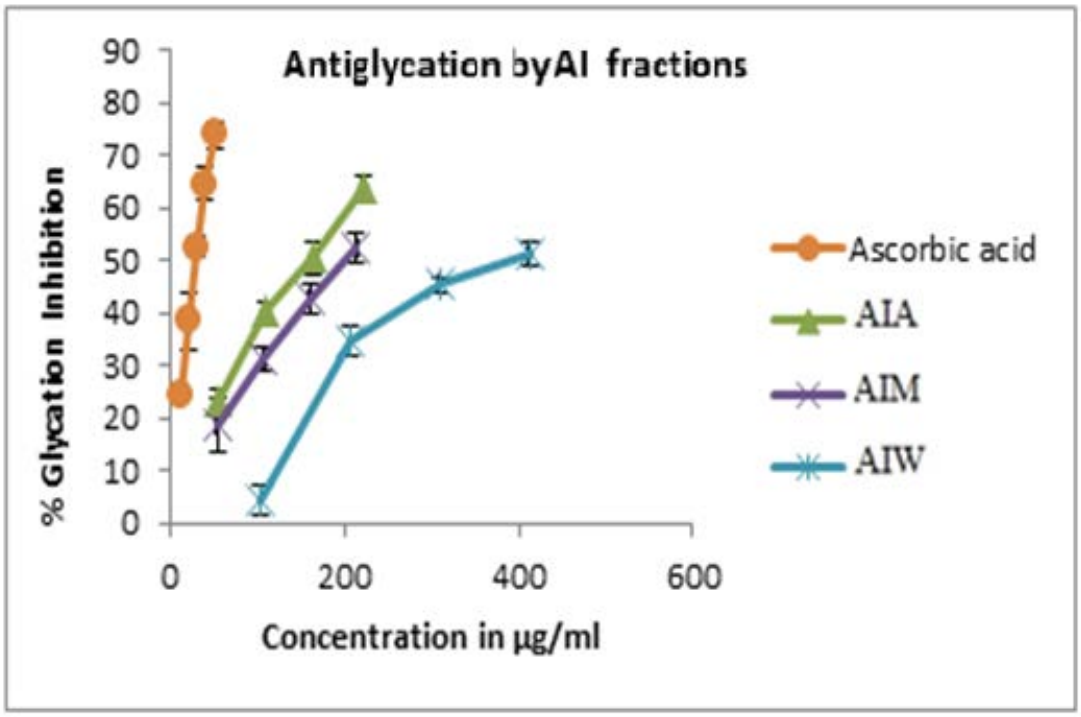

Figure 2.9: % Inhibition of glycation by different extracts of *A. indica* rhizome

Table 2.3: TPC, DPPH radical scavenging, α-amylase inhibition, α-glucosidase inhibition and antiglycation by hexane (H), acetone (A), methanol (M) and water (W) fractions of AI.

Fractions	TPC (mg GAE/g dry weight)	DPPH (IC_{50}-µg/mL)	*α*-amylase (IC_{50}-µg/mL)	*α*-glucosidase (IC_{50}-µg/mL)	Antiglycation (IC_{50}-µg/mL)
AI-H	7.67±0.146	1086.4±0.246	NIL	NIL	NIL
AI-A	133.02±2.055	25.46±0.441	100.44±0.762	23.20±0.690	161.71±0.357
AI-M	119.04±0.139	41.15±0.146	155.86±0.122	133.2±0.267	200.66±0.670
AI-W	67.63±0.522	120.2±0.521	255.17±0.590	219.3±0.987	392.09±0.982
Standard	-	3.01±0.245 (Gallic acid)	5.69±0.119 (Acarbose)	45.29±0.128 (Acarbose)	28.11±0.527 (Ascorbic acid)

All data are represented as mean ± standard deviation (n=3).

2.4. Isolation and characterization of compounds from *Ampelocissus indica* rhizome

The antioxidant and antidiabetic activity screening of different extracts of AI acetone extract has showed the highest activity compared to other extracts. Therefore, further isolation and purification of chemical constituents of acetone extract was performed. After studying the TLC, 45 g of the acetone extract was subjected to column chromatographic purification using silica gel (100-200 mesh). Column elution was initiated using 100 % hexane and polarity was increased by increasing the amount of ethyl acetate. Final elution was carried out with 15 % methanol in ethyl acetate. A total of 250 fractions of approximately 200 mL each were collected. According to the similarity in TLC, they were pooled into 60 major fraction pools (FrA.1- FrA. 60).

Fraction pools 6-8 (FrA. 6-8), obtained by eluting the column with 25 % ethyl acetate - hexane showed the presence of a UV active compound with minor impurities. It was again subjected to purification using silica gel column chromatography (230-400 mesh). Subfractions 3-8 obtained by eluting the column with 20 % ethyl acetate in hexane yielded 39 mg (0.0052 %) of light brownish solid, which was labelled as compound **1**. IR spectrum of the compound showed a broad signal at 3411 cm^{-1}, indicating the presence of hydroxyl group. In ^{1}H NMR, (Figure 2.11) the signals at δ 8.55 and 8.28 ppm indicated the presence of phenolic hydroxyl group. Signals at δ 7.03 and 6.90 ppm as a doublet each integrating for one proton with coupling constant value J = 16.5 Hz could be attributed to *trans* olefinic protons. Signals at δ 7.43 and 6.85 ppm, each integrating two for protons with coupling constant J value 8 Hz can be attributed to aromatic protons at C2*'*,C 6*'* and C3*'*, C5*'* respectively. Two protons on the carbon C2 and C6 appeared at δ 6.56 ppm as a singlet. The proton at C4 resonated as a singlet at δ 6.28 ppm. In ^{13}C NMR, (Figure 2.12) the peaks at δ 158.7 and 157.3 ppm indicated the presence of aromatic carbon attached to the hydroxyl group. The *trans* olefinic carbon resonated at δ 128.2 and 125.9 ppm. The mass spectrum of the compound **1** showed the molecular ion peak at m/z 229.0868, which is the $[M+H]^{+}$ peak. From all the spectral data and on comparison with the literature reports [Lambert *et al*., **2013**], the compound was confirmed as ***E*-Resveratrol** (3,5,4′-trihydroxy-*trans*-stilbene). The compound is being reported for the first time from *Ampelocissus* genus. The structure of the compound is shown below (Figure 2.10).

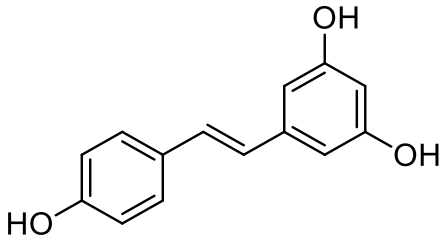

Figure 2.10: *E*-Resveratrol (**1)**

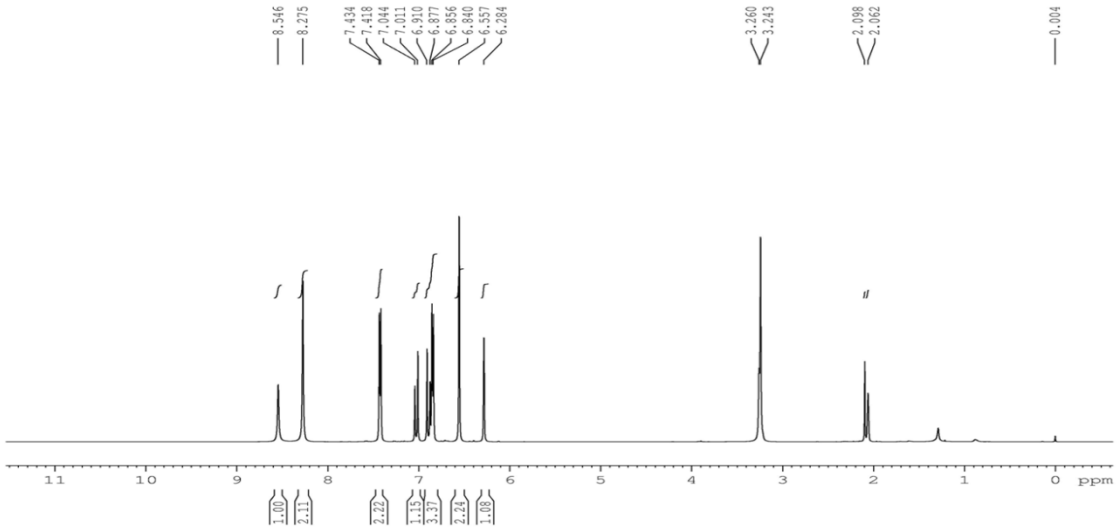

Figure 2.11: ^{1}H NMR spectrum of *E*-resveratrol

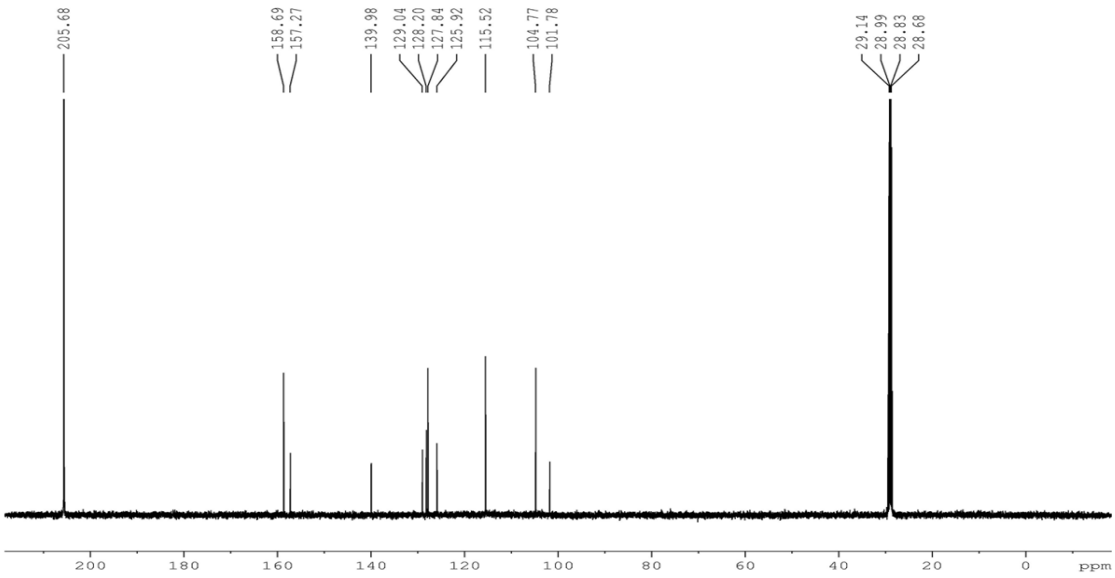

Figure 2.12: ^{13}C NMR spectrum of *E*-resveratrol

Fraction pools 11-15 (FrA.11- Fr.A.15), obtained by eluting the column with 35 % ethyl acetate in hexane yielded 17 mg (0.0023 %) of a yellow amorphous solid which showed blue fluorescence under UV light was labelled as compound **2**. IR spectrum of the compound **2** showed broad absorption at 3388 cm^{-1} indicating the presence of a hydroxyl group, and absorption at 2961 and 1603 cm^{-1} suggested the presence of aromatic C-H and C-C bonds. In ^{1}H NMR spectrum, (Figure 2.14) the peaks at δ 8.58 and 8.35 ppm indicating the presence of phenolic hydroxyl groups. The signals at δ 6.91 and 6.70 ppm as a doublet each integrating one proton with *J* value 16.5 Hz could be attributed to *trans* olefinic protons. The protons of stereocenter 7a and 8a resonated at δ 5.43 and 4.47 ppm as a doublet with coupling constant *J* value 5.5 Hz respectively. In ^{13}C NMR, (Figure 2.15) the signals at δ 161.5, 159.0, 158.8, 157.4 and 157.4 ppm are the diagnostic peaks for aromatic carbons attached to the hydroxyl group. The stereocenter carbon 7a, carbon directly attached to oxygen atom resonated at δ 93.0 ppm and another stereocenter carbon 8a appeared at δ 56.2 ppm. The mass spectra of the compound **2** gave molecular ion peak 455.1497 which is the $(M+H)^{+}$. From all these spectral data and on comparison with the literature reports [Takaya *et al*., **2002**], the compound was confirmed as *ε*-viniferin **2**, has the relatively uncommon distinction of being a natural product found in naturally in both enantiomeric forms. (−)-*ε*-Viniferin is found in several plant species in Dipterocarpaceae, Gnetaceae, Cyperaceae, and Fabaceae family, while its enantiomer, (+)-ε-viniferin, is exclusively found in plants from the family Vitaceae [Keylor *et al*., **2015**]. The absolute configuration of *ε*-viniferin **2** was established on the basis of optical activity $[\alpha]^{25}_{D}$ +46.7° (c 0.1, MeOH); which was in agreement with the reported value $[\alpha]^{22}_{D}$ +49.1° (c 0.1, MeOH) [Takaya *et al*.,**2002**; Ito and Niwa **1996**]. Finally, compound **2** was confirmed as (+)-*ε*-viniferin (Figure 2.13). The structure of the compound is shown below. Biosynthetic pathway of (+)-*ε*-viniferin will be discussed in chapter 3B.

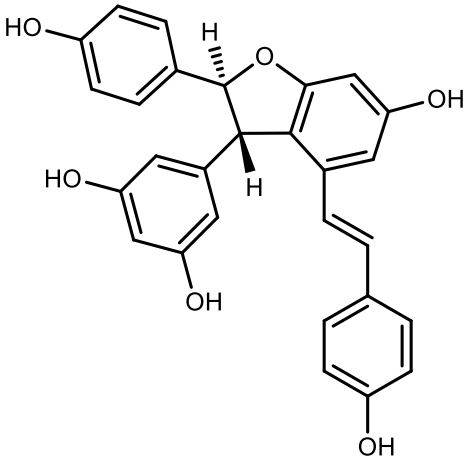

Figure 2.13: (+)-*ε*-Viniferin **(2)**

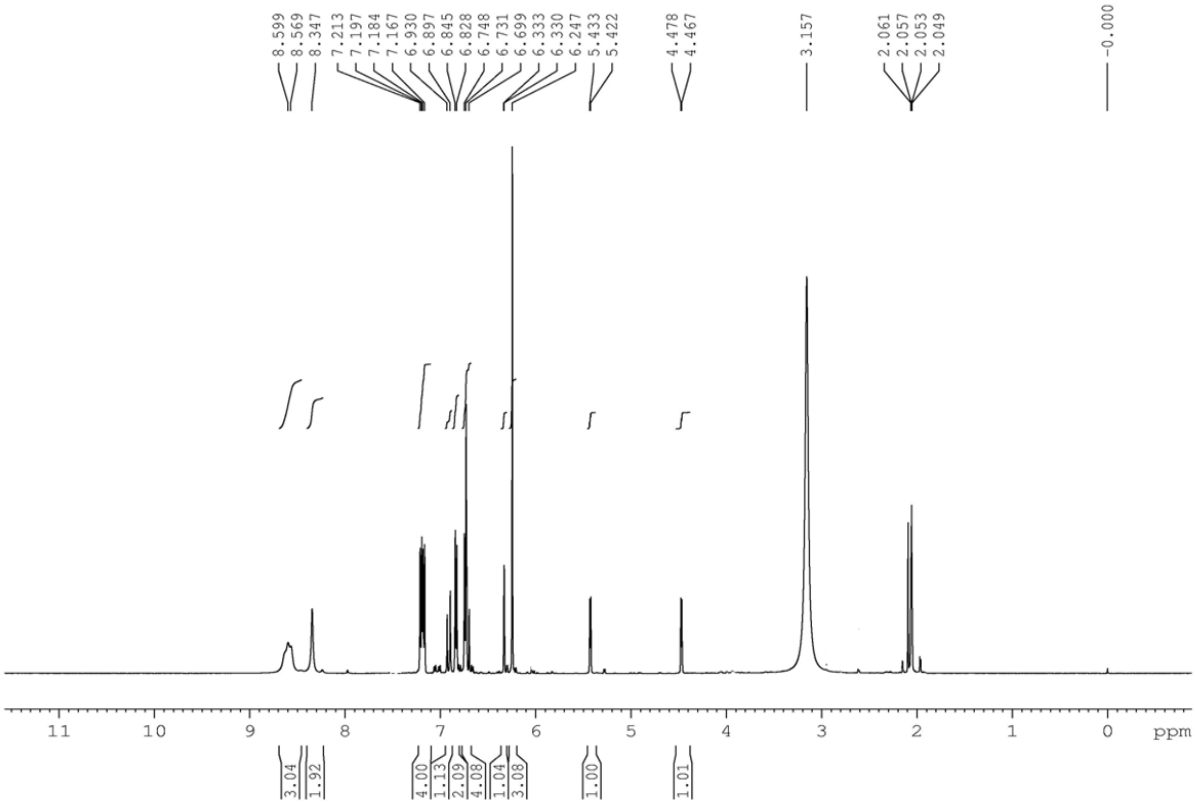

Figure 2.14: ^{1}H NMR spectrum of (+)-*ε*-viniferin

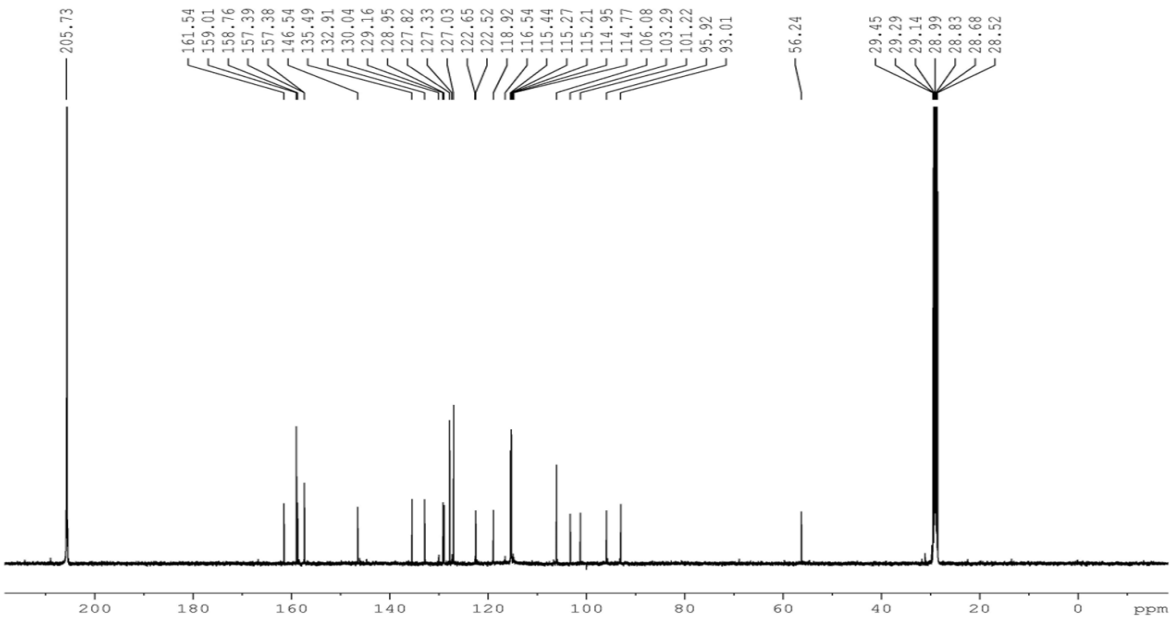

Figure 2.15: ^{13}C NMR spectrum of (+)-*ε*-viniferin

Compound **3** (5 mg; 0.00067 %) was isolated as a pale yellow coloured amorphous powder from fractions 21-24 obtained by repeating column chromatography with 60 % ethyl acetate in hexane and was assigned the molecular formula $C_{42}H_{33}O_9$ from the analysis of the HRESIMS at *m/z* 681.1970 $[M + H]^+$. IR spectrum of the compound showed absorption at 3278 and 2959 cm^{-1} suggesting the presence of hydroxyl –OH and aromatic –CH groups respectively. The ^{1}H NMR spectrum in CD_3COCD_3 (Figure 2.17) exhibited signals for eight phenolic hydroxyl groups (δ 8.42-7.94 ppm) which disappeared upon addition of D_2O. Considering the molecular formula, the remaining oxygen would contribute to the ether linkage. Other 2D spectroscopic details including ^{13}C NMR, ^{1}H–^{1}H COSY, HMQC and HMBC spectra (Figure 2.17- Figure 2.21) exhibited signals due to six aromatic rings as follows; three *p*-hydroxyphenyl groups (A1, C1 and B1), a 1,2,3,5-tetrasubstituted aromatic ring (A2), a 1,2,3,5,6-pentasubstituted aromatic ring which is directly attached to furan ring (B2) and a 3,5- dihydroxyphenyl group (ring C2). The presence of a set of mutually coupled aliphatic protons (H-7a/H-8a) and a sequence of four aliphatic protons (H-7b/H-8b/H-7c/H-8c) were also shown. The ^{1}H–^{1}H coupling pattern of the stereocenter protons (H-7a/H-8a) was characteristic of a dihydrobenzofuran ring, and of the latter (H-7b/H-8b/H-7c/H-8c) was similar to a partial structure of vaticanol A, [Tanaka *et al*., **2000**] which suggested a bicyclo[5,2,0]decadiene ring system. The planar structure was confirmed by the following

evidence. The correlations in the HMBC spectrum (Figure 2.22) were observed between H-7a/ C-(2a,6a), H-7b/C-(2b,6b), H-7c/C-(2c,6c), H-8a/C-14a, H-7b/C-8b, C-10a, H-8b,/C-9b and H-8c/C-(10c,14c), which indicated the presence of six aromatic ring and six methine units.

To confirm the relative stereochemistry, NOESY experiments were conducted (Figure 2.21). The clear cross peaks between H-7a/H-14a, H-8a/H-(2a, 6a) were observed which substantiated that the relative stereochemistry of the methine protons at 7a and 8a are in *trans* orientation. The relationship between four methine protons (H-7b, H-8b, H-7c and H-8c) and the dihydrobenzofuran ring was determined as follows. NOE interactions between H-8a/ H-(2b,6b) indicated that the ring B1 is oriented in *β*-configuration, alternatively H-7b is oriented in α-configuration. The significant NOEs observed between H-(2c,6c)/H-8c, H-(10c,14c)/H-8b and H-(10c,14c)/H-7c also indicated that the relative configuration of methine protons at C-7b, C-8b, C-7c and C-8c were *α, α, α* and *β* configurations (Figure 2.22). Also correlation between protons at 7b and 7c indicated that these protons are in *α*-orientation. On the basis of these correlations, the relative stereo chemistry of compound **3** was confirmed. The absolute configuration of compound **3** was established on the basis of optical activity which was found to be $[\alpha]^{25}_{D}$ +145^{o} (c 0.1, MeOH). From all the above spectral details and on comparison with the literature reports [Ito *et al*., **2003**], the compound was confirmed as **(+)-Pauciflorol A**. Biosynthetic pathway of pauciflorol starts from the resveratrol dimer ε-viniferin. The oxidative radical cyclization of ε-viniferin and resveratrol would generate para-quinone methide through the formation of the C_{8b}–C_{7c} bond. A 7-*exo-trig* cyclization (C_{10a}–C_{7b}) yields 5, 7-fused indane skeleton found in the natural products (+)-Pauciflorol A [Keylor *et al*., **2015**]. The structure of the compound is shown below.

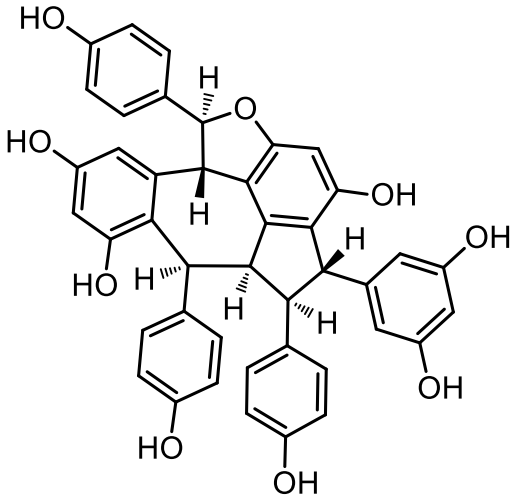

Figure 2.16: (+)-Pauciflorol A **(3)**

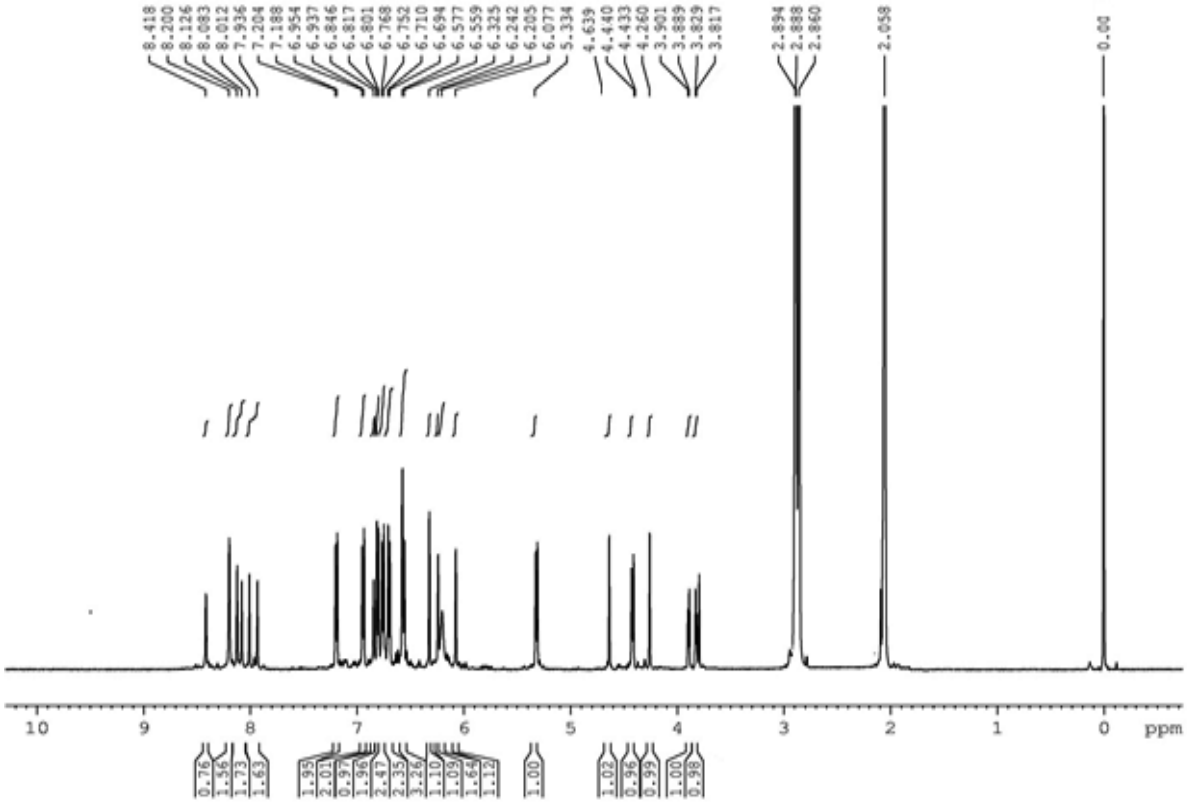

Figure 2.17: ^{1}H NMR spectrum of (+)-pauciflorol A

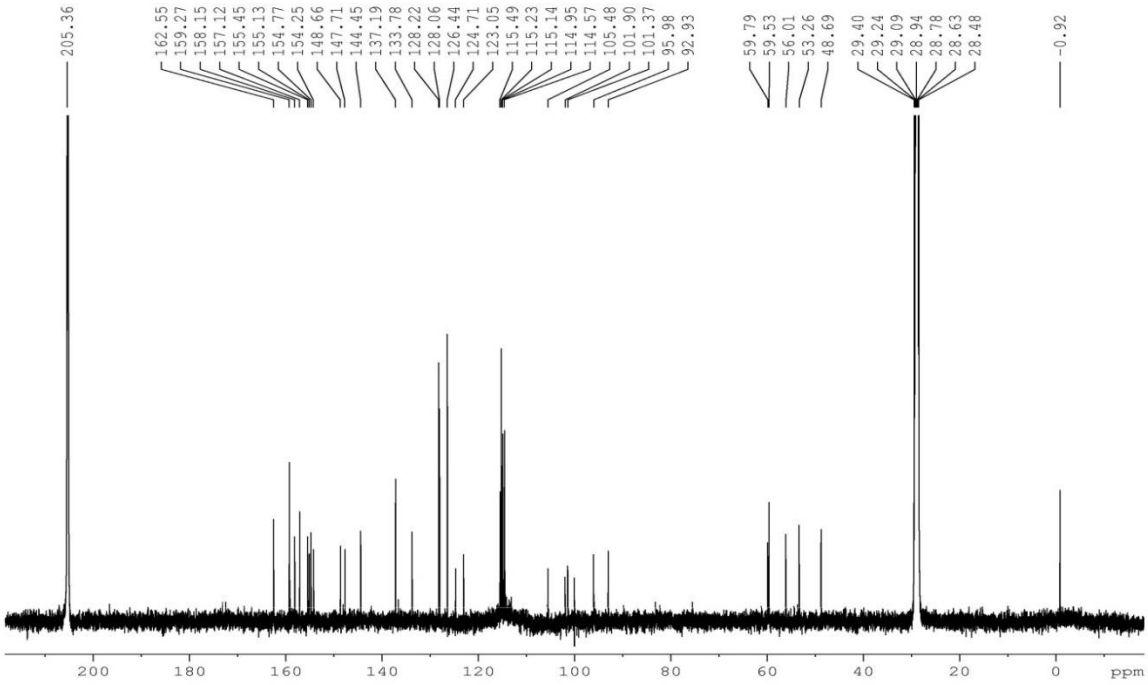

Figure 2.18: ^{13}C NMR spectrum of (+)-pauciflorol A

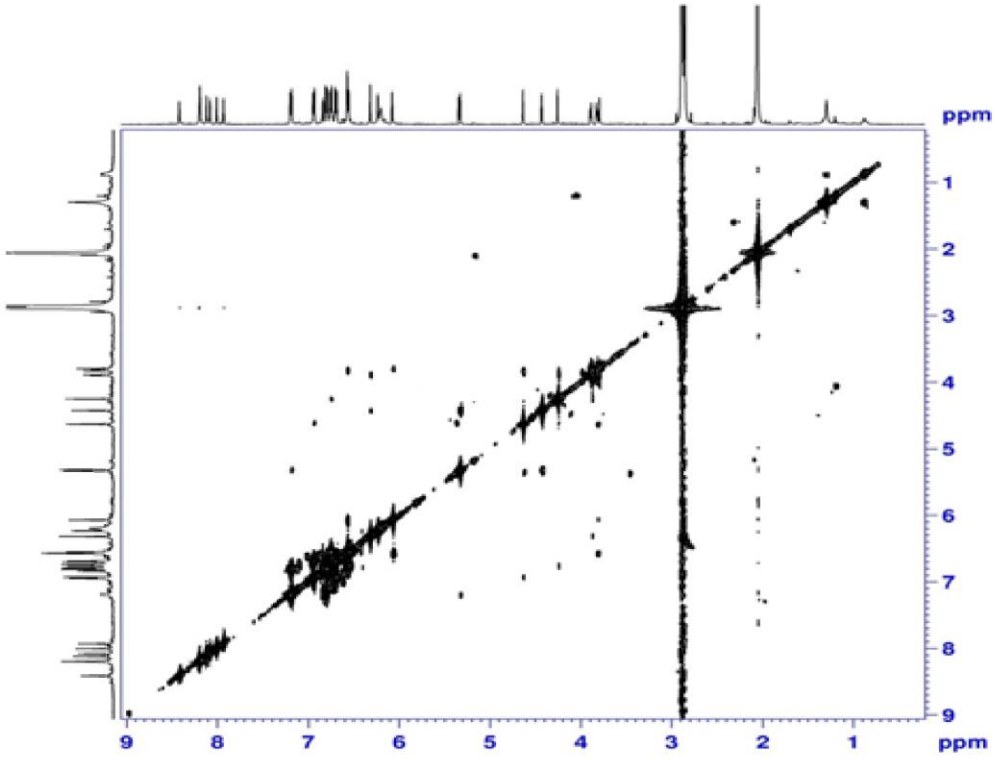

Figure 2.19: ^{1}H-^{1}H COSY NMR spectrum of (+)-pauciflorol A

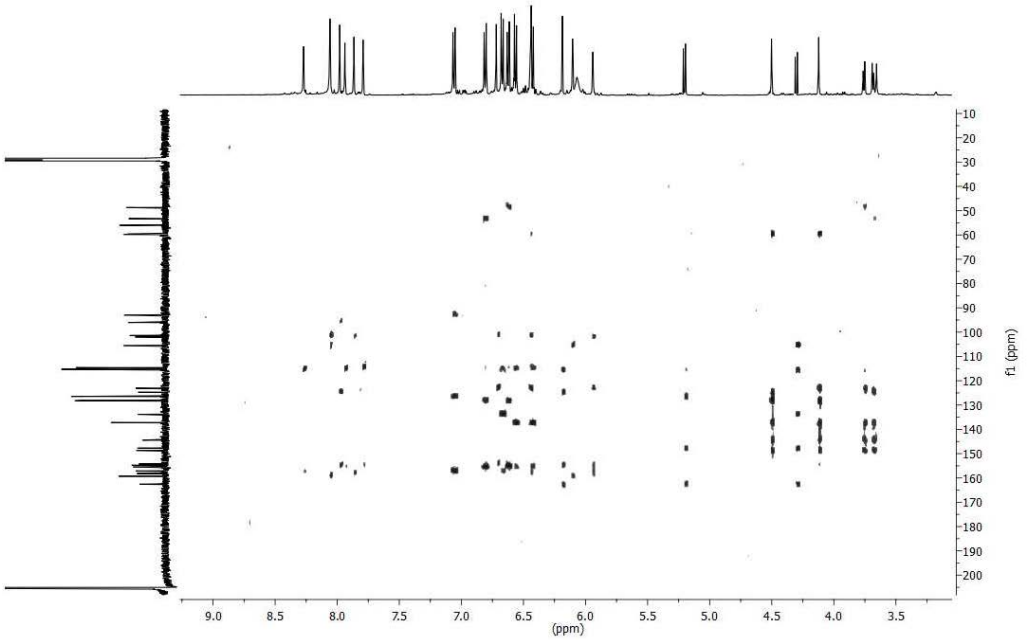

Figure 2.20: HMBC spectrum of (+)-pauciflorol A

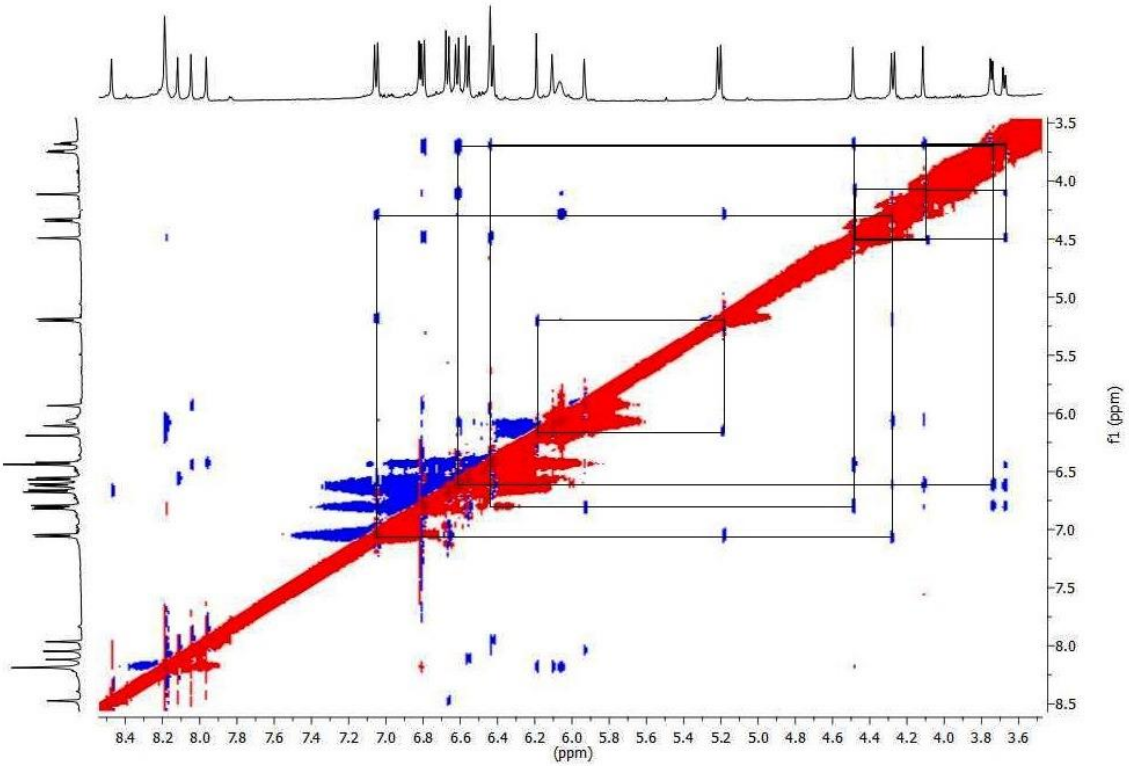

Figure 2.21: ^{1}H-^{1}H NOESY spectrum of (+)-pauciflorol A

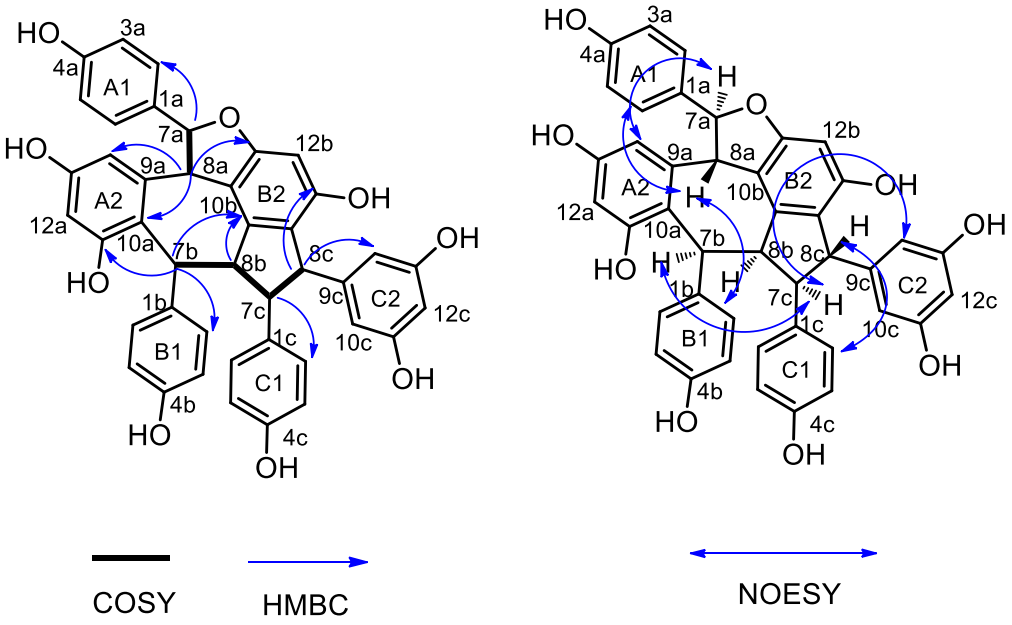

Figure 2.22: Selected COSY, HMBC and NOESY correlations of (+)-pauciflorol A

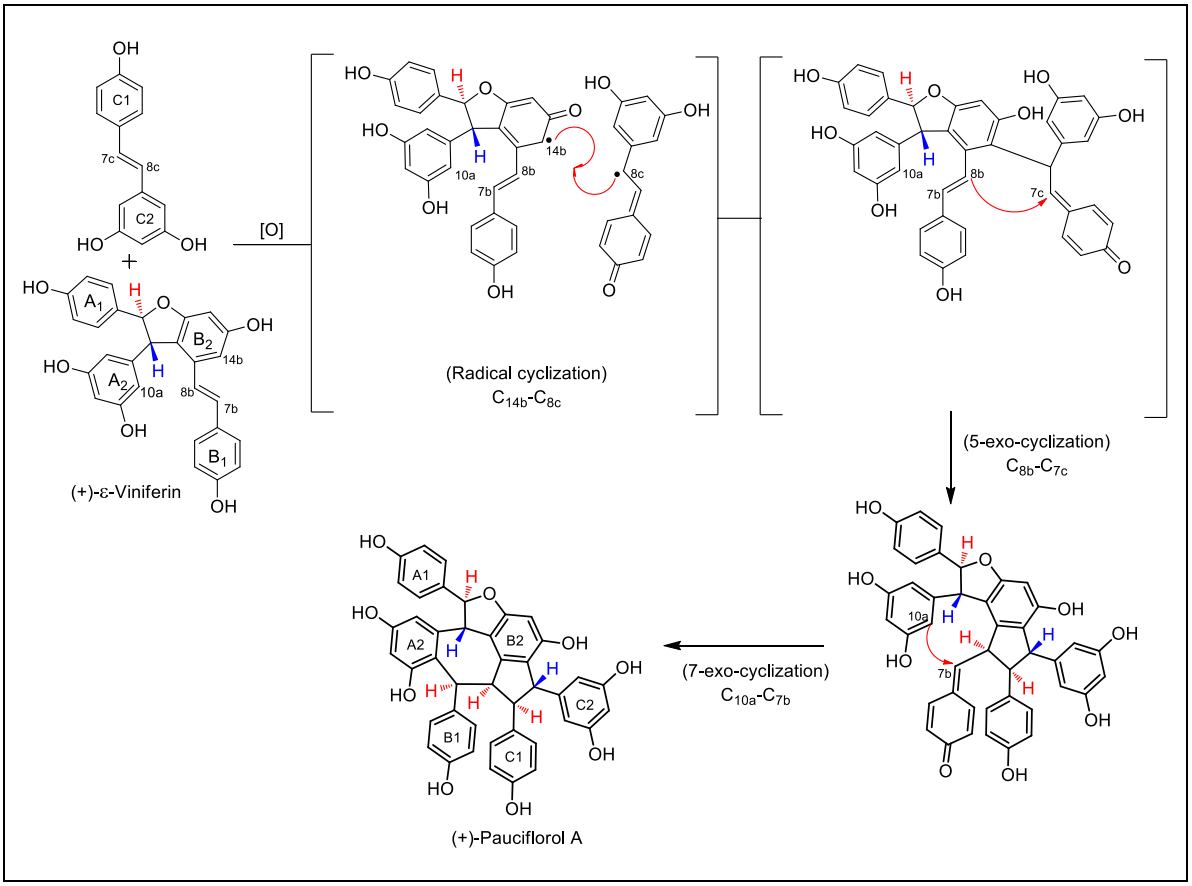

Scheme 2.1: Biosynthetic pathway of (+)-pauciflorol A

Compound **4** (450 mg; 0.06 %) was isolated as a white solid from fractions Fr.A.25-Fr.A.40 obtained by repeated column chromatography with 70 % ethyl acetate in hexane. The compound was assigned the molecular formula $C_{56}H_{42}O_{12}$ following analysis of the HRESIMS at *m/z* 907.2756 $[M + H]^+$. IR spectrum of the compound showed absorption at 3379 and 1689 cm^{-1} suggesting the presence of hydroxyl –OH and aromatic C–C groups respectively. The ^1H and ^{13}C NMR and in comparison with HRMS suggest that the isolated compound has two dimeric stilbene moieties with the same configuration. The ^1H NMR spectrum in CD_3COCD_3 (Figure 2.25) exhibited signals for five phenolic hydroxyl groups (δ 8.65-7.52 ppm) which disappeared upon addition of D_2O. Considering the molecular formula, the remaining oxygen would contribute to the ether linkage. Other 2D spectroscopic details including ^{13}C NMR, ^1H–^1H COSY, HMQC and HMBC spectra (Figure 2.26-Figure 2.30) exhibited signals due to four aromatic rings as follows; two *p*-hydroxyphenyl groups (A1 and B1) and two 1,2,3,5-tetrasubstituted aromatic ring (A2 and B2). The presence of a set of mutually coupled aliphatic protons (H-7a/H-8a) and a sequence of two aliphatic protons (H-7b/H-8b) were also shown. The ^1H–^1H coupling pattern of the stereocenter protons (H-7a/H-8a) was characteristic of a dihydrobenzofuran ring, and the latter (H-7b/H-8b) was similar to a partial structure of ampelopsin B, [Takaya *et al*., **2002**] which suggested a heptadiene ring system. The planar structure was confirmed by the following evidence. The correlations in the HMBC spectrum (Figure 2.24) were observed between H-7a/C-(2a,6a), C-8a, C-9a, 8a/C-14a, C-10a, C-10b, H-7b/C-(2b,6b), C-8b, C-10a, C-9b, C-9a, H-8b/C-9b,C-14b, C-10a), H-7b/C-8b, C-10a and H-8b/C-9b, which indicated that presence of four aromatic rings and four methine units.

To confirm the relative stereochemistry, NOESY experiments were conducted (Figure 2.30). In the spectrum, clear cross peaks between H-7a/H-14a, H-8a/H-(2a,6a), H-(2b,6b), H-8b were observed. These cross peaks substantiated that the relative stereochemistry of the methine protons at 7a and 8a are *trans* orientation. The relationship between two methine protons (H-7b and H-8b) and the dihydrobenzofuran ring was determined as follows. NOE interactions between H-8a/H-(2b,6b) indicated that the ring B1 is oriented in *β*-configuration, alternatively H-7b is oriented in *α*-configuration. The significant NOEs observed between H-7b/ H-14a, and H-8b/H-8a, H-14b, H-(2b,6b) also indicated that the relative configuration of methine protons at C-7b and C-8b are *α*, and *β* configuration respectively (Figure 2.24). On

the basis of these correlations, the relative stereochemistry of compound **4** was confirmed. The absolute configuration of compound **4** was established on the basis of optical activity $[\alpha]^{25}_{D}$ +384° (c 0.1, MeOH) which was in agreement with the reported value $[\alpha]^{25}_{D}$ +366° (c 0.17 MeOH) [Guebailia *et al*., **2006**]. From all the above spectral details and in comparison with the literature reports [Guebailia *et al*., **2006**, Aisha *et al*., **2014**], the compound was confirmed as (+)-hopeaphenol. Biosynthetic pathway of (+)-hopeaphenol will be discussed in chapter 3B. Finally the structure and stereochemistry of the (+)-hopeaphenol was unequivocally established by single crystal X-ray analysis (Figure 2.31). We carried out the crystallization using MeOH : DCM (60:40) solvent system. Brown colored crystals were observed at room temperature. Crystal structure was resolved in Bruker APEX-II-CCD. The crystals had orthorhombic crystal system. The structure of the compound is shown below.

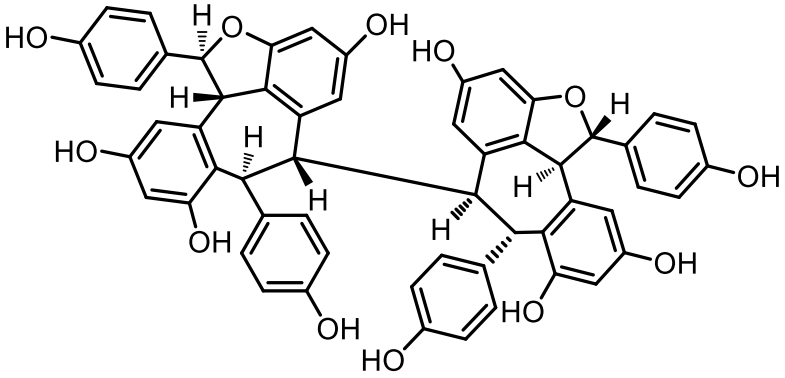

Figure 2.23: (+)-Hopeaphenol **(4)**

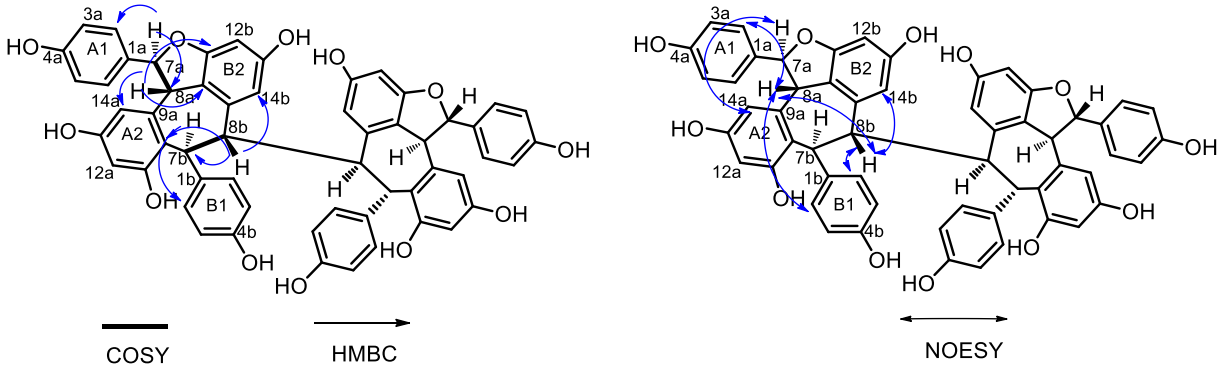

Figure 2.24: Selected COSY, HMBC and NOESY correlations of (+)-hopeaphenol

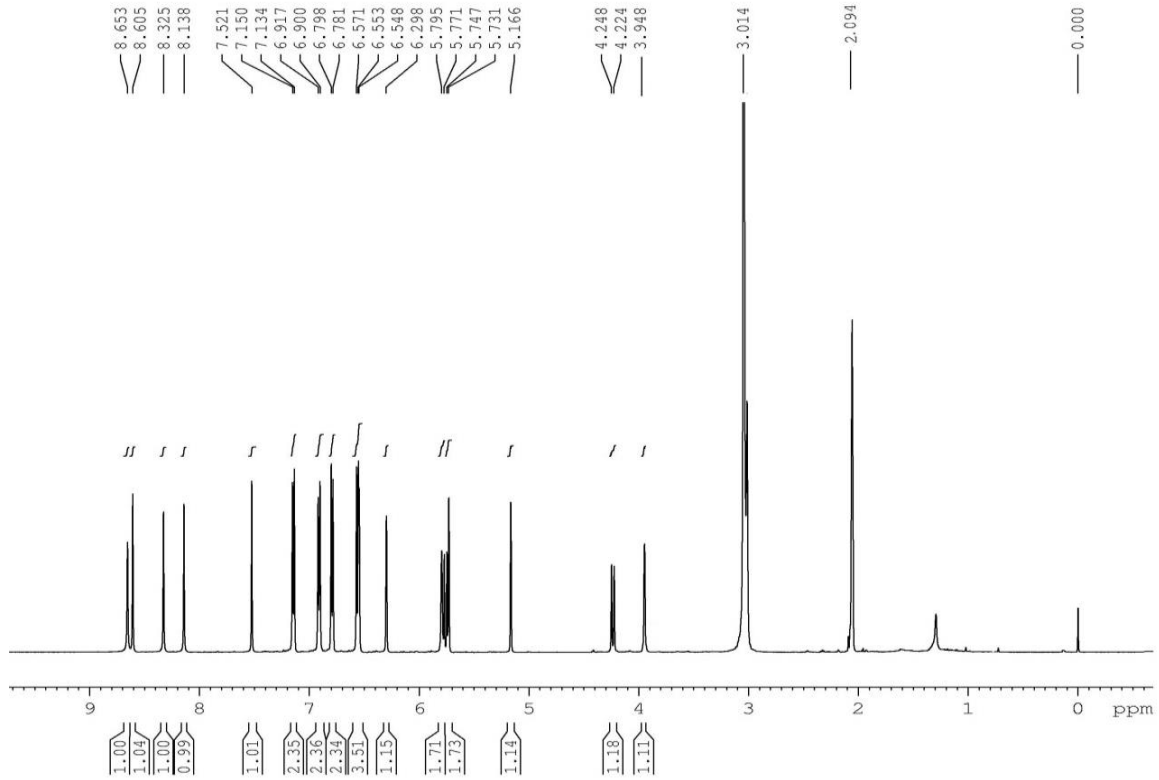

Figure 2.25: ^{1}H NMR spectrum of (+)-hopeaphenol

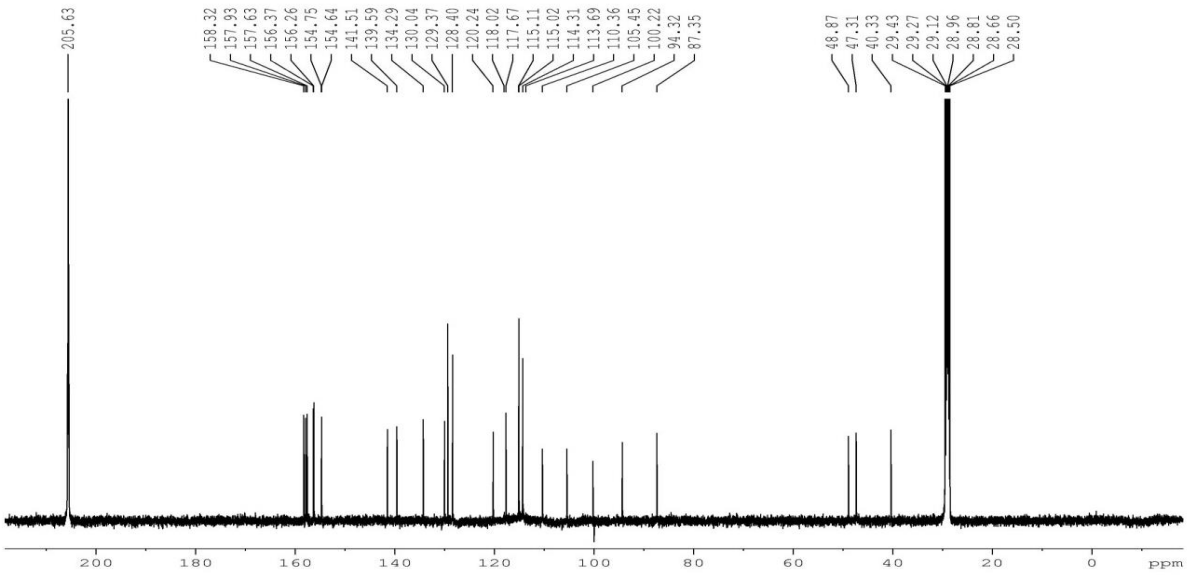

Figure 2.26: ^{13}C NMR spectrum of (+)-hopeaphenol

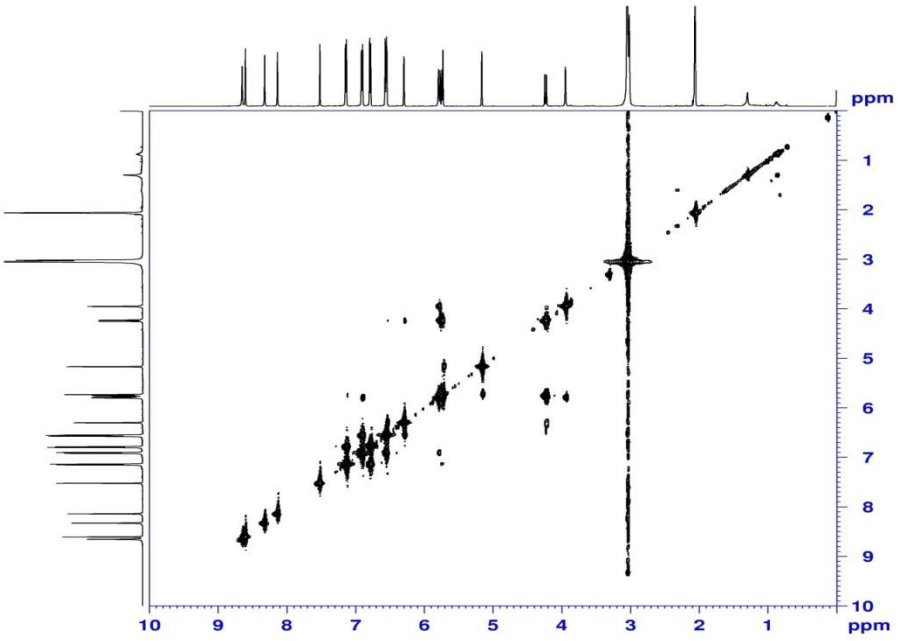

Figure 2.27: ^{1}H-^{1}H COSY NMR spectrum of (+)-hopeaphenol

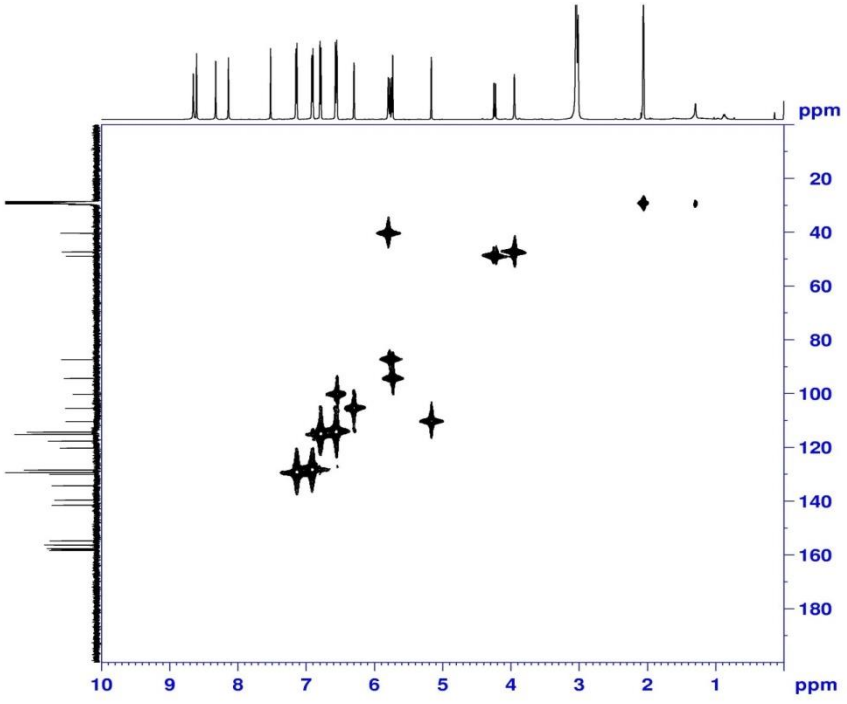

Figure 2.28: HMQC spectrum of (+)-hopeaphenol

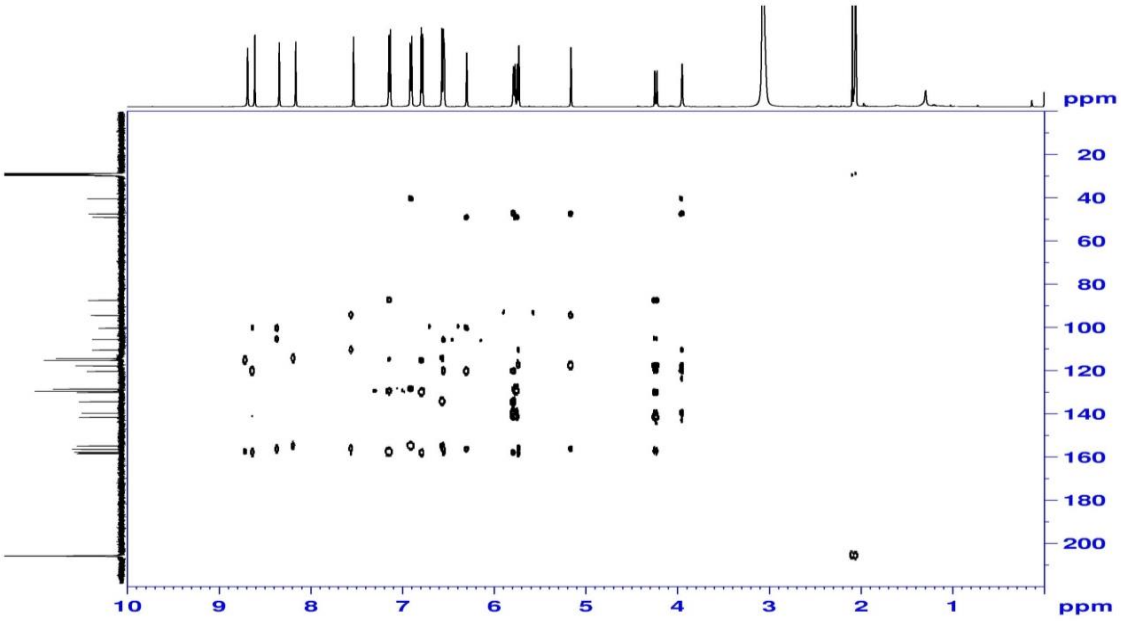

Figure 2.29: HMBC spectrum of (+)-hopeaphenol

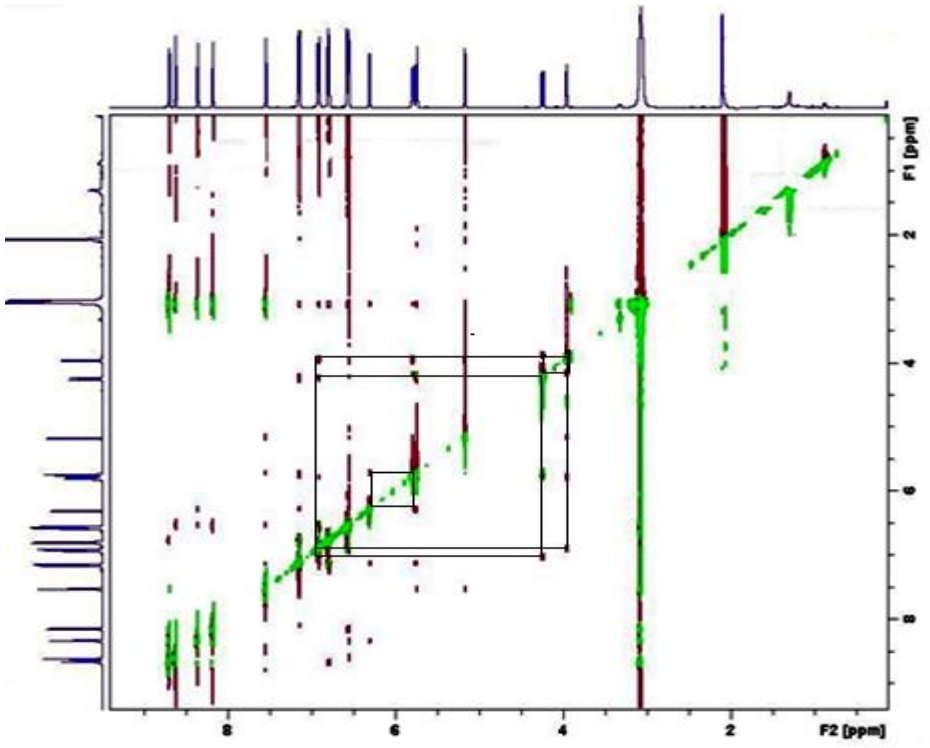

Figure 2.30: ^{1}H-^{1}H NOESY spectrum of (+)-hopeaphenol

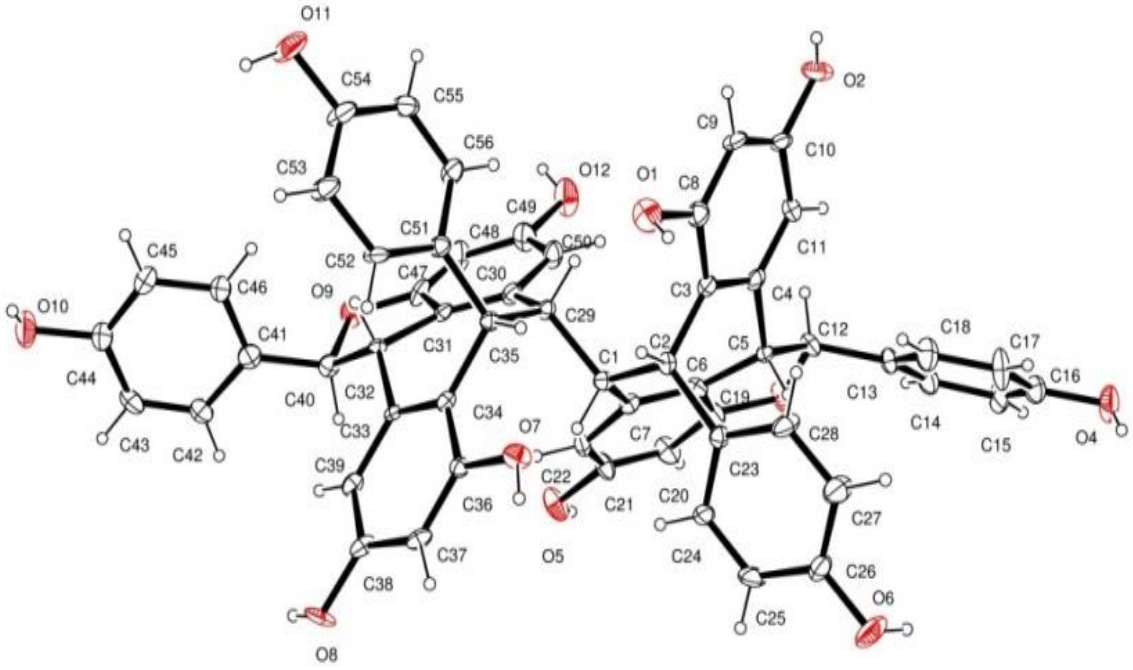

Figure 2.31: Single crystal X-ray structure of (+)-hopeaphenol

Fraction pools 46-55 (FrA.46- Fr.A.55), obtained by eluting the column with 100 % ethyl acetate yielded 17 mg of the compound **5** as white amorphous solid. IR spectrum of the compound showed broad absorption at 3395 cm^{-1}, suggesting the presence of a hydroxyl group. The ^{1}H NMR spectrum, the proton from sterol group which is directly attached to glucose ring appeared as a multiplet at δ 3.66 ppm. A doublet at δ 5.32 ppm was characteristic of the double bond present in the sterol ring. A doublet at δ 4.22 ppm integrating to one proton with *J* value 8.5 Hz could be attributed to the anomeric proton of glucose, which is in *β*-configuration. ^{13}C NMR indicated that the compound **5** consists of 35 carbons, 29 from sterol moiety and 6 from glucose ring. The mass spectra of the compound **5** gave molecular ion peak 599.4284 which is the $[M+Na]^{+}$. The compound was successfully characterized as ***β*-sitosterol-3-O-*β*-D-glucopyranoside** based on the spectral data obtained (IR, ^{1}H NMR (Figure 2.33), ^{13}C NMR (Figure 2.34) and HRESIMS) and in comparison with the literature reports [Kojima *et al*., **1990**]. The structure of the compound is shown below.

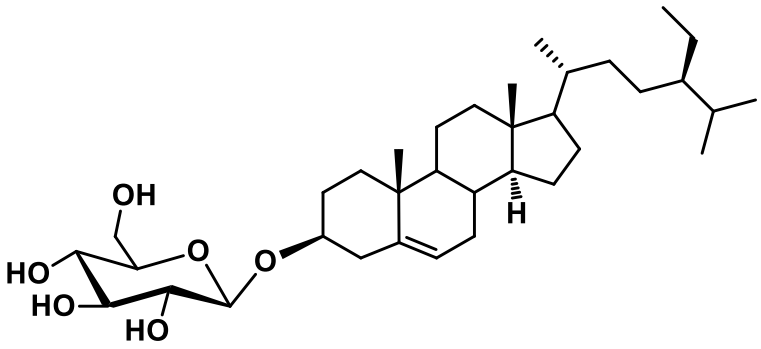

Figure 2.32: *β*-Sitosterol-3-*O*-*β*-D-glucopyranoside **(5)**

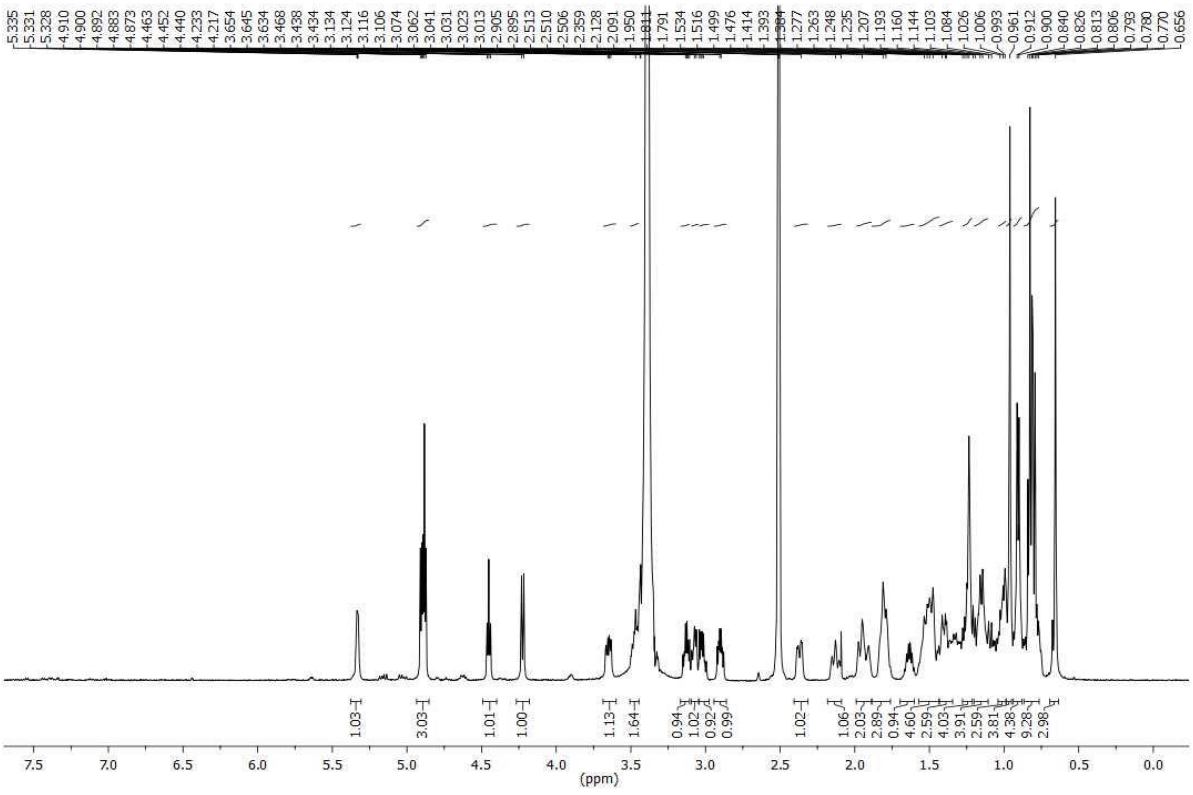

Figure 2.33: ^{1}H NMR spectrum of *β*-sitosterol-3-*O*-*β*-D-glucopyranoside

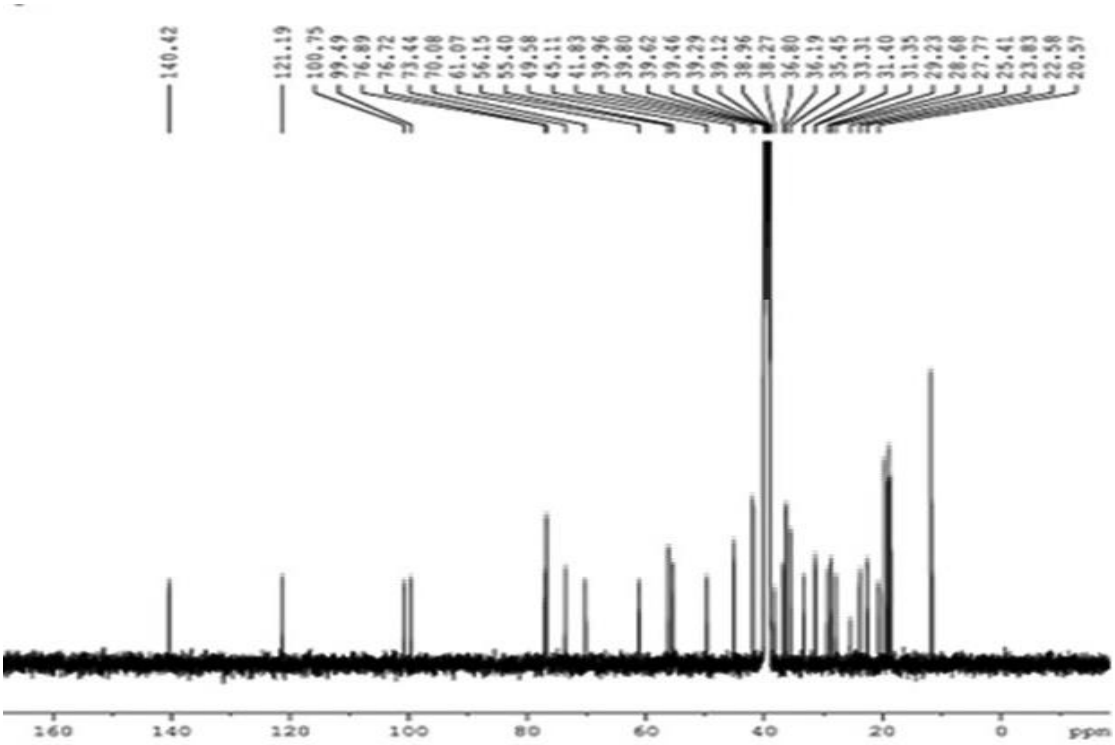

Figure 2.34: ^{13}C NMR spectrum of *β*-sitosterol-3-*O*-*β*-D-glucopyranoside

2.4.1. Isolation of compounds from hexane extract

After studying the TLC, 2.25 g of the hexane extract was subjected to column chromatographic purification using silica gel (100-200 mesh) with gradient elution. Elution was initiated with 100 % hexane and ceased with 50 % ethyl acetate in hexane. A total of 25 fractions of approximately 200 mL each were collected. According to the similarity in TLC, they were pooled into 6 major fraction pools (FrH.1- FrH.6).

Fraction pool 1-2 (Fr.H.1-Fr.H.2), obtained by eluting the column with 10 % ethyl acetate in hexane on crystallization using the same solvent yielded 14 mg (0.0019 %) of colourless needle-like crystals of compound **6**, which was characterized as the common phytosterol, ***β*-sitosterol**, based on various spectral data (IR, ^{1}H NMR, ^{13}C NMR and HRMS) obtained. The compound structure was further confirmed by TLC co-spotting with an authentic sample of *β*-sitosterol. The structure of the compound is shown below.

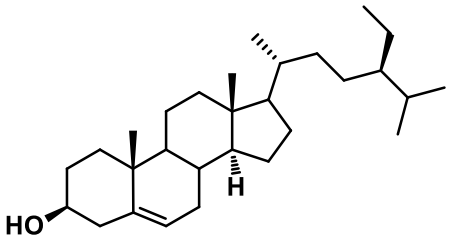

Figure 2.35: *β*-Sitosterol **(6)**

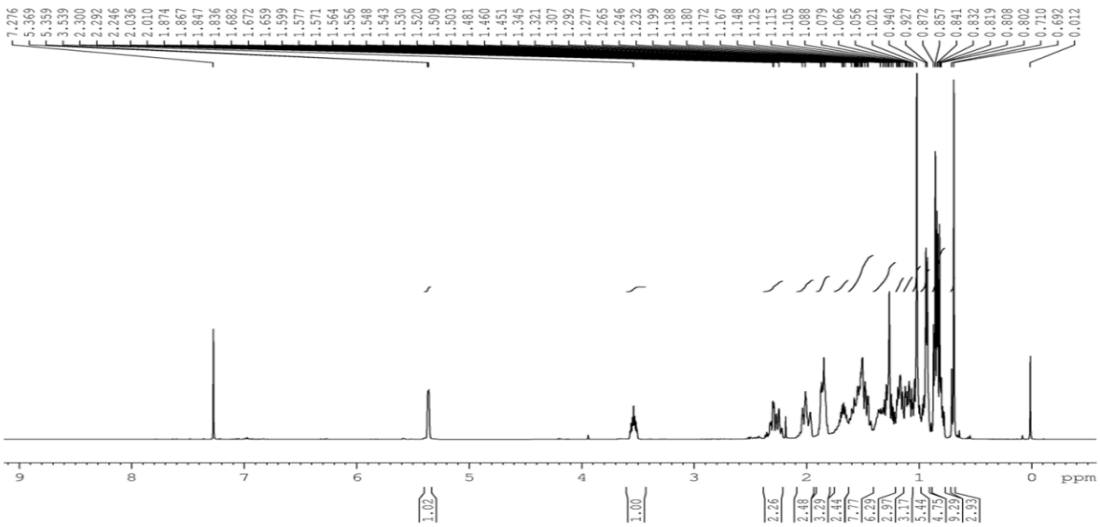

Figure 2.36: ^{1}H NMR spectrum of *β*-sitosterol

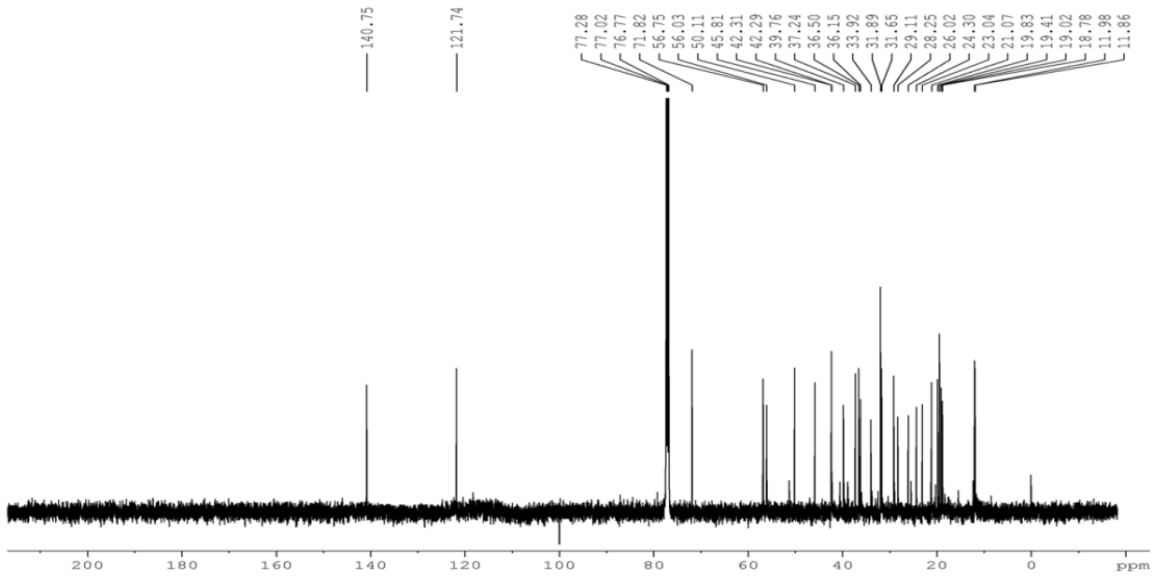

Figure 2.37: ^{13}C NMR spectrum of *β*-sitosterol

TLC of fraction 4 (Fr.H.4) obtained by eluting the column with 10 % ethyl acetate in hexane showed the presence of blue charring spot in McGill solution. This fraction was subjected to another column chromatographic separation, using a different solvent system, which on crystallization yielded 27 mg (0.0036 %) of compound **7**. The compound was found to be the phytosterol, **stigmasterol**, by using various spectroscopic techniques and by comparison with data reported in the literature [De-eknamkul and Potduang **2003**]. The structure of the compound is shown below.

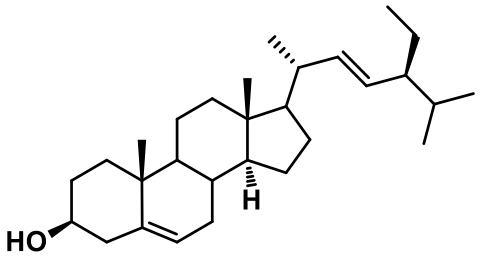

Figure 2.38: Stigmasterol **(7)**

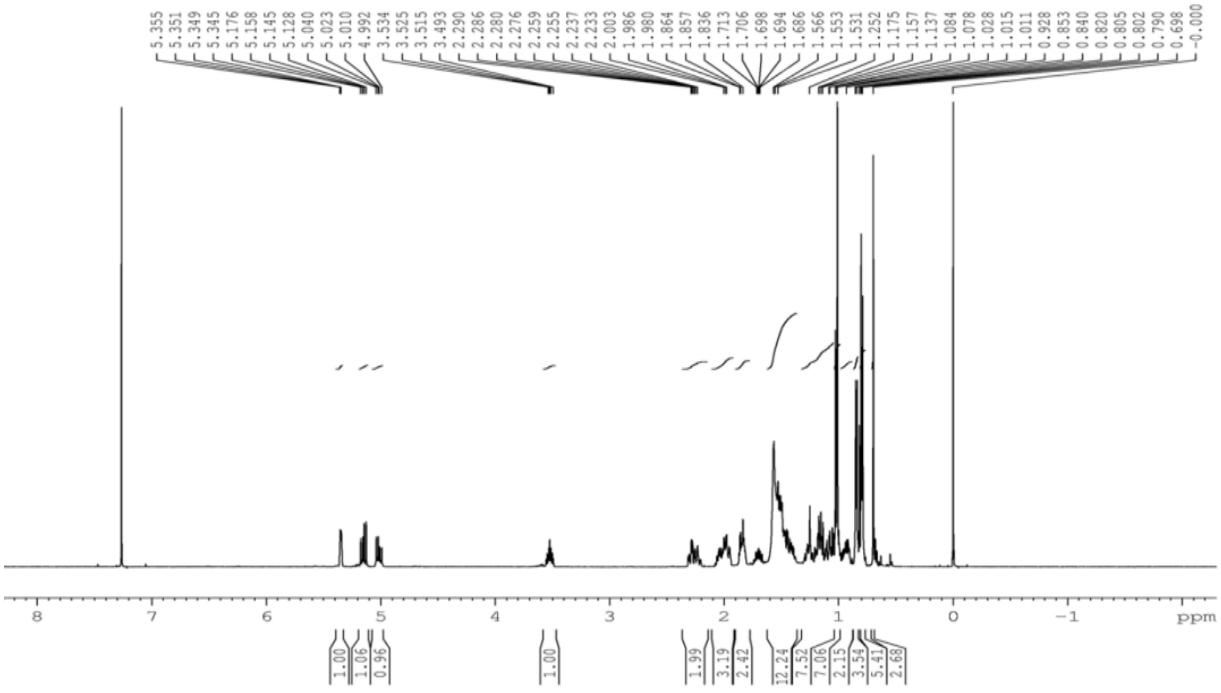

Figure 2.39: ^{1}H NMR spectrum of stigmasterol

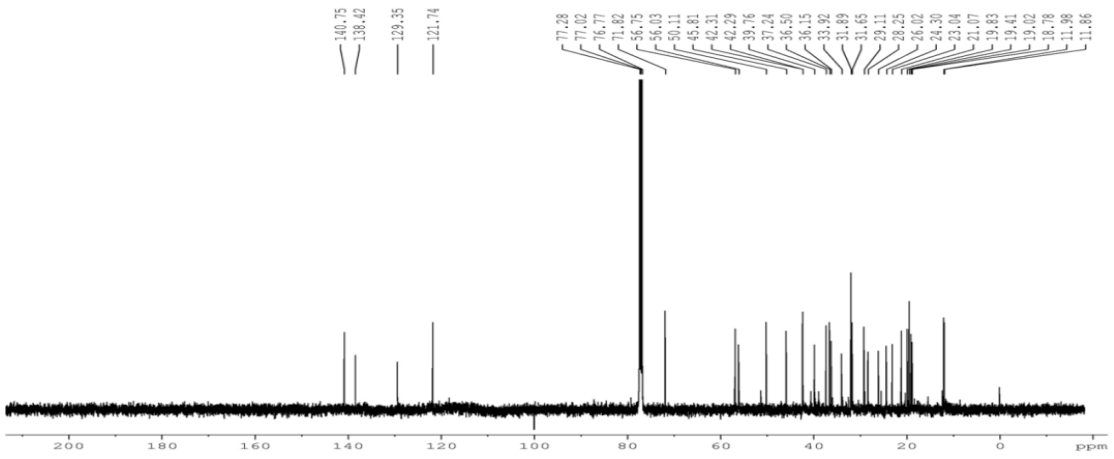

Figure 2.40: ^{13}C NMR spectrum of stigmasterol

Fraction pool 6 (Fr.H.6), obtained by eluting the column with 35 % ethyl acetate in hexane showed the presence of a UV active compound with minor impurities. It was again subjected to purification using silica gel column chromatography (230-400 mesh). Subfractions 1-5 obtained by eluting the column with 30 % ethyl acetate in hexane yielded 9 mg (0.0012 %) of white amorphous solid, which was labelled as compound **8**. IR spectrum of the compound showed a broad signal at 3115 and 1700 cm^{-1}, indicating the presence of hydroxyl and ester group. In ^{1}H NMR, (Figure 2.42) the signal at δ 5.85 ppm indicates the presence of phenolic hydroxyl group and a three hydrogen singlet at δ 3.93 could be attributed to methoxy group attached to the aromatic ring. The signals at δ 7.60 and 6.29 ppm each integrating one proton with *J* value 16 Hz could be attributed to *trans* olefinic protons. In ^{13}C NMR, (Figure 2.43) the signal at δ 166.05 ppm is the diagnostic peak for ester carbonyl carbon. Methoxy carbon resonated at δ 55.8 ppm. The mass spectrum of the compound **8** showed molecular ion peak at *m/z* 223.0970, which is the $[M+H]^+$ peak. From all the above spectral details and in comparison with the literature reports [Souza Chaves *et al*., **2017**] the compound was confirmed as **Ethyl ferulate.** The structure of the compound is shown below.

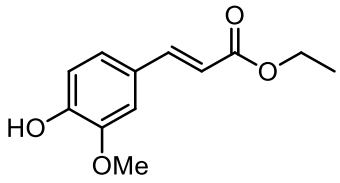

Figure 2.41: Ethyl ferulate **(8)**

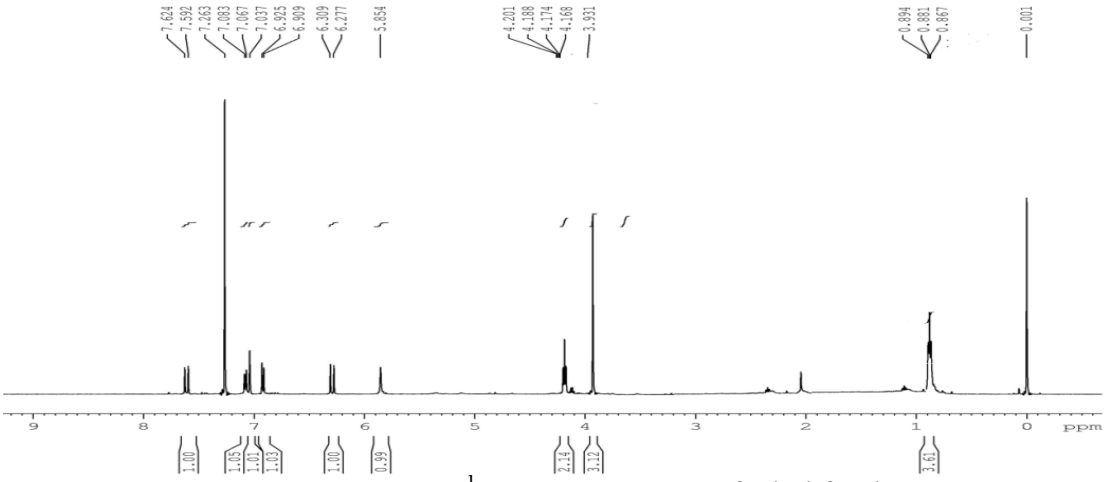

Figure 2.42: ^{1}H NMR spectrum of ethyl ferulate

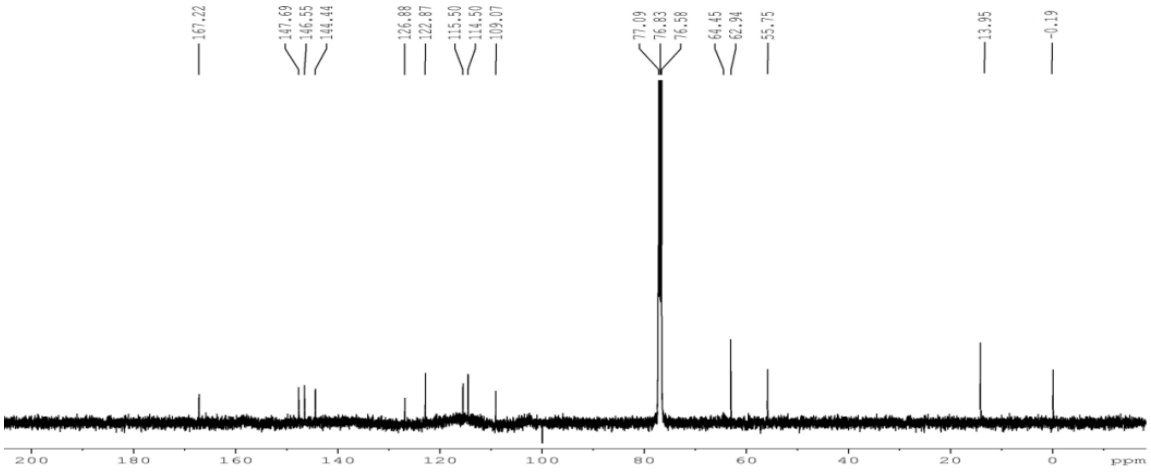

Figure 2.43: ^{13}C NMR spectrum of ethyl ferulate

After the successful isolation and characterization of compounds from *A. indica* rhizome, we extended our effort to isolate phytochemicals from the fruits of *A. indica*.

2.5. Extraction, isolation and characterization of compounds from *Ampelocissus indica* fruits

2.5.1. Plant material and extraction

The fruits of *Ampelocissus indica* (L.) were collected in June 2017 from Kasaragod district of Kerala. The plant material was authenticated by the taxonomist of Jawaharlal Nehru Tropical Botanical Garden and Research Institute (JNTBGRI), Palode, Thiruvananthapuram, voucher specimen (JNTBGRI 83500) and deposited in the herbarium

repository of the institute. The fruits were thoroughly cleaned and dried in a hot air oven maintained at 50 ^{o}C for three days. It was then coarsely powdered. Approximately 350 g of the powdered material was subjected to repeated extraction three times with acetone (2.5L x 48h) at room temperature. Thin layer chromatography indicated that the extraction was complete after six days. The total extract was then concentrated under reduced pressure using a Heidolph rotary evaporator. This yielded about 25 g of crude acetone extract (A). The above mentioned extraction procedures were repeated using ethanol (E) and water (W). Ethanol extract yielded about 12 g, and finally we got about 5 g of water extract on lyophilisation. Thin layer chromatography of all the extracts was carried out. Among the four different extracts, the acetone extract displayed the intense UV active spots and UV inactive spots were identified using McGill solution. Rest of the extracts did not show any spots in TLC, so we focused on the acetone extract for further isolation.

After studying the TLC, 25 g of the acetone extract was subjected to column chromatographic purification using silica gel (100-200 mesh). Column elution was started using 100 % hexane and increase in polarity was made by increasing the amount of ethyl acetate. Final elution was carried out using 5 % methanol in ethyl acetate. A total of 125 fractions of approximately 200 mL each were collected. According to the similarity in TLC, they were pooled into 40 major fraction pools (Fr.A.1- Fr.A. 40).

TLC of fractions 2-5 (Fr.A.2- Fr.A.5) obtained by eluting the column with 10 % ethyl acetate in hexane showed the presence of a single compound, which on crystallization in hexane yielded 57 mg (0.016 %) of compound **9** as white crystals. This was characterized as the phytosterol, **lupeol**. In ^{1}H NMR two singlets at δ 4.77 and 4.53 ppm each integrating for one proton respectively, indicated the presence of exocyclic double bond. Proton which is directly attached to the hydroxyl carbon resonated as a multiplet at δ 3.44-3.40 ppm. Peaks at δ 148.8 and 106.8 ppm in the ^{13}C spectrum confirmed the presence of olefinic carbons. Finally, the structure was confirmed using various spectroscopic data and in comparison with reports in literature [Fotie *et al*., **2006**]. The structure of the compound is shown below.

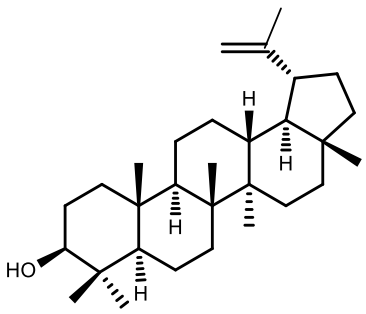

Figure 2.44: Lupeol **(9)**

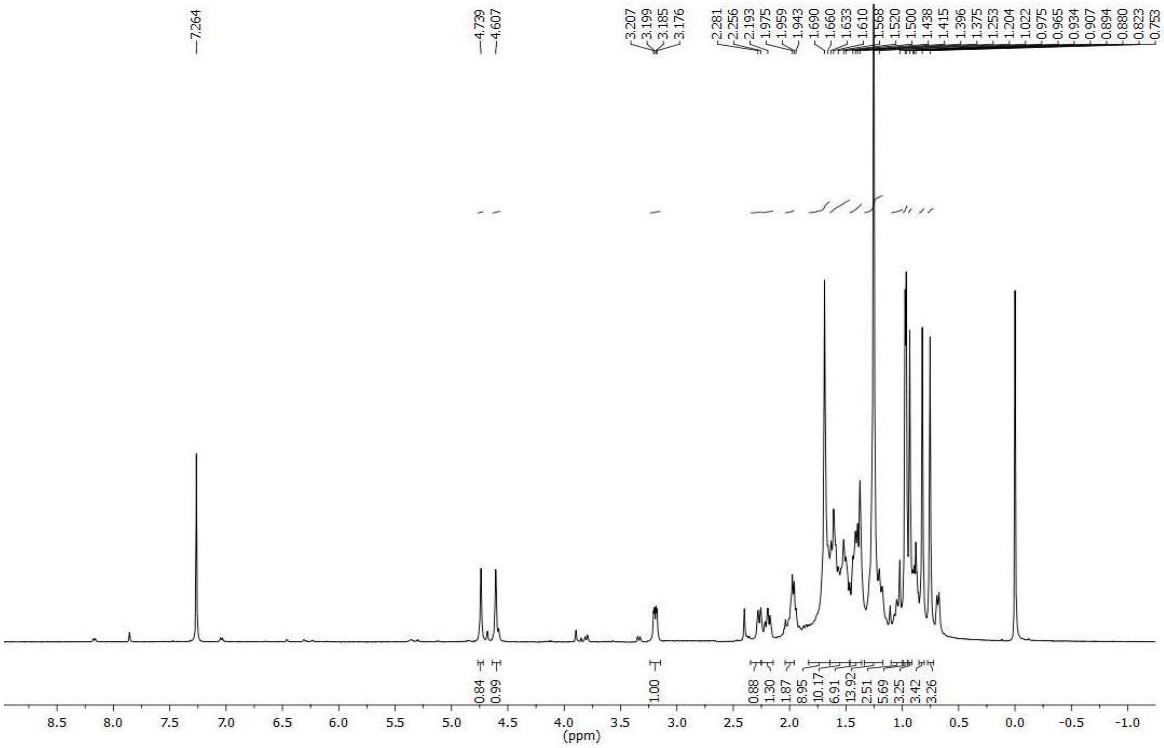

Figure 2.45: ^{1}H NMR spectrum of lupeol

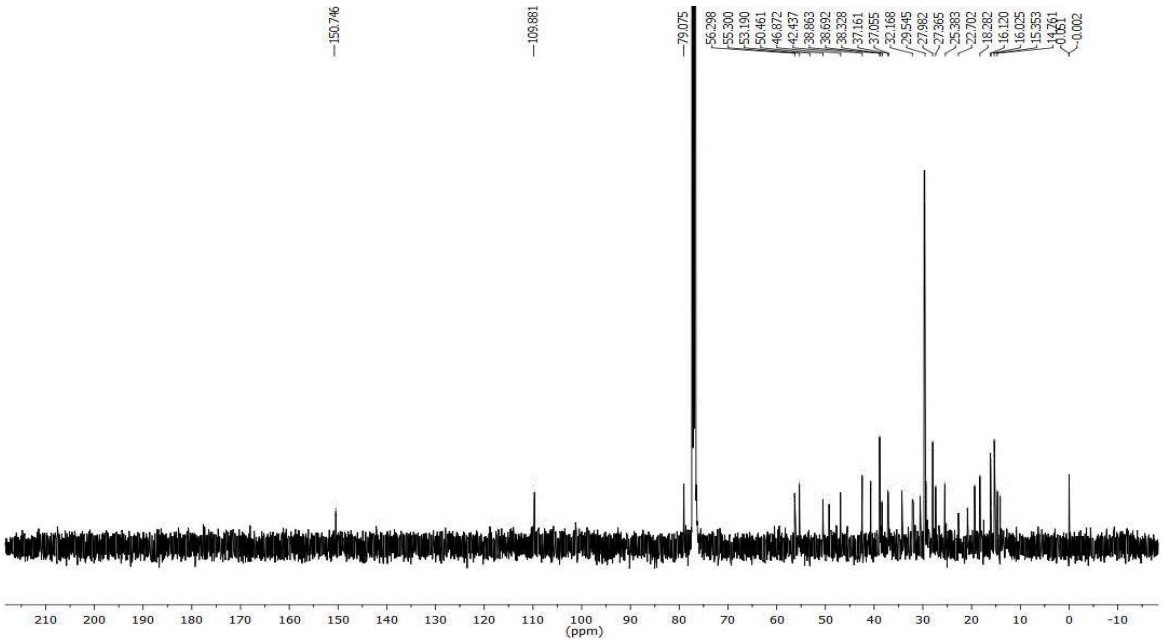

Figure 2.46: ^{13}C NMR spectrum of lupeol

Compound **10** (11 mg; 0.0031 %) was obtained as a colorless solid from fractions 15-17, (Fr.A.15- Fr.A.17) by eluting the column with 70 % ethyl acetate in hexane. The compound was found to be UV inactive, suggesting that the compound does not contain any chromophore in it. The TLC was sprayed with Mc-Gill reagent and identified the UV inactive compound. IR spectrum of the compound showed absorption at 1697 cm^{-1} suggesting the presence of an acid group. ^{1}H NMR (Figure 2.48) and ^{13}C NMR spectra (Figure 2.49) of the compound was suggestive of steroidal acid. Triplet at δ 5.28 ppm integrating for one proton could be attributed to the olefinic proton. Proton attached to the carbon bearing hydroxyl group resonated as a multiplet at δ 3.23-3.20 ppm. The signals at δ 2.83-2.80 ppm attributed to the proton adjacent to the acid group. All other aliphatic protons appeared in between δ 1.99 to 0.70 ppm. ^{13}C NMR spectrum of the compound showed the presence of thirty carbon atoms. Comparison of the ^{13}C NMR spectral values, and DEPT-135 spectra suggested that there are seven methyl groups, ten methylene groups, four methine groups and six quaternary carbons in the molecule (Figure 2.50). Carbon bearing the hydroxyl group resonated at δ 79.0 ppm. Acid carbonyl carbon was discernible at δ 183.1 ppm. The mass spectrum of the compound **10** showed molecular ion peak at *m/z* 455.3525,

which is the $[M-H]^+$ peak. By incorporating all the spectral details and in comparison with the literature [Hlila *et al*., **2016**], the compound was found to be **Oleanolic acid**.

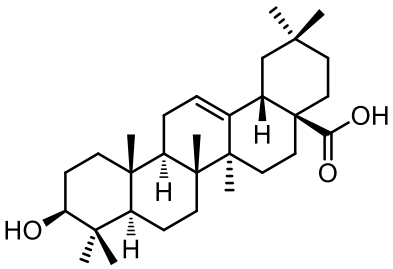

Figure 2.47: Oleanolic acid **(10)**

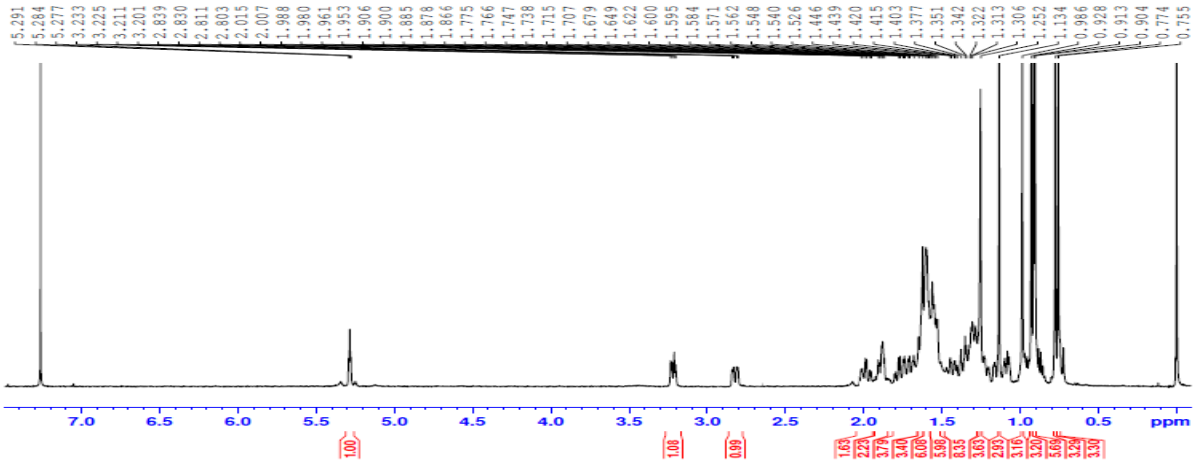

Figure 2.48: ^{1}H NMR spectrum of oleanolic acid

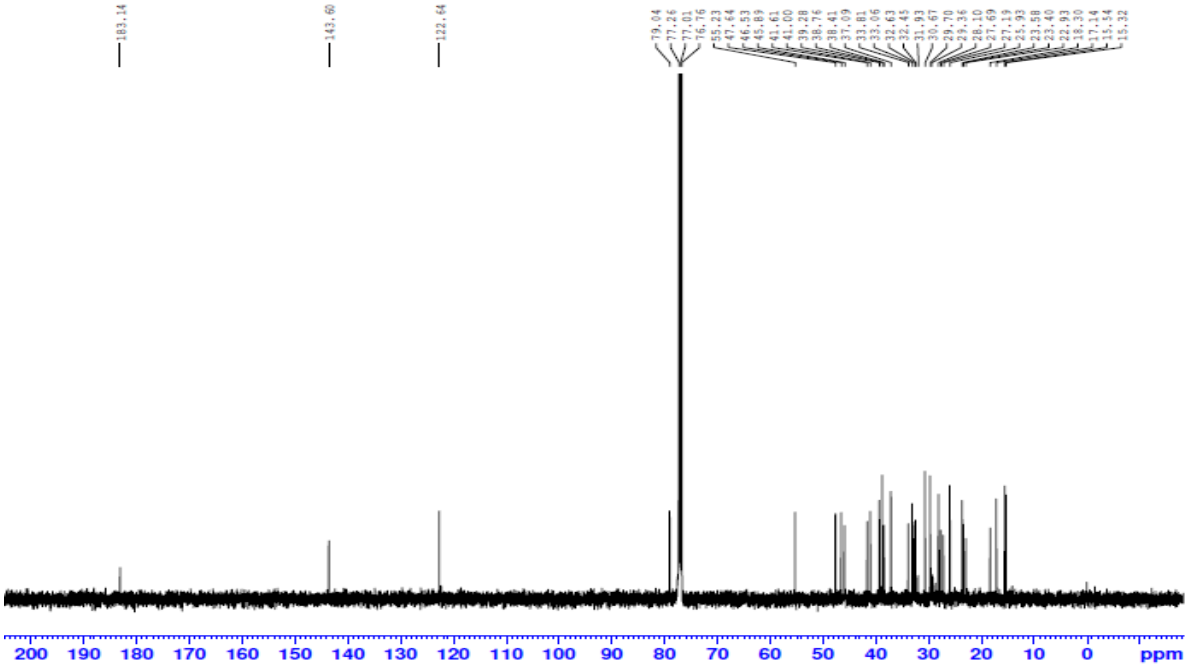

Figure 2.49: ^{13}C NMR spectrum of oleanolic acid

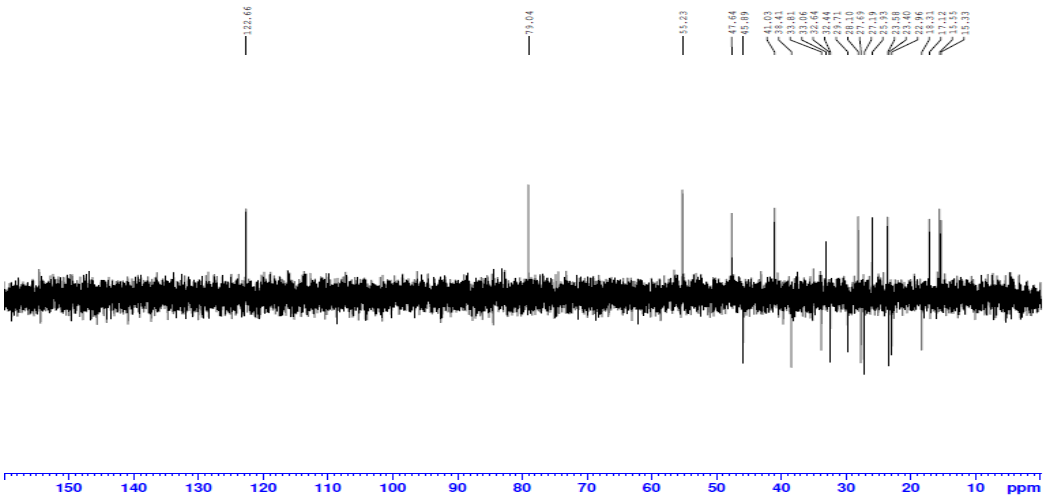

Figure 2.50: DEPT-135 NMR spectrum of oleanolic acid

Compound **11** (27 mg; 0.0077) was isolated from the fraction pool 19-21, (Fr.A.19-Fr.A.21) by eluting the column with 80 % ethyl acetate in hexane. Compound **11** was obtained as a white solid. Spectral data in detail (IR, ^{1}H and ^{13}C NMR) confirmed that the compound **11** is similar to compound **10** (oleanolic acid) obtained earlier. The DEPT-135 spectrum of compound **11** showed only nine methylene groups (Figure 2.54), whereas in oleanolic acid ten methylene carbons were observed. This is due to the shift of one methyl group from fifth cyclohexane ring to the adjacent position. Finally, by incorporating all the spectral details and in comparison with the literature [Luna-Vázquez *et al*., **2016**], the compound was found to be **Ursolic acid**. The structure of the compound is shown below.

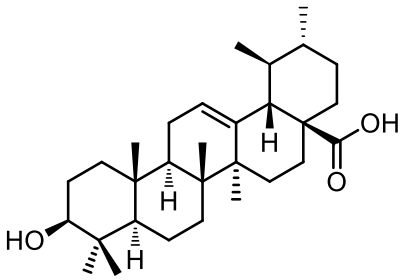

Figure 2.51: Ursolic acid **(11)**

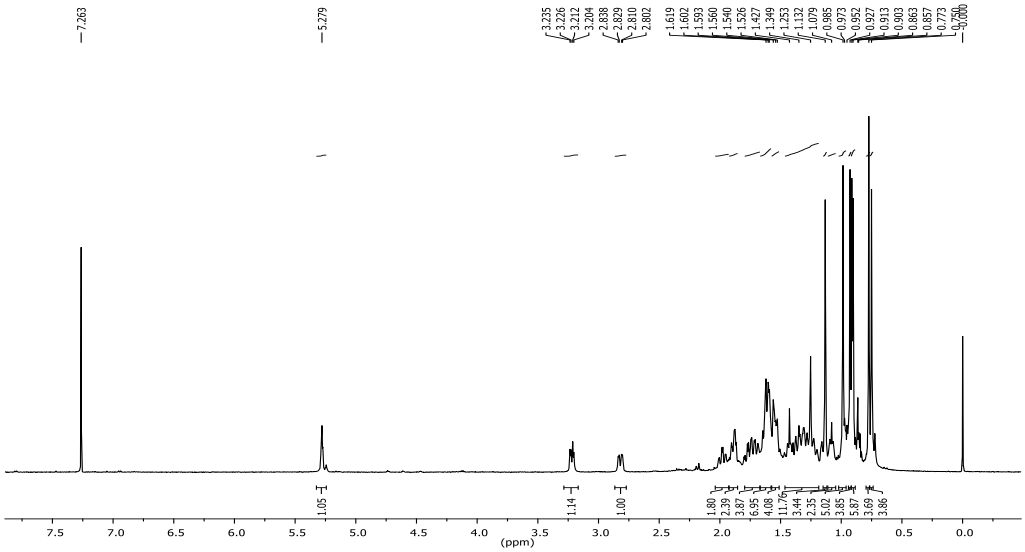

Figure 2.52: ^{1}H NMR spectrum of ursolic acid

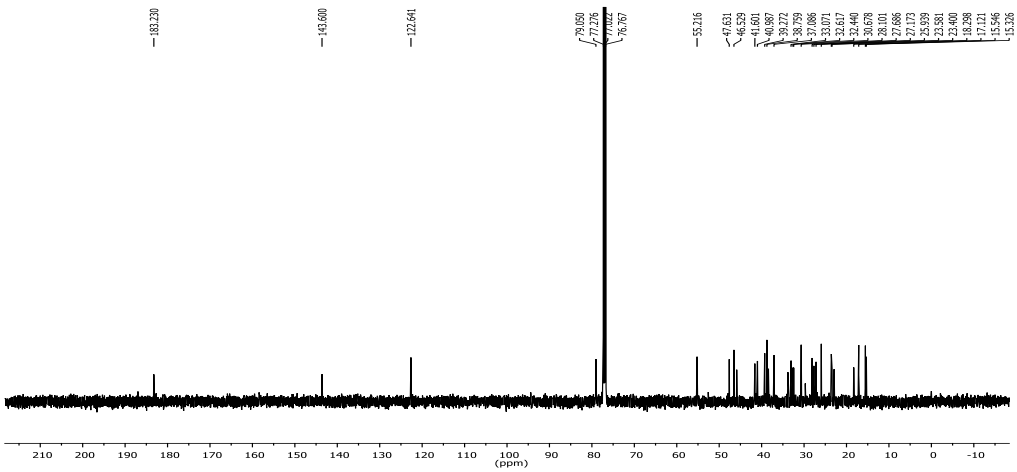

Figure 2.53: ^{13}C NMR spectrum of ursolic acid

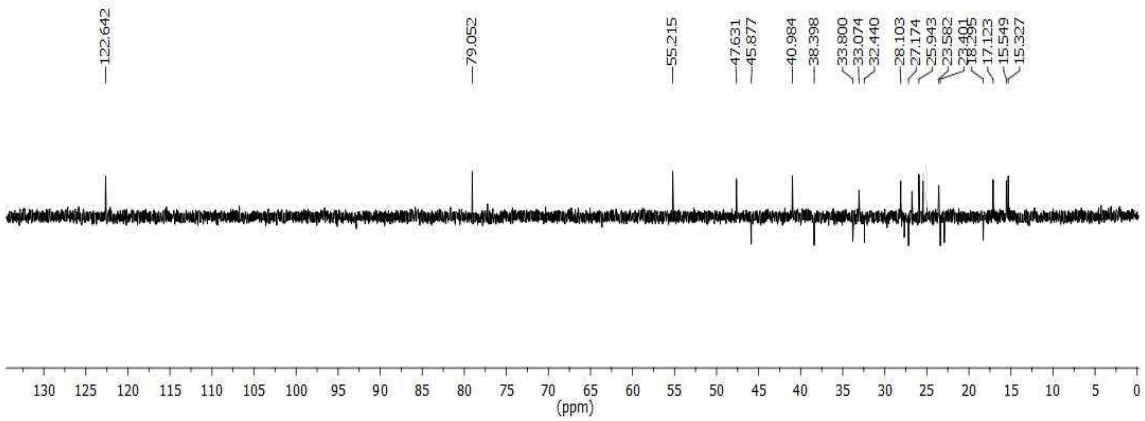

Figure 2.54: DEPT-135 NMR spectrum of ursolic acid

Fraction pools 22-24 (Fr.A.22- Fr.A.24) was subjected to column chromatography using silica gel by eluting with 100 % ethyl acetate, which gave compound **12** (16 mg; 0.0046 %) as a yellow powder. One singlet at δ 7.02 ppm in the ^{1}H NMR (Figure 2.56) spectrum integrating for two protons, suggested the presence of identical aromatic protons. Broad singlet at δ 8.52 ppm indicated the presence of aromatic hydroxyl groups. Peaks at δ 172.9 ppm in the ^{13}C NMR (Figure 2.57) spectrum confirmed the presence of an acid group. Mass spectrum of the compound gave molecular ion peak at 169.0136 which is the $[M-H]^{+}$ peak. Based on these spectral details, compound **12** was confirmed to be **gallic acid** [Shaheen *et al*., **2017**] and the structure is shown below.

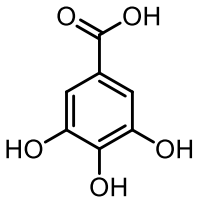

Figure 2.55: Gallic acid **(12)**

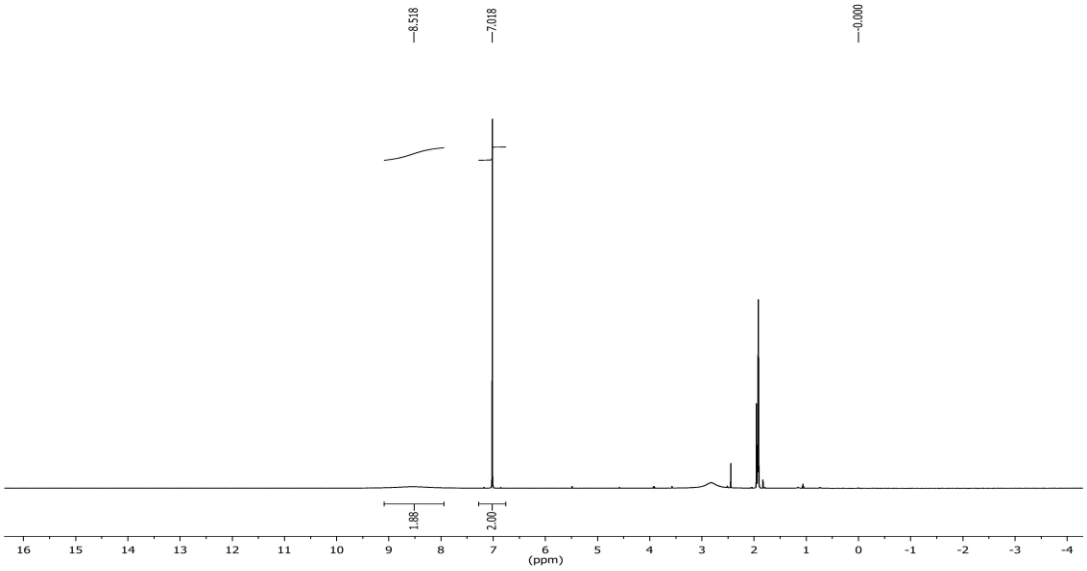

Figure 2.56: ^{1}H NMR spectrum of gallic acid

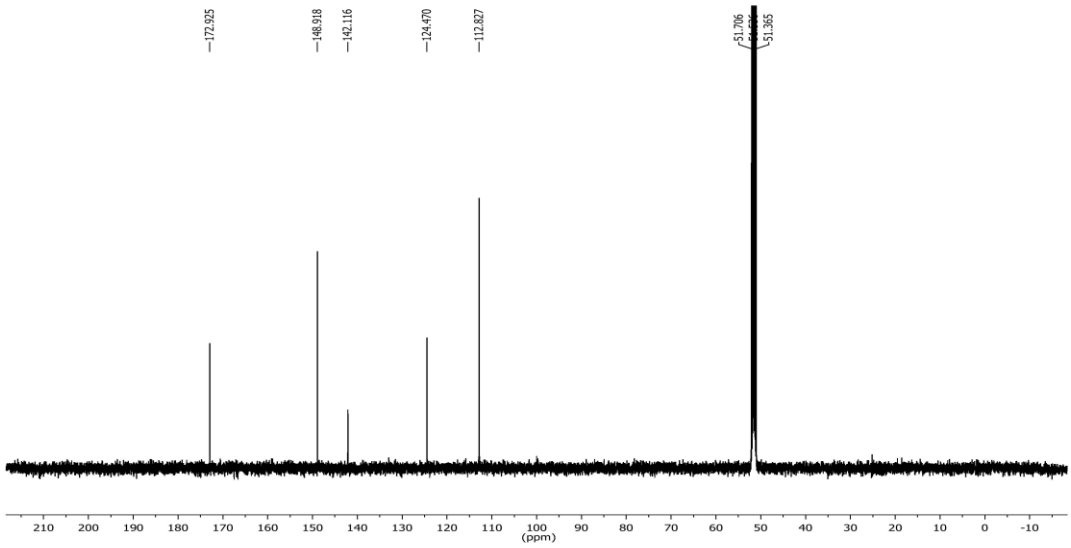

Figure 2.57: ^{13}C NMR spectrum of gallic acid

Fraction pools 25-35, (Fr.A.25- Fr.A.35) obtained by eluting the column with 100 % ethyl acetate yielded the mixture of compound **13** and compound **14**. This solid mixture was further subjected to silica gel column chromatography by eluting with ethyl acetate-hexane (9:1) which gave ten sub fractions.

Sub fractions 1-3 on crystallization in methanol-chloroform mixture afforded compound **13** (10 mg; 0.0029 %) as a white solid. IR spectrum of compound **13** showed a broad absorption peak at 3409 cm^{-1}, which indicated the presence of hydroxyl group. Signals at δ 10.77 ppm in the ^{1}H NMR (Figure 2.59) spectrum suggested the presence of two phenolic hydroxyl groups. A singlet at δ 7.53 ppm in the ^{1}H NMR spectrum, integrating for two protons indicated the presence of two identical aromatic protons. A singlet at δ 4.04 ppm integrating for six protons in ^{1}H NMR spectrum suggested the presence of two identical -OMe groups. Signals at δ 158.9 ppm in the ^{13}C NMR (Figure 2.60) spectrum confirmed the presence of carbonyl carbon of *δ*-lactone rings. Peaks in between δ 111.9-152.7 ppm in the ^{13}C NMR spectrum confirmed the presence of aromatic carbons. Signals at δ 61.5 ppm also supported the presence of two -OMe groups. The mass spectrum of the compound gave the molecular ion peak at 329.0297 which is the $[M-H]^{+}$ peak. Based on these spectral details and in comparison with literature data compound **13** was confirmed to be **3,3'-di-*O*-methylellagic acid** [Nawwar *et al*., **1982**] and the structure is shown below.

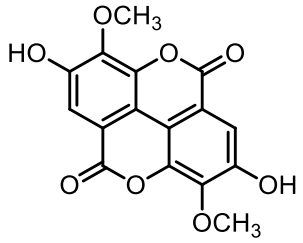

Figure 2.58: 3,3'-Di-*O*-methylellagic acid (**13**)

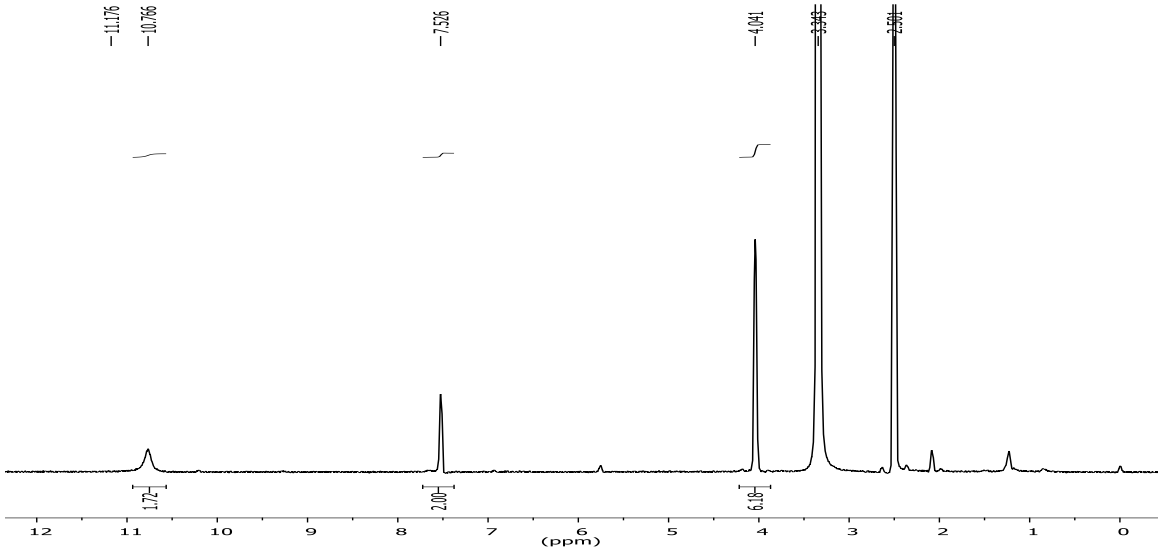

Figure 2.59: ^{1}H NMR spectrum of 3,3'-di-*O*-methylellagic acid

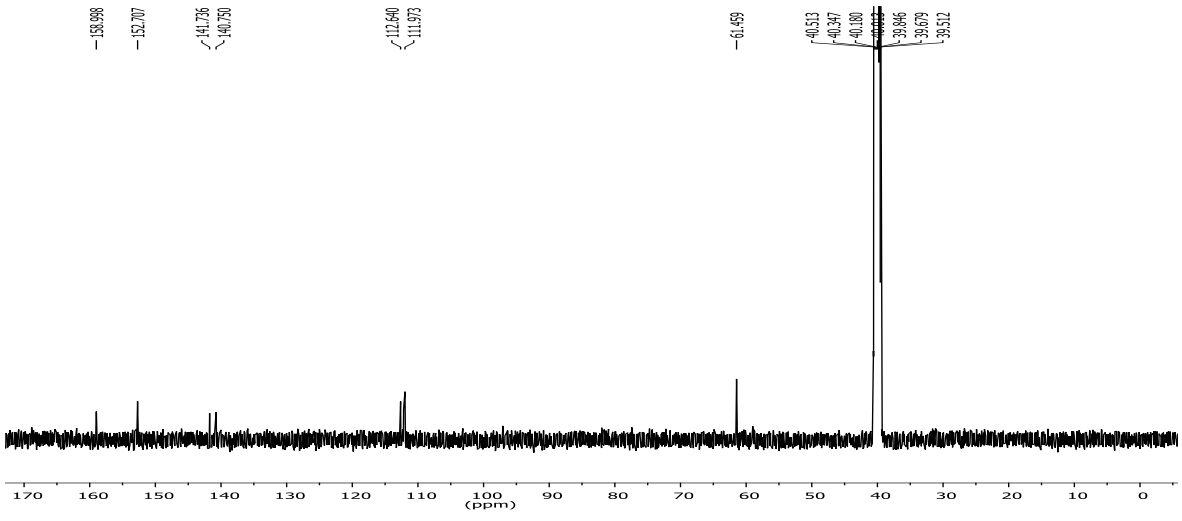

Figure 2.60: ^{13}C NMR spectrum of 3,3'-di-*O*-methylellagic acid

Sub fractions 5-10 on crystallization in methanol afforded compound **14** (350 mg; 0.1 %) as white solid. Spectral data in detail (IR, ^{1}H and ^{13}C NMR) confirmed that the compound **14** is similar to compound **13** (3,3'-di-O-methylellagic acid) obtained earlier. The mass spectrum of the compound gave the molecular ion peak at 301.1407 which is the $[M-H]^{+}$ peak. Based on ^{1}H and ^{13}C NMR spectral details and in comparison with literature data compound **14** was confirmed to be **ellagic acid** [Shaheen *et al*., **2017**] and the structure is shown below.

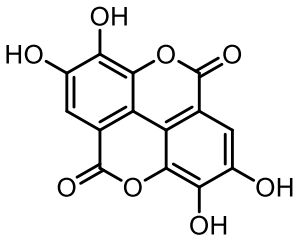

Figure 2.61: Ellagic acid (**14**)

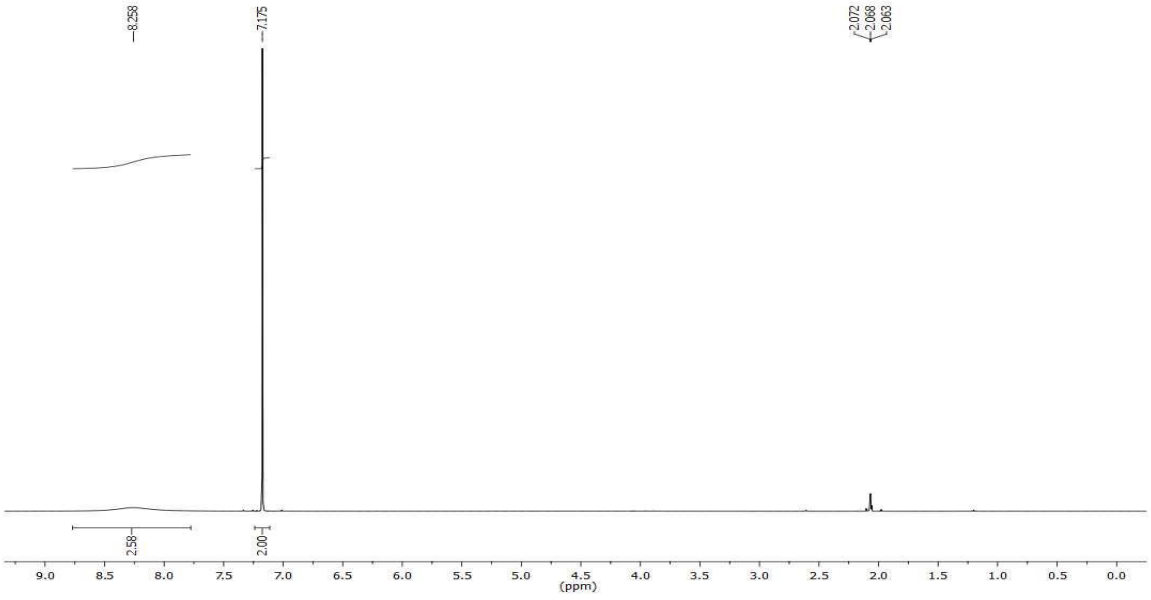

Figure 2.62: ^{1}H NMR spectrum of ellagic acid

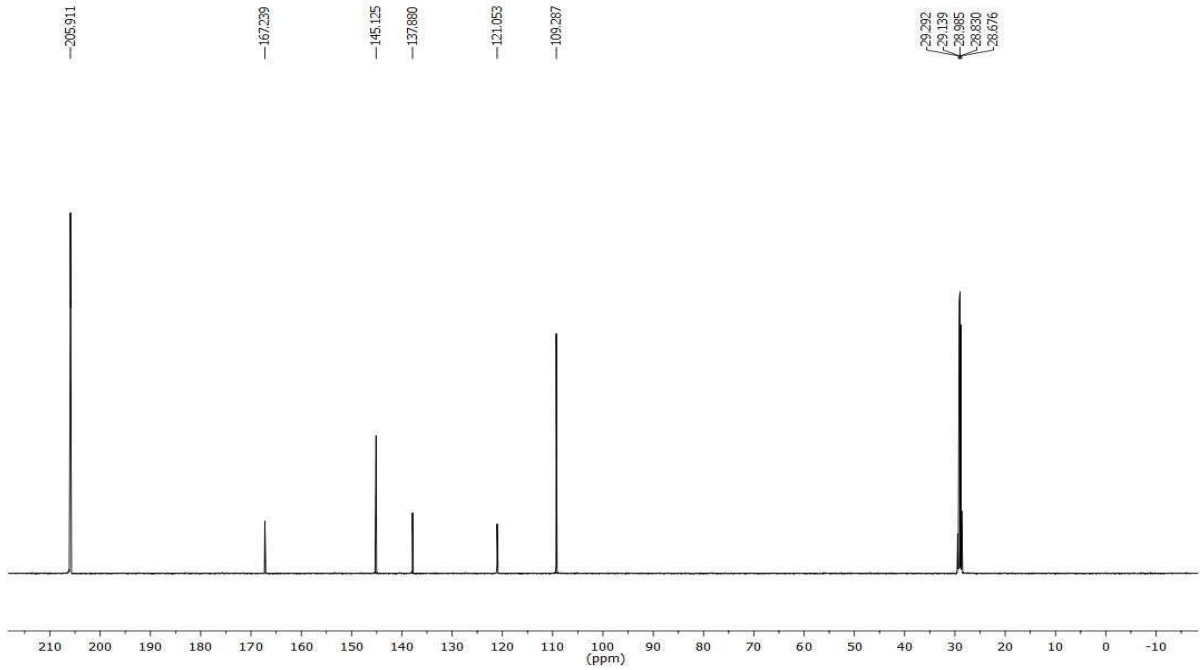

Figure 2.63: ^{13}C NMR spectrum of ellagic acid

2.6. Conclusion

In this chapter, the isolation of chemical constituents from various parts of *A. indica* has been carried out. This plant has hitherto uninvestigated and therefore the extracts prepared from *A. indica* rhizome were subjected to detailed antioxidant and antidiabetic studies. Eight compounds have been isolated from the rhizome of *A. indica*, *viz*., *E*-resveratrol, (+)-ε-viniferin**,** (+)-pauciflorol A, (+)-hopeaphenol, *β*-sitosterol-3-O-*β*-D-glucopyranoside, *β*-sitosterol, stigmasterol and ethyl ferulate. Similarly, *A. indica* fruits were subjected to phytochemical investigations. Six compounds *viz*., lupeol, oleanolic acid, ursolic acid, gallic acid, 3,3'-di-*O*-methylellagic acid and ellagic acid were isolated. To the best of our knowledge, chemical constituents from *A. indica* were reported for the first time. The compound level antidiabetic screening of *A. indica* will be discussed in the coming chapter.

2.7. Experimental Section

2.7.1. General experimental details

Melting point was determined by a Fisher-Jones Melting Point apparatus and is uncorrected. IR spectra were recorded on Bruker FTIR spectrometer. ^{1}H and ^{13}C NMR spectra were recorded at 500 and 125 MHz respectively using deuterated chloroform ($CDCl_3$), deuterated acetone (CD_3COCD_3) and deuterated dimethyl sulfoxide (CD_3SOCD_3)

on Bruker AMX 500 MHz spectrometer. Tetramethylsilane (TMS) was used as internal standard and chemical shifts were expressed in δ-scale. Abbreviations used in ^{1}H NMR are *s* - singlet, *d* - doublet, *dd* - doublet of doublet, *brs* - broad singlet, *q* - quartet and *m* - multiplet. HRMS-ESI was recorded on a Thermo Scientific Exactive mass spectrometer (column used: C18 reverse phase column) at 61,800 resolution. Optical activity was recorded on a Jasco P-1020 Polarimeter using spectroscopic grade methanol as solvent. For *α*-glucosidase and *α*-amylase inhibition assay, acarbose was used as the standard and ascorbic acid as the standard for antiglycation assay.

Analytical thin layer chromatography (TLC) was performed on Merck silica gel 60 F_{254} aluminium sheets, visualization was effected with UV and/or by staining with Enholm yellow/Mc-Gill solution. For column chromatography, silica gel of different pore size 100–200, 230–400 were used. All the solvents used for chromatography were of commercial grade and were distilled prior to use. The solvents used for column chromatography were removed under reduced pressure using Büchi/Heidolph rotary evaporator. Drying of the plant material was carried out in RRLT-NC natural convection air drier at 45-50 °C.

2.7.2. Extraction of *A. indica* rhizome

The rhizomes of *Ampelocissus indica* were collected from Calicut district, Kerala. This was thoroughly cleaned and dried in drier maintained at 50^{o}C and powdered. The powdered rhizome (750 g) was subjected to repeated extraction using hexane, acetone ethanol and water (2.5 L X 48h) at room temperature. After extraction, the solvent was removed under reduced pressure using Büchi rotary evaporator. The acetone extract (45 g) and hexane extract (2.25 g) was then subjected to column chromatographic separation.

2.7.3. Chromatographic separation of acetone extract of *A. indica* rhizome

The acetone extract (45 g) of the rhizomes of *A. indica* dissolved in minimum quantity of acetone and was adsorbed in silica gel (100-200) loaded on the top of silica gel column filled with slurry of 100-200 mesh silica gel in hexane. The column was eluted successively with gradient mixtures of hexane and ethyl acetate of increasing polarities and finally with 10 % methanol in ethyl acetate. A total of 250 fractions of approximately 200 mL each were collected. According to the similarity in TLC, they were pooled into 60 major fraction pools (FrA.1- FrA. 60). Hexane extract (2.25 g) was subjected to column chromatographic purification using silica gel (100-200 mesh) with gradient elution. Elution was started with

100 % hexane and ends with 50 % ethyl acetate in hexane. A total of 25 fractions of approximately 200 mL each were collected. According to the similarity in TLC, they were pooled into 6 major fraction pools (FrH.1- FrH.6). Pictorial representation of the procedure for the isolation of the compound is shown in Figure 2.64.

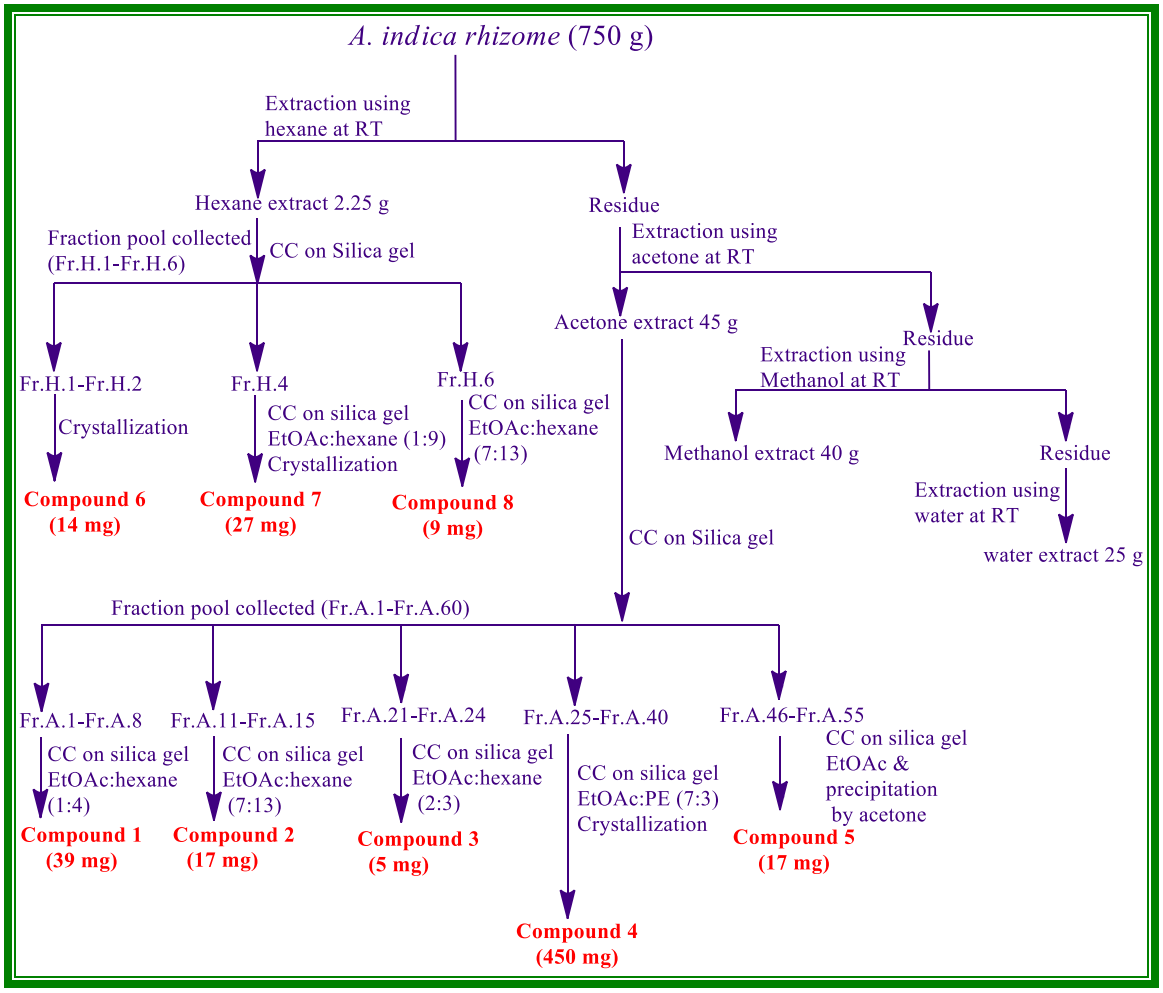

Figure 2.64: Pictorial representation of isolation of compounds from *A. indica rhizome*

2.7.3.1. Isolation of compound 1

The isolation procedure of compound **1** is represented in Figure 2.64. Compound **1** (39 mg) was obtained as a light brownish solid, on eluting the column with 20 % ethyl acetate in hexane. IR, ^{1}H NMR, ^{13}C NMR and mass spectral studies of this compound and on comparison with literature values [Lambert *et al*., **2013**], confirmed it to be *E*-Resveratrol.

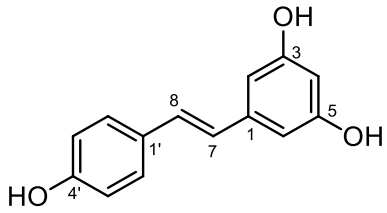

Melting point	:	270-272 ^{o}C
FT-IR (NaCl) υ_{max}	:	3411, 2924, 2858, 1582, 1506, 1440, 1379, 1143 cm^{-1}.
^{1}H NMR (500 MHz, CD_3COCD_3)	:	δ 8.55 (s, 1H, -OH), 8.28 (s, 2H, -OH), 7.43 (d, *J* = 8 Hz, 2H, H-2', H-6'), 7.03 (d, *J* = 16.5 Hz, 1H, H-8), 6.90 (d, *J* = 16.5 Hz, 1H, H-7), 6.85 (d, *J* = 8 Hz, 2H, H-3', H-5'), 6.56 (s, 2H, H-2, H-6), 6.28 (s, 1H, H-4) ppm.
^{13}C NMR (125 MHz, CD_3COCD_3)	:	δ 158.7 (2C, C-3, C-5), 157.3 (C-4'), [139.9, 129.0, 128.2, 127.8, 125.9, 115.5, 104.8, 101.8, (Other aromatic carbon)] ppm.
HR-ESIMS *m/z*	:	229.0868 $[M+H]^{+}$ (calcd for $C_{14}H_{13}O_3$, 229.0868)

2.7.3.2. Isolation of compound 2

Fraction pool 11-15 showed the presence of a UV active compound, which was re purified with 35 % ethyl acetate in hexane to obtain (+)-*ε*-viniferin in 17 mg yield as yellowish amorphous solid. The structure of the compound was confirmed as shown below by comparing the IR, ^{1}H NMR, ^{13}C NMR and mass spectral details of the compound with those reported in the literature [Takaya *et al*.,**2002**].

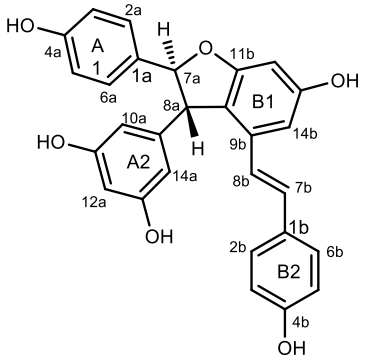

$[\alpha]^{25}_{D}$	:	+46.7 ^{o} (c 0.1, MeOH)
FT-IR (NaCl) υ_{max}	:	3388, 2961, 2933, 2872, 1721, 1603, 1513, 1448, 1373,

1225, 1165, 1128, 1074, 1001, 966 cm^{-1}.

^{1}H NMR (500 MHz, CD_3COCD_3)	:	δ 8.58 (brs, 3H, -OH), 8.35 (brs, 2H, -OH), 7.21 (d, *J* = 8 Hz, 2H, H-2a, H-6a), 7.18 (d, *J* = 8.5 Hz, 2H, H-2b, H-6b) 6.91 (d, *J* = 16.5 Hz, 1H, H-7b), 6.84 (d, *J* = 8.5 Hz, 2H, H-3a, H-5a), 6.75-6.73 (m, 3H, H-3b, H-5b, H-14b), 6.70 (d, *J* = 16.5 Hz, 1H, H-8b), 6.33 (d, *J* = 1.5 Hz, 1H, H-12a), 6.25 (s, 3H, H-10a, H-14a, H-12b), 5.43 (d, *J* = 5.5 Hz, 1H, H-7a), 4.47 (d, *J* = 5.5 Hz, 1H, H-8a) ppm.
^{13}C NMR (125 MHz, CD_3COCD_3)	:	δ 161.5 (C-OH), 159.0 (C-OH), 158.8 (C-OH), 157.4 (C-OH), 157.4 (C-OH), 146.5 (C-11b), 135.5 (C-7b), 132.9 (C-1a), 129.2 (C-10b), 127.8 (2C, C-2a, C-6a), 127.0 (2C, C-2b, C-6b), 118.9 (C-1a), 115.4 (C-3b), 115.3 (C-5b), 115.2 (C-9b), 114.9 (C-1b), 114.8 (C-14b), 106.1 (C-10a, C-14a), 103.3 (C-12b), 101.2 (C-8b), 95.9 (C-12a), 93.0 (C-7a), 56.2 (C-8a) ppm.
HR-ESIMS *m/z*	:	455.1497 $[M+H]^+$ (calcd for $C_{28}H_{23}O_6$, 455.1494)

NMR Spectral assignments were made on the basis of 1D and 2D NMR analysis and in comparison with the literature reports.

2.7.3.3. Isolation of compound 3

Fraction pool 21-24 on repeated purification with column chromatography by 60 % ethyl acetate in hexane gave (+)-Pauciflorol A as pale yellow amorphous powder. The absolute configuration of the compound was established by optical activity $[\alpha]^{25}_D$ +145 (c 0.1, MeOH). From all the 1D, 2D, HRMS data and on comparison with the literature reports [Ito *et al*., **2003**], the compound was confirmed. The structure of the compound is shown below.

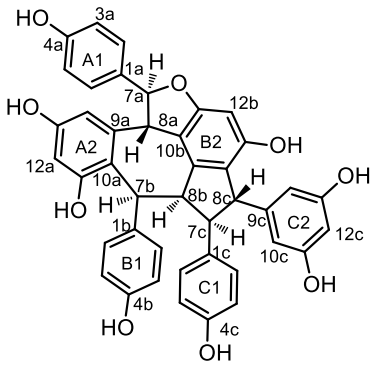

$[\alpha]^{25}_{D}$	:	$+145^{o}$ (c 0.1, MeOH)
FT-IR (NaCl) υ_{max}	:	3278, 2959, 2933, 2872, 1720, 1513, 1440, 1373, 1165, 1128, 1104, 1001 cm^{-1}.
^{1}H NMR (500 MHz, CD_3COCD_3)	:	δ 8.42 (brs, 1H, -OH), 8.20 (brs, 2H, -OH), 8.13 (brs, 1H, -OH), 8.08 (brs, 1H, -OH), 8.01 (brs, 1H, -OH), 7.94 (s, 1H, -OH), 7.20 (d, *J* = 8.5 Hz, 2H, H-2b, H-6b), 6.95 (d, *J* = 8.5 Hz, 2H, H-2a, H-6a), 6.85 (brs, 1H, -OH), 6.81 (d, *J* = 8.5 Hz, 2H, H-3b, H-5b), 6.76 (d, *J* = 8 Hz, 2H, H-2c, H-6c), 6.70 (d, *J* = 8 Hz, 2H, H-3a, H-5a), 6.58 (brs, 2H, H-3c, H-5c), 6.56 (brs, 2H, H-10c, H-14c), 6.32 (s, 1H, H-14a), 6.24 (s, 1H, H-12a), 6.20 (brs, 1H, H-12b), 6.08 (s, 1H, H-12c), 5.33 (d, *J* = 8.5 Hz, 1H, H-7a), 4.64 (s, 1H, H-7c), 4.43 (d, *J* = 8.5 Hz, 1H, H-8a) 4.26 (s, 1H, H-7b), 3.89 (d, *J* = 6.5 Hz, 1H, H-8c), 3.82–3.81 (m, 1H, H-8b) ppm.
^{13}C NMR (125 MHz, CD_3COCD_3)	:	δ 162.6 (C-OH), 159.3 (C-OH), 158.1 (C-OH), 157.1 (C-OH), 155.5 (C-OH), 155.2 (C-OH), 154.8 (C-OH), 154.3 (C-OH), 148.7 (C-11b), 144.5 (C-10b), 137.2 (C-9a), 133.8 (C-14b), 128.2 (2C, C-2c, C-6c), 128.1 (2C, C-2a, C-6a), 126.4 (2C, C-2b, C-6B), 124.9 (C-1c), 123.0 (C-1a), 115.5 (2C, C-3b, C-5b), 115.2 (C-1c), 114.9 (2C, C-3a, C-5a), 114.6 (2C, 3c, 5c), 105.5 (C-12b), 101.9 (C-12a), 101.4 (C-12c), 96.0 (C-14a), 92.9 (C-7a), 59.8 (C-8b), 59.5 (C-8c), 56.0 (C-8a), 53.3 (C-7c), 48.7 (C-7b) ppm.
HR-ESIMS *m/z*	:	681.1970 $[M+H]^{+}$ (calcd for $C_{42}H_{33}O_9$, 681.2124)

NMR Spectral assignments were made on the basis of ^{1}H-^{1}H COSY, HMQC, HMBC, NOESY analysis and in comparison with the literature reports.

2.7.3.4. Isolation of compound 4

Compound **4** (+)-hopeaphenol, (450 mg) was isolated as a white solid from fractions 25-40 obtained by repeated column chromatography with 70 % ethyl acetate in hexane. Further, the compound was purified by precipitation method by using chloroform followed by crystallization in MeOH:DCM (60:40). From all the 1D, 2D, HRMS data and on comparison with the literature reports [Guebailia et al., **2006**, Aisha *et al*., **2014**], the compound was confirmed. The structure of the compound is shown below.

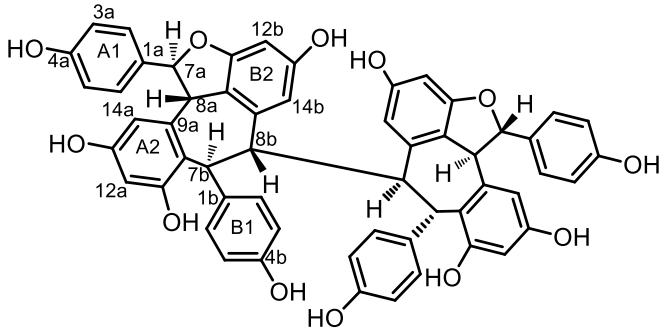

Melting point	:	> 280 ^{o}C decomposing
$[\alpha]^{25}_{D}$	:	+384 ^{o} (c 0.17, MeOH)
FT-IR (NaCl)	:	3379, 1689, 1591, 1507, 1437, 1336, 1210, 1168, 1124, 1081, 989 cm^{-1}.
^{1}H NMR (500 MHz, CD_3COCD_3)	:	δ 8.65(s, 1H, -OH), 8.60(s, 1H, -OH), 8.33(s, 1H, -OH), 8.14 (s, 1H, -OH), 7.52 (s, 1H, -OH), 7.14 (d, *J* = 8.5 Hz, 2H, H-2a, H-6a), 6.91 (d, *J* = 8.5 Hz, 2H, H-2b, H-6b), 6.79 (d, *J* = 8.5 Hz, 2H, H-3a, H-5a), 6.57 (s, 1H, H-12a), 6.55 (d, *J* = 8.5 Hz, 2H, H-3b, H-5b), 6.30 (s, 1H, H-14a), 5.80 (s, 1H, H-7b), 5.76 (d, *J* = 12 Hz, 1H, H-7a), 5.73 (s, 1H, H-12b), 5.17 (s, 1H, H-14b), 4.24 (d, *J* = 12 Hz, 1H, H-8a), 3.95 (s, 1H, H-8b) ppm.
^{13}C NMR (125 MHz, CD_3COCD_3)	:	δ 158.3 (C-OH), 157.9 (C-OH), 157.6 (C-OH), 156.4 (C-OH), 156.3 (C-OH), 154.7 (C-11b), 141.5 (C-9a), 139.6 (C-9b), 134.3 (C-1a), 130.0 (C-1b), 129.4 (2C, C-2a, C-6a), 128.4 (2C, C-2b, C-6b), 120.2 (C-10a), 118.0 (C-

10b), 115.1 (C-3a, C-5a), 114.3 (2C, C-3b, C-5b), 113.7, 110.4 (C-14b), 105.4 (C-14a), 100.2 (C-12a), 94.3 (C-12b), 87.4 (C-7a), 48.9 (C-8a), 47.3 (C-8b), 40.3 (C-7b) ppm.

HR-ESIMS *m/z* : 907.2756 $[M+H]^+$ (calcd for $C_{56}H_{43}O_{12}$, 907.2754)

NMR Spectral assignments were made on the basis of ^1H-^1H COSY, DEPT, HMQC, HMBC, NOESY analysis and in comparison with the literature reports. (+)-Hopeaphenol was crystallized in MeOH: DCM (60:40) mixture at room temperature to give brown coloured crystal. Crystal structure was resolved with Bruker APEX-II CCD. (+)-Hopeaphenol belong to orthorhombic space group crystal system, cell length a =11.2283(4), b =20.8486(7), c =24.0242(9), $\alpha = \beta = \gamma = 90^o$. The cif crystallographic data for (+)-hopeaphenol was deposited at the Cambridge Crystallographic Data Centre, under the reference number CCDC **1035198.**

2.7.3.5. Isolation of compound 5

Fraction pool (46-55), obtained by eluting the column with 100 % ethyl acetate, gave 17 mg of compound **5** as a white amorphous powder. The compound was successfully characterized as ***β*-sitosterol-3-*O*-*β*-D-glucopyranoside** based on the spectral data obtained and on comparison with the literature reports [Kojima *et al*., **1990**].

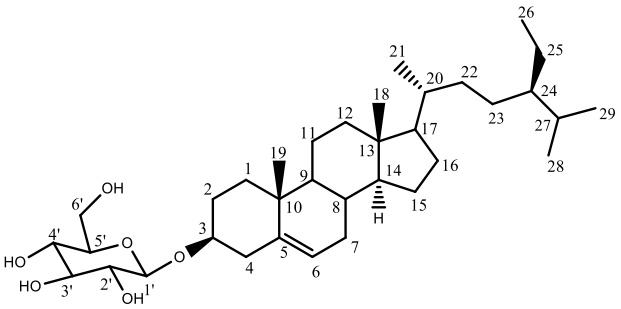

FT-IR (NaCl) υ_{max} : 3400, 2900, 2935, 2863, 1645, 1459, 1374, 1316, 1257, 1190, 1099, 1054, 1024, 958, 802 cm^{-1}.

^1H NMR (500 MHz, CD_3SOCD_3) : δ 5.34 (d, J = 5 Hz, 1H, H-6), 4.90-4-87 (m, 3H, 2', 3', 4'-OH), 4.46-4.44 (m, 1H, 6'-OH), 4.23 (d, J = 8 Hz, 1H, H-1'), 3.64-3.63 (m, 1H, H-2'), 3.47-3.43 (m, 2H, H-6'), 3.13-3.12 (m, 1H, H-5'), 3.10-3.07 (m, 1H, H-4',

H3' merged), 3.02-3.01 (m, 1H), 2.90-2.89 (m, 1H, H-3), 2.36-2.35 (m, 1H, H-4a), 2.13-2.10 (m, 1H, H-4b), 1.95-1.94 (m, 2H, H-2), [1.81-1.79 (m, 3H), 1.53-1.51 (m, 1H), 1.51-1.40 (m, 6H), 1.28-1.23 (m, 6H), 1.21-1.19 (m, 4H), 0.96 (s, 3H), 0.91 (s, 5H), 0.82-0.81 (m, 9H), 0.66 (s, 3H) (other aliphatic hydrogens)] ppm.

^{13}C NMR (125 MHz, CD_3SOCD_3) : δ 140.4 (C-5), 121.2 (C-6), 100.7 (C-1'), [99.5, 76.9, 76.7, 73.4, 70.1, 61.1, (C-Glu)], [56.1, 55.4, 49.6, 45.1, 41.8, 38.3, 36.8, 36.2, 35.4, 33.3, 31.4, 31.3, 29.2, 28.7, 27.8, 25.4, 23.8, 22.6, 20.6, 19.7, 19.1, 18.9, 18.6, 11.8, 11.6, aliphatic carbons)] ppm.

HR-ESIMS *m/z* : 599.4284$[M+Na]^+$ (calcd for $C_{35}H_{60}O_6Na$, 599.4287)

NMR Spectral assignments were made on the basis of DEPT-135 and 2D NMR analysis and in comparison with the literature reports.

2.7.3.6. Isolation of compound 6

The fractions 1-2 obtained on column chromatographic separation of hexane extract observed colorless needle-like crystal. This was further purified by crystallization using hexane-ethyl acetate mixture. The compound was successfully characterized as ***β*-sitosterol,** based on the spectral data obtained and on comparison with the literature reports [De-eknamkul and Potduang **2003**].

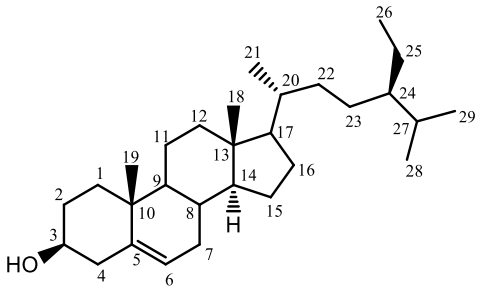

Melting point : 128-130 ^oC

FT-IR (NaCl) υ_{max} : 3408, 2935, 2863, 1645, 1459, 1374, 1316, 1257, 1190, 1099, 1054, 1024, 958, 802 cm^{-1}.

^{1}H NMR : δ 5.37 (d, J = 5 Hz, 1H, H-6), 3.53-3.54 (m, 1H, H-3),

(500 MHz, $CDCl_3$)		[2.30-2.29 (m, 2H), 2.04-1.87 (m, 2H), 1.87-1.84 (m, 3H), 1.68-1.66 (m, 2H), 1.60-1.45 (m, 7H), 1.32-1.23 (m, 6H), 1.20-1.10 (m, 3H), 1.09-1.96 (m, 3H) (other aliphatic hydrogens)], 1.02 (s, 3H, Me), 0.94- 0.93 (m, 3H, Me), 0.87-0.71 (m 9H, Me), 0.69 (s, 3H, Me) ppm.
^{13}C NMR	:	δ 140.8 (C-5), 121.7 (C-6), 71.8 (C-3), [56.8, 56.0, 50.1,
(125 MHz,$CDCl_3$)		45.8, 42.3, 42.3, 39.8, 37.2, 36.5, 36.2, 33.9, 31.9, 31.7, 29.1, 28.3, 26.0, 24.3, 23.0, 21.1, 19.8, 19.4, 19.0, 18.8, 11.9, 11.9 (other aliphatic carbons)] ppm.
HR-ESIMS *m/z*	:	415.3928 $[M+H]^+$ (calcd for $C_{29}H_{51}O$, 415.3939)

2.7.3.7. Isolation of compound 7

TLC of fraction (Fr.H.4) obtained by eluting the column with 10 % ethyl acetate in hexane showed the presence of blue charring spot in McGill solution. This fraction was subjected to another column chromatographic separation, followed by crystallization yielded compound **7**, **stigmasterol**, by using various spectroscopic techniques and by comparison with data reported in the literature [De-eknamkul and Potduang **2003**]. The structure of the compound is shown below.

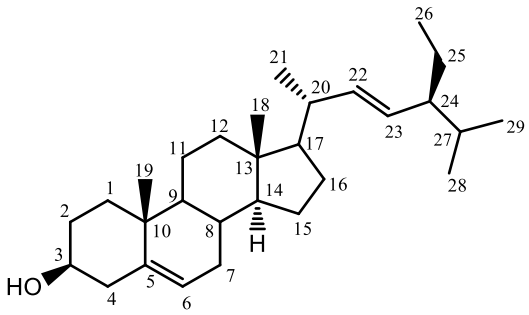

Melting point	:	162-165 ^oC
FT-IR (NaCl) υ_{max}	:	3410, 3272, 2935, 2863, 1645, 1459, 1374, 1316, 1257, 1190, 1099, 1054, 1024 cm^{-1}.
^1H NMR	:	δ 5.35 (d, J = 2Hz, 1H, H-6), 5.15 (dd, J_1 = 15.5 Hz, J_2 =
(500 MHz, $CDCl_3$)		11 Hz, 1H, H-22), 5.02 (dd, J_1=15 Hz, J_2 = 13.5 Hz, 1H, H-23), 3.53-3.52 (m, 1H, H-3), [2.29-2.00 (m, 2H), 1.99-1.83 (m, 3H), 1.57-1.55 (m, 2H), 1.54-1.25 (m, 12H),

1.8-1.14 (m, 7H), 1.10-1.04 (m, 7H), 1.03-1.00 (m, 2H), 0.85-0.82 (m, 3H), 0.80-0.70 (m, 5H), 0.68 (s, 3H), (other aliphatic hydrogens)] ppm.

^{13}C NMR (125 MHz,$CDCl_3$) : δ 140.8 (C-5), 138.4 (C-22), 129.4 (C-23), 121.7 (C-6), 71.8 (C-3), [56.8, 56.0, 50.1, 45.8, 42.3, 42.3, 39.7, 37.2, 36.5, 36.2, 33.9, 31.9, 29.11, 28.6, 26.0, 24.3, 23.0, 21.1, 19.8, 19.4, 19.0, 18.8, 11.98, 11.7, (other aliphatic carbons)] ppm.

HR-ESIMS *m/z* : 413.3763 $[M+H]^+$ (calcd for $C_{29}H_{49}O$, 413.3783)

2.7.3.8. Isolation of compound 8

Compound **8 ethyl ferulate** obtained by eluting the column with 30 % ethyl acetate in hexane from the fraction pool Fr. H.6 as a white amorphous solid. The structure of the compound was confirmed as shown below by comparing the IR, ^{1}H NMR, ^{13}C NMR and mass spectral details of the compound with those reported in the literature.

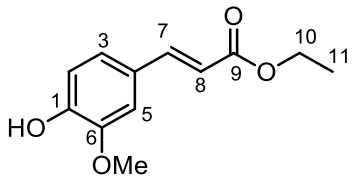

FT-IR (NaCl) υ_{max} : 3115, 2935, 2863, 1700 cm^{-1}.

^{1}H NMR (500 MHz, $CDCl_3$) : δ 7.61(d, *J* = 16 Hz, 1H, H-7), 7.07 (d, *J* = 8 Hz, 1H, H-3), 7.04 (s, 1H, H-5), 6.92 (d, *J* = 7.5 Hz, 1H, H-2), 6.29 (d, *J* = 16 Hz, 1H, H-8), 5.85 (s, 1H, 1-OH), 4.18 (q, *J* = 7.5 Hz, 2H, H-10), 3.93 (s, 3H, 6-OMe), 0.88 (s, 3H, 11-Me) ppm.

^{13}C NMR (125 MHz,$CDCl_3$) : δ 167.2 (C-9), 147.7 (C-1), 146.6 (C-6), 144.4 (C-4), 126.9 (C-7), 122.9 (C-3), 115.5 (C-2), 114.5 (C-), 109.1 (C-5), 62.9 (C-10), 55.7 (C-OMe), 13.9 (C-11) ppm.

HR-ESIMS *m/z* : 223.0970 $[M+H]^+$ (calcd for $C_{12}H_{15}O_4$, 223.0971)

2.7.4. Extraction and isolation of compounds from *A. indica* fruits

The fruit of *Ampelocissus indica* was collected from Kasaragod district, Kerala. This was thoroughly cleaned and dried in drier maintained at 50°C and powdered. The powdered fruits (350 g) were subjected to repeated extraction using acetone ethanol and water (2.5 L X 48h) at room temperature. After extraction, the solvent was removed under reduced pressure using Büchi rotary evaporator. The acetone extract (25 g) was then subjected to column chromatographic separation. Column elution was started using 100 % hexane and increase in polarity was carried out by increasing the amount of ethyl acetate. Final elution was carried out using 5 % methanol in ethyl acetate. A total of 125 fractions of approximately 200 mL each were collected. According to the similarity in TLC, they were pooled into 40 major fraction pools (Fr.A.1- Fr.A. 40). Pictorial representation of the procedure for the isolation of the compound is shown in Figure 2. 65.

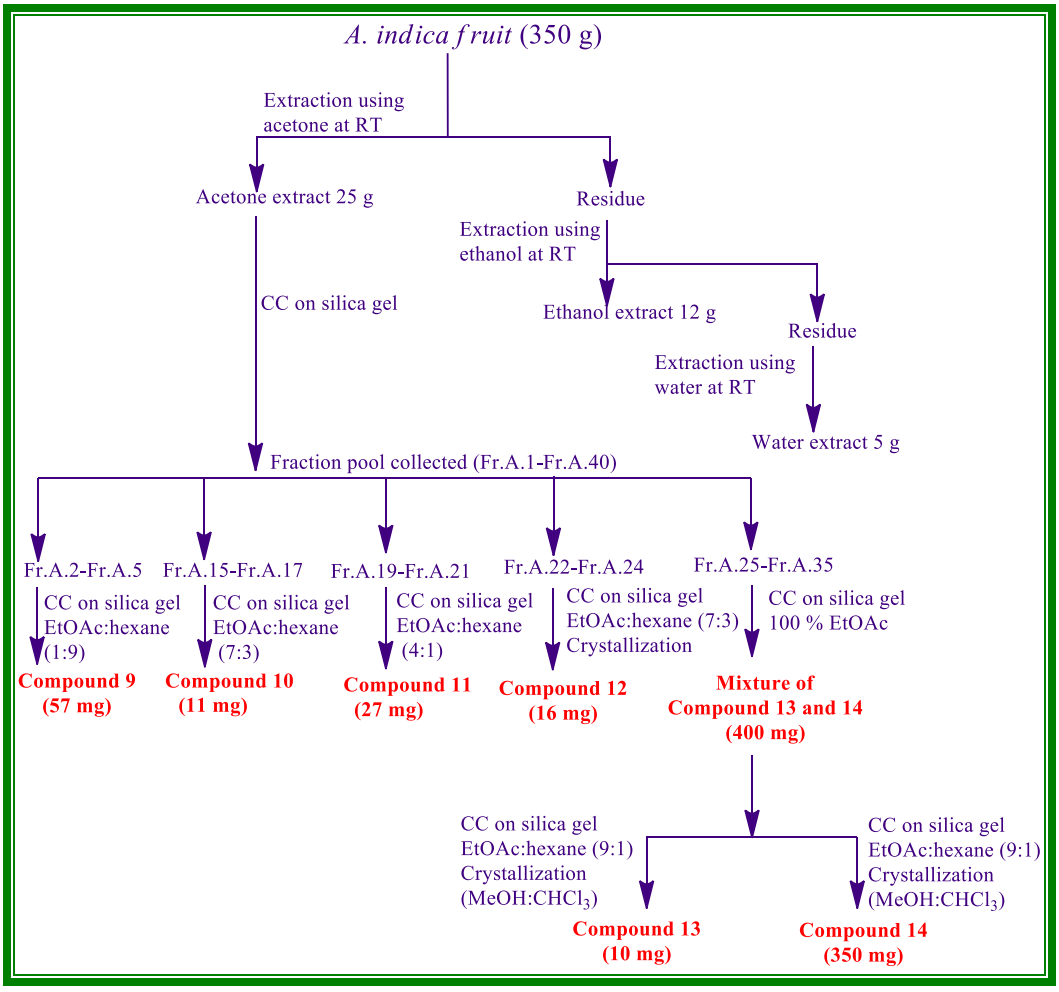

Figure 2.65: Pictorial representation of isolation of compounds from *A. indica* fruit

2.7.4.1. Isolation of compound 9

The isolation procedure of compound **9** is represented in Figure 2. 65. Compound **9** (57 mg) was obtained as a colorless solid, on eluting the column with 10 % ethyl acetate in hexane. ^{1}H NMR, ^{13}C NMR and mass spectral studies of this compound and on comparison with literature values [Fotie *et al*., **2006**], confirmed it to be lupeol.

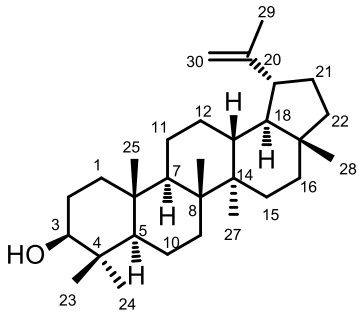

Melting point	:	215-217 ^{o}C
FT-IR (NaCl) υ_{max}	:	3410, 2934, 2863, 1646, 1469, 1374, 1316, 1257, 1190, 1099, 1054, 1024 cm^{-1}.
^{1}H NMR (500 MHz, $CDCl_3$)	:	δ 4.74 (s, 1H), 4.61 (s, 1H), 3.19 (dd, J_1 = 11.5, J_2= 4.4 Hz, 2H), 2.28-2.17 (m, 2H), 2.03-1.94 (m, 2H), 1.69-1.66 (m, 9H), 1.63 – 1.61 (m, 10H), 1.59-1.37 (m, 20H), 1.25 (s, 3H), 0.97 (s, 3H), 0.96 (s, 3H), 0.93 (s, 3H), 0.82 (S, 3H), 0.75 (s, 3H) ppm.
^{13}C NMR (125 MHz,$CDCl_3$)	:	δ 150.7, 109.9, 79.1, 56.3, 55.3, 53.2, 50.5, 46.9, 42.4, 38.9, 38.3, 37.2, 37.1, 32.2, 29.5, 27.9, 25.4, 22.7, 18.3, 16.1, 16.0, 15.3, 14.6, 14.2 ppm.
HR-ESIMS *m/z*	:	427.3938 $[M + H]^+$ (calcd for $C_{30}H_{51}O$ 427.3936)

2.7.4.2. Isolation of compound 10

Compound **10** (11 mg) obtained as colorless solid from fractions 15-17, (Fr.A.15-Fr.A.17) obtained by eluting the column with 70 % ethyl acetate in hexane, was found to be UV inactive, The TLC was sprayed with Mc-Gill reagent and identified the UV inactive spot. ^{1}H, ^{13}C, DEPT-135 NMR and mass spectral studies of this compound and on comparison with literature values [Hlila *et al*., **2016**], confirmed it to be Oleanolic acid.

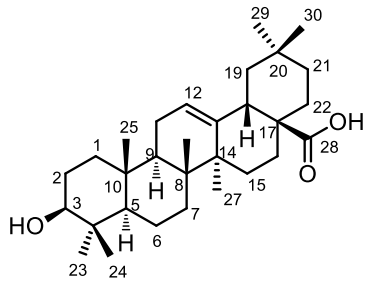

Melting point	:	308-310 ^{o}C
FT-IR (NaCl) υ_{max}	:	3449, 2945, 2866, 1701, 1460, 1385, 1363, 1267, 1161, 1009 cm^{-1}.
^{1}H NMR (500 MHz, $CDCl_3$)	:	δ 5.28 (t, J = 3.5 Hz, 1H, H-12), 3.23 (dd, J_1 = 11.5, J_2 = 4.5 Hz, 1H, H-3), 2.82 (dd, J_1 = 13, J_2= 4 Hz, 1H, H-18), [2.01-1.99 (m, 2H), 1.98-1.96 (m, 2H), 1.88-1.71 (m, 4H), 1.79-1.59 (m, 6H), 1.58-1.53 (m, 6H), 1.45-1.40 (m,8H), 1.38-1.31 (m, 4H), (aliphatic hydrogens)], 1.25 (s, 3H, Me), 1.13 (s, 3H, Me), 0.99 (s, 3H, Me), 0.93 (s, 3H, Me), 0.92 (s, 3H, Me), 0.77 (s, 3H, Me). 0.76 (s, 3H, Me) ppm.
^{13}C NMR (125 MHz,$CDCl_3$)	:	δ 183.2 (C-28), 143.6 (C-13), 122.6 (C-12), 79.1 (C-3), [55.2, 47.6, 46.5, 45.9, 41.6, 40.9, 39.3, 38.8, 38.4, 37.1, 33.8, 33.1, 32.6, 32.4, 30.7, 28.1, 27.7, 27.2, 25.9, 23.6 (aliphatic carbons)]. (C-Me), 23.4 (C-Me), 22.9 (C-Me), 18.3 (C-Me), 17.1(C-Me), 15.6 (C-Me), 15.33 (C-Me) ppm.
HR-ESIMS *m/z*	:	455.3525 $[M-H]^{+}$ (calcd for $C_{30}H_{47}O_3$, 455.3610)

2.7.4.3. Isolation of compound 11

Compound **11** (27 mg) obtained as colourless solid from fractions 19-21, (Fr.A.19-Fr.A.21) obtained by eluting the column with 80 % ethyl acetate in hexane. Finally, by incorporating all the spectral details and on comparison with oleanolic acid and literature data [Luna-Vázquez *et al*., **2016**], the compound was found to be Ursolic acid.

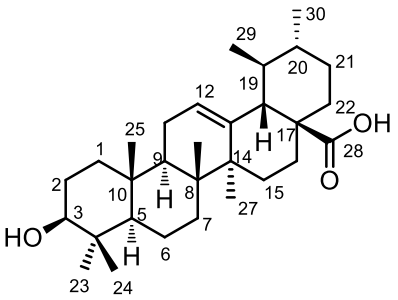

Melting point	:	286-287 ^{o}C
FT-IR (NaCl) υ_{max}	:	3449, 2955, 2866, 1700, 1560, 1385, 1361, 1267 cm^{-1}.
^{1}H NMR (500 MHz, $CDCl_3$)	:	δ 5.28 (t, J = 3.5 Hz, 1H, H-12), 3.22 (dd, J_1 = 11.5, J_2 = 4.5 Hz, 1H, H-3), 2.82 (dd, J_1 = 13, J_2= 4 Hz, 1H, H-18), [2.0-1.95 (m, 2H), 1.90-1.87 (m, 3H), 1.78 – 1.71 (m, 3H), 1.62–1.52 (m, 12H), 1.43–1.23 (m, 11H), (aliphatic hydrogens)], 1.13 (s, 3H, Me), 0.99 (s, 3H, Me), 0.93 (s, 3H, Me), 0.91 (s, 3H, Me), 0.90 (s, 3H, Me), 0.77 (s, 3H, Me), 0.75 (s, 3H, Me) ppm.
^{13}C NMR (125 MHz,$CDCl_3$)	:	δ 183.1 (C-28), 143.6 (C-13), 122.6 (C-12), 79.0 (C-3), 55.2, 47.6, 46.5, 45.9, 41.6, 41.0, 39.3, 38.8, 38.4, 37.1, 33.8, 33.1, 30.7, 29.7, 29.4, 28.1, 27.7, 27.2, 25.9, (aliphatic carbons)], 23.6 (C-Me), 23.4 (C-Me), 22.9 (C-Me), 18.3 (C-Me), 17.1 (C-Me), 15.5 (C-Me), 15.3 (C-Me) ppm.
HR-ESIMS *m/z*	:	455.3525 $[M-H]^{+}$ (calcd for $C_{30}H_{47}O_3$, 455.3610)

2.7.4.4. Isolation of compound 12

The fractions 22-24 (Fr.A.22- Fr.A.24) obtained on column chromatographic separation of acetone extract afforded compound **12** (16 mg) as a yellow powder. This was further purified by crystallization using methanol-chloroform mixture. The compound was successfully characterized as gallic acid**,** based on the spectral data obtained and on comparison with the literature reports [Shaheen *et al*., **2017**].

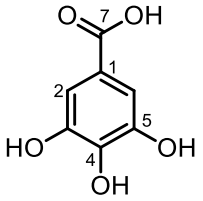

Melting point	:	> 280 ^{o}C decomposing
FT-IR (NaCl) υ_{max}	:	3435, 2810, 2810, 1738 cm^{-1}.
^{1}H NMR (500 MHz, CD_3SOCD_3)	:	δ 8.52 (brs, 3H, -OH), 7.02 (s, 2H, H-2, H-6) ppm.
^{13}C NMR (125 MHz, CD_3SOCD_3)	:	δ 172.9 (C-7), 148.9 (2C, C-3, C-5), 142.1 (C-4), 124.5 (C-1), 112.8 (2C, C-2, C-6) ppm.
HR-ESIMS *m/z*	:	169.0136 $[M-H]^{+}$ (calcd for $C_7H_5O_5$, 169.0137)

2.7.4.5. Isolation of compound 13

The fractions 25-35, (Fr.A.25- Fr.A.35) obtained by eluting the column with 90 % ethyl acetate in hexane yielded 10 sub fractions. Sub fractions 1-3 on crystallization in methanol chloroform afforded compound **13**, 3,3'-di-O-methylellagic acid (10 mg). Based on the spectral data obtained and on comparison with the literature reports [Nawwar *et al*., **1982**], the compound was characterized.

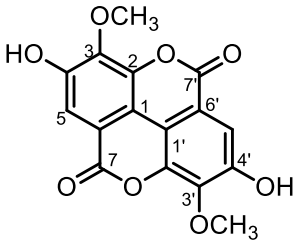

Melting point	:	334-336 ^{o}C
FT-IR (NaCl) υ_{max}	:	3300, 2960, 2840, 1730, 1582, 1506, 1440 cm^{-1}.
^{1}H NMR (500 MHz, CD_3SOCD_3)	:	δ 10.77 (brs, 2H, -OH), 7.53 (s, 2H, H-5, H-5'), 4.04 (s, 6H, 3,3'-OMe) ppm.
^{13}C NMR (125 MHz, CD_3SOCD_3)	:	δ 159.0 (2C, C-7, 7'), 152.7 (4C, C-4, 4', C-2, 2'), 141.7 (2C, C-6, 6'), 140.8 (2C, C-3, 3'), 112.6 (2C, C-1,

1'), 111.9 (2C, C-5, 5'), 61.5 (2C, C-OMe) ppm.

HR-ESIMS *m/z* : 329.0297 $[M-H]^+$ (calcd for $C_{16}H_9O_8$, 329.0295)

2.7.4.6. Isolation of compound 14

Sub fractions 5-10 on crystallization in methanol afforded compound **14** (350 mg) as white solid. Spectral data in detail (IR, ^1H and ^{13}C NMR) and comparison with literature data [Shaheen *et al*., **2017**], the isolated compound was confirmed as ellagic acid.

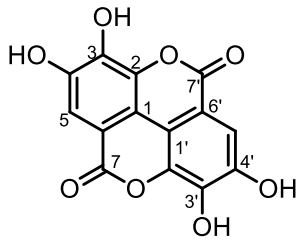

Melting point : > 300 ^oC decomposing

FT-IR (NaCl) υ_{max} : 3313, 2966, 1700, 1440, 1397 cm^{-1}.

^1H NMR (500 MHz, CD_3COCD_3) : δ 8.26 (brs, 4H, -OH), 7.18 (s, 2H, H-5, H-5') ppm.

^{13}C NMR (125 MHz, CD_3COCD_3) : δ 167.2 (2C, C-7,7'), 145.1 (6C, C-2,2',C-4,4', C-3,3') 137.9 (2C, C-6,6'), 121.1 (2C, C-1, C-1'), 109.3 (2C, C-5,5') ppm.

HR-ESIMS *m/z* : 301.1407 $[M-H]^+$ (calcd for $C_{15}H_5O_8$, 301.1847)

2.7.5. Antioxidant and antidiabetic activity studies on *A. indica* rhizome extracts

2.7.5.1. Total Phenolic Content (TPC)

The total phenolic content of the various solvent fractions were determined using Folin-Ciocalteau reagent and was expressed in mg GAE/g of the dry extract. [Singleton and Rossi, **1965**] Absorbance was measured at 725 nm using a multiplate reader (Synergy, Biotek, USA).

2.7.5.2. DPPH radical scavenging activity

DPPH radical scavenging activity of different extracts were estimated according to the method reported by Brand-Williams. Various concentrations of the extracts

were added to 1 mL of DPPH solution (0.2 mM) and kept for incubation at room temperature in dark for about 30 minutes. A control and blank were also performed simultaneously. Gallic acid was used as the standard. The absorbance was measured at 517 nm using a multiplate reader (Synergy 4 Biotek. USA). The percentage radical scavenging capacity was determined using the formula,

$$\% \text{ RSA} = [(A_0 - A_S)/A_0] \times 100$$

A_0 is the absorbance of control and A_S is the absorbance of tested samples. A graph was plotted with a concentration along X-axis and absorbance along Y-axis and the IC_{50} value was calculated and expressed in µg/mL. IC_{50} value signifies the concentration of tested samples to scavenge 50 % of the DPPH radical [Brand-Williams *et al*., **1995**].

2.7.5.3. α-Amylase inhibition assay

α-Amylase inhibition activity was carried out in a microlitre plate according to Xiao *et al.* based on the starch-iodine test [Xiao *et al*., **2006**]. Starch containing a *α*-amylase solution (1U/mL) and different concentrations of extracts were incubated at 50ºC for 30min. After incubation, the reaction was stopped with 1M HCl and 100 µL of iodine reagent was added to the reaction mixture. The absorbance was read at 580 nm on a microplate reader using Synergy 4 Biotek multiplate reader (USA). The known α-amylase inhibitor, acarbose, was used a positive control. The percentage inhibition was calculated using following equation.

$$\% \text{ Inhibition} = \frac{\text{Absorbance of Control - Absorbance of Sample}}{\text{Absorbance of Control}} \times 100$$

A graph was plotted with concentration along the x axis and percentage inhibition along the y axis to obtain the IC_{50} value

2.7.5.4. α-Glucosidase inhibition assay

α-Glucosidase inhibitory activity was assayed as described by Adisakwattana. Different concentrations of extracts containing α-glucosidase solution (1U/mL) were vortexed and kept at room temperature for 5 min, after incubation 250 µL of PNPG was added and incubated at 37ºC for 20 min. The reaction was stopped with 500 µL of

9.4 mM Na_2CO_3. Sample without compounds serves as a control, and commercially available acarbose was used as the standard. The absorbance was measured at 405 nm using a multimode reader (Synergy 4 Biotek multiplate reader, USA). The α-glucosidase inhibitory activity was expressed as the inhibition percentage and was calculated as follows:

$$\% \text{ Inhibition} = \frac{\text{Absorbance of Control - Absorbance of Sample}}{\text{Absorbance of Control}} \times 100$$

A graph was plotted with concentration along the x axis and percentage inhibition along the y axis to obtain the IC_{50} value [Adisakwattana *et al*., **2011**].

2.7.5.5. Anti glycation assay

It was performed according to the methods reported by Jedsadayanmata with slight modifications [Jedsadayanmata **2005**]. About 500 µL of albumin (1 mg/mL final concentration) was incubated with 400 µL of glucose (500 mM) in the presence of 100 µL of extracts at different concentrations, the reaction was allowed to proceed at 60 °C for 24 h and thereafter reaction was stopped by adding 10 µL of 100 % TCA. Then the mixture was kept at 4 °C for 10 min before subjected to centrifugation (Kuboto, Japan) at 10000 xg. The precipitate was redissolved in 500 µL alkaline PBS (pH 10) and immediately quantified for the relative amount of glycated BSA based on fluorescence intensity at 370 nm (excitation) and 440 nm (emission) by Synergy 4 Biotek multiplate reader, USA . Ascorbic acid was used as the positive control.

CHAPTER 3A

Isolation and characterization of bioactives from *Vateria indica* Linn.

3a.1. An overview of Dipterocarpaceae

Dipterocarpaceae is a well-known family of Asian rain forests, consisting of 17 genera which include *Anisoptera*, *Cotylelobium, Dipterocarpus*, *Stemonoporus*, *Upuna*, *Vateria*, *Vateriopsis*, *Vatica, Dryobalanops, Hopea, Neobalanocarpus, Parashorea, Shorea, Marquesia, Monotes, Pseudomonotes* and *Pakaraimaea,* with approximately 600 species. Generally they are trees reaching heights of 40–70 m tall, some even over 80 m. The family name is derived from a Greek word *Dipterocarpus* means "two winged fruit". The species of this family are of major importance in the timber trade and this family produces a wide variety of natural products such as terpenoids, flavonoids, arylpropanoids and resveratrol oligomers. Structural variations in these genera have been examined and about 120 new resveratrol oligomers have been reported from different species [Ito, **2011**]. These resveratrol oligomers have been suggested to play an important role in the prevention of a number of pathological conditions, serious health problems faced by human kind such as anti-cancer [Ito *et al*., **2003**], anti-bacterial [Davis *et al*., **2014**], and anti-HIV [Zeng *et al*., **2017**].

The genus *Vateria*, belonging to dipterocarpaceae family is one of the least explored genus in the family and it consists of nearly 27 species of mainly tropical lowland rainforest trees, distributed in India and Sri Lanka. The name and distribution of most important plant species belonging to the genus *Vateria* are given in Table 3a.1.

Table 3a.1: *Vateria s*pecies and their distribution

SI. No	***Vateria* species**	**Distribution**
1	*V. acuminata* Hayne	Sri Lanka
2	*V. acuminata* Thwaites	Sri Lanka
3	*V. affinis* Thwaites	Sri Lanka
4	*V. ceylanica* Wight	Sri Lanka
5	*V. copallifera* (Retz.) Alston	India, Sri Lanka

		Table 3a.1 contd…
6	*V. flexuosa* Lour.	Vietnam
7	*V. gardneri* Thwaites	Sri Lanka
8	*V. indica* L.	India, Sri Lanka
9	*V. indica* C.F.Gaertn.	India
10	*V. jucunda* Thwaites ex Dyer	United Kingdom
11	*V. lanceolaria* Roxb.	India
12	*V. lanceolata* Thwaites	Sri Lanka
13	*V. lancifolia* Thwaites	Sri Lanka
14	*V. macrocarpa* K.M.Gupta	India
15	*V. malabarica* Blume	India
16	*V. moonii* Thwaites	Sri Lanka
17	*V. nervosa* Thwaites ex Trimen	Sri Lanka
18	*V. oblongifolia* Thwaites	Sri Lanka
19	*V. reticulata* Thwaites	Sri Lanka
20	*V. rigida* Thwaites	Sri Lanka
21	*V. scabriuscula* Thwaites	Sri Lanka
22	*V. wightii* Thwaites	Sri Lanka

3a.2. *Vateria indica*

Vateria indica is also known as the "Indian copal tree" and "dhupa". This plant belongs to the family dipterocarpaceae. The plant *V. indica* used by our ancestors from the prehistoric time and is now at the edge of extinction. Rapid industrialization has led to an impetuous human interference to its habitat and the plant was industrially over exploited for its wood in the 1960's leading to the present condition of extinction. Now the plant is delineated as one of the critically endangered species in the red list of International Union for Conservation of Nature (IUCN Red list - August 2010), needs an urgent attention for Conservation.

Dipterocarpaceous plants are well known to have an abundance in stilbene oligomers which are the building blocks of resveratrol based polymers. The plant *V. indica* also characteristics of the family in a greater extend that it can be considerd as a factory of versatile resveratrol oligomers [Ito *et al.*, **2010**].

Morphology: It is a large evergreen tree that can grow taller than 15 meters, with greyish, smooth bark. The leaf-stalks are 2-3 cm long, swollen at the apex and nearly hairless. The leaves are simple and elliptic-oblong in shape, with caduceus-shaped stipples. The tip of the leaf is abruptly long-pointed or blunt and the leaf base varies in shape from rounded to heart-shaped, flowers are white and possess aroma, the flowering starts inbetween February to March.

Medicinal uses: *V. indica* Linn is mentioned in almost all ancient Ayurvedic literatures with the names Sarja, Sarjaka, Ajakarna. The resin collected from the plant has been used as a traditional medicine for sore throat, chronic bronchitis, piles, rheumatism, obesity, lipid disorders, anaemia, genitourinary diseases, diarrhoea and diseases due to vitiated blood; externally in gout, abscesses, skin diseases, burns. Leaf juice is used for curing burns and blood diseases.The bark is used as an antidote against poison and infections. Resin from this plant is used in chronic rheumatism, and other painful affections, carbuncles and other ulcerations [Hari *et al.,* **2010**; Nadkarni, **1976**].

3a.3. Scientific classification

Table 3a.2: Scientific classification of *Vateria indica*

Kingdom	**Plantae**
Phylum	***Tracheophyta***
Class	**Magnoliopsida- Dicotyledons**
Subclass	**Dilleniidae**
Order	**Theales**
Family	**Dipterocarpaceae - Meranti family**
Genus	***Vateria***
Species	***Vateria indica***

Figure 3a.1: Picture of *Vateria indica* plant, bark and Seeds

3a.4. *Vateria indica* - Literature survey

Vateria indica Linn. is an evergreen medicinal tree that grows up to 30 m height, indigenous to evergreen forests of Western Ghats from North Karnataka to Kerala. The resin exuded by the tree is known as piney resin, white dammer or Dhupa. The resin is known as Sarja rasa in Ayurveda and Vellai kungiliyam in Siddha [Venkateshwarlu *et al*., **2011**]. The resin finds its use in traditional Indian system of medicine like Ayurveda and Siddha for health and healing diseases. It is credited with tonic, carminative and expectorant properties and it is used for the treatment of respiratory disorders like chronic bronchitis, tubercular gland, boils, piles diarrhoea and so on. Mishima *et al*., have reported the antitumor activity of the ethanol extract from the stem bark of *V. indica*, which contains four resveratrol oligomers and bergenin as the major constituent. Both *in vitro* and *in vivo* study showed the growth of inoculated S-180 cells in mice was retarded by oral administration of the extract in a dose-

dependent manner [Mishima *et al*., **2003**]. Ito *et al*., reported the first resveratrol octamer vateriaphenol A from the stem bark of *V. indica* and their cytotoxicity against KB cell lines [Ito *et al*., **2001**]. The same group also reported the isolation of new oligostilbene with dihydrobenzofuran from the stem bark of *V. indica* [Ito et al., **2003**]. In 2010 Ito and co-workers reported the comprehensive re-investigation of the chemical constituents in the leaves of *Vateria indica* resulted in the isolation of a novel resveratrol dimeric dimer vateriaphenol F, and two new O-glucosides of resveratrol oligomers, vateriosides A and B along with a known resveratrol oligomers and its derivatives [Ito *et al*., **2010**]. Recently the same group reported the rotational isomeric shoreaketone, identified as a skeletal member of resveratrol tetramers, from three species of Dipterocarpaceaeous plants including *V. indica*.

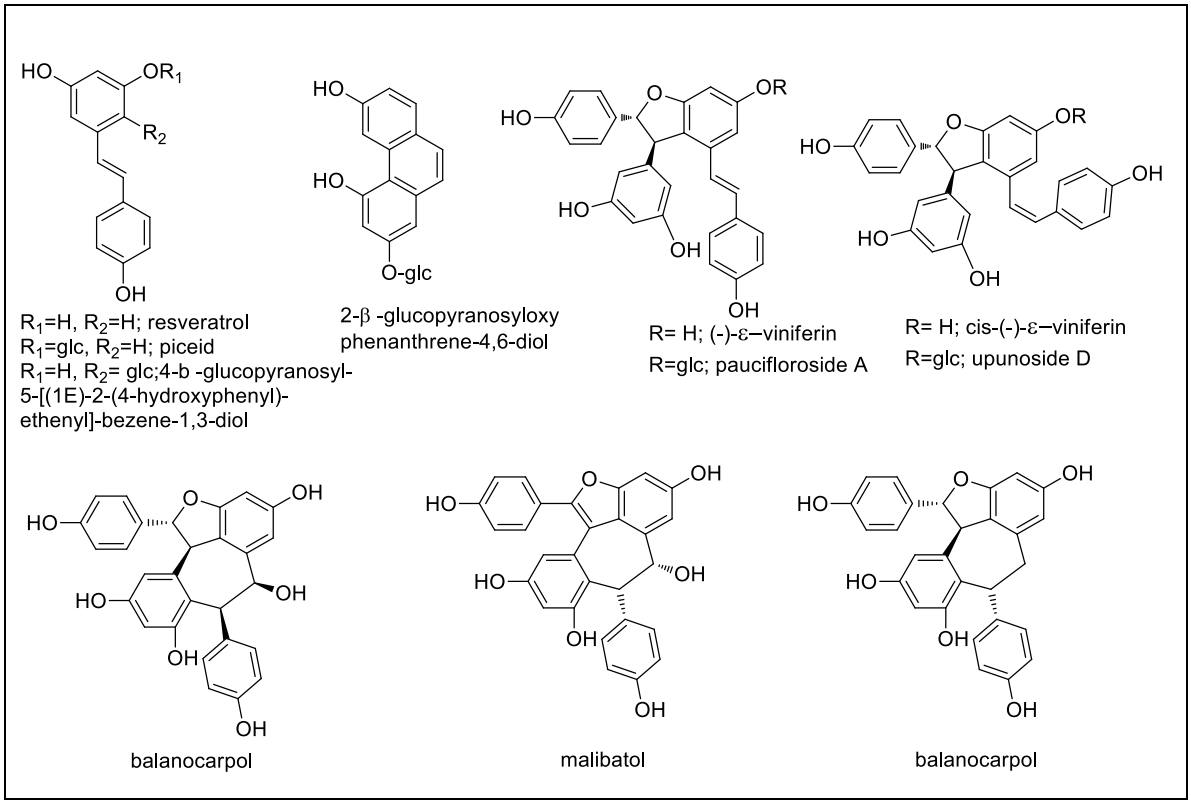

Figure 3a.2: Known phytochemicals from *V. indica*

Figure 3a.2 Contd…

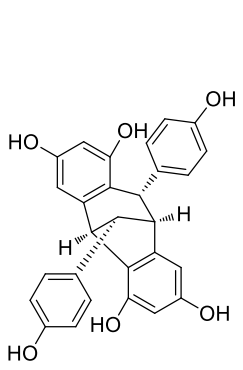

(-)-ampelopsin F

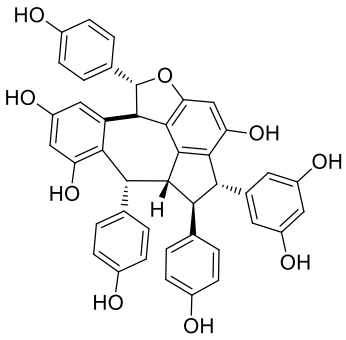

paucifloral B

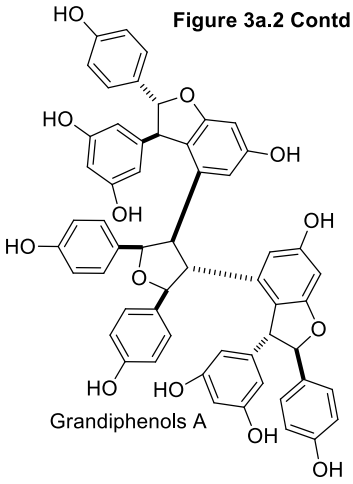

Grandiphenols A

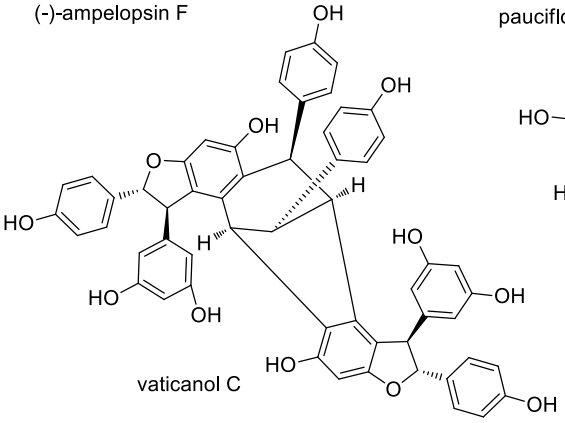

vaticanol C

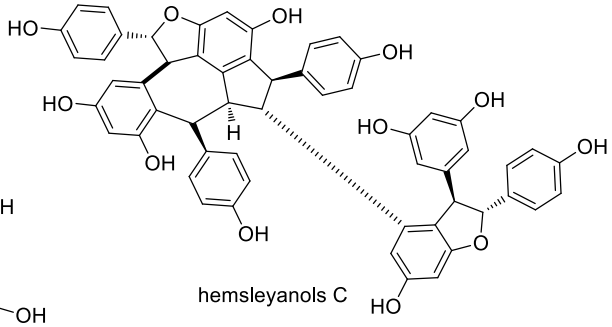

hemsleyanols C

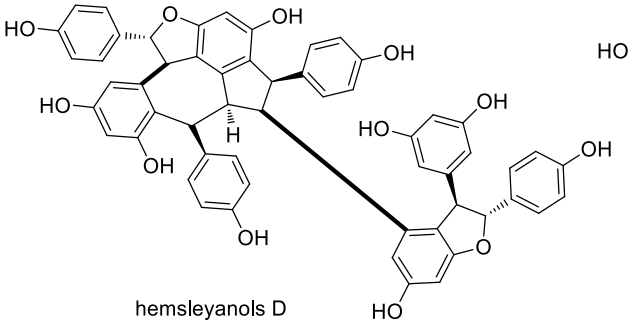

hemsleyanols D

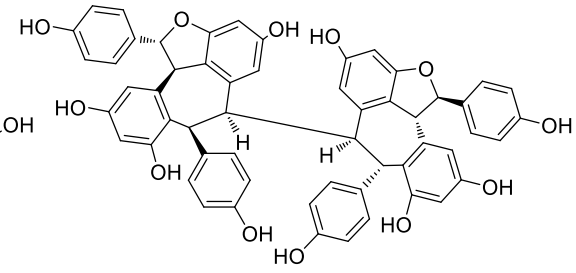

pauciflorol C

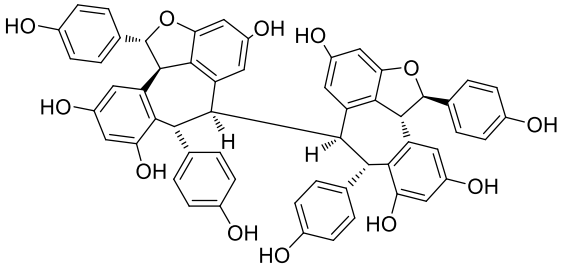

vateriaphenol B

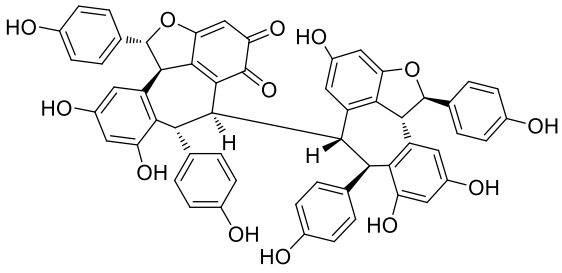

nepalensinol G

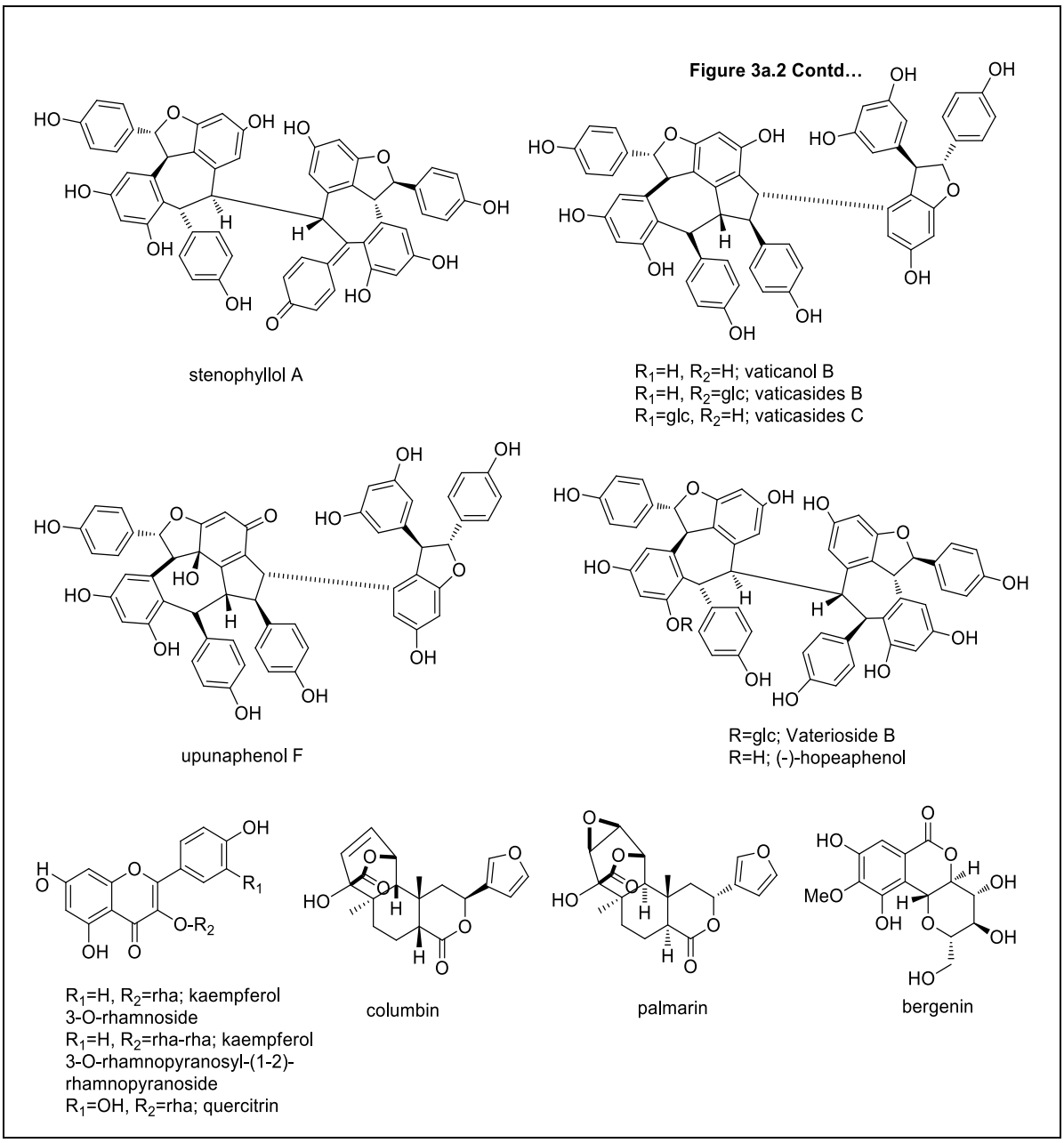

3a.5. Aim and scope of the present work

Vateria indica Linn is a large evergreen tree, belongs to Dipterocarpaceae family. The tree grows mostly in moist evergreen forests, deciduous forests and adjoining rivers. This plant is endemic to India; usually found in the state of Karnataka, Kerala and Tamil Nadu. It is a multipurpose tree which has economic and medicinal significance. The various parts of this plant are used in the treatment of chronic bronchitis, scrofula, ringworm, wounds, rheumatism, urinary discharges, piles, amenorrhoea, syphilis and gonorrhoea. In Ayurveda

this plant has been used for the treatment of anaemic disorder, ear disorder, skin disorder and diabetes mellitus. Even though the preliminary phytochemical analysis of *V. indica* bark and leaves revealed the presence of sterols and stilbenoids in them, there has been no detailed report on the phytochemical and pharmacological investigation of the *V. indica*. Now the plant is delineated as one of the critically endangered species in the red list of International Union for Conservation of Nature (IUCN Red list-August 2010), needs an urgent attention for conservation. Therefore it is timely and relevant to carry out the phytochemical investigation of *V. indica.* So, as part of this Ph.D. program, a detailed study of *V. indica* bark and seed was undertaken. Evaluation of chemical indices of acetone extract of *V. indica* bark, preliminary *in vitro* antioxidant and antidiabetic potentials of the extracts have been carried out. Detailed identification and separation of fatty acids from *V. indica* seed by using GCMS has been carried out, and the results are described in this chapter.

3a.6. Extraction and biological activities of *Vateria indica* bark

3a.6.1. Plant material and extraction

The bark of *Vateria indica* Linn. was collected in June 2014 from Wayanad district of Kerala. The plant material was authenticated by the taxonomist of M. S. Swaminathan Research Foundation, Wayanad, Kerala (Voucher no. M.S.S.H.0763) and was deposited in the herbarium repository of the institute. This was thoroughly cleaned and dried in a hot air oven maintained at 50 ^{o}C for three days. It was then coarsely powdered. It weighed approximately 1 kg. The powdered material was subjected to repeated extraction three times with hexane (2.5L x 48h) at room temperature. Thin layer chromatography indicated that the extraction was complete after six days. The total extract was then concentrated under reduced pressure using a Heidolph rotary evaporator. This yielded about 3.55 g of crude hexane extract (H). The above mentioned extraction procedures were repeated using acetone (A), ethanol (E) and water (W). Acetone extract yielded about 56 g, methanol extract yielded about 45 g and we obtained about 29.25 g of water extract after lyophilisation. These extracts were analysed for their antioxidant and antidiabetic activities.

3a.7. Extract level antioxidant and antidiabetic activities

3a.7.1. Total phenolic content

Polyphenols are the major group of compounds that contribute to the antioxidant properties. The main principle of this method was its ability to reduce phenol functional

group. It is an electron transfer reaction between Folin-ciocalteu reagent and the phenolic compound. In the present study the acetone, hexane, ethanol and water extracts were prepared to examine the total phenolic content. The phenolic contents in the examined plant extracts using Folin-Ciocalteus reagent is expressed in terms of gallic acid equivalents. The TPC was calculated using the following linear equation based on calibration curve obtained by plotting standard gallic acid (1mg/mL):

$$y = 0.100x - 0.116$$

Here, y is the absorbance & x is the observed phenol content (µg). The highest concentration of phenols was measured in acetone extract (117.93± 0.21mg GAE/g). Hexane extract contains considerably smaller concentration of phenol (17.00± 0.64 mg GAE/g).

3a.7.2. DPPH radical scavenging activity

The DPPH stable free radical method is an easy, rapid and sensitive way to survey the antioxidant activity of specific plant extracts. 2,2-diphenyl-1-picrylhydrazyl (DPPH radical) (i) is a stable free radical. When it reacts with an antioxidant compound (ii) which can donate H radical, DPPH free radical is reduced to 2, 2- diphenyl-1-picrylhydrazine (iii). DPPH radical is characterized by violet colour. The antioxidants in the sample scavenge the free radicals & turn it into yellow colour [Reddy *et al.,* **2005**].

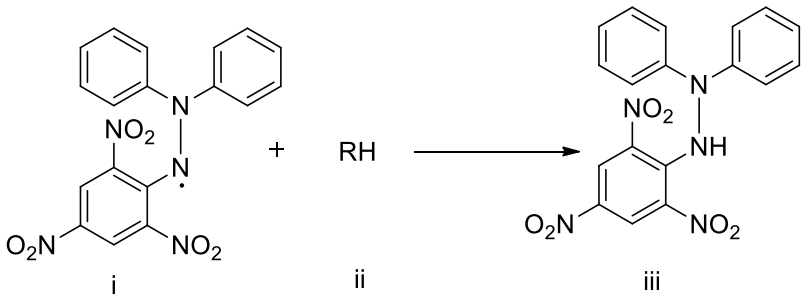

Scheme 3a.1: Represents the reaction of DPPH radical with anti-oxidant compound

Thus antioxidant molecules can quench DPPH free radicals by providing hydrogen atom or by electron donation, a colourless stable molecule 2, 2- diphenyl-1-picrylhydrazine is formed and as a result of which the absorbance (at 517 nm) of the solution is decreased.

The free radical scavenging activity of different solvent extracts of *Vateria indica* stem bark were determined by the DPPH method and the results were compared with standard gallic acid.

From the dose dependent curve of DPPH radical scavenging activity of different extracts of *V. indica*, it was observed that the acetone extract had higher radical scavenging activity (IC_{50}29.58±0.91). The values obtained were plotted in **Figure 3a.3**. From the Figure 3a.3 it is clear that the concentration of extract increases, the percentage of inhibition also increases.

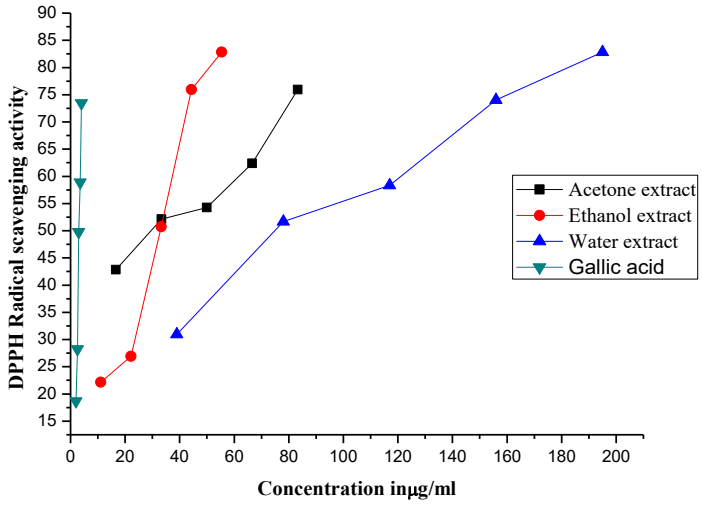

Figure 3a.3: Extract level DPPH radical scavenging activity of *V. indica* stem bark

3a.7.3. Antidiabetic activity

Diabetes mellitus is the most common disease in the world. α-Amylase & α- glucosidase are enzymes that catalyse the breakdown of starch to glucose. One therapeutic approach for treating diabetes is inhibition of α- amylase and α- glucosidase activities to reduce blood glucose level. In this context we assess antidiabetic potential of different extracts in terms of their inhibition towards the enzymes *α*- amylase and *α*- glucosidase

3a.7.4. *α*–Amylase inhibition assay

α-Amylase inhibition assay was determined using acarbose as the positive control. Acarbose has been used in the clinical management of early diabetes. The principle of the method is Iodine reagent complexes with starch to form a blue colour. Any starch that has not yet been hydrolyzed by the amylase will turn blue, with the intensity of the blue colour being proportional to the amount of starch remaining. Percentage *α*- amylase inhibition of the plants extracts and seven compounds from bark were plotted as a function of concentration in comparison with acarbose. The results indicate that out of the four extracts, acetone extract

exhibited good anti-α amylase activity (IC_{50} 17.12±0.22). Hexane extract showed the least inhibitory activity (IC_{50} 68.08±0.822).Water extract have no *α*-amylase inhibition.

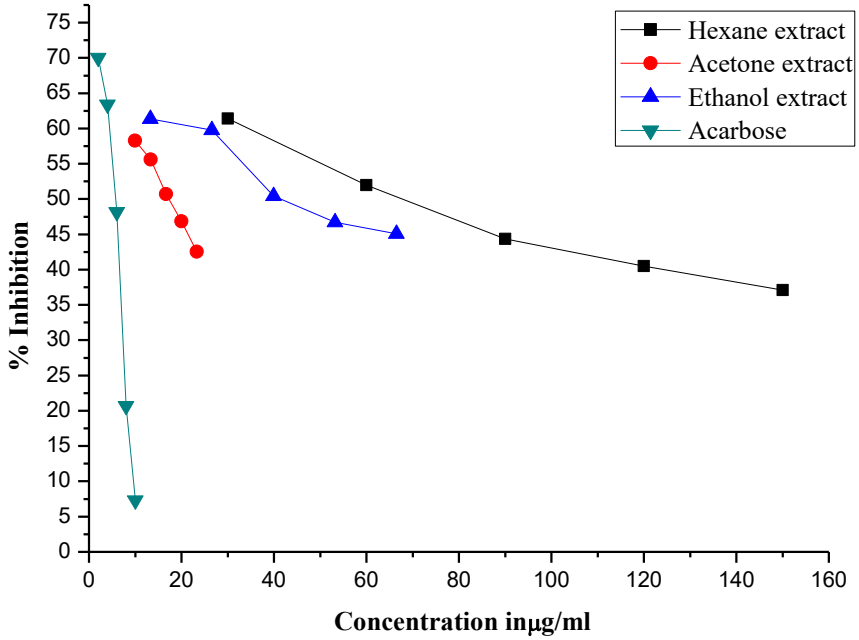

Figure 3a.4: *α*-Amylase inhibitory activity of different extracts of *V. indica* stem bark

3a.7.5. *α*-Glucosidase inhibition assay

The principle of this method is *α*-glucosidase converts the substrate *p*-nitrophenyl *α*-D-glucopyranoside into *α*-D-glucopyranoside and *p*-nitrophenol. The yellow colour of *p*-nitrophenol is measured spectrophotometrically.

It was observed that the Acetone extract of *V. indica* exhibits higher *α*-glucosidase activity (IC_{50}1.47 ± 0.693 µg/mL). From the Figure 3a.5, it is clear that percentage *α*-glucosidase inhibition increases as the concentration of the extract increases. Hexane extract showed least inhibitory activity.

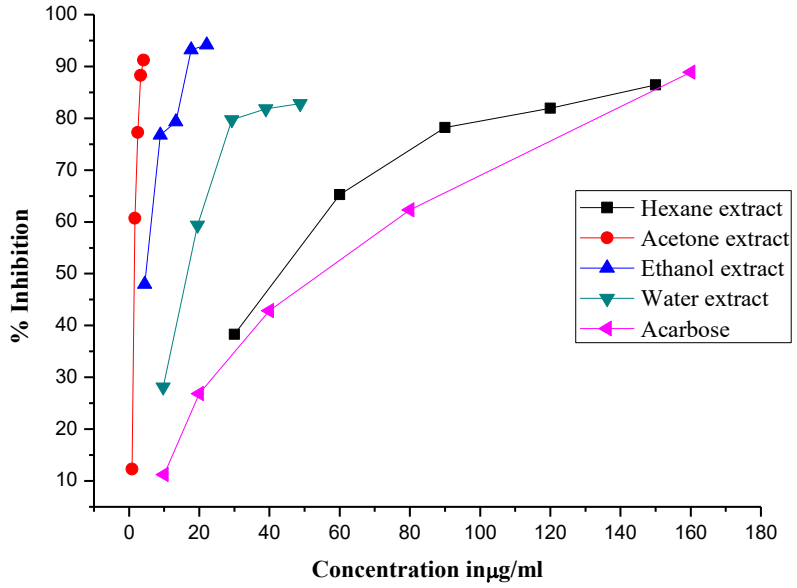

Figure 3a.5: α-Glucosidase inhibitory activity of different extracts of *V. indica* stem bark

Table 3a.3. IC_{50} values of different extracts of *V. indica* in α-amylase inhibition, α-glucosidase inhibition and antiglycation assay

Fractions	**TPC (mg GAE/g dry weight)**	**DPPH (IC_{50}-μg/mL)**	***α*-amylase (IC_{50}-μg/mL)**	***α*-glucosidase (IC_{50}-μg/mL)**	**Antiglycation (IC_{50}-μg/mL)**
VI-H	17.00± 0.64	NIL	68.08±0.822	42.86±0.785	NIL
VI-A	117.93± 0.21	29.589±0.91	17.12±0.22	1.47±0.693	NIL
VI-E	26.27±1.00	32.69±0.76	40.37±0.38	4.60±1.12	NIL
VI-W	37.34 ±0.035	74.12±1.2	NIL	16.54±0.77	NIL
Standard	-	3.58±0.31 (Gallic acid)	5.65±0.23 (Acarbose)	54.73±0.92 (Acarbose)	NIL (Ascorbic acid)

All data are represented as mean ± standard deviation (n=3).

3a.8. Isolation and characterization of compounds from *Vateria indica* bark

The antioxidant and antidiabetic activity screening confirmed that the acetone extract has the highest activity compared to other extracts. Therefore, further isolation, purification

and characterization of chemical constituents were performed on the acetone extract. After studying the TLC extensively, 56 g of the acetone extract was subjected to column chromatographic purification using silica gel (100-200 mesh). Column elution was initiated using 100 % hexane and polarity was increased by increasing the amount of ethyl acetate. Final elution was carried out using 15 % methanol in ethyl acetate. A total of 200 fractions of approximately 200 mL each were collected. According to the similarities in TLC, they were pooled into 62 major fraction pools (FrA.1- FrA. 62).

Fraction pool 1-2 (FrA.1-2), obtained by eluting the column with 10 % ethyl acetate in hexane on crystallization using the same solvent yielded 40 mg of colourless needle like crystals of a common phytosterol, ***β*-sitosterol.** Fraction pool 3 (FrA.3), obtained by eluting the column with 10 % ethyl acetate in hexane on crystallization using the same solvent yielded 25 mg of colourless needle like crystals of **stigmasterol.** Both *β*-sitosterol and stigmasterol were characterized based on various spectral data (^{1}H NMR, ^{13}C NMR and HRMS) obtained. The compound was further confirmed by TLC co-spotting with authentic samples.

Fraction pool 4-6 (FrA.4-6), obtained by eluting the column with 20 % ethyl acetate in hexane yielded 65 mg of the mixture of compound **15** and compound **16**. This was further purified by using silica gel (230-400 mesh) column chromatography by eluting column with 20 % ethyl acetate in hexane. Subfractions 3-10 obtained by eluting the column with 20 % ethyl acetate in hexane yielded 20 mg (0.002 %) of compound **15** as a colourless crystals, which was found to be UV inactive, suggesting that the compound does not contain any chromophore in it. The TLC was sprayed with Mc-Gill reagent and identified the UV inactive spot. ^{1}H NMR (Figure 3a.7) and ^{13}C NMR spectra (Figure 3a.8) of the compound was suggestive of steroid moiety. Triplet at δ 5.18 ppm integrating for one proton could be attributed to the olefinic proton. Proton attached to the carbon bearing hydroxyl group resonated as a multiplet at δ 3.24-3.21 ppm. All other aliphatic protons appeared in between δ 2.17 to 0.79 ppm. ^{13}C NMR spectrum of the compound showed the presence of thirty carbon atoms indicating that the compound **15** is a pentacyclic triterpene. Comparison of the ^{13}C NMR spectral values, and DEPT-135 spectra suggested that there are eight methyl groups, ten methylene groups, five methine groups and seven quaternary carbons in the molecule (Figure 3a.9). Carbon bearing the hydroxyl group resonated at δ 79.0 ppm. The

olefinic carbon atributed at δ 145.2 and 121.7 ppm. The mass spectrum of the compound **15** showed molecular ion peak at m/z 427.3941, which is the $[M+H]^+$ peak. By incorporating all the spectral details and on comparison with the literature [Okoye *et al.,* **2014**], the compound was confirmed as ***β*-amyrin**. The compound is being reported for the first time from *V. indica*. The structure of the compound is shown below.

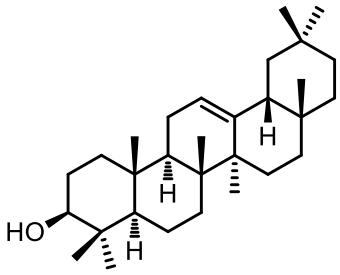

Figure 3a.6: *β*-Amyrin **(15)**

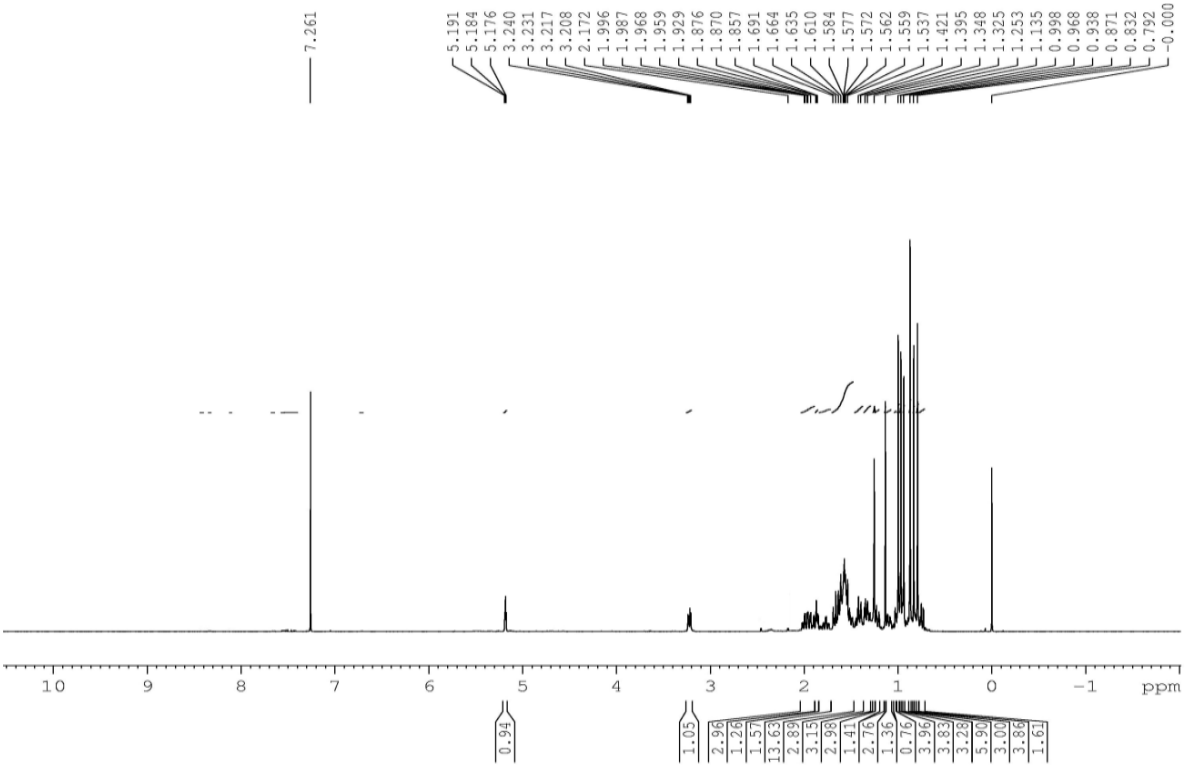

Figure 3a.7: ^{1}H NMR spectrum of *β*-amyrin

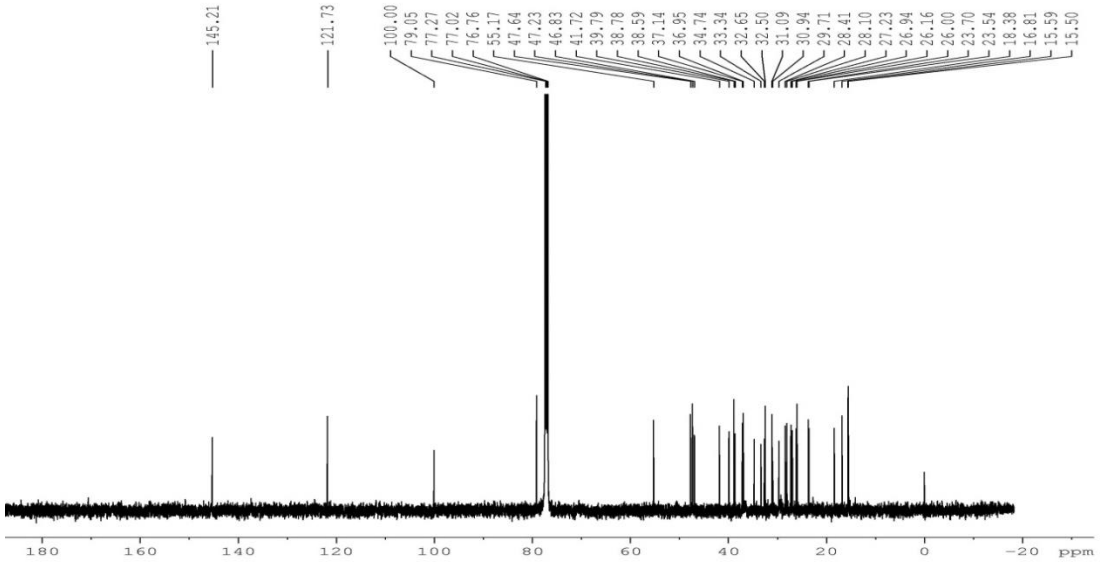

Figure 3a.8: ^{13}C NMR spectrum of *β*-amyrin

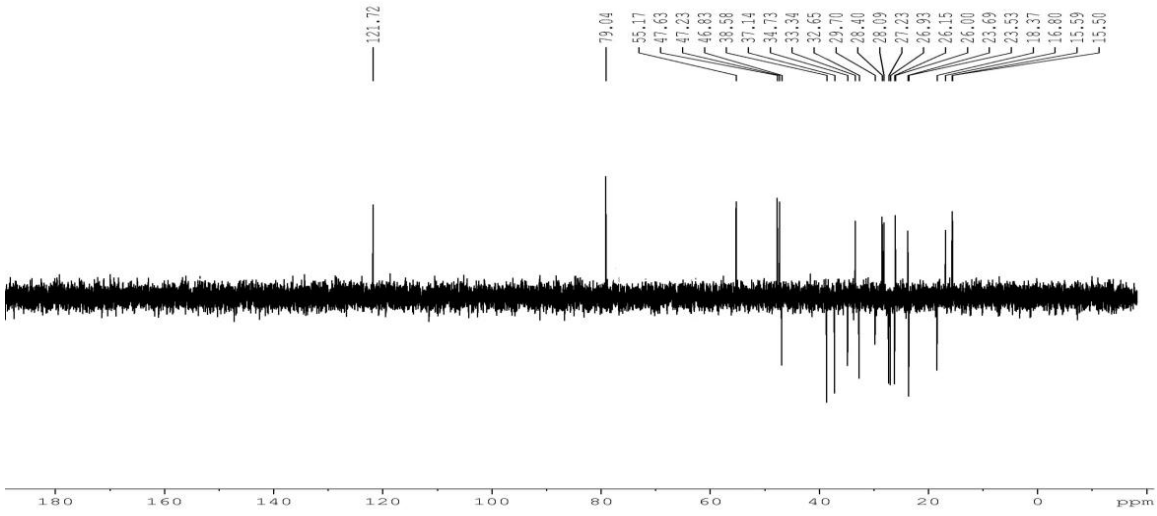

Figure 3a.9: DEPT-135 NMR spectrum of *β*-amyrin

Subfractions 10-15 obtained from fraction pool 4-6 (FrA.4-6), by eluting the column with 20 % ethyl acetate in hexane yielded 37 mg (0.0037 %) of compound **16** as a colourless crystal, which was found to be UV inactive. The TLC was sprayed with Mc-Gill reagent and identified the UV inactive spot. ^{1}H NMR (Figure 3a.11) and ^{13}C NMR spectra (Figure 3a.12) of the compound **16** is similar to that of compound **15**. In ^{1}H NMR spectrum triplet at δ 5.25 ppm integrating for one proton could be attributed to the olefinic proton. Proton attached to the carbon bearing ester group resonated as a multiplet at δ 3.62-3.58 ppm. The deshielding

nature of proton is due to the presence of ester group. All other aliphatic protons appeared in between δ 2.07 to 0.81 ppm. ^{13}C NMR spectrum of the compound showed the presence of ester carbon at δ 178.97 ppm. Comparison of the ^{13}C NMR and DEPT-135 spectral values with compound **15**, the compound **16** was characterized. The mass spectrum of the compound **16** showed molecular ion peak at m/z 469.4039, which is the $[M+H]^+$ peak. By incorporating all the spectral details and on comparison with the literature [Okoye *et al.,* **2014**], the compound was found to be ***β*-amyrin acetate**. This is the first report of the isolation of *β*-amyrin acetate from any part of *V. indica*. The structure of the compound is shown below.

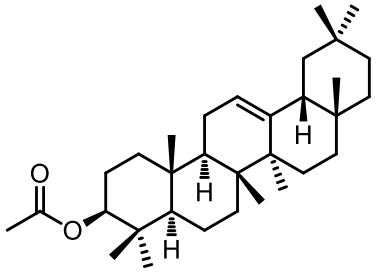

Figure 3a.10: *β*-Amyrin acetate **(16)**

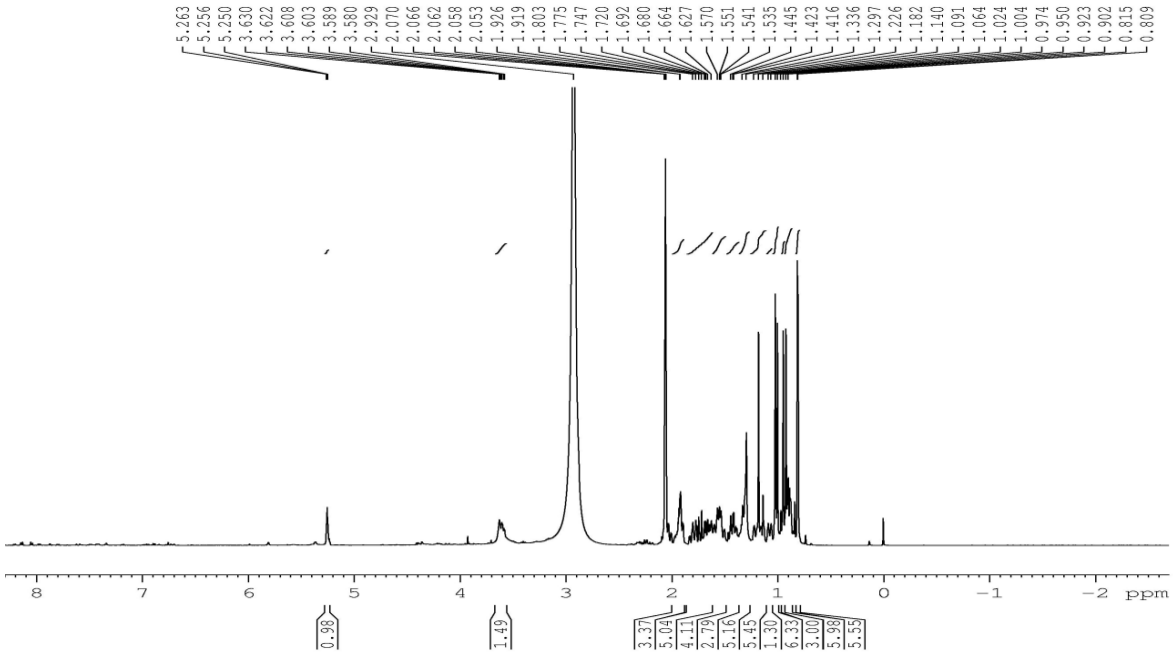

Figure 3a.11: ^{1}H NMR spectrum of *β*-amyrin acetate

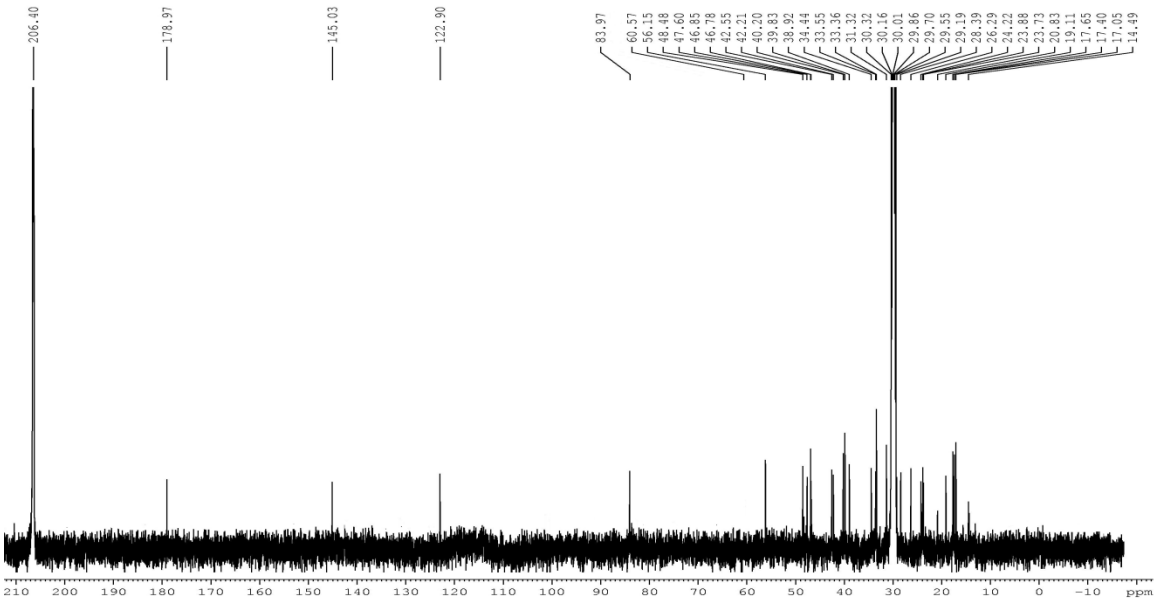

Figure 3a.12: ^{13}C NMR spectrum of *β*-amyrin acetate

Fraction pool 6-8 (FrA.6-8) which on precipitation by using acetone, a white pasty mass of Compound **17** (11 mg; 0.0011 %) was yielded. IR spectrum of the compound gave absorptions at 3498 and 1737 cm^{-1} suggesting the presence of hydroxyl and ester groups. ^{1}H NMR spectrum (Figure 3a.14) and ^{13}C NMR spectrum (Figure 3a.15) of the compound clearly indicated that the compound is a steroidal glucoside with long chain fatty acid ester. In ^{1}H NMR signal at δ 5.36 indicated the presence of an olefinic proton. The anomeric proton from the glucose ring resonated at δ 4.38 ppm as a doublet with coupling constant value J = 7.5 Hz indicating that the glucose ring which is attached to the sterol moiety is in *β*-orientation. Signals at δ 4.46 and 4.27 ppm attributed to the diasterotopic ester methylene protons. The remaining protons from the glucose moiety appeared in the region δ 3.58-3.36 ppm. All other aliphatic protons resonated in the region δ 2.78-0.68 ppm. In ^{13}C NMR, the signal at δ 174.7 ppm could be attributed to ester carbonyl carbon. The olefinic quarternary and methine carbon resonated at δ 140.3 and 122.2 ppm respectively. Anomeric carbon appeared at δ 101.2 ppm. Methine carbon which is directly attached to the hydroxy group resonated in the region 79.6- 70.1 ppm. Signal at δ 63.2 ppm attributed to the ester methylenic carbon which was further confirmed from DEPT-135 spectrum (Figure 3a.16). Remaining all other signals in ^{13}C NMR is good agreement with the *β*–sitosterol. Finally the mass spectra of compound **17** gave 837.2183 $[M + Na]^{+}$ as the molecular ion peak. Presence

of palmitic acid, glucose ring and tetracyclic sterol moiety were further confirmed by mass fragmentation pattern (palmitic acid; m/z-255.0654, glucose; m/z-181.0654, tetracyclic sterol moiety; m/z-337.0686). Deducing from all the spectral details and in comparison with the literature [Ren *et al.,* **2015**], the compound was found to be **sitoindoside I**. The structure of the compound is shown below. To the best of our knowledge this is the first report on the isolation of **sitoindoside I** from any part of *V. indica* and the compound is being reported for the first time from Dipterocarpaceae family.

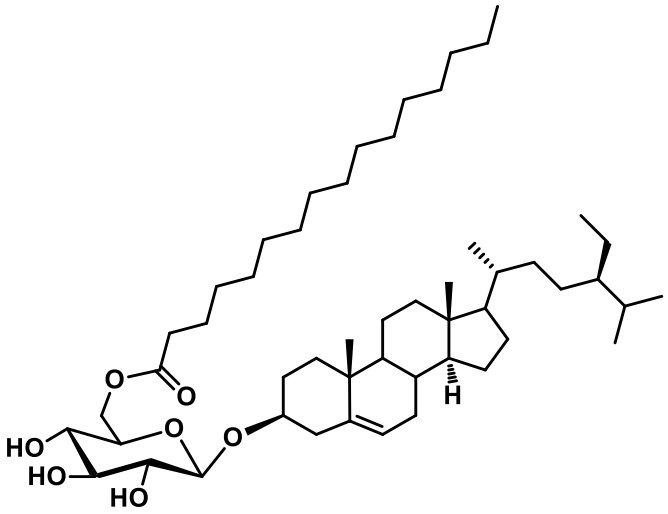

Figure 3a.13: Sitoindoside I **(17)**

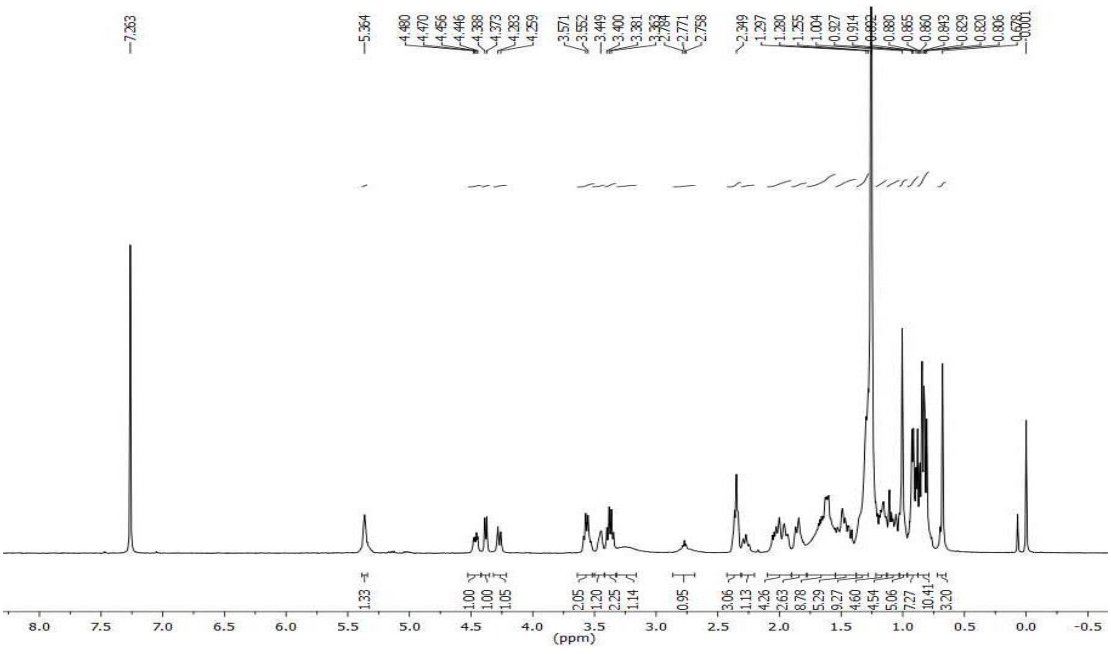

Figure 3a.14: ^{1}H NMR spectrum of sitoindoside I

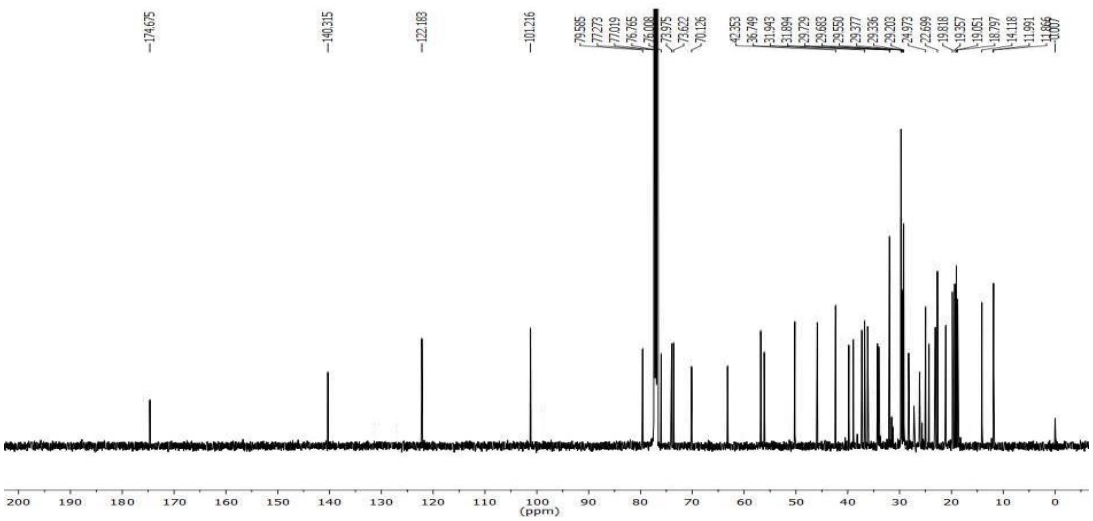

Figure 3a.15: ^{13}C NMR spectrum of sitoindiside I

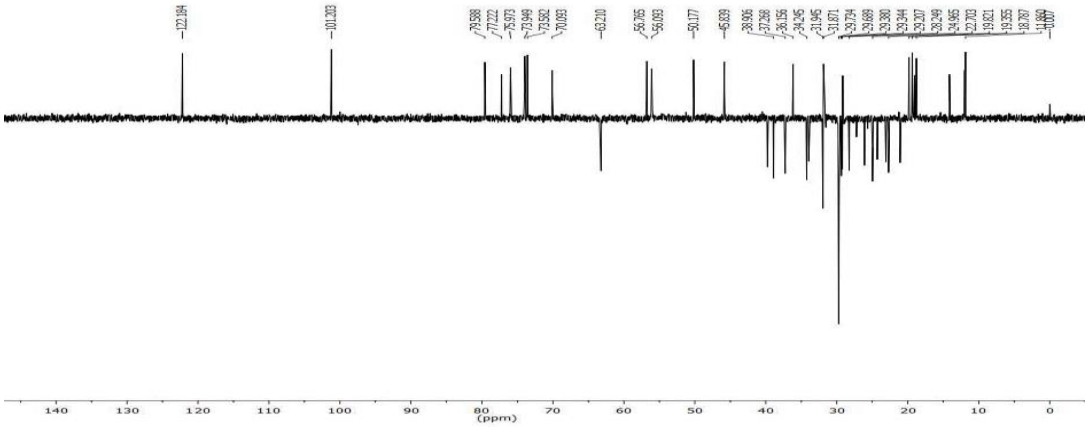

Figure 3a.16: DEPT-135 NMR spectrum of sitoindoside I

Fraction pool 9 (FrA. 9), obtained by eluting the column with 30 % ethyl acetate in hexane showed the presence of a UV active compound. It was again subjected to purification using silica gel column chromatography (230-400 mesh) yielded 18 mg (0.0018 %) of light brownish solid, which was labelled as compound **18**. Compound **18** was confirmed to be ***E*-Resveratrol**, which was earlier isolated from *A. indica* rhizome (chapter 2).

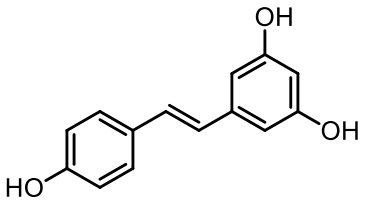

Figure 3a.17: *E*-Resveratrol **(18)**

Fraction pool 11-15 (FrA.11- Fr.A.15), obtained by eluting the column with 35 % ethyl acetate in hexane yielded 17 mg (0.0017 %) of yellowish amorphous solid which showed blue fluorescence in UV light labelled as compound **19**. IR, ^{1}H, ^{13}C and HRESIMS spectrum of the compound **19** is similar to that of compound **2**. In ^{1}H NMR spectrum (Figure 3a.19) δ 8.58 and 8.35 ppm indicating the presence of phenolic hydroxyl groups. The signals at δ 6.91 and 6.70 ppm as a doublet each integrating one proton with *J* value 16.5 Hz could be attributed to *trans* olefinic protons. The protons of stereocenter resonated at δ 5.43 and 4.47 ppm with coupling constant *J* value 5.5 Hz respectively. In ^{13}C NMR, (Figure 3a.20) the signals at δ 161.5, 159.0, 158.8, 157.4 and 157.4 ppm are the diagnostic peaks for aromatic carbons attached to the hydroxyl group. The stereocenter carbon directly attached to oxygen atom resonated at δ 93.0 and another methine stereocenter carbon appeared at δ 56.2 ppm. The mass spectra of the compound **19** gave molecular ion peak 455.1497 which is the $[M+H]^{+}$. As already discussed in chapter 2 most of the resveratrols which are enantiomerically pure form isolated from vitaceae family are in (+) form. While its enantiomer, (-)-form is exclusively found in plants from the family Dipterocarpaceae [Keylor *et al*., **2015**]. The absolute configuration of compound **19** was established on the basis of optical activity $[\alpha]^{25}_{D}$ -31.5^{o} (c, 0.1 MeOH); which was in agreement with the reported value $[\alpha]^{23}_{D}$ -27.9^{o} (c 0.843, MeOH) [Kurihara *et al*.,**1990]**. Finally, compound **19** was identified as **(-)-*ε*-viniferin** (Figure 3a.18). Biosynthetic pathway of (-)-*ε*-viniferin will be discussed in chapter 3B.

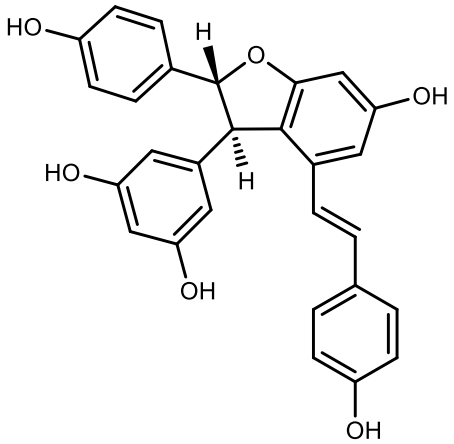

Figure 3a.18: (-)-*ε*-Viniferin **(19)**

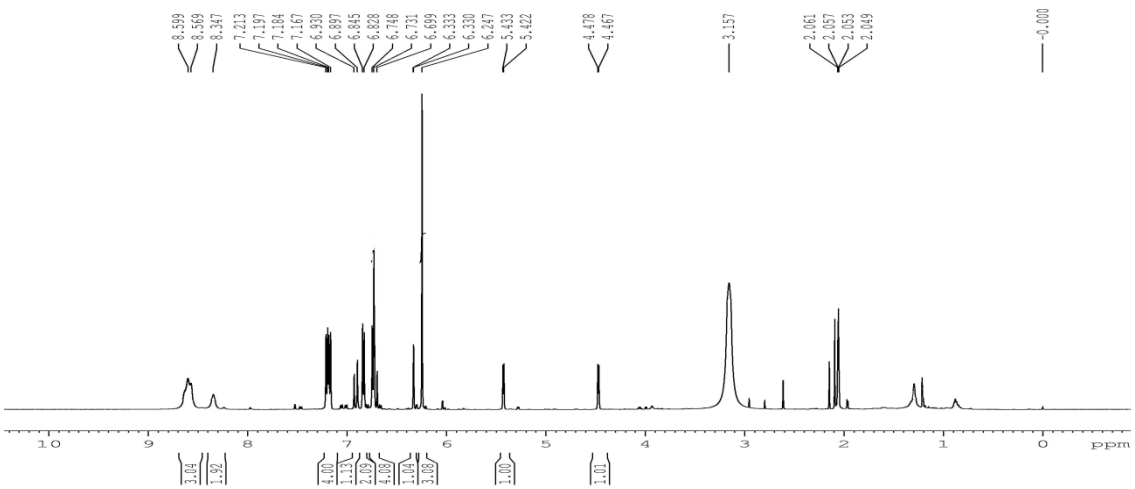

Figure 3a.19: ^{1}H NMR spectrum of (-)-ε-viniferin

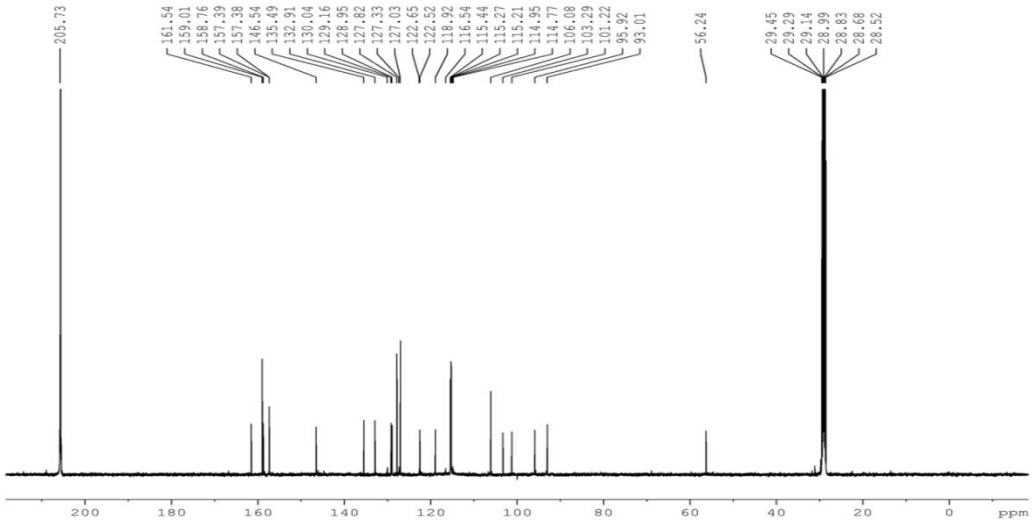

Figure 3a.20: ^{13}C NMR spectrum of (-)-ε-viniferin

Compound **20** (4 g; 0.4 %) was isolated as a white solid from fractions Fr.A.17- Fr.A.30 obtained by repeated column chromatography with 70 % ethyl acetate in hexane. The compound was assigned the molecular formula $C_{56}H_{42}O_{12}$ following analysis of the HRESIMS at m/z 907.2737 $[M + H]^+$. IR, 1D and 2D NMR spectrum of the compound **20** was similar to that of compound **4**. The ^{1}H and ^{13}C NMR and in comparison with HRMS suggest that the isolated compound has two dimeric stilbene moieties with the same configuration. The ^{1}H NMR spectrum in CD_3COCD_3 (Figure 3a.23) exhibited signals for five phenolic hydroxyl groups (δ 8.56-7.45 ppm) which disappeared upon addition of D_2O. Considering the molecular formula, the remaining oxygen would contribute to the ether

linkage. Other 2D spectroscopic details including ^{13}C NMR, $^{1}H–^{1}H$ COSY, HMQC and HMBC spectra (Figure 3a.24-Figure 3a.27) exhibited signals due to four aromatic rings as follows; two *p*-hydroxyphenyl groups (A1 and B1) and two 1,2,3,5-tetrasubstituted aromatic ring (A2 and B2). The presence of a set of mutually coupled aliphatic protons (H-7a/H-8a) and a sequence of two aliphatic protons (H-7b/H-8b) were also shown. The $^{1}H–^{1}H$ coupling pattern of the stereocenter protons (H-7a/H-8a) was characteristic of a dihydrobenzofuran ring, and of the latter (H-7b/H-8b) was similar to a partial structure of ampelopsin B, [Takaya *et al*., **2002**] which suggested that a heptadiene ring system. The planar structure was confirmed by the following evidence. The correlations in the HMBC spectrum (Figure 3a. 27) were observed between H-7a/C-(2a,6a), C-8a, C-9a, 8a/C-14a, C-10a, C-10b, H-7b/C-(2b,6b), C-8b, C-10a, C-9b, C-9a, H-8b/C-9b,C-14b, C-10a), H-7b/C-8b, C-10a and H-8b/C-9b which indicated the presence of four aromatic rings and four methine units.

To confirm the relative stereochemistry, NOESY experiments were conducted (Figure 3a.28). In the spectrum, clear cross peaks between H-7a/H-14a, H-8a/H-(2a,6a), H-(2b,6b), H-8b were observed. These cross peaks substantiated that the relative stereochemistry of the methine protons at 7a and 8a are in *trans* orientation. The relationship between two methine protons (H-7b and H-8b) and the dihydrobenzofuran ring was determined as follows. NOE interactions between H-8a/ H-(2b,6b) indicated that the ring B1 is oriented in α-configuration, alternatively H-7b is oriented in β-configuration. The significant NOEs observed between H-7b/ H-14a, and H-8b/H-8a, H-14b, H-(2b,6b) also indicated that the relative configuration of methine protons at C-7b and C-8b are β and α respectively (Figure 3a.22). On the basis of these correlations, the relative stereochemistry of compound **20** was confirmed. The absolute configuration of compound **20** was established on the basis of optical activity $[\alpha]^{25}_{D}$ -369^{o} (c 0.1, MeOH) which was in agreement with the reported value $[\alpha]^{25}_{D}$ -407^{o} (c 0.1 EtOH) [Coggon *et al*., **1965**]. From all the above spectral details and in comparison with the literature reports [Coggon *et al*., **1966**, Aisha *et al*., **2014**], the compound was confirmed as **(-)-hopeaphenol**. Biosynthetic pathway of (-)-hopeaphenol will be discussed in chapter 3B. Finally the structure and stereochemistry of the (-)-hopeaphenol was unequivocally established by single crystal X-ray analysis (Figure 3a.29). We carried out the crystallization using MeOH : DCM (60:40) solvent system. Brown colored crystals were

observed at room temperature. Crystal structure was resolved in Bruker APEX-II-CCD. The crystals had orthorhombic crystal system. The structure of the compound is shown below.

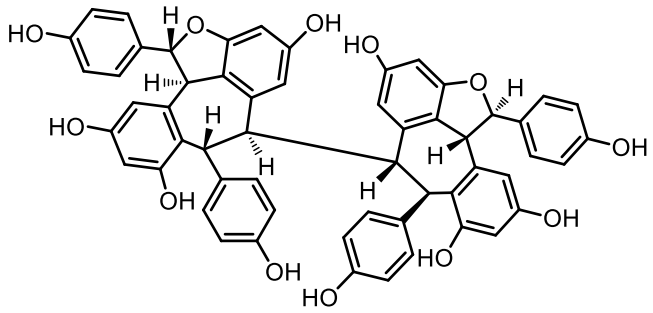

Figure 3a.21: (-)-Hopeaphenol **(20)**

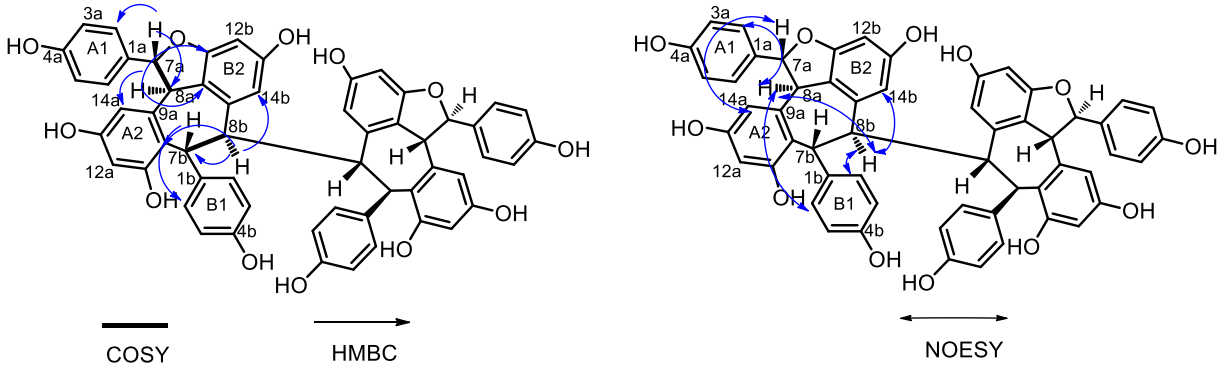

Figure 3a.22: Selected COSY, HMBC and NOESY correlations of (-)-hopeaphenol

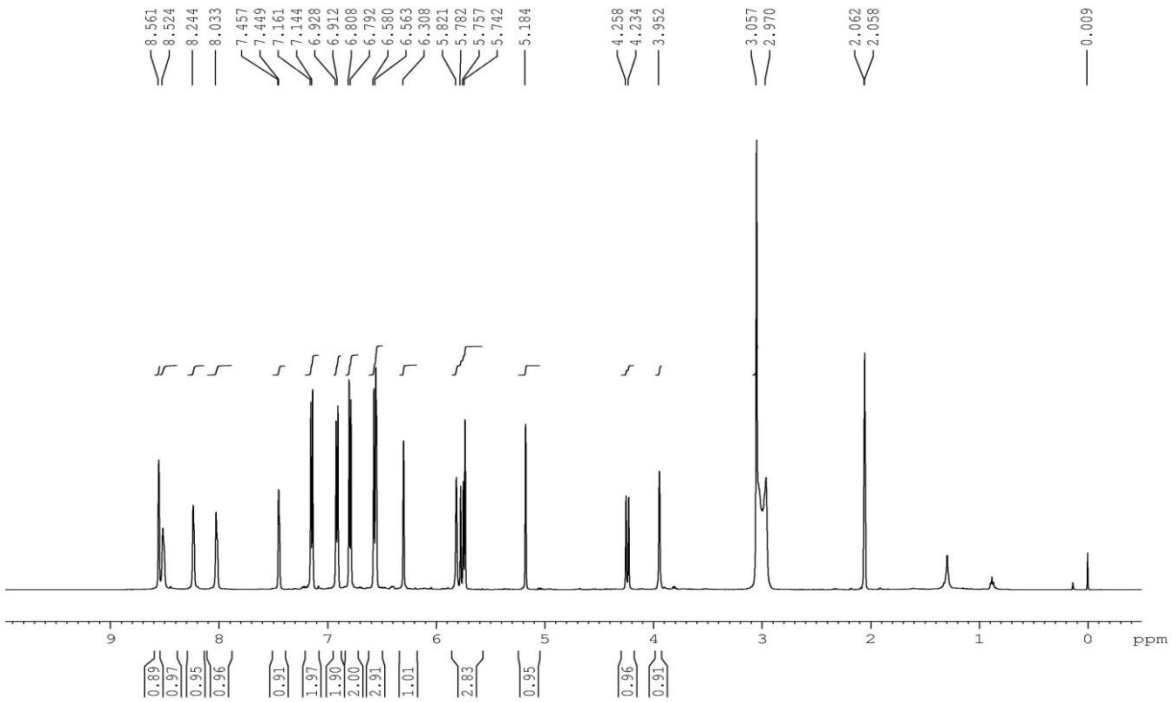

Figure 3a.23: ^{1}H NMR spectrum of (-)-hopeaphenol

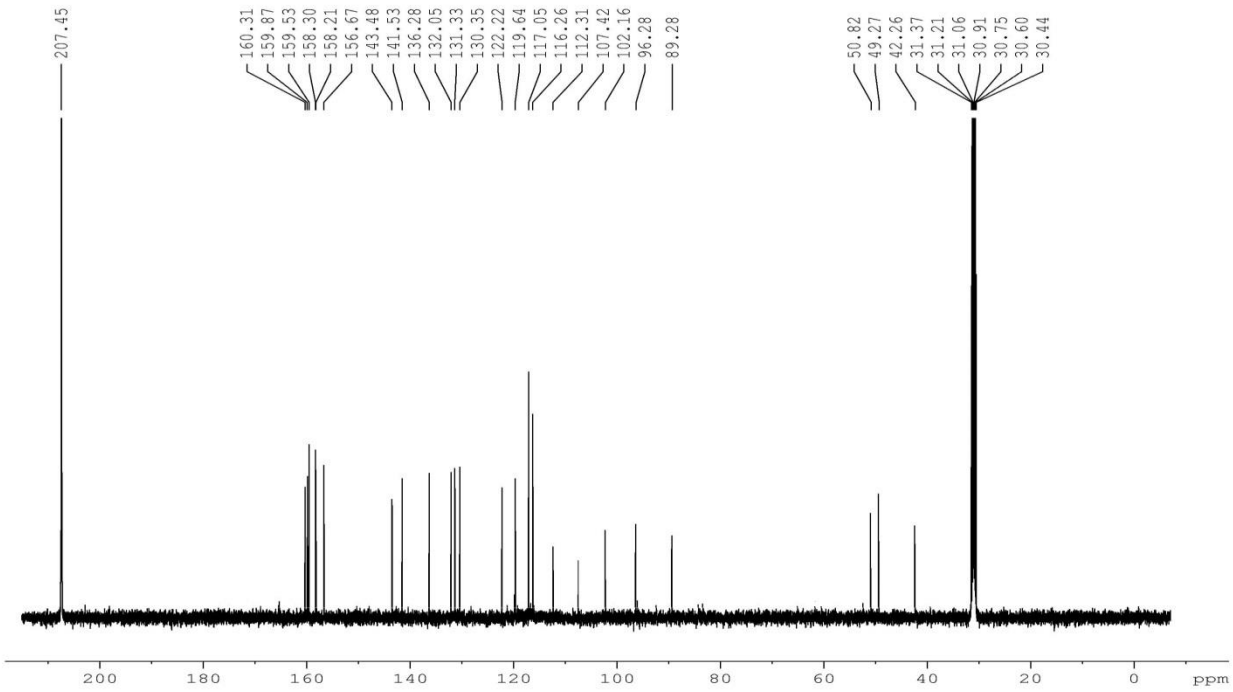

Figure 3a.24: ^{13}C NMR spectrum of (-)-hopeaphenol

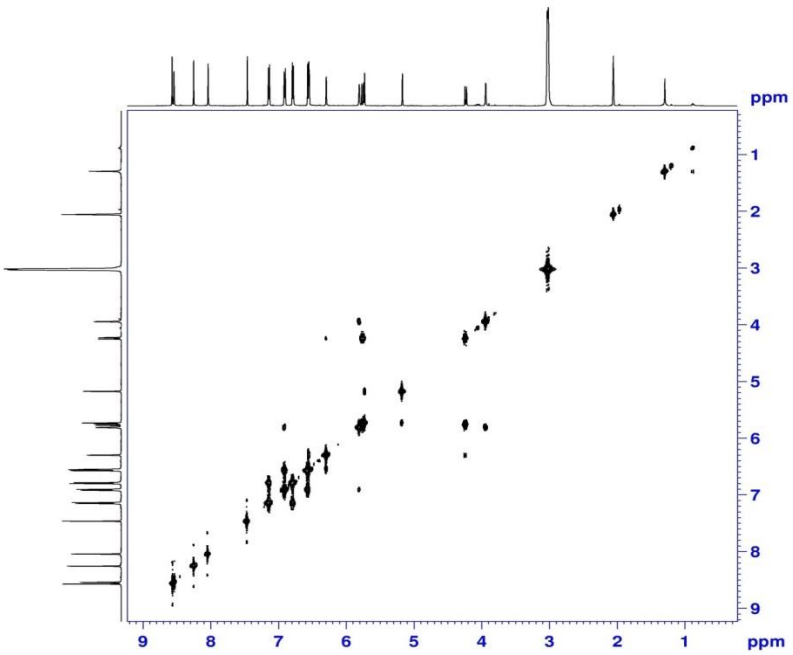

Figure 3a.25: ^{1}H-^{1}H COSY NMR spectrum of (-)-hopeaphenol

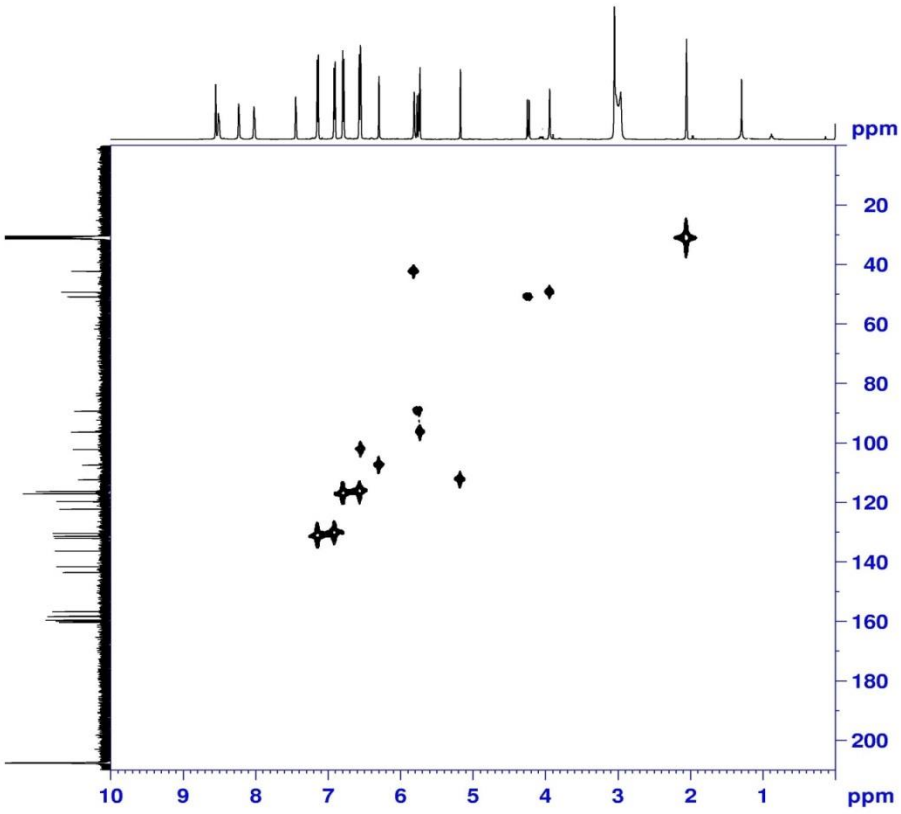

Figure 3a.26: HMQC spectrum of (-)-hopeaphenol

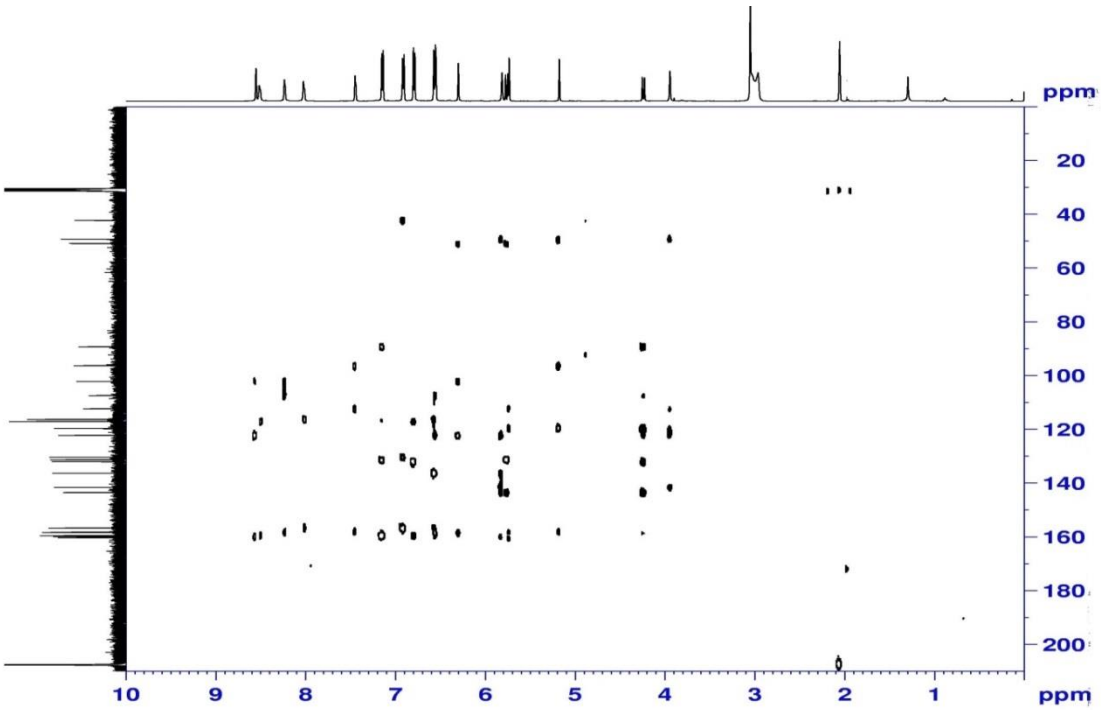

Figure 3a.27: HMBC spectrum of (-)-hopeaphenol

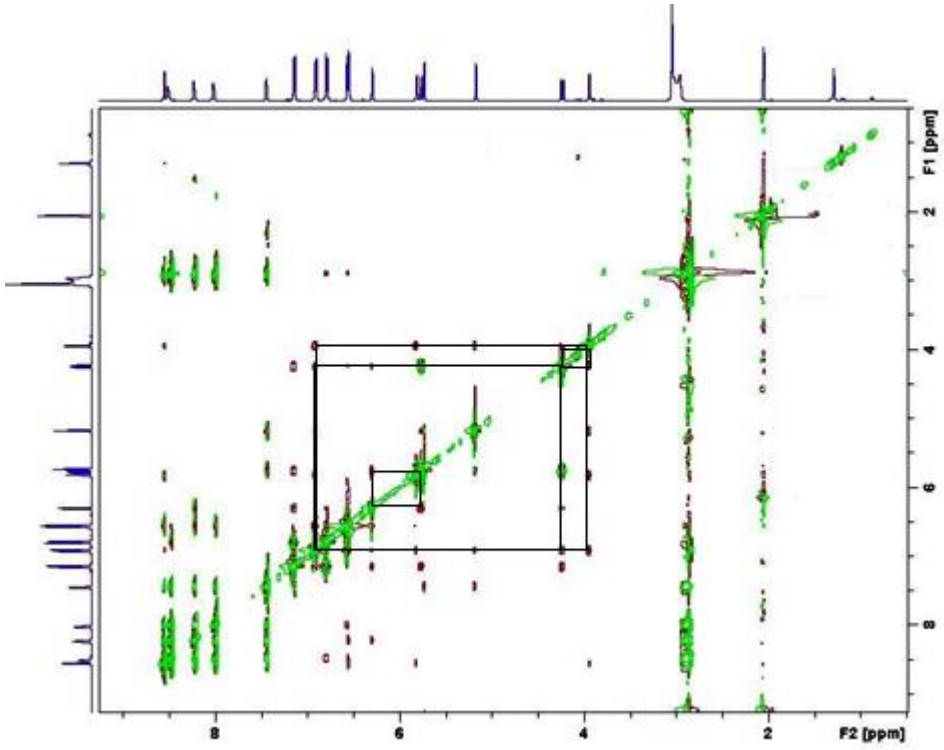

Figure 3a.28: ^{1}H-^{1}H NOESY spectrum of (-)-hopeaphenol

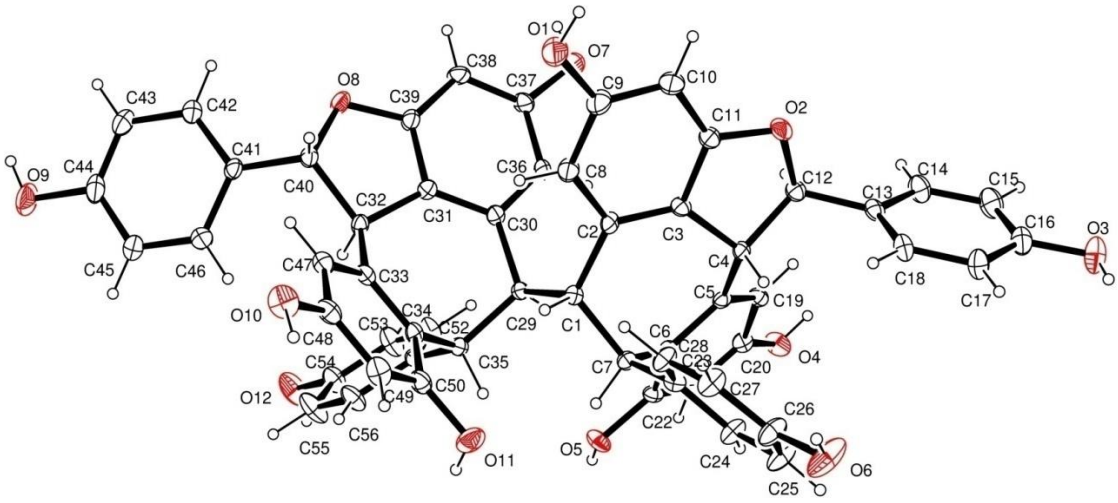

Figure 3a.29: Single crystal X-ray structure of (-)-hopeaphenol

Compound **21** (85 mg; 0.0085 %) was isolated as a brown solid from fractions Fr.A.31-Fr.A.35 obtained by repeated column chromatography with 80 % ethyl acetate in hexane. The compound was assigned the molecular formula $C_{56}H_{42}O_{12}$ following analysis of the HRESIMS at m/z 907.2745 $[M + H]^+$. In the IR spectrum of **21**, a strong absorption band at 3365 cm^{-1} indicated the presence of hydroxyl groups. The ^1H and ^{13}C NMR and in comparison with HRMS suggest that the isolated compound has four resveratrol units. The ^1H NMR spectrum in CD_3COCD_3 (Figure 3a.33) exhibited signals for ten phenolic hydroxyl groups (δ 8.47-7.46 ppm) which disappeared upon addition of D_2O. Considering the molecular formula, the remaining oxygen would contribute to the ether linkage. Other 2D spectroscopic details including ^{13}C NMR, ^1H–^1H COSY, HMQC and HMBC spectra (Figure 3a.34-Figure 3a.37) exhibited signals due to eight aromatic rings as follows; four *p*-hydroxyphenyl groups (A1, B1, C1 and D1), two 1,2,3,5-tetrasubstituted aromatic ring (A2 and C2), one 1,2,3,4,5-pentasubstituted aromatic ring (B2) and one 1,3,5-trisubstituted aromatic ring (D2). The presence of eight mutually coupled aliphatic protons (H-7a/H-8a, H-7b/H-8b, H-7c/H-8c, H-7d/H-8d) were also observed. The ^1H–^1H coupling pattern of the stereocenter protons (H-7a/H-8a and H-7d/H-8d) were characteristic of a dihydrobenzofuran rings, and the remaining (H-7b/H-8b) was similar to a partial structure of ampelopsin B, [Takaya *et al*., **2002**] which suggested that a heptadiene ring system. In addition to that there is an additional pentacyclic ring system including the two center (H-7c/H-8c). The planar

structure was confirmed by the following evidence. The correlations in the HMBC spectrum (Figure 3a.31) were observed between H-7a/C-(2a,6a), C-8a, C-9a, H-8a/C-9a, C-14a, C-10a, C-10b, H-7b/C-1b, C-(2b,6b), C-8b, C-10a, C-9b, C-9a, H-8b/C-7b, C-9b,C-14b, C-10a) and H-7c/C-(2c,6c), C-1c, C-8c, C-9c which indicated that presence of five aromatic ring and six methine units. The additional correlations from the HMBC spectra H-8c/C-7c, C-1c, C-14b, C-9c, C-10c, C-14c, H-8d/C-10c, C-9c, C-11c, C-9d, C-(10d,14d), indicated the presence of ε-viniferin moiety attached to the pentacyclic ring (C3).

To confirm the relative stereochemistry, NOESY experiments were conducted (Figure 3a.38). In there the clear cross peaks between H-7a/H-14a, H-8a/H-(2a, 6a), H-(2b,6b) were observed. These cross peaks substantiated that the relative stereochemistry of the methine protons at 7a and 8a are in *trans* orientation. The relationship between four methine protons H-7b, H-8b and H-7c, H-8c was determined as follows. NOE interactions between H-7b/H-8b, (2c, 6c) indicated that the ring B1 is oriented in *β*-configuration; alternatively H-7b is oriented in *α*-configuration. The *β*-configuration of B1 ring was further confirmed by the correlation of H-8a/H-(2b,6b). The significant NOEs observed between H-8b/ H-7b, and H-8b/H-(2c,6c), H-7c/H-(2b,6b), H-8c/H-(2c,6c), H-8c/H-10d, H-8c/H-14d also indicated that the relative configuration of methine protons H-8b, H-7c and H-8c are *α, β* and *α* respectively (Figure 3a.32). The *trans* stereochemistry of H-7c and H-8c were further confirmed the coupling constant with J value 11.5 Hz respectively. On the basis of these correlations, the relative stereochemistry of compound **21** was confirmed. The absolute configuration of compound **21** was established on the basis of optical activity $[\alpha]^{25}_{D}$ -28^{o} (c 0.1, MeOH) which was in agreement with the reported value $[\alpha]^{25}_{D}$ -29^{o} (c 0.1 MeOH) [Seo *et al*., **1999**]. From all the above spectral details and in comparison with the literature reports [Seo *et al*., **1999**], the compound was confirmed as **vaticaphenol A**. The structure of the compound is shown below. Biosynthetic pathway of vaticaphenol A starts from the 8−8′ oxidative dimerization of two molecules of ε-viniferin (Scheme 3a.2). This bis-para-quinone methide can undergo cyclization modes (C-10a-C-7b and C-14b-C-7c), delivering vaticaphenol A [Keylor *et al*., **2015**].

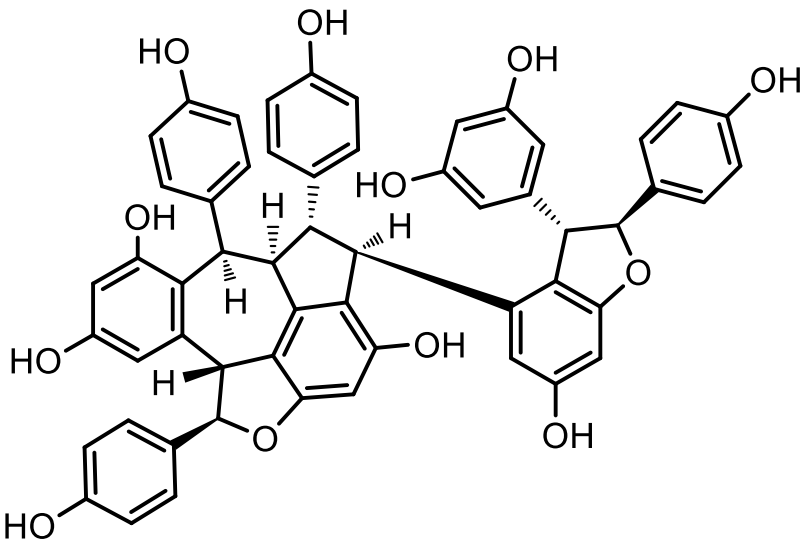

Figure 3a.30: Vaticaphenol A **(21)**

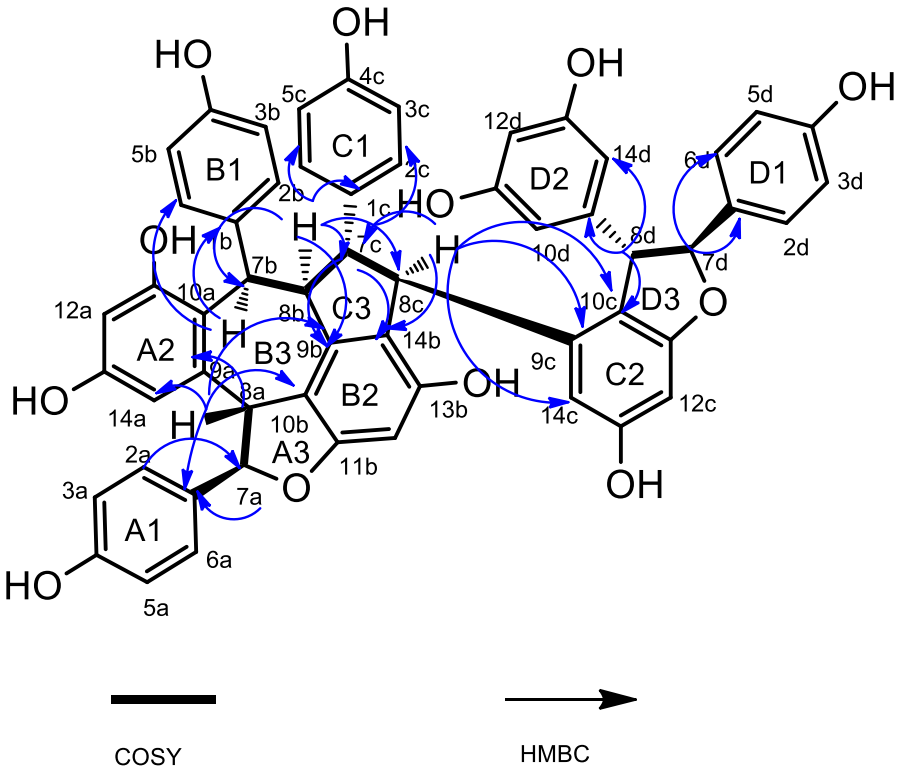

Figure 3a.31: Selected COSY and HMBC correlations of vaticaphenol A

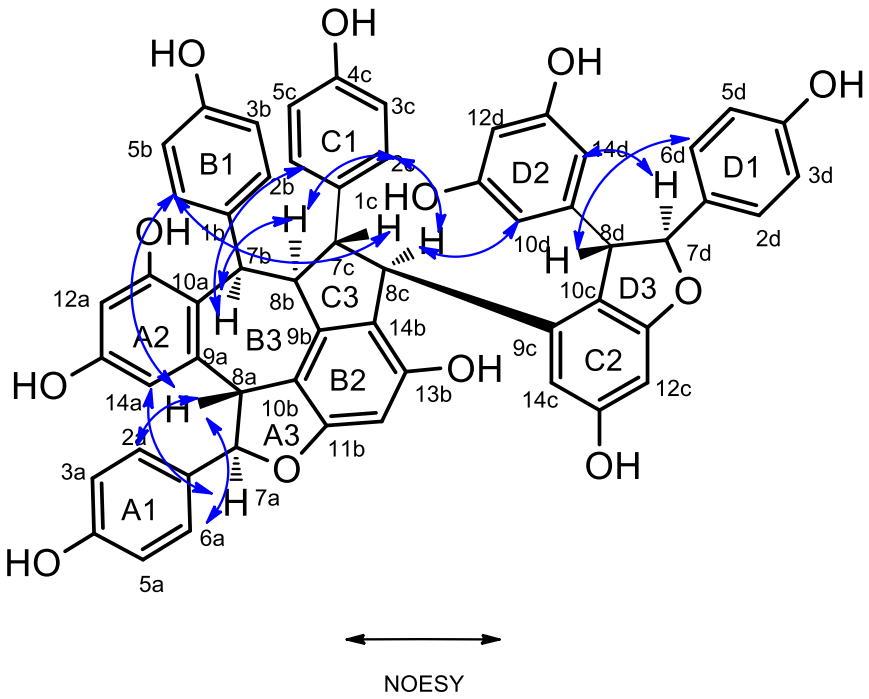

Figure 3a.32: Selected NOESY correlations of vaticaphenol A

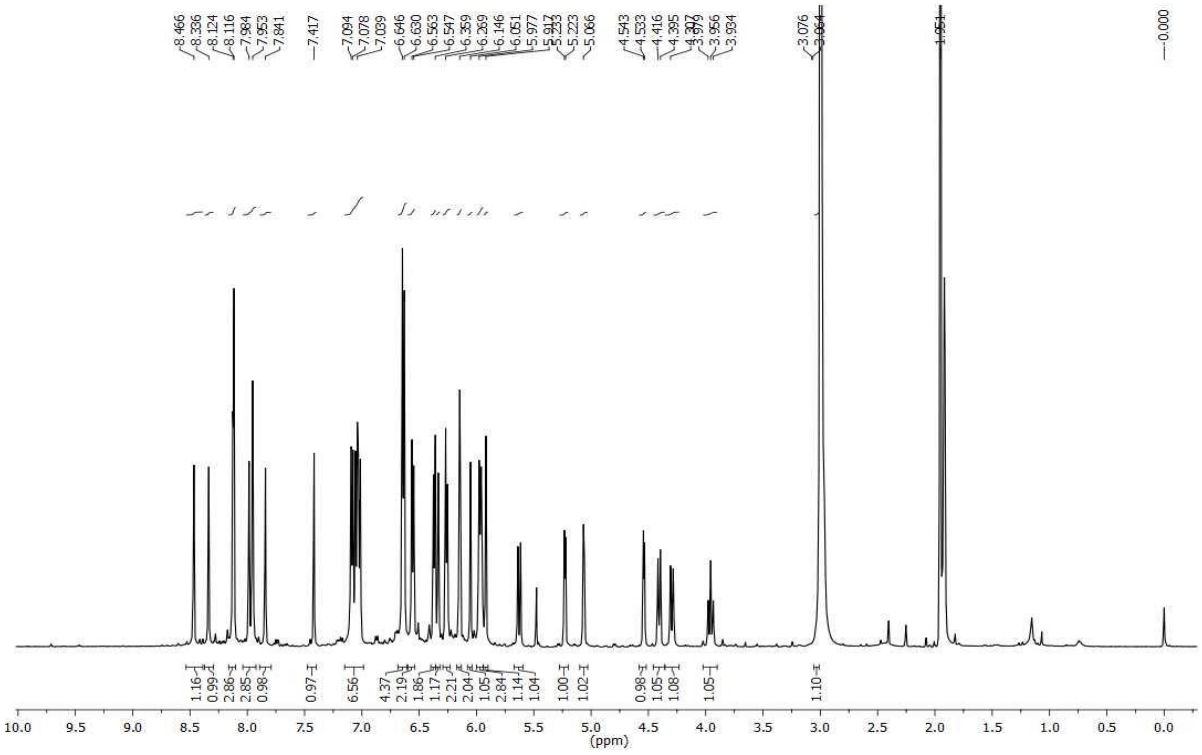

Figure 3a.33: ^{1}H NMR spectrum of vaticaphenol A

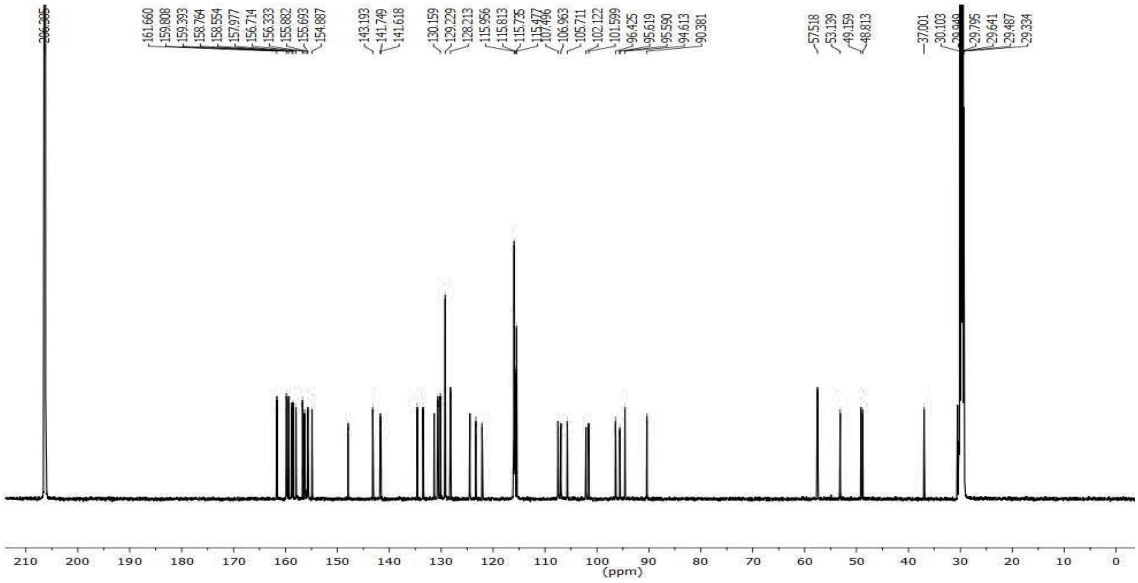

Figure 3a.34: ^{13}C NMR spectrum of vaticaphenol A

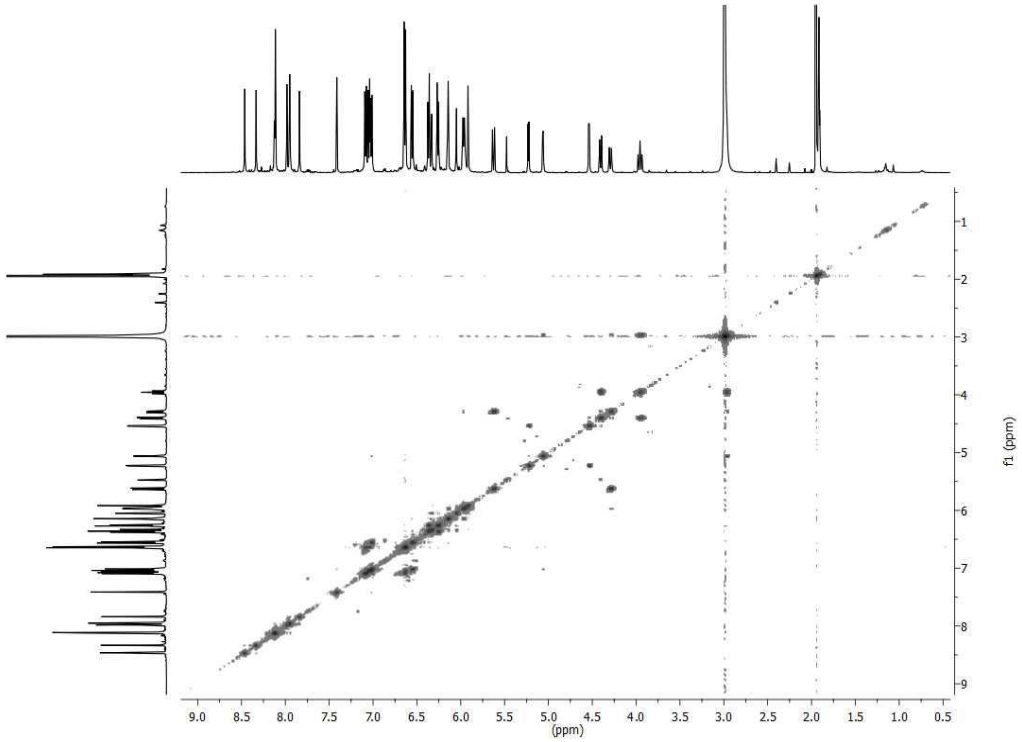

Figure 3a.35: ^{1}H-^{1}H COSY NMR spectrum of vaticaphenol A

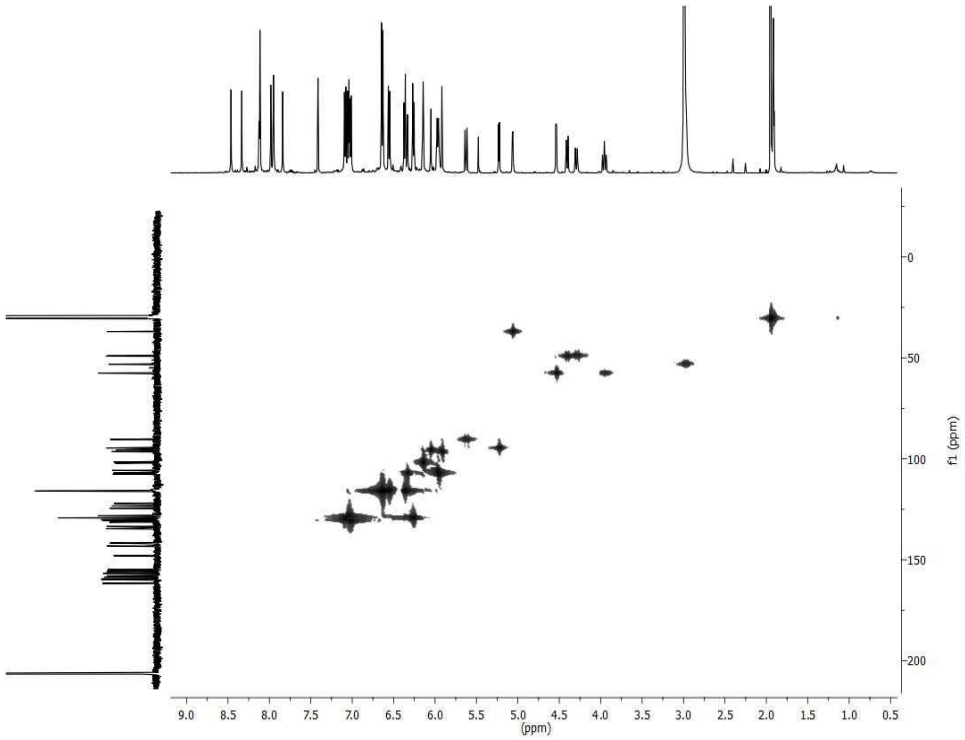

Figure 3a.36: HMQC spectrum of vaticaphenol A

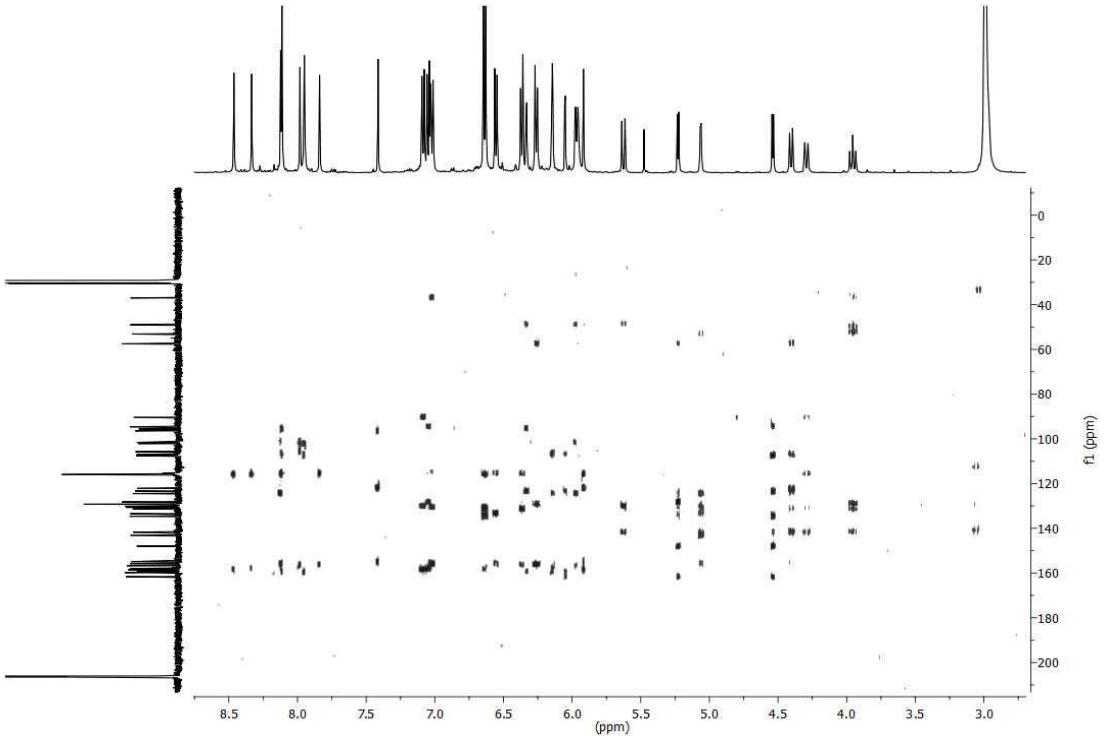

Figure 3a.37: HMBC spectrum of vaticaphenol A

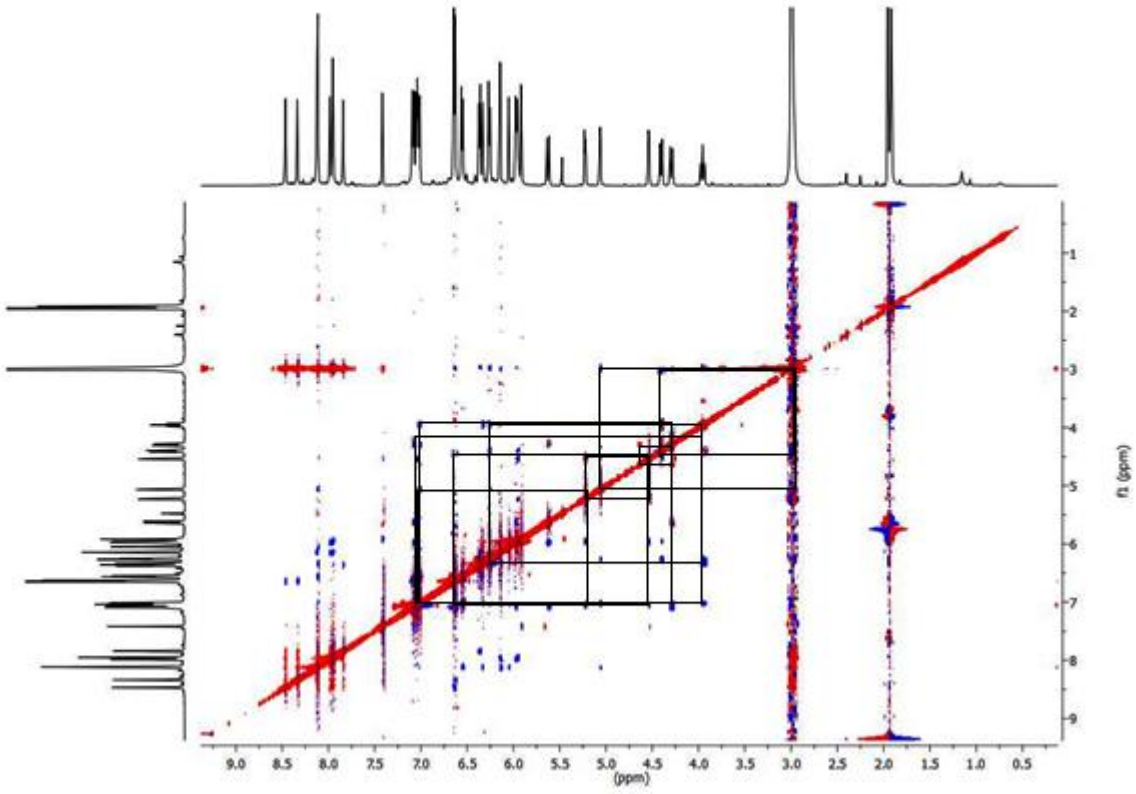

Figure 3a.38: ^{1}H-^{1}H NOESY spectrum of vaticaphenol A

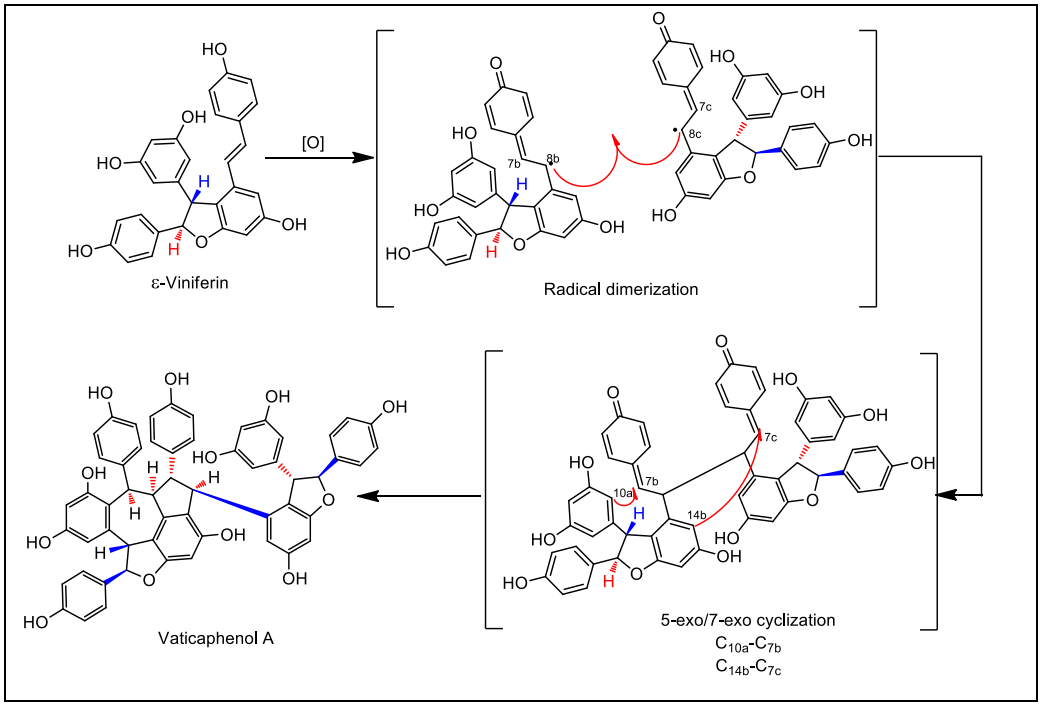

Scheme 3a.2: Biosynthetic pathway of vaticaphenol A

Fraction pool 37-57 (FrA.37- Fr.A.57), obtained by eluting the column with 100 % ethyl acetate and 5 % methanol in ethyl acetate yielded 4.5 g (0.45 %) of white crystalline solid which showed dark UV active spots in UV light labelled as compound **22**. In the IR spectrum of **22**, a strong absorption band at 3388 cm^{-1} indicated the presence of hydroxyl groups. In the ^{1}H NMR spectrum, (Figure 3a.40) signals at δ 9.83 and 8.50 ppm appeared as a broad singlet indicating the presence of two phenolic hydroxyl groups. The signals at δ 7.04 ppm integrating one proton could be attributed to the aromatic proton. The secondary hydroxyl protons resonated at δ 5.71 and 5.49 ppm with coupling constant *J* value 5 Hz. The signals at δ 5.03 ppm integrating one proton could be attributed to the stereocenter methine proton which is directly attached to the carbon bearing hydroxyl group. In ^{13}C NMR, (Figure 3a.41) the signal at δ 163.8 ppm could be attributed to the carbonyl carbon of the lactone ring. Signals at δ 151.4, 148.5 and 141.0 ppm are the diagnostic peaks for aromatic carbons attached to the hydroxyl group. Methoxy carbon resonated at δ 60.3 ppm. All other observed signals are in good agreement with the reported literature value [Seo *et al*., **1999**]. The mass spectra of the compound **22** gave molecular ion peak 329.0874 which is the $[M+H]^{+}$ and was identified as **bergenin**. Finally the structure and stereochemistry of the bergenin was unequivocally established by single crystal X-ray analysis (Figure 3a.42). We carried out the crystallization using methanol. Colorless crystals were observed at room temperature. Crystal structure was resolved in Bruker APEX-II-CCD. The structure of the compound is shown below (Figure 3a.39).

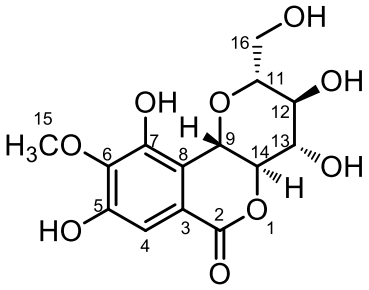

Figure 3a.39: Bergenin **(22)**

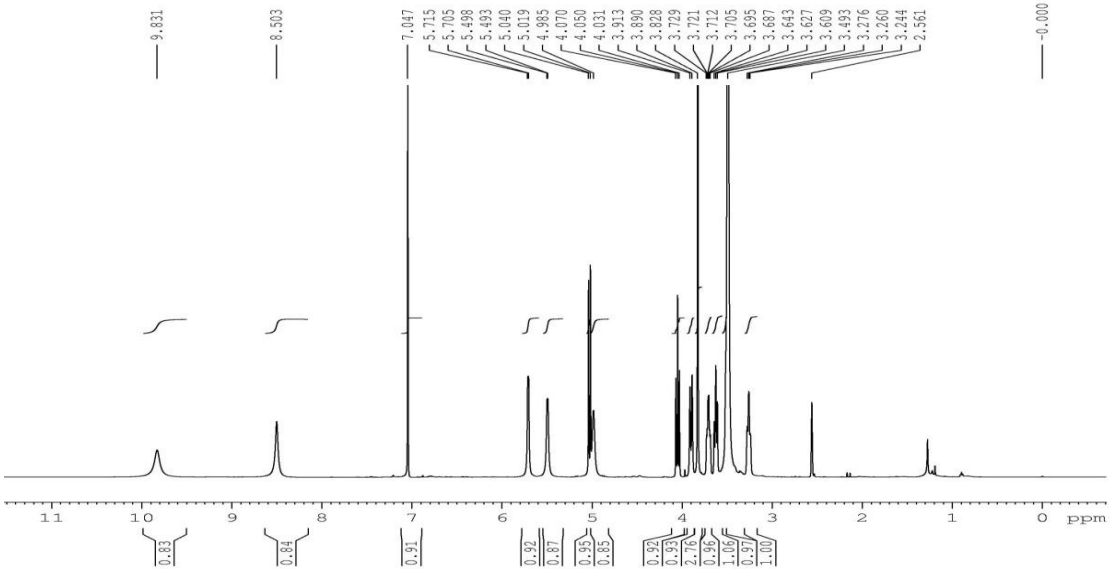

Figure 3a.40: ^{1}H NMR spectrum of bergenin

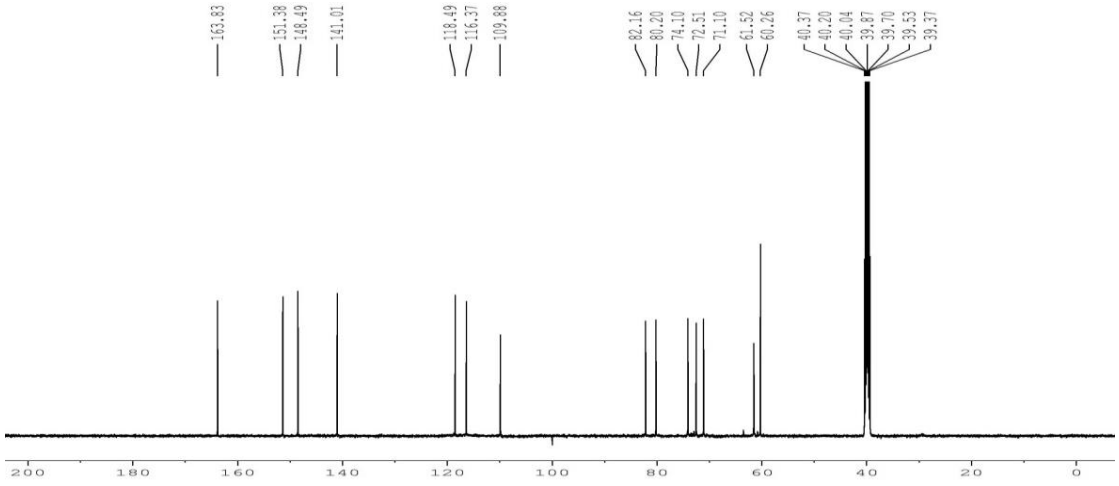

Figure 3a.41: ^{13}C NMR spectrum of bergenin

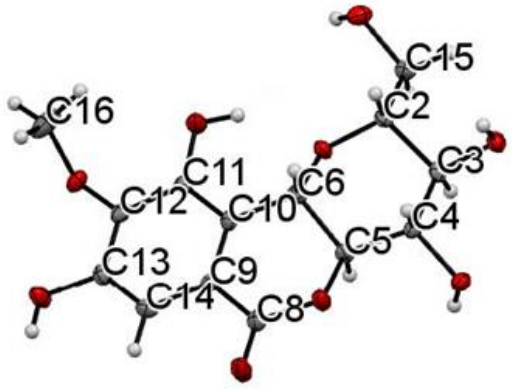

Figure 3a.42: Single crystal X-ray structure of bergenin

3a.9. Isolation of major constituents from *Vateria indica* seed

3a.9.1. Plant material and extraction

The seeds of *Vateria indica* (L.) was collected in June 2014 from Wayanad district of Kerala. The plant material was authenticated by the taxonomist of M. S. Swaminathan Research Foundation, Wayanad, Kerala (Voucher no. M.S.S.H.0763) and was deposited in the herbarium repository of the institute. This was thoroughly cleaned and dried in a hot air oven maintained at 50 ^{o}C for three days. It was then coarsely powdered. It weighed approximately 1kg. The powdered material was subjected to repeated extraction three times with acetone (2.5L x 48h) at room temperature. Thin layer chromatography indicated that the extraction was complete after six days. The total extract was then concentrated under reduced pressure using a Heidolph rotary evaporator. This yielded about 85 g of crude acetone extract (A). Further the extraction was continued with ethanol yielded 25 g of ethanol extract (E).
After studying the TLC, 85 g of the acetone extract was subjected to column chromatographic purification using silica gel (100-200 mesh). Column elution was initiated using 100 % hexane and increase in polarity was made by increasing the amount of ethyl acetate. Final elution was carried out using 10 % methanol in ethyl acetate. A total of 105 fractions of approximately 200 mL each were collected. According to the similarities in TLC, they were pooled into 35 major fraction pools (Fr.A.1- Fr.A. 35).

TLC of fractions 1-10 (Fr.A.1- Fr.A.10) obtained by eluting the column with 10 % ethyl acetate in hexane showed the presence of UV inactive spots which was identified by spraying McGill solution, yielded 11g of mixture of triglycerides. In ^{1}H NMR two signals at 4.30 and 4.14 ppm each integrating for two proton as a doublet of doublet with coupling constant 12 and 4 Hz respectively, indicated the presence of ester methylene protons. The ester methine proton appeared as a multiplet at δ 5.27-5.25 ppm and the olefinic protons from the fatty acid resonated as a doublet of doublet with coupling constant 8 and 5.5 Hz represented the *cis* confirmation. Peaks at δ 173.2-172.7 ppm in the ^{13}C spectrum confirmed the presence of ester carbonyl carbon. Signals at δ 129.9 and 129.7 ppm could be attributed to the olefinic carbons. Finally, the structures were confirmed using GC-MS analysis and will be discussed in the following section.

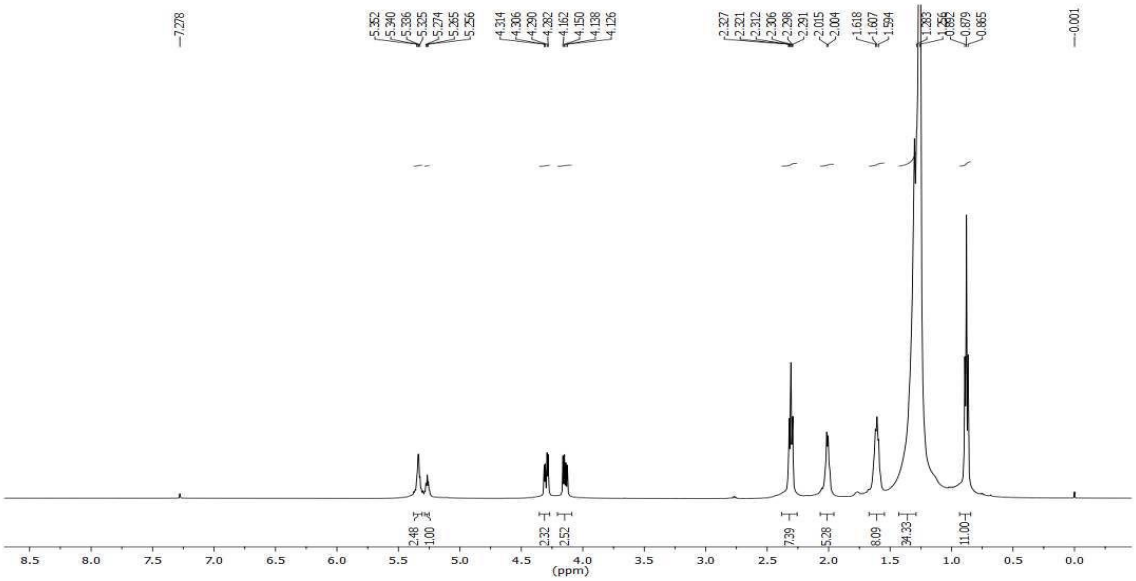

Figure 3a.43: ^{1}H NMR spectrum of triglycerides

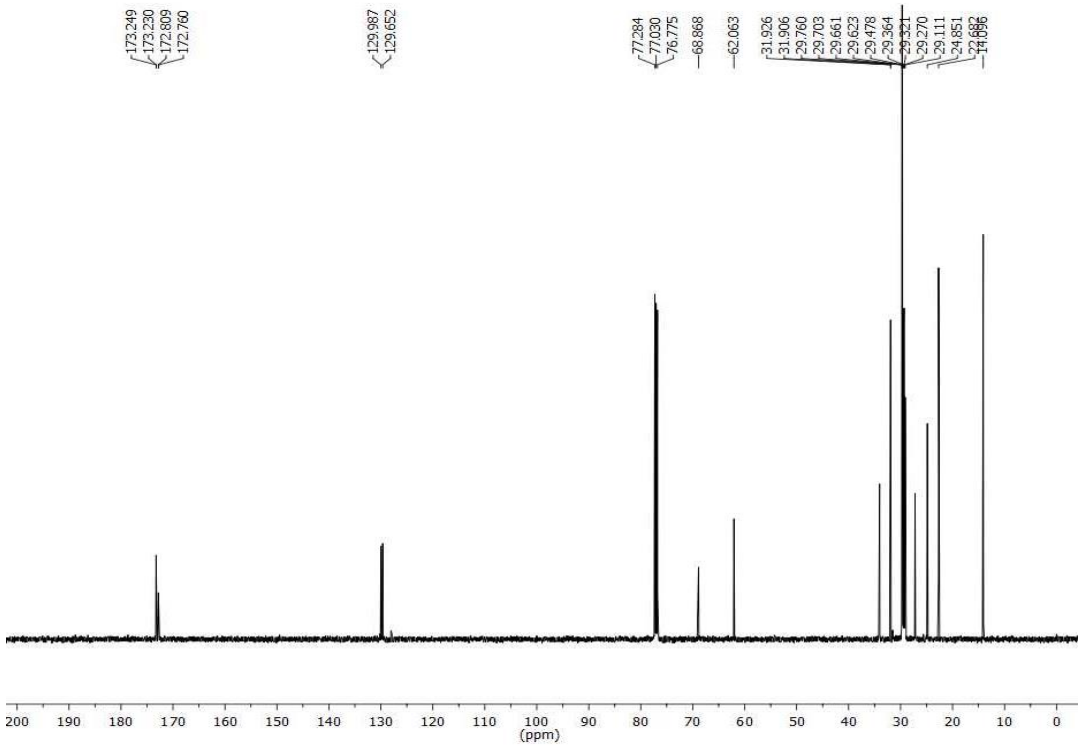

Figure 3a.44: ^{13}C NMR spectrum of triglycerides

Fraction pool 11-15 (FrA.11- Fr.A.15), obtained by eluting the column with 30 % ethyl acetate in hexane yielded 30 mg of yellow amorphous solid which showed blue fluorescence in UV light. IR, ^{1}H, ^{13}C, HMQC, HMBC and HRESIMS spectrum of the compound **23** is similar to that of compound **19** namely **(-)-ε-viniferin** and was previously isolated from the stem bark. Fraction pool 17-20 was subjected to column chromatography silica gel using 70

% ethyl acetate in hexane afforded compound **24** (7.4 g) which was confirmed to be **(-)-hopeaphenol**. The structure and stereochemistry was further confirmed by comparison with previously isolated compound **20**. Fraction pool 22 (510 mg) was submitted to repeated column chromatography on silica gel (mesh 230-400) using 80 % ethyl acetate in hexane to yield another resveratrol oligomers namely **vaticaphenol A 25** (200 mg). Finally the major compound present in the *V. indica* seed namely **bergenin 26** (9 g) was isolated from the fraction pool 23-30 (FrA.23- Fr.A.30), by eluting 100 % ethyl acetate and 5 % methanol in ethyl acetate, and it was further recrystallized in methanol. Further evidence was made by comparing the TLC with that of compound **22** isolated earlier.

3a.10. Separation and identification of fatty acids from *V. indica* seed by GC-MS analysis

3a.10.1. Hydrolysis of the triglycerides from *V. indica* seed hexane extract

The triglyceride (1g) from *V. indica* seed on hydrolysis using methanolic potassium hydroxide followed by acidification yielded mixture of long chain fatty acids like Palmitic acid, Linoleic acid, Stearic acid etc.

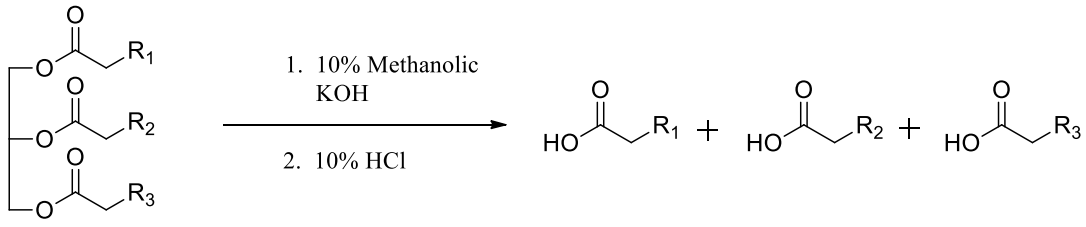

R_1, R_2, R_3 = Palmitic acid, Linoleic acid, Oleic acid, Stearic acid, Arachidic acid, Heneicosanoate acid etc.

Scheme 3a.3: Saponification of triglycerides

3a.10.2. GCMS analysis

Gas chromatographic analysis was performed using GCMS-TQ8030 SHIMADZU instrument. 1µL of sample was injected on to a GC equipped with a MS and a medium polar capillary column Rxi-5Sil MS, (30m X 0.25mm I. D., 0.25µm), the oven program had an initial temperature of 60^{o}C for 2 min, increased to 200^{o}C for 2min at the rate of 5^{o}C /min followed by the temperature was increased to 220^{o}C for 1min at the rate of 3^{0}C /min. Finally temperature was increased to 250 at the rate of 6^{o}C /min for 7min.Total run time was 50min.

The detector temperature and injection temperature was 250°C, helium is used the carrier gas with purity 99.999 % at a flow rate of 1mL/min. The samples were injected in the splitless mode. The ion energy used for the electron impact ionization (EI) mode was 70eV. The mass range scanned was 100 - 1000 *m/z*.

The essential chemical constituents were identified by matching mass spectra with spectra of reference compounds in mass spectral library of NIST and WILEY. The relative amounts of individual components were expressed as percentage peak areas relative to total peak area. The methyl esters of fatty acid profile in GCMS as shown in (Figure 3a.45). The major fatty acids present were Palmitic acid **27** (12.38%) (m/z = 270.45), Linoleic acid **28** (3.29 %) (m/z = 294.52), Oleic acid **29** (32.77 %) (m/z = 296.49), Stearic acid **30** (44.89 %) (m/z = 298.50), Arachidic acid **31** (3.46%) (m/z = 326.55), Heneicosanoate acid **32** (1.11 %) (m/z = 340.58) (Figure 3a.46).

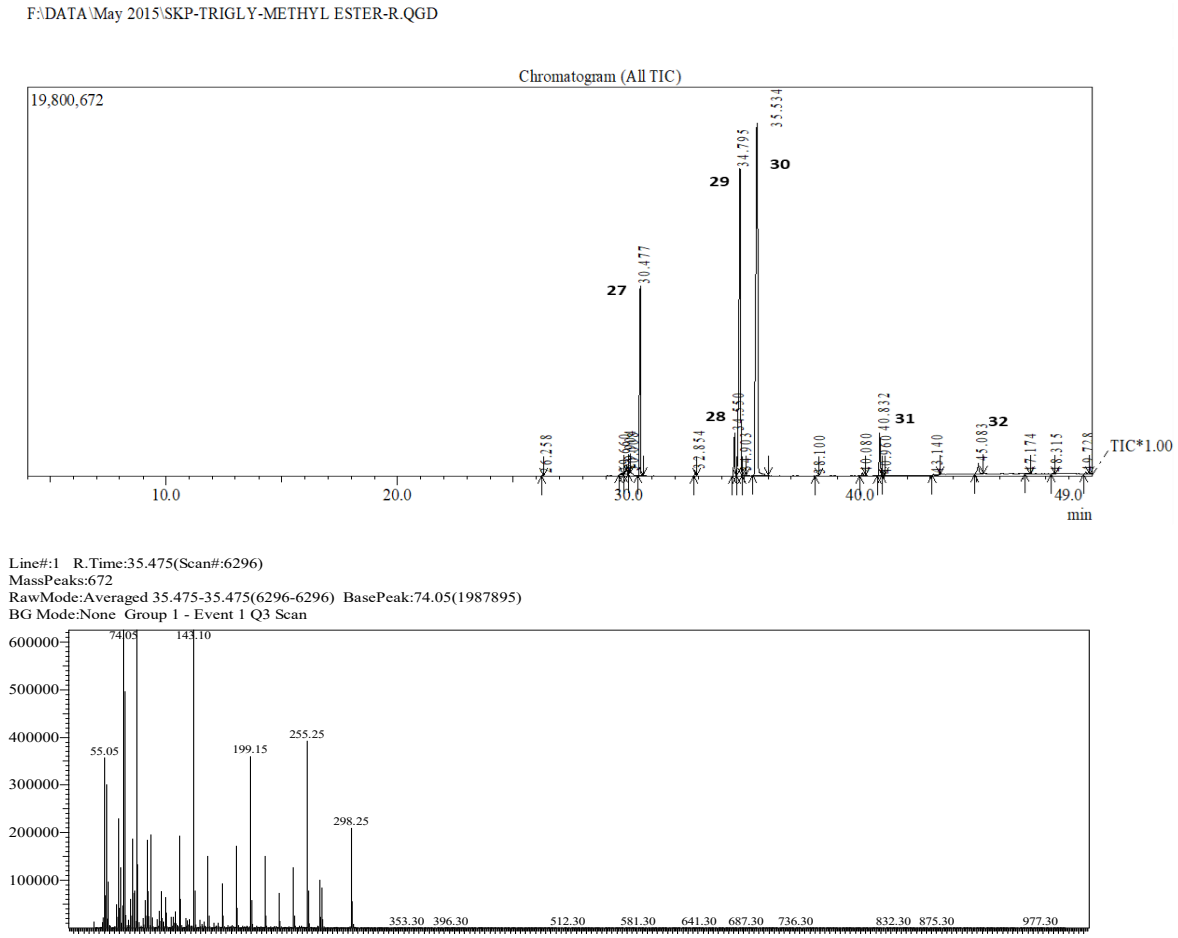

Figure 3a.45: GCMS spectrum of triglycerides

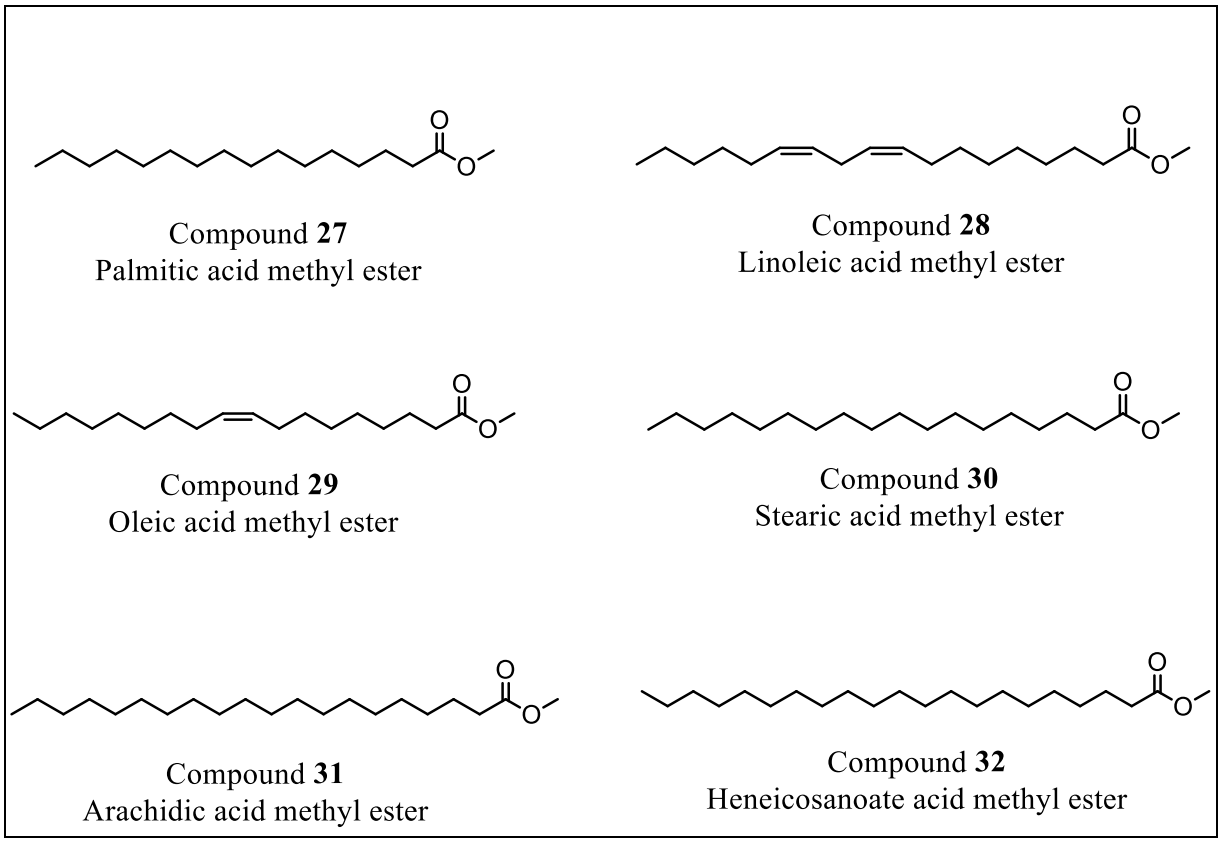

Figure 3a.46: Structure of fatty acids **(27-32)**

3a.11. Conclusion

In this chapter, the isolation of chemical constituents from various parts of *V. indica* has been carried out. The different extracts prepared from *V. indica* stem bark were subjected to detailed antioxidant and antidiabetic studies. Eight compounds have been isolated from the stem bark of *V. indica viz*., *β*-amyrin, *β*-amyrin acetate, sitoindoside I, *E*-resveratrol, (-)-ε-viniferin, (-)-hopeaphenol, vaticaphenol A and bergenin. Similarly, *V. indica* seeds were subjected to phytochemical investigations. Four major compounds along with fatty acids *viz*., (-)-ε-viniferin, (-)-hopeaphenol, vaticaphenol A and bergenin in high yield were isolated. From best of our knowledge, *β*-amyrin, *β*-amyrin acetate and sitoindoside I from *V. indica* stem bark were reported for the first time. This is the first report of resveratrol oligomers from the seeds of *V. indica.* The detailed antidiabetic screening of resveratrol oligomers will be discussed in the coming chapter.

3a.12. Experimental Session

General experimental details and procedure for antioxidant and antidiabetic activity studies are given in Chapter 2.

3a.12.1. Extraction of *V. indica* stem bark

The bark of *Vateria indica* was collected from Wayanad district, Kerala. This was thoroughly cleaned and dried in drier maintained at 50^{o} C and powdered. The powdered rhizome (1 kg) was subjected to repeated extraction using hexane, acetone ethanol and water (2.5 L X 48 h) at room temperature. After extraction, the solvent was removed under reduced pressure using Büchi rotary evaporator. The acetone extract (56 g) was then subjected to column chromatographic separation.

3a.12.2. Chromatographic separation of acetone extract of *V. indica* stem bark

The acetone extract (56 g) of the stem bark of *V. indica* dissolved in minimum quantity of acetone and was adsorbed in silica gel (100-200) loaded on the top of silica gel column filled with slurry of 100-200 mesh silica gel in hexane. The column was eluted successively with gradient mixtures of hexane and ethyl acetate of increasing polarities and finally with 10 % methanol in ethyl acetate. A total of 200 fractions of approximately 200 mL each were collected. According to the similarity in TLC, they were pooled into 62 major fraction pools (FrA.1- FrA. 62). Pictorial representation of the procedure for the isolation of the compound is shown in Figure 3a.47.

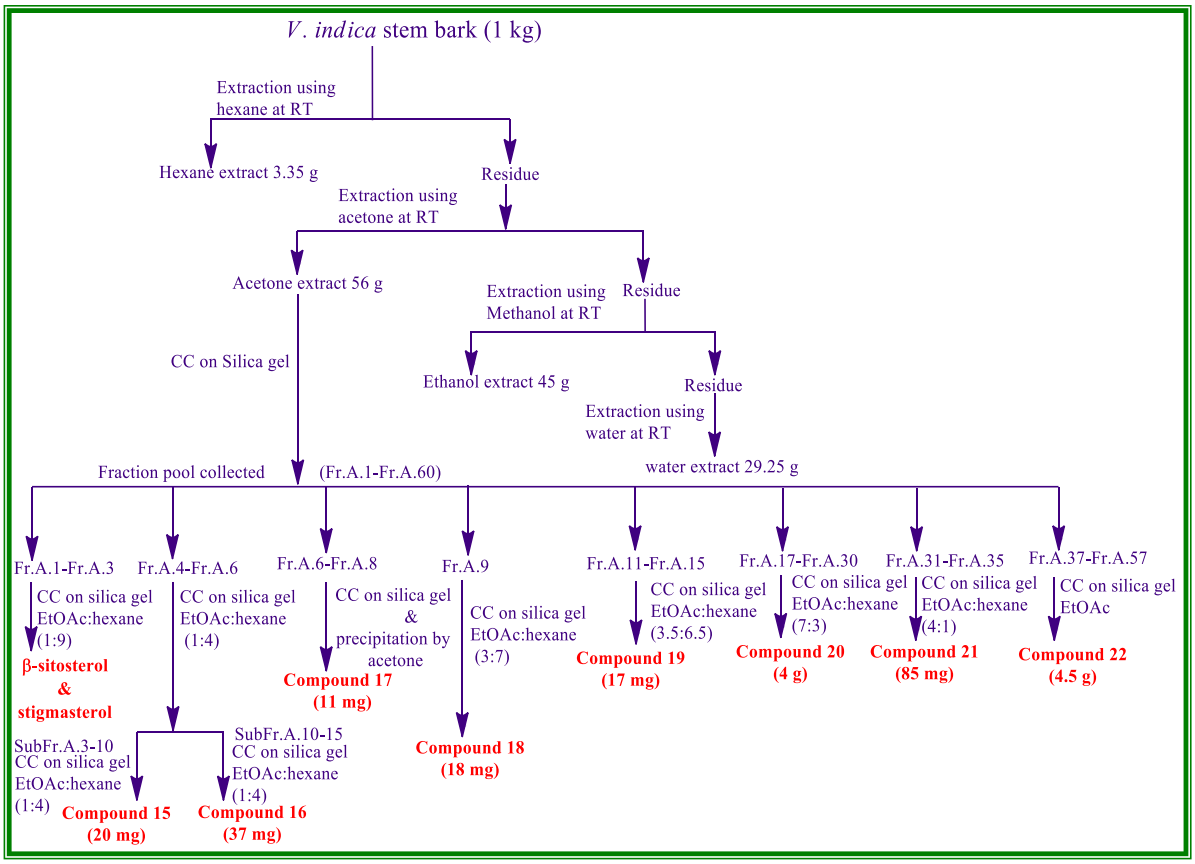

Figure 3a.47: Pictorial representation of isolation of compounds from *V.indica* stem bark

3a.12.3. Isolation of compound 15

The isolation procedure of compound **15** is represented in Figure 3a.47. Compound **15** (20 mg) was obtained as a colourless crystal, on eluting the column with 20 % ethyl acetate in hexane. IR, ^{1}H NMR, ^{13}C NMR and mass spectral studies of this compound and on comparison with literature values [Okoye *et al.,* **2014**], confirmed as *β*-amyrin.

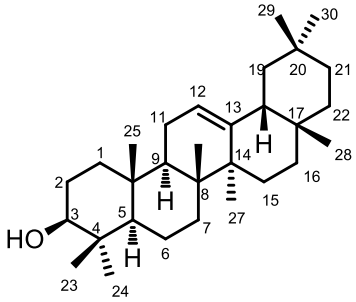

Melting point : 197-198 ^{o}C

FT-IR (NaCl) υ_{max} : 3408, 2935, 2863, 1645, 1459, 1374, 1316, 1257, 1190,

1099, 1054, 1024 cm^{-1}.

^{1}H NMR (500 MHz, $CDCl_3$)	:	δ 5.18 (t, *J* = 3.5 Hz, 1H, H-12), 3.24-3.21 (m, 1H, H-3), [2.17-1.99 (m, 3H), 1.99-1.97 (m, 1H), 1.96-1.93 (m, 1H), 1.88-1.86 (m, 13H), 1.69-1.64 (m, 3H), 1.61-1.58 (m, 3H), 1.57-1.56 (m, 3H), 1.56-1.54 (m, 1H), 1.42-1.40 (m, 3H), 1.35-1.33 (m, 1H), 1.32-1.25 (m, 1H) (aliphatic hydrogens)], 1.13 (s, 3H, Me), 1.00 (s, 3H, Me), 0.99 (s, 3H, Me), 0.97 (s, 3H, Me), 0.94 (s, 3H, Me), 0.87 (s, 3H, Me), 0.83 (s, 3H, Me), 0.79 (s, 3H, Me) ppm.
^{13}C NMR (125 MHz, $CDCl_3$)	:	δ 145.2 (C-13), 121.7 (C-12), 79.1 (C-3), [55.2, 47.6, 47.2, 46.8, 41.7, 39.8, 38.8, 38.6, 37.1 (aliphatic carbons)], 36.9, 34.7, 36.9, 34.7, 33.3 (C-Me), 32.6, 31.1, 30.9 (C-CH_2), 29.7 (C-CH_2), 28.4 (C-Me), 28.1(C-Me), 27.2 (C-Me), 26.9 (C-CH_2), 26.2 (C-CH_2), 26.0 (C-Me), 23.7 (C-Me), 23.5 (C-Me), 18.4 (C-CH_2), 16.8 (C-CH_2), 15.6 (C-Me), 15.5 (C-Me) ppm.
HR-ESIMS *m/z*	:	427.3941[$(M+H)^+$ (calcd for $C_{30}H_{51}O$, 427.3939)

3a.12.4. Isolation of compound 16

The isolation procedure of compound **16** is represented in Figure 3a.47. Compound **16** (37 mg) was obtained as a colourless crystal, on eluting the column with 20 % ethyl acetate in hexane. IR, ^{1}H NMR, ^{13}C NMR and mass spectral studies of this compound and on comparison with literature values [Okoye *et al.,* **2014**], confirmed as *β*-amyrin acetate.

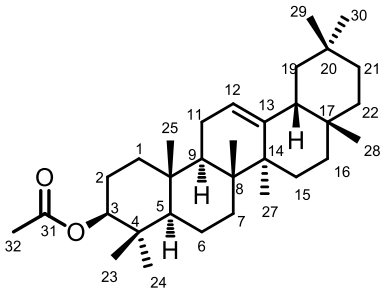

Melting point	:	240-242 ^{o}C
FT-IR (NaCl) υ_{max}	:	3411, 2924, 2858, 1739, 1582, 1506, 1440, 1379, 1143 cm^{-1}.
^{1}H NMR (500 MHz, CD_3COCD_3)	:	δ 5.26 (t, *J* = 3.5 Hz, 1H, H-12), 3.63-3.58 (m, 1H, H-3), 2.07- (s, 3H, H-32), [2.06-2.05 (m, 5H), 1.93-1.69 (m, 4H), 1.68-1.63 (m, 3H), 1.57-1.53 (m, 5H), 1.44-1.23 (m, 5H), (aliphatic hydrogens)], 1.02 (s, 3H, Me), 1.00 (s, 3H, Me), 0.97 (s, 3H, Me), 0.95 (s, 3H, Me), 0.92(s, 3H, Me), 0.90 (s, 3H, Me), 0.82 (s, 3H, Me), 0.81 (s, 3H, Me) ppm.
^{13}C NMR (125 MHz, CD_3COCD_3)	:	δ 178.9 (C-31), 145.0 (C-13), 122.9 (C-12), 83.9 (C-3), [60.6, 56.2, 48.5, 47.6, 46.8, 46.7, 42.6, 42.2, 40.2, 39.8, 38.9, 34.4, 33.6, 33.4, 31.3, 30.3, 30.2, 30.0, 29.9, 29.7, 29.6, 29.2, 28.4, 26.3, 24.2, 23.9, 23.7, 20.8, 19.1, 17.6, 17.4, 14.5 (Other aliphatic carbons)] ppm.
HR-ESIMS *m/z*	:	469.4039 $[M+H]^{+}$ (calcd for $C_{32}H_{53}O_2$, 469.4045)

3a.12.5. Isolation of compound 17

Fraction pool 6-8 (FrA.6-8) which on precipitation by using acetone, a white pasty mass of Compound **17** (11 mg) was yielded The compound was successfully characterized as **sitoindoside I** based on the spectral data obtained and in comparison with the literature reports literature [Ren *et al.,* **2015**].

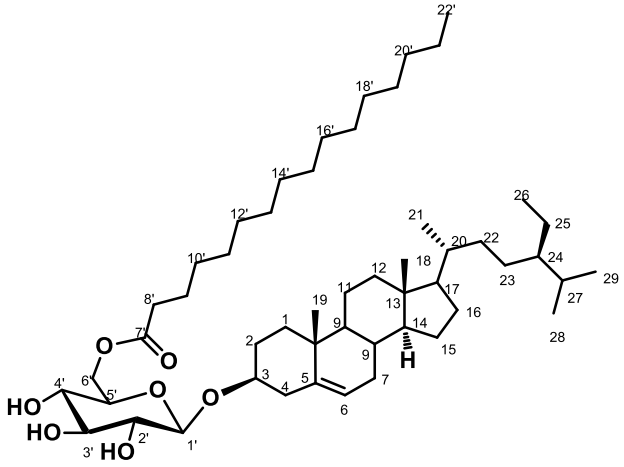

FT-IR (NaCl) υ_{max}	:	3400, 2900, 2935, 2863, 1735, 1645, 1459, 1374, 1316, 1257, 1190, 1099, 1054, 1024, 958, 802 cm^{-1}.
^1H NMR (500 MHz, $CDCl_3$)	:	δ 5.36 (s, 1H, H-6), 4.46 (dd, J_1 = 12.0, J_2 = 5.0 Hz, 1H, H-6'), 4.38 (d, J = 8 Hz, 1H, H-1'), 4.27 (d, J = 11.5 Hz, 1H, H-6'), 3.59 – 3.55 (m, 2H, H-2', H-3'), 3.45 (bs, 1H, -OH), 3.37 (dd, J_1= 18, J_2 = 9 Hz, 2H, H-4', H-5'), 3.26 (bs, 1H, -OH), [2.77 (t, J = 6.5 Hz, 1H), 2.36-2.33 (m, 3H), 2.27 (t, J = 11.5 Hz, 1H), 2.04 – 1.96 (m, 4H), 1.87-1.84 (m, 2H), 1.66-1.60(m, 9H), 1.49 – 1.47 (m, 5H), 1.29-1.26 (m, 9H), 1.22-1.57 (m, 4H), 1.11-1.09 (m, 4H), 1.00 (s, 5H), 0.93-0.88 (m, 7H), 0.86-0.81 (m, 10H), 0.68 (s, 3H), (Other aliphatic hydrogens)] ppm.
^{13}C NMR (125 MHz, $CDCl_3$)	:	δ 174.7 (C-7'), 140.3 (C-5), 122.2 (C-6), 101.2 (C-1'), 79.6 (C-3), [76.0, 73.9, 73.6, 70.1 (C-2',C-3',C-4',C-5')], 63.2 (C-6'), [56.8, 56.1, 50.2, 45.9, 42.3, 39.8, 38.9, 37.3, 36.8, 36.2, 34.2, 33.9, 31.9, 31.9, 31.5, 29.7, 29.7, 29.6, 29.4, 29.3, 29.2, 28.2, 27.2, 26.1, 24.9, 24.3, 23.1, 22.7, 21.1, 19.8, 19.4, 19.0, 18.8, 14.1, 11.9, 11.9, (Other aliphatic carbons)] ppm.
HR-ESIMS *m/z*	:	837.2183 $[M+Na]^+$ (calcd for $C_{51}H_{90}NaO_7$, 837.2158)

3a.12.6. Isolation of compound 18

Compound **18** (18 mg) was obtained as a light brown colour solid, on eluting the column with 30 % ethyl acetate in hexane. IR, ^1H NMR, ^{13}C NMR and mass spectral studies of this compound and on comparison with compound **1**, previously isolated from *A. indica* rhizome [Chapter 2], confirmed it to be *E*-resveratrol.

3a.12.7. Isolation of compound 19

Compound **19** (17 mg) was obtained as a yellowish amorphous solid, on eluting the column with 35 % ethyl acetate in hexane. IR, ^1H NMR, ^{13}C NMR and mass spectral studies of this compound and on comparison with compound **2**, previously isolated from *A. indica* rhizome [Chapter 2], confirmed it to be resveratrol dimer viniferin. The absolute

configuration of compound 19 was established on the basis of optical activity $[\alpha]^{25}_{D}$ -31.5 (c, 0.1 MeOH); Finally, compound 19 was identified as (-)-ε-viniferin.

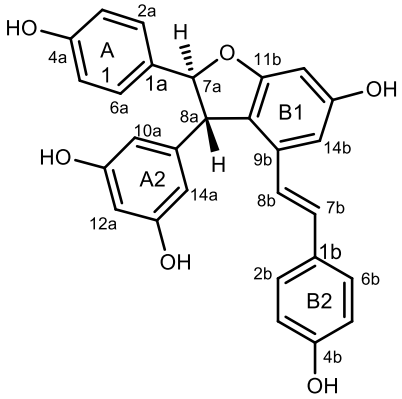

$[\alpha]^{25}_{D}$	:	-31.5° (c 0.1, MeOH)
FT-IR (NaCl) υ_{max}	:	3388, 2961, 2933, 2872, 1721, 1603, 1513, 1448, 1373, 1225, 1165, 1128, 1074, 1001, 966 cm^{-1}.
^{1}H NMR (500 MHz, CD_3COCD_3)	:	δ 8.58 (brs, 3H, -OH), 8.35 (brs, 2H, -OH), 7.21 (d, *J* = 8 Hz, 2H, H-2a, H-6a), 7.18 (d, *J* = 8.5 Hz, 2H, H-2b, H-6b) 6.91 (d, *J* = 16.5 Hz, 1H, H-7b), 6.84 (d, *J* = 8.5 Hz, 2H, H-3a, H-5a), 6.75-6.73 (m, 3H, H-3b, H-5b, H-14b), 6.70 (d, *J* = 16.5 Hz, 1H, H-8b), 6.33 (d, *J* = 1.5 Hz, 1H, H-12a), 6.25 (s, 3H, H-10a, H-14a, H-12b), 5.43 (d, *J* = 5.5 Hz, 1H, H-7a), 4.47 (d, *J* = 5.5 Hz, 1H, H-8a) ppm.
^{13}C NMR (125 MHz, CD_3COCD_3)	:	δ 161.5 (C-OH), 159.0 (C-OH), 158.8 (C-OH), 157.4 (C-OH), 157.4 (C-OH), 146.5 (C-11b), 135.5 (C-7b), 132.9 (C-1a), 129.2 (C-10b), 127.8 (2C, C-2a, C-6a), 127.0 (2C, C-2b, C-6b), 118.9 (C-1a), 115.4 (C-3b), 115.3 (C-5b), 115.2 (C-9b), 114.9 (C-1b), 114.8 (C-14b), 106.1 (C-10a, C-14a), 103.3 (C-12b), 101.2 (C-8b), 95.9 (C-12a), 93.0 (C-7a), 56.2 (C-8a) ppm.
HR-ESIMS *m/z*	:	455.1497 $[M+H]^{+}$ (calcd for $C_{28}H_{23}O_6$, 455.1494)

3a.12.8. Isolation of compound 20

Compound **20** (-)-hopeaphenol, (4 g) was isolated as a white solid from fractions 17-30 obtained by repeated column chromatography with 70 % ethyl acetate in hexane. Further, the compound was purified by precipitation method by using chloroform followed by crystallization in MeOH:DCM (60:40). From all the 1D, 2D, HRMS data and on comparison with the literature reports [Coggon *et al*., **1966**, Aisha *et al*., **2014**], the compound was confirmed. The structure of the compound is shown below.

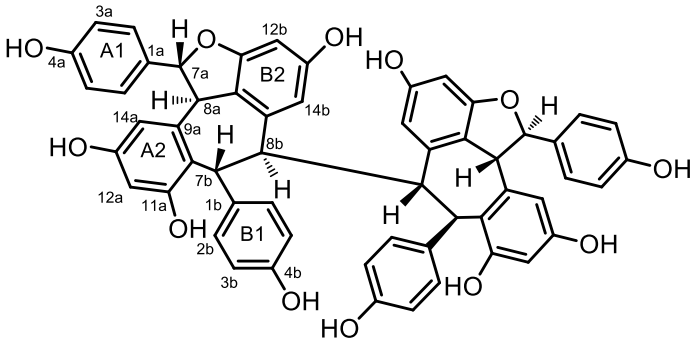

Melting point	:	above 280 ^{o}C decomposing
$[\alpha]^{25}_{D}$	:	-369 ^{o} (c 0.1, MeOH)
FT-IR (NaCl) υ_{max}	:	3379, 1689, 1591, 1507, 1437, 1336, 1210, 1168, 1124, 1081, 989 cm^{-1}.
^{1}H NMR (500 MHz, CD_3COCD_3)	:	δ 8.56 (s, 1H, -OH), 8.52 (s, 1H, -OH), 8.24 (s, 1H, -OH), 8.03 (s, 1H, -OH), 7.45 (s, 1H, -OH), 7.15 (d, *J* = 8.5 Hz, 2H, H-2a, H-6a), 6.92 (d, *J* = 8.5 Hz, 2H, H-2b, H-6b), 6.79 (d, *J* = 8.5 Hz, 2H, H-3a, H-5a), 6.56 (s, 1H, H-12a), 6.55 (d, *J* = 8.5 Hz, 2H, H-3b, H-5b), 6.31 (s, 1H, H-14a), 5.82 (s, 1H, H-7b), 5.77 (d, *J* = 12 Hz, 1H, H-7a), 5.74 (s, 1H, H-12b), 5.18 (s, 1H, H-14b), 4.24 (d, *J* = 12 Hz, 1H, H-8a), 3.95 (s, 1H, H-8b) ppm.
^{13}C NMR (125 MHz, CD_3COCD_3)	:	δ 160.3 (C-OH), 159.9 (C-OH), 159.5 (C-OH), 158.3 (C-OH), 158.2 (C-OH), 156.7 (C-11b), 143.5 (C-9a), 141.5 (C-9b), 136.3 (C-1b), 132.1 (C-1a), 131.3 (2C, C-2a, C-6a), 130.4 (2C, C-2b, C-6b), 122.2 (C-10a), 119.6 (C-

10b), 116.3 (C-3a, C-5a), 117.1 (2C, C-3b, C-5b), 113.7, 112.3 (C-14b), 107.4 (C-14a), 102.2 (C-12a), 96.3 (C-12b), 89.3 (C-7a), 50.8 (C-8a), 49.3 (C-8b), 42.3 (C-7b) ppm.

HR-ESIMS *m/z* : 907.2737 $[M+H]^+$ (calcd for $C_{56}H_{43}O_{12}$, 907.2754)

NMR Spectral assignments were made on the basis of ^{1}H-^{1}H COSY, DEPT, HMQC, HMBC, NOESY analysis and in comparison with the literature reports. (-)-Hopeaphenol was crystallized in MeOH: DCM (60:40) mixture at room temperature to give brown coloured crystal. Crystal structure was resolved with Bruker APEX-II CCD. (-)-Hopeaphenol belongs to orthorhombic space group crystal system with cell length *a* =11.2315(2), *b* =20.8456(5), *c* =24.0263(6), $\alpha = \beta = \gamma = 90^o$. The cif crystallographic data for (-)-hopeaphenol was deposited at the Cambridge Crystallographic Data Centre, under the reference number CCDC **1061115**.

3a.12.9. Isolation of compound 21

Compound **21** vaticaphenol A, (85 mg) was isolated as a white solid from fractions 31-35 obtained by repeated column chromatography with 80 % ethyl acetate in hexane. From all the 1D, 2D, HRMS data and on comparison with the literature reports [Seo *et al*., **1999**], the compound was confirmed. The structure of the compound is shown below.

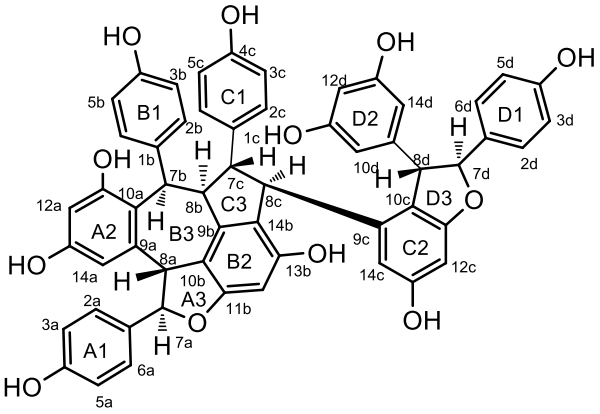

Melting point : above 300 ^{o}C decomposing

$[\alpha]^{25}_D$: -28 ^{o} (c 0.1, MeOH)

FT-IR (NaCl) υ_{max} : 3175, 2961, 2933, 2872, 1689, 1591, 1507, 1437, 1336,

1210, 1124, 1081, 989 cm^{-1}.

^{1}H NMR (500 MHz, CD_3COCD_3)	:	δ 8.47 (s, 1H, -OH), 8.34 (s, 1H, -OH), 8.12 (s, 1H, -OH), 8.11 (s, 2H, -OH), 7.98 (s, 1H, -OH), 7.95 (s, 1H, -OH), 7.84 (s, 1H, -OH), 7.42 (s, 1H, -OH), 7.09 (d, *J* = 8 Hz, 2H, H-2a, H-6a), 7.05 (d, *J* = 7.5 Hz, 2H, H-2d, H-6d), 7.02 (d, *J* = 8 Hz, 2H, H-2b, H-6b), 6.64 (d, *J* = 8 Hz, 4H, H-3a, H-5a, H-3d, H-5d), 6.56 (d, *J* = 8 Hz, 2H, H-3b, H-5b), 6.37 (d, *J* = 8 Hz, 2H, H-3c, H-5c), 6.33 (s, 1H, H-14c), 6.26 (d, *J* = 8 Hz, 2H, H-2c, H-6c), 6.15 (s, 2H, H-12a, H-12d), 6.05 (s, 1H, H-12c), 5.98 (s, 1H, H-14a), 5.96 (s, 2H-10d, H-14d), 5.92 (s, 1H, H-12b), 5.63 (d, *J* = 11.5 Hz, 1H, H-7a), 5.23 (d, *J* = 5.0 Hz, 1H, H-7d), 5.07 (s, 1H, H-7b), 4.54 (d, *J* = 5.0 Hz, 1H, H-8d), 4.41 (d, *J* = 10.5 Hz, 1H, H-8c), 4.30 (d, *J* = 11.5 Hz, 1H, H-8a), 3.96 (t, *J* = 11.5 Hz, 1H, H-7c), 3.07 (d, *J* = 6.5 Hz, 1H, H-8b) ppm.
^{13}C NMR (125 MHz, CD_3COCD_3)	:	δ 161.7 (C-OH), 159.8 (C-OH), 159.4 (C-OH), 158.8 (C-OH), 158.6 (C-OH), 157.9 (C-OH), 156.7 (C-OH), 156.3 (C-OH), 155.9 (C-OH), 155.7 (C-OH), 154.9 (C-OH), 147.9 (C-9d), 143.2 (C-9b), 141.8 (C-9a), 141.6 (C-9c), 134.6 (C-1d), 133.5 (C-1b), 131.4 (C-1c), 130.8 (C-2b, C-6b), 130.7 (C-1a), 130.2 (C-2a, C-6a), 129.2 (C-2c, C-6c), 128.2 (C-2d, C-6d), 124.5 (C-10a), 123.3 (C-10c), 122.1 (C-14b), 115.9 (C-3a, C-5a), 115.8 (C-3c, C-5c), 115.7 (C-3d, C-5d), 115.5 (C-3b, C-5b), 107.5 (C-10d, C-14d), 106.9 (C-14c), 105.7 (C-14a), 102.1 (C-12d), 101.6 (C-12a, C-12d), 96.4 (C-12b), 95.6 (C-12c), 94.6 (C-7d), 90.4 (C-7a), 57.5 (C-7c, C-8d), 53.1 (C-8b), 49.2 (C-8c), 48.8 (C-8a), 37.0 (C-7b) ppm.
HR-ESIMS *m/z*	:	907.2737 $[M+H]^+$ (calcd for $C_{56}H_{43}O_{12}$, 907.2754)

NMR Spectral assignments were made on the basis of ^{1}H-^{1}H COSY, DEPT, HMQC, HMBC, NOESY analysis and in comparison with the literature reports.

3a.12.10. Isolation of compound 22

Fraction pools (37-57), obtained by eluting the column with 100 % ethyl acetate, gave 4.5 g of compound **22** as a white crystalline solid. The compound was successfully characterized as bergenin based on the spectral data obtained and on comparison with the literature reports [Seo *et al*., **1999**].

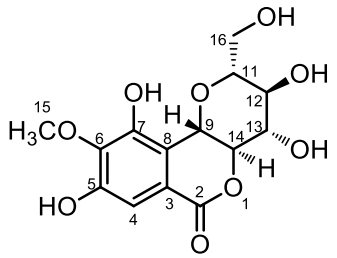

Melting point	:	236-238 ^{o}C
FT-IR (Neat) ν_{max}	:	3388, 3199, 1697, 1609, 1528, 1457, 1372, 1131, 1292, 1231, 1128, 1066, 958 cm^{-1}.
^{1}H NMR (500 MHz, DMSO d6)	:	δ 9.83 (bs, 1H, 5-OH), 8.50 (bs, 1H, 7-OH), 7.05 (s, 1H, H-4), 5.71 (d, 1H, *J* = 5 Hz, 13-OH), 5.49 (d, 1H *J* = 2.5 Hz, 12-OH), 5.03 (d, 1H, *J* = 10.5 Hz, H-9), 4.98 (bs, 1H, 16-OH), 4.05 (t, 1H, *J* = 10 Hz, H-16a), 3.90 (d, 1H *J* = 11.5 Hz, H-13), 3.83 (s, 3H, H-15), 3.73-3.69 (m, 1H, H-13), 3.63 (t, 1H, *J* = 8 Hz, H-11), 3.49 (1H, H-16b, merged), 3.26 (t, 1H, *J* = 8 Hz, H-12) ppm.
^{13}C NMR (125 MHz, DMSO d6)	:	δ 163.8 (C-2), 151.4 (C-7), 148.5 (C-6), 141.0 (C-5), 118.5 (C-8), 116.4 (C-3), 109.9 (C-4), 82.2 (C-11), 80.2 (C-14), 74.10 (C-13), 72.5 (C-9), 71.1 (C-12), 61.5 (C-6), 60.3 (C-15) ppm.
HR-ESIMS *m/z*	:	329.0874 $[M+H]^{+}$ (calcd for $C_{14}H_{17}O_9$, 329.0872)

NMR Spectral assignments were made on the basis of ^{1}H-^{1}H COSY, DEPT, HMQC, HMBC analysis and in comparison with the literature reports.

3a.12.11. Extraction and isolation of major phytochemicals from acetone extract of *V. indica* seed

The seeds of *Vateria indica* were collected from Wayanad district, Kerala. This was thoroughly cleaned and dried in a drier maintained at 50°C and powdered. The powdered seeds (1 kg) was subjected to repeated extraction using acetone (2.5 L X 48h) at room temperature. After extraction, the solvent was removed under reduced pressure using Büchi rotary evaporator. The acetone extract (85 g) was then subjected to column chromatographic separation. The column was eluted successively with gradient mixtures of hexane and ethyl acetate of increasing polarities and finally with 10 % methanol in ethyl acetate. A total of 105 fractions of approximately 200 mL each were collected. According to the similarity in TLC, they were pooled into 35 major fraction pools (FrA.1- FrA. 35). Pictorial representation of the procedure for the isolation of the compound is shown in Figure 3a.48.

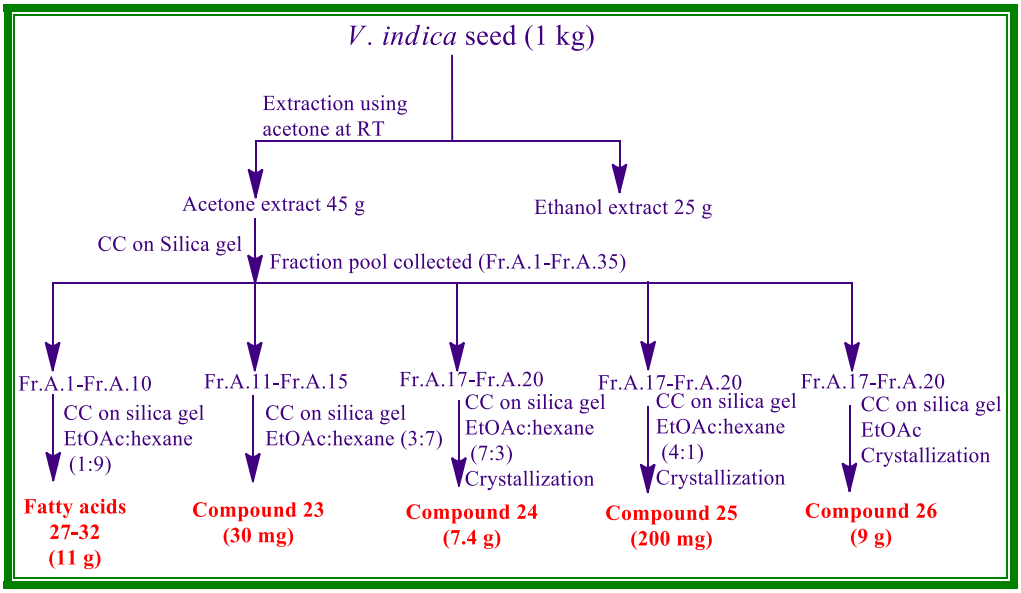

Figure 3a.48: Pictorial representation of isolation of compounds from *V. indica* seed

3a.12.12. Isolation of compound 23

Fractions pools 11-15 combined together and subjected to column chromatography on silica gel to afford compound **23** which was identified as (-)-ε-viniferin, isolated earlier from *V. indica* stem bark (compound **19**).

3a.12.13. Isolation of compound 24

Compound **24** was isolated from the seeds of *V. indica* as represented in Figure 3a.48

Compound **24** (7.4 g) was obtained as white solid by eluting the column with 70 % ethyl acetate in hexane. On evaluation of the structure of compound **24** and on comparison with 1D and 2D NMR spectrum, it was confirmed as (-)-hopeaphenol which was isolated earlier from the stem bark of *V. indica* (compound **20**).

3a.12.14. Isolation of compound 25

Figure 3a.48 represents the isolation procedure for compound **25**. It is obtained as brown solid. Detailed investigation of various spectroscopic data of compound **25** revealed that it was vaticaphenol A. Further evidence was made by comparing the 1D and 2D NMR data with that of compound **21** isolated earlier from the stem bark of *V. indica*.

3a.12.15. Isolation of compound 26

Fractions pools 23-30 combined together and recrystallized in methanol to afford colourless crystals of compound **26** which was identified as bergenin, isolated earlier from *V. indica* stem bark (compound **22**).

3a.12.16. Saponification of triglycerides

About 1g of triglyceride was dissolved in 100 mL 10 % methanolic potassium hydroxide and stirred for four hours at room temperature. The solution was evaporated under reduced pressure and was stirred with diethyl ether (50 mL) and water (250 mL). Ether layer was discarded and aqueous layer was acidified with dilute (10 % HCl). Then the acidified solution was extracted with ethyl acetate. The ethyl acetate solution was dried over anhydrous sodium sulphate and evaporated under reduced pressure.

3a.12.17. Fatty acid methyl esterification (FAME)

The saponified fatty acids were separated in aqueous phase by fractionation with water hexane mixture. The pure free fatty acids were then converted to FAME using 5 mL of acidified methanol (MeOH : HCl, 5:1), and incubating at 70°C for 5 hours. It was then fractionated in a separating funnel and extracted as hexane phase. The FAME samples were de-moisturized using anhydrous Sodium sulphate, filtered and stored in air tight vials at 0-4°C.

3a.12.18. Identification of fatty acids 27-32

The major fatty acids were identified by GCMS analysis and matching mass spectra with spectra of reference compounds in mass spectral library of NIST and WILEY.

CHAPTER 3B

Comparison of (+) and (-)-hopeaphenol, a pair of enantiomers and their antidiabetic activity

3b.1. An overview of hopeaphenol

Polyphenols, constituting oligomers of resveratrol ranging from dimer to octamer are found abundantly in plants belonging to Vitaceae, Dipterocarpaceae, Leguminosae and Cyperaceae families. These naturally occurring polyphenols are the common building blocks of a large number of complex natural products in terms of structure and stereochemistry. The biological activities such as anti-bacterial [Zetterström *et al*., **2013**], anti-HIV [Dai *et al*., **1998**], anti-inflammatory [Annabi *et al*., **2012**], anti-proliferative property [Empl *et al*., **2012**], make resveratrols a potential drug candidate. The evaluation of the mechanism underlying the biological activities of resveratrol oligomers would provide a substantial clue in the development of new drug leads. Due to the pharmaceutical importance of resveratrols, the research group of Snyder and Nicolaou independently developed protocols for the total synthesis of resveratrols despite of their structural complexity [Snyder *et al*., **2009**; Nicolaou *et al*., **2009**]. The first resveratrol oligomer ever characterized was hopeaphenol, a resveratrol tetramer isolated from *Hopea odorata* and *Balinocarpus heimii* by Coggon *et al.,* [Coggon *et al*., **1965**]. Further the absolute configuration of hopeaphenol was confirmed by single-crystal XRD of a dibromo-decamethyl ether derivative [Coggon *et al*., **1966**]. Among the resveratrol oligomers, the tetramer hopeaphenol shows a wide range of biological activities. In 2006, Merillon and co-workers isolated (+)-hopeaphenol from commercially available wine from North Africa [Guebailia *et al*., **2006**]. Recently Davis *et al*., reported the isolation of (-)-hopeaphenol from Anisoptera species which inhibit the bacterial virulence type III secretion system (T3SS) [Davis *et al*., **2014**].

It is evident from the literature that resveratrols are also accountable for antidiabetic activity and the recent works by Sharma *et al*., proved the efficacy of resveratrol as an effective therapeutic adjuvant for diabetes mellitus [Sharma *et al*., **2011**]. Most of the available drugs used for curing type 2 diabetes causes serious side effects such as obesity,

sexual and urologic complications. Kahn *et al*., reported a single mechanism to explain the link between obesity, insulin resistance and type 2 diabetes [Evans *et al*., **2002**]. The pervasiveness of type 2 diabetes is growing globally, and thus there is urgency for new antidiabetic drugs with less/no side effects. The plant derived antidiabetic drugs available in market reveals the potential of phytochemicals to regulate this metabolic disorder, compelling the search for new naturally inspired antidiabetic drug leads.

3b.2. Structural comparison of hopeaphenols

As already discussed in previous chapters, being impressed by the promising antidiabetic activity of the acetone extract, we column chromatographed the acetone extract of *A. indica* (L.) rhizome yielded (+)-hopeaphenol as the marker compound. To resolve the structure and stereochemistry of hopeaphenol with a known sample, we extended our effort to isolate the similar molecule from the plant *V. indica* Linn. which was identified as a source of (-)-hopeaphenol.

(+)-Hopeaphenol: We were delighted to isolate (+)-hopeaphenol from *A. indica.* The compact tetrameric structure was elucidated following 1D and 2D NMR data analysis and also by comparison with literature report [Aisha *et al*., **2014**]. The absolute configuration was established on the basis of optical activity $[\alpha]^{25}_{D}$= +384^{o} (c 0.1 MeOH), which was in agreement with the reported value $[\alpha]^{25}_{D}$= +366^{o} (c 0.17 MeOH) [Guebailia *et al*., **2006**]. The UV spectrum of the compound in CH_3CN showed an absorption maximum at 227 and 281 nm (Figure 3b.2a). Finally the structure and absolute configuration of (+)-hopeaphenol was unambiguously established by single crystal X-ray analysis. To the best of our knowledge, we are reporting the single X-ray structure of (+)-hopeaphenol without any derivatization for the first time (Chapter 2; Figure 2.31).

(-)-Hopeaphenol: (-)-Hopeaphenol was isolated from the stem and bark of *V. indica* Linn. All the 1D and 2D NMR spectroscopic data were consistent with the literature values and finally confirmed by single crystal X-ray analysis (Chapter 3A; Figure 3a. 29). Optical activity $[\alpha]^{25}_{D}$ = -369^{o} (c 0.1 MeOH) was also in good agreement with the reported values $[\alpha]^{25}_{D}$= -407^{o} (c 0.1 EtOH) [Coggon *et al*., **1965**]. The structure and absolute configuration of (-)-hopeaphenol was determined in 1965 by Coggon *et al.* from the X-ray crystallographic studies of dibromodecamethyl derivties [Coggon *et al*.,

1966]. From the optical activity studies, CD data (Figure 3b.2b) and by comparison with literature values we came to know that both compounds are enantiomers.

3b.3. Biosynthetic pathway of hopeaphenol

Resveratrol oligomerization appears to proceed *via* the coupling of oxidatively generated phenoxyl radicals. The dimerization typically occurs through three regioisomeric modes: the 8−10′, 8−8′ and 8−12′ coupling. Plants found in the Vitaceae and Dipterocarpaceae family synthesize an array of highly oxidized and structurally rearranged 8−10′ dimers that are unique to this plant family. ε-Viniferin forms via 8−10′ stereospecific radical dimerization of two resveratrol. The 8−8′ oxidative dimerization of two molecules of ε-viniferin as the presumed biosynthetic intermediate for a diverse series of resveratrol tetramers (Scheme 3b.1). This bis-para-quinone methide can undergo symmetric cyclization modes (C-10a-C-7b), delivering products such as hopeaphenol [Keylor *et al*., **2015**].

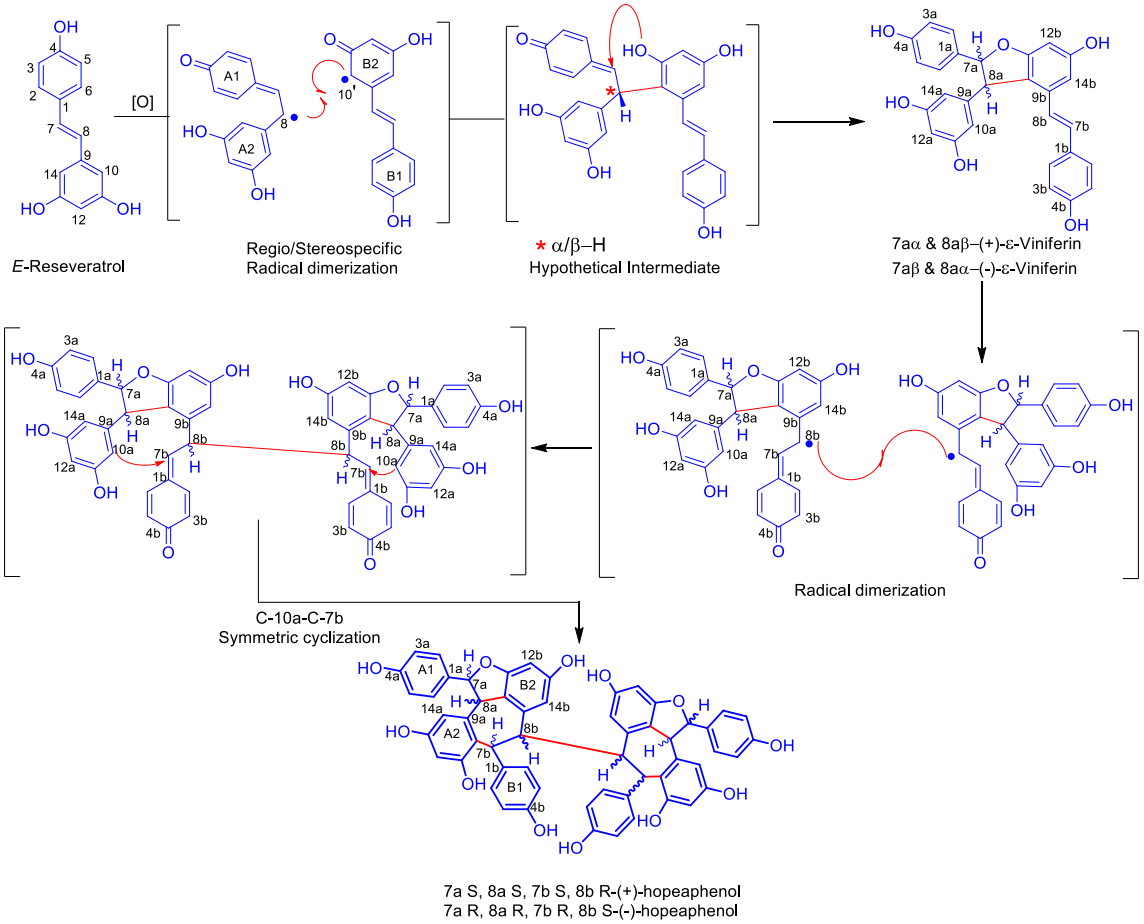

Scheme 3b.1: Biosynthetic pathway of hopeaphenol

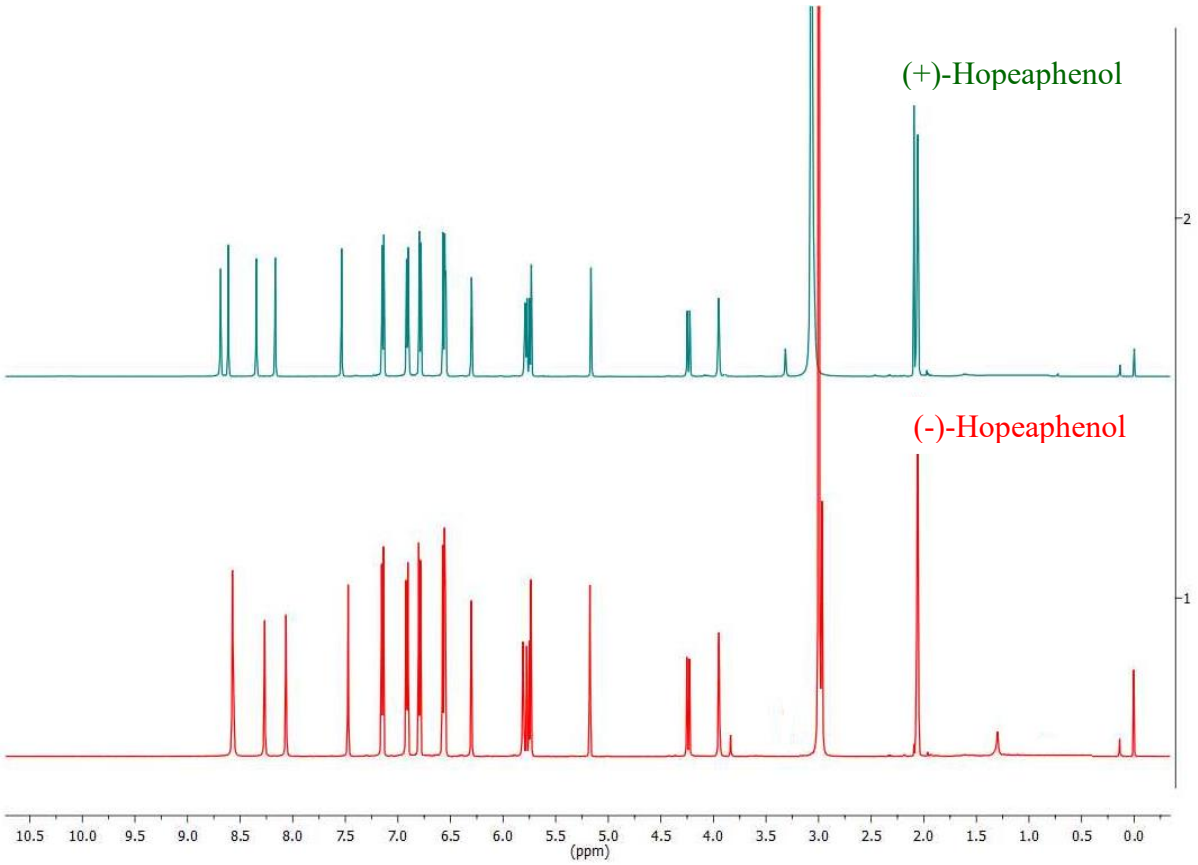

Figure 3b.1: ^{1}H NMR spectrum of (+) and (-)-hopeaphenol

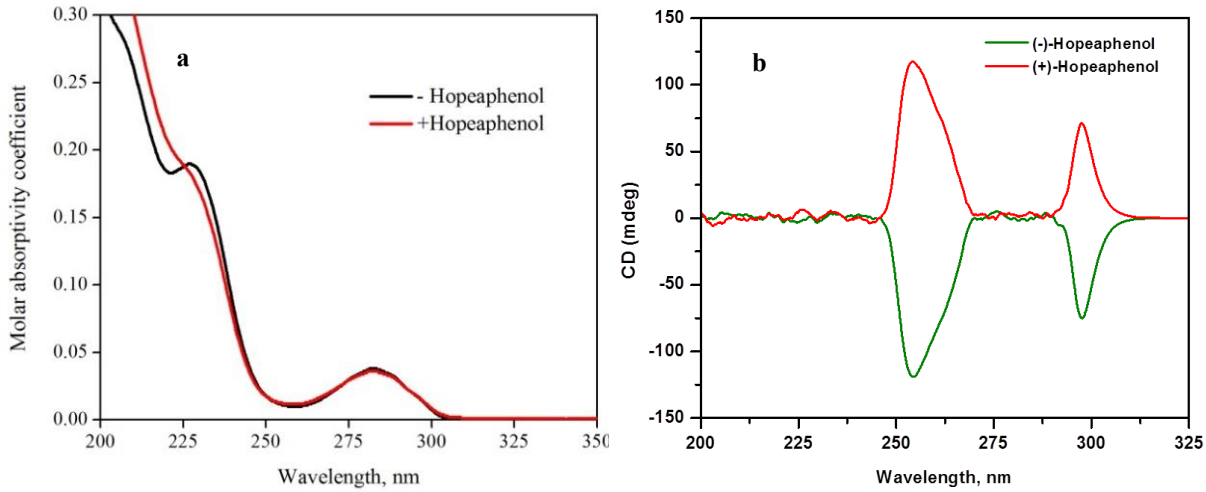

Figure 3b.2: (a) UV spectrum and (b) CD spectrum of (+) and (-)-hopeaphenol

3b.4. Biological screening of (+) and (-)-hopeaphenol

In order to showcase the biological activity of compounds, we investigated the hypoglycemic properties in terms of *α*-amylase, *α*-glucosidase, antiglycation and glucose uptake. The α-amylase enzyme found in the pancreatic juice and saliva, catalyses the hydrolysis of 1, 4-glucosidic linkages of starch, glycogen and various oligosaccharides into absorbable simpler sugars which are readily available for the intestinal absorption. Inhibitors of these enzymes delay the breakdown of carbohydrates in the small intestine, decreasing the absorption of glucose from starch and thereby diminishing the postprandial blood glucose excursion [Chen *et al*., **2010**]. The enzymes, *α*-glucosidase and *α*-amylases, are important therapeutic targets for the modulation of postprandial hyperglycemia which is the earliest metabolic abnormality to occur in type 2 diabetes mellitus. Unfortunately, the continuous administration of these synthetic drugs such as acarbose and miglitol, causes adverse side effects like diarrhoea, flatulence and hepatotoxicity [Nathan *et al*., **2009**] In the present scenario, natural products are explored with substantial interest for the management of diabetes owing to the side effects of currently available drugs. Therefore, (+) and (-)-hopeaphenol were investigated for its anti diabetic potential.

3b.4.1. α-Glucosidase inhibition assay

α-Glucosidase inhibitors which act as competitive inhibitors of intestinal α-glucosidase which can delay the digestion and subsequent absorption of elevated blood glucose levels. *α*-glucosidase activity was measured by determining the color developed by the release of p-nitrophenol arising from the hydrolysis of substrate PNPG by *α*– glucosidase using spectrophotometric method.

The *α*-glucosidase inhibitory activity was performed with different concentrations of (+) and (-) hopeaphenol. The results of *in vitro α*-glucosidase inhibitory study are summarized in Table 3b.1. The effectiveness of enzymatic inhibition of (+) and (-) hopeaphenol were determined by calculating IC_{50} value. The compounds showed a concentration-dependent inhibition of enzyme activity and seems to be more effective in *α*-glucosidase inhibitory potential compared to acarbose. The IC_{50} of (+) and (-) hopeaphenol was found to be 21.21 ± 0.987 and 9.47 ± 0.967 µM. Acarbose with the concentration required for 50 % inhibition (IC_{50}) found to 81.3 ± 1.10 µM

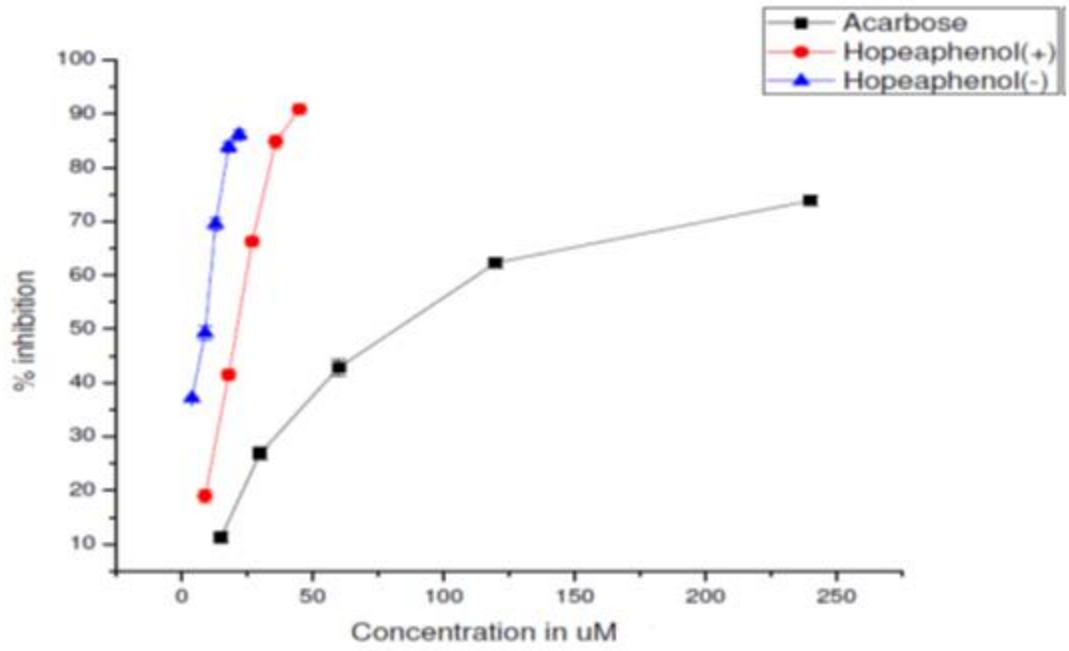

Figure 3b.3: α-Glucosidase inhibitory activity of (+) and (-) hopeaphenol

3b.4.2. α-Amylase inhibition assay

α-Amylase is an enzyme that catalyzes the hydrolysis of alpha-bonds in alpha-linked polysaccharides such as glycogen and starch to produce glucose and maltose. It is the major form of amylase in many biological organisms such as humans and other mammals. α-Amylase is found in saliva and pancreatic juice. The effect of the hopeaphenols on the enzymatic inhibition was determined by IC_{50} value. Acarbose used as positive control which shows IC_{50} = 8.5 ± 0.898 µM. The results showed that the hopeaphenols have not much effective in alpha amylase inhibition activity. (+) and (-) Hopeaphenol showed an IC_{50} of 68.75 ± 0.876 and 71.63 ± 0.987 µM respectively.

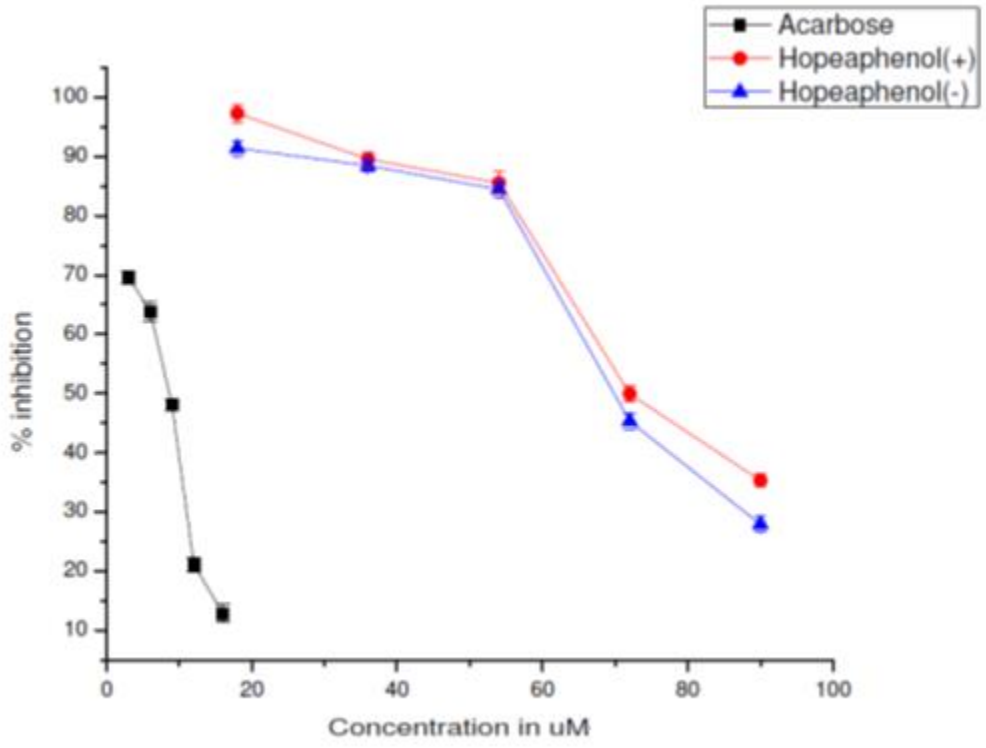

Figure 3b.4: α-Amylase inhibitory activity of (+) and (-) hopeaphenol

3b.4.3. Antiglycation assay

Protein glycation referred to as nonenzymatic glycosylation is the first part of the Maillard reaction and occurs when a sugar carbonyl group reacts with a protein amino group. Glycated proteins can undergo further reactions to form complex heterogeneous, cross-linked fluorescent molecules called advanced glycation end products (AGEPs). Increased glycation and accumulation of tissues AGEPs can alter protein conformation and impair function by altering enzyme activity.

Oxidation-reduction of proteins results in the formation of advanced glycated end products, which assumed to play an important role in the pathogenesis of diabetes. Thus, agents that inhibit the formation of advanced glycated end products are supposed to have therapeutic potential in patients with diabetes and age-related disease. By comparing to positive control acarbose (IC_{50} = 158.23 ± 0.718 µM), both (+) and (-)-hopeaphenol showed better glycation inhibition activity of IC_{50} value 81.9 ± 1.176 and 50.96 ± 0.897 µM.

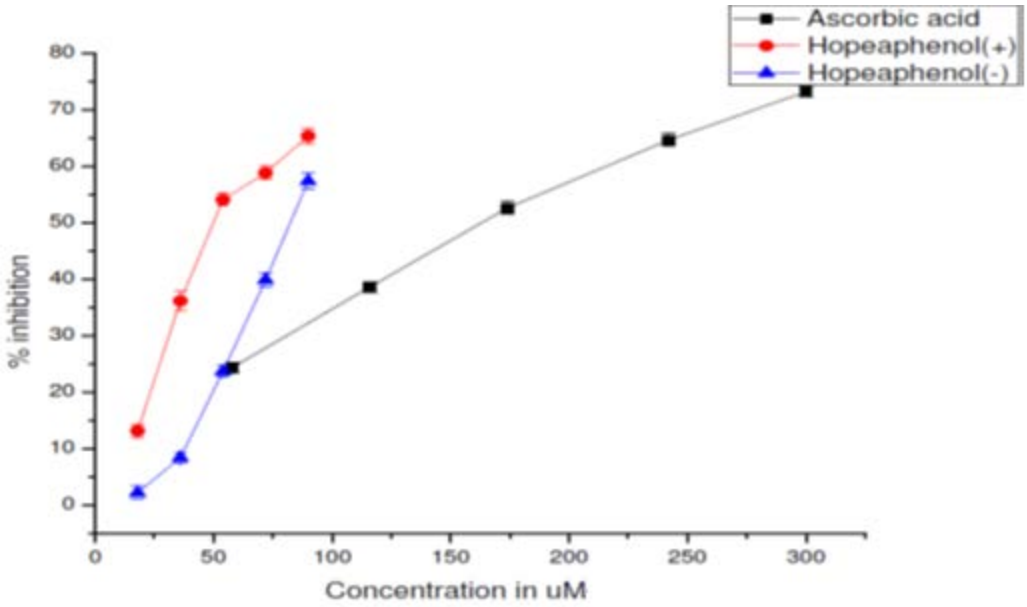

Figure 3b.5: % Inhibition of glycation by (+) and (-) hopeaphenol

Table 3b.1. IC_{50} values of (+) and (-)-hopeaphenol in α-amylase inhibition, α-glucosidase inhibition and antiglycation assay

Sr. No	Compounds	IC_{50} values (µM ±SD)		
		α-amylase inhibition	α-glucosidase inhibition	Antiglycation
1	(+)-Hopeaphenol	68.75 ± 0.876	21.21 ± 0.987	81.9 ± 1.176
2	(-)-Hopeaphenol	71.63 ± 0.987	9.47 ± 0.967	50.96 ± 0.897
3	Standard	8.5 ± 0.898 (Acarbose)	81.3 ± 1.10 (Acarbose)	158.23 ± 0.718 (Ascorbic acid)

3b.4.4. Cell viability assay

The MTT (3-[4,5-dimethylthiazol-2-yl]-2,5 diphenyl tetrazolium bromide) assay is a colorimetric assay based on the conversion of MTT into formazan crystals by living cells, which determines mitochondrial activity. This assay measures the reduction of yellow MTT by mitochondrial succinate dehydrogenase. The MTT enters the cells and passes into mitochondria where it is reduced to an insoluble, coloured (dark purple) formazan product. The cells are then solubilised with an organic solvent and the released, solubilised formazan reagent is measured spectrophotometrically. Since the reduction of MTT can only occur in metabolically active cells, the level of activity is the measurement of viability cells.

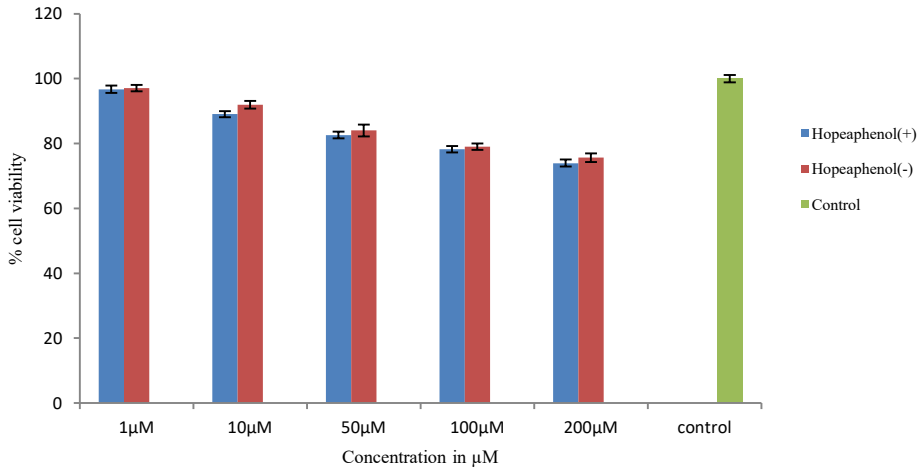

Figure 3b.6: Cell viability assay by MTT

Cytotoxicity of the sample was determined by MTT assay. The OD value of control cells (sample free) was taken as 100 % and then calculated as the percentage of reduction of absorbance in compound exposed cells. The data showed that both (+) and (-) hopeaphenols are not toxic to cells upto 200 µM concentration. Different concentration treated cells showed above 75 % cell viability. Sub toxic concentration was calculated from absorbance and which is used for glucose uptake.

3b.4.5. Glucose uptake assay by 2- NBDG

The entry of glucose into cells depends on different parameters, including expression of the appropriate glucose transporters in the target tissues and hormonal regulation of their function. Cells take up glucose by facilitated diffusion, via glucose transporters (GLUTs) associated with the plasma membrane. Stimuli leading to the increase in translocation of GLUT4 to the plasma membrane facilitate entry of glucose into the cells. Glucose uptake assay was performed by 2-NBDG in L6 rat skeletal muscle cells using flow cytometry (BD FACS Aria II, USA) [Chen *et al*., **2010**]. Differentiated L6 cells were pre-incubated with (+) and (-) hopeaphenol at two different concentrations. After incubation, 2-NBDG added to the cells for 30min and washed out the remaining glucose analogue with PBS. Then trypsinized the treated cells and cell lysate used for flow cytometric analysis. Rosiglitazone (100 nM) served as control.

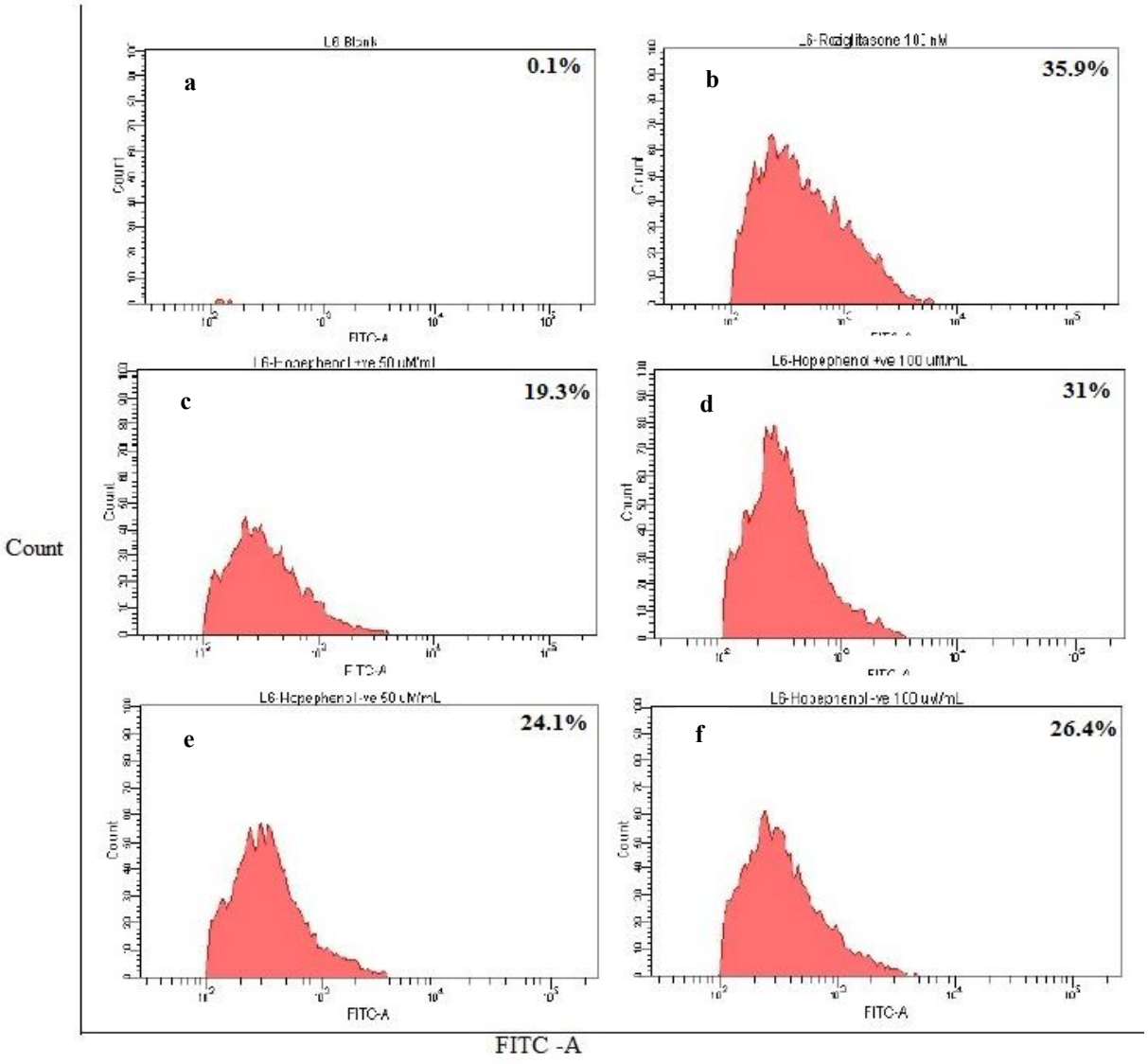

Figure 3b.7: 2-NBDG uptake in L6 myotubes. Glucose transport in differentiated myoblast was assessed by the uptake of a) control cells b) rosiglitazone treated c) and d) 50 and 100 µM (+)-hopeaphenol treated cells e) and f) 50 and 100 µM (-)- hopeaphenol treated cells.

Effect of both (+) and (-) hopeaphenol on glucose uptake by cells was checked by glucose fluorescent analogue, 2-NBDG (10 µM). Results indicated that both (+) and (-) hopeaphenol were able to enhance uptake of 2-NBDG at sub lethal concentrations (50µM and 100 µM) with 19.3 %, 31 % and 24.1 % and 26.4 % increase in probe uptake. It is interesting to observe that both hopeaphenols significantly increases glucose uptake in cells suggesting the stimulatory activity for glucose uptake. The effect was compared with standard drug rosiglitazone (100 nM), which showed 35.9 % increase in probe uptake.

3b.5. Docking interaction studies of the compounds with proteins

In order to envisage the probable binding modes of (+) and (-)-hopeaphenol on digestive enzymes, we selected porcine pancreatic α-amylase (PDB-1BVN), Saccharomyces cerevisiae (PDB-3A4A) and (PDB-3AJ7) for molecular docking studies based on the homology. The molecular docking score of (-)-hopeaphenol and (+)-hopeaphenol with the protein 1BVN are -12.0251 and -13.1447 kcal/mol respectively. Using LigPlot analysis the binding interactions of the ligands with proteins were studied. No prominent interactions were observed for (-)-hopeaphenol with this protein. But it shows an indirect hydrogen bonding interaction with a polar amino acid residue Asn53. Binding of (+)-hopeaphenol shows a backbone donor bonding interaction with a polar amino acid residue GlyA106 (2.04Å, 12 %).

The blue smudges that are drawn behind the groups represent the amount of solvent exposure. The molecular docking score of these compounds with the protein 3A4A are -6.4507 and -15.3920 kcal/mol respectively. The binding mode detected for the compound (-)-hopeaphenol gives a sidechain acceptor bonding interactions with a polar amino residue Ser240 (2.02 Å, 25 %). Binding of (+)-hopeaphenol shows an arene-cation bonding interaction with basic amino acid residue His280. Comparatively very high molecular docking scores were observed for the compounds with the protein 3AJ7. There is no prominent interactions observed for (-)-hopeaphenol with this targeted protein. It showed a docking score of -22.8589 kcal/mol (Table 3b. 2). The binding mode detected for the compound (+)-hopeaphenol gives an arene-arene-cation bonding interactions with basic amino residue His280 (1.8 Å, 66 %). And the dotted outline that is the proximity contour near this side of the ligand indicates the closeness of the groups present in that region of the ligand to the active site. It also shows a hydrogen bonding with both acidic amino acid residue Glu332 with a docking score of -19.3913 kcal/mol. The blue smudges that are drawn behind some of groups in certain cases represent the amount of solvent exposure (Figure 3b.8).

Table 3b.2. Molecular docking scores of (-)-hopeaphenol and (+)-hopeaphenol with various proteins 1BVN, 3A4A and 3AJ7

COMPOUNDS	E Score kcal/mol		
	1BVN	3A4A	3AJ7
(-)-hopeaphenol	-12.0251	-6.4507	-22.8589
(+)-hopeaphenol	-13.1447	-15.3920	-19.3913

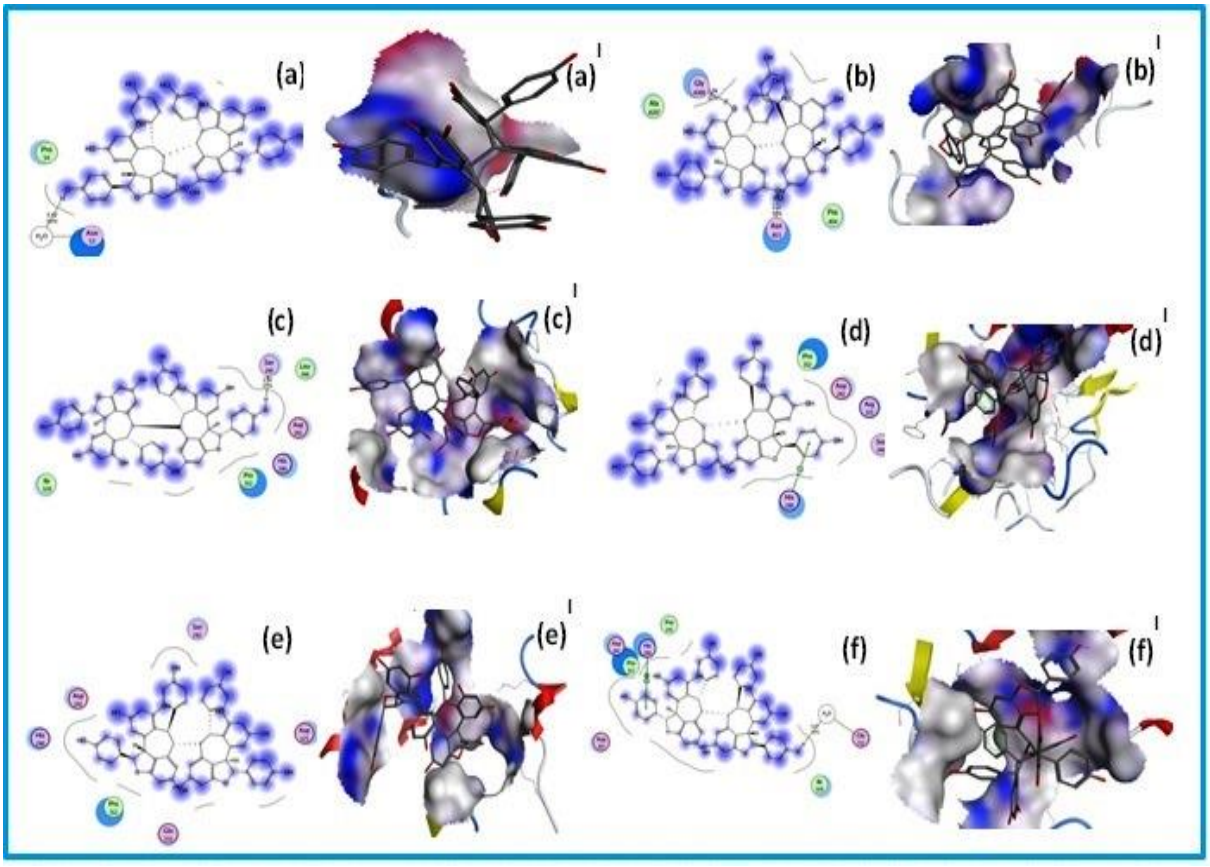

Figure 3b.8: Docking interaction studies of the compounds with Proteins; (a, a^I) and (b, b^I) molecular docking studies of (-)-hopeaphenol and (+)-hopeaphenol with protein 1BVN, ; (c, c^I) and (d, d^I) molecular docking studies of (-)-hopeaphenol and (+)-hopeaphenol with

protein 3A4A and ; (e, e^{I}) and (f, f^{I}) molecular docking studies of (-)-hopeaphenol and (+)-hopeaphenol with protein 3AJ7 respectively.

3b.6. Conclusion

In conclusion, these *in vitro* results suggest that the compounds exert its antidiabetic effects through digestive enzyme inhibition and increased glucose uptake by the muscle cells. These multiple modes of action increase the interest in the use of (+) and (-)-hopeaphenol as a therapeutic intervention for diabetes. In order to find out how these two molecules interact with the target proteins, molecular docking studies were carried out. The results demonstrated that both compounds effectively bind with the target proteins. To the best of our knowledge, exciting antidibetic activity of (+) and (-)-hopeaphenol are reported for the first time. *In vivo* studies in the appropriate animal models are the next step in validating the antidiabetic potential of these isolated compounds.

3b.7. Experimental session

General experimental details and procedure for enzymatic antidiabetic activity studies are given in Chapter 2.

3b.7.1. Cell culture

L6 cell lines were obtained from NCCS, Pune, India. The cells were maintained in DMEM supplemented with 10% FBS and 1 % antibiotic/antimycotic solution, with 5 % CO_2 at 37°C. Differentiation of cells was induced by medium supplemented with 2 % FCS) [Tagami *et al*., **1986**]. Experimental assays were performed in differentiated myotubes.

3b.7.2. Cell viability assay

The effect of compounds on the viability of L6 cells was determined by the MTT assay [Mosmann **1983**]. L6 cells were seeded into 96 multi-well plates and cultured for 24 h. cells were treated with different concentrations of (+) and (-)- hopeaphenol in a fresh medium containing 10 % FBS DMEM for 24 h. After removing the medium, 100 µL of MTT (0.5 mg/mL) was added to each well and incubated for 4 h. After removing the MTT medium, 200 µL of DMSO was added to dissolve the formazan

crystals. After shaking, optical density (OD) at 570 nm was measured on a microplate reader by Synergy 4 Biotek multiplate reader, USA. Untreated cells used as control.

$$\% \text{ cell viability} = \frac{\text{Absorbance of Sample}}{\text{Absorbance of Control}} \times 100$$

3b.7.3. Glucose uptake assay

Glucose uptake was performed in confluent and differentiated L6 myotubes were incubated for 24 h in medium (DMEM with low glucose) containing 100 μM concentration of the (+) and (-)-hopeaphenol. Compound free media and Rosiglitazone (100 nM) were used as negative and positive controls, respectively. After incubation, cells were washed twice with prewarmed (37 °C) phosphate buffer, pH 7.4 and then incubated with 2-NBDG in the same buffer for 30 min at 37 °C. After 30 min, cells were rinsed three times with phosphate buffer, pH 7.4 (37 °C) and cell lysate were used for flow cytometric analysis (BD FACS Aria II).

3b.7.4. Molecular docking

The molecular docking studies of (+) and (-)-hopeaphenol with various proteins 1BVN, 3A4A and 3AJ7 were carried out using MOE 2009.10. For identifying the active site of the proteins the default 'Site Finder' tool was used.

CHAPTER 4

Phytochemical and antidiabetic evaluation of *Hopea ponga* (Dennst.) Mabb.

4.1. *Hopea ponga*-an overview

Hopea ponga belongs to the family Dipterocarpaceae (in malayalam it is popularly known as "Irumbakam or Kambakam") which is found in the tropical evergreen forests of south western India and distributed all along the Western Ghats of Kerala. *H. ponga* is endemic to India and it has been categorized as an endangered plant under the International Union for Conservation of Nature red list of threatened species [Hidayathulla *et al*., **2014**]. Plants belonging to the genus *Hopea* are well known for their stilbene oligomers which are the building blocks of several resveratrol based oligomers.

4.1.1. Morphology

It is a large tree with oblong leaves; flowers are pink in colour with glabrous racemose panicles. Fruits are green, turns red when it matures. The tree is economically important as timber; the bark is also a good tanning material and astringent with the slow speed of diffusion [Hidayathulla *et al*., **2014**] (Figure 4.1).

4.1.2. Ethnopharmacological relevance

Hopea ponga (Dennst.) Mabb. is endemic to India. This plant was reported to be used in traditional herbal formulations for diabetes, piles and snake bite [Muralikrishnan *et al.,* **1997**]. Recently Rose and co-workers reported the antioxidant and antibacterial activities of methanol and aqueous extracts of *H. ponga* [Rose *et al*., **2013**]. Apart from these, there is no report on the detailed phytochemical and pharmacological evaluations of *H. ponga*.

Figure 4.1: Picture of *Hopea ponga* tree, flower and seed

4.2. Scientific classification of *Hopea ponga*

Table 4.1. Scientific classification of *Hopea ponga*

Kingdom	***Plantae***
Phylum	***Tracheophyta***
Class	***Magnoliopsida***
Order	***Malvales***
Family	***Dipterocarpaceae***
Genus	***Hopea***
Species	***H. ponga***

4.3. An introduction to *Hopea* genus

As already discussed in the chapter 3A, Dipterocarpaceae is a well-known family of Asian rain forests, consisting of 17 genera. *Hopea* is one of the plant genus in Dipterocarpaceae family which consists about 104 species, distributed in India, Sri Lanka, China, and southward throughout Malaysia to New Guinea. The genus *Hopea* is usually tropical trees with simple leaves, fragrant flowers with one-sided spikes or racemes and often with hard heavy wood. Plants of this genus are known to elaborate mainly resveratrol oligomers [Keylor *et al.,* **2015**]. Resveratrol oligomers from Dipterocarpaceae exhibit diverse biological activities. Till now, only a few natural resveratrol oligomers have been isolated from *Hopea* genus. Atun *et al*, reported the isolation of resveratrol derivatives from the stem bark of *Hopea odorata*, *H. mengarawan* and *H. nigra* [Atun *et al*., **2008**]. Recently Ge and co-workers reported the isolation of unusual and potent immunosuppressive resveratrol oligomers from a tropical Dipterocarpaceae plant *Hopea chinensis* [Ge *et al*., **2010**]. Some of the previously reported resveratrol oligomers from *Hopea* genus are summarised in figure 4.2.

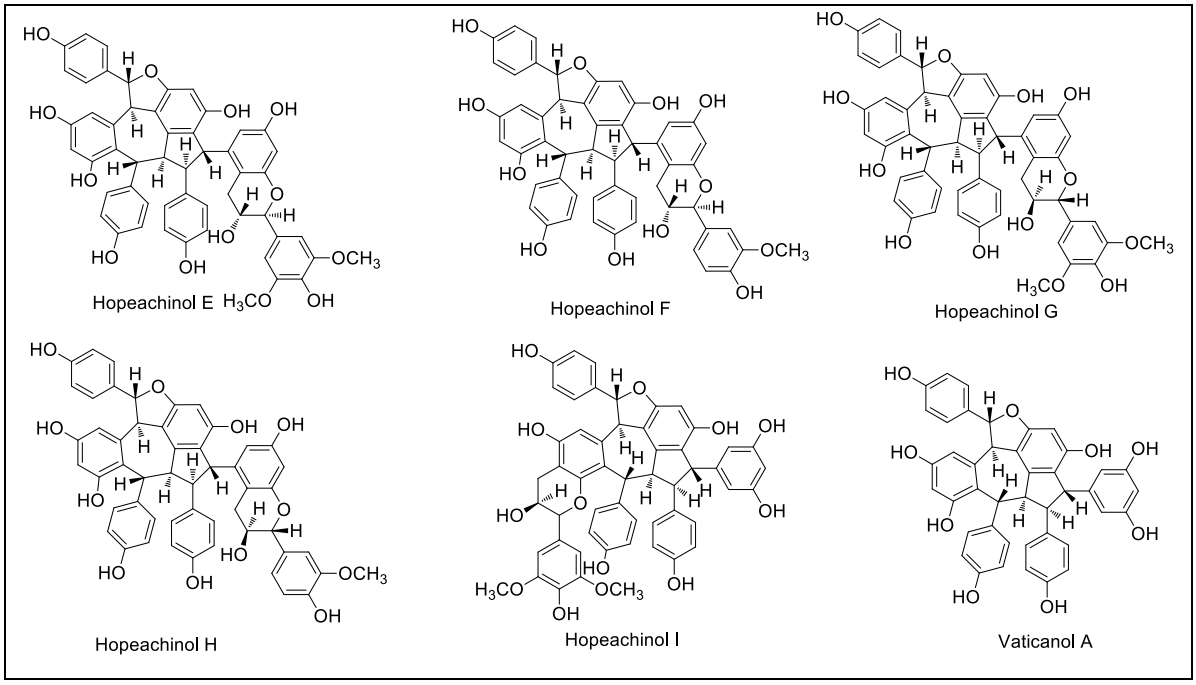

Figure 4.2: Resveratrol oligomers from *Hopea* genus

Figure 4.2 Continues...

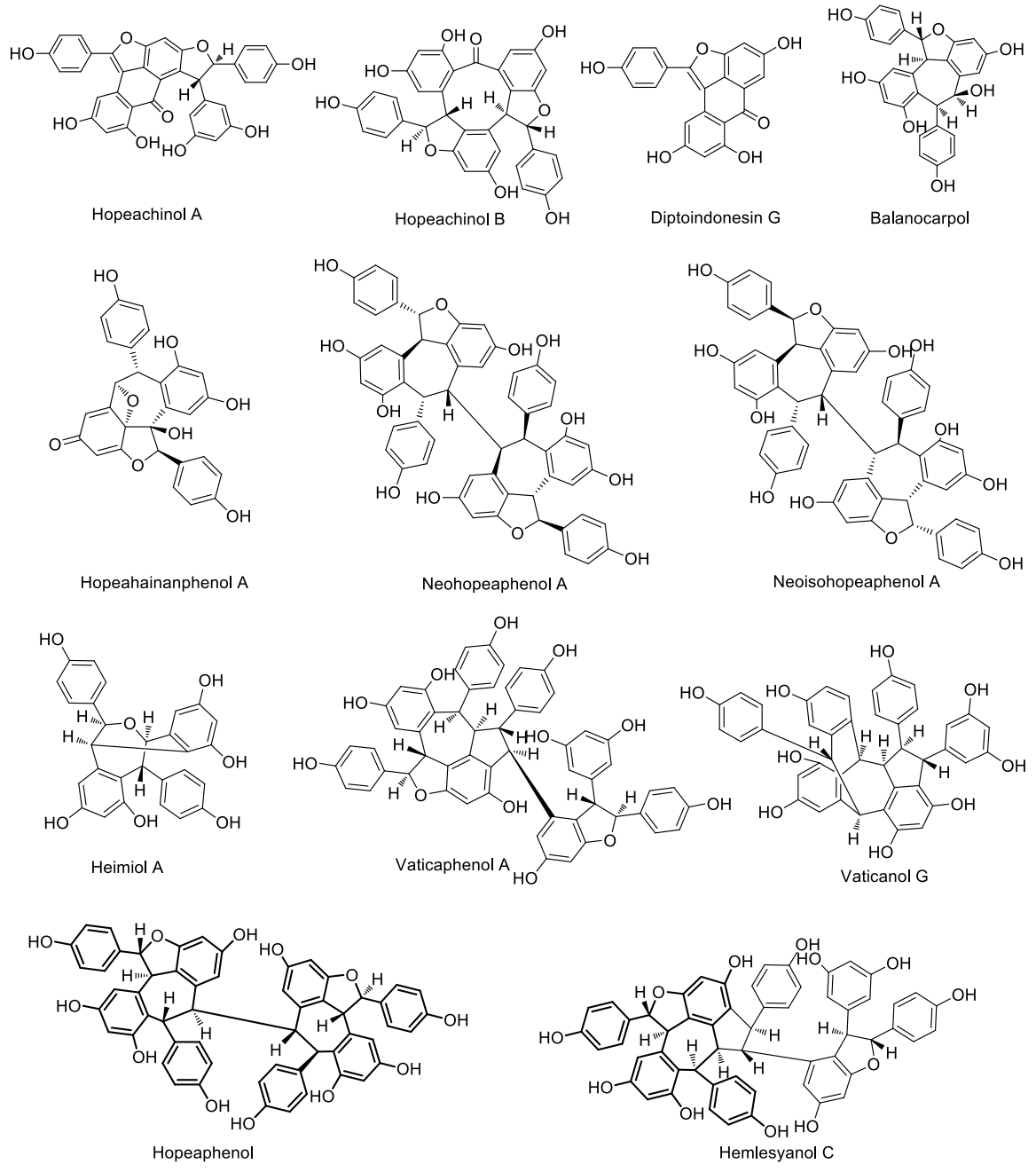

4.4. Aim and scope of the present work

Hopea ponga was reported to be used in traditional medicine for the treatment of diabetes, piles and snake bite. Recently Rose *et al* reported the antioxidant and antibacterial activities of methanol and aqueous extracts of *H. ponga*. Apart from these, there is no report on detailed phytochemical and pharmacological evaluations of *H. ponga*. Now the plant is

delineated as one of the endangered species in the red list of International Union for Conservation of Nature (IUCN Red list-August 2010), needs an urgent attention for conservation. Therefore it appeared timely and relevant to carry out the phytochemical and pharmacological evaluation of *H. ponga.* So as part of this Ph.D. program, a detailed study of *H. ponga* stem bark was undertaken. Evaluation of chemical indices of two different extracts of *H. ponga* stem bark, preliminary *in vitro* antidiabetic potentials of the extracts and the effect of antidiabetic modulation of digestive enzymes, protein glycation and glucose uptake in L6 myocytes of the isolated compounds have been carried out and the results are described in this chapter.

4.5. Extraction, Isolation and antidiabetic activity of *Hopea ponga* stem bark

4.5.1. Plant material

The stem bark of *Hopea ponga* (Dennst.) Mabb. was collected from the Western Ghats region (Wayanad District) of Kerala state, India. The plant material was authenticated by the taxonomist of M. S. Swaminathan Research Foundation (MSSRF), Kerala, India and a voucher specimen (M.S.S.H. 1542) was deposited in the herbarium repository of the same institute.

4.5.2. Extraction and antidiabetic screening of *H. ponga* (HP)

The air-dried stem bark of the *H. ponga* (1.2 kg) was extracted successively with acetone (A), ethanol (E) and water (W). The supernatant liquid was decanted and filtered. The extracts were then concentrated under reduced pressure in a rotary vacuum evaporator to remove the residual solvent which yielded 100 g (8.33 %) acetone (A), 25 g (2.08 %) ethanol (E) and 7 g (0.58 %) of water (W) crude extracts. These extracts were analyzed for α-glucosidase, α-amylase and glycation inhibitory activities. The results showed that the acetone and ethanol extracts of HP possessed α-glucosidase inhibitory activity (IC_{50} 11.21 ± 0.47 and 22.42 ± 0.24 µg/mL, respectively) which was significantly higher than that of the standard inhibitor acarbose (IC_{50} 45.37 ± 0.68 µg/mL). The antiglycation activity observed with acetone and ethanol extracts (IC_{50} 8.94 ± 0.02 and 19.36 ± 0.15 µg/mL) were also expressively higher than that of ascorbic acid standard (IC_{50} 48 ± 0.87 µg/mL). There was no significant reduction in α-amylase activity with the extracts tested. The IC_{50} values of HP extracts along with respective standards are shown in Table 4.2.

Table 4.2. Antidiabetic activity screening of different extracts of *H. ponga* (HP)[a]

Extracts	α-Glucosidase inhibition (IC_{50} µg/mL)	α-Amylase inhibition (IC_{50} µg/mL)	Antiglycation (IC_{50} µg/mL)
HPA	11.21 ± 0.47	122.40 ± 0.25	8.94 ± 0.02
HPE	22.42 ± 0.24	165.85 ± 0.49	19.36 ± 0.15
HPW	138.08 ± 0.51	265.44 ± 0.23	221.22 ± 0.76
Acarbose	45.37 ± 0.68	5.53 ± 0.36	------
Ascorbic acid	------	------	48 ± 0.87

[a] (A) acetone, (E) ethanol and (W) water fractions of *H. ponga*. All data are represented as mean ± standard deviation (n=3).

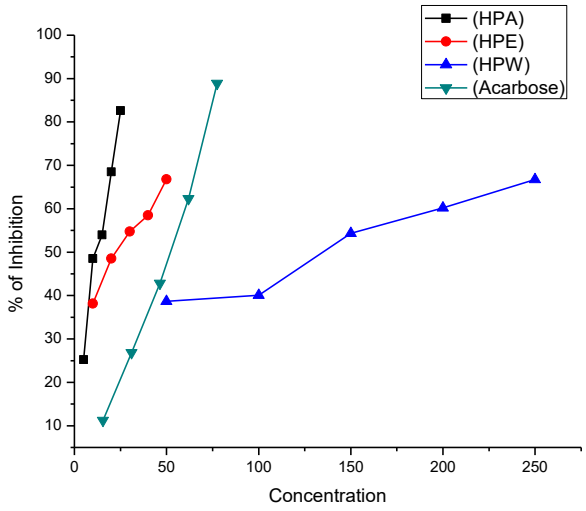

Figure 4.3: α-glucosidase inhibition activity of different extracts of HP

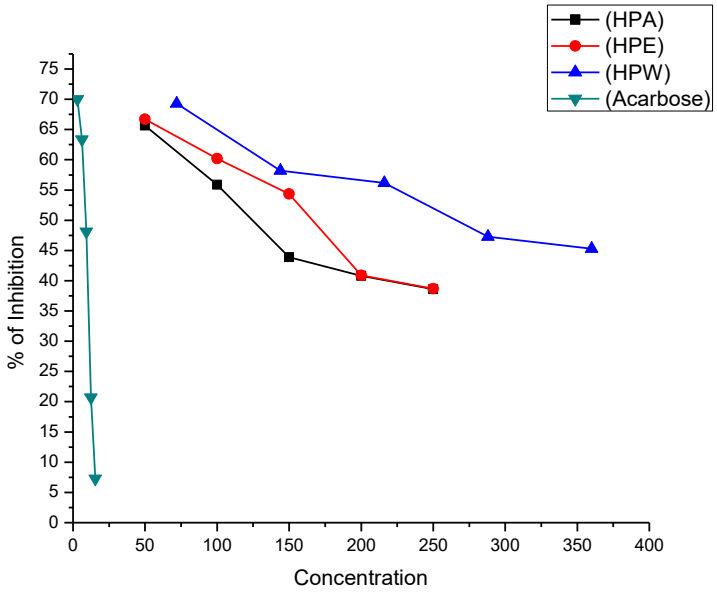

Figure 4.4: α-Amylase inhibition activity of different extracts of HP

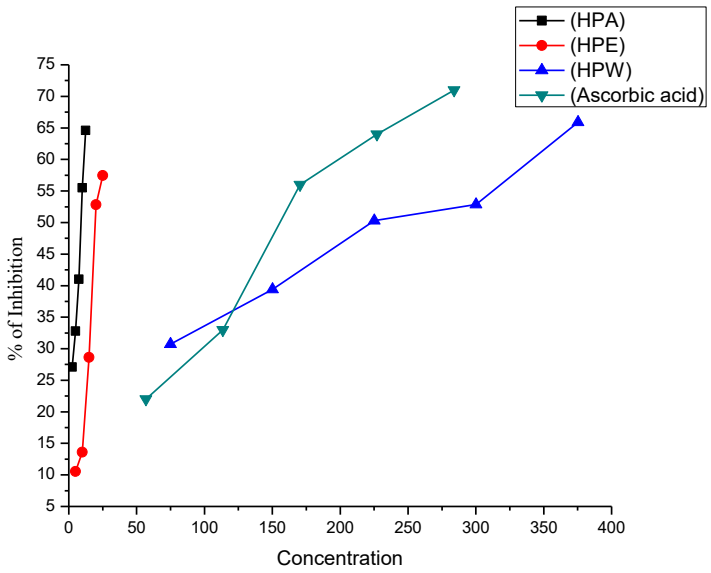

Figure 4.5: Glycation inhibitory activity of different extracts of HP

4.5.3. Isolation and characterization of compounds

The antidiabetic activity screening confirmed that the acetone and ethanol extracts were having the highest antidiabetic activity compared to water extract. Therefore, further isolation and purification of chemical constituents were focused on the acetone and ethanol extracts. The acetone extract (100 g) was fractionated using silica gel (100-200 mesh) column and eluted with n-hexane/EtOAc gradient (100 % n-hexane to 100 % EtOAc). Each fraction was analyzed by TLC (n-hexane-EtOAc), and those displaying the same TLC profile were combined to afford fourty fractions (FrA.1-FrA.40).

Fraction pool 1-5 (FrA.1-5), obtained by eluting the column with 10-20 % ethyl acetate in hexane upon crystallization using the same solvent yielded a mixture of phytosterol, ***β*-sitosterol** and compound **33.** This was further column chromatographed using silica gel (100-200 mesh) and a white pasty mass was (6 mg; 0.0005 %) obtained. IR spectrum of the compound showed broad signals at 3114 and 1703 cm^{-1}, indicating the presence of hydroxyl and ester groups. In ^{1}H NMR, (Figure 4.7) the signal at δ 5.88 ppm indicates the presence of phenolic hydroxyl group and a three hydrogen singlet at δ 3.93 ppm was attributed to the methoxy group attached to the aromatic ring. The signals at δ 7.61 and 6.29 ppm each integrating one proton with *J* value 16 Hz could be attributed to *trans* olefinic protons. In ^{13}C NMR, (Figure 4.8) the signal at δ 166.5 ppm is the diagnostic peak for ester carbonyl carbon. Methoxy carbon resonated at δ 55.9 ppm. The mass spectrum of the compound **33** showed molecular ion peak at m/z 531.4335, which is the $[M+H]^{+}$ peak. From all the above spectral details and in comparison with the literature reports [Xiang *et al*., **2008**] the compound was confirmed as **tetracosyl ferulate**. The structure of the compound is shown below.

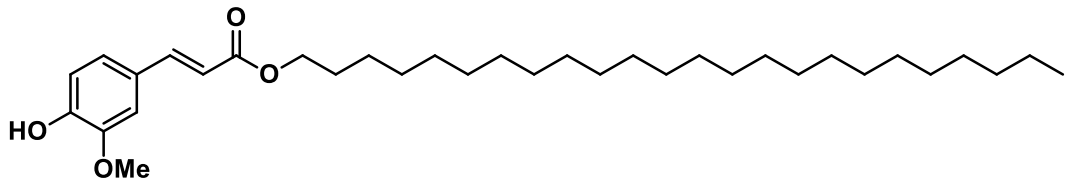

Figure 4.6: Tetracosyl ferulate **(33)**

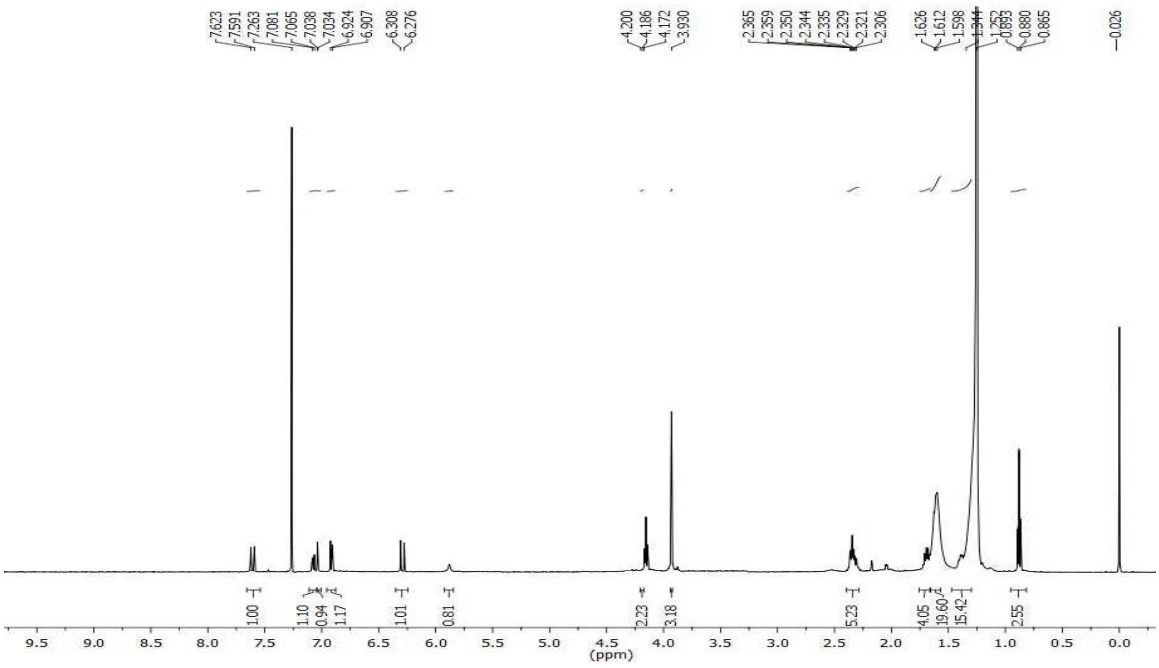

Figure 4.7: ^{1}H NMR spectrum of tetracosyl ferulate

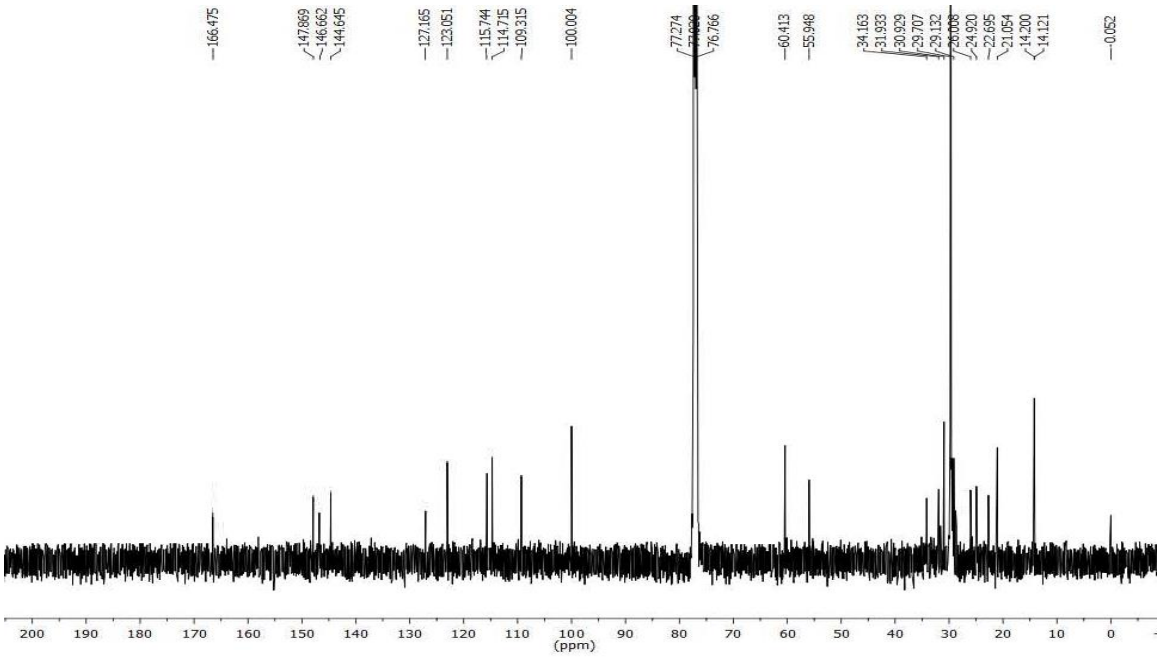

Figure 4.8: ^{13}C NMR spectrum of tetracosyl ferulate

Fraction pool 6-8 (FrA. 6-8), obtained by eluting the column with 35 % ethyl acetate in hexane showed the presence of a UV active compound. It was again subjected to purification

using silica gel column chromatography (100-200 mesh) yielding 12 mg (0.001 %) of light brown solid, which was labelled as compound **34**. Compound **34** was confirmed to be ***E*-Resveratrol**, which was earlier isolated from *A. indica* rhizome (Chapter 2) and *V. indica* stem bark (Chapter 3A).

Fraction pool 9-12 (FrA.9- Fr.A.12), obtained by eluting the column with 40 % ethyl acetate in hexane yielded 27 mg (0.0023 %) of a yellow amorphous solid with characteristic blue fluorescence in UV light. IR, ^{1}H, ^{13}C, HMQC, HMBC and HRESIMS spectra of the compound **35** was found to be similar to that of compound **19** namely **(-)-*ε*-viniferin** which was previously isolated from the *V. indica* stem bark and seed (Chapter 3A).

Compound **36** (350 mg; 0.03 %) was isolated as a pale yellow solid from fractions 14-24 by repeating column chromatography with 60 % ethyl acetate in hexane and was assigned the molecular formula $C_{42}H_{31}O_9$ following analysis of the HRESIMS at *m/z* 679.1967 $[M+H]^+$. IR spectrum of the compound showed absorption at 3389cm^{-1} suggesting the presence of hydroxyl group. The ^{1}H NMR spectrum in CD_3COCD_3 (Figure 4.11) exhibited signals for six phenolic hydroxyl groups (δ 8.42-8.21 ppm) which disappeared upon addition of D_2O. Considering the molecular formula, the remaining oxygen would contribute to the ether linkage. Other 2D spectroscopic details including ^{1}H–^{1}H COSY, HMQC and HMBC spectra (Figure 4.13-Figure 4.16) exhibited signals due to six aromatic rings as follows; three *p*-hydroxyphenyl groups (A1, B1 and C1) and three 1,2,3,5-tetrasubstituted aromatic ring (A2, B2 and C2) connected through 9 membered ring. The structure of compound **35** was characterized by the presence of three 7-8 ring junctions wherein the H7-H8 vicinal coupling values show significant differences in the 3 monomeric subunits. In the ^{1}H-^{1}H COSY NMR spectrum the presence of two sets of mutually coupled aliphatic stereocenter protons (H-7a/H-8a) and (H-7b/H-8b) with coupling constant 10 Hz and 6.5 Hz respectively and the remaining stereocenter protons at H-7c/H-8c appeared as broad singlet. The correlations in the HMBC spectrum (Figure 4.10) were observed between H-7a/C-8a, C-(2a,6a), H-8a/C-7a, C-9a, C-9c, C-10c, H-7b/C-8b, C-(2b,6b), H-8b/C-7b, C-9b, C-10a, H-7c/C-8c, C-1c, C-2c, C-6c, H-8c/C-7c, C-11b, C-9c, which indicated the presence of six aromatic rings and six methine units.

To confirm the relative stereochemistry, NOESY experiments were conducted (Figure 4.16). In the spectrum, clear cross peaks between H-8a/H-8b, H-(2a,6a) were observed.

These cross peaks substantiated that the relative stereochemistry of the methine protons at 8a and 7a are in *trans* orientation and protons at 8a and 8b are in *cis* orientation. The *trans* stereochemistry of the protons at 8b and 7b was confirmed by coupling constant with J value 6.5 Hz. NOE interactions between H-8b/ H-(2b,6b) indicated that the ring B1 is oriented in α-configuration and H-8b is oriented in α-configuration. There was no notable correlation between H-8b/H-8c and H-8c/H-8a which indicates that the proton at 8c is in β-orientation. On the basis of these correlations and observed coupling constant, the relative stereo chemistry of compound **36** was confirmed as *trans-cisoid-trans-transoid-trans*. The absolute configuration of compound **36** was established on the basis of optical activity $[\alpha]^{25}_{D}$ -49^{o} (c 0.1, MeOH). From all the above spectral details, on comparison with the biosynthetic pathway (Scheme 4.1) and literature reports [Pryce and Langcake **1977**; Mattivi *et al*., **2011**; Keylor *et al*., **2015**], the compound was confirmed as (-)-α-Viniferin. The structure of the compound is shown below.

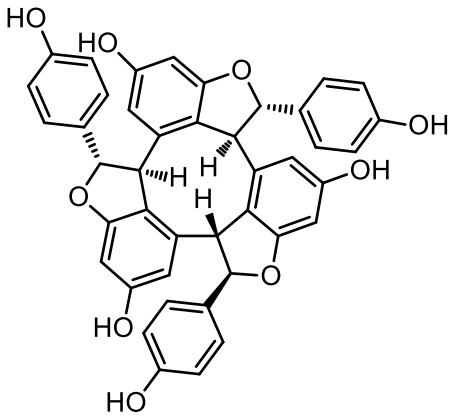

Figure 4.9: (-)-α-Viniferin **(36)**

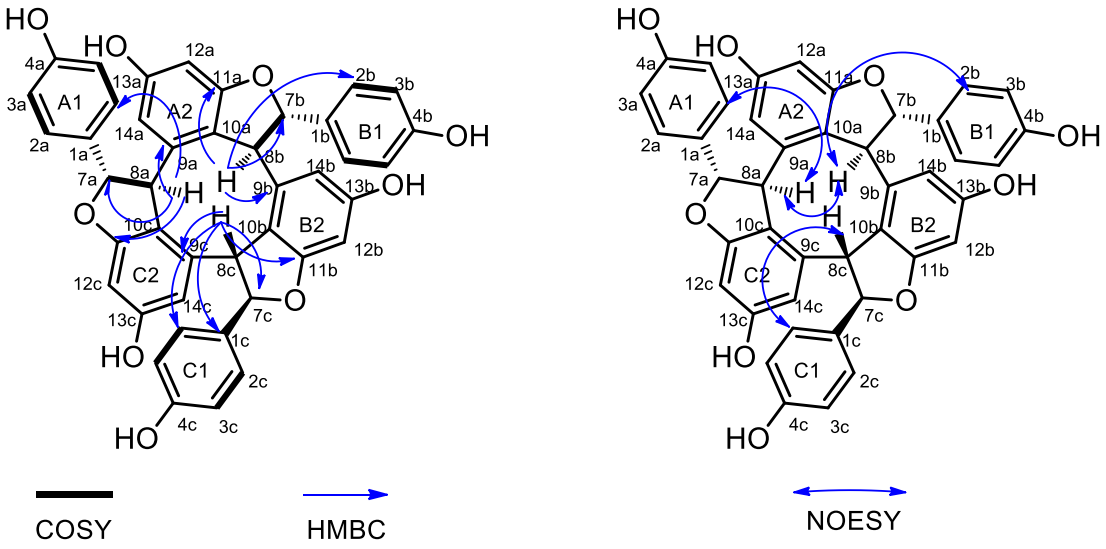

Figure 4.10: Selected COSY, HMBC and NOESY correlations of (-)-*α*-viniferin

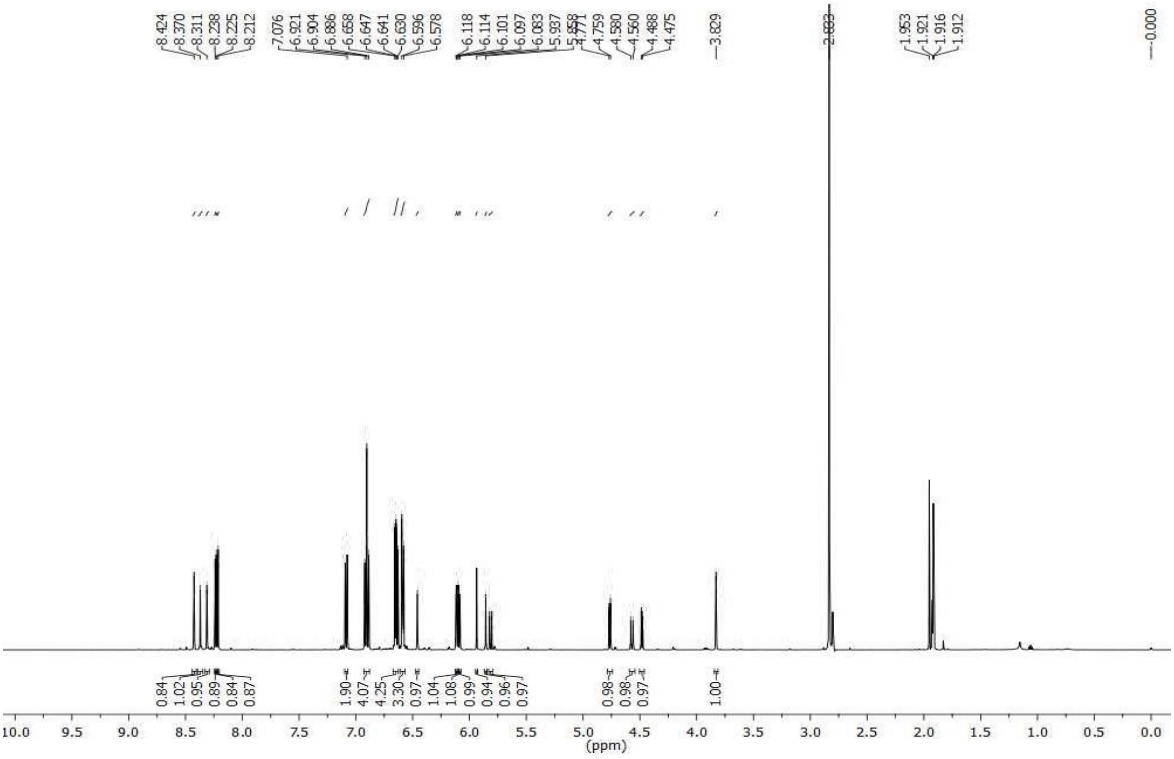

Figure 4.11: ^{1}H NMR spectrum of (-)-*α*-viniferin

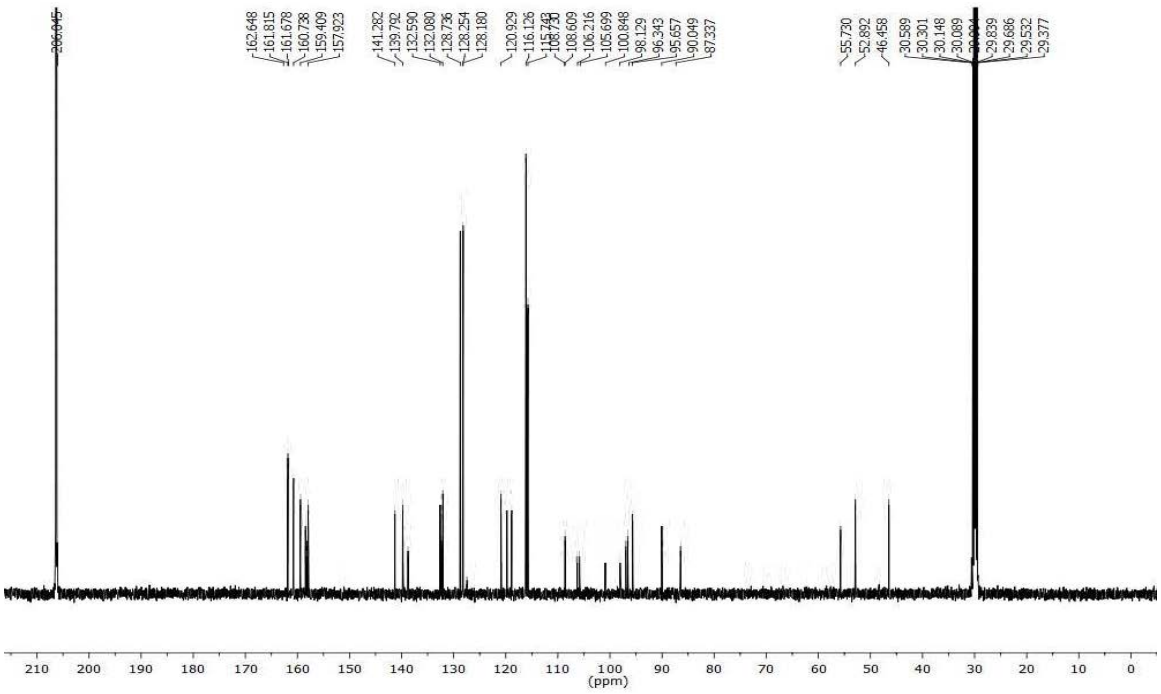

Figure 4.12: ^{13}C NMR spectrum of (-)-*α*-viniferin

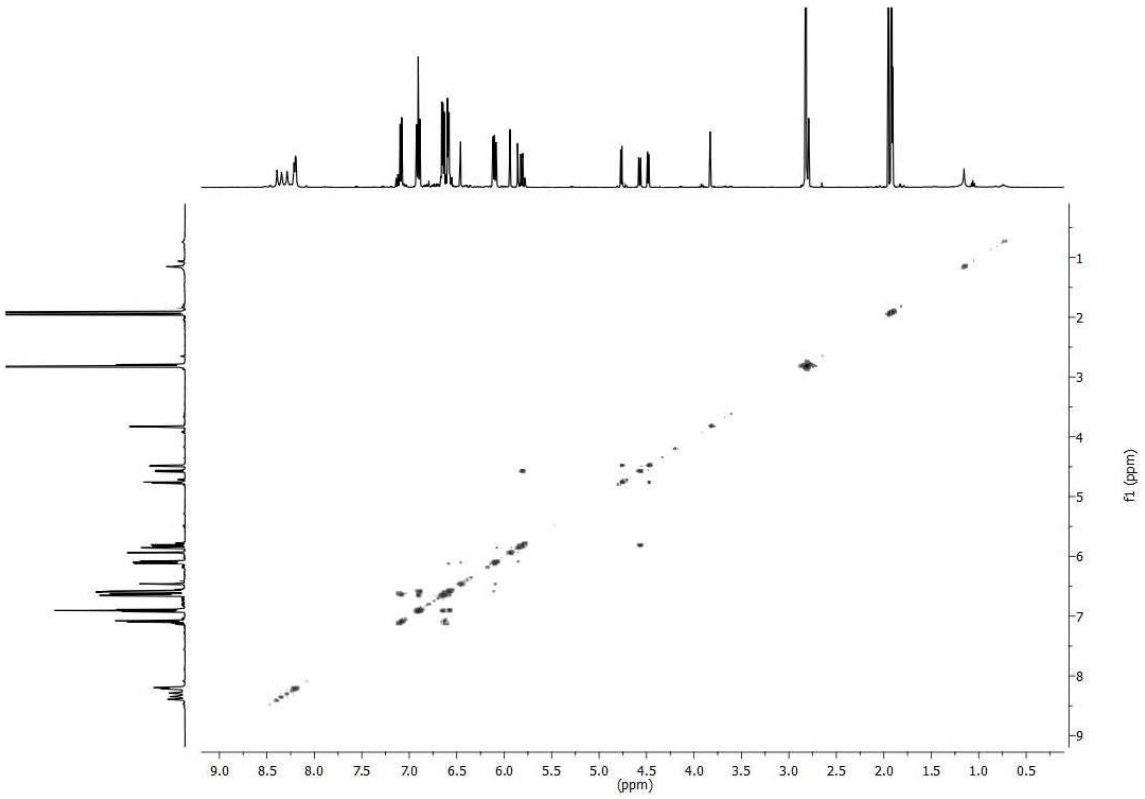

Figure 4.13: ^{1}H-^{1}H COSY NMR spectrum of (-)-*α*-viniferin

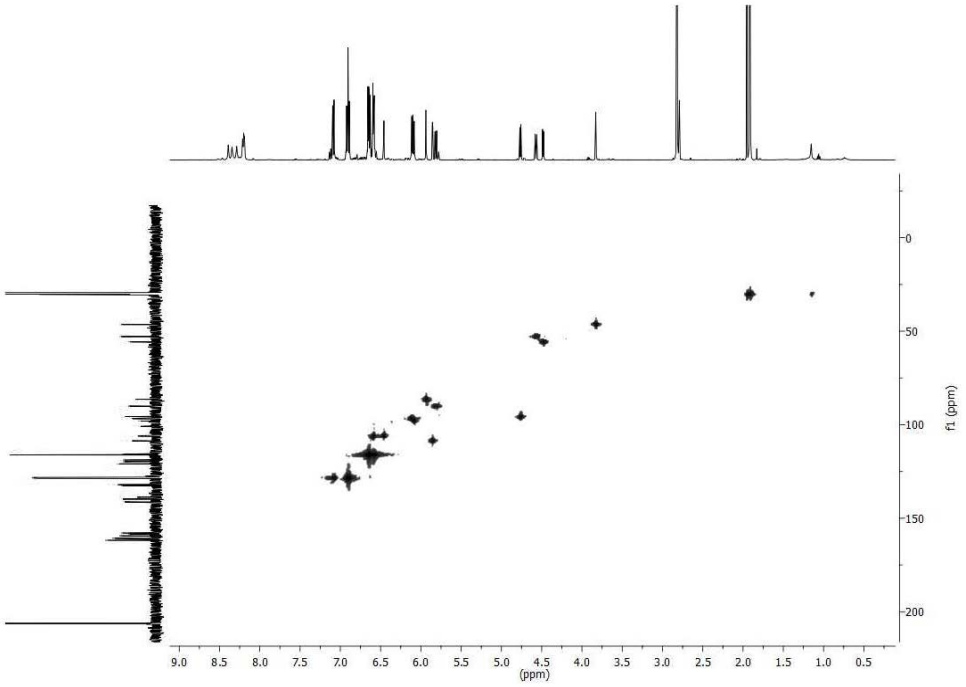

Figure 4.14: HMQC spectrum of (-)-*α*-viniferin

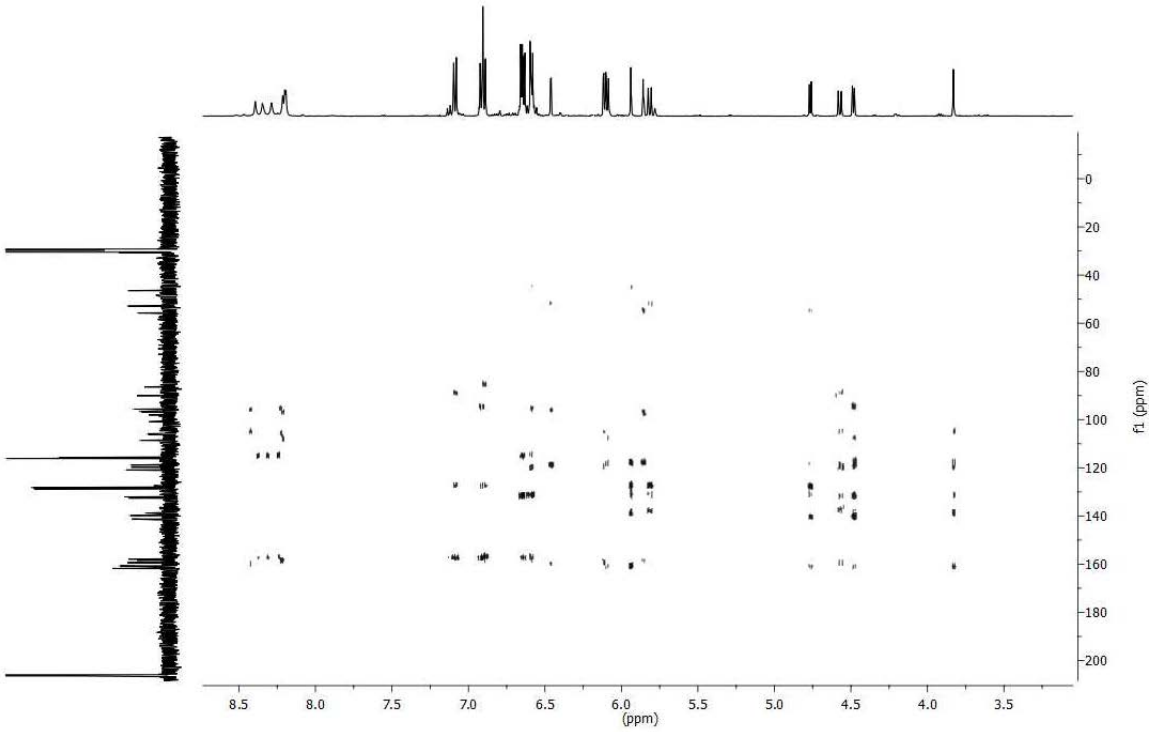

Figure 4.15: HMBC spectrum of (-)-*α*-viniferin

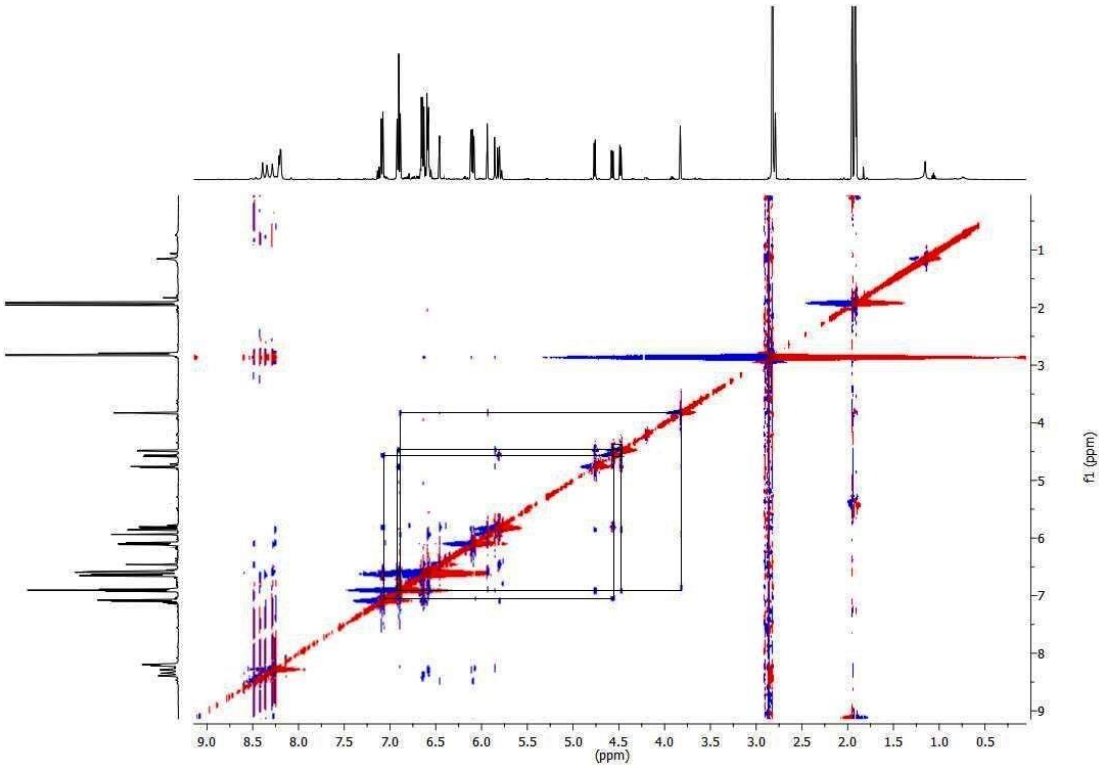

Figure 4.16: ^{1}H-^{1}H NOESY spectrum of (-)-*α*-viniferin

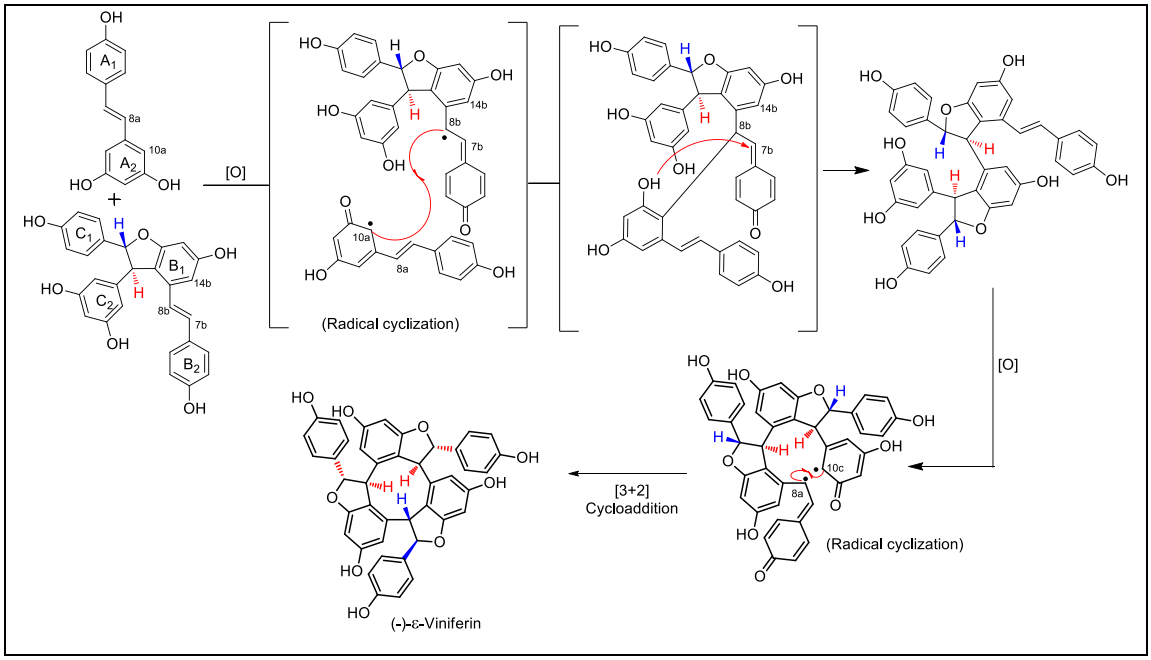

Scheme 4.1: Biosynthetic pathway of (-)-*α*-viniferin

Fraction pool 25 (FrA.25) on precipitation using acetone, furnished a white pasty compound **37** in 5 mg (0.00042 %). NMR and HRMS spectrum of compound 37 was similar to that of compound **17**, namely **sitoindoside I**, which was previsiouly isolated from *Vateria indica* stem bark. Fraction pool 26-30 was subjected to silica gel column chromatography using 70 % ethyl acetate in hexane which afforded compound **38** (2 g; 0.17 %). The structure and stereochemistry was further confirmed by comparison with single crystal X-ray structure of previously isolated compound **20**. We have solved the single crystal X-ray structure of compound **38** (Figure 4.17, red colour ORTEP), and it was overlaid with single crystal X-ray structure of compound **20** (Figure 4.17, green colour ORTEP) and it was unambiguously confirmed as **(-)-hopeaphenol**.

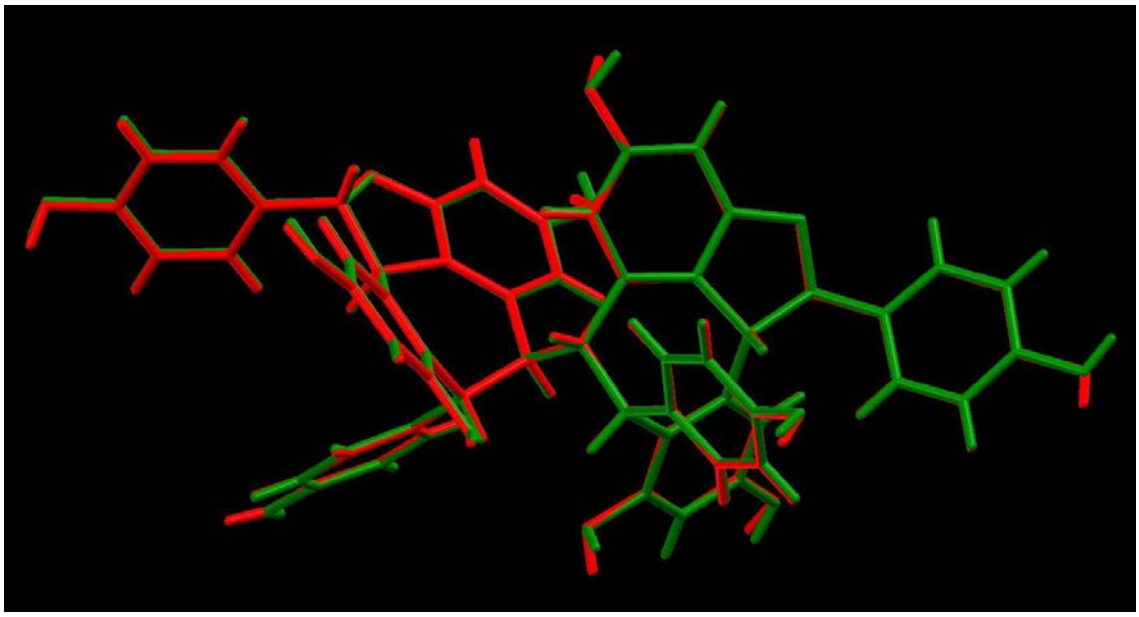

Figure 4.17: Single crystal X-ray overlay structure of (-)-hopeaphenol

Fraction pool 31-33 was submitted to repeated column chromatography on silica gel (mesh 230-400) using 80 % ethyl acetate in hexane to yield another resveratrol oligomer namely **vaticaphenol A 39** (7 mg; 0.00058), which was previously isolated from *V. indica* bark and seed. Fraction pool 34-39 was subjected to precipitation by using acetone which afforded the compound **40** (57 mg, 0.0048) and was confirmed to be ***β*-sitosterol-3-*O*-*β*-D-glucopyranoside**, earlier isolated from *A. indica* rhizome.

The ethanol extract (25 g) was also fractionated on a silica gel (230-400 mesh) column eluted with n-hexane/EtOAc of increasing polarity to afford eight fractions (FrE.1-FrE.8). Crude brown solid (1.5 g) precipitated from FrE.1-6 were chromatographed over silica gel (MeOH/EtOAc of increasing polarity) gave compound **41** (900 mg; 0.08 %) as a brown solid. IR spectrum of the compound showed a broad absorption at 3349 cm^{-1} suggesting the presence of a hydroxyl group. The broad signals at δ 8.24 and 7.52 ppm in ^{1}H NMR spectrum indicates the presence of phenolic hydroxyl groups. Four *ortho*-coupled aromatic protons resonated at δ 7.41 and 6.82 ppm with coupling constant value J = 8.5 Hz. The signal at δ 4.97 ppm integrating one proton with J value 9.5 Hz could be attributed to an anomeric proton with β linkage. ^{13}C NMR indicated that the compound **41** consists of 20 carbons, 14 from phenanthrene moiety and 6 from the glucose ring. The signals at δ 158.6, 158.5 and 158.1 ppm could be attributed to the carbons bearing hydroxyl group. The signals at δ 81.6-62.3 ppm are characteristic of glucose ring. The mass spectra of the compound **41** gave a molecular ion peak at 411.1056 which is the $[M+Na]^{+}$. The compound was successfully characterized as **trihydroxyphenanthrene glucoside** (**THPG**) based on the spectral data obtained (^{1}H NMR (Figure 4.19), ^{13}C NMR (Figure 4.20) and HRESIMS) and on comparison with the literature reports [Baderschneider and Winterhalter **2000**]. The structure of the compound is shown below.

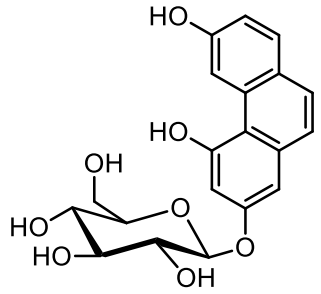

Figure 4.18: Trihydroxyphenanthrene glucoside (**41**)

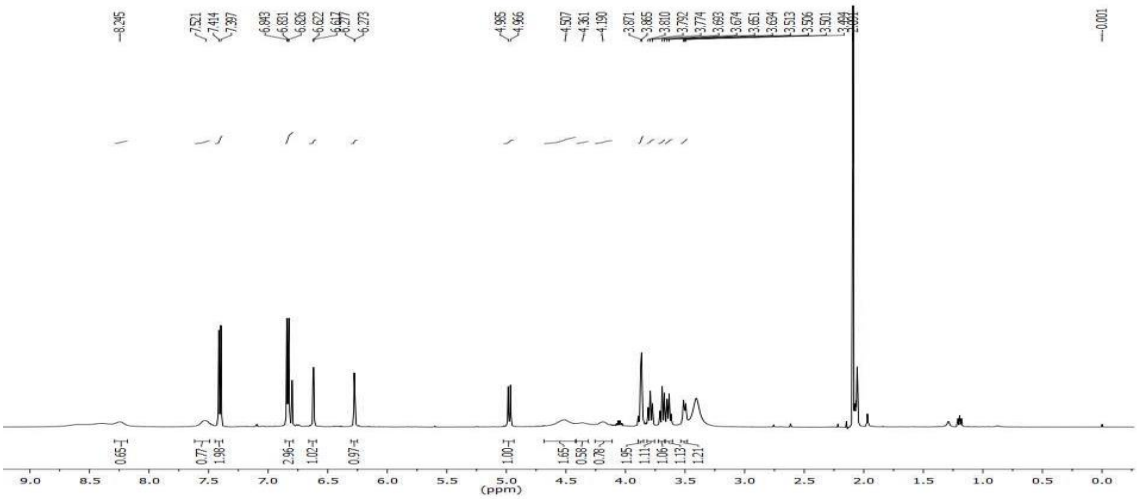

Figure 4.19: ^{1}H NMR spectrum of trihydroxyphenanthrene glucoside

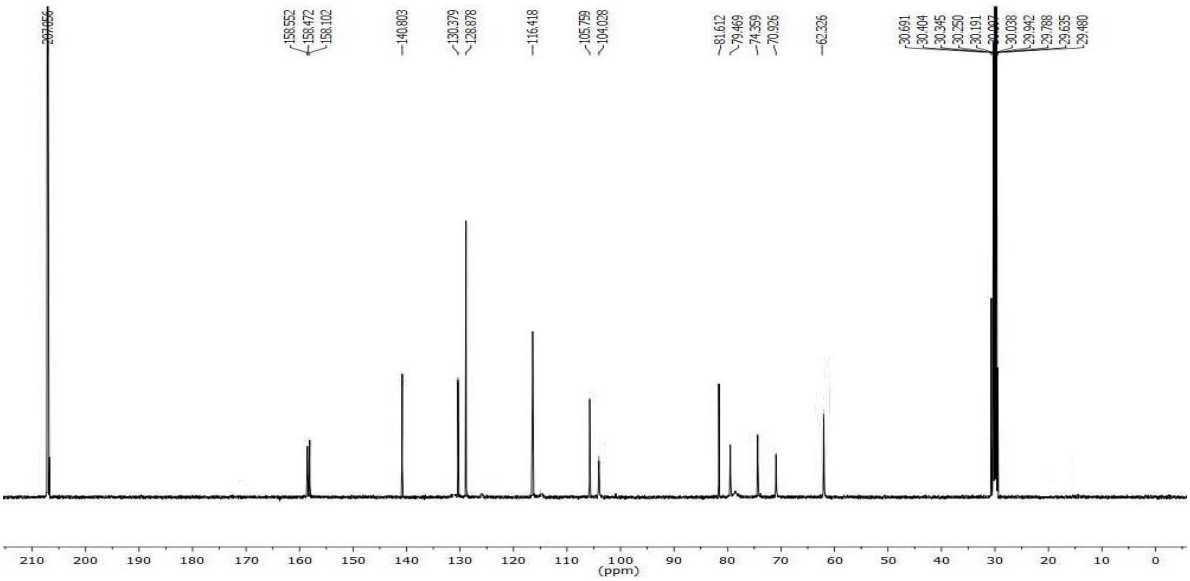

Figure 4.20: ^{13}C NMR spectrum of trihydroxyphenanthrene glucoside

4.5.4. Antidiabetic activity of isolated compounds

Diabetes is a chronic disorder associated with the metabolism of carbohydrate, protein and fat owing to absolute or corresponding deficiency of insulin secretion with or without fluctuating degree of insulin resistance [Defronzo *et al*., **2015**]. According to WHO, the people with diabetes has quadrupled in the world since 1980 and its prevalence is still growing in most regions. Diabetes accounts for 3.7 million deaths in 2012, many of which could be prevented (WHO, 2016). Elevation in the glucose and insulin levels are the

principal features of acquired insulin resistance furnishing remarkably to the pathogenesis of the disease [Huang *et al*., **2002**]. The skeletal muscle is the cardinal tissue for the insulin stimulated glucose uptake and accounts for approximately 80 % absorption presenting its role in energy balance. Type 2 diabetes patients unveil a reduction in insulin stimulated glucose uptake in skeletal muscles [Bailey and Turner **2004**]. Throughout the past, different medicaments and drugs have been used to treat Diabetes mellitus, including insulin, prior to realization of its mechanism of action. A few of them has been included in the therapeutic array of medicine and some are used as combination therapy in patients with hyperglycemia in which most of them have been acquired from plants or microbes [Rios *et al*., **2015**]. Polyphenols impart relevant protection against the progression of many chronic conditions which include diabetes, cancer, cardiovascular disease, etc. [Pandey and Rizvi **2009**]. Diabetes and its associated complications could be minimized by plant derived polyphenols according to the recent studies on account of its diverse biological effects [Bhattacharya and Sil **2018**].

As part of our ongoing search for novel antidiabetic agents of plant origin, [Ajish *et al*., **2014**; Sasikumar *et al*., **2016**] acetone and ethanol extracts of the stem bark of *H. ponga*, were used for the present study. Antidiabetic activity of different extracts and successive compound(s) level *in vitro* antidiabetic assays are described. This plant was hitherto uninvestigated and therefore the extracts prepared were subjected to detailed phytochemical investigation followed by *in vitro* antidiabetic studies. The *in vitro* antidiabetic results for the compounds seem to be highly promising and warranted further evaluation.

In order to check the antidiabetic activity of resveratrol oligomers ranging from monomer to tetramers, we examined the *α*-glucosidase, *α*-amylase and glycation inhibitiory properties. The results obtained are summarised in table 4.3. All the tested compounds showed a promising *α*-glucosidase inhibition compared to the standard acarbose. In particular, *E*-resveratrol and *α*-viniferin showed excellent *α*-glucosidase inhibitory activity with IC_{50} values of 12.56 ± 1.00 and 7.17 ± 1.10 μM, respectively. The results also showed that *α*-viniferin effectively inhibited α-amylase (IC_{50} 4.85 ± 0.06 μM) which was higher than that of acarbose used (IC_{50} 8.99 ± 0.48 μM). The higher level of glucose in the blood increases the glycation of proteins which leads to the formation of advanced glycated end

products (AGEs). These AGEs play a key role in the pathogenesis of diabetic complications like retinopathy, nephropathy, neuropathy, cardiomyopathy etc. From our study, it is evident that *E*-resveratrol, (-)-*ε*-viniferin, (-)-*α*-viniferin, THPG and Vaticaphenol A possessed prominent antiglycation activity (IC_{50} 125.92 ± 0.53, 27.10 ± 0.04, 84.45 ± 0.46 and 35.78 ± 0.37 µM, respectively) (Figure 4.21 and Table 4.3).

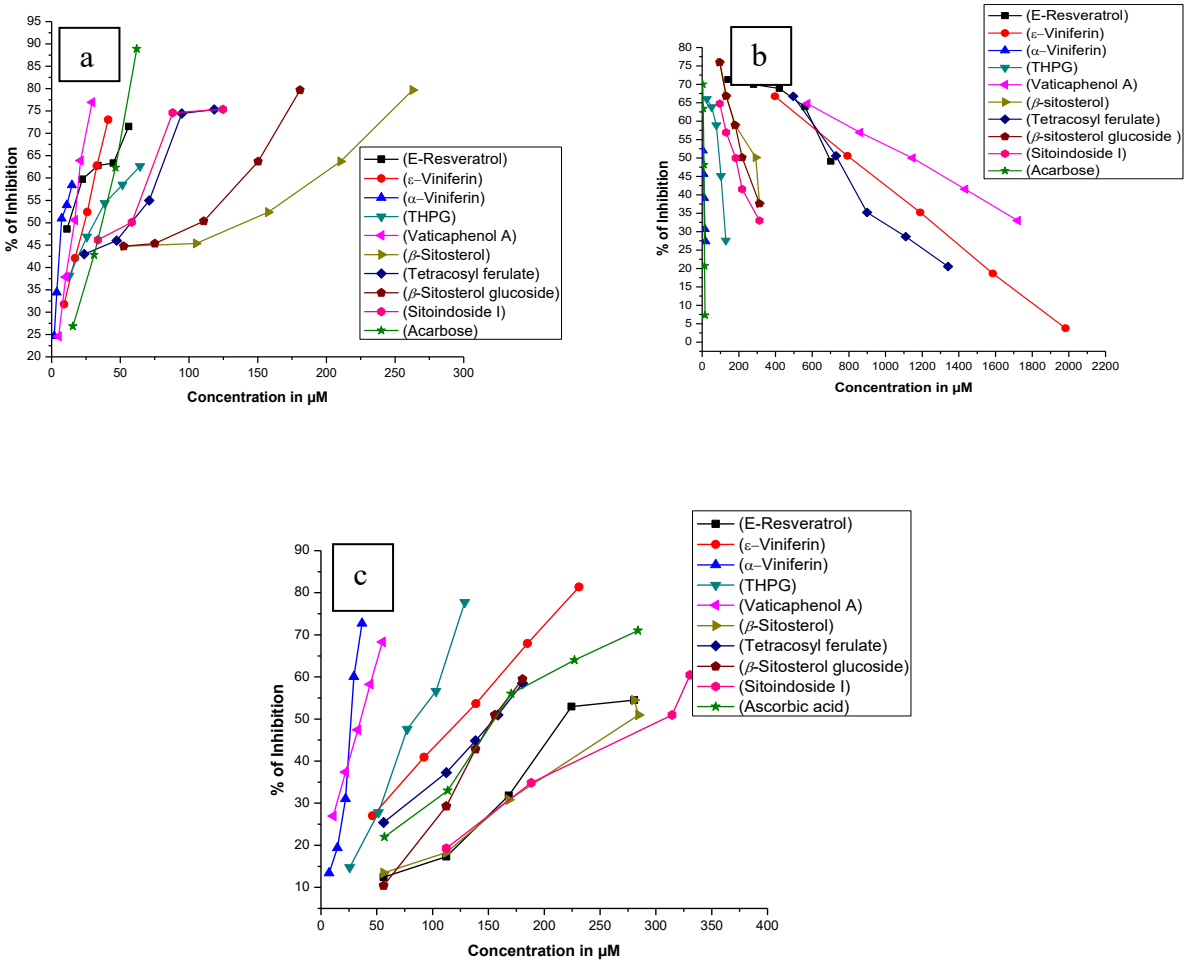

Figure 4.21: a) *α*-Glucosidase, b) *α*-amylase c) glycation inhibition activity of isolated compounds

Table 4.3. Antidiabetic activity of isolated compounds

Compounds	*α*-Glucosidase inhibition (IC_{50} µM ± SD)	*α*-Amylase inhibition (IC_{50} µM ± SD)	Antiglycation (IC_{50} µM ± SD)
E-Resveratrol	12.56 ± 1.00	690.50 ± 0.05	218.25 ± 0.05
ε-Viniferin	23.98 ± 1.11	793.64 ± 0.18	125.92 ± 0.53
α-Viniferin	7.17 ± 1.10	4.85 ± 0.06	27.10 ± 0.04
THPG	31.74 ± 0.42	94.53 ± 0.07	84.45 ± 0.46
Vaticaphenol A	16.95 ± 0.39	1139.50 ± 0.17	35.78 ± 0.37
β-sitosterol	145.75 ± 0.79	292.02 ± 0.11	284.48 ± 0.90
Tetracosyl ferulate	58.95 ± 1.29	727.90 ± 0.18	158.90 ± 1.18
β-sitosterol glucoside	110 ± 0.65	218.15 ± 0.05	155.82 ± 1.50
Sitoindoside I	88.37 ± 0.98	182.82 ± 0.75	314.48 ± 0.45
Acarbose	52.87 ± 0.22	8.99 ± 0.48	…….
Ascorbic acid	…….	…….	154.63 ± 0.49

The data is represented as mean ± standard deviation (n=3)

4.5.5. Molecular docking studies

Based on the *in vitro α*-glucosidase inhibitory activity of all the isolated compounds, molecular docking studies of resveratrol oligomers were carried out. Which will help to find possible conformations and orientations of the ligands at the binding site. Studies of the protein-ligand interactions observed using LigPlot helped to identify the polar, hydrophobic, acidic and basic residues easily. It also helped to visualize the solvent exposed ligand atoms and residues in close contact with the ligand atoms as well as side chain and backbone acceptor and donor interactions.

4.5.5.1. Binding interaction studies of compounds with 3A4A

The docking score of (-)-*α*-viniferin was -25.3174 kcal/mol. Binding of (-)-*α*-viniferin had a polar side chain donor interaction between the –OH group and the amino acid residue

Ser180 (3.09 Å, 15 %). No other prominent interactions were observed for this compound, but showed some indirect hydrogen bonding interactions with greasy amino acid residues Pro149 and Phe166. The blue smudges that were drawn behind some of the ligand atoms represent the amount of solvent exposure. No prominent interactions were observed for THPG where the docking score was -22.0623 kcal/mol. The binding mode detected for the compound *E*-resveratrol showed an arene-arene interaction between the ligand and the basic amino acid residue His280. The docking score was found to be -16.8758 kcal/mol.

The compound, (-)-*ε*-viniferin showed a molecular docking score of -20.6144 kcal/mol. The binding interaction of the compound showed an acidic side chain donor interaction between the –OH group and the amino acid residue Asp307 at a distance of 2.14 Å (19 %). The docking score of vaticaphenol A was -27.8206 kcal/mol, which is comparatively very high, this is due to the presence of more hydroxyl group present in them. The binding interaction showed an arene-cation interaction between one of the phenolic group and the basic amino acid residue His280. Some of the –OH groups present in the ligand showed indirect hydrogen bonding interactions with respect to the various amino acid residues. From these docking studies it was found that compounds having more phenolic hydroxyl group could effectively bind to the targeted protein 3A4A with high docking score and thus inhibiting the enzyme.

4.5.5.2. Binding interaction studies of compounds with 3AJ7

The molecular docking of (-)-*α*-viniferin with respect to the protein 3AJ7 gave a comparatively high docking score of -25.0834 kcal/mol and the binding interaction showed two prominent interactions. One was an arene-arene interaction between the ligand and a basic amino acid residue His280 and another was a side chain donor interaction with respect to an acidic amino acid residue Asp307 at a distance of 2.29 Å (34 %). It was seen that some of the –OH groups present in the compound gave indirect hydrogen bonding interactions with various amino acid residues. The observed docking results are comparable with the data obtained from *α*-glucosidase inhibition activity. Compound THPG, showed three prominent binding interactions. One was an arene-arene interaction between one of the phenolic group attached to the glucose ring and a basic amino acid residue His280. Another interaction was between one of the –OH groups present in the glucose ring and a greasy amino acid residue

Pro312 and a polar residue Sre240, which gives a backbone donor and side chain donor interactions respectively. One indirect hydrogen bonding interaction was also observed here. The compound showed a docking score of -22.7632 kcal/mol.

The binding mode observed in *E*-resveratrol showed an arene-arene interaction between the benzenediol ring and a basic amino acid residue His280. The docking score was found to be -16.5986 kcal/mol. (-)-ε-Viniferin showed an arene-cation interaction between phenol ring of the ligand and a basic amino acid residue His280. This compound also gave an indirect hydrogen bonding interaction. It showed a molecular docking score of -23.6175 kcal/mol. Vaticaphenol A showed a docking score of -24.3830 kcal/mol. The binding interaction showed a side chain donor interaction between one of the –OH group present in the ligand and an acidic amino acid residue Asp325 at a distance of 2.05 Å (21 %). Table 4.4 represents the molecular docking scores of these compounds on the selected target proteins (Figure 4.22).

Table 4.4. Molecular docking score of resveratrol oligomers

Ligands	**E-SCORE (kcal/mol)**	
	3A4A	**3AJ7**
E-Resveratrol	-16.8758	-16.5986
(-)-ε-Viniferin	-20.6144	-23.6175
(-)-α-Viniferin	-25.3174	-25.0834
THPG	-22.0623	-22.7632
Vaticaphenol A	-27.8206	-24.383

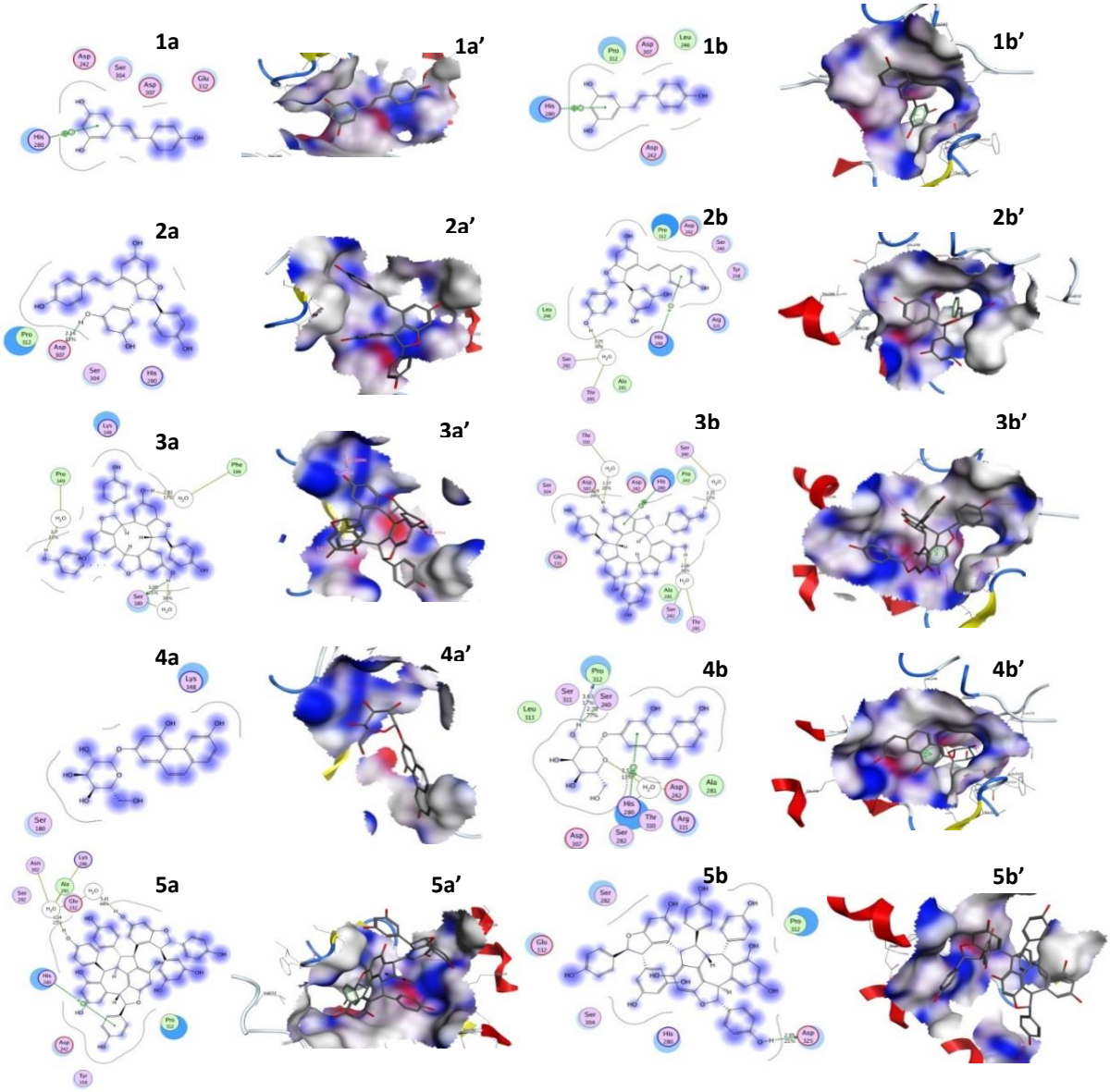

Figure 4.22: 1D and 2D molecular docking interaction studies of compounds [(1a, 1a') and (1b, 1b') are of *E*-resveratrol (**1**); (2a, 2a') and (2b, 2b') *ε*-viniferin (**2**); (3a, 3a') and (3b, 3b') *α*-viniferin (**3**); (4a, 4a') and (4b, 4b') THPG (**4**); and (5a, 5a') and (5b, 5b') vaticaphenol A (**5**) with proteins 3A4A and 3AJ7, respectively].

4.5.6. MTT assay

All the resveratrol oligomers were selected for the cell line based assays owing to their prominent antidiabetic potential in inhibiting the digestive enzymes and protein glycation, whereas the antidiabetic potential of the major compound (-)-hopeaphenol was deliberated in

previous chapter (Chapter 3A). The cytotoxicities of the resveratrol oligomers were measured at different concentrations (25, 50, 75 and 100 µM) by means of MTT assay for 24 h. (-)-*α*-Viniferin was found to be less toxic (<10 %) even at 100 µM concentration. Both (-)-*ε*-viniferin and THPG showed a dose-dependent increase in toxicity (Figure 4.23). THPG showed to be more toxic on increasing concentrations and it is least toxic at a concentration of 25 µM (<20 %). *E*-resveratrol and vaticaphenol A showed a moderate toxicity (<25 %) at 100 µM concentration. These toxicity evaluations helped us to fix a safe dose range for 2-NBDG uptake antidiabetic studies.

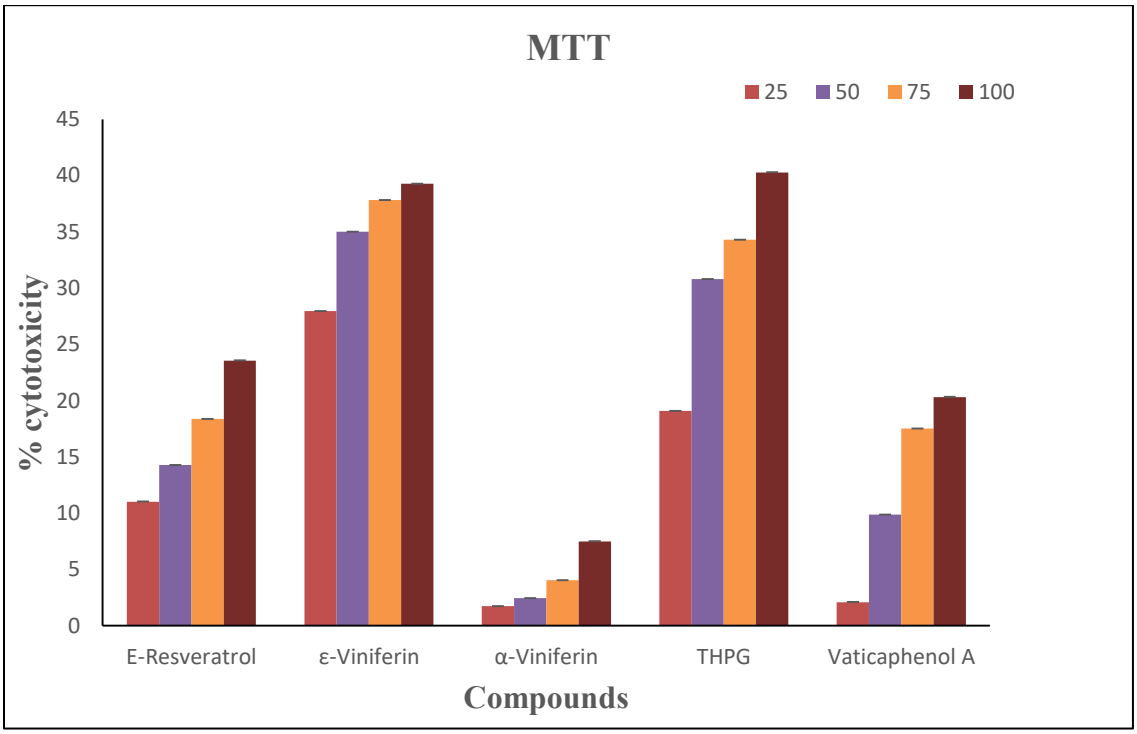

Figure 4.23: MTT cytotoxicity assay of resveratrol oligomers. L6 myoblasts were treated with various concentrations of compounds (0, 25, 50, 75, 100 µM) for 24h and cytotoxicity was determined by MTT assay. All data are represented as means ± SD (n=3)

4.5.7. 2-NBDG assay by flow cytometry

The flow cytometry analysis of 2-NBDG uptake in L6 rat myoblast cells were done by detecting the fluorescence within the cells. After 24 h, the untreated cells showed 24.8 % of glucose uptake. While the cells pretreated with *α*-viniferin (75 µM), vaticaphenol A (75 µM), and THPG (25 µM) remarkably increased the glucose uptake by 49.6 %, 45.2% and 38.8 %

respectively, which is higher than that of metformin standard (100 µM), showed only 36 % (Figure 4.24). Whereas 75 µM of *E*-resveratrol and 25 µM of (-)-ε-viniferin increased the glucose uptake by 32.5 % and 34.9 % respectively. Herein, antidiabetic potential of resveratrol oligomers were reported for the first time. Both α-viniferin and THPG demand further molecular studies for finding the underlying pathway of inducing glucose uptake in the cells.

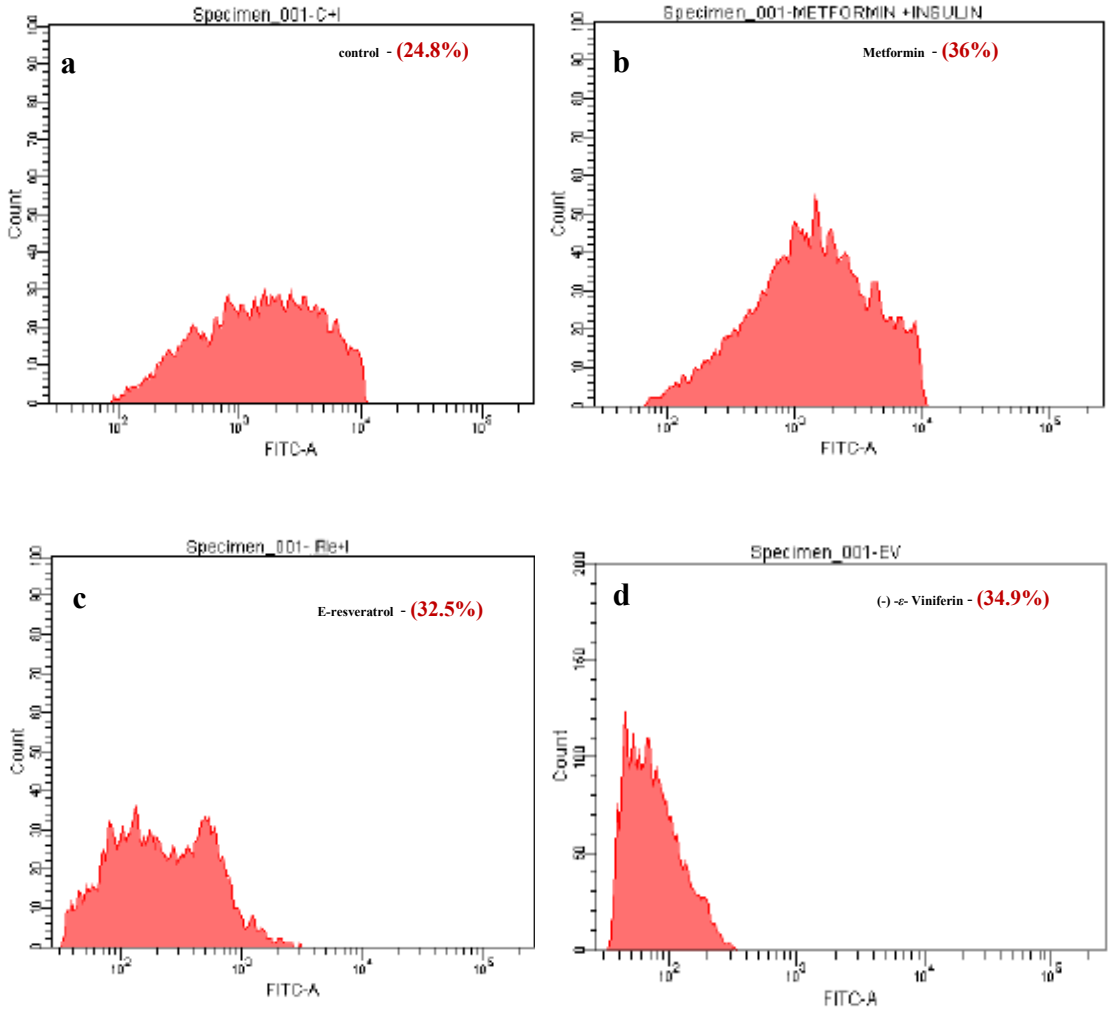

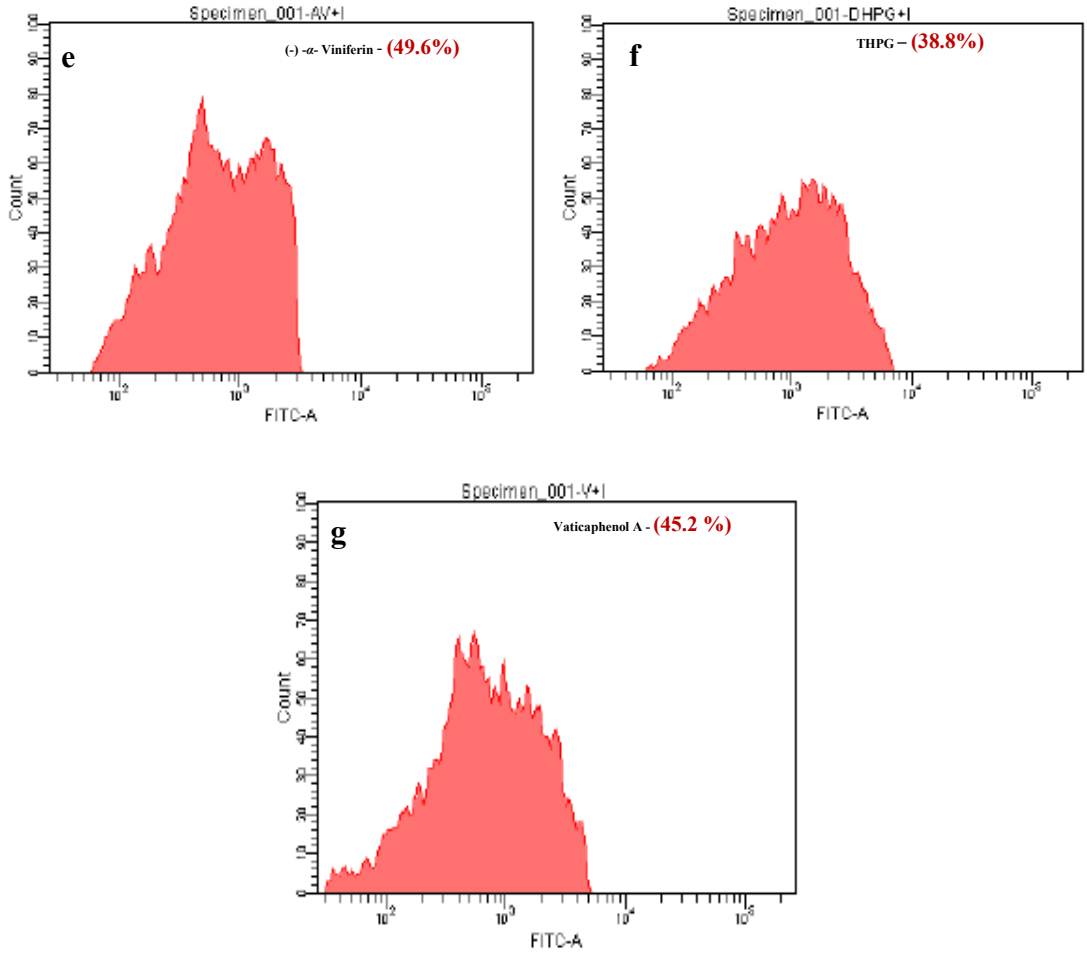

Figure 4.24: 2-NBDG assay by flow cytometry in L6 rat myoblast cells: The representative histogram shows cells with fluorescent intensity (539 nm emission) which indicates the 2-NBDG uptake. FITC histograms in (**a**) untreated cells (24.8 %); (**b**) 100 µM metformin (36 %); (**c**) 75 µM *E*-resveratrol (32.5 %); (**d**) 25 µM (-)-*ε*-viniferin (34.9 %); (**e**) 75 µM (-)-*α*-viniferin (49.6 %); and (**f**) 25 µM THPG (38.8 %); (**g**) 75 µM vaticaphenol A (45.2 %). Data are representative histograms from three independent experiments.

4.6. Separation and identification of volatile components and fatty acids from *Hopea ponga* seed by GCMS analysis

4.6.1. Preparation of extract and GCMS analysis

The seeds were shadow dried and it was made as a powder. About 1 g of the dried seeds was extracted with acetone (GC grade) and kept for 24 h. Then the extract was filtered by using PTFE syringe filter. This extract was used for the GC-MS analysis to find the bioactive components. 1µL of sample was injected in to a GC equipped with a MS (GCMS-TQ8030

SHIMADZU) and a medium polar capillary column Rxi-5Sil MS, (30m X 0.25mm I. D., 0.25µm), the oven program had an initial temperature of 60^{o}C for 2 min, increased to 200^{o}C for 2min at the rate of 5^{o}C /min followed by the temperature was increased to 220^{o}C for 1min at the rate of 3^{0}C /min. Finally temperature was increased to 250 at the rate of 6^{o}C /min for 7min. Total run time was 50min.

The essential chemical constituents were identified by matching mass spectra with spectra of reference compounds in mass spectral library of NIST and WILEY. The relative amounts of individual components were expressed as percentage peak areas relative to total peak area. GCMS profile of *H. ponga* seeds shown in figure 4.25. The major phytochemicals identified *viz.,* bicycloelemene **42** (6.21 %) (RT = 16.69, *m/z* = 204.3510), ethylcyclopropanecarboxylate **43** (4.44 %) (RT = 16.85, *m/z* = 114.1424), α-copaene **44** (0.69 %) (RT = 17.80, *m/z* = 204.3510), caryophyllene **45** (5.67 %) (RT = 19.00, *m/z* = 204.3510), 1H-cycloprop(e)azulene **46** (5.36 %) (RT = 19.50, *m/z* = 204.3510), α-gurjunene **47** (1.00 %) (RT = 19.80, *m/z* = 204.3510), α-humulene **48** (1.54 %) (RT = 19.90, *m/z* = 204.3510), β-selinene **49** (3.88 %) (RT = 20.80, *m/z* = 190.3224), myristic acid **50** (0.75 %) (RT = 26.88, *m/z* = 228.3709), palmitic acid **51** (16.88 %) (RT = 31.16, *m/z* = 256.4220), stearic acid **52** (10.56 %) (RT = 35.38, *m/z* = 284.4772), oleic acid **53** (12.08 %) (RT = 35.66, *m/z* = 282.4613) and 1-heptacosanol **54** (3.89 %) (RT = 48.46, *m/z* = 396.7329) figure 4.26.

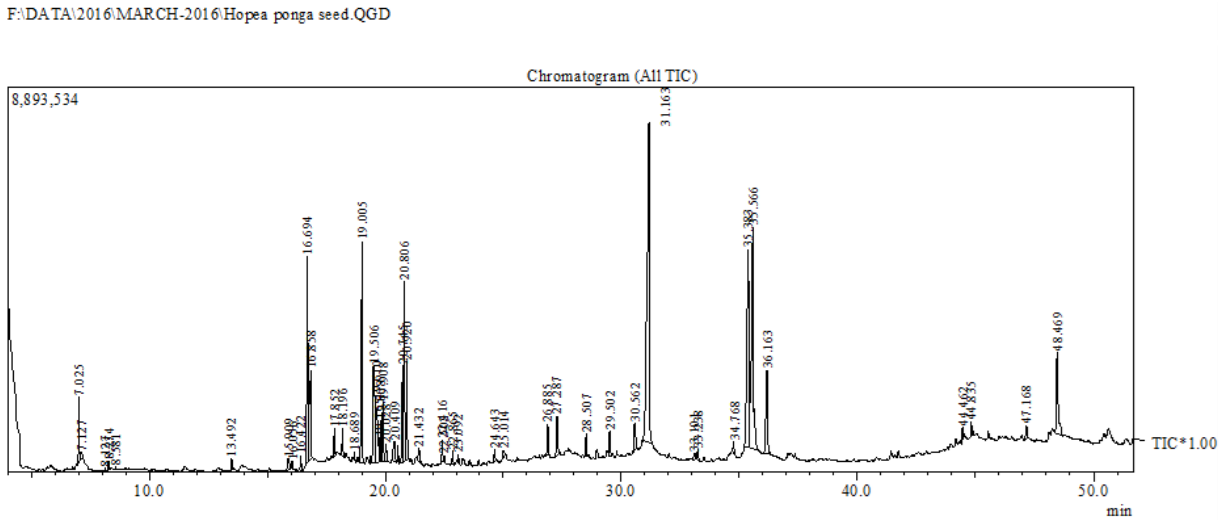

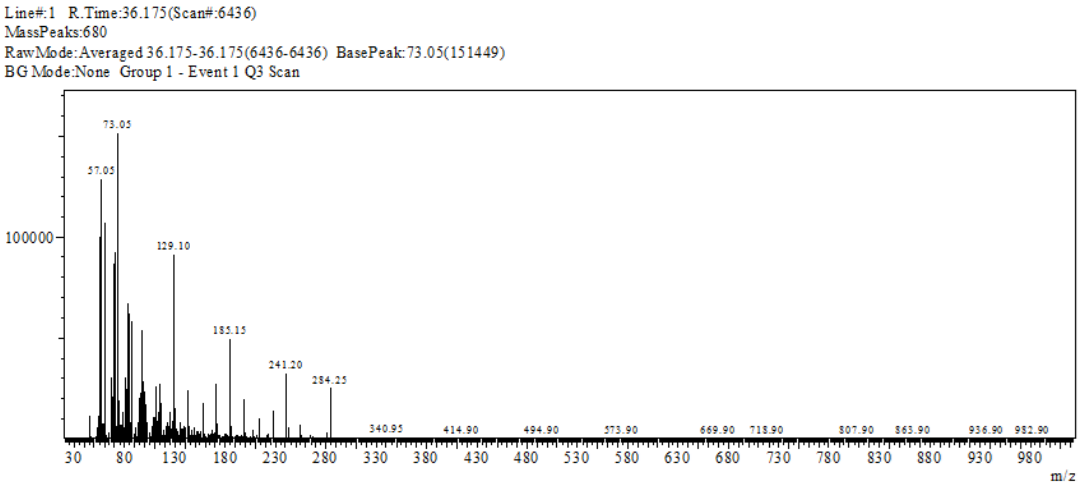

Figure 4.25: GCMS spectrum of *H. ponga* seed acetone extract

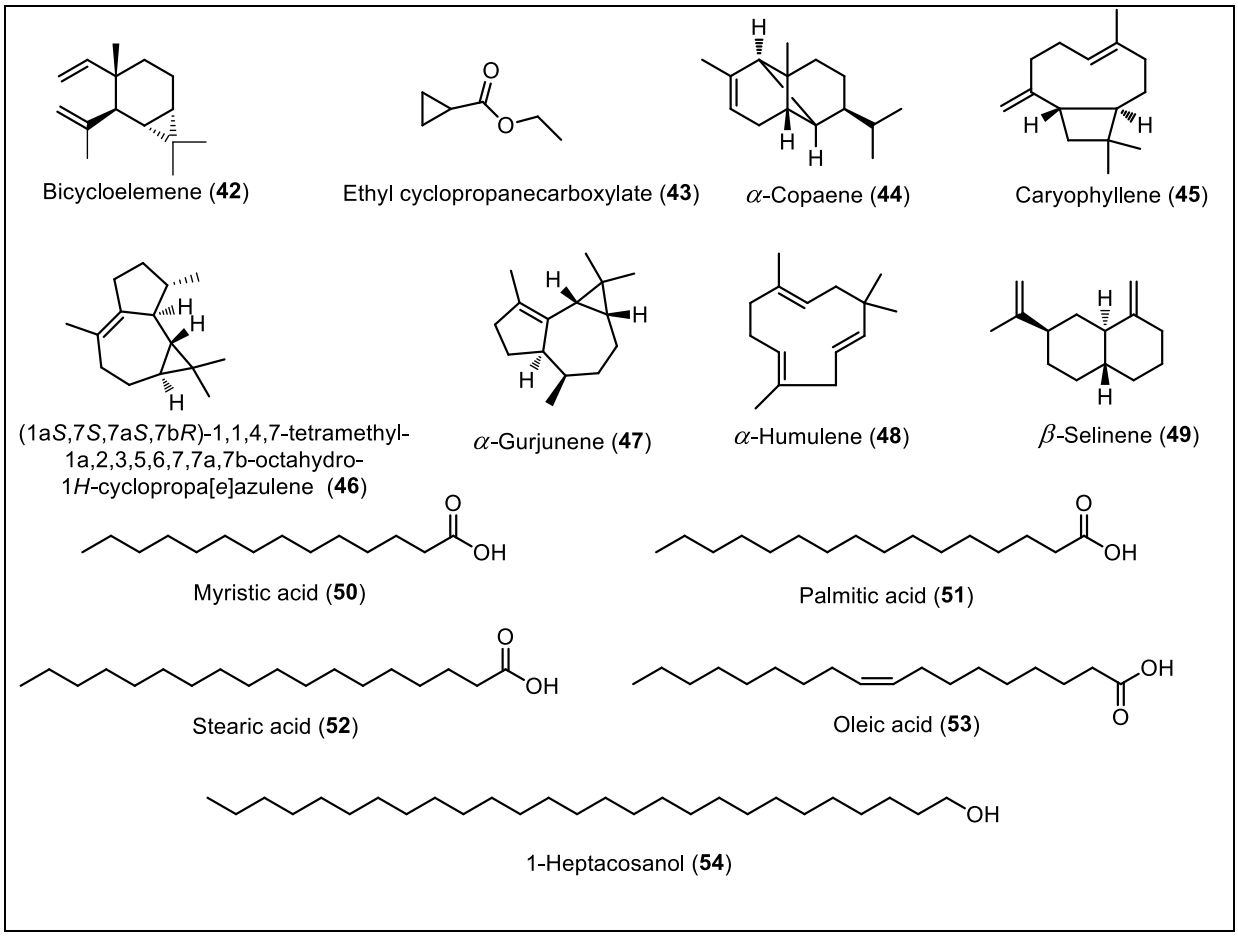

Figure 4.26: Structure of volatile compounds and fatty acids **(42-54)**

4.7. Conclusion

In this chapter, we have isolated and structurally characterized 10 compounds from the stem bark of *H. ponga viz*., *E*-resveratrol, (-)-*ε*-viniferin, (-)-*α*-viniferin, vaticaphenol A, (-)-hopeaphenol, *β*-sitosterol, tetracosyl ferulate, *β*-sitosterol-3-O-*β*-D-glucopyranoside, sitoindoside I and THPG. To the best of our knowledge, chemical constituents from *H. ponga* and their antidiabetic activity are reported for the first time. In particular, (-)-*α*-viniferin, showed a prominent *α*-glucosidase, *α*-amylase and glycation inhibitory activities. Molecular docking studies demonstrate that the resveratrol oligomers bind effectively with the target proteins. It is also interesting to observe that both *α*-viniferin, vaticaphenol A and THPG, signifcantly increased glucose uptake in cells. The increased glucose uptake by *α*-viniferin, vaticaphenol A and THPG may be either by AMPK activation or due to PI3-K/Akt mediated pathways, eventually leading to translocation of glucose transporter (GLUT-4) to the cell membrane which could be revealed through molecular pathway studies. In addition, we are reporting the GCMS analysis of acetone extract of *H. ponga* seeds lead to the identification of 13 major compounds including sesquiterpenes and fatty acids for the first time.

4.8. Experimental session

General experimental details and procedure for antidiabetic activity studies are given in Chapter 2 and Chapter 3B.

4.8.1. Extraction of *H. ponga* stem bark

The stem bark of *H. ponga* was collected from Wayanad district, Kerala. This was thoroughly cleaned and dried in drier maintained at 50^{o} C and powdered. The powdered stem bark (1.2 kg) was subjected to repeated extraction using hexane, acetone, ethanol and water (2.5 L X 48 h) at room temperature. After extraction, the solvent was removed under reduced pressure using Büchi rotary evaporator. The acetone extract (100 g) and ethanol extract (25 g) was then subjected to column chromatographic separation.

4.8.2. Isolation of compounds from *H. ponga* stem bark

The acetone extract (100 g) of the stem bark of *H. ponga* dissolved in minimum quantity of acetone and was adsorbed in silica gel (100-200) loaded on the top of silica gel column filled with slurry of 100-200 mesh silica gel in hexane. The column was eluted successively with gradient mixtures of hexane and ethyl acetate of increasing polarities and finally with 10

% methanol in ethyl acetate. A total of 220 fractions of approximately 200 mL each were collected. According to the similarity in TLC, they were pooled into 40 major fraction pools (FrA.1- FrA. 40). Ethanol extract (25 g) was subjected to column chromatographic purification using silica gel (100-200 mesh) with gradient elution. A total of 25 fractions of approximately 200 mL each were collected. According to the similarity in TLC, they were pooled into 8 major fraction pools (FrE.1- FrE.8). Pictorial representation of the procedure for the isolation of the compound is shown in figure 4.27.

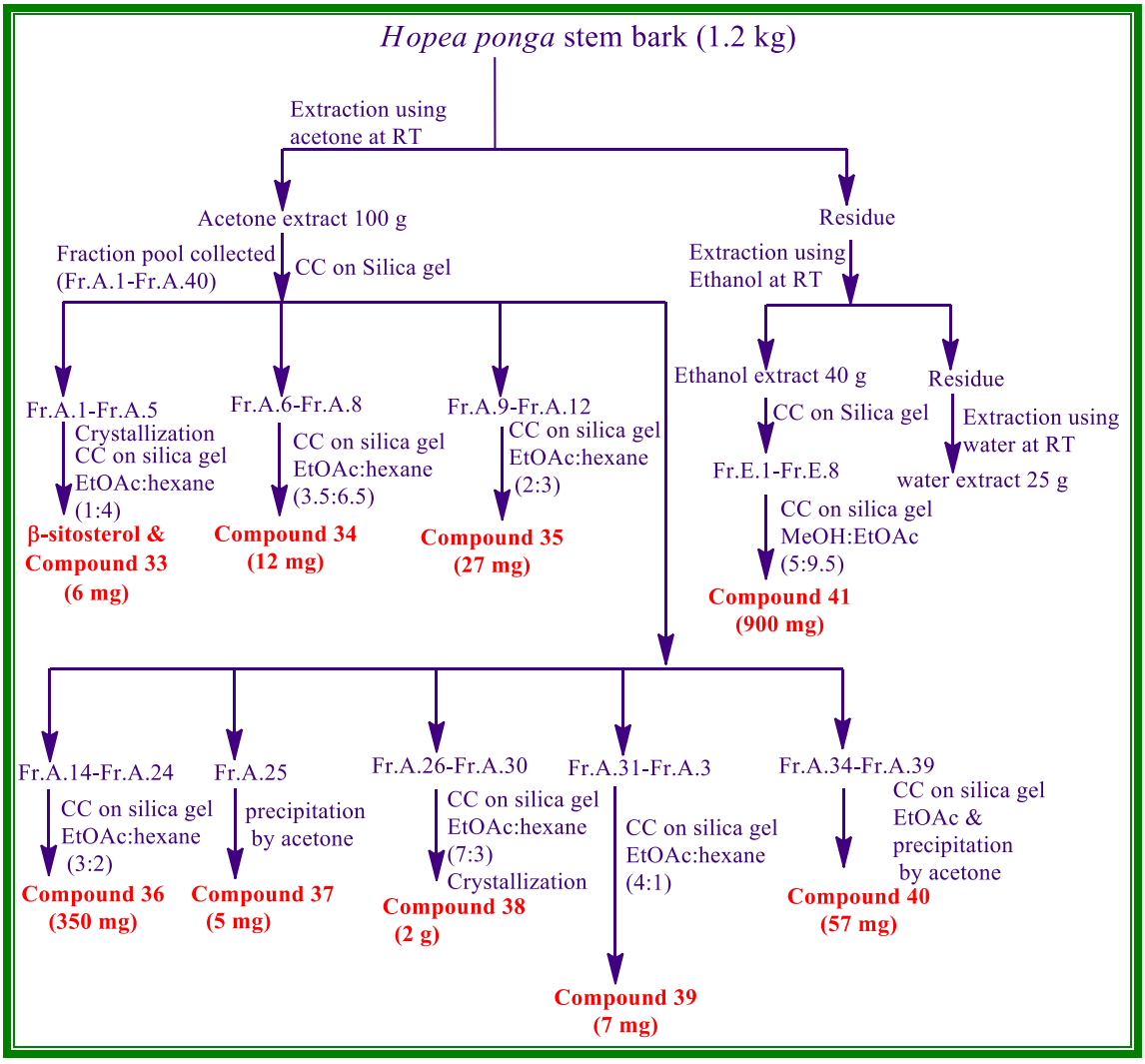

Figure 4.27: Pictorial representation of isolation of compounds from *H. ponga* stem bark

4.8.3. Isolation of compound 33

The isolation procedure of compound **33** is represented in figure 4.27. Compound **33** (6 mg) was obtained as a white pasty mass, on eluting the column with 20 % ethyl acetate in

hexane. IR, ^{1}H NMR, ^{13}C NMR and mass spectral studies of this compound and in comparison with literature values [Xiang *et al*., **2008**], confirmed it to be tetracosyl ferulate.

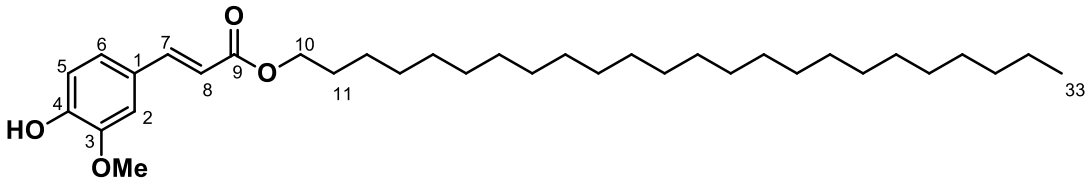

Melting point	:	270-272 ^{o}C
FT-IR (NaCl) υ_{max}	:	3411, 2924, 2858, 1582, 1506, 1440, 1379, 1143 cm^{-1}.
^{1}H NMR (500 MHz, $CDCl_3$)	:	δ 7.61 (d, *J* = 16 Hz, 1H, H-7), 7.07 (d, *J* = 8 Hz, 1H, H-6), 7.04 (d, *J* = 1.5 Hz, 1H, H-2), 6.92 (d, *J* = 8 Hz, 1H, H-5), 6.29 (d, *J* = 16 Hz, 1H, H-8), 5.88 (s, 1H, 4-OH), 4.19 (t, *J* = 6.5 Hz, 2H, H-10), 3.93 (s, 3H, 3-OMe), [2.36-2.31 (m, 5H), 1.70-1.66 (m, 4H), 1.63-1.59 (m, 19H), 1.39-1.34 (m, 15H), (other aliphatic protons)], 0.88 (t, *J* = 7 Hz, 3H, CH_3-33) ppm.
^{13}C NMR (125 MHz, $CDCl_3$)	:	δ 166.5 (C-9), 147.9 (C-4), 146.7 (C-3), 144.7 (C-7), 127.2 (C-1), 123.0 (C-5), 115.7 (C-2), 114.7 (C-8), 109.3 (C-6), 60.4 (C-10), 55.9 (C-3 OMe), [34.2, 31.9, 30.9, 29.7, 29.1, 26.0, 24.9, 22.7, 21.0, 14.2 (Other aliphatic carbons)], 14.1 (C-33) ppm.
HR-ESIMS m/z	:	531.4345 $[M+H]^+$ (calcd for $C_{34}H_{59}O_4$, 531.4345)

4.8.4. Isolation of compound 34

Compound **34** (12 mg) was obtained as a light brown colour solid, on eluting the column with 30 % ethyl acetate in hexane. IR, ^{1}H NMR, ^{13}C NMR and mass spectral studies of this compound and in comparison with compound **1**, previously isolated from *A. indica* rhizome [Chapter 2], confirmed it to be *E*-resveratrol.

4.8.5. Isolation of compound 35

Compound **35** (27 mg) was obtained as a yellowish amorphous solid, on eluting the column with 40 % ethyl acetate in hexane. IR, ^{1}H NMR, ^{13}C NMR and mass spectral studies

of this compound and in comparison with compound **19**, previously isolated from *V. indica* stem bark [Chapter 3A], confirmed it to be (-)-*ε*-viniferin.

4.8.6. Isolation of compound 36

350 mg of compound **36** was obtained as a pale yellow solid on repeated purification of the fraction pool 14-24 (Fr. A.14-24). Compound **36** was characterized as the resveratrol trimer, (-)-*α*-viniferin based on the spectral data obtained as given below and comparison with literature reports.

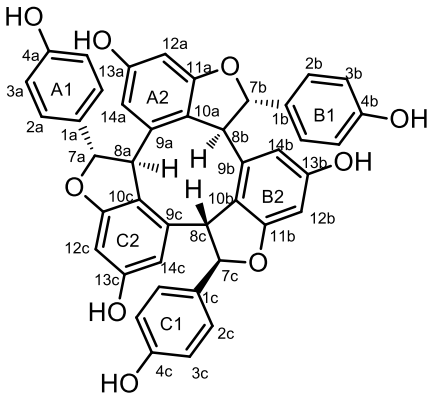

Melting point	:	231 ^{o}C
$[\alpha]^{25}_{D}$	:	-49^{o} (c 0.1, MeOH)
FT-IR (NaCl) υ_{max}	:	3389, 2927, 2853, 1698, 1614, 1514, 1443, 1365, 1240, 1172, 1120, 1073, 998, 834, 771 cm^{-1}.
^{1}H NMR (500 MHz, CD_3COCD_3)	:	δ 8.42 (bs, 1H, -OH), 8.37 (bs, 1H, -OH), 8.31 (bs, 1H, -OH), 8.24(bs, 1H, -OH), 8.22 (bs, 1H, -OH), 8.21 (bs, 1H,-OH), 7.07 (d, *J* = 8.5 Hz, 2H, H-2a, H-6a), 6.91 (t, *J* = 8.5 Hz, 4H, H-2b, H-6b, H-2c, H-6c), 6.65 (d, *J* = 8.5 Hz, 2H, H-3a, H-5a), 6.64 (d, *J* = 8.5 Hz, 2H, H-3b, H-5b), 6.59-6.58 (m, 3H, H-3c, H-5c, H-14c), 6.46 (d, *J* = 2.0 Hz, 1H, H-14a), 6.12 (d, *J* = 2 Hz, 1H, H-12c), 6.10 (d, *J* = 2.0 Hz, 1H, H-12a), 6.09 (d, *J* = 2 Hz, 1H, H-14b), 5.94 (s, 1H, H-7c), 5.86 (d, *J* = 2 Hz, 1H, H-14c), 5.82 (d, *J* = 10 Hz, 1H, H-7a), 4.77 (d, *J* = 6.5 Hz, 1H, H-7b), 4.57 (d, *J* = 10 Hz, 1H, H-8a), 4.48 (d, *J* = 6.5 Hz,

1H, H-8b), 3.83 (s, 1H, H-8c) ppm.

^{13}C NMR (125 MHz, CD_3COCD_3)	:	δ 162.6 (C-OH), 161.8 (C-11b), 161.7 (C-11a), 160.7 (C-11c), 159.4 (C-OH), 158.4 (C-OH), 158.3 (C-OH), 159.4 (C-OH), 157.9 (C-OH), 141.3 (C-9b), 139.8 (C-9c), 138.8 (C-9a), 132.6 (C-1b), 132.1 (C-1a), 131.9 (C-1c), 128.7 (C-2b, C-6b), 128.2 (C-2a, C-6a), 128.1 (C-2c, C-6c), 120.9 (C-10c), 119.8 (C-10a), 118.9 (C-10b), 116.1 (C-3a, C-5a, C-3b, C-5b), 115.7 (C-3c, C-5c), 108.6 (C-14b), 106.3 (C-14c), 105.8 (C-14a), 98.1 (C-12b), 96.9 (C-12a), 95.7 (C-7b), 90.0 (C-7a), 86.5 (C-7c), 55.7 (C-8b), 52.9 (C-8a), 46.4 (C-8c) ppm.
HR-ESIMS m/z	:	679.1967 $[M+H]^+$ (calcd for $C_{42}H_{31}O_9$, 679.1968)

NMR Spectral assignments were made on the basis of 1D and 2D NMR analysis and in comparison with the literature reports.

4.8.7. Isolation of compound 37

Fraction pool 25 (FrA.25) which on precipitation by using acetone, a white pasty mass of compound **37** (5 mg) was yielded. The structure of the compound **37** was confirmed in comparison with the NMR data of compound **17**, namely sitoindoside I, which was previously isolated from *Vateria indica* stem bark.

4.8.8. Isolation of compound 38

Compound **38** (2 g) was obtained as a white solid by eluting the column with 70 % ethyl acetate in hexane. On evaluation of the structure of compound **38** and in comparison with 1D and 2D NMR spectrum, it was confirmed as (-)-hopeaphenol which was isolated earlier from the stem bark of *V. indica* (Chapter 3A, Compound **20**).

4.8.9. Isolation of compound 39

Figure 4.27 represents the isolation procedure for compound **39**. It was obtained as a brown solid. Detailed investigation of various spectroscopic data of compound **39** revealed that it was vaticaphenol A. Further evidence was made by comparing the 1D and 2D NMR data with that of compound **21** isolated earlier from the stem bark of *V. indica*.

4.8.10. Isolation of compound 40

Fraction pool 34-39 was subjected to precipitattion by using acetone afforded compound **40** (57 mg) which was confirmed to be ***β*-sitosterol-3-*O*-*β*-D-glucopyranoside**, earlier isolated from *A. indica* rhizome.

4.8.11. Isolation of compound 41

Crude brown solid (1.5 g) precipitated from ethanol fraction FrE.1-6 were chromatographed over silica gel (MeOH/EtOAc of increasing polarity) to give a compound **41** THPG, (900 mg) as a brown solid.

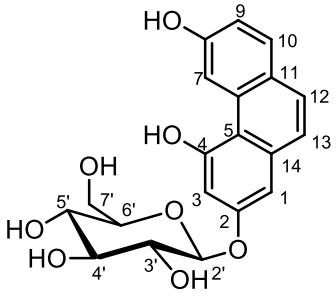

Melting point	:	260 ^{o}C
FT-IR (NaCl) υ_{max}	:	3349, 2925, 1695, 1600, 1512, 1450, 1360, 1235, 1148, 1148, 1081, 1016, 897 cm^{-1}.
^{1}H NMR (500 MHz, CD_3COCD_3)	:	δ 8.25 (bs, 1H, OH), 7.52 (bs, 1H, OH), 7.40 (d, *J* = 8.5 Hz, 2H,, H-10, H-12), 6.83 (d, *J* = 6 Hz, 2H, H-9, H-13), 6.82 (s, 1H, H-7), 6.62 (d, *J* = 2.5 Hz, 1H, H-1), 6.27 (d, *J* = 2.5 Hz, 1H, H-3), 4.97 (d, *J* = 9.5 Hz, 1H, H-2'), 4.51 (bs, 2H, -OH), 4.36 (bs, 1H, -OH), 4.19 (bs, 1H, -OH), [3.87-3.49 (m, 6H, Protons from glucose ring)] ppm.
^{13}C NMR (125 MHz, CD_3COCD_3)	:	δ 158.6 (C-8), 158.5 (C-4), 158.1 (C-2), 140.8 (C-5, C-6), 130.4 (C-7), 128.9 (C-10, C-12, C-11, C14, merged), 116.4 (C-9, C-13), 105.8 (C-1), 104.0 (C-3), 81.6 (C-2'), [79.5, 74.4, 70.9, 62.3 (Other carbons from glucose ring)] ppm.

HR-ESIMS m/z : 411.1056 $[M+Na]^+$ (calcd for $C_{20}H_{20}NaO_8$, 411.1055)

4.8.12. Identification of fatty acids and sesquiterpenes 42-54

The major fatty acids and sesquiterpenes were identified by GCMS analysis and matching mass spectra with spectra of reference compounds in mass spectral library of NIST and WILEY.

CHAPTER 5

Isolation and antidiabetic screening of phytochemicals from *Artocarpus camansi* Blanco and *Artocarpus lakoocha* Roxb.

5.1. Moraceae-An overview

Moraceae, one of the famous mulberry family comprising about 50 genera and over 1400 species. Most of this species are widespread in tropical and subtropical regions and less in temperate climates. Plants belonging to Moraceae are a rich source of important biologically active molecules, and since many of them find extensive application in traditional systems of medicine, they have been well explored for their phytochemistry and pharmacology. Moraceae family gaining lots of research attention in the recent times for its nutritional and health benefits. Among the genera, *Artocarpus, Morus, Broussonetia, Strebulus Ficus* and *Maclura* are the most important sources of flavonoids and other polyphenols. Of these studies, the majority of work was performed on the economically important *Artocarpus* species [Venkataraman, **1972**; Hakim, **2010**]. Flavonoids are widely considered phytoalexins in Moraceae family for their role in plant resistance to fungal pathogens.

5.2. *Artocarpus*

The genus *Artocarpus* (Moraceae) comprises about 50 species of evergreen and deciduous trees. A number of *Artocarpus* species are used as food and for traditional folk medicines in South-East Asia, Indonesia, Western part of Java and India [Perry, **1980**; Heyne, **1987**]. The genus *Artocarpus* is gaining lots of research attention in the recent times for its nutritional and health benefits [Swami *et al*., **2012**]. It has been established by lot of research groups by the consumption of tropical fruits can reduces the risk of fast growing diseases like diabetes, cancer, coronary heart disease, neurodegenerative ailment [Rajurkar *et al.*, **2012**].

The *Artocarpus* species are rich in phenolic compounds including flavonoids, arylbenzofurans and stilbenoids [Hakim *et al*., **2006**, Jagtap and Bapat **2010**]. The biological

activities such as anti-bacterial [Sato *et al*., **1996**], antimalarial effects [Namdaung *et al*., **2006**], antitubercular activity [Boonphong *et al*., **2007**], antiviral activity [Likhitwitayawuid *et al*., **2005**], antifungal activity [Trindade *et al*., **2006**] and anti-inflammatory activity [Wei *et al*., **2005**], make this phenolic compounds as a potential drug candidates.

5.2.1. Ethnopharmacological relevance

Many species from the *Artocarpus* genus are reported to be used for treatment of inflammation, diabetes, malarial fever, diarrhoea, and tapeworm infection [Perry, **1980**., Heyne, **1987**]. The latex mixed with vinegar promotes healing of abscesses, snakebite and glandular swellings. The leaves and stem barks of many of the *Artocarpus* species have been used to treat asthma, anaemia, diarrhoea, dermatitis, cough and as an expectorant [Balbach and Boarim, **1992**]. The hot aqueous extract of *Artocarpus lakoocha* Roxb. heartwood has been used as a traditional anthelmintic drug for treatment of tapeworm infection in Thailand [Charoenlarp *et al*., **1981**; Salguero, **2003**]. Fruit pulp and leaves of *Artocarpus camansi* are used as tonic for liver, to treat liver cirrhosis, hypertension and diabetes [Jagtap and Bapat, **2010**].

5.2.2. *Artocarpus camansi*

Artocarpus camansi, (breadnut) has often been considered to be a seeded breadfruit belonging to Moraceae family native to New Guinea and possibly in India. It is utilized as vegetable. The decoction of *A. camansi* leaves is used for diabetes and baths of people with rheumatism. It was also found to be an effective natural product to treat allergic contact dermatitis [Salonga *et al*., **2014**]. *β*-Sitosterol propionate isolated from the hexane extract from the leaves of *A. camansi* showed antidiabetic properties [Nasution *et al*., **2014**]. The extracts of *A. camansi* leaves were considered as highly cytotoxic against the selected human cancer cell lines [Ourlad *et al*., **2015**].

5.2.3. *Artocarpus lakoocha*

Monkey Jack fruit (*Artocarpus lakoocha* Roxb., Moraceae) is a tropical fruit and originated from India. Fruits are highly nutritious and important food item in the human diet and are rich source of vitamins and minerals those act as antioxidant [Jahan *et al*., **2011**]. In several studies it revealed that *A. lakoocha* has many medicinal uses such as anti-inflammatory, antiviral, anticancer and anti-HIV properties [Kirtikar and Basu **2007**].

Figure 5.1: Picture of *Artocarpus camansi* tree, leaves and fruit

5.3. Scientific classification of *Artocarpus camansi* and *Artocarpus lakoocha*

Table 5.1: Scientific classification of *A. camansi* and *A. lakoocha*

Kingdom	***Plantae***	***Plantae***
Phylum	***Tracheophyta***	***Tracheophyta***
Class	***Magnoliopsida***	***Magnoliopsida***
Order	***Rosales***	***Rosales***
Family	***Moraceae***	***Moraceae***
Genus	***Artocarpus***	***Artocarpus***
Species	***A. camansi***	***A. lakoocha***

Figure 5.2: Picture of *Artocarpus lakoocha* tree, leaves and fruit

5.4. Phytochemistry of *Artocarpus* - an overview

An extended literature survey of *Artocarpus* revealed that, it is a rich source of triterpenoids, isoprenylated flavonoids, stilbenes and miscellaneous compounds.

5.4.1. Triterpenoids

Most of the triterpenoids isolated from *Artocarpus* belong to cycloartane group [Barik *et al*., **1994;** Altman *et al*., **1976;** Tsai *et al*., **2013**]. There are 16 cycloartane type triterpenoids reported from *Artocarpus*. The majority of triterpenoids have been reported from the different parts of *A. heterophyllus.* Some of the previously reported cycloartane type triterpenoids from *Artocarpus* genus are summarised in figure 5.3.

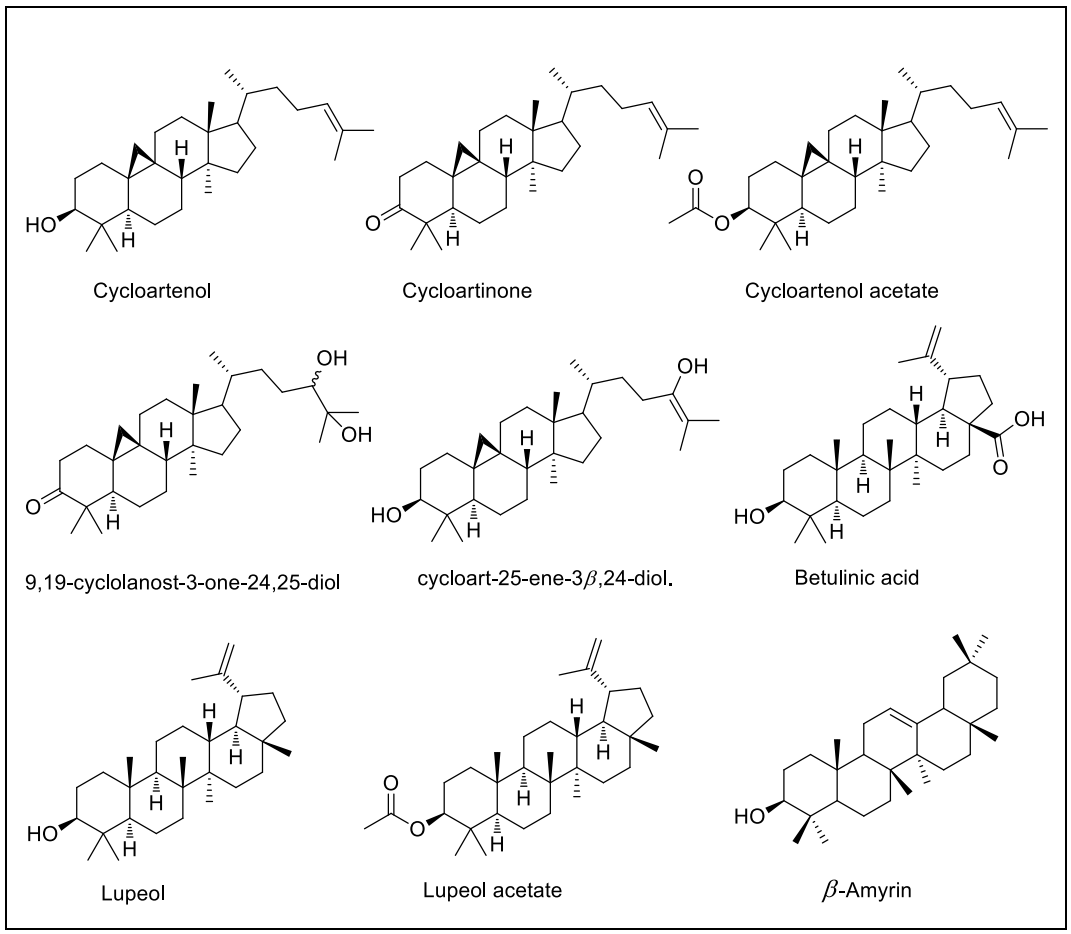

Figure 5.3: Structures of triterpenoids isolated from *Artocarpus*

5.4.2. Flavonoids and prenylated flavonoids

Majority of the flavonoids reported from the genus *Artocarpus* are flavone derivatives. Flavones with mono, di and tri-prenyl as well as dimethyl chromeno and furano derivatives are reported in the genus. Isoprenylated flavonoids are the most abundant class of compounds in *Artocarpus*. The flavonoids from *Artocarpus* are further classified into flavones, flavanones and flavonol glycosides. Some of the reported flavonoids and prenylated flavonoids from *Artocarpus* are shown in figure 5.4 [Zheng *et al*., **2008**; Lu *et al*., **1994**; Hakim, **2010**].

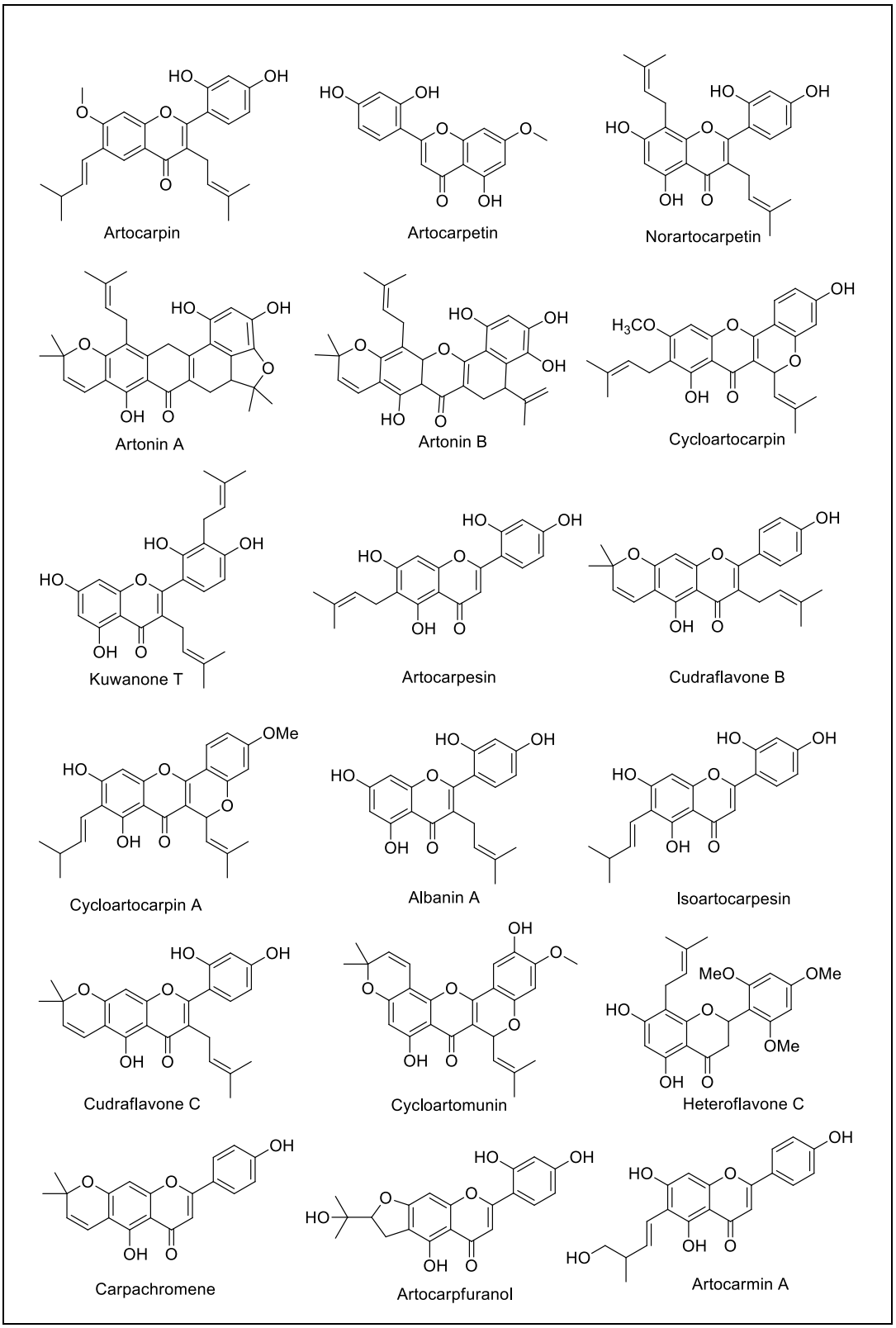

Figure 5.4: Structures of flavonoids and prenylated flavonoids from *Artocarpus*

5.4.2.1. Biosynthetic pathway of flavonoids

Both flavonoids and resveratrols, share a common phenylpropanoid biosynthetic pathway. Phenylalanine, a product of the shikimate pathway, undergoes a series of enzymatic reactions to produce a linear tetraketide. This intermediate is critical for the synthesis of flavonoids through constitutively expressed chalcone synthase (Scheme 5.1).

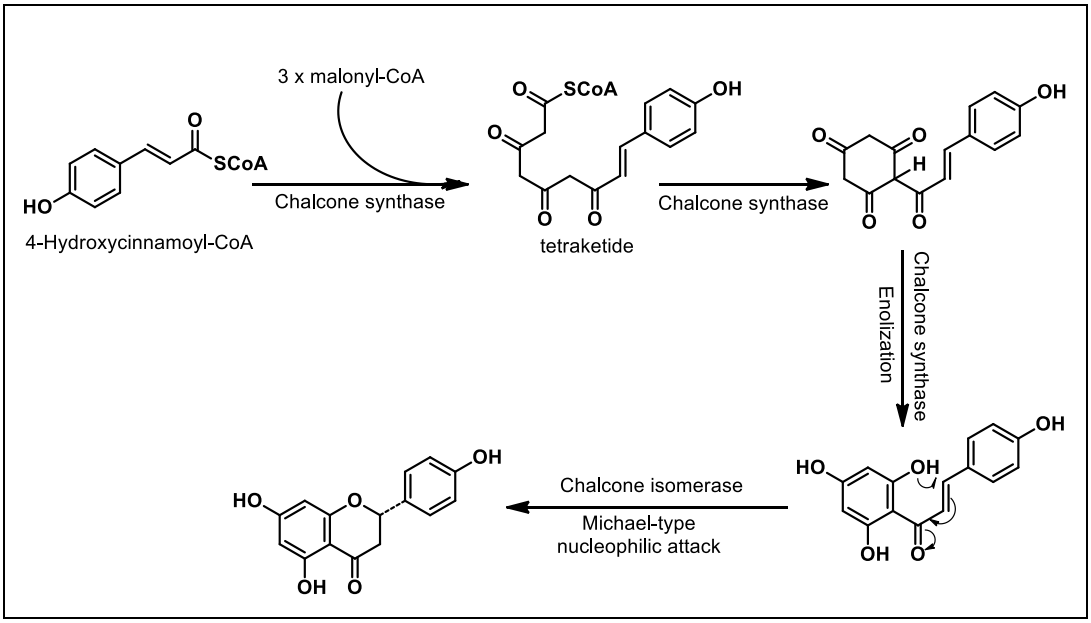

Scheme 5.1: Biosynthetic pathway of flavonoids

5.4.3. Stilbenes and its derivatives

As already discussed in the chapter 2, stilbene monomer is a building block of many of the resveratrol oligomers. In *Artocarpus* genus only prenylated or geranylated stilbenes are reported. Among them tetrahydroxy stilbene (Oxyresveratrol) and its derivatives are the major phytoconstituients.

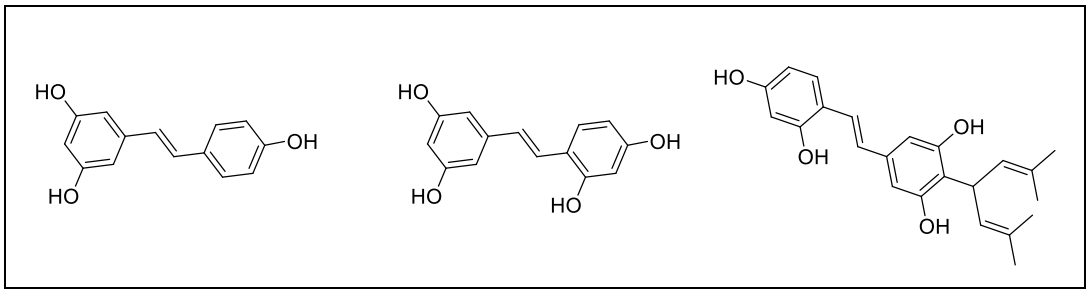

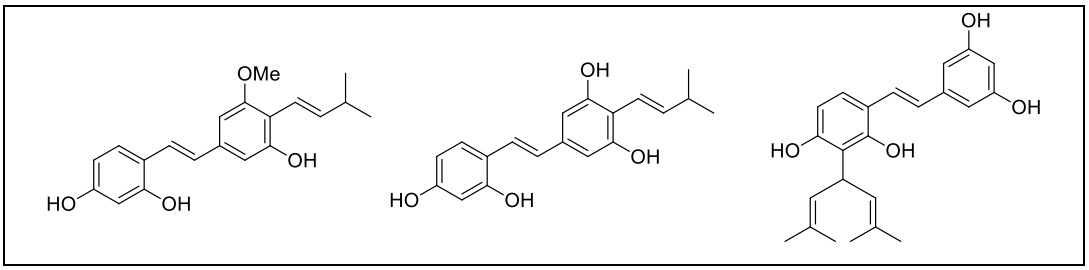

Figure 5.5: Structures of stilbenes and its derivatives from *Artocarpus*

5.5. Aim and scope of the present work

The genus *Artocarpus* is gaining lots of research attention in the recent times for its nutritional and health benefits. It has been established by a number of research groups that consumption of tropical fruits can reduce the risk of fast growing diseases like diabetes, cancer, coronary heart disease, neurodegenerative ailment [Rajurkar and Gaikwad, **2012**]. So as part of this Ph.D. program and due to our continuing interest in the chemical profiling of the plants of ethnobotanical importance [Sasikumar *et al*., **2016**; Ajish *et al*., **2014**], we selected the two plant species namely *A. camansi* and *A. lakoocha*. Even though there are some literatures on the isolation of phytochemicals from these plants, [Tsai *et al*., **2013**; Pandey and Bhatnagar **2009**] it is essential to conduct more scientific research on wild edible fruits that can be further exploited for value added products in the form of neutraceuticals and health products. Evaluation of chemical indices of acetone extract of stem bark of *A. camansi and A. lakoocha*, preliminary *in vitro* antidiabetic potentials of the extracts and the effect of antidiabetic modulation of digestive enzymes, protein glycation and glucose uptake in L6 myotubes of the isolated compounds have been carried out and the results are described in this chapter.

5.6. Extraction and Isolation of the stem bark of *A. camansi* and *A. lakoocha*

5.6.1. Plant material

The stem bark of *Artocarpus camansi* and *Artocarpus lakoocha* were collected from Thrissur and Calicut, Kerala. The plant material was authenticated by the taxonomist of M. S. Swaminathan Research Foundation (MSSRF), Kerala, India and a voucher specimen (Voucher no. M.S.S.H. 1631 and M.S.S.H 1801) were deposited in the herbarium repository of the same institute.

5.6.2. Extraction of *Artocarpus camansi* stem bark

The air-dried stem bark of *A. camansi* (400 g) was extracted successively with acetone (A) and ethanol (E). The supernatant liquid was decanted and filtered. The extracts were then concentrated under reduced pressure in a rotary vacuum evaporator to remove the residual solvent, which yielded 30 g (7.5 %) of acetone (A) and 18 g (4.5 %) (E) of crude ethanol extracts.

5.6.3. Isolation and characterization of compounds from *A. camansi* acetone extract

Based on the TLC analysis further isolation, purification and characterisation of chemical constituents were focused on the acetone extract. The acetone extract (30 g) was fractionated on a silica gel (100-200 mesh) column and eluted with n-hexane/EtOAc gradient (100 % n-hexane to 100 % EtOAc). Each fraction was analyzed by TLC (n-hexane-EtOAc), and those displaying the same TLC profile were combined to afford fourty fractions (FrA.1-FrA.45).

Fraction pools 1-2 (FrA.1-2), obtained by eluting the column with 10 % ethyl acetate in hexane on crystallization using the same solvent yielded the mixture of compound **55** and compound **56.** This was further column chromatographed using Sephadex LH-20 (Methanol), 230 mg (0.06 %) and 135 mg (0.03 %) of white solids were obtained. IR spectrum of the compound **55** showed a broad signal at 1733 cm^{-1}, indicating the presence of ester group. In ^{1}H NMR spctrum, (Figure 5.7) signal at δ 5.10 ppm integrating one proton could be attributed to an olefinic proton. δ 4.57 ppm could be attributed to the proton which is directly attached to the ester group. The diastereotopic methylene protons from the cyclopropane ring was discernable at δ 0.57 and 0.34 ppm. In ^{13}C NMR spectrum, (Figure 5.8) the signal at δ 171.0 ppm is the diagnostic peak for ester carbonyl carbon. The mass spectrum of the compound **55** showed molecular ion peak at m/z 469.4045, which is the $[M+H]^{+}$ peak. From all the above spectral details and in comparison with the literature reports [Teresa *et al*., **1987**; Tsai *et al*., **2013**] the compound was confirmed as **cycloartenol acetate**. The structure of the compound is shown below.

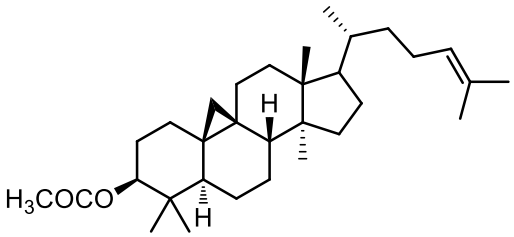

Figure 5.6: Cycloartenol acetate **(55)**

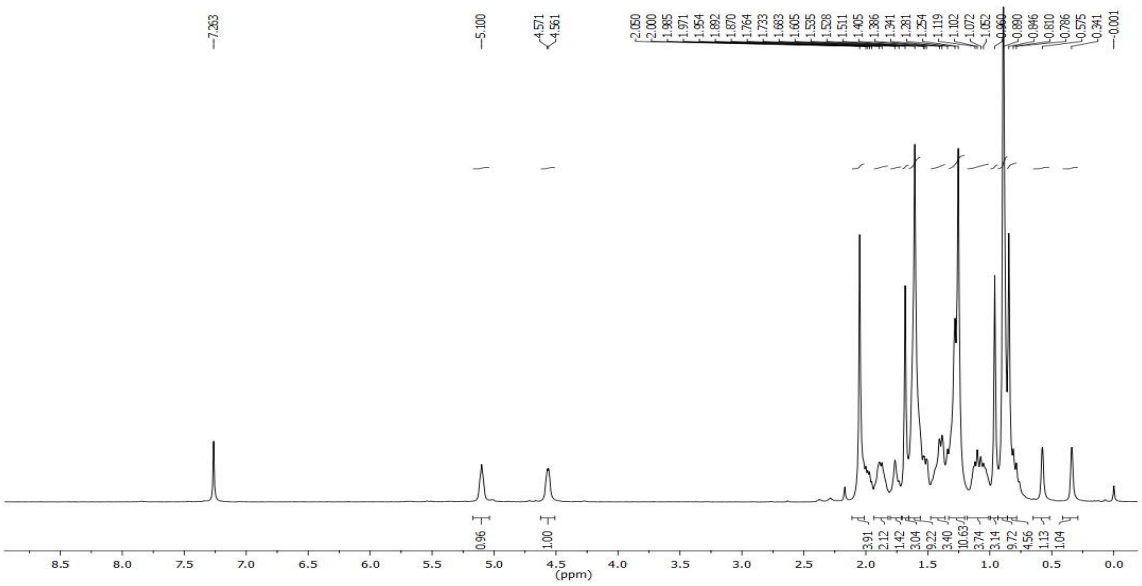

Figure 5.7: ^{1}H NMR spectrum of cycloartenol acetate

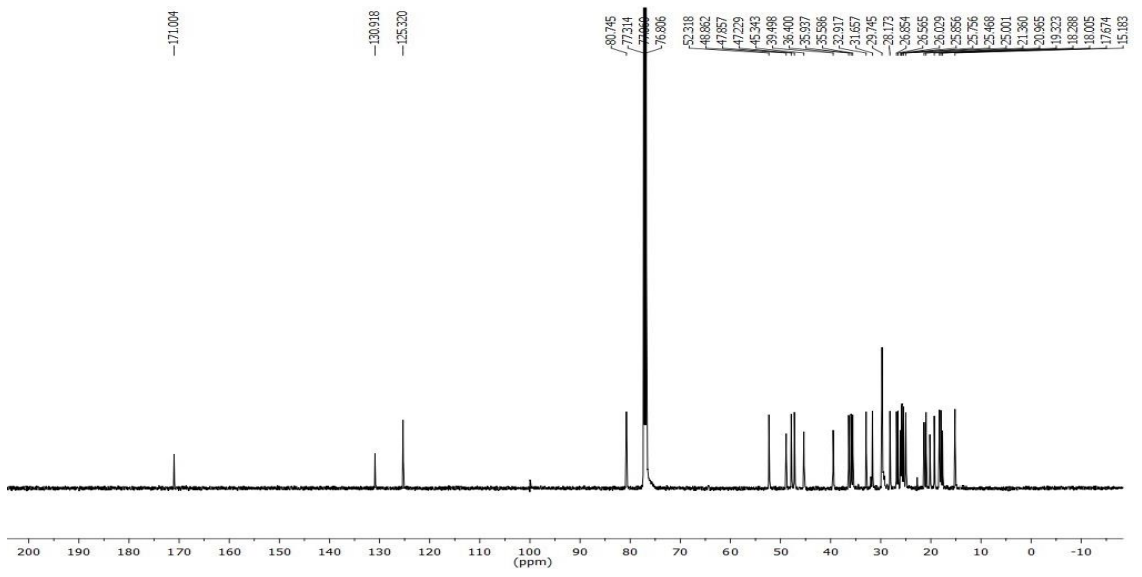

Figure 5.8: ^{13}C NMR spectrum of cycloartenol acetate

In ^{1}H NMR spectrum of compound **56** (Figure 5.10) signal at δ 5.03-5.01 ppm integrating one proton could be attributed to olefinic proton. δ 3.30-3.27 ppm could be attributed to the proton which is directly attached to the hydroxyl group. The diastereotopic methylene protons from the cyclopropane ring are discernable at δ 0.56 and 0.33 ppm. In ^{13}C NMR spectrum, (Figure 5.11) the signals at δ 134.5 and 130.7 ppm are the diagnostic peak for olefinic carbon. The mass spectrum of the compound **56** showed molecular ion peak at m/z 427.3938, which is the $[M+H]^{+}$ peak. From all the above spectral details and in comparison with the literature reports [Teresa *et al*., **1987**; Tsai *et al*., **2013**] the compound was confirmed as **cycloartenol**. The structure of the compound is shown below.

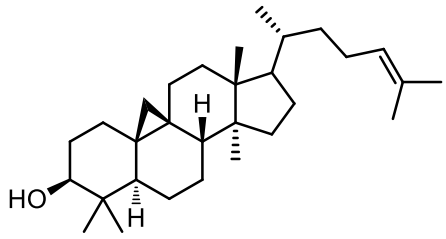

Figure 5.9: Cycloartenol **(56)**

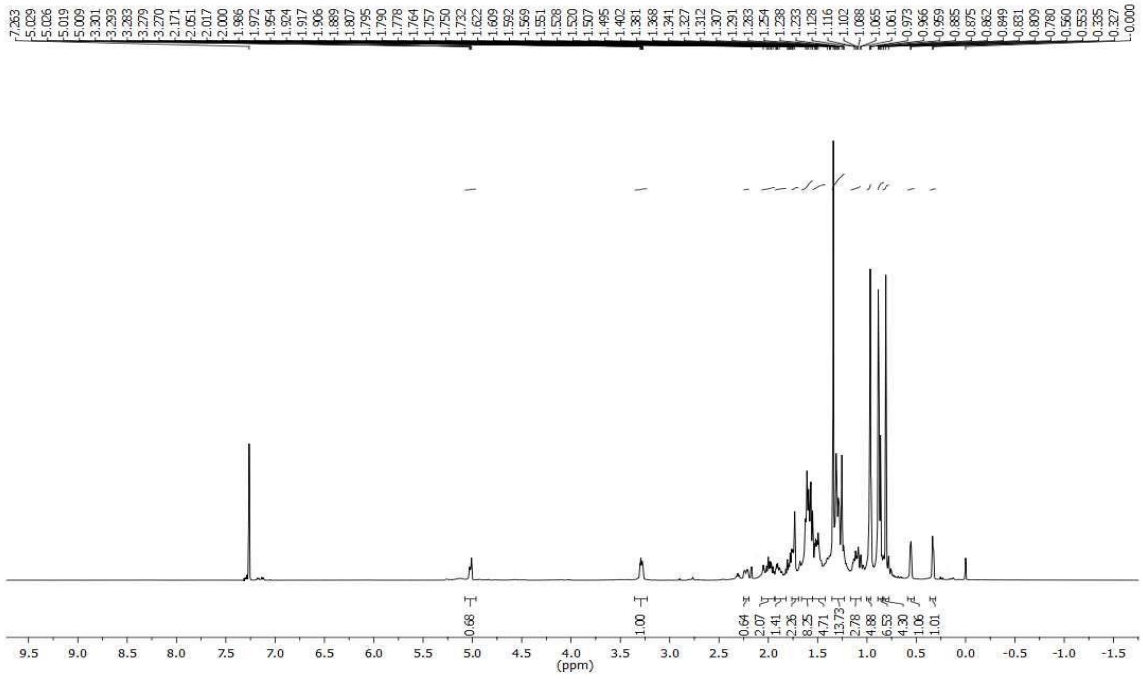

Figure 5.10: ^{1}H NMR spectrum of cycloartenol

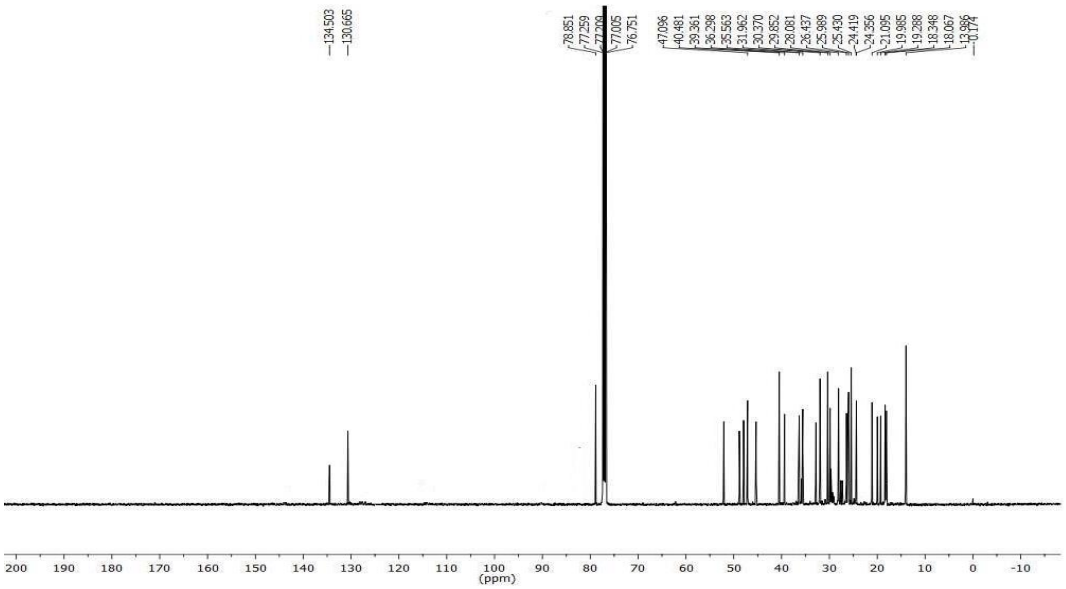

Figure 5.11: ^{13}C NMR spectrum of cycloartenol

Fraction pools 3-6 (FrA. 3-6), obtained by eluting the column with 20 % ethyl acetate in hexane showed the presence of a UV inactive compound. It was again subjected to purification by using silica gel column chromatography (100-200 mesh) yielded 30 mg (0.0008 %) of a white solid, which was labelled as compound **57**. IR, ^{1}H, ^{13}C and HRESIMS spectrum of the compound **57** is similar to that of compound **16** namely ***β*-amyrin acetate** and was previously isolated from the *V. indica* stem bark and seed (Chapter 3A).

Fraction pools 8-11 (FrA.8- Fr.A.11), obtained by eluting the column with 30 % ethyl acetate in hexane yielded 32 mg (0.008 %) of white solid of compound **58**. IR spectrum of the compound **58** showed a broad signal at 1693 cm^{-1}, indicating the presence of an acid group. In ^{1}H NMR spectrum, (Figure 5.13) signal at δ 12.07 ppm integrating one proton could be attributed to acid hydroxyl proton. Signals at δ 4.69 and 4.56 ppm could be attributed to the olefinic methylene protons. In ^{13}C NMR spectrum, (Figure 5.14) the signal at δ 177.7 ppm is the diagnostic peak for acid carbonyl carbon. The mass spectrum of the compound **58** showed molecular ion peak at m/z 455.3525, which is the $[M-H]^{+}$ peak. From all the above spectral details and the literature reports [Bisoli *et al*., **2008**; Bringmann *et al*., **1997**] the compound was confirmed as **betulinic acid**. The structure of the compound is shown below.

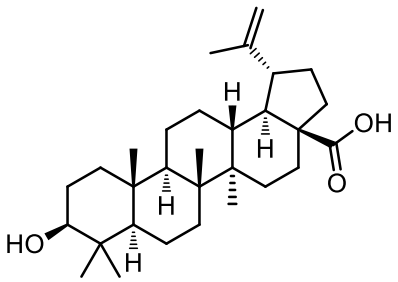

Figure 5.12: Betulinic acid **(58)**

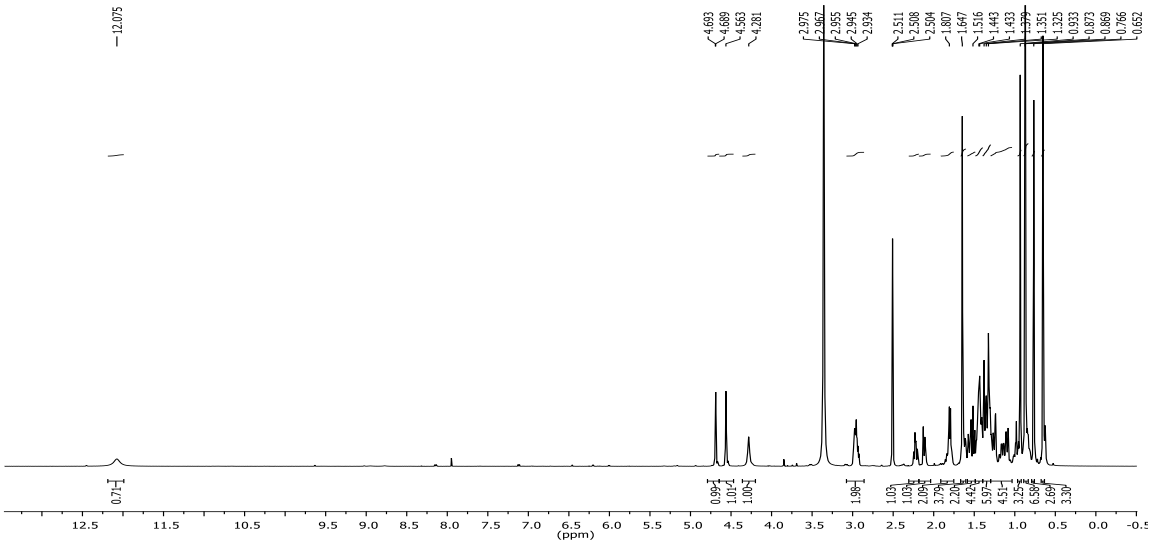

Figure 5.13: ^{1}H NMR spectrum of betulinic acid

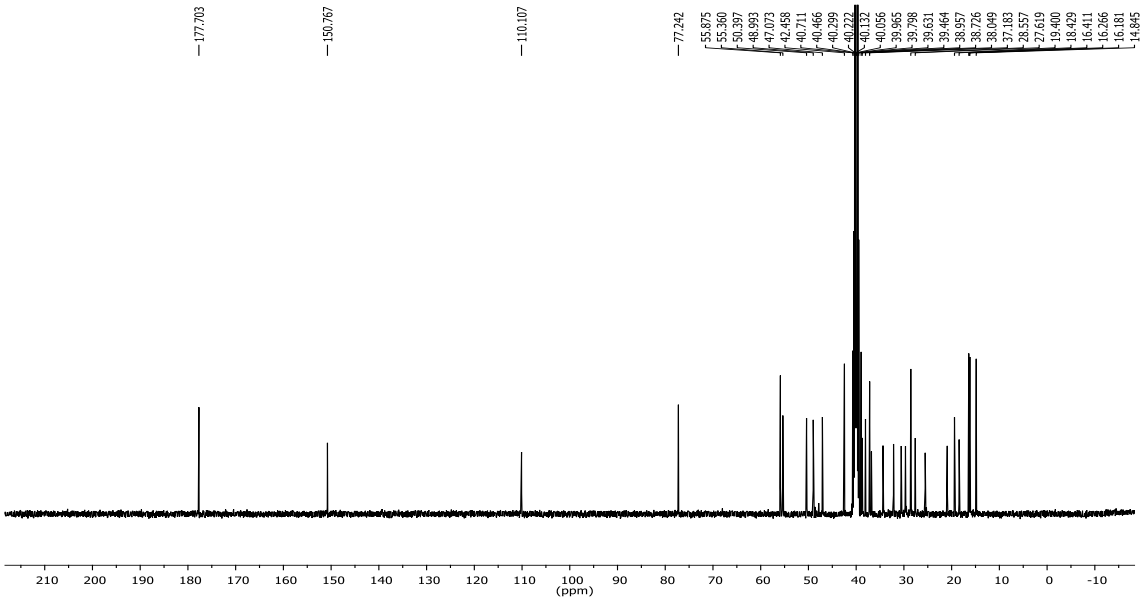

Figure 5.14: ^{13}C NMR spectrum of betulinic acid

Fraction pool 12-14 (FrA.12-14), obtained by eluting the column with 40 % ethyl acetate in hexane yielded 22 mg (0.006 %) of a light brownish solid, which was labelled as compound **59**. Compound **59** was confirmed to be ***E*-resveratrol,** which was earlier isolated from *A. indica* rhizome (chapter 2), *V. indica* stem bark (Chapter 3A) and *H. ponga* stem bark (Chapter 4).

Fraction pool 17-20 (FrA.17-20), obtained by eluting the column with 50 % ethyl acetate in hexane yielded yellowish solid, which on further purified by column chromatography on sephadex–LH 20 afford a compound **60** (12 mg; 0.003 %). IR spectrum of the compound **60** showed a broad signal at 1642 cm^{-1}, indicating the presence of carbonyl group. In ^{1}H NMR, (Figure 5.16) signal at δ 12.27 ppm integrating one proton could be attributed to the hydrogen bonded (O-H-O) hydroxyl proton. Signal at δ 5.16-5.13 ppm could be attributed to the olefinic proton. Methylene proton resonated at δ 3.21 ppm. In ^{13}C NMR, (Figure 5.17) the signal at δ 183.5 ppm is the diagnostic peak for carbonyl carbon. Methylene carbon resonated at δ 21.9 ppm. The mass spectrum of the compound **60** showed molecular ion peak at m/z 355.1185, which is the $[M+H]^{+}$ peak. From all the above spectral details and the literature reports [Zheng *et al*., **2008**] the compound was confirmed as **artocarpesin**. The structure of the compound is shown below.

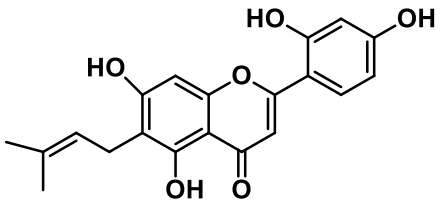

Figure 5.15: Artocarpesin **(60)**

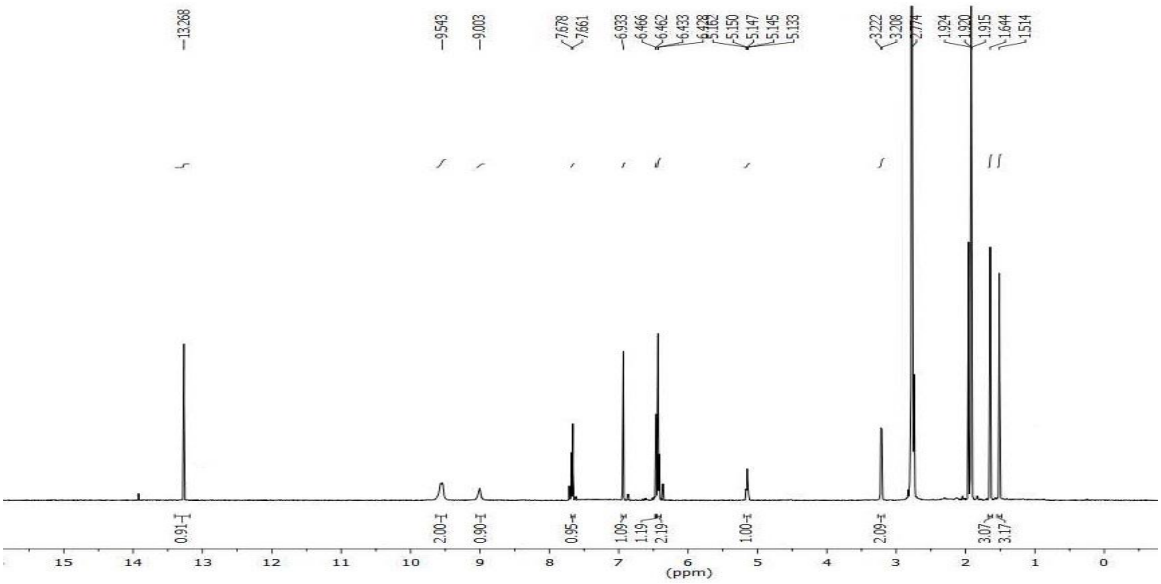

Figure 5.16: ^{1}H NMR spectrum of artocarpesin

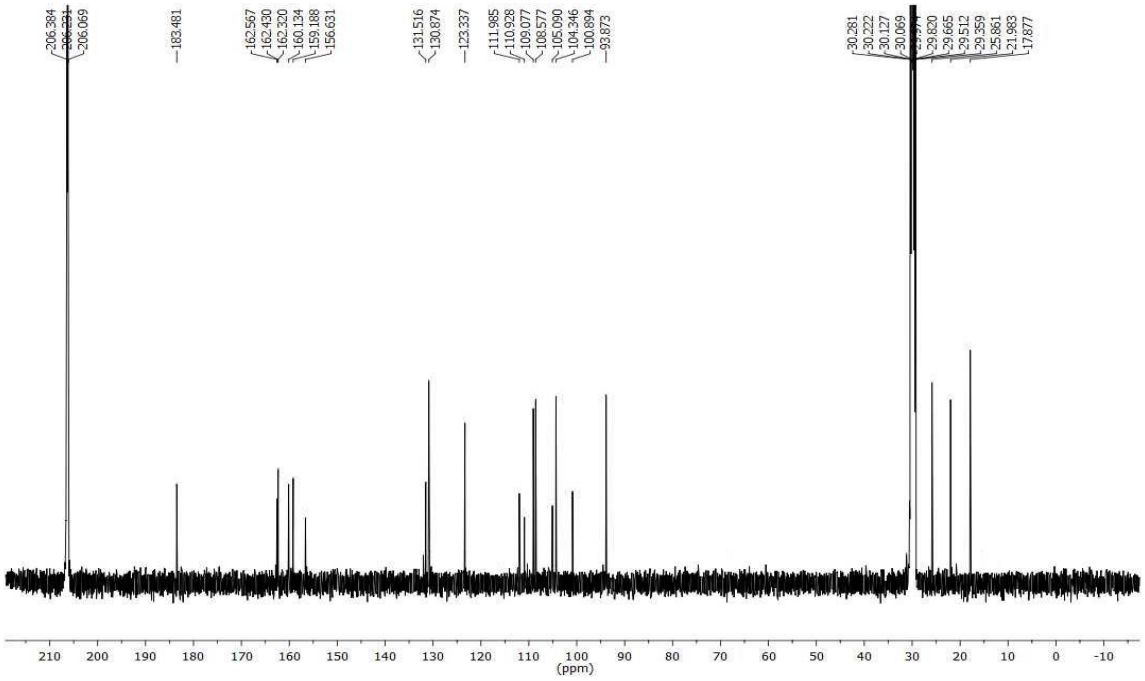

Figure 5.17: ^{13}C NMR spectrum of artocarpesin

Fraction pools 21-24 (FrA.21-24), obtained by eluting the column with 55 % ethyl acetate in hexane, which on further purified by column chromatography on sephadex–LH 20 in methanol afford a compound **61** (23 mg; 0.006 %). IR spectrum of the compound **61** showed a broad signal at 1642 cm^{-1}, indicating the presence of carbonyl group. In ^{1}H NMR

spectrum, (Figure 5.19) the signal at δ 13.72 ppm integrating one proton could be attributed to the hydrogen bonded (O-H-O) hydroxyl proton. Signal at δ 5.24 ppm could be attributed to the olefinic proton from the prenylated group. Methylene proton from prenylated group resonated at δ 3.32 ppm. Signals at δ 3.23 and 2.36 ppm could be attributed to the diastereotopic methylene protons. In ^{13}C NMR, (Figure 5.20) the signal at δ 181.5 ppm is the diagnostic peak for carbonyl carbon. Methylene carbon from prenylated group resonated at δ 25.9 ppm. Methine carbon from the furan ring discernible at δ 47.6 ppm. The mass spectrum of the compound **61** showed molecular ion peak at m/z 501.1920, which is the $[M-H]^+$ peak. From all the above spectral details and in comparison with the literature reports [Hano *et al*., **1989**; Chung *et al*., **1995**], the compound was confirmed as **Artonin A**. The structure of the compound is shown below.

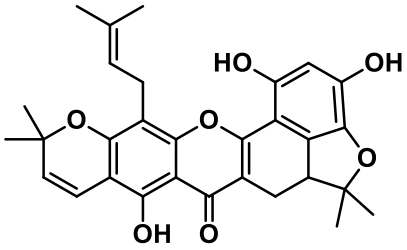

Figure 5.18: Artonin A **(61)**

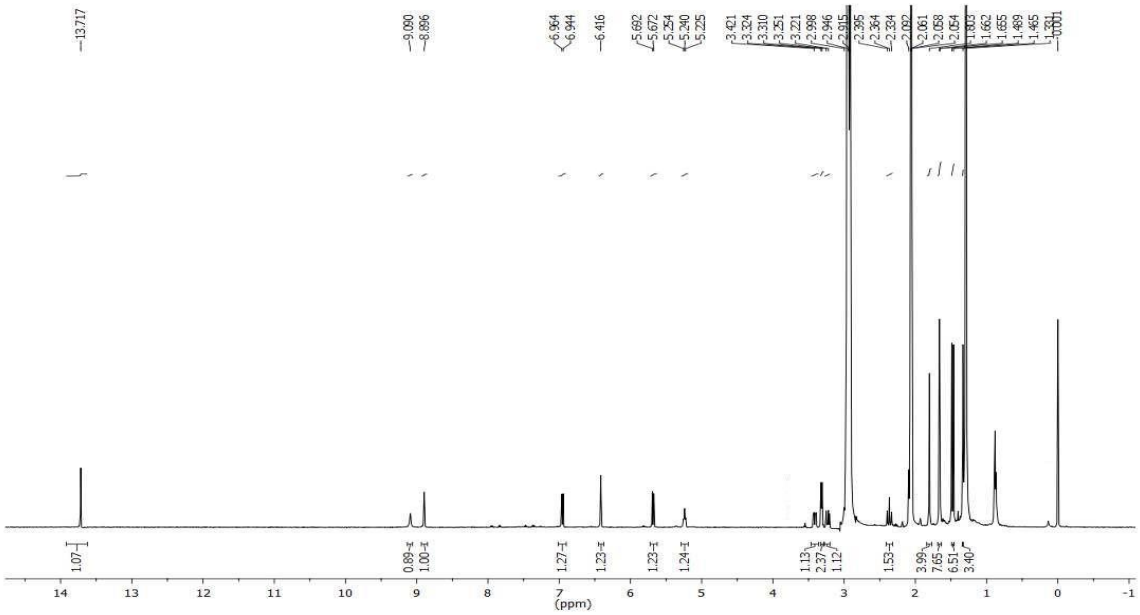

Figure 5.19: ^{1}H NMR spectrum of artonin A

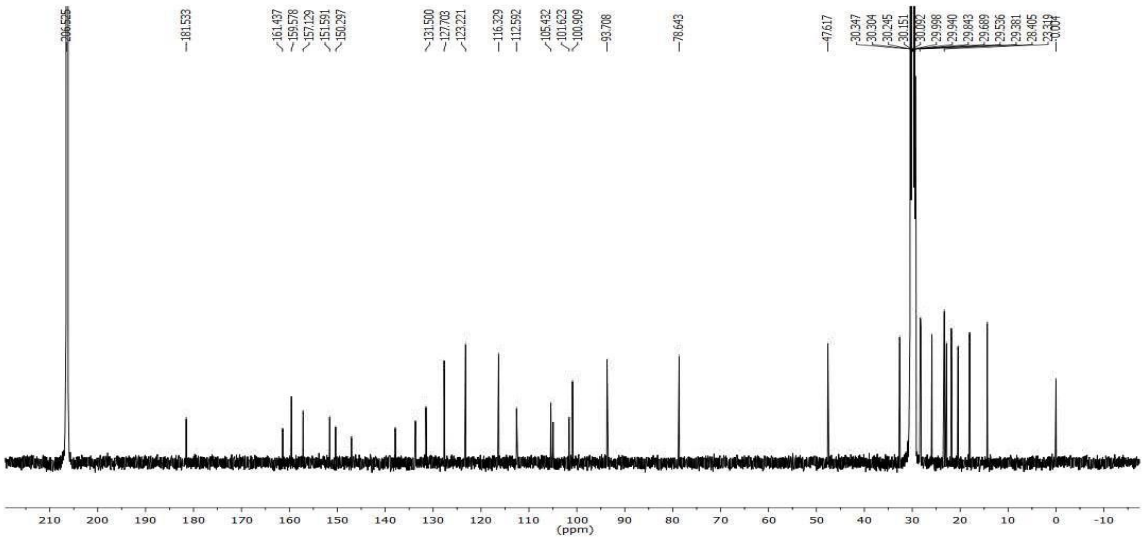

Figure 5.20: ^{13}C NMR spectrum of artonin A

Compound **62** (11 mg; 0.003 %) was obtained as a dark yellow solid from fraction 26-29, (Fr.A.26-Fr.A.29) and it was further purified by sephadex-LH 20 column. IR spectrum of the compound **62** showed a broad signal at 1642 cm^{-1}, indicating the presence of carbonyl group. In ^{1}H NMR, (Figure 5.22) signal at δ 12.51 ppm integrating one proton could be attributed to the hydrogen bonded (O-H-O) hydroxyl proton. Signals at δ 4.82 and 4.58 ppm as a singlet could be attributed to the exocyclic methylene olefinic proton. Signal at δ 3.44 and 2.67 ppm could be attributed to the diastereotopic methylene proton. In ^{13}C NMR spectrum, (Figure 5.23) the signal at δ 180.3 ppm is the diagnostic peak for carbonyl carbon. Olefinic methylene carbon resonated at δ 113.2 ppm. Methine carbon from the cyclohexene ring discernible at δ 35.3 ppm. The mass spectrum of the compound **62** showed molecular ion peak at m/z 435.1441, which is the $[M+H]^+$ peak. From all the above spectral details and in comparison with the literature reports [Uvais *et al*., **1989;** Sritularak *et al*., **2010**] the compound was confirmed as **Artobiloxanthone**. The structure of the compound is shown below.

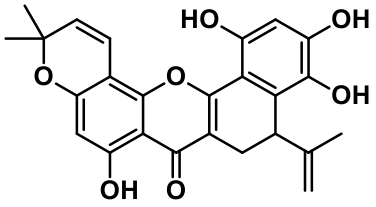

Figure 5.21: Artobiloxanthone **(62)**

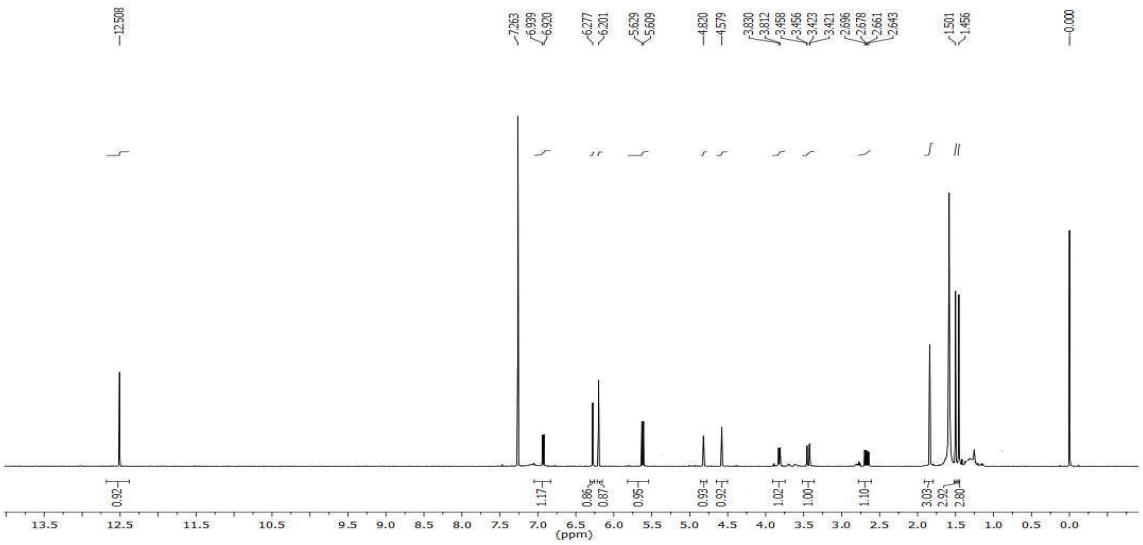

Figure 5.22: ^{1}H NMR spectrum of artobiloxanthone

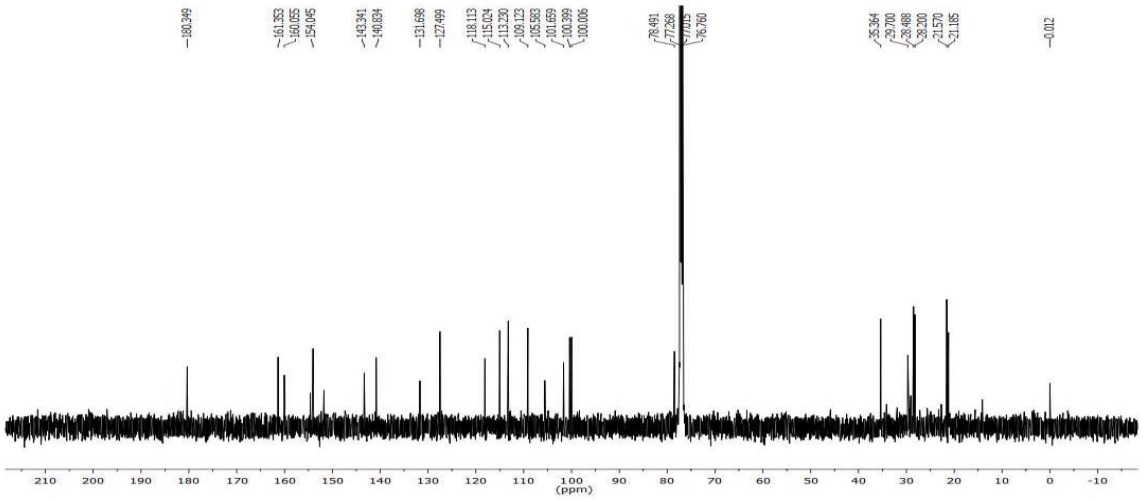

Figure 5.23: ^{13}C NMR spectrum of artobiloxanthone

Compound **63** (25 mg; 0.006 %) was obtained as a yellow solid from fraction 30-32, (Fr.A.30-Fr.A.32) by sephadex-LH 20 column. IR spectrum of the compound **63** showed a broad signal at 1622 cm^{-1}, indicating the presence of carbonyl group. In ^{1}H NMR, (Figure 5.25) signal at δ 13.39 ppm integrating one proton could be attributed to the hydrogen bonded (O-H-O) hydroxyl proton. Signals at δ 3.21 and 2.31 ppm could be attributed to the diastereotopic methylene proton. Methine proton from the furan ring discernible at δ 3.43 ppm. In ^{13}C NMR spectrum, (Figure 5.26) the signal at δ 181.4 ppm is the diagnostic peak

for carbonyl carbon. Methine carbon from the furan ring discernible at δ 47.5 ppm. Signal at δ 20.34 ppm attributed to the methylene carbon from cyclohexane ring. The mass spectrum of the compound **63** showed molecular ion peak at m/z 435.1438, which is the $[M+H]^+$ peak. From all the above spectral details and on comparison with the literature reports [Uvais *et al*., **1989**; Lan *et al*., **2013**] the compound was confirmed as **cycloartobiloxanthone**. The structure of the compound is shown below.

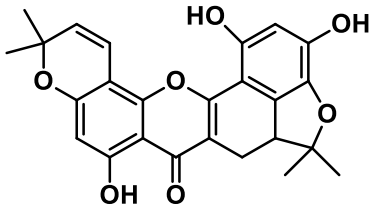

Figure 5.24: Cycloartobiloxanthone **(63)**

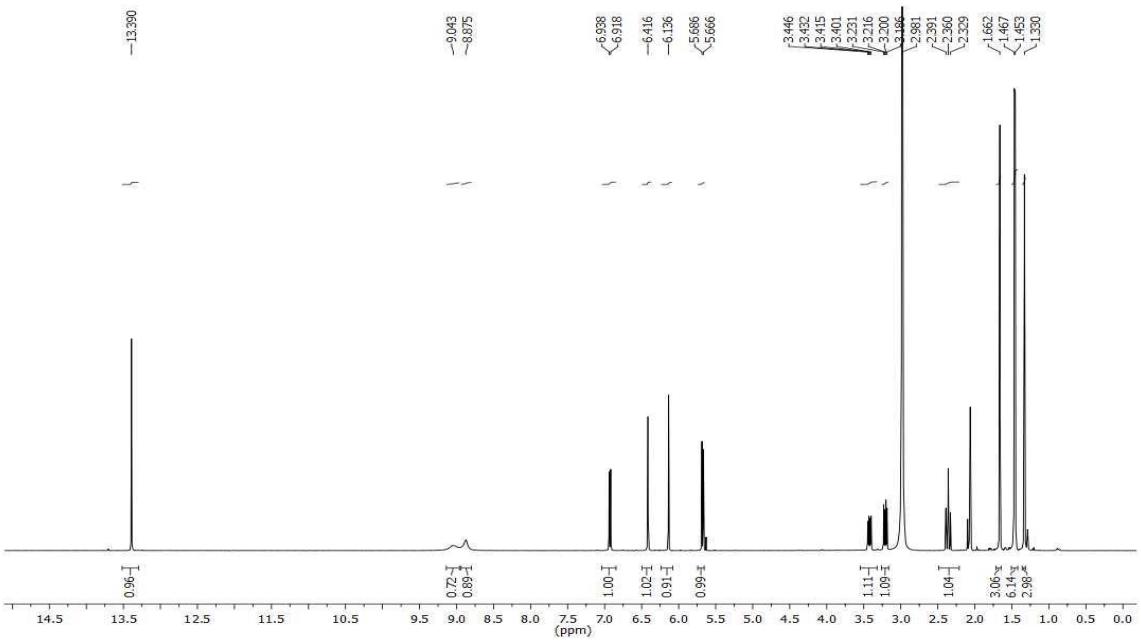

Figure 5.25: ^{1}H NMR spectrum of cycloartobiloxanthone

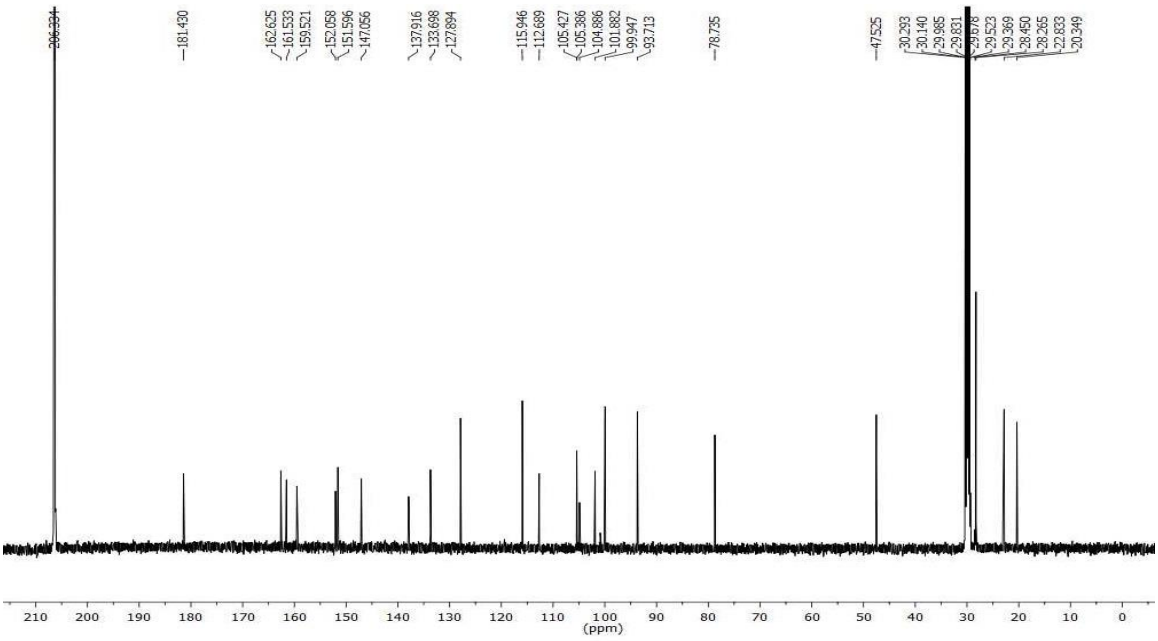

Figure 5.26: ^{13}C NMR spectrum of cycloartobiloxanthone

Compound **64** (9 mg; 0.002 %) was obtained as a brown amorphous solid from fraction (Fr.A.33-Fr.A.36), and it was further purified by Sephadex-LH 20 column in methanol. IR spectrum of the compound **62** showed a broad signal at 1641 cm^{-1}, indicating the presence of carbonyl group. Spectral details of compound **64** is similar to compound **62** (artobiloxanthone), only difference is there is a shifts in NMR values. In ^{1}H NMR, (Figure 5.28) signal at δ 13.02 ppm integrating one proton could be attributed to the hydrogen bonded (O-H-O) hydroxyl proton. Signals at δ 4.78 and 4.47 ppm could be attributed to the exocyclic methylene olefinic proton. Signal at δ 3.36 and 2.60 ppm could be attributed to the diastereotopic methylene proton. In ^{13}C NMR, (Figure 5.29) the signal at δ 180.1 ppm is the diagnostic peak for carbonyl carbon. Olefinic methylene carbon from resonated at δ 112.6 ppm. Methine carbon from the cyclohexene ring discernible at δ 37.9 ppm. The mass spectrum of the compound **64** showed molecular ion peak at m/z 435.1441, which is the $[M+H]^+$ peak. From all the above spectral details and in comparison with the literature reports [Syah *et al*., **2006**] the compound was confirmed as **Artoindonesianin A-3**. The structure of the compound is shown below.

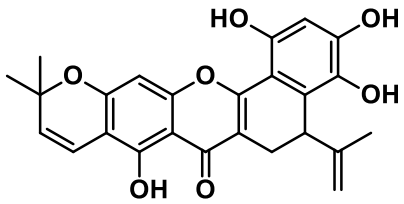

Figure 5.27: Artoindonesianin A-3 **(64)**

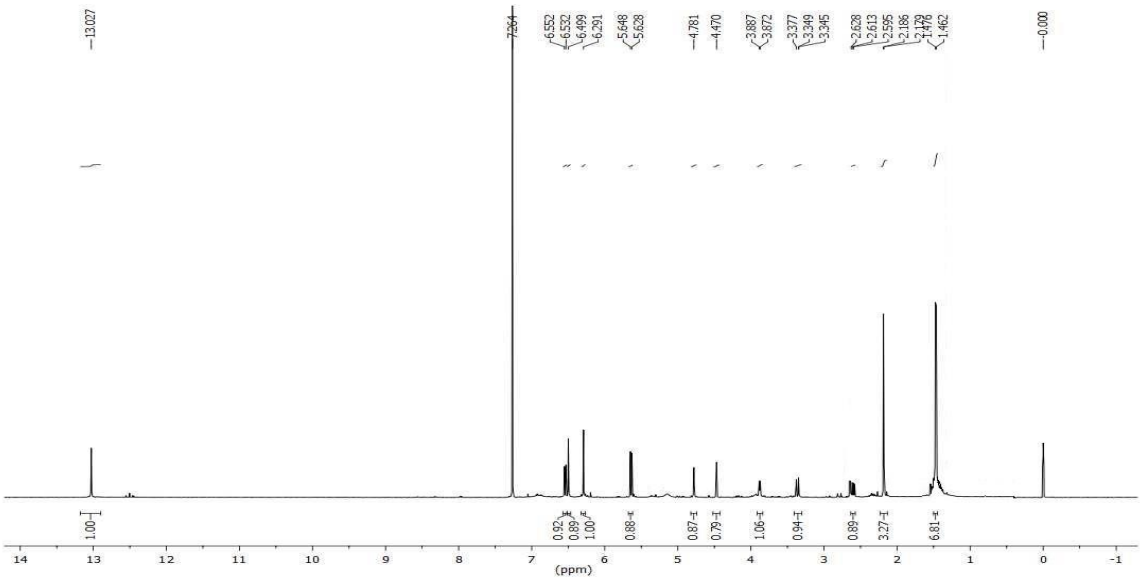

Figure 5.28: ^{1}H NMR spectrum of artoindonesianin A-3

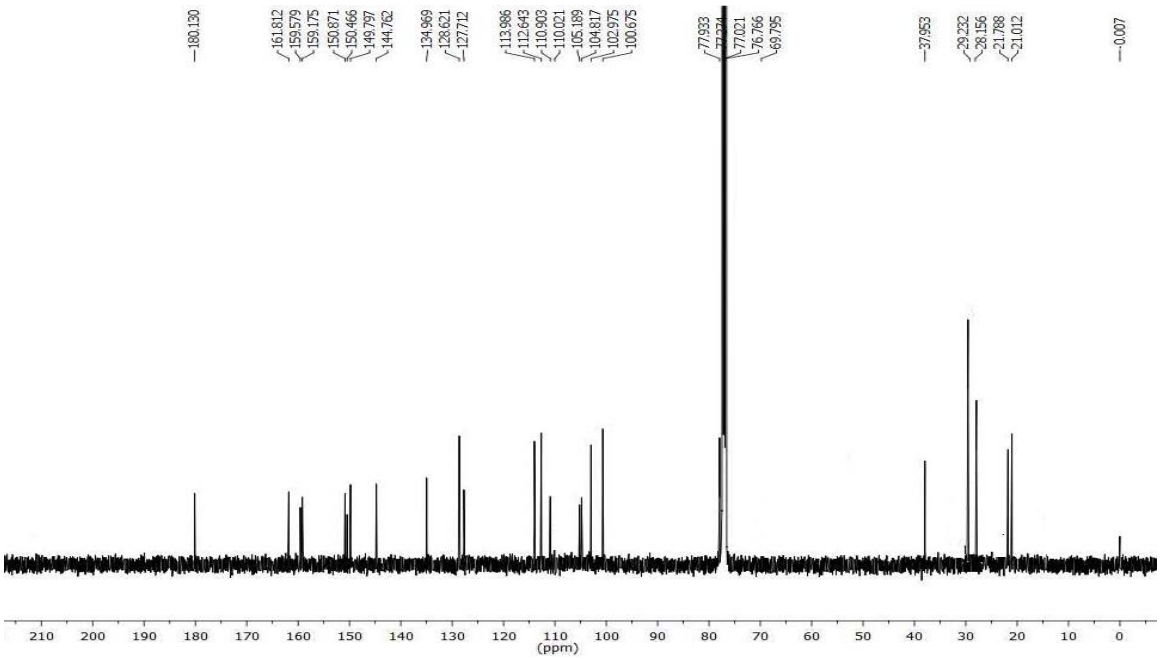

Figure 5.29: ^{13}C NMR spectrum of artoindonesianin A-3

Fraction pool 40 (FrA.40), obtained by eluting the column with 60 % ethyl acetate in hexane, which on further purified by column chromatography on sephadex–LH 20 in methanol afford a compound **65** (12 mg; 0.003 %). IR spectrum of the compound **65** showed a broad signal at 1643 cm^{-1}, indicating the presence of carbonyl group. In ^{1}H NMR, (Figure 5.31) signal at δ 12.49 ppm integrating one proton could be attributed to the hydrogen bonded (O-H-O) hydroxyl proton. Signal at δ 6.60 and 5.64 ppm could be attributed to the olefinic protons. In ^{13}C NMR, (Figure 5.32) the signal at δ 198.4 and 179.2 ppm is the diagnostic peak for carbonyl carbon of the acetophenone and chromanone moiety. Signal at δ 166.7 ppm attributed to the carbonyl carbon of the lactone ring. The mass spectrum of the compound **65** showed molecular ion peak at m/z 419.1128, which is the $[M-H]^{+}$ peak. From all the above spectral details and the literature reports [Aida *et al*., **1997**; Lan *et al*., **2013**], the compound was confirmed as **Artonol B**. A single-crystal X-ray diffraction experiment was performed on compound **65** (Figure 5.33), which unambiguously established the structure of compound **65**. The structure of the compound is shown below.

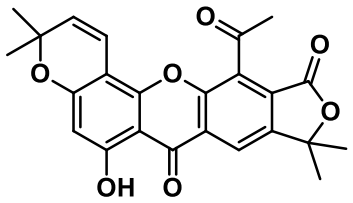

Figure 5.30: Artonol B **(65)**

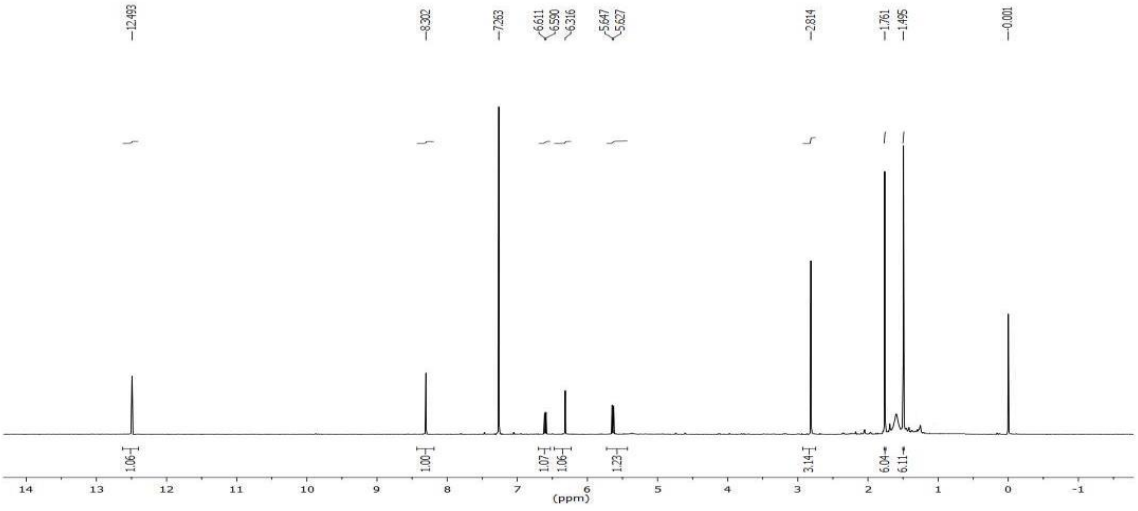

Figure 5.31: ^{1}H NMR spectrum of artonol B

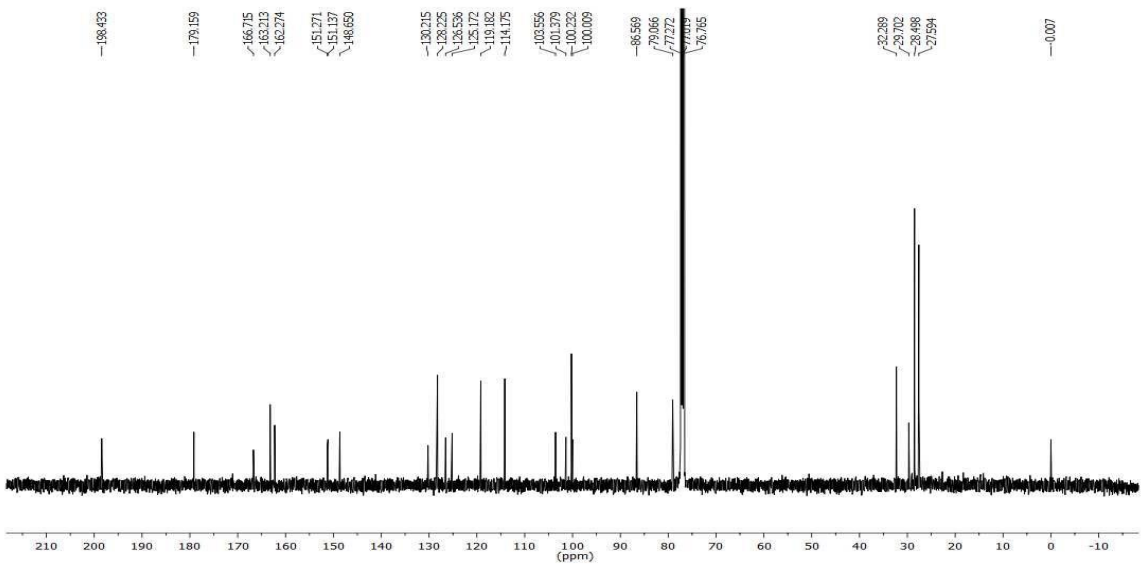

Figure 5.32: ^{13}C NMR spectrum of artonol B

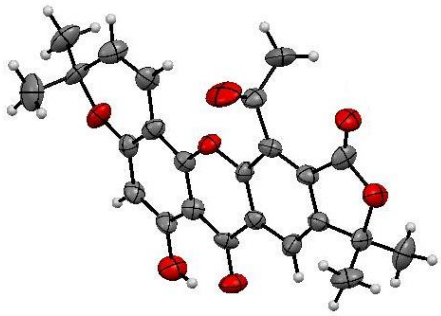

Figure 5.33: ORTEP structure of artonol B

Compound **66** (90 mg; 0.02 %) was obtained as a white solid from fraction (Fr.A.41-Fr.A.44), and it was further purified crystallization in water. In ^{1}H NMR spectrum, (Figure 5.35) signal at δ 8.75-8.39 ppm could be attributed to the hydroxyl proton. Signal at δ 7.35 and 6.91 ppm could be attributed to the *trans* olefinic proton. In ^{13}C NMR spectrum, (Figure 5.36) the signals at δ 159.5, 159.1 and 156.9 ppm are the diagnostic peak for oxygenated aromatic carbon. *Trans* olefinic carbons resonated at δ 128.3 and 124.4 ppm. The mass spectrum of the compound **66** showed molecular ion peak at m/z 245.0812, which is the $[M+H]^{+}$ peak. From all the above spectral details and in comparison with the literature reports [Takasugi *et al*., **1978**; Hanawa *et al*., **1992**] the compound was confirmed as **oxyresveratrol**. The structure of the compound is shown below.

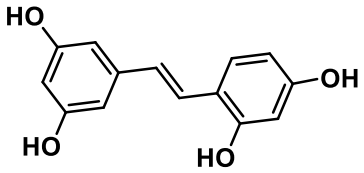

Figure 5.34: Oxyresveratrol **(66)**

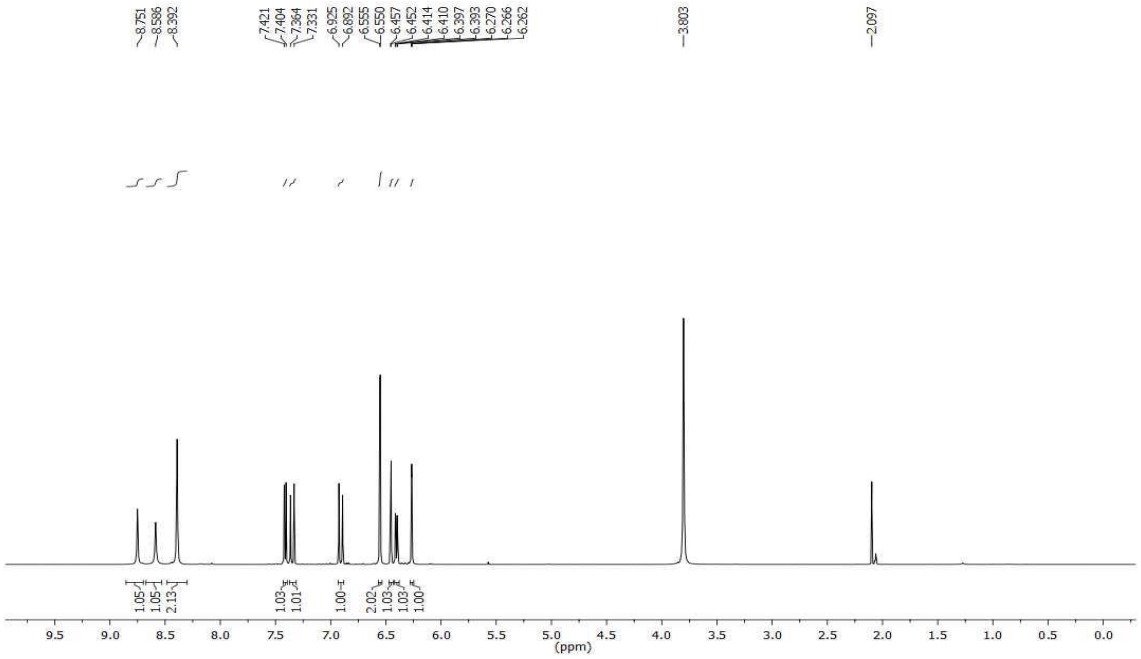

Figure 5.35: ^{1}H NMR spectrum of oxyresveratrol

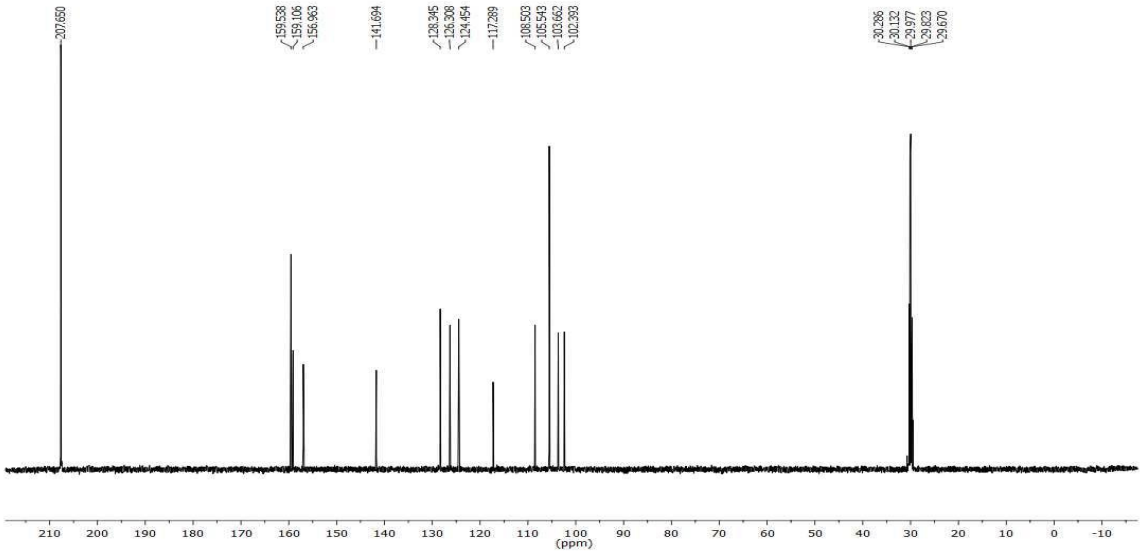

Figure 5.36: ^{13}C NMR spectrum of oxyresveratrol

5.7. Extraction of *Artocarpus lakoocha* stem bark

The air-dried stem bark of *A. lakoocha* (750 g) was extracted successively with acetone (A) and ethanol (E). The supernatant liquid was decanted and filtered. Then the extracts were concentrated under reduced pressure in a rotary vacuum evaporator to remove the residual solvent, which yielded 25.5 g (3.4 %) (A) and 22 g (2.9 %) (E) of crude extracts.

5.8. Isolation of compounds from *A. lakoocha* acetone extract

Based on the TLC analysis further isolation, purification and characterisation of chemical constituents were focused on the acetone extract. The acetone extract (25.5 g) was fractionated on a silica gel (100-200 mesh) column and eluted with n-hexane/EtOAc gradient (100 % n-hexane to 100 % EtOAc). Each fraction was analyzed by TLC (n-hexane-EtOAc), and those displaying the same TLC profile were combined to afford twenty fractions (FrA.1-FrA.20).

Fraction pool 1-2 (FrA.1-2), obtained by eluting the column with 10 % ethyl acetate in hexane on crystallization using the same solvent yielded the mixture of ***β*-sitosterol and stigmasterol.**

Fraction pool 3-6 (FrA.3-6), obtained by eluting the column with 20 % ethyl acetate in hexane yielded 25 mg (0.0003 %) of a light brownish solid, which was labelled as compound **67**. Compound **67** was confirmed to be ***E*-resveratrol,** which was earlier isolated from *A. camansi* (compound **59**). *E*-Resveratrol is commonly found in vitaceae and dipterocarpaceae family (Chapter 2, Chapter 3A and Chapter 4).

Compound **68** (2.5 mg; 0.0003 %) was obtained as an yellow amorphous solid from fraction (Fr.A.8-Fr.A.11), and it was further purified by column chromatography by using 30 % ethyl acetate in hexane. In ^{1}H NMR spectrum, (Figure 5.38) signal at δ 8.53 and 8.28 ppm could be attributed to the hydroxyl proton. *Trans*-olefinic protons discernible at δ 6.64 and 6.08 ppm. Signal at δ 2.36-2.33 ppm attributed to the isoprenyl methine proton. In ^{13}C NMR spectrum, (Figure 5.39) the signal at δ 31.8 ppm is the diagnostic peak for aliphatic methine carbon and methyl carbon resonated at δ 22.1 ppm. The mass spectrum of the compound **68** showed molecular ion peak at m/z 311.1182, which is the $[M+H]^{+}$ peak. From all the above spectral details and in comparison with the literature reports [Kapche *et al*., **2009**] the compound was confirmed as **moracin S**.

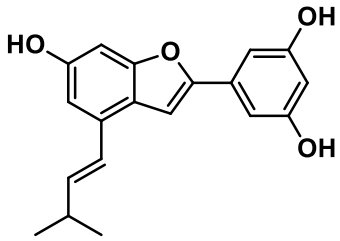

Figure 5.37: Moracin S **(68)**

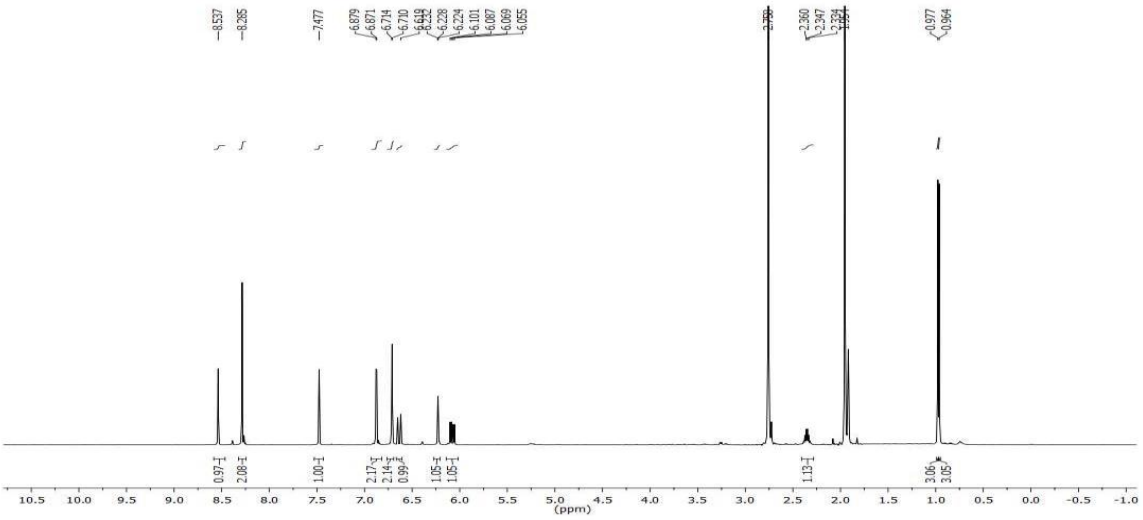

Figure 5.38: ^{1}H NMR spectrum of moracin S

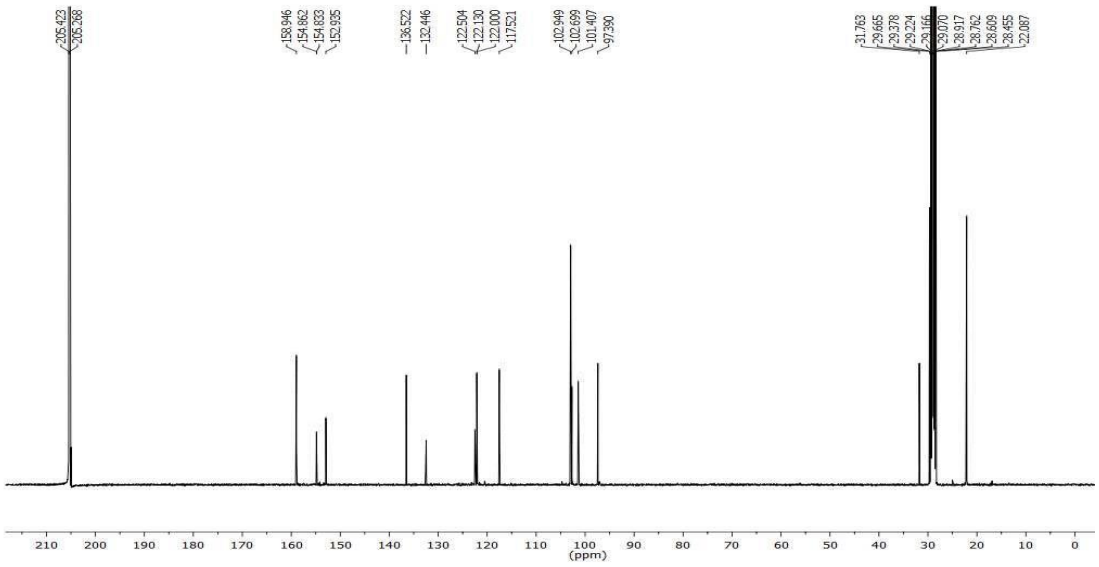

Figure 5.39: ^{13}C NMR spectrum of moracin S

Fraction pool 12-19 (FrA.12-19), obtained by eluting the column with 90 % ethyl acetate in hexane yielded 16 g (2.13 %) of a white solid and it was recrystallized in water, labelled as compound **69**. Compound **69** was confirmed to be **oxyresveratrol,** which was earlier isolated from *A. camansi* stem bark (compound **66**).

Compound **70** (3 mg; 0.0004 %) was obtained as a yellow solid from fraction Fr.A.20, and it was further purified by column chromatography by using 90 % ethyl acetate in hexane. In ^{1}H NMR spectrum, (Figure 5.41) signal at δ 8.53 and 8.28 ppm could be attributed to the hydroxyl proton. *Trans*-olefinic protons discernible at δ 7.13 and 6.69 ppm. Signal at δ 5.17 ppm attributed to the olefinic isoprenyl proton. Methylene proton resonated at δ 5.17 ppm. In ^{13}C NMR spectrum, (Figure 5.42) the signal at δ 17.9 ppm is the diagnostic peak for methylene carbon. The mass spectrum of the compound **70** showed molecular ion peak at m/z 313.1439, which is the $[M+H]^{+}$ peak. From all the above spectral details and in comparison with the literature reports [Takasugi *et al*., **1978**], the compound was confirmed as **4-Prenyl oxyresveratrol**.

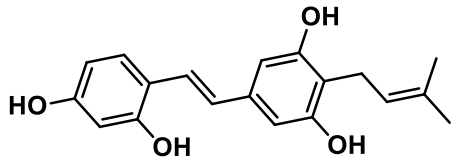

Figure 5.40: 4-Prenyl oxyresveratrol **(70)**

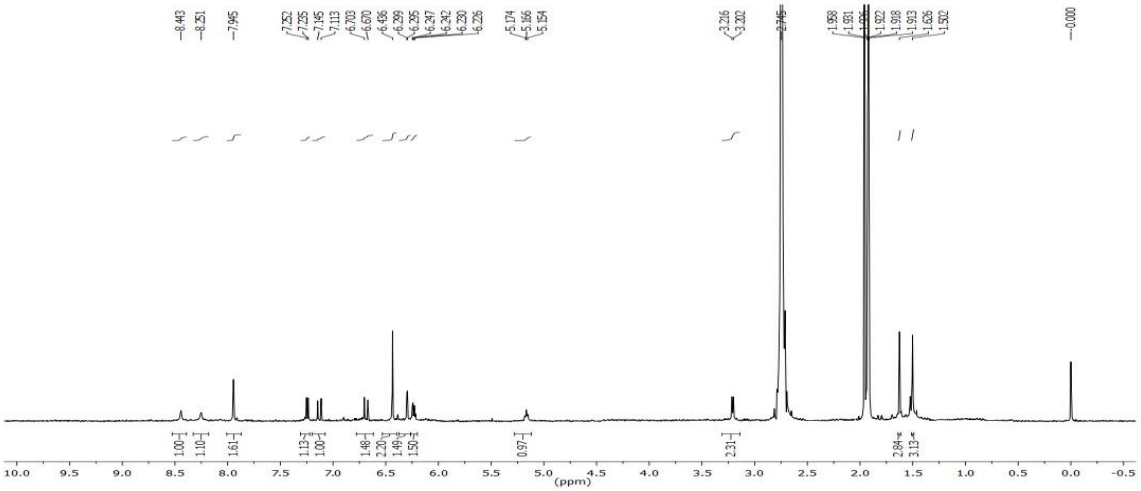

Figure 5.41: ^{1}H NMR spectrum of 4-Prenyl oxyresveratrol

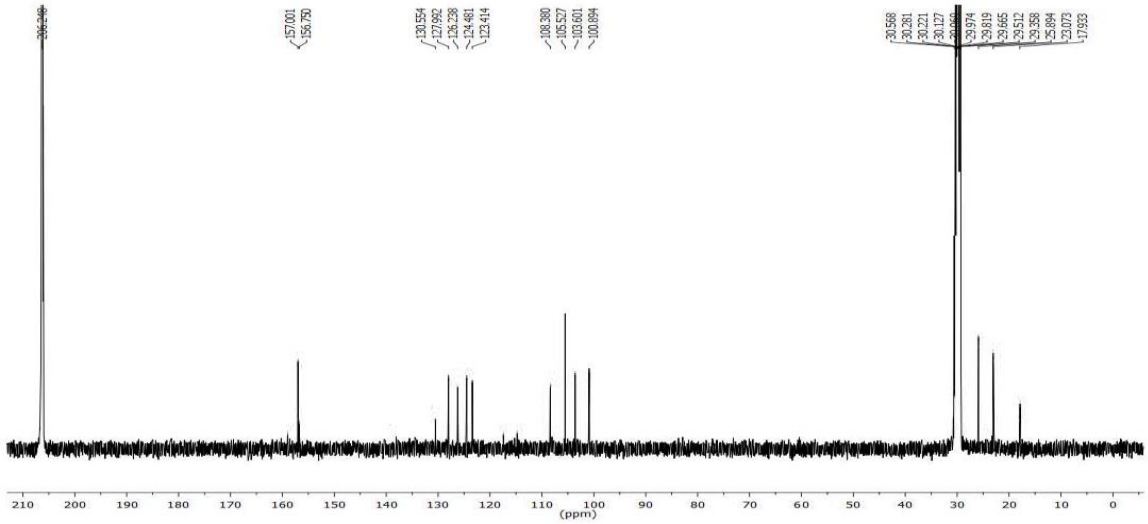

Figure 5.42: ^{13}C NMR spectrum of 4-Prenyl oxyresveratrol

5.9. Isolation of oxyresveratrol from *A. lakoocha* heartwood

The air-dried inner bark of *A. lakoocha* (500 g) was extracted with acetone : water (9:1) which yielded 65 g (13 %) of crude acetone extract. The solid acetone extract (65 g) was recrystallized in hot water to afford 46 g (9.2 %) of oxyresveratrol.

5.10. Extract level antidiabetic activity of *A. camansi* (AC) and *A. lakoocha* (AL)

In order to check the antidiabetic activity of these plants, different extracts were analysed for α-glucosidase, α-amylase and glycation inhibitory activity. The results from the study showed that the acetone fraction of AC effectively inhibits α-glucosidase and α-amylase enzyme (IC_{50} 49.54 ± 0.344 and 27.18 ± 0.144 µg/mL), which is comparable to the standard acarbose used (IC_{50} 45.37 ± 0.681 and 5.53 ± 0.367 µg/mL). The result from our study depicts that acetone fraction of AC showed a prominent antiglycation property with an IC_{50} 4.90 ± 0.205 µg/mL, which is better than the standard ascorbic acid used (IC_{50} 48.00 ± 0.876 µg/mL). Whereas ethanol extract of AL shows a prominent α-amylase inhibitory activity (IC_{50} 26.00 ± 0.264 µg/mL) compared with the acetone extract (Table 5.2).

Table 5.2. Extract level antidiabetic activity

Extracts	*α*-glucosidase (µg/mL)	*α*-amylase (µg/mL)	Antiglycation (µg/mL)
ACA	49.54 ± 0.344	27.18 ± 0.144	4.90 ± 0.205
ACE	81.31 ± 0.511	80.81 ± 0.571	95.26 ± 0.554
ALA	63.02 ± 0.513	265.44 ± 0.230	84.70 ± 0.571
ALE	64.28 ± 0.405	26.00 ± 0.264	85.64 ± 0.663
Acarbose	45.37 ± 0.681	5.53 ± 0.367	……
Ascorbic acid	……	……	48 ± 0.876

5.11. Antidiabetic activity of isolated compounds

In order to showcase the biological activity of isolated compounds, we examined the hypoglycemic properties in terms of *α*-glucosidase, *α*-amylase, antiglycation and glucose uptake. Except triterpinoids and moracin S, all the tested compounds showed a moderate *α*-glucosidase inhibition compared to acarbose. In particular, *E*-resveratrol, oxyresveratrol, artobiloxanthone and artoindonesianin A-3 showed prominent *α*-glucosidase inhibitory activity with IC_{50} values of 12.56 ± 1.00, 37.38 ± 1.11, 53.74 ± 0.76 and 54.04 ± 0.40 µM, respectively. The results also showed that artobiloxanthone inhibited α-amylase (IC_{50} 19.69 ± 0.06 µM) which was comparable with that of standard, acarbose, used (IC_{50} 8.99 ± 0.48 µM). The higher level of glucose in the blood increases the glycation of proteins which leads to the formation of advanced glycated end products (AGEs). From our study, it is evident that artocarpesin and artonol B possessed prominent antiglycation activity (IC_{50} 50.10 ± 0.25 and 94.77 ± 0.53 µM, respectively) (Figure 5.43 and Table 5.3).

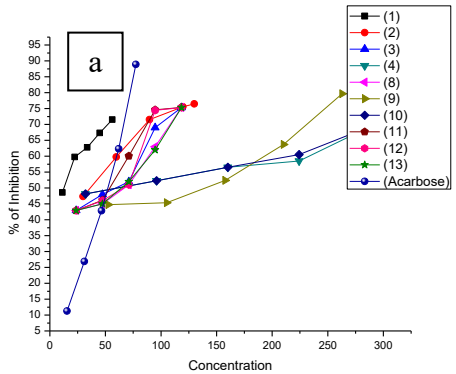

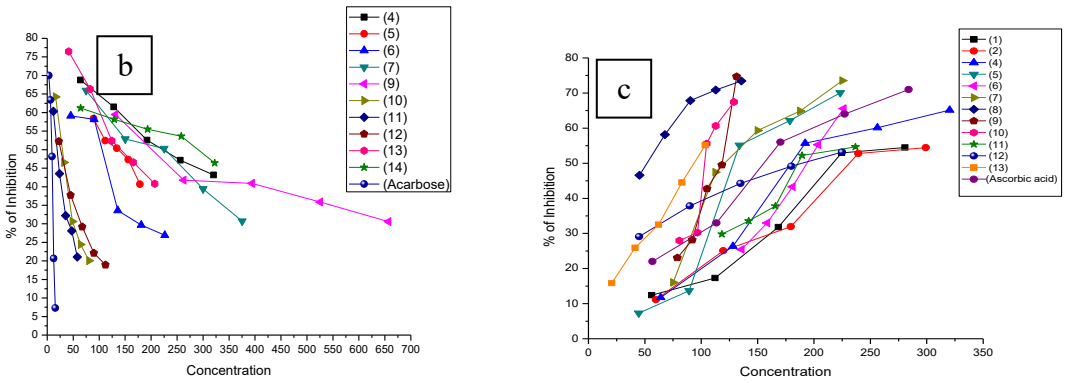

Figure 5.43: a) *α*-Glucosidase, b) *α*-amylase c) glycation inhibition activity of isolated compounds

Table 5.3. Antidiabetic activity of isolated compounds

Sl. No	Compound	*α* - glucosidase (µM)	*α*- amylase (µM)	Antiglycation (µM)
1	*E*-Resveratrol	12.56 ± 1.00	690.50 ± 0.05	218.25 ± 0.05
2	Oxyresveratrol	37.38 ± 1.11	2363.34 ± 0.08	232.15 ± 0.53
3	4-Prenyl oxyresveratrol	62.00 ± 0.45	789.50 ± 0.08	917.58 ± 0.98
4	*β*-Amyrin acetate	61.51 ±0 .84	215.33 ± 0.44	180.02 ± 0.58
5	Betulinic acid	328.25 ± 0.55	136.25 ± 0.17	128.86 ± 0.37
6	Cycloartenol acetate	296.25 ± 0.05	104.28 ± 0.06	195.42 ± 0.23
7	Cycloartenol	218.25 ± 0.42	221.22 ± 0.76	120.78 ± 0.28
8	Artocarpesin	67.66 ± 0.30	537.50 ± 0.26	50.10 ± 0.25
9	Artonin A	142.24 ± 1.03	144.24 ± 0.58	118.55 ± 0.36
10	Cycloartobiloxanthone	63.64 ± 0.31	29.00 ± 0.05	103.43 ± 0.50
11	Artobiloxanthone	53.74 ± 0.76	19.69 ± 0.06	179.78 ± 0.06
12	Artoindonesianin A-3	54.04 ± 0.40	25.93 ± 0.65	191.05 ± 0.53
13	Artonol B	65.66 ± 0.31	139.86 ± 0.93	94.77 ± 0.53
14	Moracin S	418.25 ± 0.11	286.31 ± 0.76	618.25 ± 0.12
15	Acarbose	52.87 ± 0.22	8.99 ± 0.48	…….
16	Ascorbic acid	…….	…….	154.63 ± 0.49

All data are represented as mean ± standard deviation (n=3)

5.12. MTT assay

All the isolated compounds were selected for the cell line based assays owing to their prominent antidiabetic potential in inhibiting the digestive enzymes and protein glycation. The cytotoxicities of the compounds were measured at different concentrations (0, 1, 5, 10, 15 and 25 µM) by means of MTT assay for 24 h. All the tested compounds were found to be less toxic in a dose dependent manner (<20 %) even at 5 µM concentration (Figure 5.44). These toxicity evaluations helped us to fix a safe dose range for 2-NBDG uptake antidiabetic studies.

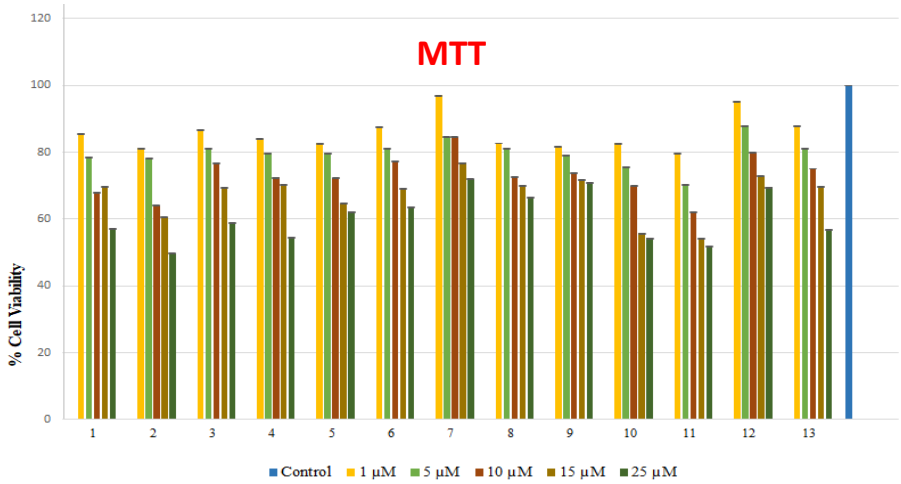

Figure 5.44: MTT cytotoxicity assay of isolated compounds**.** L6 myoblasts were treated with various concentrations of compounds (0, 1, 5, 10, 15, 25 µM) for 24 h and cytotoxicity was determined by MTT assay. All data are represented as means ± SD (n=3)

5.13. 2-NBDG uptake assay by fluorescent microscopy

2-NBDG is a fluorescent tagged deoxy-glucose analogue that has been used to monitor glucose uptake in living cells. In the present study, the L6 rat myotubes were challenged with isolated compounds at 5 µM concentration for 24 h. Among them *E*-resveratrol, oxyresveratrol, artobiloxanthone and artonol exhibited optimum glucose uptake (Fig. 5.45 showing high intense fluorescence) which is comparable to the standard metformin (100 µM). The fluorescent intensity of the images was analysed using BD Image Data Explorer software and was represented as mean ± SD (standard deviation) from duplicate measurements of three different experiments.

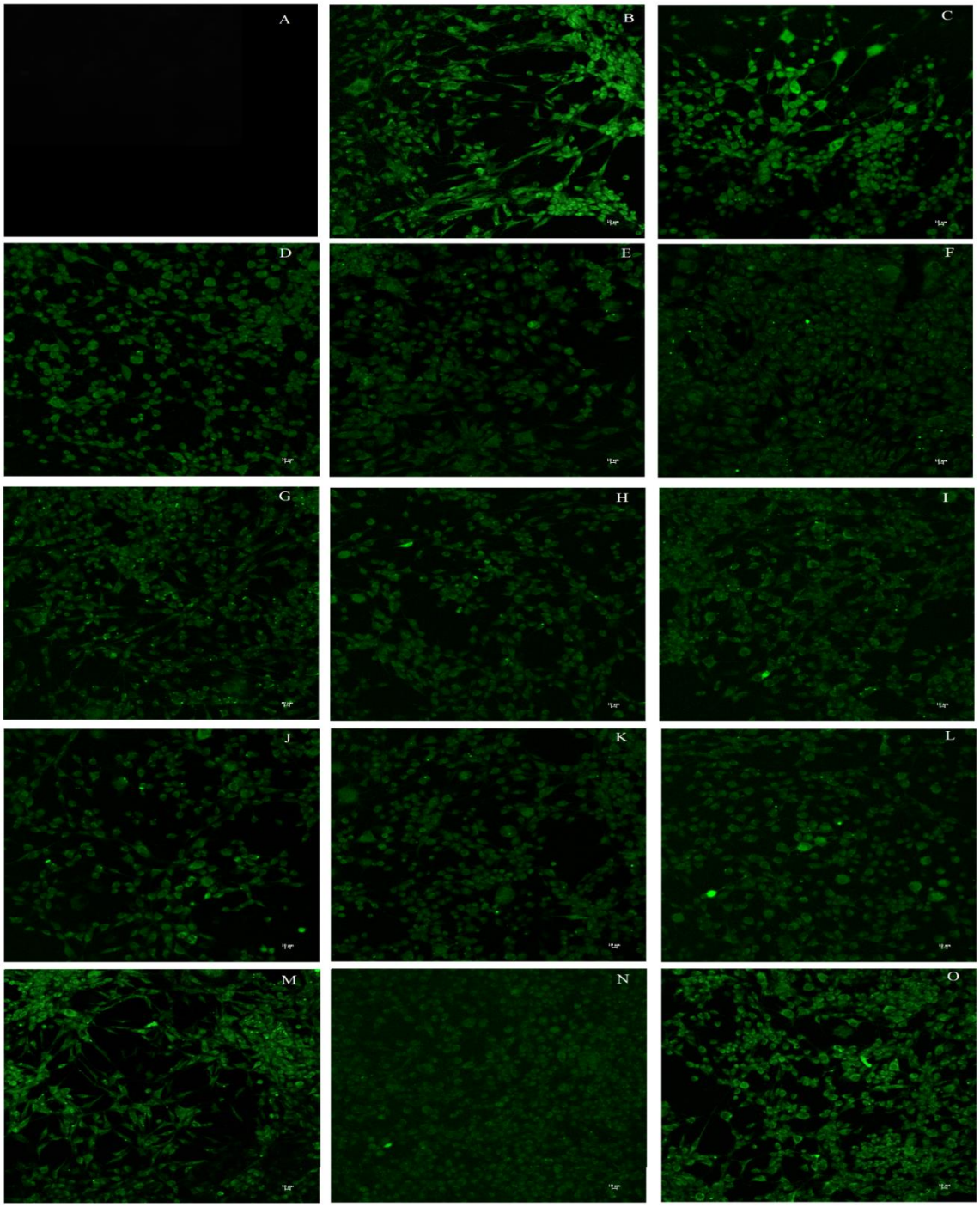

Figure 5.45: 2-NBDG uptake assay by fluorescent microscopy in L6 rat myotubes: (A) untreated cells, (B) 100 µM metformin (C) *E*-Resveratrol (D) Oxyresveratrol. (E) 4-Prenyl oxyresveratrol, (F) *β*-Amyrin acetate, (G) Betulinic acid, (H) Cycloartenol acetate, (I) Cycloartenol, (J) Artocarpesin, (K) Artonin A, (L) Cycloartobiloxanthone, (M)

Artobiloxanthone, (N) Artoindonesianin A-3, (O) Artonol B, All data are represented as means ± SD (n=3).

5.14. Conclusion

In this chapter, we have isolated and structurally characterized 12 compounds from the stem bark of *A. camansi* and 4 compounds from *A. lakoocha viz*., *E*-resveratrol, oxyresveratrol, 4-prenyl oxyresveratrol, *β*-amyrin acetate, betulinic acid, cycloartenol acetate, cycloartenol, artocarpesin, artonin A, cycloartobiloxanthone, artobiloxanthone, artoindonesianin A-3, artonol B and morcin. To the best of our knowledge, all the chemical constituents except triterpenoids from *A. camansi* and their antidiabetic activity are reported for the first time. In particular, *E*-resveratrol, oxyresveratrol, artobiloxanthone and artonol B, signifcantly increased glucose uptake in L6 cells.

5.15. Experimental session

General experimental details and procedure for antidiabetic activity are given in Chapter 2 and Chapter 3B.

5.15. 1. Extraction of *A. camansi* stem bark

The stem bark of *A. camansi* was collected from Thrissur district, Kerala. This was thoroughly cleaned and dried in a drier maintained at 50^{o} C and powdered. The powdered stem bark (400 g) was subjected to repeated extraction using acetone and ethanol (2.5 L X 48 h) at room temperature. After extraction, the solvent was removed under reduced pressure using Büchi rotary evaporator. The acetone extract (30 g) was then subjected to column chromatographic separation.

5.15.2. Isolation of compounds from *A. camansi* stem bark

The acetone extract (30 g) of the stem bark of *A. camansi* dissolved in minimum quantity of acetone and was adsorbed in silica gel (100-200) loaded on the top of silica gel column filled with slurry of 100-200 mesh silica gel in hexane. The column was eluted successively with gradient mixtures of hexane and ethyl acetate of increasing polarities and finally with 50 % methanol in ethyl acetate. A total of 175 fractions of approximately 200 mL each were collected. According to the similarity in TLC, they were pooled into 45 major fraction pools (FrA.1- FrA. 45). Pictorial representation of the procedure for the isolation of the compound is shown in figure 5.46.

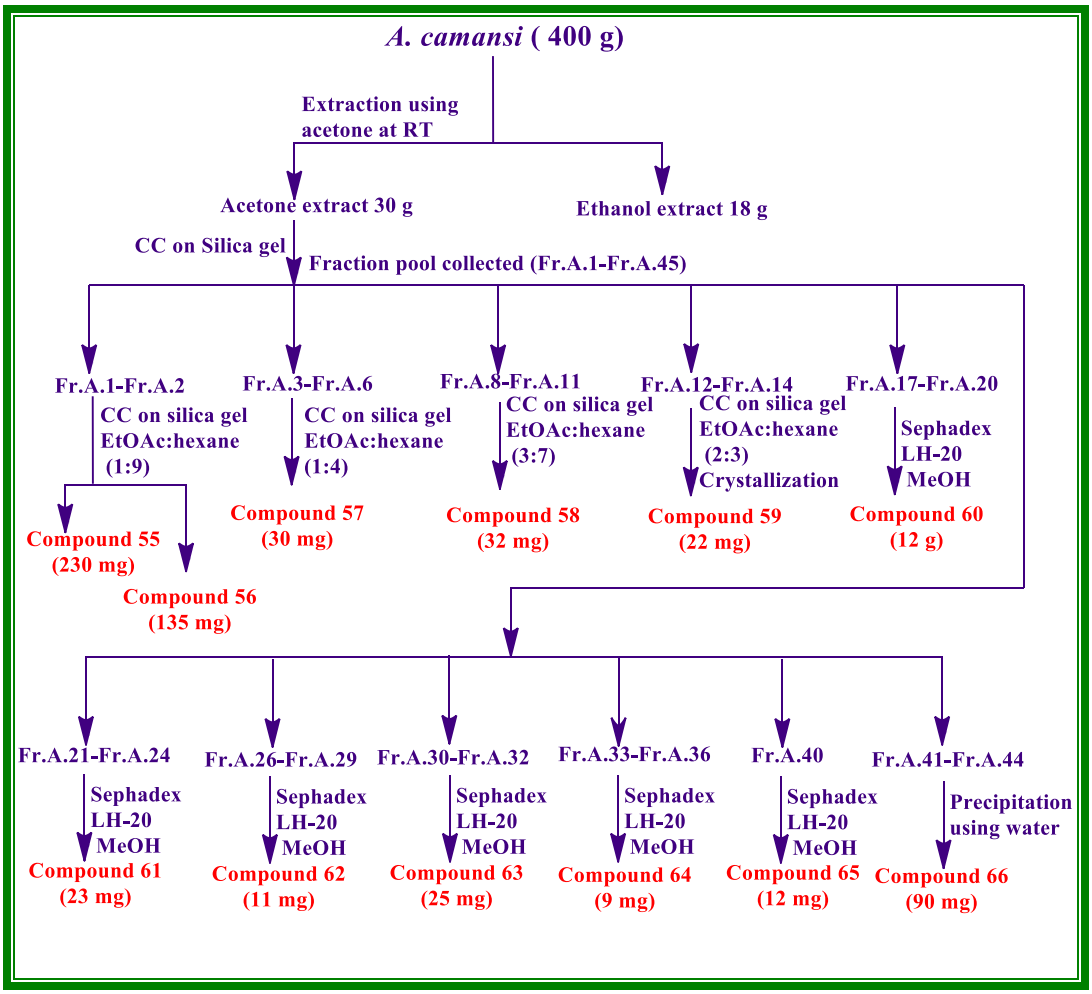

Figure 5.46: Pictorial representation of isolation of compounds from *A. camansi* stem bark

5.15.2.1. Isolation of compound 55

The isolation procedure of compound **55** is represented in figure 5.46. Compound **55** (230 mg) was obtained as a white solid, on eluting the column with 10 % ethyl acetate in hexane. IR, ^{1}H NMR, ^{13}C NMR and mass spectral studies of this compound and on comparison with literature values [Teresa *et al*., **1987**; Tsai *et al*., **2013**], confirmed it to be cycloartenol acetate.

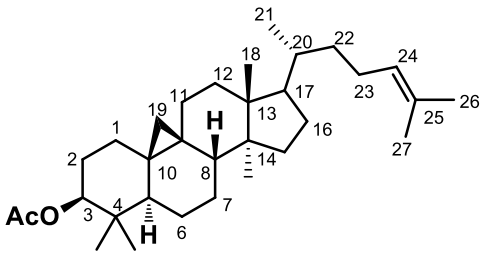

Melting point	:	119-120 ^{o}C
$[\alpha]^{25}_{D}$	:	+52^{o} (c 0.25, $CHCl_3$)
FT-IR (NaCl) υ_{max}	:	2102, 1733, 1643, 1464, 1372, 1248 cm^{-1}.
^{1}H NMR (500 MHz, $CDCl_3$)	:	δ 5.10 (bs, 1H, H-24), 4.57 (d, *J* = 5 Hz, 1H, H-3), 2.05 (s, 3H, OAc-3), [2.00-1.95 (m, 1H), 1.89-1.87 (m, 2H), 1.76-1.73 (m, 1H), 1.68 (s, 3H), 1.60-1.51 (m, 9H), 1.40-1.34 (m, 3H), 1.28-1.25 (m, 10H), 1.12-1.05 (m, 4H), 0.96 (s, 3H), 0.89 (s, 9H), 0.81(s, 3H), (Other aliphatic protons)] 0.58 (bs, 1H, H-19), 0.34 (bs, 1H, H-19) ppm.
^{13}C NMR (125 MHz, $CDCl_3$)	:	δ 171.0 (OAc-3), 130.9 (C-25), 125.3 (C-24), 80.7 (C-3), 52.3 (C-17), 48.9 (C-14), 47.9 (C-8), 47.2 (C-5), 45.3 (C-13), 39.5 (C-4), 36.4 (C-22), 35.9 (C-20), 35.6 (C-12), 32.9 (C-15), 31.7 (C-1), 29.7 (C-14), [28.2, 26.9, 26.6, 26.0, 25.9, 25.8, 25.5, 25.0, 21.4, 20.9, 20.2, 19.3, 18.3, 18.0, 17.7, 15.2 (Other aliphatic carbon)] ppm.
HR-ESIMS m/z	:	469.4041 $[M+H]^{+}$ (calcd for $C_{32}H_{53}O_2$, 469.4045)

5.15.2.2. Isolation of compound 56

Compound **56** (135 mg) was obtained as a white solid, on eluting the column with 10 % ethyl acetate in hexane. IR, ^{1}H NMR, ^{13}C NMR and mass spectral studies of this compound and in comparison with literature values [Teresa *et al*., **1987**; Tsai *et al*., **2013**], confirmed it to be cycloartenol.

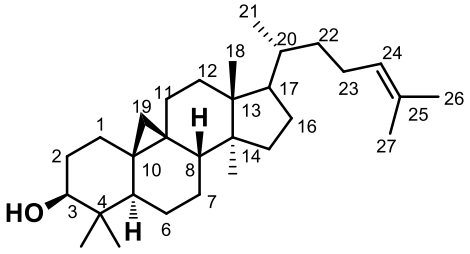

Melting point	:	106-108 ^{o}C
$[\alpha]^{25}_{D}$	:	+40^{o} (c 0.25, $CHCl_3$)
FT-IR (NaCl) υ_{max}	:	3423, 2923, 1641 cm^{-1}.
^{1}H NMR (500 MHz, $CDCl_3$)	:	δ 5.03-5.01 (m, 1H, H-24), 3.3-3.27 (m, 1H, H-3), [2.23 (d, *J* = 13 Hz, 1H), 2.05-1.95 (m, 2H), 1.92-1.89 (m, 1H), 1.78-1.73 (m, 2H), 1.62-1.55 (m, 8H), 1.55-1.49 (m, 4H), 1.40-1.23 (m, 13H), 1.13-1.06 (m, 3H), 0.97-0.96 (m, 5H), 0.86-0.85 (m, 6H), 0.81 (s, 3H) (Other aliphatic protons)], 0.56 (d, *J* = 3.5 Hz, 1H, H-19), 0.33 (d, *J* = 4.0 Hz, 1H, H-19) ppm.
^{13}C NMR (125 MHz, $CDCl_3$)	:	δ 134.5 (C-25), 130.7 (C-24), 78.85 (C-3), 52.1 (C-17), 48.8 (C-14), 47.9 (C-8), 47.1 (C-5), 45.3 (C-13), 40.5 (C-4), 36.3 (C-22), 35.6 (C-20), 31.9 (C-1), [30.4, 29.9, 28.1, 26.5, 26.4, 26.1, 25.9, 25.4, 24.4, 24.4, 21.1, 19.9, 19.3, 19.3, 18.3, 18.1, 18.01, 13.9 (Other aliphatic carbon)] ppm.
HR-ESIMS m/z	:	427.3938 $[M+H]^{+}$ (calcd for $C_{30}H_{51}O$, 427.3939)

5.15.2.3. Isolation of compound 57

Compound **57** (30 mg) was obtained as a white solid, on eluting the column with 20 % ethyl acetate in hexane. IR, ^{1}H NMR, ^{13}C NMR and mass spectral studies of this compound and on comparison with compound **16**, previously isolated from *V. indica* stem bark [Chapter 3A], confirmed it to be *β*-amyrin acetate.

5.15.2.4. Isolation of compound 58

Compound **58** (32 mg) was obtained as a white solid, on eluting the column with 30 % ethyl acetate in hexane. IR, ^{1}H NMR, ^{13}C NMR and mass spectral studies of this compound and on comparison with literature values [Bisoli *et al*., **2008**], confirmed it to be betulinic acid.

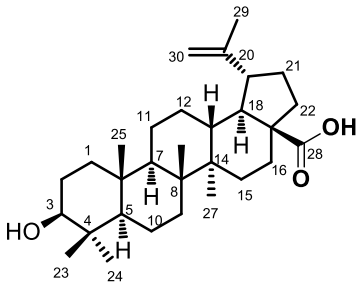

Melting point	:	312-314 ^{o}C
$[\alpha]^{25}_{D}$	:	+6^{o} (c 0.25, MeOH)
FT-IR (NaCl) υ_{max}	:	3428, 3075, 2944, 2671, 1693, 1454, 1440, 1379, 1143 cm^{-1}.
^{1}H NMR (500 MHz, DMSO d6)	:	δ 12.08 (s, 1H, OH-28), 4.69 (d, *J* = 2 Hz, 1H, H-30), 4.56 (s, 1H, H-30), 4.28 (s, 1H, OH-3), 3.02-2.93 (m, 2H, H-3, H-18), [2.25-2.19 (m, 1H), 2.12-2.09 (m, 1H), 1.84-1.77 (m, 2H), 1.65 (s, 3H), 1.54-1.08 (m, 20H), 0.93 (s, 3H), 0.87 (s, 6H), 0.77 (s, 3H), 0.65 (s, 3H) (Other aliphatic protons)] ppm.
^{13}C NMR (125 MHz, DMSO d6)	:	δ 177.7 (C-28), 150.8 (C-20), 110.1 (C-30), 77.2 (C-3), [55.9, 55.4, 50.4, 48.9, 47.1, 42.5, 38.9, 38.7, 38.0, 37.2, 36.8, 34.4, 32.2, 30.6, 29.7, 28.6, 27.6, 25.5, 20.9, 19.4, 18.4, 16.4, 16.3, 16.2, 14.8 (Other aliphatic carbon)] ppm.
HR-ESIMS m/z	:	455.3525 $[M-H]^{+}$ (calcd for $C_{30}H_{47}O_3$, 455.3525)

5.15.2.5. Isolation of compound 59

Fraction pool 12-14 (FrA.12-14) which on column chromatographed by using 40 % ethyl acetate in hexane, a white solid of compound **59** (22 mg) was obtained. The structure of the compound **59** was confirmed as in comparison with the NMR data of compound **1**, namely *E*-resveratrol, previously isolated from *A. indica* rhizome, *Vateria indica* stem bark and *Hopea ponga* stem bark [Chapter 2, Chapter 3A and Chapter 4].

5.15.2.6. Isolation of compound 60

Compound **60** (12 mg) was obtained as a yellow solid, on eluting the sephadex-LH 20 column with methanol. IR, ^{1}H NMR, ^{13}C NMR and mass spectral studies of this compound and on comparison with literature values [Zheng *et al*., **2008**], confirmed it to be artocarpesin.

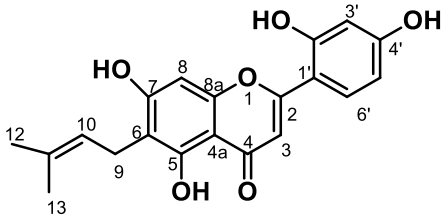

Melting point	:	231-232 ^{o}C
FT-IR (NaCl) υ_{max}	:	3429, 3150, 2087, 1642, 1431 cm^{-1}.
^{1}H NMR (500 MHz, CD_3COCD_3)	:	δ 13.27 (s, 1H, OH-5), 9.54 (s, 2H, OH-3', OH-5'), 9.00 (s, 1H, OH-7), 7.67 (d, *J* = 8.5 Hz, 1H, H-6'), 6.93 (s, 1H, H-3), 6.46 (d, *J* = 2 Hz, 1H, H-3'), 6.45-6.39 (m, 2H, H-5', H-8, merged), 5.16- 5.13 (m, 1H, H-10), 3.21 (d, *J* = 7.5 Hz, 2H, H-9), 1.64 (s, 3H, H-12), 1.51 (s, 3H, H-13) ppm.
^{13}C NMR (125 MHz, CD_3COCD_3)	:	δ 183.5 (C-4), 162.6 (C-OH), 162.4 (C-OH), 162.3 (C-OH), 160.1 (C-OH), 159.2 (C-O-C), 156.6 (C-O-C), 131.5 (C-11), 130.9 (C-6'), 123.3 (C-10), [111.9, 110.9, 109.1, 108.6, 105.1, 104.3, 100.9, 93.9 (Other aromatic carbon)], 25.9 (C-12), 21.9 (C-9), 17.9 (C-13) ppm.
HR-ESIMS m/z	:	355.1185 $[M+H]^{+}$ (calcd for $C_{20}H_{19}O_6$, 355.1181)

NMR Spectral assignments were made on the basis of 1D and 2D NMR analysis the literature reports.

5.15.2.7. Isolation of compound 61

Fraction pool 21-24 (FrA. 21-24) which on column chromatographed by sephadex-LH 20 in methanol, a yellow solid of compound **61** (23 mg) was obtained. IR, ^{1}H NMR, ^{13}C NMR and mass spectral studies of this compound and on comparison with literature values [Hano *et al*., **1989**; Chung *et al*., **1995**], confirmed it to be artonin A.

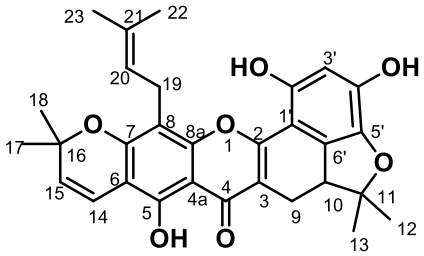

Melting point	:	239-240 ^{o}C
FT-IR (NaCl) υ_{max}	:	3428, 3150, 2099, 1642, 1550, 1475, 1430 cm^{-1}.
^{1}H NMR (500 MHz, CD_3COCD_3)	:	δ 13.72 (s, 1H, OH-5), 9.09 (s, 1H, OH-2'), 8.90 (s, 1H, OH-4'), 6.95 (d, J = 10.0 Hz, 1H, H-14), 6.42 (s, 1H, H-3'), 5.68 (d, J = 10 Hz, 1H, H-15), 5.24 (t, J = 7.5 Hz, 1H, H-20), 3.41 (dd, J_1 = 15, J_2 = 7 Hz, 1H, H-10), 3.32 (d, J = 7 Hz, 2H, H-19), 3.23 (dd, J_1 = 15, J_2 = 7 Hz, 1H, H-9), 2.36 (t, J = 15 Hz, 1H, H-9), 1.80 (s, 3H, Me-22), [1.66 (s, 6H), 1.49 (s, 3H), 1.46 (s, 3H), 1.33 (s, 3H) (Other CH_3 protons)] ppm.
^{13}C NMR (125 MHz, CD_3COCD_3)	:	δ 181.5 (C-4), 161.4 (C-2), 159.6 (C-5'), 157.1 (C-7), 151.6 (C-2'), 150.3 (C-4'), 131.5 (C-21), 127.7, 123.2 (C-20), 116.3 (C-14), 112.6 (C-3), 105.4 (C-1'), 101.6, 100.9, 93.7 (C-11), 78.6 (C-16), 47.6 (C-10), 32.6, 28.3 (C-17), 28.2 (C-18), 25.9 (C-22), 22.9 (C-13), 21.8 (C-19), 20.4 (C-9), 18.0 (C-23), 14.3 (C-12) ppm.
HR-ESIMS m/z	:	501.1920 $[M-H]^{+}$ (calcd for $C_{30}H_{29}O_7$, 501.1913)

NMR Spectral assignments were made on the basis of 1D and 2D NMR analysis and in comparison with the literature reports.

5.15.2.8. Isolation of compound 62

Compound **62** (11 mg) was obtained as a dark yellow solid, on eluting the sephadex-LH 20 column with methanol. IR, ^{1}H NMR, ^{13}C NMR and mass spectral studies of this compound and on comparison with literature values [Uvais *et al*., **1989**], confirmed it to be artobiloxanthone.

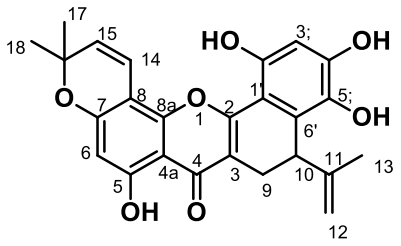

Melting point	:	163-164 ^{o}C
FT-IR (NaCl) υ_{max}	:	3421, 3150, 2097, 1622, 1431 cm^{-1}.
^{1}H NMR (500 MHz, $CDCl_3$)	:	δ 12.51 (s, 1H, OH-5), 6.93 (d, *J* = 10 Hz, 1H, H-14), 6.28 (s, 1H, H-6), 6.20 (s, 1H, H-3'), 5.62 (d, *J* = 10.0 Hz, 1H, H-15), 4.82 (s, 1H, H-12), 4.58 (s, 1H, H-12), 3.82 (d, *J* = 8.5 Hz, 1H, H-10), 3.44 (dd, J_1 = 17.5, J_2 = 1.0 Hz, 1H, H-9), 2.67 (dd, J_1 = 17.5, J_2 = 9.0 Hz, 1H, H-9), 1.84 (s, 3H, Me-13), 1.50 (s, 3H, Me-17), 1.46 (s, 3H, Me-18) ppm.
^{13}C NMR (125 MHz, $CDCl_3$)	:	δ 180.3 (C-4), 161.3 (C-OH), 160.1 (C-OH), 154.0 (C-OH), 143.3 (C-O-C), 140.8 (C-O-C), 131.7 (C-11), 127.5 (C-15), 118.1 (C-1'), 115.0 (C-14), 113.2 (C-12), 109.1(C-8), 105.6 (C-4a), 100.4, 100.0 (C-6), 78.5 (C-16), 35.4 (C-10), 28.5 (C-17), 28.2 (C-18), 21.6 (C-13), 21.2 (C-9) ppm.
HR-ESIMS m/z	:	435.1441 $[M+H]^{+}$ (calcd for $C_{25}H_{23}O_7$, 435.1443)

NMR Spectral assignments were made on the basis of 1D and 2D NMR analysis and in comparison with the literature reports.

5.15.2.9. Isolation of compound 63

Fraction pools 30-32 (FrA. 30-32) which on column chromatographed by sephadex-LH 20 in methanol, a yellow solid of compound **63** (25 mg) was obtained. IR, ^{1}H NMR, ^{13}C NMR and mass spectral studies of this compound and in comparison with literature report [Uvais *et al*., **1989**], confirmed it to be cycloartobiloxanthone.

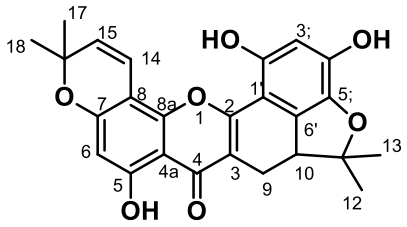

Melting point	:	286-287 ^{o}C
FT-IR (NaCl) υ_{max}	:	3404, 3100, 2975, 1640, 1622, 1431 cm^{-1}.
^{1}H NMR (500 MHz, CD_3COCD_3)	:	δ 13.39 (s, 1H, OH-5), 9.04 (s, 1H, OH-2'), 8.88 (s, 1H, OH-4'), 6.93 (d, *J* = 10.0 Hz, 1H, H-14), 6.42 (s, 1H, H-6), 6.14 (s, 1H, H-3'), 5.68 (d, *J* = 10.0 Hz, 1H, H-15), 3.42 (dd, J_1 = 15, J_2 = 7 Hz, 1H, H-10), 3.21 (dd, J_1 = 15, J_2 = 7 Hz, 1H, H-9), 2.36 (t, *J* = 15 Hz, 1H, H-9), 1.66 (s, 3H, Me-17), 1.47 (s, 3H, Me-18), 1.45 (s, 3H, Me-12), 1.33 (s, 3H, Me-13) ppm.
^{13}C NMR (125 MHz, CD_3COCD_3)	:	δ 181.4 (C-4), 162.6 (C-OH), 161.5 (C-OH), 159.5 (C-O-C), 152.1 (C-O-C), 151.6 (C-5), 147.1 (C-4'), 137.9 (C-5'), 133.7 (C-6'), 127.9 (C-15), 115.9 (C-14), 112.7 (C-1'), 105.4 (C-3'), 105.3(C-10), 104.9 (C-8), 99.9 (C-6), 93.7 (C-11), 78.7 (C-16), 47.5 (C-10), 28.4 (C-17), 28.3 (C-18), 22.8 (C-12), 20.3 (C-13) ppm.
HR-ESIMS m/z	:	435.1438 $[M+H]^+$ (calcd for $C_{25}H_{23}O_7$, 435.1443)

NMR Spectral assignments were made on the basis of 1D and 2D NMR analysis and in comparison with the literature reports.

5.15.2.10. Isolation of compound 64

Compound **64** (9 mg) was obtained as brown amorphous solid, on eluting the sephadex-LH 20 column with methanol. IR, ^{1}H NMR, ^{13}C NMR and mass spectral studies of this compound and in comparison with literature values [Syah *et al*., **2006**], confirmed it to be artoindonesianin A-3.

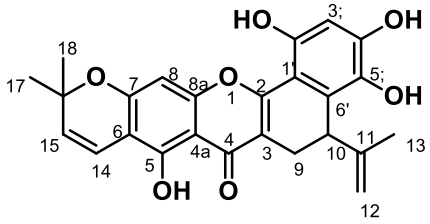

FT-IR (NaCl) υ_{max}	:	3404, 3100, 2975, 1640, 1622, 1431 cm^{-1}.
^{1}H NMR (500 MHz, $CDCl_3$)	:	δ 13.03 (s, 1H, OH-5), 6.54 (d, *J* = 10.0 Hz, 1H, H-14), 6.50 (s, 1H, H-3'), 6.29 (s, 1H, H-8), 5.64 (d, *J* = 10.0 Hz, 1H, H-15), 4.78 (s, 1H, H-12), 4.47 (s, 1H, H-12), 3.88 (d, *J* = 7 Hz, 1H, H-10), 3.36 (dd, *J* = 16.5, 2.0 Hz, 1H, H-9), 2.60 (dd, J_1 = 16.4, J_2 = 7.4 Hz, 1H, H-9), 2.18 (d, *J* = 3.0 Hz, 3H, Me-13), 1.48 (s, 3H, Me-17), 1.46 (s, 3H, Me-18) ppm.
^{13}C NMR (125 MHz, $CDCl_3$)	:	δ 180.1 (C-4), 161.8 (C-2), 159.6 (C-7), 159.2 (C-8a), 150.9 (C-2'), 150.5 (C-4'), 149.8, 144.8 (C-11), 134.9 (C-5'), 128.6 (C-15), 127.7 (C-6'), 113.9 (C-14), 112.6 (C-12), 110.9 (C-3), 110.0, 105.2 (C-6), 104.8, 102.9 (C-3'), 100.7 (C-8), 77.9 (C-16), 37.9 (C-10), 29.2 (C-17), 28.2 (C-18), 21.7 (C-9), 21.0 (C-13) ppm.
HR-ESIMS m/z	:	435.1441 $[M+H]^+$ (calcd for $C_{25}H_{23}O_7$, 435.1443)

NMR Spectral assignments were made on the basis of 1D and 2D NMR analysis and in comparison with the literature reports.

5.15.2.11. Isolation of compound 65

Compound **65** (12 mg) was obtained as white solid, on eluting the sephadex-LH 20 column with methanol. IR, ^{1}H NMR, ^{13}C NMR and mass spectral studies of this compound and in comparison with literature values [Aida *et al*., **1997**; Chun Lan *et al*., **2013**], confirmed it to be artonol B.

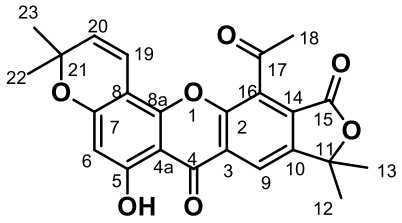

Melting point	:	190-192 ^{o}C
FT-IR (NaCl) υ_{max}	:	3432, 3100, 2100, 1740, 1715, 1643, 1622 cm^{-1}.
^{1}H NMR (500 MHz, $CDCl_3$)	:	δ 12.49 (s, 1H, OH-5), 8.30 (s, 1H, H-9), 6.60 (d, *J* = 10 Hz, 1H, H-19), 6.32 (s, 1H, H-6), 5.64 (d, *J* = 10 Hz, 1H, H-20), 2.81 (s, 3H, Me-18), 1.76 (s, 6H, Me-22, Me-23), 1.49 (s, 6H, Me-12, Me-13) ppm.
^{13}C NMR (125 MHz, $CDCl_3$)	:	δ 198.4 (C-17), 179.2 (C-4), 166.7 (C-15), 163.2 (C-OH), 162.3 (C-O-C), 151.3 (C-O-C), 151.1 (C-O-C), 148.7 (C-10), 130.2 (C-16), 128.2 (C-20), 126.5 (C-14), 125.2 (C-3), 119.2 (C-9), 114.2 (C-19), 103.6 (C-4a), 101.4 (C-8), 100.2 (C-6), 86.6 (C-11), 79.1 (C-21), 32.3 (C-18), 28.5 (2C, C-22, C-23), 27.6 (2C, C-12, C-13) ppm.
HR-ESIMS m/z	:	419.1128 $[M-H]^{+}$ (calcd for $C_{24}H_{19}O_7$, 419.1130)

NMR Spectral assignments were made on the basis of 1D and 2D NMR analysis and in comparison with the literature reports.

5.15.2.12. Isolation of compound 66

Fraction pool 41-44 was subjected to precipitate by using water afforded compound **66** (90 mg) which was confirmed to be oxyresveratrol.

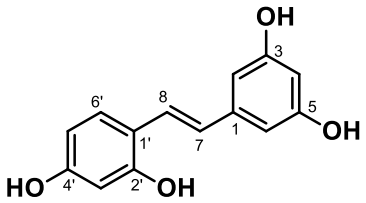

Melting point	:	200-202 ^{o}C
FT-IR (NaCl) υ_{max}	:	3209, 2921, 1589 cm^{-1}.
^{1}H NMR (500 MHz, CD_3COCD_3)	:	δ 8.75 (s, 1H, OH-4'), 8.59 (s, 1H, OH-2'), 8.39 (s, 2H, OH-3, OH-5), 7.41 (d, *J* = 8.5 Hz, 1H, H-6'), 7.35 (d, *J* = 16.5 Hz, 1H, H-7), 6.91 (d, *J* = 16.5 Hz, 1H, H-8), 6.55 (d, *J* = 2.1 Hz, 2H, H-2, H-6), 6.45 (d, *J* = 2 Hz, 1H, H-3'), 6.40 (dd, J_1 = 8.5, J_2 = 2.5 Hz, 1H, H-5'), 6.27 (t, *J* = 2 Hz, 1H, H-4) ppm.
^{13}C NMR (125 MHz, CD_3COCD_3)	:	δ 159.5 (2C, C-3, C-5), 159.1 (C-4'), 156.9 (C-2'), 141.7 (C-1), 128.3 (C-6'), 126.3 (C-7), 124.4 (C-8), 117.3 (C-1'), 108.5 (C-5'), 105.5 (2C, C-2, C-6), 103.7 (C-3'), 102.4 (C-4) ppm.
HR-ESIMS m/z	:	245.1802 $[M+H]^+$ (calcd for $C_{14}H_{13}O_4$, 245.1803)

5.15.3. Extraction of *A. lakoocha* stem bark

The stem bark of *A. camansi* was collected from Calicut district, Kerala. This was thoroughly cleaned and dried in drier maintained at 50 ^{o}C and powdered. The powdered stem bark (750 g) was subjected to repeated extraction using acetone and ethanol (2.5 L X 48h) at room temperature. After extraction, the solvent was removed under reduced pressure using Büchi rotary evaporator. The acetone extract (25.5 g) was then subjected to column chromatographic separation.

5.15.4. Isolation of compounds from *A. lakoocha* stem bark

The acetone extract (25.5 g) of the stem bark of *A. lakoocha* dissolved in minimum quantity of acetone and was adsorbed in silica gel (100-200) loaded on the top of silica gel column filled with slurry of 100-200 mesh silica gel in hexane. The column was eluted successively with gradient mixtures of hexane and ethyl acetate of increasing polarities and

finally with 10 % methanol in ethyl acetate. A total of 105 fractions of approximately 200 mL each were collected. According to the similarity in TLC, they were pooled into 20 major fraction pools (FrA.1- FrA. 20). Pictorial representation of the procedure for the isolation of the compound is shown in figure 5.47.

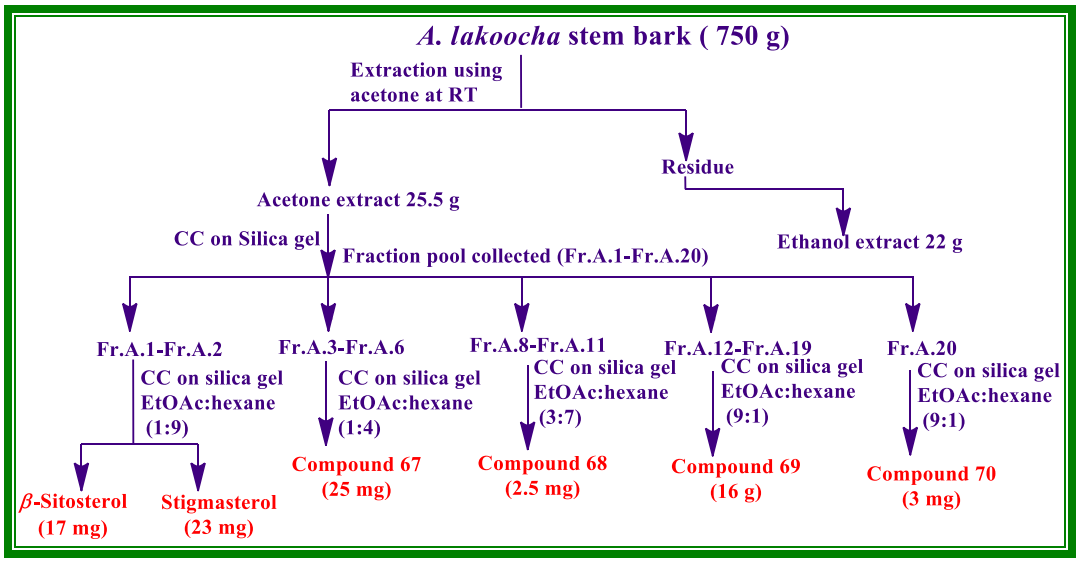

Figure 5.47: Pictorial representation of isolation of compounds from *A. lakoocha* stem bark

5.15.4.1. Isolation of compound 67

The isolation procedure of compound **67** is represented in figure 5.47. Compound **67** (25 mg) was obtained as a white solid, on eluting the column with 20 % ethyl acetate in hexane. IR, ^{1}H NMR, ^{13}C NMR and mass spectral studies of this compound made a comparison with the literature compound **59**, confirmed as *E*-resveratrol, previously isolated from *A. camansi* stem bark.

5.15.4.2. Isolation of compound 68

Compound **68** (12 mg) was obtained as white solid, on eluting the column with 30 % ethyl acetate in hexane. IR, ^{1}H NMR, ^{13}C NMR and mass spectral studies of this compound and in comparison with literature values [Kapche *et al*., **2009**], confirmed it to be moracin S.

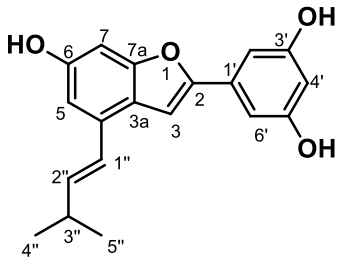

FT-IR (NaCl) υ_{max}	:	3419, 1697, 1622, 1578, 1423, 1157 cm^{-1}.
^1H NMR (500 MHz, CD_3COCD_3)	:	δ 8.54 (s, 1H, OH-6), 8.29 (s, 2H, OH-3', OH-5'), 7.48 (s, 1H, H-3), 6.88 (s, 1H, H-5), 6.87 (s, 1H, H-7), 6.71 (d, *J* = 2 Hz, 2H, H-2', H-6'), 6.64 (d, *J* = 16 Hz, 1H, H-1"), 6.23 (t, *J* = 2.0 Hz, 1H, H-4'), 6.08 (dd, J_1 = 16.0, J_2 = 7.0 Hz, 1H, H-2"), 2.39-2.32 (m, 1H, H-3"), 0.98 (s, 3H, Me-4"), 0.96 (s, 3H, Me-5") ppm.
^{13}C NMR (125 MHz, CD_3COCD_3)	:	δ, 158.9 (2C, C-3', C-5'), 154.9 (C-7a), 154.8 (C-2), 152.9 (C-6), 136.5 (C-2"), 132.4 (C-1'), 122.5 (C-3a), 122.1(C-1"), 122.0, 117.5 (C-3), 102.9 (2C, C-2'. C-6'), 102.7 (C-4'), 101.4 (C-5), 97.4 (C-7), 31.8 (C-3"), 22.1 (2C, C-4", C-5") ppm.
HR-ESIMS m/z	:	311.1281 $[M+H]^+$ (calcd for $C_{19}H_{19}O_4$, 311.1283)

NMR Spectral assignments were made on the basis of ^{13}C, DEPT NMR analysis and in comparison with the literature reports.

5.15.4.3. Isolation of compound 69

The isolation procedure of compound **69** is represented in figure 5.47. Compound **69** (16 g) was obtained as a white solid, on eluting the column with 90 % ethyl acetate in hexane. IR, ^1H NMR, ^{13}C NMR and mass spectral studies of this compound and in comparison with compound **66,** confirmed as oxyresveratrol, previously isolated from *A. camansi* stem bark.

5.15.4.4. Isolation of compound 70

Compound **70** (3 mg) was obtained as white solid, on eluting the column with 90 % ethyl acetate in hexane. IR, ^1H NMR, ^{13}C NMR and mass spectral studies of this compound

and in comparison with literature values [Takasugi *et al*., **1978**], confirmed it to be 4-prenyl oxyresveratrol.

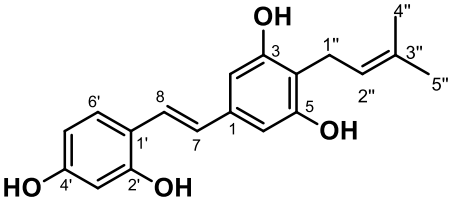

Melting point	:	196-198 ^{o}C
FT-IR (NaCl) υ_{max}	:	3220, 2920, 1569 cm^{-1}.
^{1}H NMR (500 MHz, CD_3COCD_3)	:	δ 8.44 (s, 1H, OH-4'), 8.25 (s, 1H, OH-2'), 7.95 (s, 2H, OH-3, OH-5), 7.24 (d, *J* = 8.5 Hz, 1H, H-6'), 7.13 (d, *J* = 16.5 Hz, 1H, H-7), 6.69 (d, *J* = 16.5 Hz, 1H, H-8), 6.44 (s, 2H, H-2, H-6), 6.30 (d, *J* = 2.5 Hz, 1H, H-3'), 6.24 (dd, J_1= 8.5, J_2 = 2.5 Hz, 1H, H-5'), 5.16 (t, *J* = 5 Hz, 1H, H-2"), 3.21 (d, *J* = 7.0 Hz, 2H, H-1"), 1.63 (s, 3H, Me-4"), 1.50 (s, 3H, Me-5") ppm.
^{13}C NMR (125 MHz, CD_3COCD_3)	:	δ 157.0 (3C, C-3, C-5, C-4'), 156.8 (C-2'), 130.6 (C-3"), 127.9 (C-2"), 126.2 (C-7), 124.5 (C-8), 123.4 (C-5'), 108.4 (C-6'), 105.5 (2C, C-2, C-6), 103.6 (C-3'), 100.9 (C-1), 25.9 (C-1"), 23.1 (C-4"), 17.9 (C-5") ppm.
HR-ESIMS m/z	:	314.1439 $[M+H]^+$ (calcd for $C_{19}H_{21}O_4$, 314.1439)

5.15.5. 2-NBDG uptake in L6 myotubes

L6 myoblasts seeded in 96 well black clear bottom plates (BD Bio-sciences, Franklin Lakes, NJ, USA) was differentiated to myotubes for 5 days and was evaluated by examining multinucleation. After pretreatment with the least cytotoxic concentration of compounds (5 μM) for 24 hours, medium was removed from each well and replaced with fresh culture medium in the absence and presence of 100 μM fluorescent 2-NBDG (Molecular Probes-Invitrogen), incubated for 30 min. The cells were then washed with cold PBS and the

fluorescence in cells were imaged by a fluorescent microscope (BD Pathway 855, BD Biosciences, CA, USA) equipped with filters in the fluorescein isothiocyanate (FITC) range filters (excitation, 490 nm and emission, 525 nm, bandpass filters).

CHAPTER 6A

Isolation of dihydro-*β*-agarofuran sesquiterpenoids from the seeds of *Celastrus paniculatus* Willd.

6a.1. Celastraceae an overview

The family Celastraceae is widespread in the tropical and sub-tropical regions of the world with approximately 88 genera and 1300 species, including trees, shrubs and liana plants [Spivey *et al*., **2002**; Gao *et al*., **2007**]. In India, it is distributed throughout at elevations up to 1200 m, mainly in deciduous forests. Among the 88 genera, *Maytenus*, *Tripterygium, Celastrus* and *Euonymus* are well studied for their phytochemical constituents and have been used in traditional medicine and agriculture around the world.

Over the last 30 years, a large variety of biologically-active secondary metabolites have been identified from the members of the Celastraceae which possess broad spectrum of biological activities such as antitumor [Takaishi *et al*., **1992**], anti-inflammatory [Jin *et al*., **2002**], analgesic [Ahmad *et al*., **1994**], cytotoxic [Kuo *et al*., **1994**], hypolipidemic [Patil *et al*., **2010**], anti-plasmodial [Mba'ning *et al*., **2013**], anti-HIV [Gutierrez-Nicolas *et al*., **2014**], anti-tubercular [Chou *et al*., **2007**], immunosuppressant [Luo *et al*., **2014**] and insecticidal [Jinbo *et al*., **2002**] activities.

The plants of Celastraceae are an important source of terpenoids such as triterpenes of a series of friedelane, lupane, oleanane and diterpenes such as kaurane and abietane. However, the most widespread and characteristic metabolites of this family are a large group of unusually highly oxygenated sesquiterpenoids, based on the 5, 11-epoxy-5*β*, 10*α*-eudesman-4-(14)-ene skeleton commonly known as dihydro-*β*-agarofurans (Fig. 6a.1). They are well recognized as chemotaxonomic markers or indicators of the family [Spivey *et al*., **2002**; Gao *et al*., **2007**; Ning *et al*., **2015**].

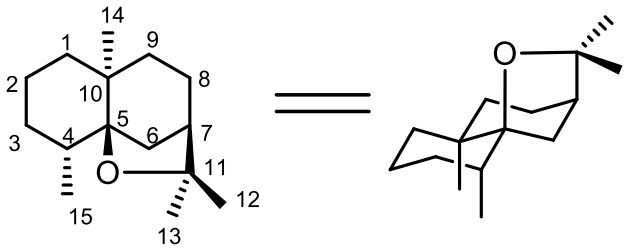

Figure 6a.1: General scaffold of dihydro-*β*-agarofuran

Among various Celastraceae species, *Celastrus paniculatus* Willd. is one of the least explored medicinally important woody liana indigenous to Western Ghats of India chiefly found in the deciduous. The genus *Celastrus,* consists of nearly 40 species of shrubs and vines. They have a wide distribution in East Asia, Australia and Africa. The name and distribution of important plant species belonging to the genus *Celastrus* are given in table 6a.1.

Table 6a.1: *Celastrus* species and their distribution

SI. No	***Celastrus* species**	**Distribution**
1	*C. aculeatus* Merr.	China
2	*C. angulatus* Maxim.	China
3	*C. casearіifolius* Lundell	Colombia
4	*C. cuneatus*	China
5	*C. flagellaris* Rupr.	South Korea and Japan
6	*C. franchetianus* Loes.	China
7	*C. gemmatus* Loes.	China
8	*C. glaucophyllus*	China
9	*C. hindsii* Benth.	Thailand
10	*C. hirsutus*	China
11	*C. hookeri* Prain	India
12	*C. hypoleucus*	China
13	*C. kusanoi Hayata*	China
14	*C. lenticellatus* Lundell	Mexico
15	*C. liebmannii* Standl.	Mexico
16	*C. madagascariensis* Loes.	Madagascar
17	*C. membranifolius* Prain	China
18	*C. monospermoides* Loes.	Malaysia and Philippines
19	*C. monospermus* Roxb.	India and Vietnam
20	*C. novoguineensis* Merr.	Papua New Guinea
21	*C. orbiculatus* Thunb.	China

		Table 6a.1 contd…
22	*C. pachyrachis* Lundell	Venezuela
23	*C. panamensis* Lundell	Panama
24	***C. paniculatus* Willd.**	India and Vietnam
25	*C. pringlei* Rose	Mexico
26	*C. punctatus* Thunb.	Japan and China
27	*C. richii* A.Gray	Fiji
28	*C. rosthornianus* Loes.	China
39	*C. scandens* L.	United States
30	*C. stylosus* Wall.	China
31	*C. subspicatus* Hook.	Australia
32	*C. vulcanicolus* Donn.Sm.	Honduras

6a.1.1. Dihydroxylated dihydro-*β*-agarofuran sesquiterpene esters

There are four dihydroxylated polyesters reported in Celastraceae family (Figure 6a.2). Three of these dihydroxylated agarofuran have been reported from the fruits of *T. wilfordii* var. [Takaishi *et al*., **1991**]. The remaining, 1*α*-Acetoxy-9*β*-*β*-phenyloxacyclobutanoyloxy dihydrob-agarofuran only found in *C. gemmatus* species [Yongqiang *et al*., **1990**].

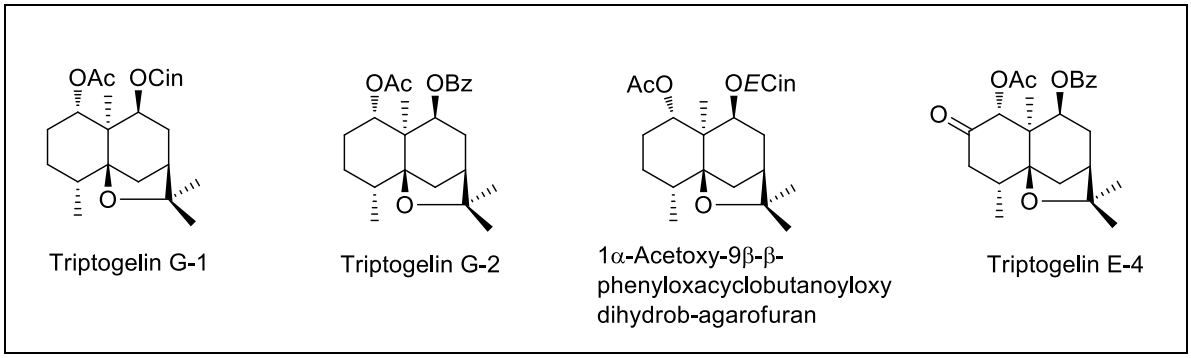

Figure 6a.2: Dihydroxylated dihydro-*β*-agarofuran from Celastraceae

6a.1.2. Trihydroxylated dihydro-*β*-agarofuran sesquiterpene esters

In 1992, Takaishi and co-workers reported the major triptogelin, trihydroxylated dihydro-*β*-agarofuran sesquiterpenes from *Tripterygium wilfordii var*. [Takaishi *et al*., **1992**]. Orbiculin and its derivatives were reported from *Celastrus orbiculatus* which are reversing multidrug resistance in cancer cells [Kim *et al*., **1998**]. Some of the trihydroxylated dihydro-*β*-agarofuran sesquiterpenes isolated from Celastraceae are shown below (Figure 6a.3).

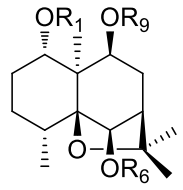

R_1 = Ac, R_6 = Cin, R_9 = Bz; Celafolin A-1
R_1 = Ac, R_6 = Bz, R_9 = Bz; Celorbicol ester
R_1 = Ac, R_6 = Fu, R_9 = Bz; Orbiculin B
R_1 = Ac, R_6 = Bz, R_9 = Fu; Orbiculin C
R_1 = Ac, R_6 = Fu, R_9 = Fu; Orbiculin D
R_1 = Ac, R_6 = Nic, R_9 = Bz; Triptogelin F-1
R_1 = Ac, R_6 = Ac, R_9 =Cin; Triptogelin F-2

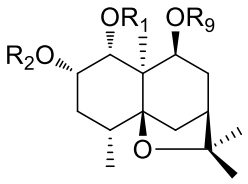

R_1 = Ac, R_2 = MeBut, R_9 = Bz; Triptogelin E-1
R_1 = Ac, R_2 = Ac, R_9 = Bz; Triptogelin E-2
R_1 = Ac, R_2 = MeBut, R_9 = Cin; Triptogelin E-3
R_1 = Ac, R_2 = nBu, R_9 = Bz; Triptogelin E-5
R_1 = Ac, R_2 = iBu, R_9 = Bz; Triptogelin E-6
R_1 = Ac, R_2 = nBu, R_9 = Cin; Triptogelin E-7
R_1 = Ac, R_2 = iBu, R_9 = Cin; Triptogelin E-8
R_1 = Ac, R_2 = H, R_9 = Cin; Celafolin B-1
R_1 = H, R_2 = Ac, R_9 = Cin; Celafolin B-2
R_1 = Ac, R_2 = Bz, R_9 = Cin; Celafolin B-3

Figure 6a.3: Trihydroxylated dihydro-*β*-agarofuran from Celastraceae

6a.1.3. Tetrahydroxylated dihydro-*β*-agarofuran sesquiterpene esters

There are 75 tetrahydroxylated dihydro-*β*-agarofuran sesquiterpene esters reported from Celastaraceae. Of these, majority of the compounds isolated from the genera *Celastraus*. Kim and co-workers reported the isolation of tetrahydroxylated dihydro-*β*-agarofuran sesquiterpene esters from the roots of *Celastrus orbiculatus* [Kim *et al*., **1999**]. Triptogelin B and C have been isolated from the achenes of *Tripterygium wilfordii* Hook fil. var. and this plant has been used as an anticancer drug by the Chinese for hundreds of years [Takaishi *et al*., **1991**]. Now this plant has been used to treat rheumatoid arthritis and spondylitis in some Chinese clinics. Angulatueoids are the class of tetrahydroxylated dihydro-*β*-agarofuran reported from the species *Celastrus angulatus* which are attracted interest as a consequence of their cytotoxic and antitumour promoter activities [Liu *et al*., **1995;** Chunquan *et al*., **1992**]. Some of the tetrahydroxylated dihydro-*β*-agarofuran reported from Celastraceae are shown below (Figure 6a.4).

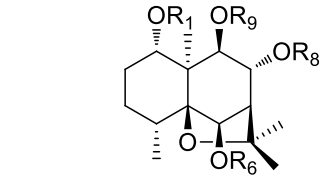

R_1 = Ac, R_6 = Ac, R_8 = Ac, R_9 = Bz; Celafolin C-1
R_1 = Ac, R_6 = Ac, R_8 = Ac, R_9 = Fu; Eumaitenin
R_1 = Ac, R_6 = Fu, R_8 = Ac, R_9 = Fu; Orbiculin H
R_1 = Bz, R_6 = Ac, R_8 = Bz, R_9 = Bz; Celafolin D-1
R_1 = Bz, R_6 = Ac, R_8 = MeBut, R_9 = Bz; Celafolin D-3
R_1 = Ac, R_6 = Ac, R_8 = Bz, R_9 = Bz; Angulatueoid H
R_1 = H, R_6 = Ac, R_8 = Bz, R_9 = Bz; Triptogelin B-1
R_1 = Nic, R_6 = Ac, R_8 = Bz, R_9 = Bz; Triptogelin B-2

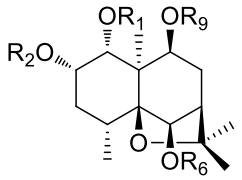

R_1 = Ac, R_2 = Ac, R_6 = Ac, R_9 = Bz; Triptogelin C-1
R_1 = Ac, R_2 = Ac, R_6 = Nic, R_9 = Bz; Triptogelin C-2
R_1 = Ac, R_2 = MeBut, R_6 = Ac, R_9 = Bz; Triptogelin C-3
R_1 = Ac, R_2 = H, R_6 = Nic, R_9 = Bz; Triptogelin C-4
R_1 = Ac, R_2 = Ac, R_6 = Bz, R_9 = Bz; Orbiculin A
R_1 = Ac, R_2 = Ac, R_6 = Fu, R_9 = Bz; Orbiculin E
R_1 = Ac, R_2 = Fu, R_6 = Fu, R_9 = Bz; Orbiculin F
R_1 = Ac, R_2 = Bz, R_6 = Bz, R_9 = Bz; Orbiculin G

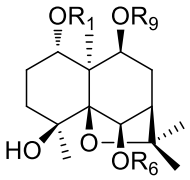

R_1 = Ac, R_6 = Fu, R_9 = Fu; Eumai(y)tenol
R_1 = Nic, R_6 = Nic, R_9 = Cin; Wilforcidine
R_1 = Bz, R_6 = H, R_9 = Bz; Triptofordin B
R_1 = Bz, R_6 = Nic, R_9 = Bz; Regelidine

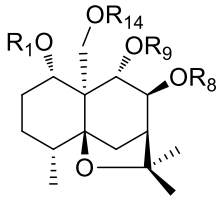

R_1 = iBu, R_8 = Ac, R_9 = Bz, R_{14} = Nic; Angulatueoid E
R_1 = Pro, R_8 = Ac, R_9 = Bz, R_{14} = Nic; Angulatueoid F
R_1 = Ac, R_8 = Ac, R_9 = Bz, R_{14} = Ac; Angulatueoids C
R_1 = Ac, R_8 = Ac, R_9 = Bz, R_{14} = Pic; Angulatueoid D
R_1 = Bz, R_8 = Nic, R_9 = Ac, R_{14} = Ac; Kupitengester II
R_1 = Bz, R_8 = Ac, R_9 = Ac, R_{14} = Ac; Kupitengester IV

Figure 6a.4: Tetrahydroxylated dihydro-*β*-agarofuran from Celastraceae

6a.1.4. Pentahydroxylated dihydro-*β*-agarofuran sesquiterpene esters

Extensive phytochemical investigation of *Reissantia buchananii* (Loes.) resulted in the isolation of 5-carboxy-N-methyl-2-pyridone (Pyd) substituent pentahydroxylated dihydro-*β*-agarofuran sesquiterpenes reissantin [Chang *et al*., **2003**]. Majority of the tetrahydroxylated dihydro-*β*-agarofuran sesquiterpenes are isolated from the genus *Tripterygzum* [Takaishi *et al*., **1991**]. Some of the previously reported pentahydroxylated agarofurans are shown in figure 6a.5.

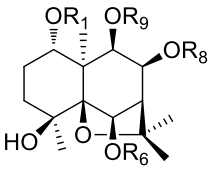

R_1 = Ac, R_6 = Pyd, R_8 = Ac, R_9 = Bz; Reissantin A
R_1 = Fu, R_6 = Ac, R_8 = Pyd, R_9 = Fu; Reissantin C
R_1 = Ac, R_6 = H, R_8 = H, R_9 = Bz; Reissantin D
R_1 = Ac, R_6 = H, R_8 = Ac, R_9 = Bz; Reissantin E
R_1 = H, R_6 = Pyd, R_8 = Ac, R_9 = Bz; Reissantin G

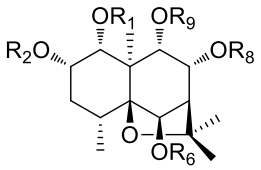

R_1 = Bz, R_2 = Bz, R_6 = Ac, R_8 = Bz, R_9 = Bz; Triptogelin A-1
R_1 = Bz, R_2 = H, R_6 = Ac, R_8 = Bz, R_9 = Bz; Triptogelin A-2
R_1 = H, R_2 = H, R_6 = Ac, R_8 = Bz, R_9 = Bz; Triptogelin A-3
R_1 = Nic, R_2 = Bz, R_6 = Ac, R_8 = MeBut, R_9 = Bz; Triptogelin A-5
R_1 = Bz, R_2 = Bz, R_6 = Ac, R_8 = Nic, R_9 = Bz; Triptogelin A-6

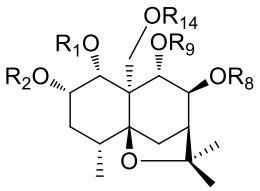

R_1 = Ac, R_2 = Ac, R_8 = Ac, R_9 = Bz, R_{14} = Pic; Angulatueoids A
R_1 = Ac, R_2 = Ac, R_8 = Ac, R_9 = Bz, R_{14} = Ac; Angulatueoids B

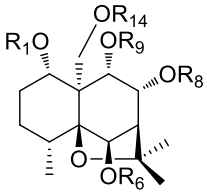

R_1 = Ac, R_6 = Ac, R_8 = Ac, R_9 = Bz, R_{14} = Ac; Celastrine A
R_1 = Ac, R_6 = Ac, R_8 = Bz, R_9 = Ac, R_{14} = Ac; Kiautschovin

Figure 6a.5: Pentahydroxylated dihydro-*β*-agarofuran from Celastraceae

6a.1.5. Biosynthetic Pathway of dihydro-*β*-agarofuran

Biosynthetic Pathway of dihydro-β-agarofuran begins with isopentenyl pyrophosphate (IPP) by mevalonic acid pathway, which on isomerization to form DMAPP by the enzyme isopentenyl pyrophosphate isomerase. The formation of GPP and FPP from DMAPP are catalyzed by prenyl transferases enzymes. Cyclization of FPP to form corresponding conformers of germacran cation (A), which on *trans*-antiparallel cyclization; a subsequent hydride migration leads to the formation of another cation (B), finally cyclization by proton splitting to form dihydro-*β*-agarofuran [Bruning *et al*., **1978**] (Scheme 6a.1).

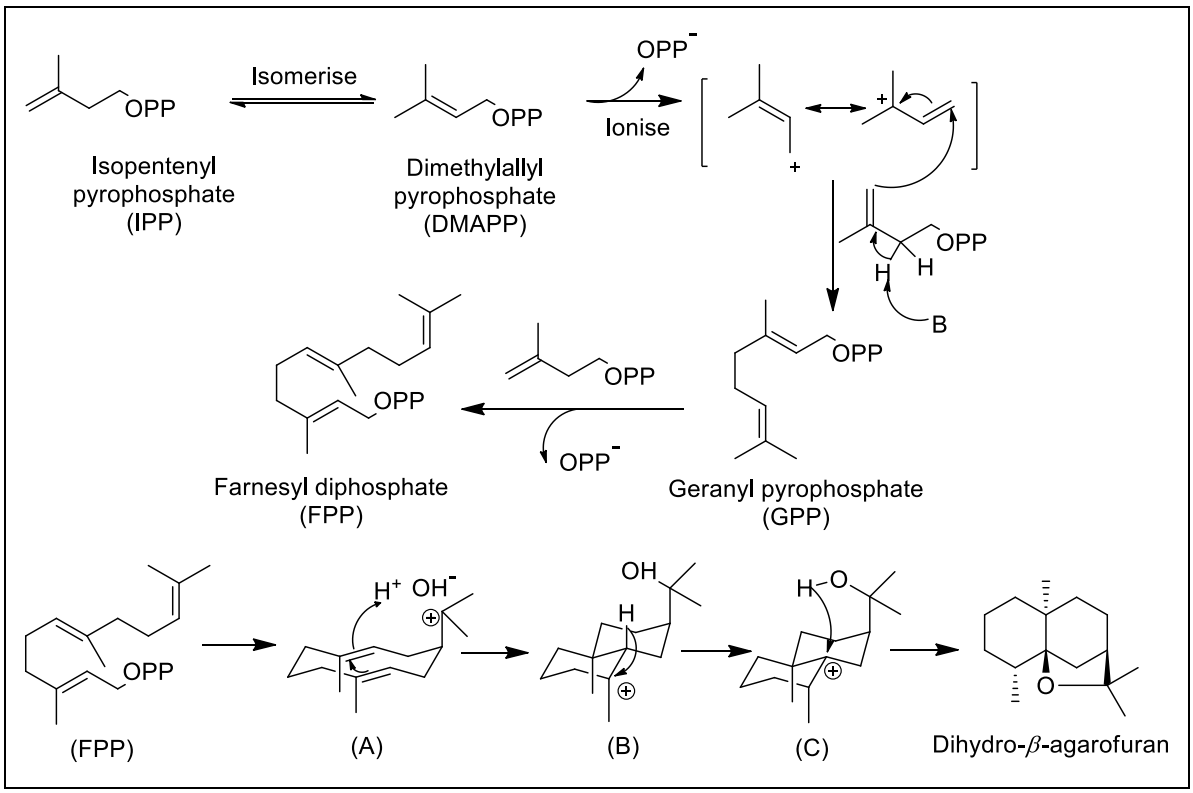

Scheme 6a.1. Biosynthetic Pathway of dihydro-*β*-agarofuran

6a.2. *Celastrus paniculatus*

Celastrus paniculatus Willd. commonly known as Killithinipanji, Jyothishmathi, Cherupunna, is a medicinally important plant belonging to the family Celastraceae. It is a deciduous twining shrub with pale brown rough and cracked bark, branchlets pubescent or glabrous, with prominent elliptic lenticels. Leaves are simple, alternate, stipules, spiral and lacinate. Flowers are pale greenish; Male flowers: long, sepals 5-lobed; Female flowers: sepals, petals, and disc as in the male flowers; stamens sterile; ovary globose; style columnar; stigma 3-lobed Seeds 3-6 with 3-5 x 2-4 mm size, brownish, smooth and arillate.

Ethnopharmacological relevance: *C. paniculatus* seed oil has a long history in traditional Indian systems of medicine and has been reported to improve memory, beneficial to psychiatric patients and increased the intelligence quotient (IQ) of mentally retarded children. *Celastrus paniculatus* seeds are used to relieve cognitive problems and promote intestinal health. Oil of this seeds is sometimes used during massage and is used to alleviate skin inflammation and has a mild sedative effect [Nadkarni, **1976**]. *Celastrus paniculatus* is one

of the plants used in 'medhya rasayanas'. Which are used for prevention and treatment of mental disorders of all the age group.

Figure 6a.6: Picture of *Celastrus paniculatus* leaves, plant, and seeds

6a.3. Scientific classification of *Celastrus paniculatus*

Table 6a.2: Scientific classification of *Celastrus paniculatus*

Kingdom	**Plantae**
Phylum	**Tracheophyta**
Class	**Magnoliopsida**

Order	**Celastrales**
Family	**Celastraceae**
Genus	***Celastrus***
Species	***C. paniculatus***

6a.4. Aim and scope of the present work

Celastrus paniculatus, is widely known as the "intellect tree," a black oil deciduous vine plant which grows natively throughout the Indian subcontinent. It has been used in various Indian cultural and medical traditions, such as Ayurveda and Unani. *C. paniculatus* has been used to both sharpen mental focus and relax the nerves. Now the plant is delineated as one of the threatened species in the red list of International Union for Conservation of Nature (IUCN Red list-August 2010), which demands an urgent attention for conservation. Therefore it appeared timely and relevant to carry out the phytochemical and pharmacological evaluation of *C. paniculatus.* As part of our ongoing search for new bioactive chemical entities based on the traditional medicinal plants, a detailed study of *C. paniculatus* seeds has been undertaken. Evaluation of chemical indices of two different extracts of *C. paniculatus* seeds have been carried out and the results are described in this chapter.

6a.5. Extraction and isolation of phytochemicals from *C. paniculatus* seeds

6a.5.1. Plant material

The seeds of *Celastrus paniculatus* Willd. were collected from the Western Ghats region (Wayanad District) of Kerala state, India. The plant material was authenticated by the taxonomist of M. S. Swaminathan Research Foundation (MSSRF), Kerala and a voucher specimen (M.S.S.H. 4396) was deposited in the herbarium repository of the institute.

6a.5.2. Extraction and isolation of *C. paniculatus* (CP)

The air-dried seed powder of the *C. paniculatus* (1 kg) was extracted successively with n-hexane (H), acetone (A), ethanol (E) and water (W). The supernatant liquid was decanted and filtered. These extracts were then concentrated under reduced pressure in a rotary

vacuum evaporator (Heidolph, Germany) to remove the residual solvent, which yielded 60.5 g (H), 15 g (A), 12 g (E) and 9 g (W) of crude extracts.

6a.5.3. Isolation and characterization of compounds

The hexane-extract (60.5 g) was fractionated on a silica gel (100-200 mesh) column and eluted with n-hexane/EtOAc gradient (100 % n-hexane to 100 % EtOAc). Each fraction was analyzed by TLC (n-hexane-EtOAc), and those displaying the same TLC profile were combined to afford thirty fractions (FrH.1-FrH.30).

Compound **71** (52 mg; 0.005 %), obtained by eluting the column with 30 % ethyl acetate in hexane as stable colourless crystals and was assigned the molecular formula $C_{38}H_{40}O_8$ following analysis of the (+)-HRESIMS sodium adduct ion at m/z 647.2625 $[M + Na]^+$ (calcd for $C_{38}H_{40}O_8Na$, 647.2620). IR spectrum of the compound showed a broad signal at 3425 and 1711 cm^{-1}, indicating the presence of hydroxyl and ester group. The ^1H NMR spectrum of compound **71** revealed the signals corresponding to four methyl groups at δ_H 1.42, 1.52, 1.57 and 1.59 ppm, three oxygenated methine protons (δ 5.14, 5.61, and 5.62 ppm), 15 protons in the aromatic region for the two benzoyl and one cinnamoyl groups at (δ 7.24, 7.32, 7.48-7.39, 7.51-7.49, 7.58-7.54 and 7.80 ppm) and the *trans* double bond from the cinnamoyl group at (δ 6.49 and 7.90 ppm, at J = 16 Hz and 15.5 Hz) respectively. The ^{13}C NMR, HMQC and ^{13}C-DEPT spectra suggested the presence of 38 carbon atoms, consisting of four methyls, three methylenes, 21 methines, and ten nonprotonated carbons. The ^{13}C NMR resonances at δ 165.3, 165.5 and 166.3 ppm were indicative of three ester groups. Two oxygenated tertiary carbon signals were observed at δ 84.5 and 91.7 ppm, which were characteristic of the ethereal carbons of a dihydro-*β*-agarofuran [Chang *et al*., **2003**; Carroll *et al*., **2009**]. Fragments H-1/H2-1/H2-2/H3-1/H3-2 and H-6/H-7/H-8/H-9 were readily established from the ^1H-^1H COSY data (Figure 6a.8). Further clarification was deduced following analysis of HMBC data. HMBC correlations from both H-1 to C-4 and C-10, as well as from H-1 to C-5, constructed a partial structure of cyclohexane ring A substituted by a methyl and hydroxyl group at C-4 (Figure 6a.8). The HMBC spectrum of **71** also showed correlations from H-6 to C-5, from H-7 to C-9, and from H-9 to C-5 and C-10, revealing the presence of another six-membered ring B, which was fused to ring A (Figure 2). HMBC correlations from H-6 to C-5 and C-11, along with the ^{13}C NMR resonances of C-5 (δ 91.7 ppm) and C-11 (δ 84.5 ppm), suggested that C-5 and C-11 were oxygenated tertiary carbons

linked through an ether bond [Chang *et al*., **2003**; Carroll *et al*., **2009**]. A gem-dimethyl group was located on the oxygenated tertiary carbon C-11 based on HMBC correlations from Me-12 and Me-13 to C-11; these correlations also confirmed the gem-dimethyl group. Further HMBC correlations from Me-15 to C-9, and C-10 located Me-15 at C-10. The presence of two benzoyl and one cinnamoyl groups was indicated by HMBC correlations from the aromatic protons at δ 7.51-7.49 and 7.58-7.54 ppm to carbonyl resonances at δ 165.3, 165.5 and 166.3 ppm respectively. These considerations indicated that the compound **71** was a dihydro-*β*-agarofuran sesquiterpenoid containing two benzoate and one cinnamoyl groups. The two benzoate moieties were attached at C-1 and C-9 based on HMBC correlations from protons at δ 5.61 and 5.14 to the ester carbonyl groups at δ 165.3, 165.5 ppm. Similarly, the one cinnamoyl group was located at C-6, on the basis of HMBC correlations from H-6 to carbonyl carbons at δ 166.3 ppm. On the basis of these data, the 2D structure of compound **71** was established. The relative configuration was assigned by following ^{1}H-^{1}H NOESY analysis (Figure 6a.8). Correlations between H-9 and H-7 and between H-9 and H-6 showed that these protons were *α*-oriented. There is no notable correlation between H-9 and H-1 indicating that the proton at C-1 is *β*-oriented.

A single-crystal X-ray diffraction experiment was performed for compound **71** (Figure 6a.16), which unambiguously established the structure and absolute configuration of compound **71** as a novel **1*α*, 9*β*-dibenzoyloxy-6*β*-cinnamoyloxy-4*β*-hydroxydihydro-*β*-agarofuran**. The structure of the compound is shown below.

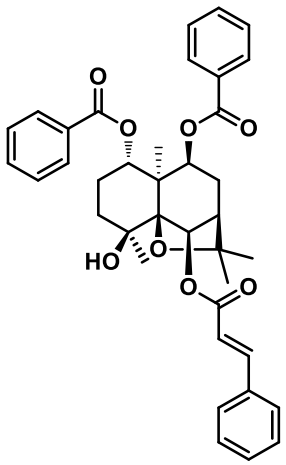

Figure 6a.7: 1*α*, 9*β*-dibenzoyloxy-6*β*-cinnamoyloxy-4*β*-hydroxydihydro-*β*-agarofuran **(71)**

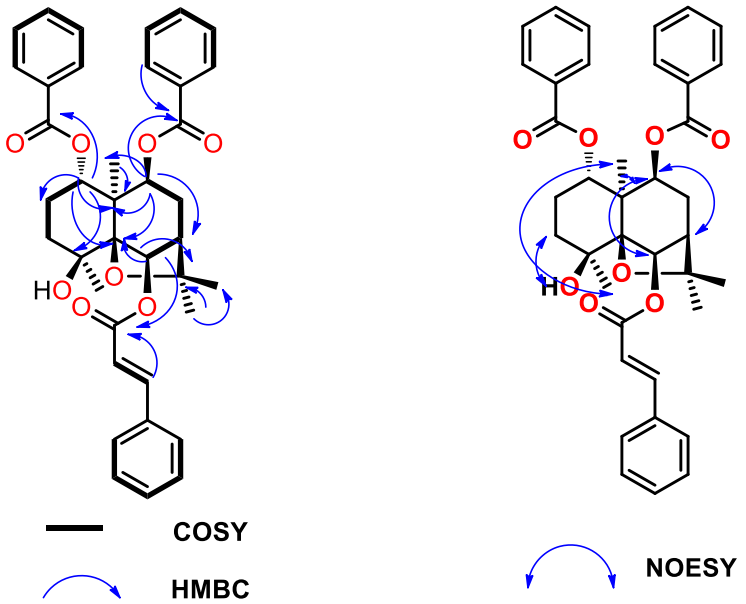

Figure 6a.8: Selected COSY, HMBC and NOESY correlations of compound **71**

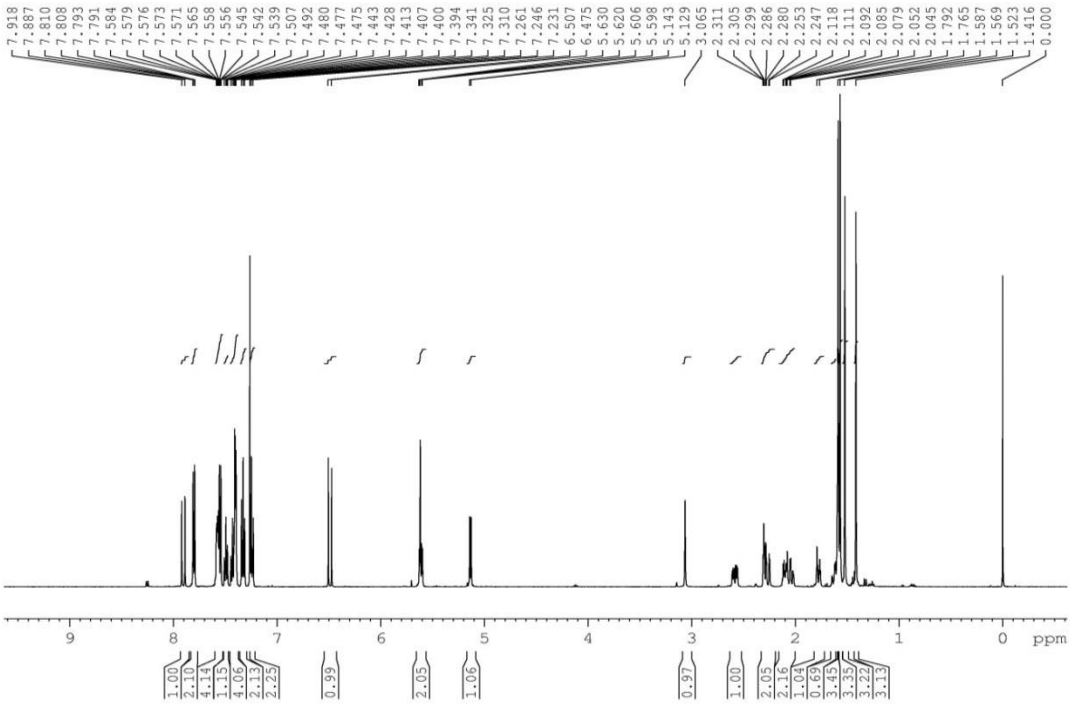

Figure 6a.9: ^{1}H NMR spectrum of compound **71**

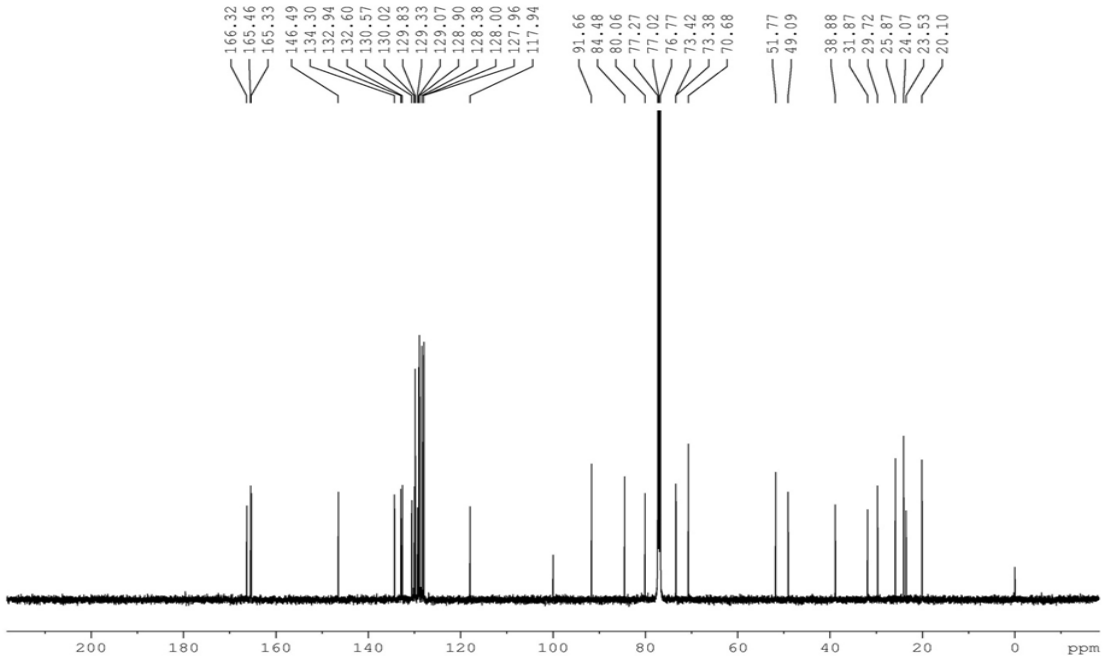

Figure 6a.10: ^{13}C NMR spectrum of compound **71**

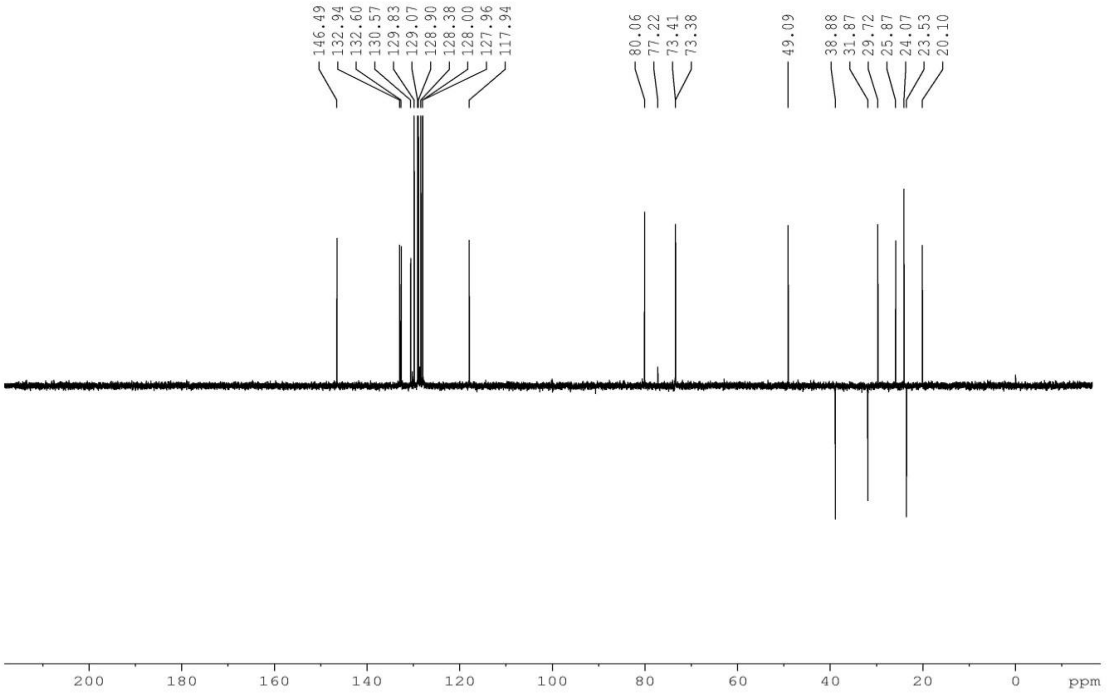

Figure 6a.11: ^{13}C DEPT 135 spectrum of compound **71**

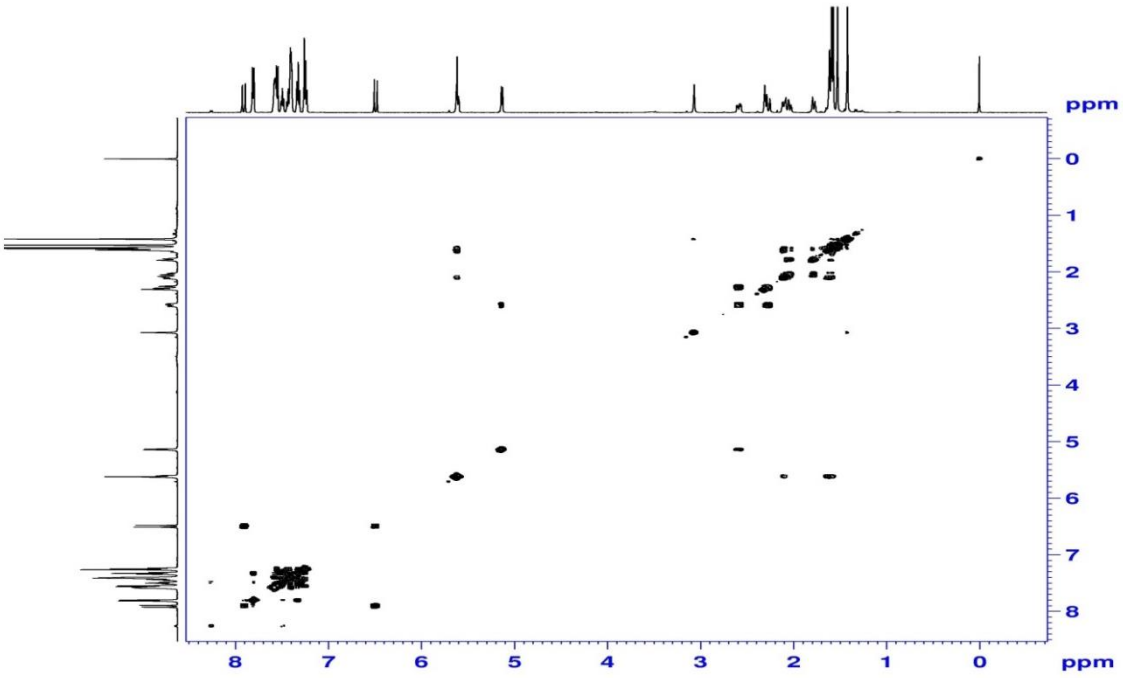

Figure 6a.12: ^{1}H-^{1}H COSY spectrum of compound **71**

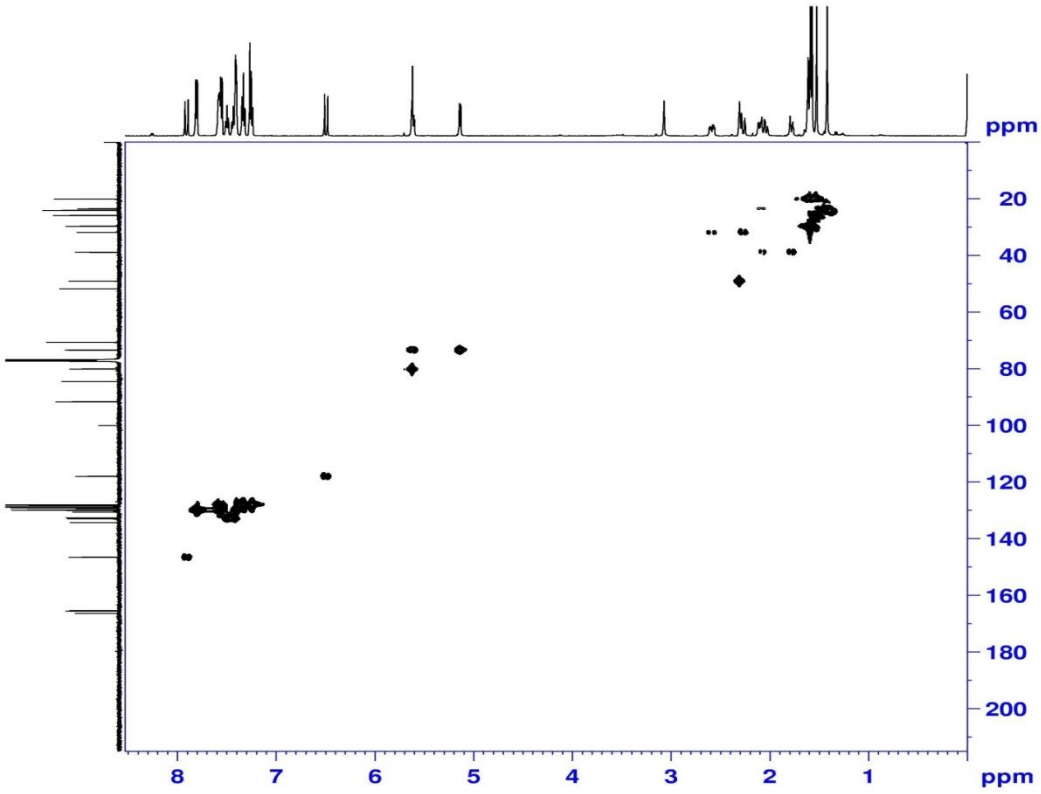

Figure 6a.13: HMQC spectrum of compound **71**

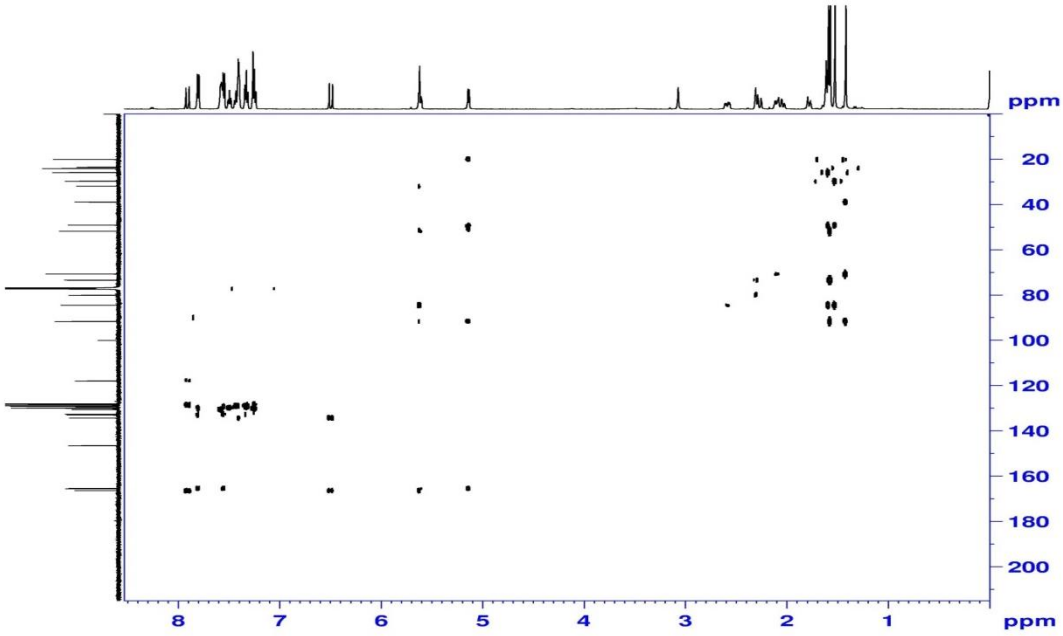

Figure 6a.14: HMBC spectrum of compound **71**

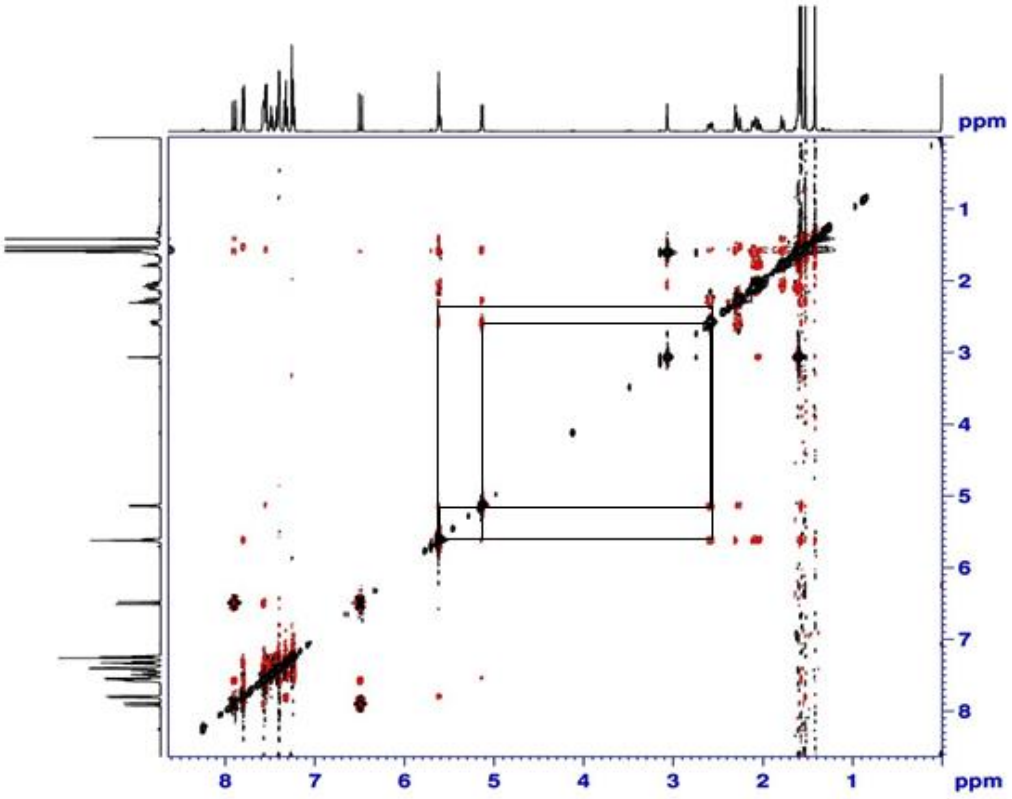

Figure 6a.15: NOESY spectrum of compound **71**

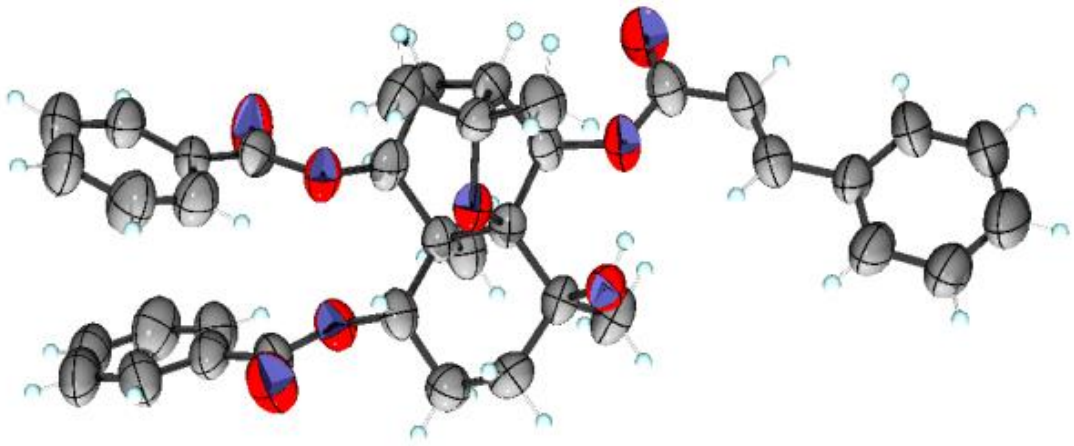

Figure 6a.16: ORTEP structure of compound **71**

Compound **72** was a novel molecule (1.38 g; 0.14 %), obtained as a white crystalline solid by eluting the column with 35 % ethyl acetate in hexane and was assigned the molecular formula $C_{28}H_{36}O_{10}$ following analysis of the (+)-HRESIMS sodium adduct ion at m/z 555.2215 $[M + Na]^+$ (calcd for $C_{28}H_{36}O_{10}Na$, 555.2206). IR spectrum of the compound showed a broad signal at 3446 and 1738 cm^{-1}, indicating the presence of hydroxyl and ester group. The ^1H NMR spectrum of compound **72** revealed the signals corresponding to six methyl groups at δ 1.31, 1.33, 1.53, 1.65, 1.88 and 2.31 ppm, three oxygenated methine protons (δ 5.28, 5.53 and 6.07 ppm), a pair of coupled oxymethylene doublets (δ 4.37, 4.96 ppm, J = 13 Hz), and one benzoyl group (5H, δ 7.44, 7.56 and 7.92 ppm). The ^{13}C NMR, HMQC and ^{13}C-DEPT spectra suggested the presence of 28 carbon atoms, consisting of six methyls, four methylenes, nine methines, and nine nonprotonated carbons. The ^{13}C NMR resonances at δ 165.7, 169.9, 170.4 and 170.5 ppm were indicative of four ester groups. Two oxygenated tertiary carbon signals were observed at δ 82.9 and 91.0 ppm, which are characteristic of the ethereal carbons of a dihydro-*β*- agarofuran [Chang *et al*., **2003**; Carroll *et al*., **2009**]. Fragments H-1/H2-1/H2-2/H3-1/H3-2 and H-6/H-7/H-8/H-9 were readily established from the ^1H-^1H COSY data (Figure 6a.18). Further confirmation was deduced from the following analysis of HMBC data. HMBC correlations from both H-1 to C-10, as well as from H-3 to C-4, constructed a partial structure of cyclohexane ring A substituted by a methyl and hydroxyl group at C-4 (Figure 6a.18). The HMBC spectrum also showed

correlations from H-6 to C-5 and C-8, from H-7 to C-5 and C-8, and from H-9 to C-10, revealing the presence of another six-membered ring B, which was fused to ring A (Figure 2). HMBC correlations from H-6 and H-7 to C-5 and C-11, along with the ^{13}C NMR resonances of C-5 (δ 91.0 ppm) and C-11 (δ 82.9 ppm), suggested that C-5 and C-11 were oxygenated tertiary carbons linked through an ether bond [Chang *et al*., **2003**; Carroll *et al*., **2009**]. A gem-dimethyl group was located on the oxygenated tertiary carbon C-11 based on HMBC correlations from Me-12 and Me-13 to C-6 and C-7; these correlations also confirmed that the gem-dimethyl group and C-7 were connected through the nonprotonated carbon C-11. Further HMBC correlations from CH_2-15 to C-1, C-5, C-9, and C-10 located CH_2-15 at C-10. The presence of three acetoxy groups was indicated by HMBC correlations from the methyl protons at δ 1.53, 1.88, 2.31 to carbonyl resonances at 170.5, 170.4 and 169.9 ppm respectively. These considerations indicated that the compound **72** was a dihydro-*β*-agarofuran sesquiterpenoid containing one benzoate and three acetoxy groups. The benzoate moiety was attached at C-9 based on HMBC correlations from both aromatic protons at δ 7.92 and 6.07 ppm (H-9) to an ester carbonyl group at δ 165.7 ppm. Similarly, the three acetoxy groups were located at C-1, C-8, and C-15 on the basis of HMBC correlations from H-1, H-8, and CH_2-15 to carbonyl carbons at δ 169.9, 170.4 and 170.5 ppm, respectively. On the basis of these data, the 2D structure of compound **72** was established. The relative configuration was assigned following analysis of ^{1}H-^{1}H NOESY data (Figure 6a.18). Correlations between H-8 and H-6, H-7 and between H-15 and CH_3-4*α* showed that these protons were *α*-oriented. Also correlation between H-1 and H-9 indicated that the proton at C-1 and C-9 are *β*-oriented.

A single-crystal X-ray diffraction experiment was performed for compound **2** (Figure 3), which unambiguously established the structure and absolute configuration of compound **72** as **1*α*, 8*β*, 15*α*-triacetoxy-9*α*-benzoyloxy-4*β*-hydroxydihydro-*β*-agarofuran**. The structure of the compound is shown below.

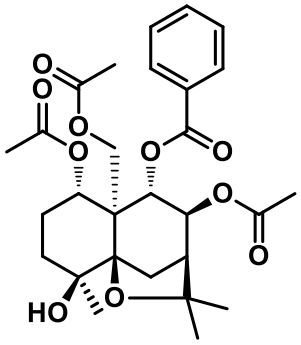

Figure 6a.17: 1*α*, 8*β*, 15*α*-triacetoxy-9*α*-benzoyloxy-4*β*-hydroxydihydro-*β*-agarofuran **(72)**

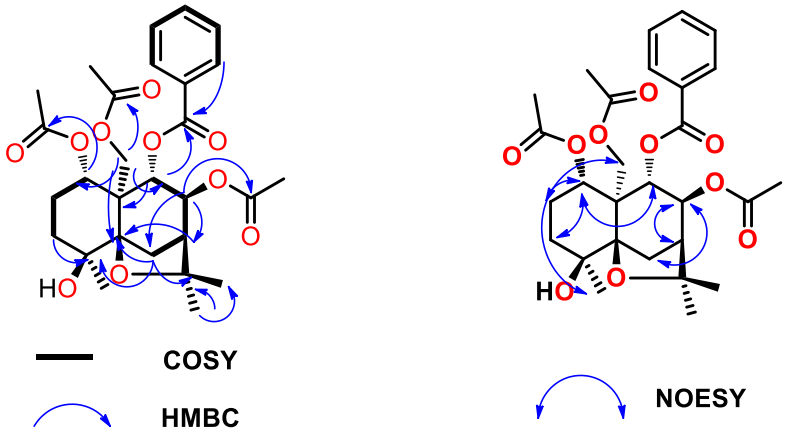

Figure 6a.18: Selected COSY, HMBC and NOESY correlations of compound **72**

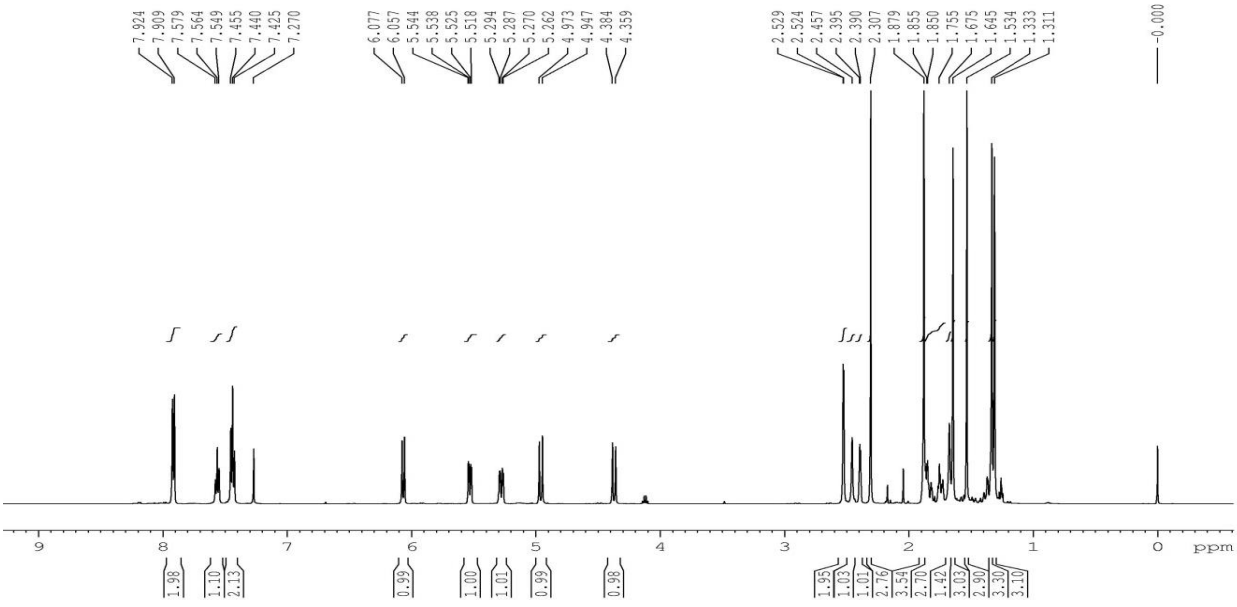

Figure 6a.19: ^{1}H NMR spectrum of compound **72**

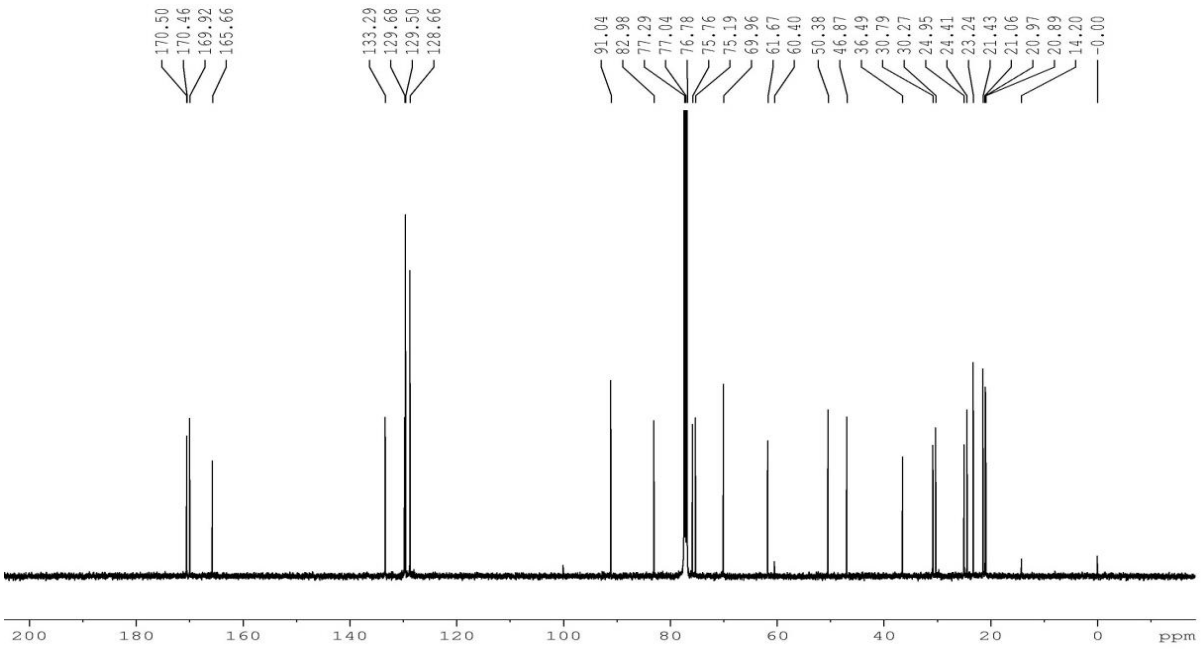

Figure 6a.20: ^{13}C NMR spectrum of compound **72**

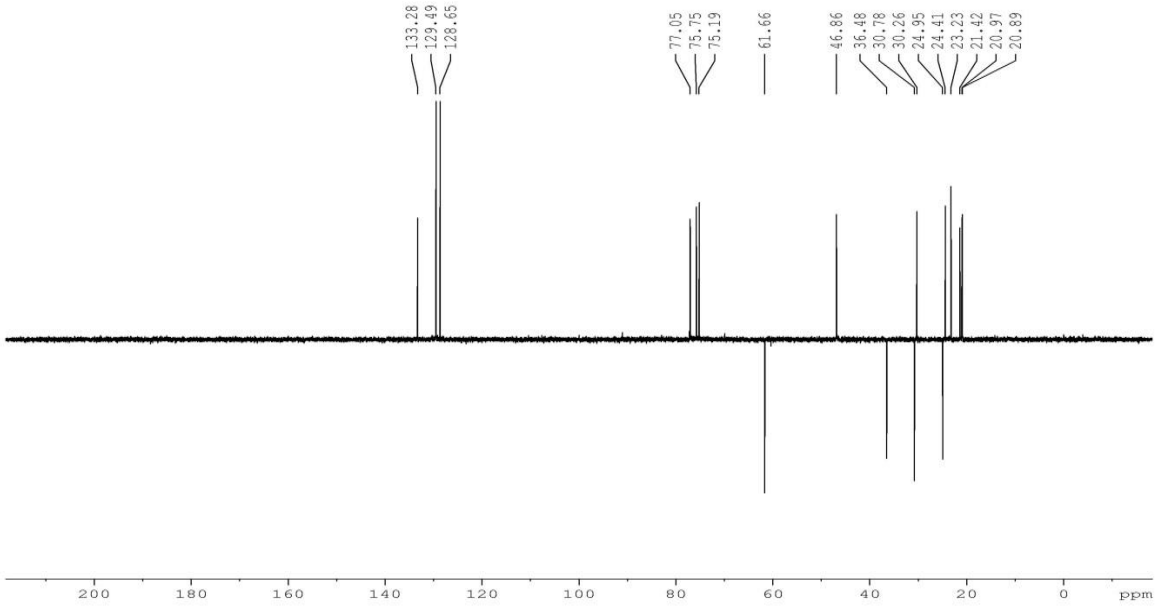

Figure 6a.21: ^{13}C DEPT 135 spectrum of compound **72**

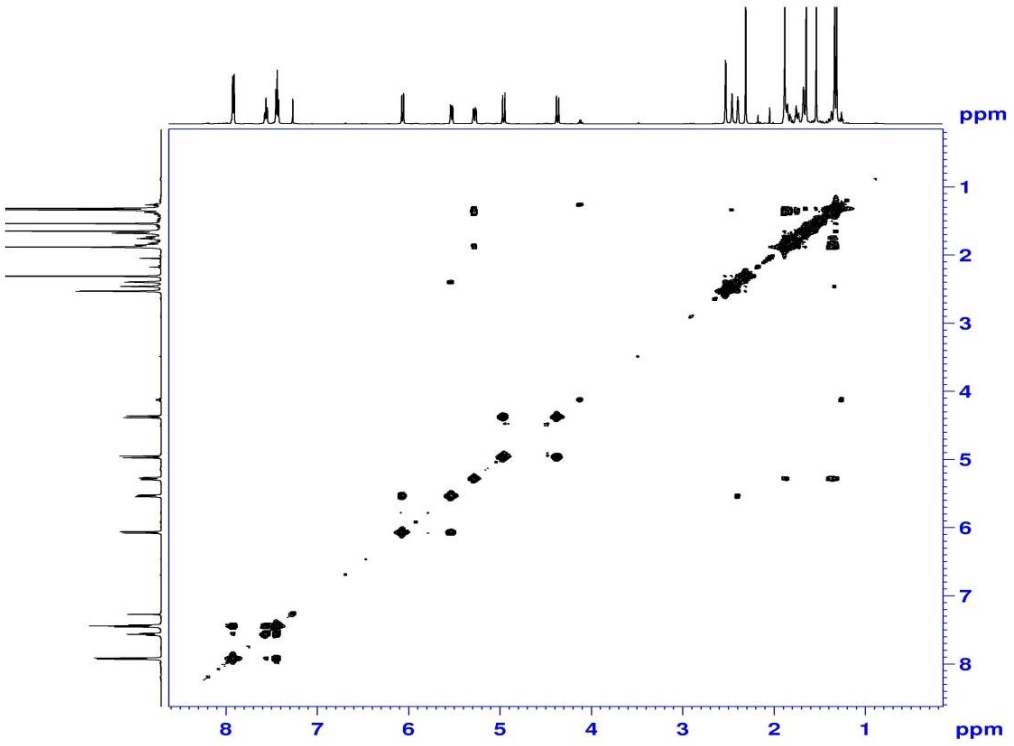

Figure 6a.22: ^{1}H-^{1}H COSY spectrum of compound **72**

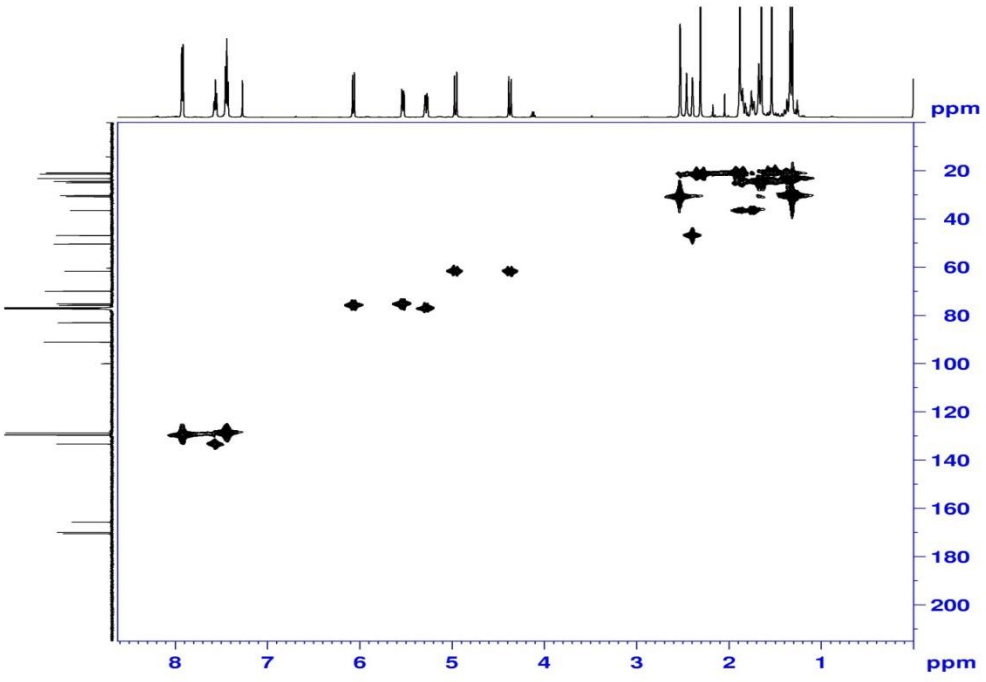

Figure 6a.23: HMQC spectrum of compound **72**

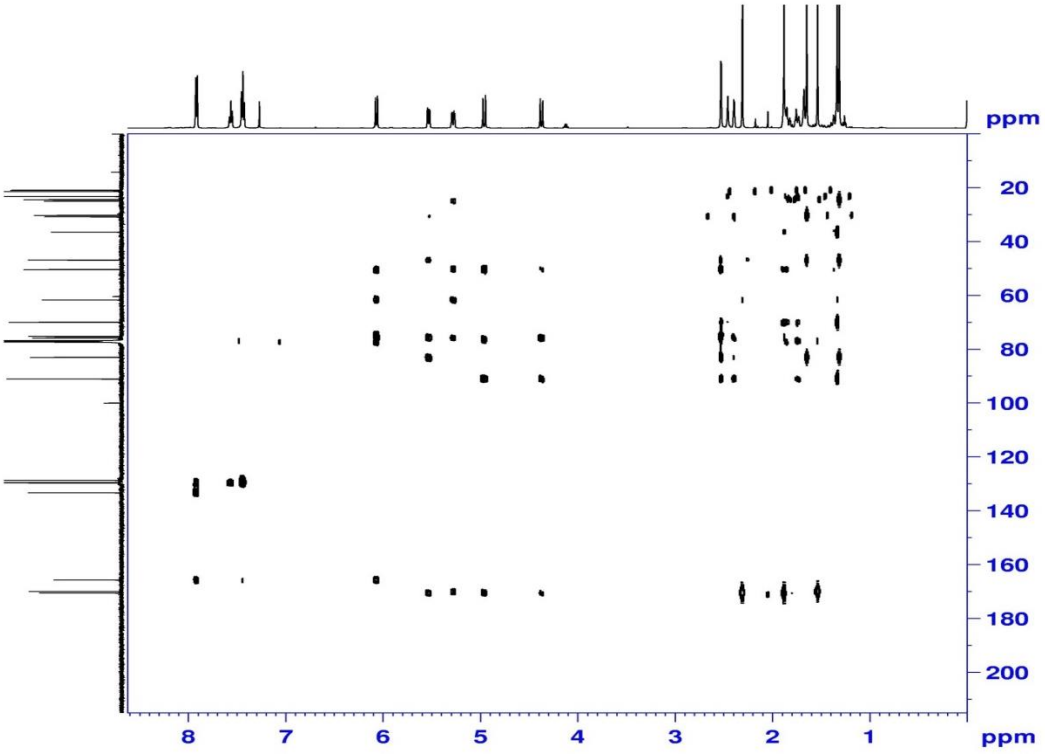

Figure 6a.24: HMBC spectrum of compound **72**

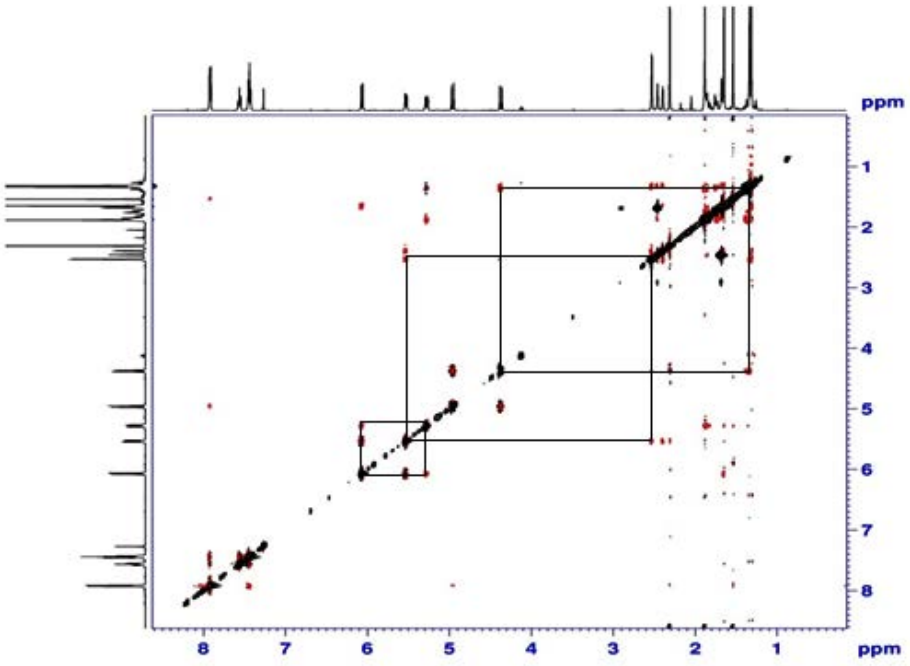

Figure 6a.25: NOESY spectrum of compound **72**

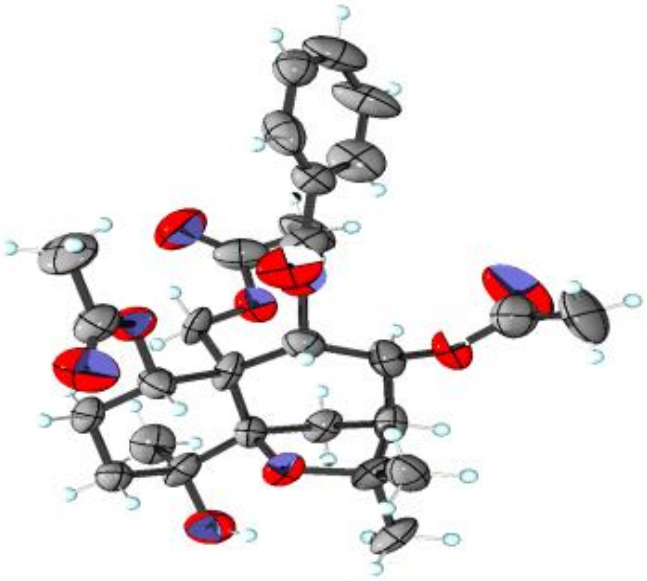

Figure 6a.26: ORTEP structure of compound **72**

Fraction pool 4 (Fr. H.4) was subjected to repeated column chromatography on silica gel (mesh 230-400) using 35 % ethyl acetate in hexane to yield compound **73** obtained as a colourless crystal and was assigned the molecular formula $C_{40}H_{42}O_{10}$ following analysis of the (+)-HRESIMS sodium adduct ion at m/z 705.2690 $[M+Na]^+$ (calcd for $C_{40}H_{42}O_{10}Na$, 705.2675). The ^1H NMR spectrum of the compound **73** was similar to that of compound **71**, except in the presence of one acetoxy group at C-2 of compound **73**. Analysis of the IR, NMR and MS data of **73** and comparison with compound **71** revealed that both compounds shared the same dihydro-*β*-agarofuran scaffold. However, the presence of acetoxy group in compound **73** was determined by HMBC correlations from H-2 (δ 5.15-5.14 ppm) to C-1 and C-4 at δ_C 72.8 and 71.2 ppm respectively. Also there is a correlation between H-2 and carbonyl carbon at δ 170.5 ppm. A single-crystal X-ray diffraction experiment was performed on compound **73** (Figure 6a.35), which unambiguously established the structure and absolute configuration of compound **73** as a novel **1*α*, 9*β*-dibenzoyloxy-2*β*-acetoxy-6*β*-cinnamoyloxy-4*β*-hydroxyldihydro-*β*-agarofuran**. The structure of the compound is shown below.

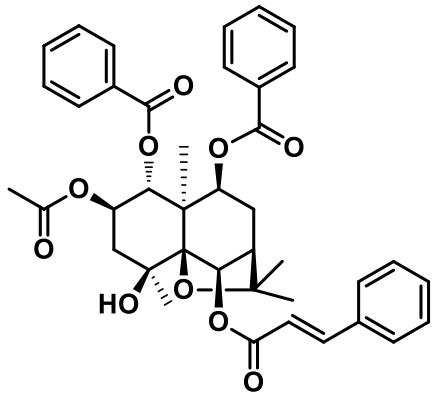

Figure 6a.27: 1*α*, 9*β*-dibenzoyloxy-2*β*-acetoxy-6*β*-cinnamoyloxy-4*β*-hydroxyldihydro-*β*-agarofuran **(73)**

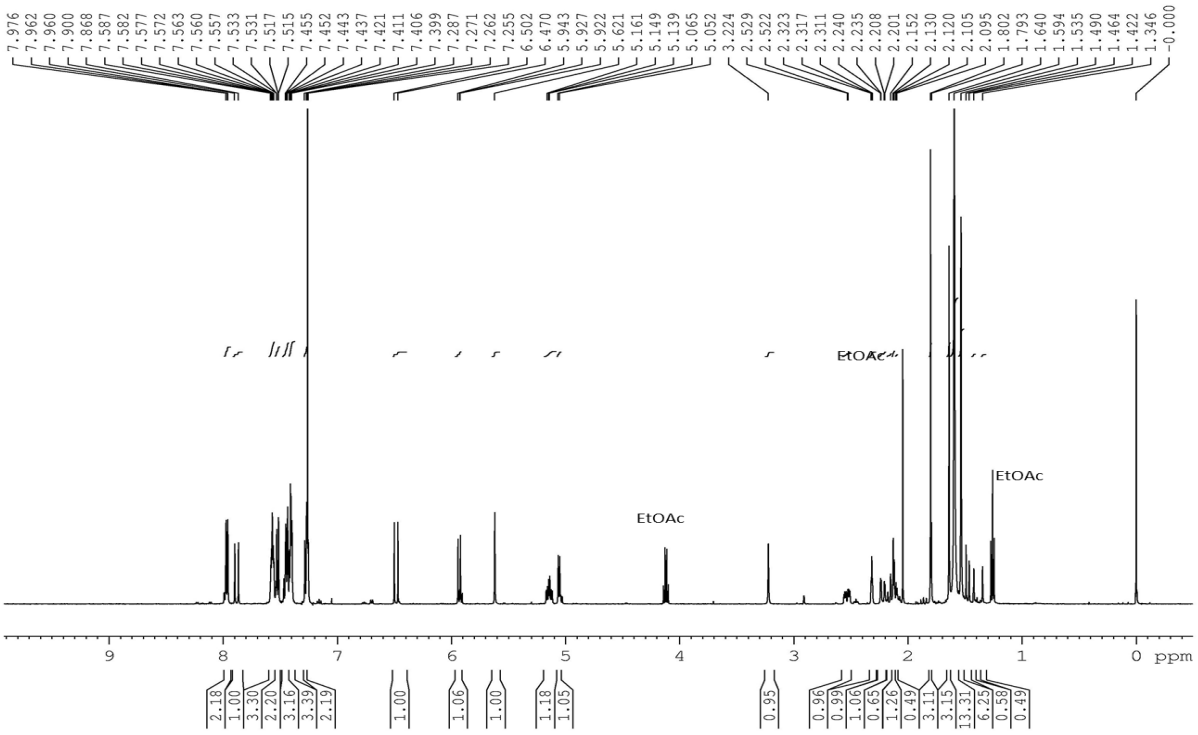

Figure 6a.28: ^{1}H NMR spectrum of compound **73**

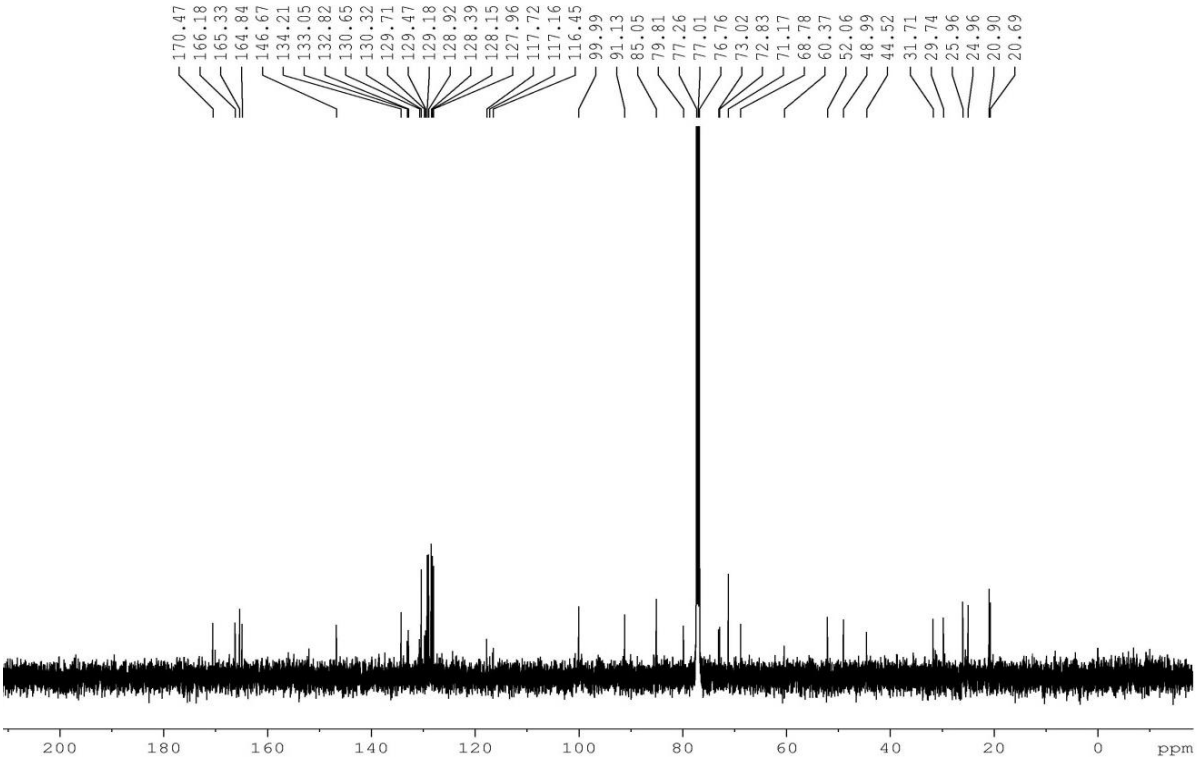

Figure 6a.29: ^{13}C NMR spectrum of compound **73**

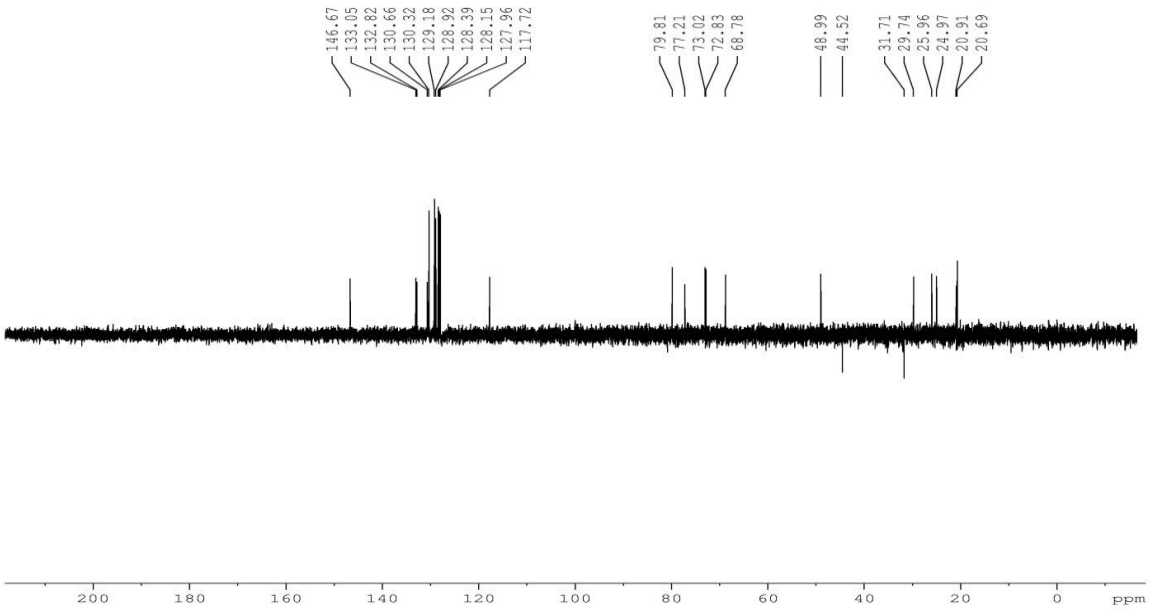

Figure 6a.30: ^{13}C DEPT 135 spectrum of compound **73**

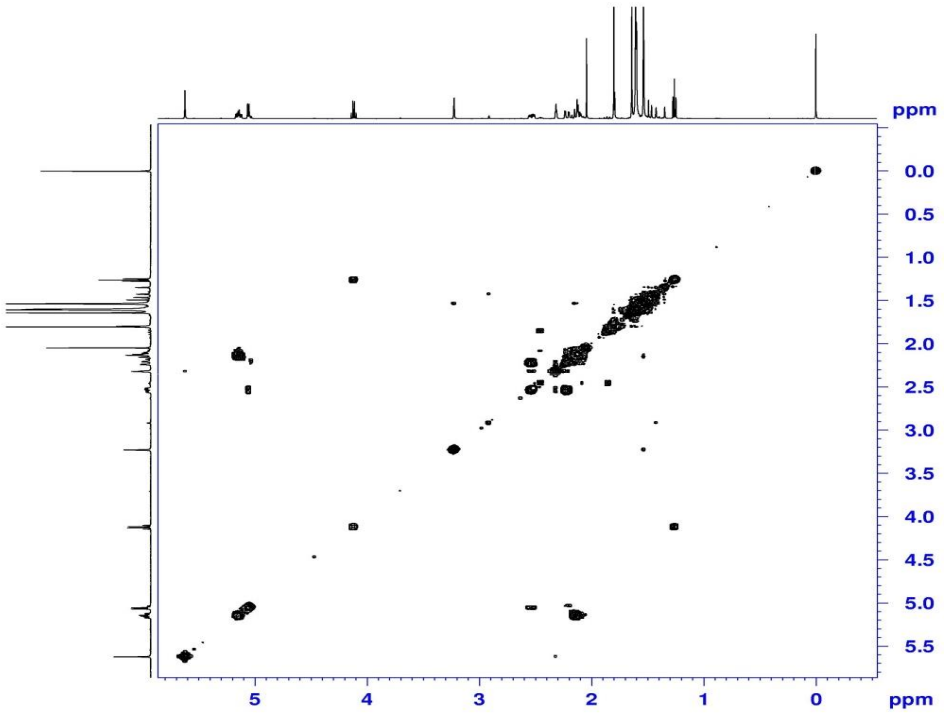

Figure 6a.31: ^{1}H-^{1}H COSY spectrum of compound **73**

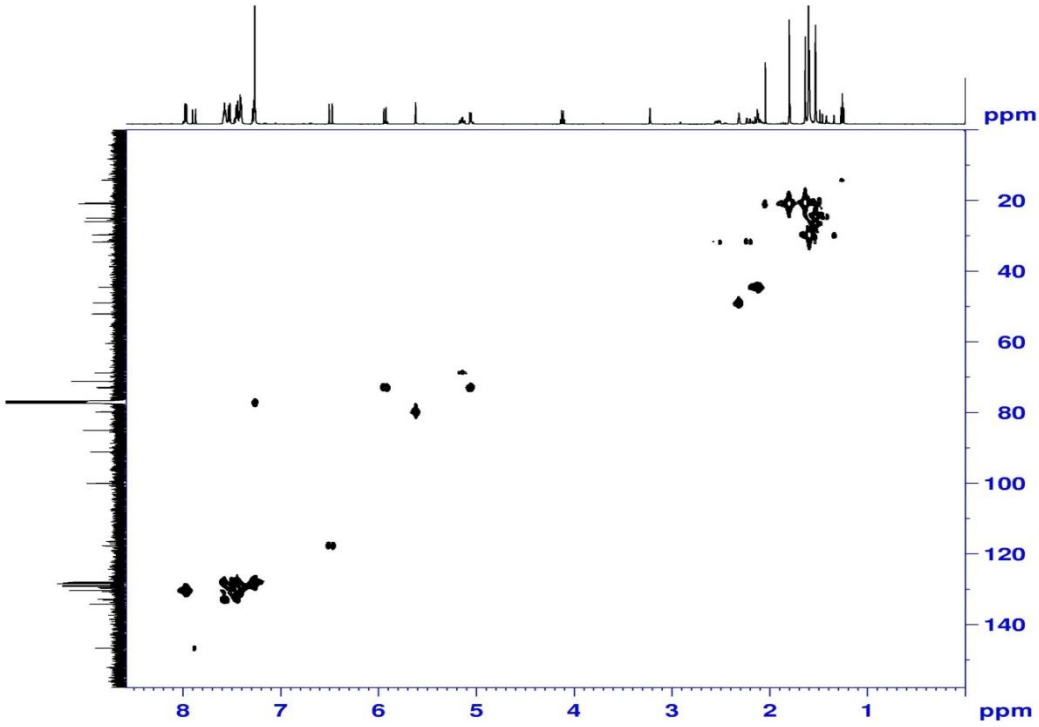

Figure 6a.32: HMQC spectrum of compound **73**

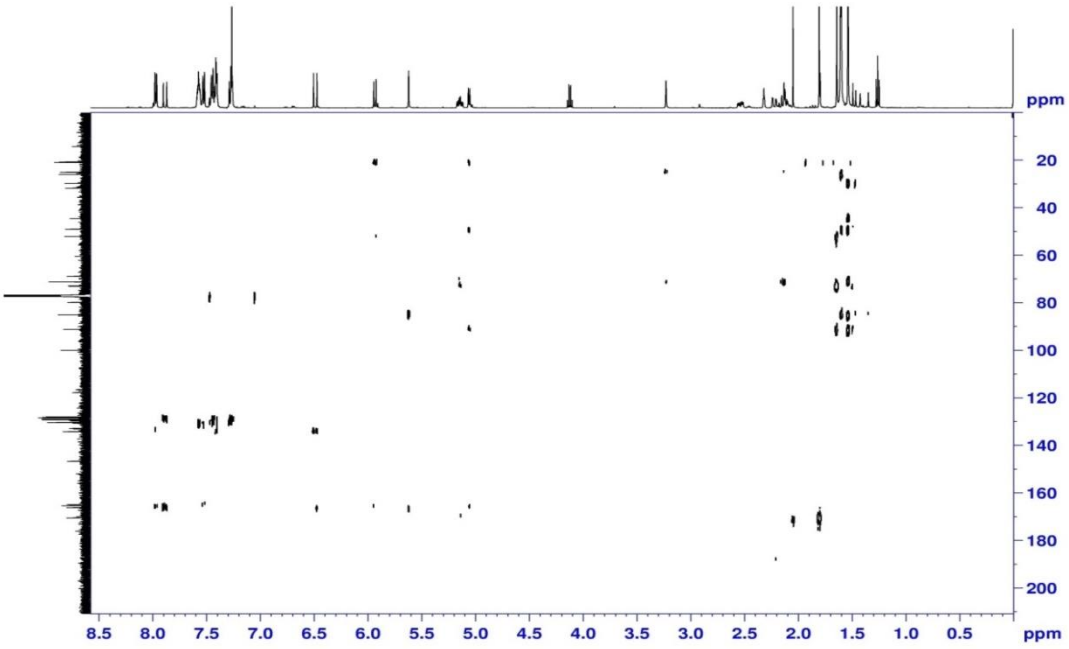

Figure 6a.33: HMBC spectrum of compound **73**

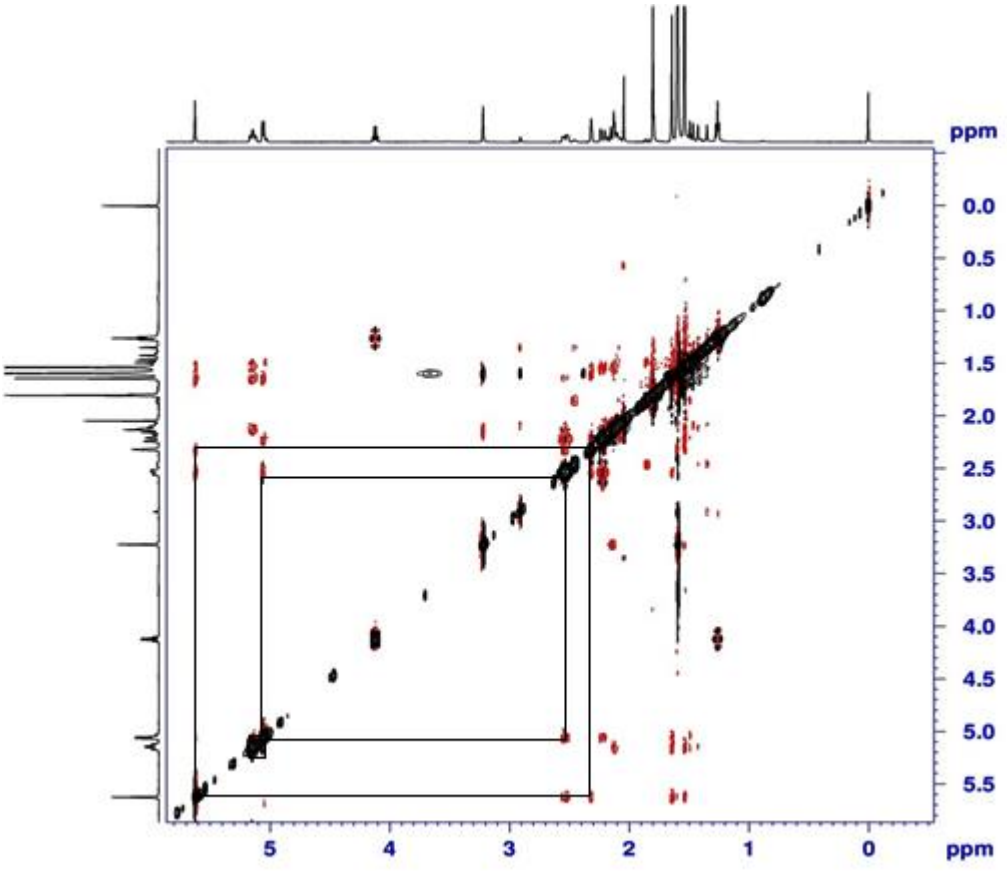

Figure 6a.34: NOESY spectrum of compound **73**

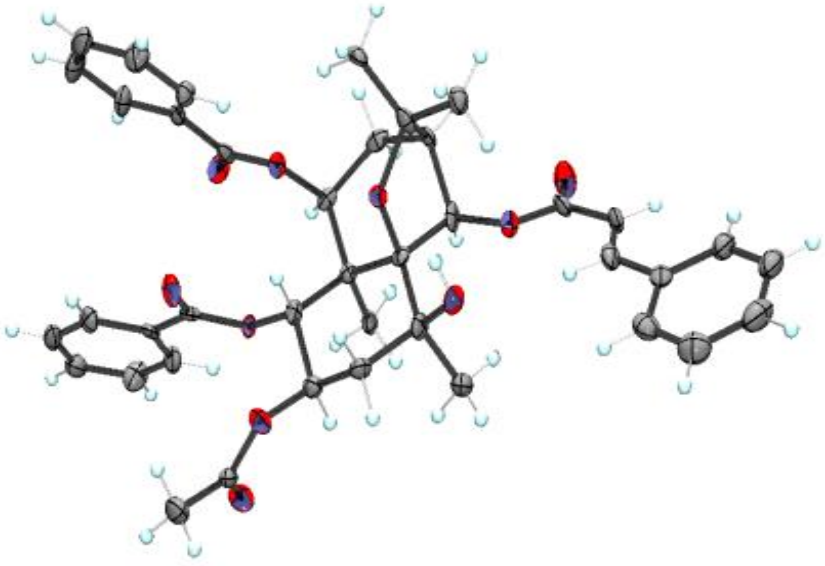

Figure 6a.35: ORTEP structure of compound **73**

Fraction pools 5-8 (Fr.H.5-Fr.H.8) were subjected to repeated column chromatography on silica gel (mesh 230-400) using 35 % ethyl acetate in hexane to yield Compound (**74**) obtained as a colourless crystal and was assigned the molecular formula $C_{40}H_{42}O_{10}$ following analysis of the (+)-HRESIMS sodium adduct ion at m/z 705.2678 $[M+Na]^+$ (calcd for $C_{40}H_{42}O_{10}Na$, 705.2675). The ^1H NMR spectrum of the compound **74** was similar to that of compound **73**, except in the position of attachment of cinnamoyloxy, benzoyloxy and acetoxy group. Analysis of the IR, NMR and MS data of compound **74** and comparison with compound **73** revealed that both compounds shared the same dihydro-*β*-agarofuran scaffold. However, the position of attachment of cinnamoyloxy group at C-8 in compound **74** was determined by HMBC correlations from H-8 to C-7 and C-9. Also there is a correlation between H-6 to C-7 and C-8 indicated that one of the benzoyloxy group attached at C-6 carbon [Tu and Chen **1993**]. A single-crystal X-ray diffraction experiment was performed on compound **74** (Figure 6a.39), which unambiguously established the structure and absolute configuration of compound **74** as **1*α*-acetoxy-6*β*, 9*α*-dibenzoyloxy-8*α* cinnamoyloxy-4*β*-hydroxydihydro-*β*-agarofuran**. The structure of the compound is shown below.

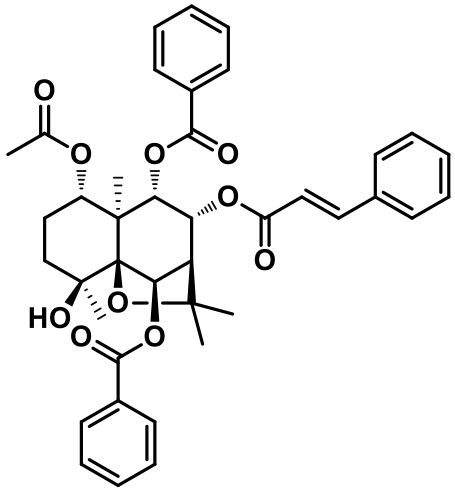

Figure 6a.36: 1*α*-acetoxy-6*β*, 9*α*-dibenzoyloxy-8*α* cinnamoyloxy-4*β*-hydroxydihydro-*β*-agarofuran **(74)**

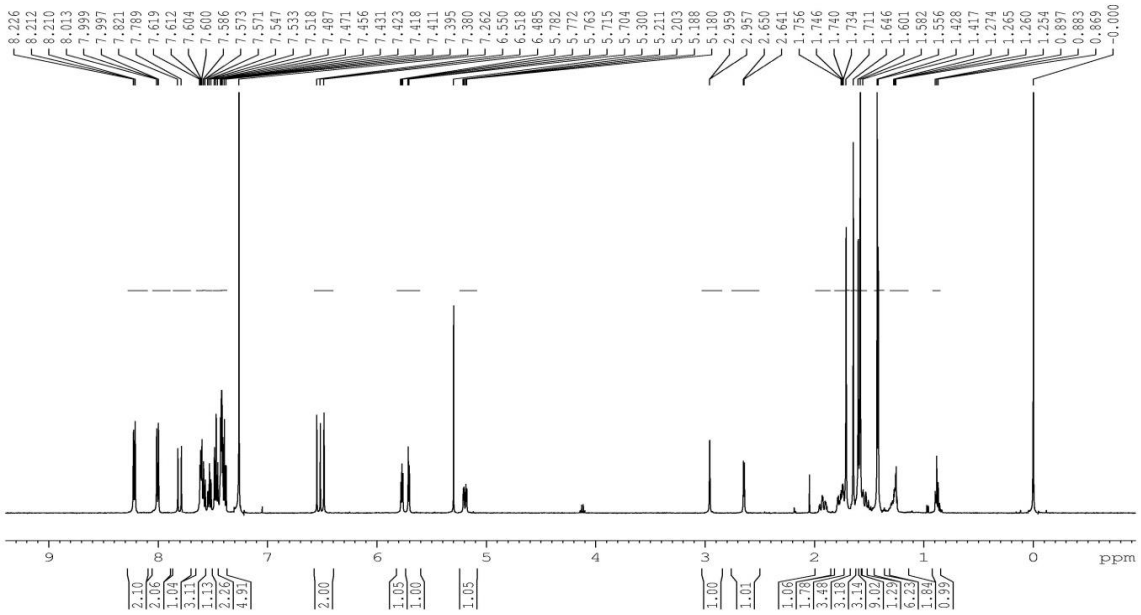

Figure 6a.37: ^{1}H NMR spectrum of compound **74**

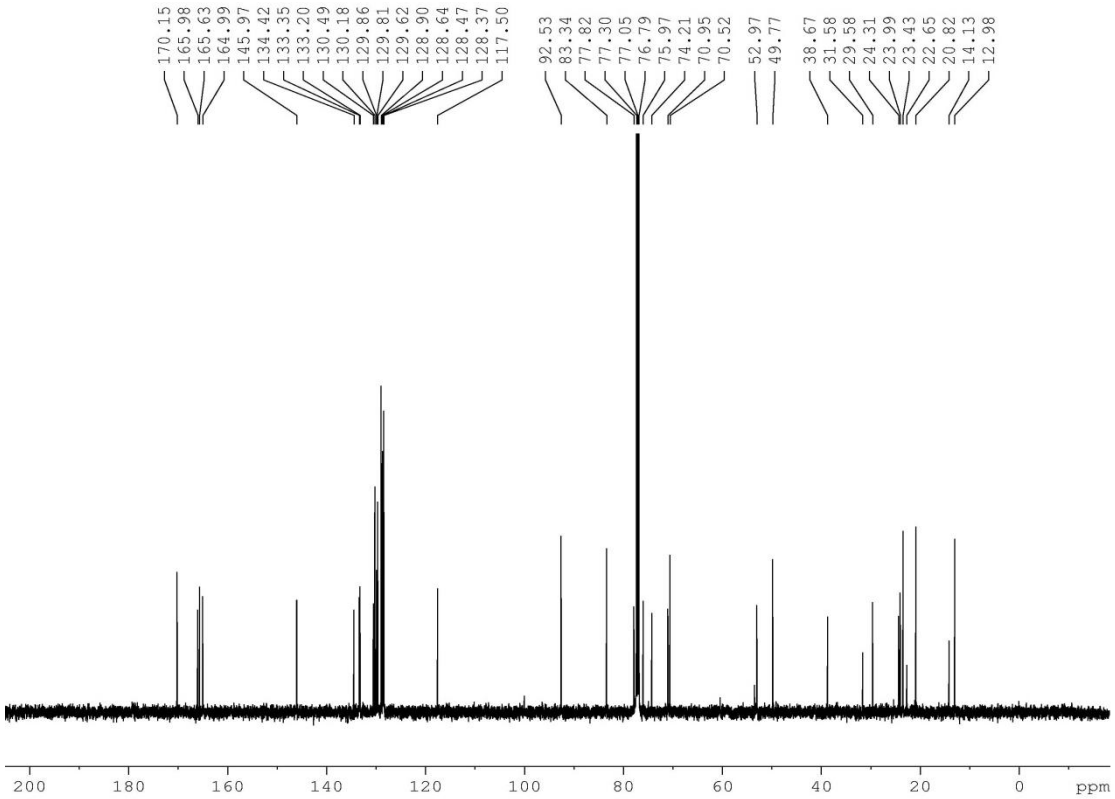

Figure 6a.38: ^{13}C NMR spectrum of compound **74**

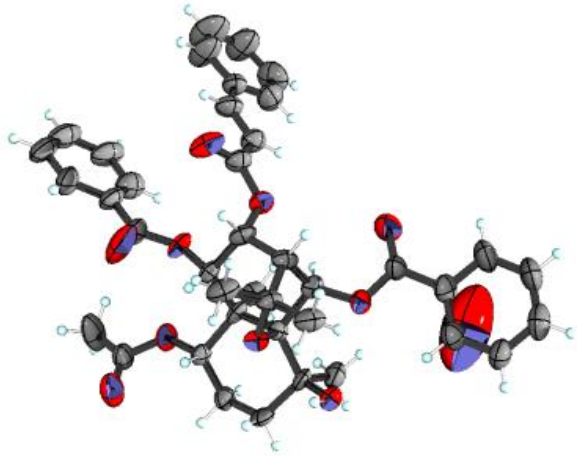

Figure 6a.39: ORTEP structure of compound **74**

Fraction pools 9-13 (FrH.9- Fr.H.13), obtained by eluting the column with 40 % ethyl acetate in hexane yielded 255 mg (0.03 %) of colourless crystals. The ^{1}H NMR spectrum of the compound 7**5** was similar to that of compound **71**. However, in compound **5** cinnomoyl group was replaced by benzoyl group at C-6. Analysis of the IR, NMR and MS data of **5** and

comparison with **71** revealed that both compounds shared the same dihydro-*β*-agarofuran scaffold. The mass spectrum of the compound **75** showed molecular ion peak at m/z 621.2486, which is the $[M+Na]^+$ peak. From all the above spectral details and on comparison with the literature reports [Zhang *et al*., **1998**] the compound was confirmed as **1*α*, 6*β*, 9*β*-tribenzoyloxy-4*β*-hydroxydihydro-*β*-agarofuran**. A single-crystal X-ray diffraction experiment was performed on compound **75** (Figure 6a.43), which unambiguously established the structure and absolute configuration of compound **75**. The structure of the compound is shown below.

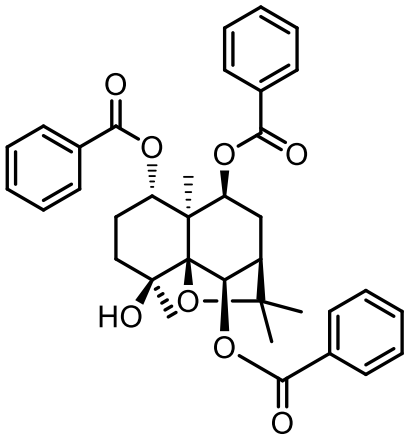

Figure 6a.40: 1*α*, 6*β*, 9*β*-tribenzoyloxy-4*β*-hydroxydihydro-*β*-agarofuran **(75)**

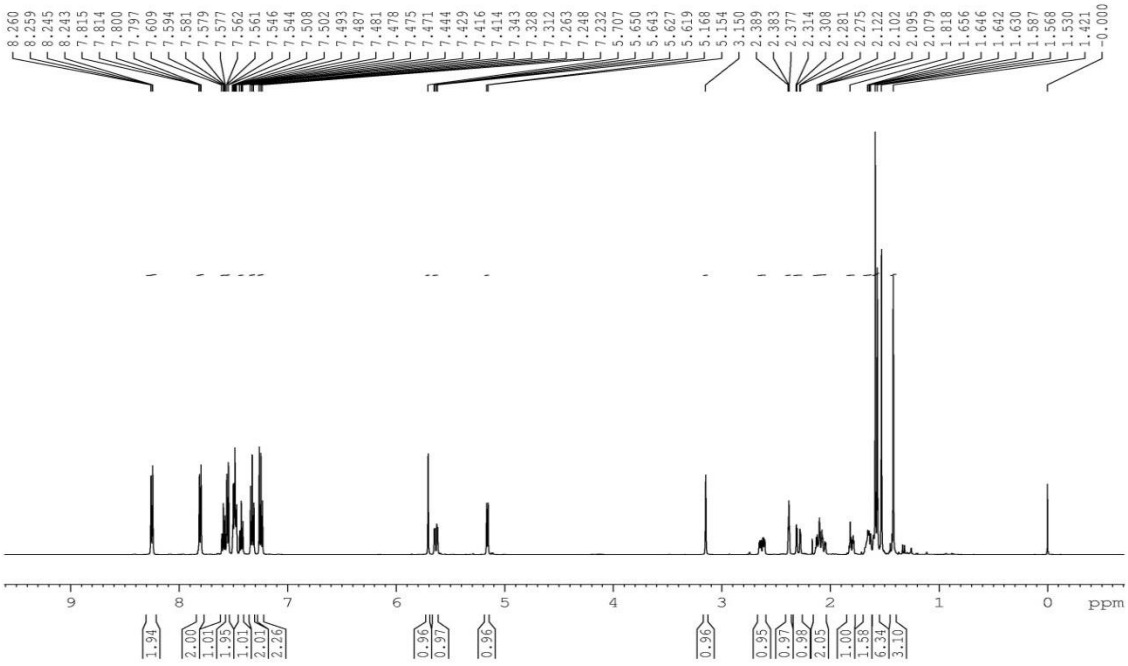

Figure 6a.41: ^{1}H NMR spectrum of compound **75**

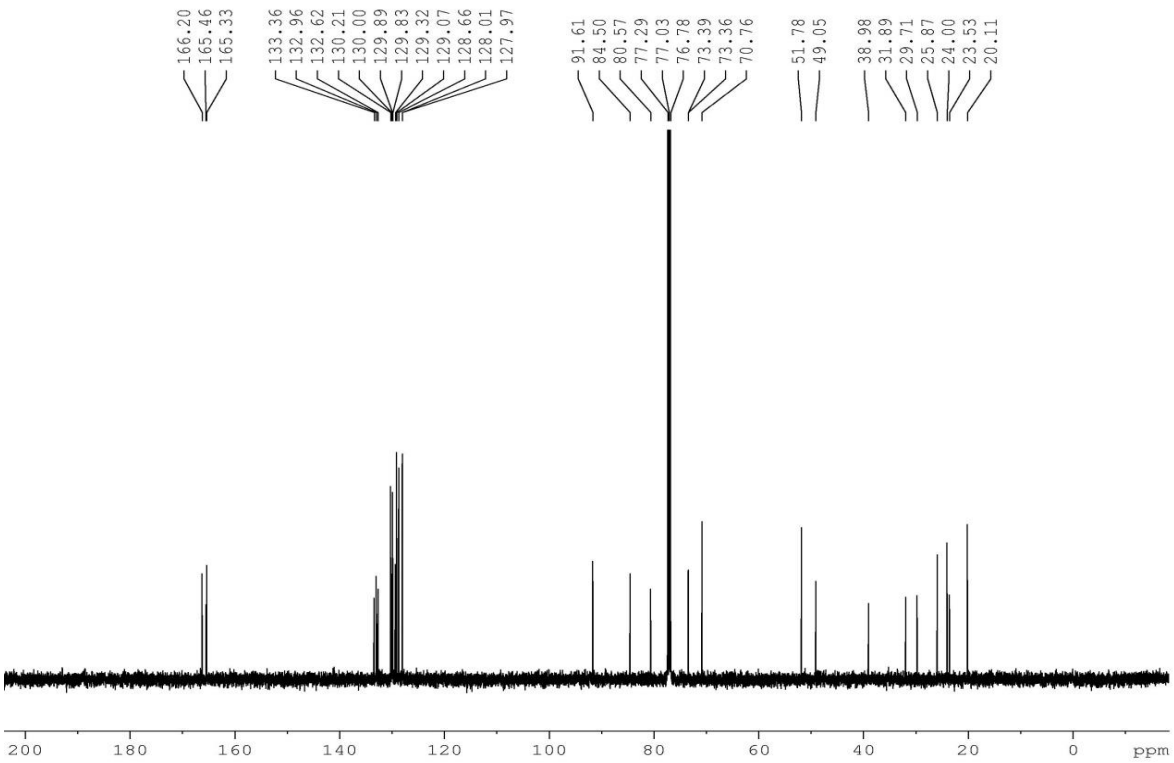

Figure 6a.42: ^{13}C NMR spectrum of compound **75**

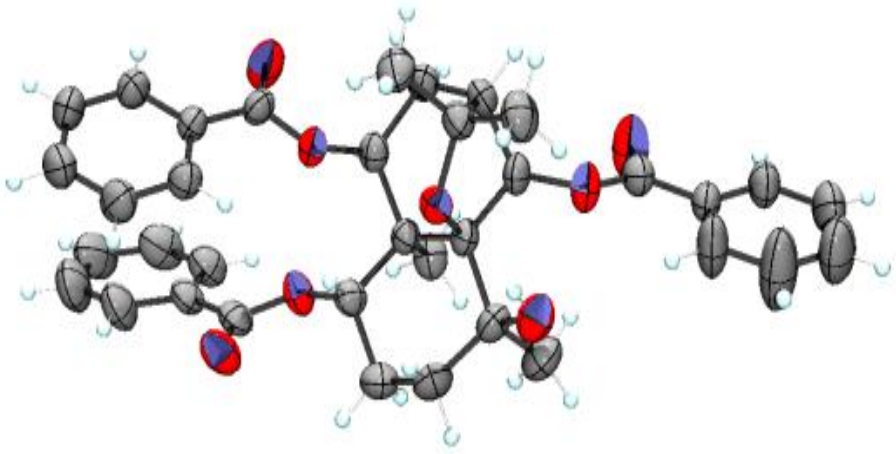

Figure 6a.43: ORTEP structure of compound **75**

Compound **76** (864 mg; 0.09 %) was isolated as a colourless crystal from fractions 14-20 obtained by repeated column chromatography with 40 % ethyl acetate in hexane and was assigned the molecular formula $C_{30}H_{38}O_{12}$ following analysis of the HRESIMS at *m/z* 613.2260 $[M+Na]^+$. IR spectrum of the compound showed absorption at 3527 and 1740 cm^{-1}

suggesting the presence of hydroxyl and ester group. The ^{1}H NMR spectrum of compound **76** revealed the signals corresponding to seven methyl groups at δ 1.34, 1.54, 1.55, 1.70, 1.88, 2.13 and 2.39 ppm, four oxygenated methine protons (δ 6.55, 6.02, 5.59 and 5.28 ppm), 5 protons in the aromatic region for the one benzoyl group at (δ 7.90, and 7.45 ppm). The ^{13}C NMR, HMQC and ^{13}C-DEPT spectra suggested the presence of 30 carbon atoms. The ^{13}C NMR resonances at δ 170.5, 169.9, 169.8, 169.7, and 165.6 ppm were indicative of five ester groups. Two oxygenated tertiary carbon signals were observed at δ 84.1 and 92.4 ppm, which were characteristic of the ethereal carbons of a dihydro-*β*-agarofuran. The position of acetoxy and benzoyloxy groups were confirmed by HMBC analysis.

From the above spectral details and on comparison with the literature reports [Chavez *et al*., **1999**], the compound was confirmed as **1*α*, 6*β*, 8*β*, 15-tetraacetoxy-9*α*-benzoyloxy-4*β*-hydroxydihydro-*β*-agarofuran**. Moreover; this is the first report on the isolation of this compound from *C. paniculatus.* The structure of the compound is shown below.

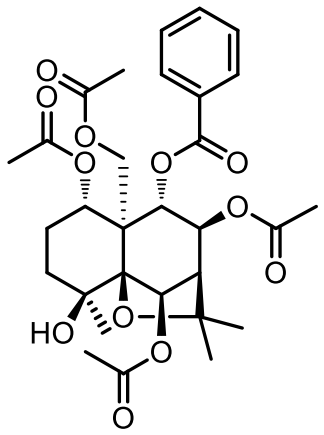

Figure 6a.44: 1*α*, 6*β*, 8*β*, 15-tetraacetoxy-9*α*-benzoyloxy-4*β*-hydroxydihydro-*β*-agarofuran **(76)**

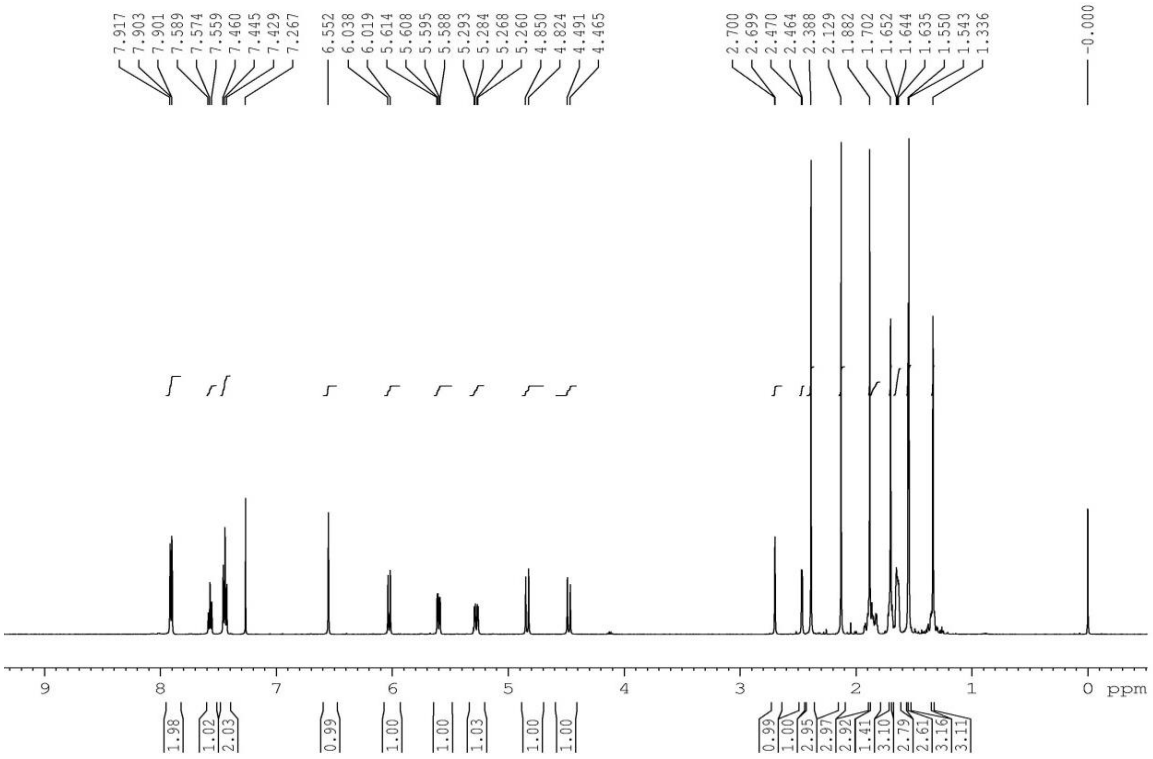

Figure 6a.45: ^{1}H NMR spectrum of compound **76**

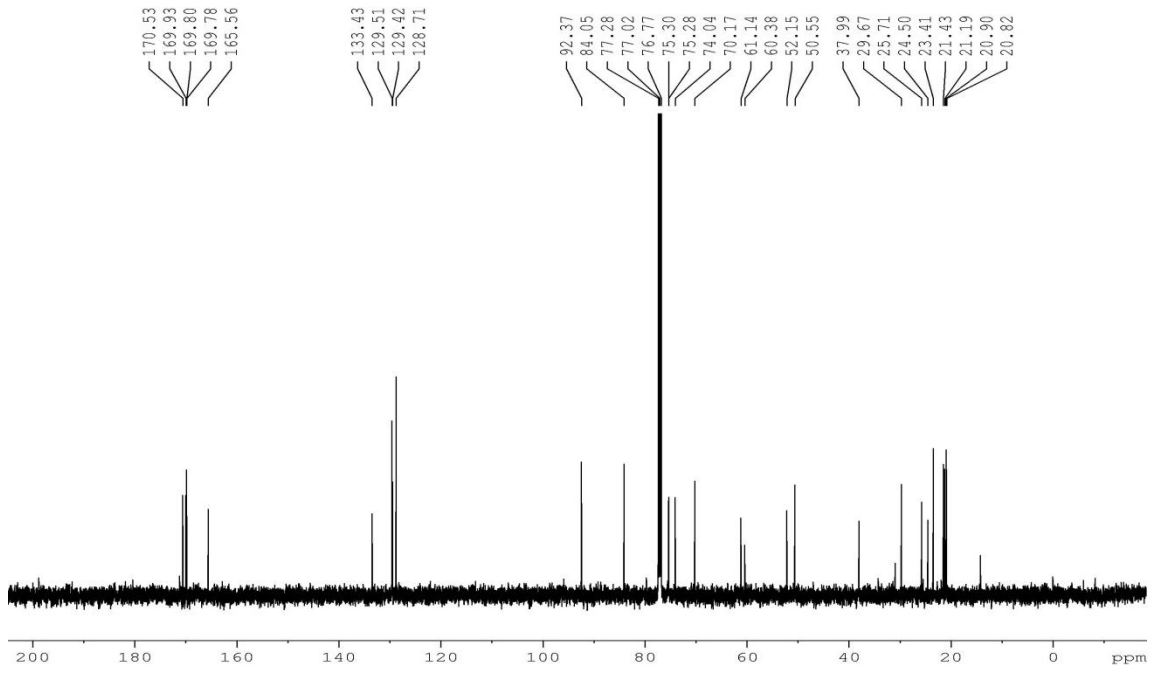

Figure 6a.46: ^{13}C NMR spectrum of compound **76**

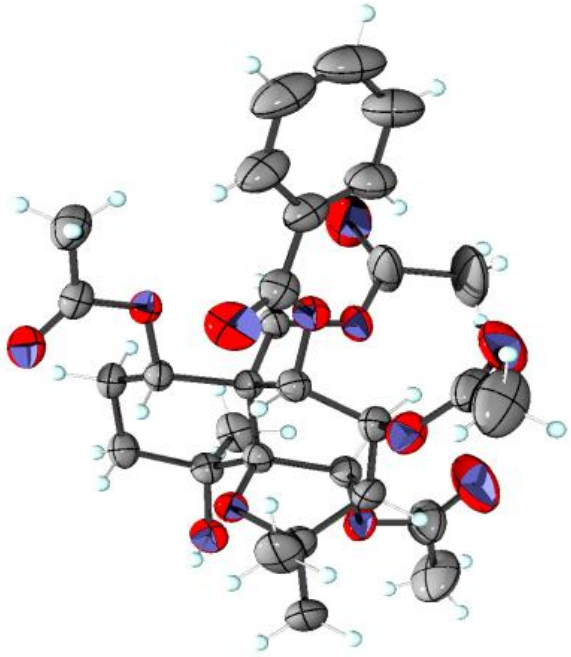

Figure 6a.47: ORTEP structure of compound **76**

Fraction pools 21-27 (Fr.H.21-27) which on repeated column chromatography with 40 % ethyl acetate in hexane obtained 96 mg of compound **77** and was assigned the molecular formula $C_{33}H_{38}O_{10}$ following analysis of the HRESIMS at m/z 617.2372 $[M+Na]^+$. IR spectrum of the compound showed absorption at 3553 and 1738 cm^{-1} suggesting the presence of hydroxyl and ester group. The ^1H NMR spectrum of compound **77** revealed the signals corresponding to six methyl groups at δ 1.36, 1.49, 1.51, 1.53, 1.70 and 1.89 ppm, four oxygenated methine protons (δ 6.00, 5.79, 5.45 and 5.17 ppm), ten protons in the aromatic region for the two benzoyl group at (δ 8.20, 8.04, 7.60-7.57 and 7.49-7.45 ppm). The ^{13}C NMR, HMQC and ^{13}C-DEPT spectra suggested the presence of 33 carbon atoms. The ^{13}C NMR resonances at δ 170.1, 169.8, 165.7 and 165.4 ppm were indicative of four ester groups (Figure 6a.50). Two oxygenated tertiary carbon signals were observed at δ 84.2 and 92.4 ppm, which were characteristic of the ethereal carbons of a dihydro-*β*-agarofuran. The position of acetoxy and benzoyloxy groups were confirmed by HMBC analysis.

From the above spectral details and on comparison with the literature reports [Torres-Romero *et al*., **2009**], the compound was confirmed **1*α*, 8*β*-diacetoxy-6*β*,9*β*-dibenzoyloxy-4*β*-hydroxydihydro-*β*-agarofuran**. However; this is the first report on the isolation of 1*α*,

8*β*-diacetoxy-6*β*,9*β*-dibenzoyloxy-4*β*-hydroxydihydro-*β*-agarofuran from *C. paniculatus.* The structure of the compound is shown below.

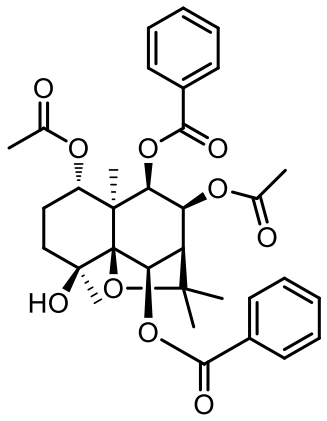

Figure 6a.48: 1*α*, 8*β*-diacetoxy-6*β*, 9*β*-dibenzoyloxy-4*β*-hydroxydihydro-*β*-agarofuran **(77)**

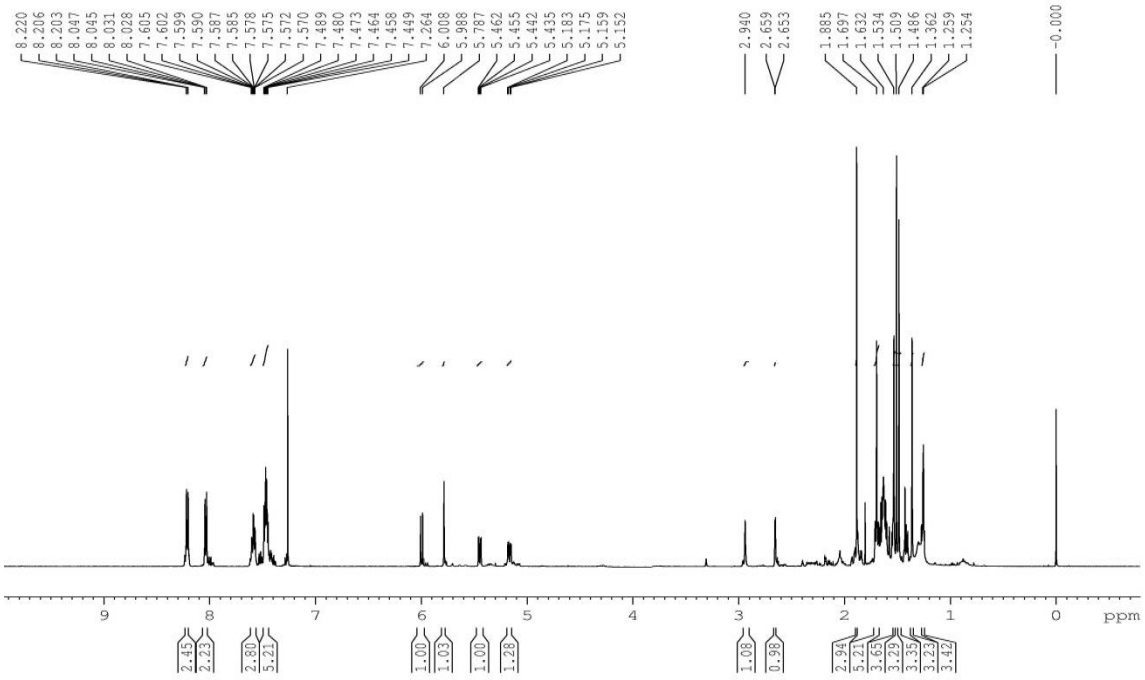

Figure 6a.49: ^{1}H NMR spectrum of compound **77**

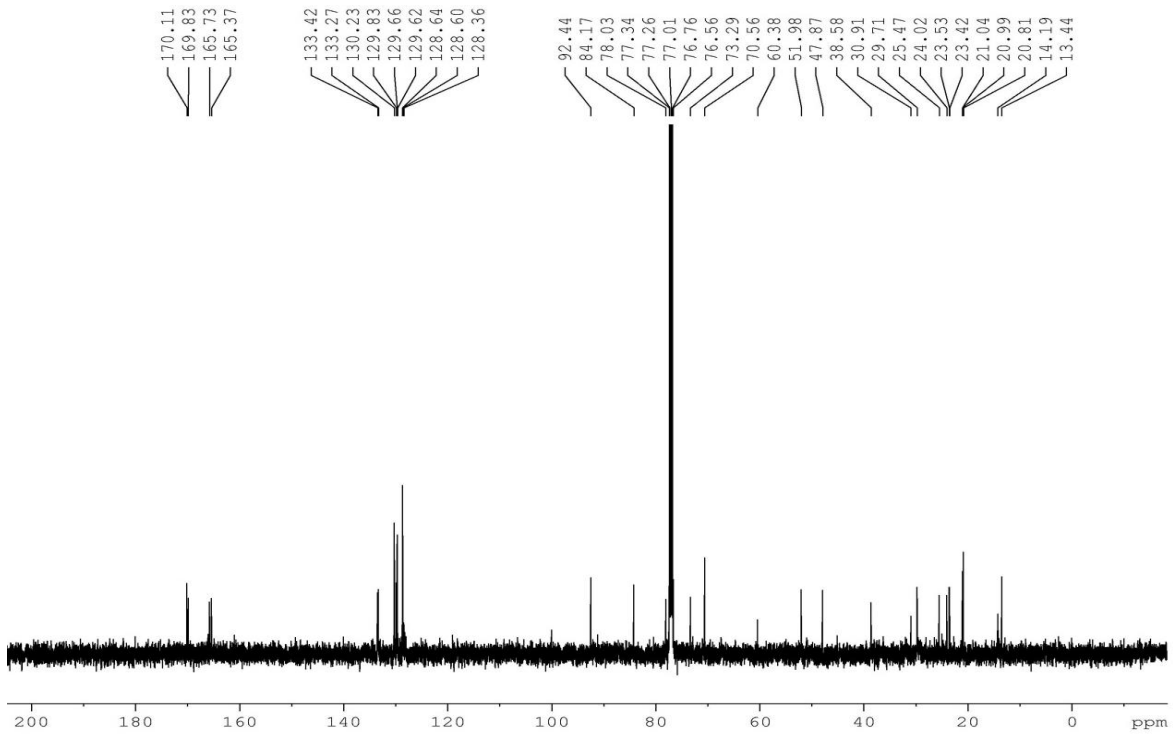

Figure 6a.50: ^{13}C NMR spectrum of compound **77**

Fraction pools 28-30 was submitted to repeated column chromatography on silica gel (mesh 230-400) using 40 % ethyl acetate in hexane to yield compound **78** (6 mg; 0.0006 %). IR spectrum of the compound showed absorption at 3543 and 1716 cm^{-1} suggesting the presence of hydroxyl and ester group. The ^{1}H NMR spectrum of compound **78** revealed the signals corresponding to four methyl groups at δ 1.34, 1.32, 1.43 and 1.45 ppm, two oxygenated methine protons (δ 5.60 and 5.11 ppm), ten protons in the aromatic region for the two benzoyl group at (δ 7.82, 7.57, 7.48, 7.46-7.41, 7.32 and 7.24 ppm). The ^{13}C NMR, HMQC and ^{13}C-DEPT spectra suggested the presence of 29 carbon atoms. The ^{13}C NMR resonances at δ 165.6 and 165.5 ppm were indicative of two ester groups. Two oxygenated tertiary carbon signals were observed at δ 83.6 and 90.6 ppm, which were characteristic of the ethereal carbons of a dihydro-*β*-agarofuran. The position of benzoyloxy groups were confirmed by HMBC analysis. The mass spectra of the compound **78** gave molecular ion peak 501.2261 which is the $[M+Na]^{+}$. A single-crystal X-ray diffraction experiment was performed on compound **78** (Figure 6a.54), which unambiguously established the structure and absolute configuration of compound **78**.

From the above spectral details and on comparison with the literature reports [Torres-Romero *et al*., **2009**], the compound was confirmed **1*α*, 9*β*-dibenzoyloxy-4*β*-hydroxydihydro-*β*-agarofuran**. To the best of our knowledge this is the first report on the isolation of 1*α*, 9*β*-dibenzoyloxy-4*β*-hydroxydihydro-*β*-agarofuran from any part of *C. paniculatus.* The structure of the compound is shown below.

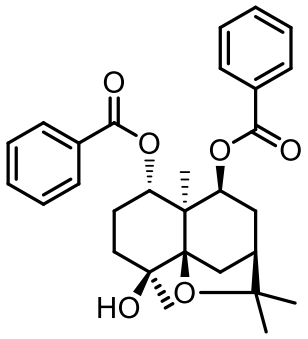

Figure 6a.51: 1*α*, 9*β*-dibenzoyloxy-4*β*-hydroxydihydro-*β*-agarofuran **(78)**

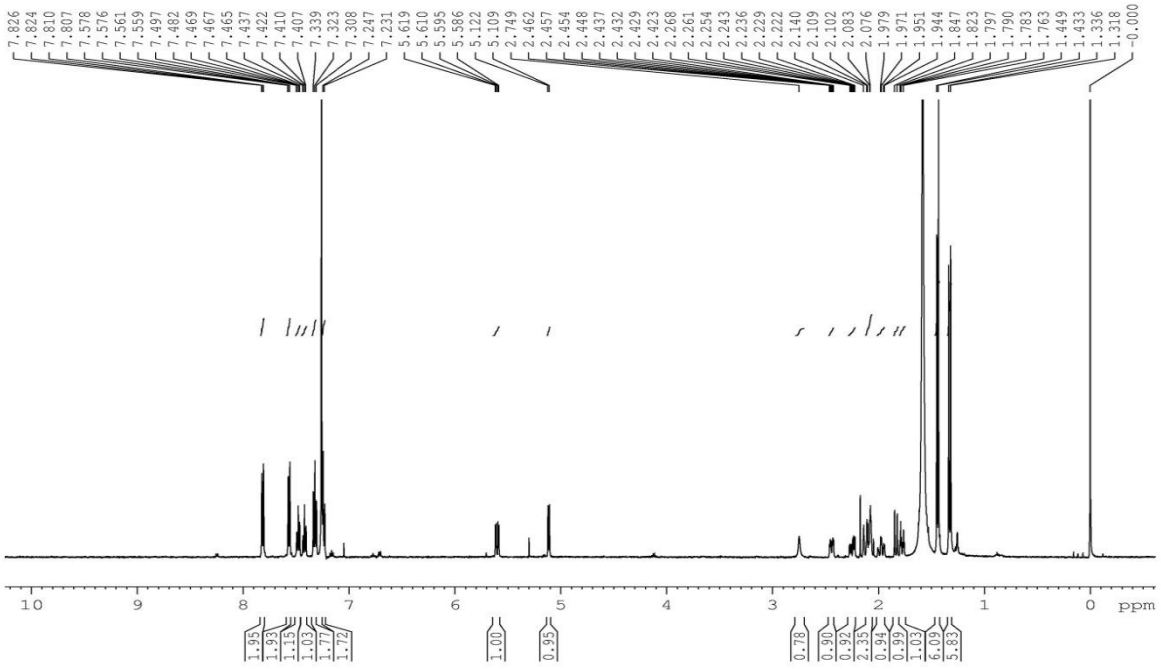

Figure 6a.52: ^{1}H NMR spectrum of compound **78**

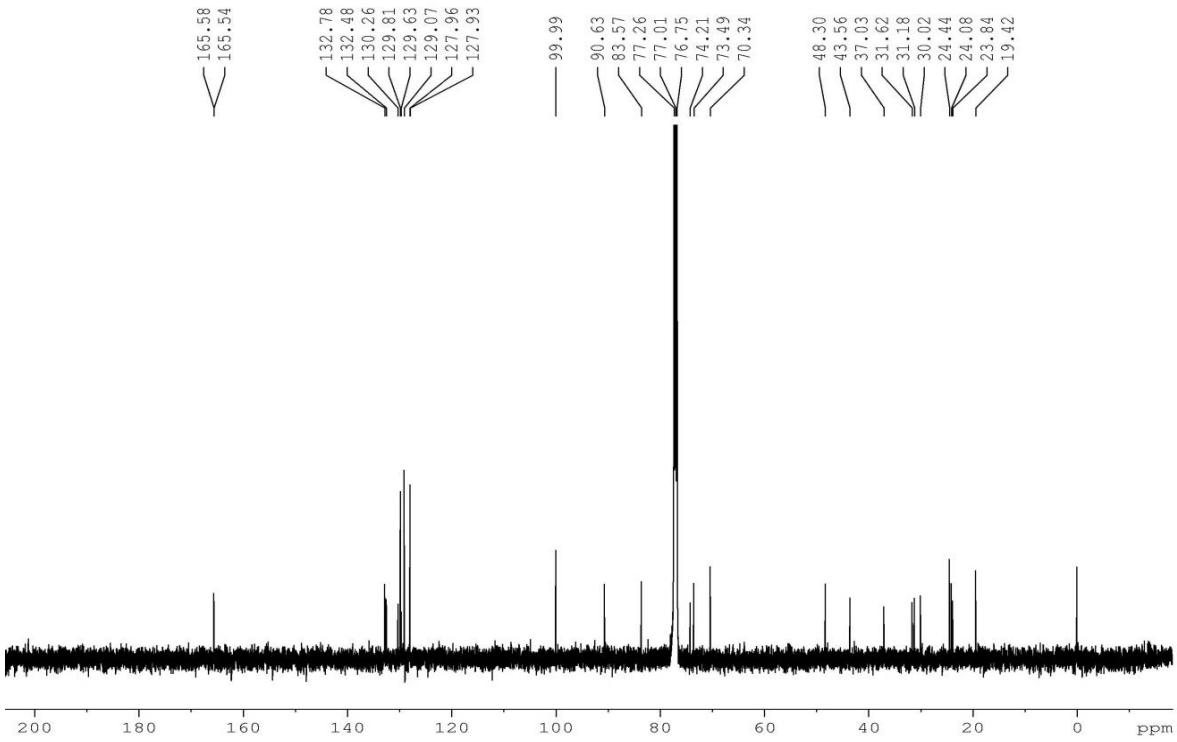

Figure 6a.53: ^{13}C NMR spectrum of compound **78**

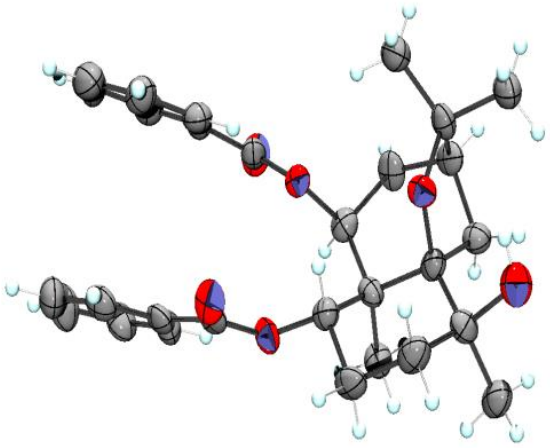

Figure 6a.54: ORTEP structure of compound **78**

The acetone extract (15 g) was also fractionated on a silica gel (100-200 mesh) column eluted with n-hexane/EtOAc of increasing polarity to afford eight fractions (FrA.1-FrA.8). Compound **79** (6 mg; 0.0006 %) was crystalized from the fraction pool FrA.2 by eluting 45

% ethyl acetate in hexane. IR spectrum of the compound showed broad absorption at 3704 and 1743 cm^{-1} suggesting the presence of a hydroxyl and ester group. The ^{1}H NMR spectrum of compound **79** revealed the signals corresponding to seven methyl groups at δ 1.43, 1.47, 1.56, 1.75, 2.09, 2.14 and 2.30 ppm, five oxygenated methine protons (δ 4.46, 5.33, 5.45, 5.87 and 6.37 ppm), five protons in the aromatic region for the one benzoyl group at (δ 7.98, 7.60 and 7.47 ppm). The diastereotopic methylene protons resonated at δ 4.96 and 4.70 ppm. The ^{13}C NMR, HMQC and ^{13}C-DEPT spectra suggested the presence of 30 carbon atoms. The ^{13}C NMR resonances at δ 171.2, 170.3, 170.0, 169.6, and 166.9 ppm were indicative of five ester groups. Two oxygenated tertiary carbon signals were observed at δ 84.3 and 92.0 ppm, which were characteristic of the ethereal carbons of a dihydro-*β*-agarofuran. The position of acetoxy and benzoyloxy groups were confirmed by HMBC analysis. The mass spectra of the compound **79** gave molecular ion peak 629.2230 which is the $[M+Na]^{+}$. A single-crystal X-ray diffraction experiment was performed on compound **79** (Figure 6a.58), which unambiguously established the structure and absolute configuration of compound **79**.

From all the above spectral details and on comparison with the literature reports [Takaishi *et al*., **1992**], the compound was confirmed as **1*α*, 2*α*, 6*β*, 15-tetraacetoxy-9*α*-benzoyloxy-4*β*, 8*β*- dihydroxydihydro-*β*-agarofuran**. The structure of the compound is shown below.

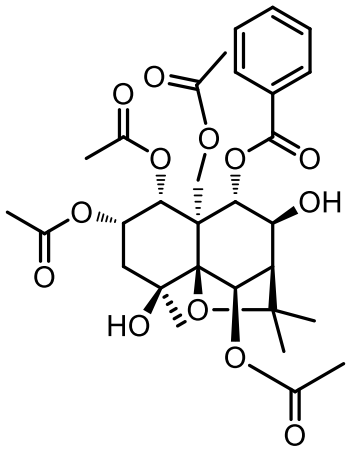

Figure 6a.55: 1*α*, 2*α*, 6*β*, 15-tetraacetoxy-9*α*-benzoyloxy-4*β*, 8*β*- dihydroxydihydro-*β*-agarofuran **(79)**

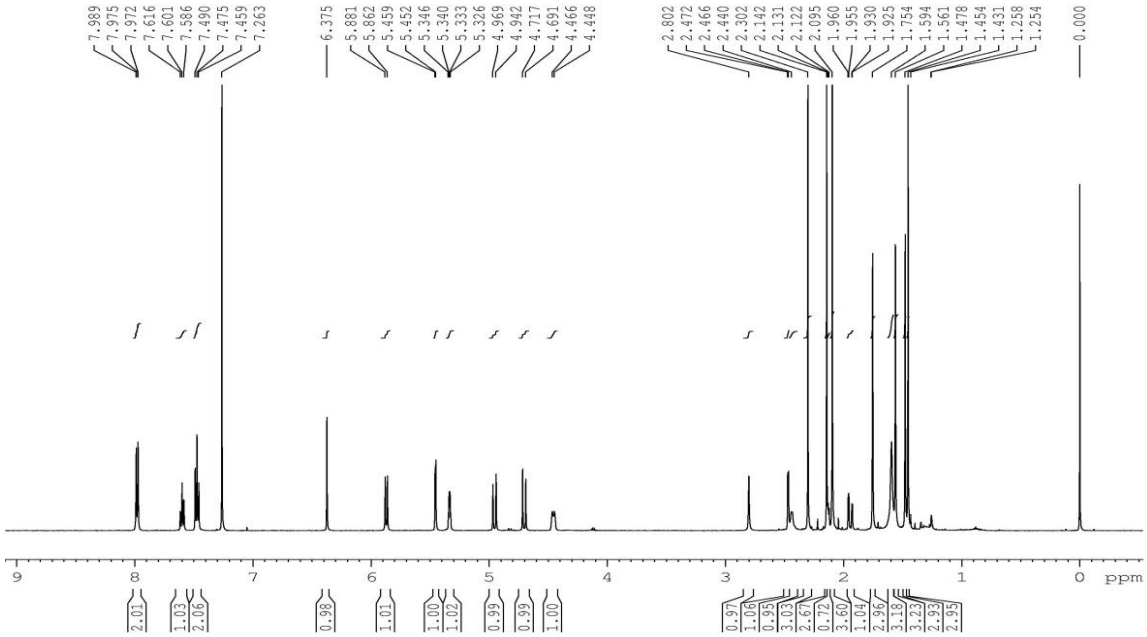

Figure 6a.56: ^{1}H NMR spectrum of compound **79**

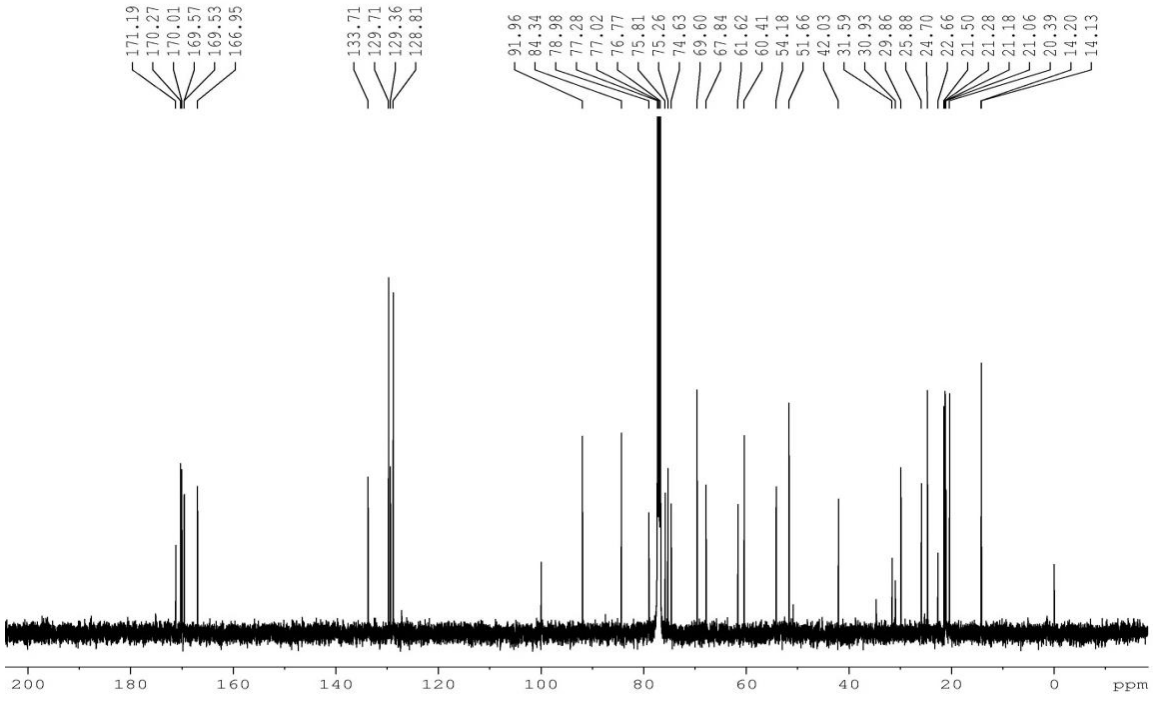

Figure 6a.57: ^{13}C NMR spectrum of compound **79**

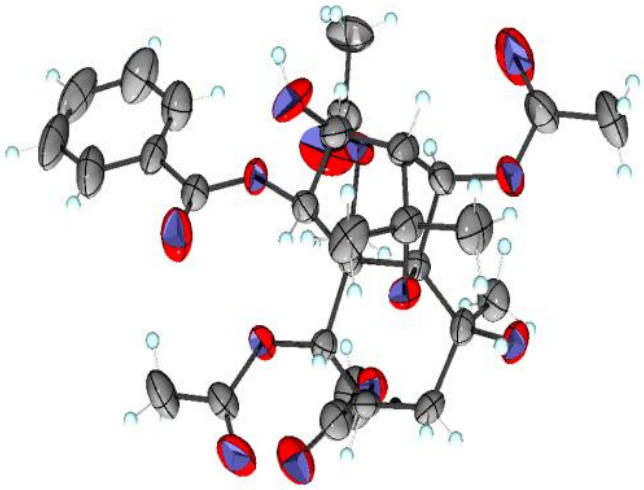

Figure 6a.58: ORTEP structure of compound **79**

Fraction pool 4-5 (FrA.4-5) was submitted to repeated column chromatography on silica gel (mesh 230-400) using 50 % ethyl acetate in hexane to yield compound **80** (30 mg; 0.003 %). IR spectrum of the compound showed absorption at 3532, 3062 and 1722 cm^{-1} indicates the presence of hydroxyl and ester group. The ^{1}H NMR spectrum of compound **80** revealed the signals corresponding to five methyl groups at δ 1.63, 1.58, 1.56, 1.42 and 1.39 ppm, four oxygenated methine protons (δ 5.53, 5.30, 5.14 and 4.48 ppm), ten protons in the aromatic region for the two benzoyl group at (δ 8.21, 8.11, 7.61-7.57, 7.61-7.56 and 7.49-7.44 ppm). The ^{13}C NMR, HMQC and ^{13}C-DEPT spectra suggested the presence of 31 carbon atoms. The ^{13}C NMR resonances at δ 170.3, 166.0 and 165.1 ppm were indicative of three ester groups. Two oxygenated tertiary carbon signals were observed at δ 83.0 and 92.7 ppm, which were characteristic of the ethereal carbons of a dihydro-*β*-agarofuran. The position of acetoxy and benzoyloxy groups were confirmed by HMBC analysis. The mass spectra of the compound **80** gave molecular ion peak 575.2267 which is the $[M+Na]^{+}$. A single-crystal X-ray diffraction experiment was performed on compound **80** (Figure 6a.62), which unambiguously established the structure and absolute configuration of compound **80**.

Comparing the above spectral details with the literature reports [Carroll *et al*., **2009**], the compound was confirmed as **1*α*-acetoxy-6*β*, 9*β*-dibenzoyloxy-8*α*, 4*β*-dihydroxydihydro-*β*-agarofuran**. To the best of our knowledge the isolation of 1*α*-acetoxy-6*β*, 9*β*-dibenzoyloxy-8*α*, 4*β*-dihydroxydihydro-*β*-agarofuran is first time from any part of *C. paniculatus*. The structure of the compound is shown below.

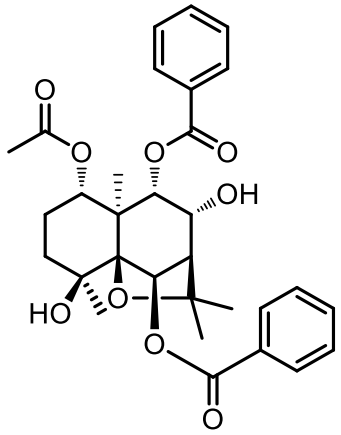

Figure 6a.59: 1α-acetoxy-6β, 9β-dibenzoyloxy-8α, 4β-dihydroxydihydro-β-agarofuran **(80)**

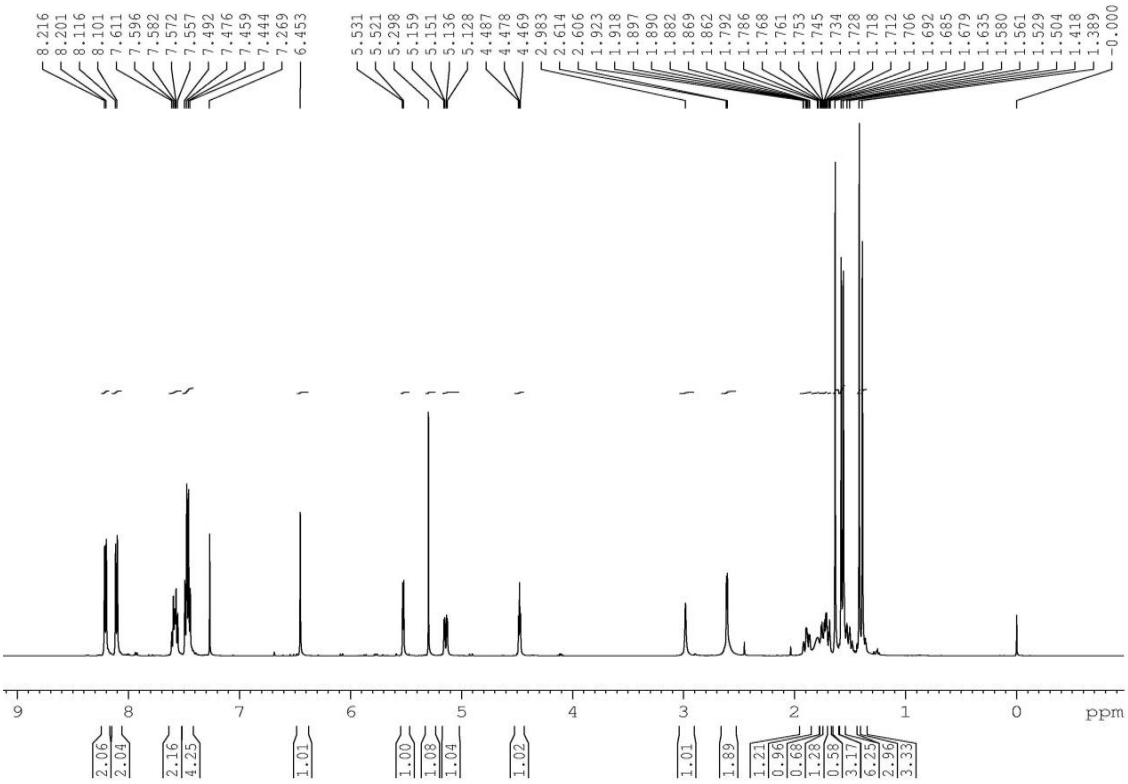

Figure 6a.60: ^{1}H NMR spectrum of compound **80**

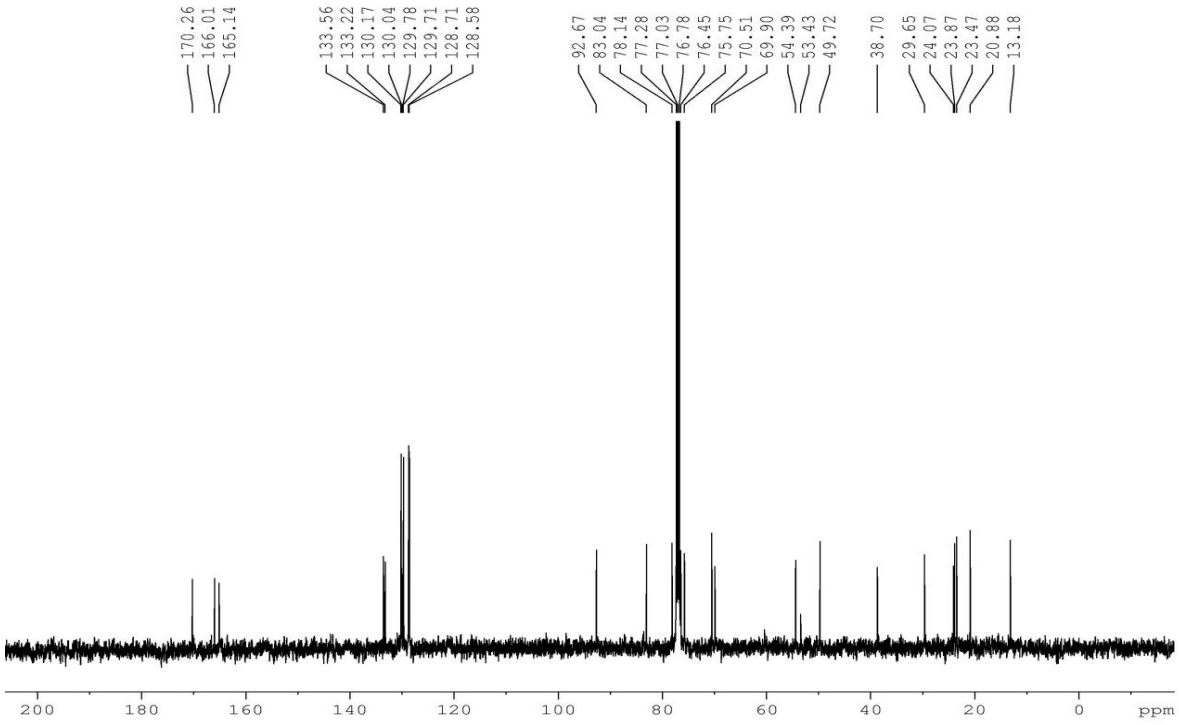

Figure 6a.61: ^{13}C NMR spectrum of compound **80**

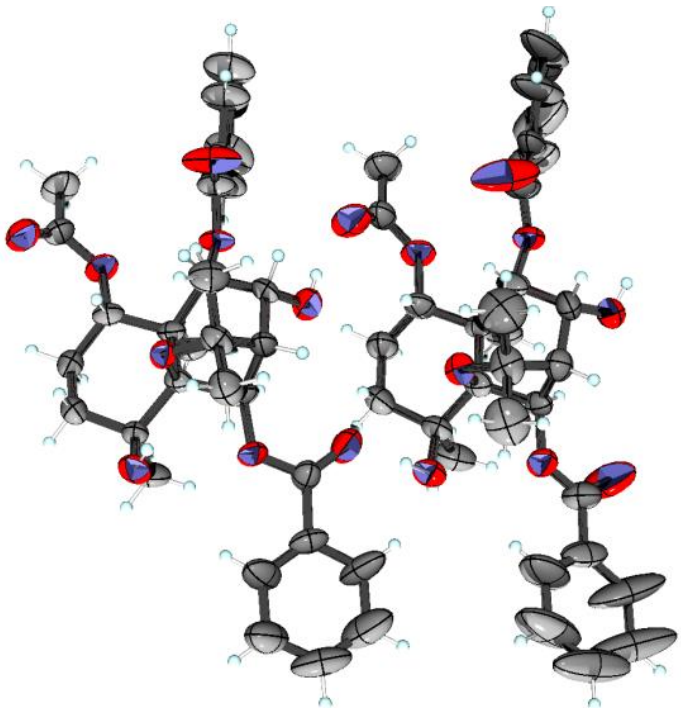

Figure 6a.62: ORTEP structure of compound **80**

Compound **81** (3 mg; 0.0003 %) was precipitated as a white solid from the fraction pool 7-8 (FrA.7-8). IR spectrum of the compound showed absorption at 3559, 3054 and 1722 cm^{-1}

indicates the presence of hydroxyl and ester group. The ^{1}H NMR spectrum of compound **81** is similar to that of compound **80**, only difference is the position of acetoxy group at C-6 carbon and that was confirmed by the HMBC correlation. The ^{13}C NMR resonances at δ 170.6, 165.9 and 165.8 ppm were indicative of three ester groups. Two oxygenated tertiary carbon signals were observed at δ 82.9 and 92.6 ppm, which were characteristic of the ethereal carbons of a dihydro-*β*-agarofuran. The mass spectra of the compound **81** gave molecular ion peak 575.2267 which is the $[M+Na]^{+}$.

From the above spectral details and on comparison with the literature reports [Gonzalez *et al*., **1993**], the compound was confirmed as **1*α*, 9*β*-dibenzoyloxy-6*β*-acetoxy-8*α*, 4*β*-dihydroxydihydro-*β*-agarofuran**. To the best of our knowledge, this is the first report of 1*α*, 9*β*-dibenzoyloxy-6*β*-acetoxy-8*α*, 4*β*-dihydroxydihydro-*β*-agarofuran from *C. paniculatus*. The structure of the compound is shown below.

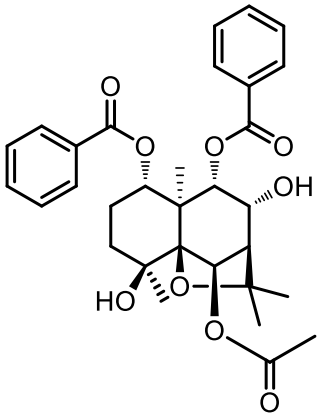

Figure 6a.63: 1*α*, 9*β*-dibenzoyloxy-6*β*-acetoxy-8*α*,4*β*-dihydroxydihydro-*β*-agarofuran **(81)**

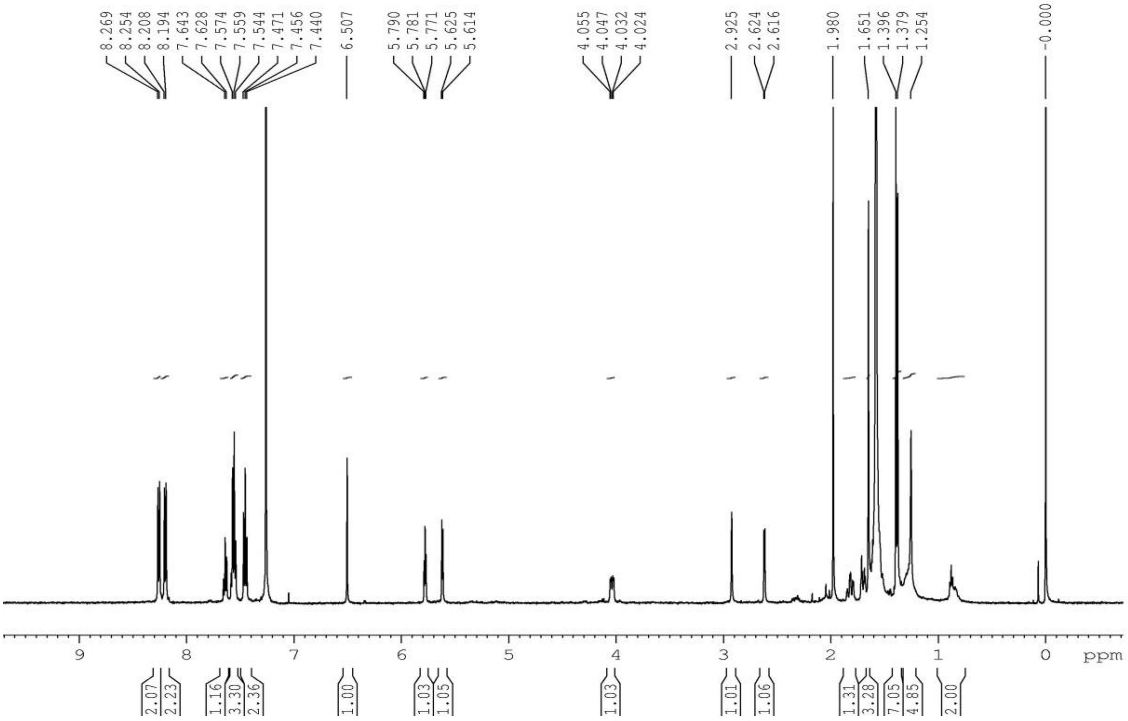

Figure 6a.64: ^{1}H NMR spectrum of compound **81**

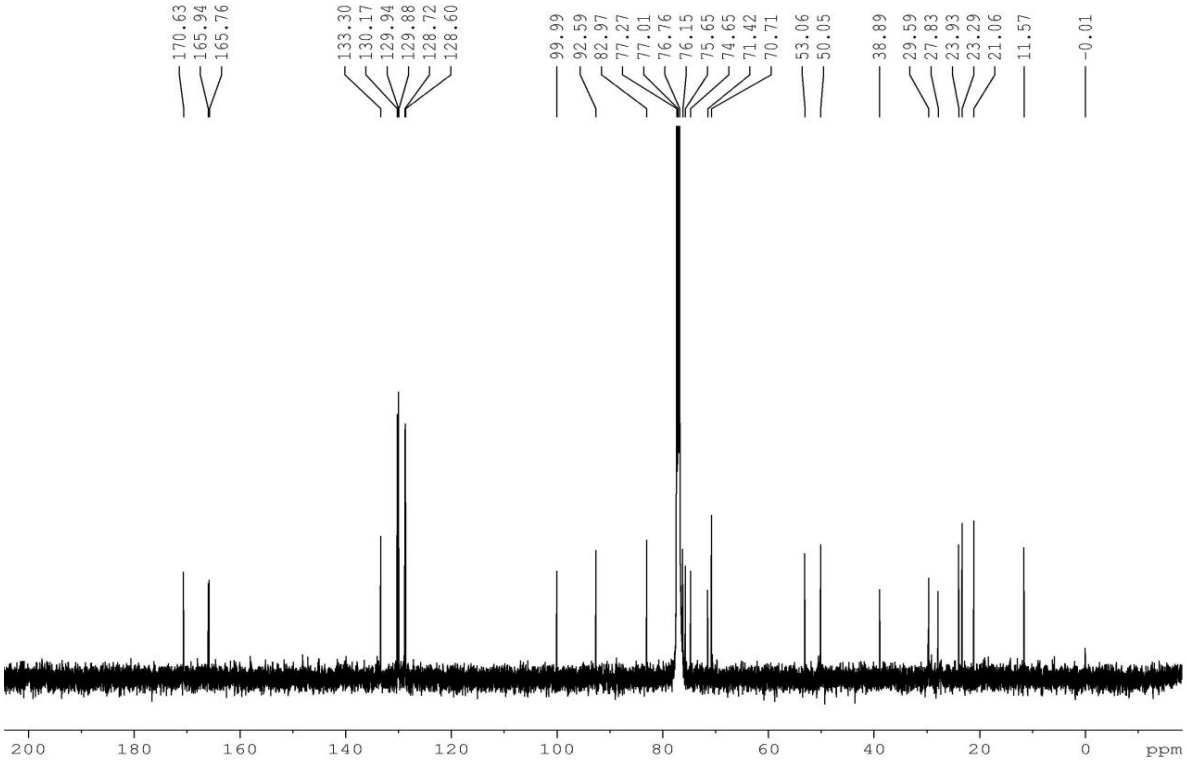

Figure 6a.65: ^{13}C NMR spectrum of compound **81**

6a.7. Conclusion

In this chapter, we have isolated 11 compounds from the seeds of *C. paniculatus* including three novel compounds *viz*., *1α, 9β-dibenzoyloxy-6β-cinnamoyloxy-4β-hydroxydihydro-β-agarofuran, 1α,8β,15α-triacetoxy-9α-benzoyloxy-4β-hydroxydihydro-β-agarofuran* and *1α,9β-dibenzoyloxy-2β-acetoxy-6β-cinnamoyloxy-4β-hydroxyldihydro-β-agarofuran* all the isolated compounds were structurally characterized by 1D and 2D NMR spectroscopy and their stereochemistry were confirmed by single crystal X-ray studies. Among the known compounds *1α, 6β, 8β, 15α-tetraacetoxy-9α-benzoyloxy-4β-hydroxydihydro-β-agarofuran, 1α, 8β-diacetoxy-6β, 9β-dibenzoyloxy-4β-hydroxydihydro-β-agarofuran, 1α, 9β-dibenzoyloxy-4β-hydroxydihydro-β-agarofuran, 1α-acetoxy-6β,9α-dibenzoyloxy-8α,4β-dihydroxydihydro-β-agarofuran* and *1α,9β-dibenzoyloxy-6β-acetoxy-8α,4β-dihydroxydihydro-β-agarofuran* are reporting for the first time from this species. To the best of our knowledge, single crystal X-ray structure of all the isolated compounds are reported for the first time.

6a.7. Experimental Session

General experimental details are given in Chapter 2.

6a.7.1. Extraction of *C. paniculatus* seeds

The stem bark of *C. paniculatus* was collected from Wayanad district, Kerala. This was thoroughly cleaned and dried in drier maintained at 50^{o} C and powdered. The powdered rhizome (1 kg) was subjected to repeated extraction using hexane, acetone, ethanol and water (2.5 L X 48 h) at room temperature. After extraction, the solvent was removed under reduced pressure using Büchi rotary evaporator. The hexane extract (60.5 g) and acetone extract (15 g) was then subjected to column chromatographic separation.

6a.7.2. Isolation of compound from *C. paniculatus* seeds

The acetone extract (60.5 g) of *C. paniculatus* seeds was dissolved in minimum quantity of dichloromethane and was adsorbed in silica gel (100-200) loaded on the top of silica gel column filled with slurry of 100-200 mesh silica gel in hexane. The column was eluted successively with gradient mixtures of hexane and ethyl acetate of increasing polarities and finally with 100 % ethyl acetate. A total of 175 fractions of approximately 200 mL each were collected. According to the similarity in TLC, they were pooled into 30 major fraction pools

(FrH.1- FrH. 30). Acetone extract (15 g) was subjected to column chromatographic purification using silica gel (100-200 mesh) with gradient elution. A total of 20 fractions of approximately 200 mL each were collected. According to the similarity in TLC, they were pooled into 8 major fraction pools (FrA.1- FrA.8). Pictorial representation of the procedure for the isolation of the compound is shown in figure 6a.66.

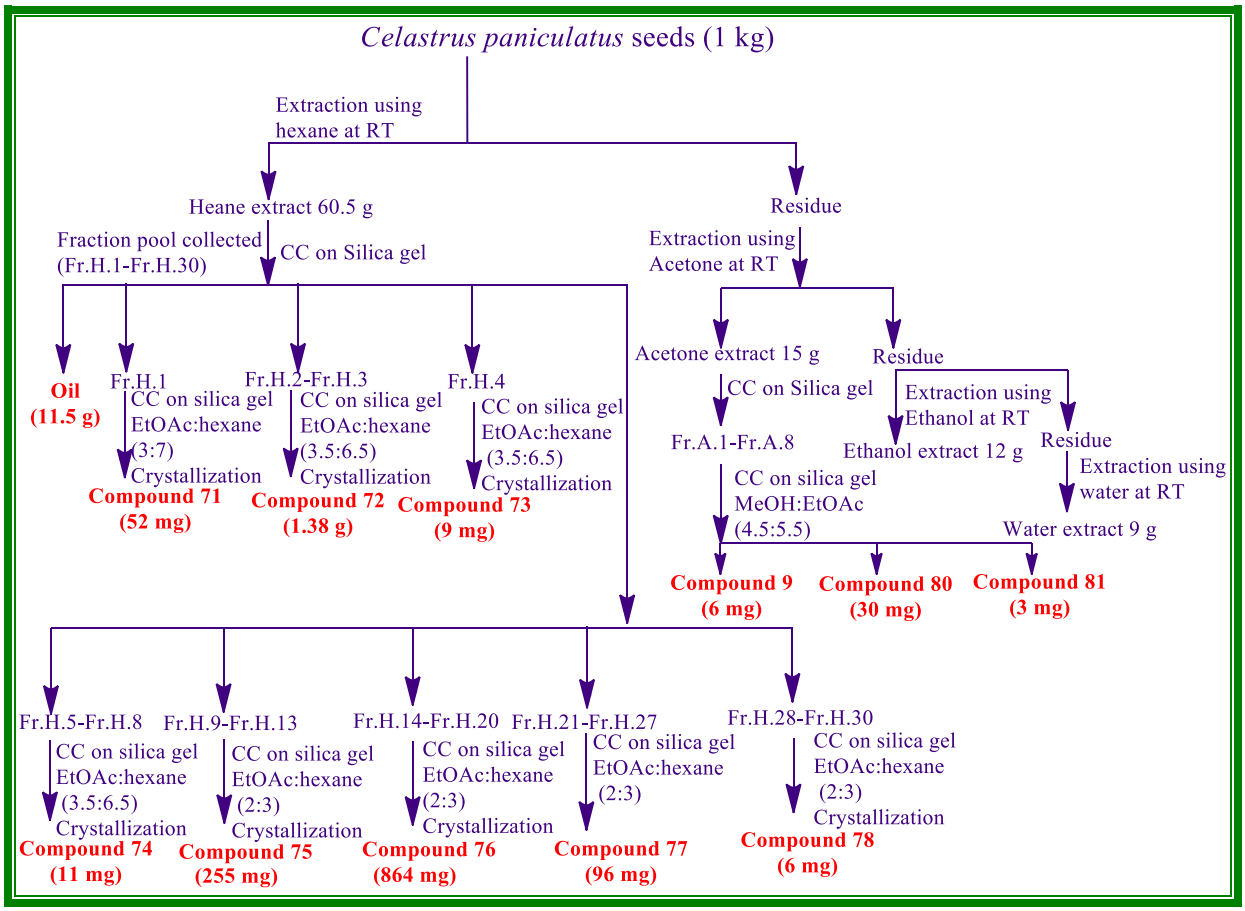

Figure 6a.66: Pictorial representation of isolation of compounds from *C. paniculatus*

6a.7.2.1. Isolation of compound 71

The isolation procedure of compound **71** is represented in figure 6a.66. Compound **71** (52 mg) was obtained as a colourless crystal, on eluting the column with 30 % ethyl acetate in hexane. IR, ^{1}H NMR, ^{13}C NMR, HMQC, HMBC, NOESY and mass spectral studies of this compound and single crystal X-ray analysis, confirmed it to be 1α, 9β-dibenzoyloxy-6β-cinnamoyloxy-4β-hydroxydihydro-β-agarofuran. Structure of the compound is shown below.

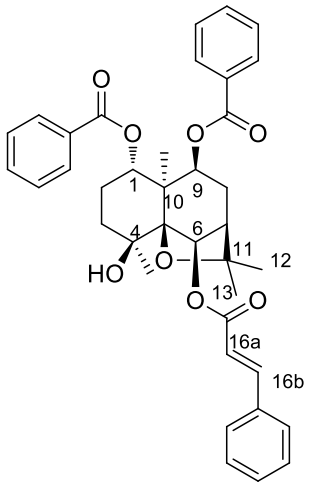

Melting point	:	228-230 ^{o}C
$[\alpha]^{25}_{D}$	:	+104.08^{o} (c 0.25, MeOH)
FT-IR (NaCl) υ_{max}	:	3425, 2954, 2359, 2114, 1711, 1637, 1487, 1451, 1388, 1277, 1168, 1027, 979, 875, 823 cm^{-1}.
^{1}H NMR (500 MHz, $CDCl_3$)	:	δ 7.90 (d, *J* = 15.5 Hz, 1H, CinO-6), 7.80 (dd, J_1 = 7 Hz, J_2 = 1 Hz, 2H, OCin-6), 7.58-7.54 (m, 4H, OCin-6, OBz-9), 7.51-7.49 (m, 1H, OBz-1), 7.48-7.39 (m, 4H, OBz-1), 7.32 (t, *J* = 8 Hz, 2H, OBz-9), 7.24 (t, *J* = 7.5 Hz, 2H, OBz-9), 6.49 (d, *J* = 16 Hz, 1H, OCin-6), 5.62 (s, 1H, H-6), 5.61 (dd, J_1 = 12 Hz, J_2 = 4 Hz, 1H, H-1), 5.14 (d, *J* = 7 Hz, 1H, H-9), 3.07 (s, 1H, OH-4), 2.61-2.56 (m, 1H, H-8*α*), 2.31-2.29 (m, 2H, H-7), 2.29-2.25 (m, 2H, H-8*β*), 2.12-2.05 (m, 2H, H-2*α,* H-3*α*), 1.79-1.76 (m, 1H, H-2*β*), 1.59 (s, 3H, Me-14), 1.57 (s, 3H, Me-15), 1.52 (s, 3H, Me-13), 1.42 (s, 3H, Me-12) ppm.
^{13}C NMR (125 MHz, $CDCl_3$)	:	δ 166.3 (C, OCin-6), 165.5 (C, OBz-1), 165.3 (C, OBz-9), [146.5, 134.3, 132.9, 132.6, 130.6, 130.2, 130.0, 129.8, 129.3, 129.1, 128.9, 128.4, 128.0, 127.9, 117.9 (C and CH, OCin-6, OBz-1, OBz-9), 91.7 (C-5) 84.5 (C-11), 80.1 (C-6), 73.4 (C-1), 73.4 (C-9), 70.7 (C-4), 51.8

(C-10), 49.1 (C-7), 38.9 (C-3), 31.9 (C-2), 29.7 (C-14), 25.9, 24.1 (C-13), 23.5 (C-12), 20.1(C-15) ppm.

HR-ESIMS m/z : 647.2625 $[M+Na]^+$ (calcd for $C_{38}H_{40}O_8Na$, 647.2620)

NMR Spectral assignments were made on the basis of 1D and 2D NMR analysis.

Crystal data for **71**: $C_{38}H_{39}O_8$. M = 623.69, Monoclinic, space group *P*21, a = 13.201(9) Å, b = 7.028(5) (3) Å, c = 17.656(12) (10) Å, α = 90 °, β = 94.700(11)°, γ = 90°, cell formula units Z = 2, crystal density = 1.269 mg/m^3, T = 302(2), 5886 reflections collected, [2272 reflections with I > 2\s(I)] R factor gt 0.0683 (CCDC 1812318).

6a.7.2.2. Isolation of compound 72

Compound **72** (1.38 g) was obtained as a colourless crystal, on eluting the column with 35 % ethyl acetate in hexane. Based on the NMR, HRMS and single crystal X-ray data, compound **72** was confirmed as 1α, 8β, 15α-triacetoxy-9α-benzoyloxy-4β-hydroxydihydro-β-agarofuran. Structure of the compound is shown below.

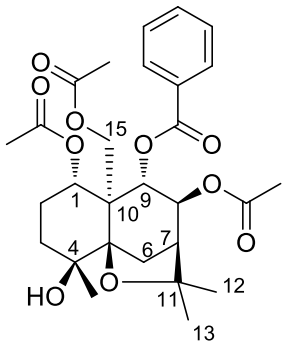

Melting point : 234-236 °C

$[\alpha]^{25}_D$: -4.16° (c 0.25, MeOH)

FT-IR (NaCl) υ_{max} : 3446, 2992, 2390, 2123, 1738, 1650, 1452, 1370, 1276, 1230, 1166, 1040, 969, 869 cm^{-1}.

^{1}H NMR (500 MHz, $CDCl_3$) : δ 7.92 (d, J = 8 Hz, 2H, OBz-9), 7.56 (t, J = 7.5 Hz, 1H, OBz-9), 7.44 (t, J = 7.5 Hz, 2H, OBz-9), 6.07 (d, J = 10 Hz, 1H, H-9), 5.53 (dd, J_1 = 9.5 Hz, J_2 = 3 Hz, 1H, H-8α), 5.28 (dd, J_1 = 12 Hz, J_2 = 3 .5 Hz, 1H, H-1), 4.96 (d, J = 13 Hz, 1H, H-15), 4.37 (d, J = 12.5 Hz, 1H, H-15),

		2.53 (d, *J* = 2.5 Hz, 2H, H-6), 2.46 (s, 1H, OH-4), 2.39 (d, *J* = 2.5 Hz, 1H, H-7), 2.31 (3H, s, OAc-1), 1.88 (3H s, OAc-8), 1.86-1.85 (m, 2H, H-2), 1.76-1.68 (m, 1H, H-3), 1.65 (s, 3H, Me-14), 1.53 (s, 3H, OAc-15), 1.33 (s, 3H, Me-13), 1.31 (s, 3H, Me-12) ppm.
^{13}C NMR (125 MHz, $CDCl_3$)	:	δ 170.5 (C, OAc-1), 170.4 (C, OAc-8), 169.9 (C, OAc-15), 165.7 (C, OBz-9), [133.3, 129.7, 129.5, 128.7, (C and CH, OBz-9)], 91.0 (C-5), 82.9 (C-11), 75.8 (C-8), 75.2 (C-9), 61.7 (C-15), 50.1 (C-10), 46.9 (C-7), 36.5 (C-2), 30.8 (C-6), 30.3 (OAc-Me), 24.9 (C-3), 24.4 (OAc-Me), 23.2 (OAc-Me), 21.4 (Me-14), 21.0 (Me-13), 20.9 (Me-12) ppm.
HR-ESIMS m/z	:	555.2215 $[M+H]^+$ (calcd for $C_{28}H_{36}O_{10}Na$, 555.2206)

NMR Spectral assignments were made on the basis of 1D and 2D NMR analysis.

Crystal data for 7**2**: $C_{28}H_{36}O_{10}$. M = 532.57, Monoclinic, space group *P*21, *a* = 11.954(14) Å, *b* = 8.967(11) Å, *c* = 12.810(16) Å, *α* = 90 °, *β* = 95.867°, *γ* = 90°, cell formula units *Z* = 2, crystal density = 1.295 mg/m^3, *T* = 302(2), 4949 reflections collected, [2070 reflections with I > 2\s(I)] R factor gt 0.0894 (CCDC 1812320).

6a.7.2.3. Isolation of compound 73

The isolation procedure of compound **73** is represented in figure 6a.66. Compound **73** (9 mg) was obtained as a colourless crystal, on eluting the column with 35 % ethyl acetate in hexane. IR, ^{1}H NMR, ^{13}C NMR, HMQC, HMBC, NOESY and mass spectral studies of this compound and single crystal X-ray analysis, confirmed it to 1*α*,9*β*-dibenzoyloxy-2*β*-acetoxy-6*β*-cinnamoyloxy-4*β*-hydroxyldihydro-*β*-agarofuran. Structure of the compound is shown below.

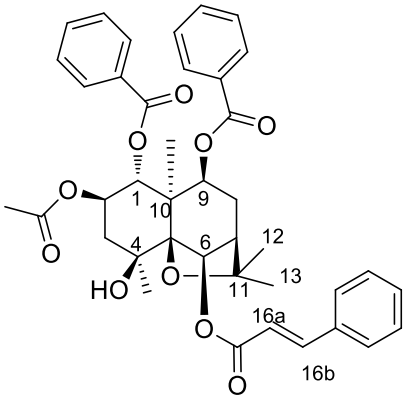

Melting point	:	236-238 ^{o}C
$[\alpha]^{25}_{D}$	:	-7.12^{o} (c 0.25, MeOH)
FT-IR (NaCl) υ_{max}	:	3429, 2934, 2539, 2114, 1715, 1480, 1461, 1392, 1267, 1168, 1055, 978, 873 cm^{-1}.
^{1}H NMR (500 MHz, $CDCl_3$)	:	δ 7.97 (t, *J* = 7 Hz, 2H, OCin-6), 7.88 (d, *J* = 16 Hz, 1H, OCin-6), 7-59-7.56 (m, 3H, OCin-6), 7.53-7.52 (m, 2H, OBz-9), 7.46-7.40 (m, 6H, OBz-1), 7.29-7.26 (m, 2H, OBz-9), 6.49(d, 1H, *J* = 16 Hz, OCin-6), 5.93 (t, *J* = 8 Hz, 1H, H-1), 5.62 (s, 1H. H-6), 5.16-5.14 (m, 1H, H-2*α*), 5.06 (d, *J* = 6.5 Hz, 1H, H-9), 3.22 (s, 1H, OH-4), 2.53-2.52 (m, 1H, H-8*α*), 2.32 (t, *J* = 3 Hz, 2H, H-7), 2.24-2.20 (m, 2H, H-8*β*), 1.80 (s, 3H, Me-14), 1.64 (s, 3H, Me-15), 1.49 (s, 3H, Me-13), 1.42 (s, 3H, Me-12) ppm.
^{13}C NMR (125 MHz, $CDCl_3$)	:	δ 170.5 (C, OAc-1), 166.2, (C, O-Cin-6) 165.3, (OBz-1), 164.8(OBz-9), [146.7, 133.1, 132.8, 130.7, 130.3, 129.7, 129.5, 129.2, 128.9, 128.4, 128.2, 127.9, (C, CH, OCin-6, OBz-1, OBz-9)], 91.1 (C-5) 85.1 (C-11), 79.8 (C-6), 73.0 (C-1), 72.8 (C-9), 71.2 (C-4), 68.8 (C-2), 52.1 (C-10), 48.9 (C-7), 44.5 (C-3), 25.9 (C-14), 24.9(C-15), 20.9 (C-13), 20.7 (C-12) ppm.
HR-ESIMS m/z	:	705.2690 $[M+Na]^{+}$ (calcd for $C_{40}H_{42}NaO_{10}$, 705.2675)

NMR Spectral assignments were made on the basis of 1D and 2D NMR analysis.

Crystal data for 7**3**: $C_{40}H_{42}O_{10}$. M = 682.74, Orthorhombic, space group *P*212121, *a* = 8.4506(14) Å, *b* = 14.262(2) Å, *c* = 28.035(5) Å, $\alpha = \beta = \gamma = 90°$, cell formula units *Z* = 4, crystal density = 1.342 mg/m^3, *T* = 150(2), 5922 reflections collected, [5271 reflections with I > 2\s(I)] R factor gt 0.0817 (CCDC 1812321).

6a.7.2.4. Isolation of compound 74

Fraction pool 5-8 (Fr.H.5-8) performed a column chromatography and on crystallization, a colourless crystals of compound **74** (11 mg) was yielded. The structure of the compound **74** was confirmed as in comparison with the NMR data of compound **73** and literature data [Tu and Chen **1993**]. Finally the structure was confirmed by single crystal X-ray analysis namely 1*α*-acetoxy-6*β*,9*α*-dibenzoyloxy-8*α*-cinnamoyloxy-4*β*-hydroxydihydro-*β*-agarofuran. Structure of the compound is shown below.

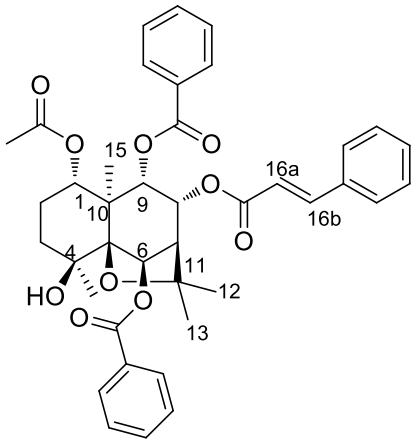

Melting point	:	242-244 ^oC
$[\alpha]^{25}_D$	:	-24.02^o (c 0.25, MeOH)
FT-IR (NaCl) υ_{max}	:	3426, 3063, 2952, 1722, 1635, 1601, 1453, 1368, 1317, 1275, 1167, 1072, 1034, 968, 863 cm^{-1}.
^{1}H NMR (500 MHz, $CDCl_3$)	:	δ [8.22 (t, *J* = 7 Hz, 2H), 8.22 (t, *J* = 7 Hz, 2H), 7.81(d, *J* = 15.5 Hz, 1H), 7.62-7.57(m, 3H), 7.53 (t, *J* = 7 Hz, 1H), 7.47 (t, *J* = 8 Hz, 2H), 7.43-7.38 (m, 5H), 6.53 (d, *J* = 16 Hz, 1H), (5H-OBz-9, 5-H-OBz-6, 7H-OCin-8)], 6.49 (s, 1H, H-6), 5.77 (t, *J* = 5 Hz, 1H, H-8), 5.71 (d, *J* = 5.5

Hz, 1H, H-9), 5.20 (dd, J_1 = 11.5 Hz, J_2 = 4 Hz, 1H, H-1), 2.96 (d, J = 1 Hz, 1H, OH-4), [2.65 (d, J = 4.5 Hz, 1H), 1.96-1.89 (m, 1H), 1.76-1.73 (m, 2H), (Aliphatic CH_2 and CH protons)], [1.71 (s, 3H), 1.65 (s, 3H), 1.60 (s, 3H), 1.58-1.57 (m, 1H), 1.43 (s, 3H), 1.42 (s, 3H), (CH_3 Protons)] ppm.

^{13}C NMR (125 MHz, $CDCl_3$) : δ 170.2 (C, OAc-1),, 165.9 (C, OBz-6), 165.6 (C, OBz-9), 165.0 (C, OCin-8), [145.9, 134.4, 133.4, 133.2, 130.5, 130.2, 129.9, 129.8, 129.6, 128.9, 128.6, 128.5, 128.4, 117.5, (C, CH, OBz-6, OCin-8, OBz-9)], 92.5 (C-5), 83.3 (C-11), 75.9 (C-6), 74.2 (C-1), 70.9 (C-8), 70.5 (C-4), [52.9, 49.8, 38.7, 31.6, 29.6, 24.3, 23.9, 23.4, 22.7, 20.8, 14.1, 12.9 (C, CH2, CH_3 Other aliphatic carbon)] ppm.

HR-ESIMS m/z : 705.2675 $[M+Na]^+$ (calcd for $C_{40}H_{42}NaO_{10}$, 705.2678)

NMR spectral assignments were made on the basis of 1D, 2D NMR analysis and on comparison with the literature reports.

Crystal data for **74**: $C_{40}H_{42}O_{10}.2H_2O$. M = 714.73, Monoclinic, space group *C*2, a = 38.80 Å, b = 8.896 Å, c = 11.406 Å, α = 90 °, β = 104.552°, γ = 90°, cell formula units Z = 4, crystal density = 1.215 mg/m^3, T = 302(2), 15151 reflections collected, [7161 reflections with I > 2\s(I)] R factor gt 0.0626 (CCDC 1812322).

6a.7.2.5. Isolation of compound 75

Compound **75** (255 mg) was obtained as colourless crystal by eluting the column with 40 % ethyl acetate in hexane. From all the 1D, 2D, HRMS data and on comparison with the literature reports [Zhang *et al*., **1998**], the compound was confirmed. Finally the structure was confirmed by single crystal X-ray analysis as 1α, 6β, 9β-tribenzoyloxy-4β-hydroxydihydro-β-agarofuran.

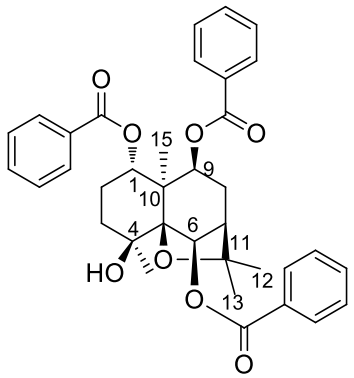

Melting point	:	218-220 ^{o}C
$[\alpha]^{25}_{D}$	:	+79.76^{o} (c 0.25, MeOH)
FT-IR (NaCl) υ_{max}	:	3528, 2956, 1741, 1443, 1374, 1272, 1103, 1043, 964, 873 cm^{-1}.
^{1}H NMR (500 MHz, $CDCl_3$)	:	δ [8.25 (dd, J_1 = 7 Hz, J_2 = 1 Hz, 2H), 7.81 (dd, J_1 = 7 Hz, J_2 = 1.5 Hz, 2H), 7.61-7.58 (m, 1H), 7.55 (dd, J_1 = 7.5 Hz, J_2 = 1 Hz, 2H), 7.51-7.47 (m, 3H), 7.44-7.41 (m, 1H), 7.33 (t, J = 7.5 Hz, 2H), 7.25 (t, J = 7.5 Hz, 2H) (15H-OBz-1, OBz-6, OBz-9)], 5.71 (s, 1H, H-6), 5.63 (dd, J_1 = 8 Hz, J_2 = 3.5 Hz, 1H, H-1), 5.16 (d, J = 7 Hz, 1H, H-9), 3.15 (s, 1H, OH-4), [2.65 – 2.60 (m, 1H), 2.38 (t, J = 3 Hz, 1H), 2.29 (dd, J_1 = 8.5 Hz, J_2 = 3 Hz, 1H), 2.12 – 2.08 (m, 2H), 1.81– 1.80 (m, 1H), 1.65 – 1.63 (m, 1H), (Aliphatic CH_2 and CH protons)], 1.59 (s, 3H), 1.57(s, 3H), 1.53 (s, 3H), 1.42 (s, 3H) (CH_3 Protons)] ppm.
^{13}C NMR (125 MHz, $CDCl_3$)	:	δ 166.2 (C, OBz-1), 165.5 (C, OBz-6), 165.3 (C, OBz-9), [133.4, 132.9, 132.6, 130.2, 130.0, 129.9, 129.8, 129.3, 129.1, 128.7, 128.0, 127.9 (C, CH, OBz-1, OBz-6, OBz-9)], 91.6 (C-5), 84.5 (C-11), 80.6 (C-1), 73.4 (C-6), 73.4 (C-4), 51.8 (C-10), [49.1, 38.9, 31.9, 29.7, 25.9, 24.0, 23.5, 20.1(C, CH2, CH_3 Other aliphatic carbon)] ppm.
HR-ESIMS m/z	:	621.2486 $[M+Na]^+$ (calcd for $C_{36}H_{38}O_8Na$, 621.2464)

NMR spectral assignments were made on the basis of 1D, 2D NMR analysis and on comparison with the literature reports.

Crystal data for 7**5**: $C_{36}H_{38}O_8$. M = 598.66, Orthorhombic, space group *P*212121, *a* = 9.0119(4) Å, *b* = 12.1099(5) Å, *c* = 28.4883(12) Å, $\alpha = \beta = \gamma = 90°$, cell formula units *Z* = 4, crystal density = 1.278 mg/m^3, *T* = 296(2), 6066 reflections collected, [3482 reflections with I > 2\s(I)] R factor gt 0.0441 (CCDC 1812324).

6a.7.2.6. Isolation of compound 76

Compound **76** (864 mg) was obtained as colourless crystal by eluting the column with 40 % ethyl acetate in hexane. From all the 1D, 2D, HRMS data and on comparison with the literature reports [Chavez *et al*., **1999**], the compound was confirmed. Finally the structure was confirmed by single crystal X-ray analysis as 1*α*, 6β, 8*β*, 15-tetraacetoxy-9*α*-benzoyloxy-4*β*- hydroxydihydro-*β*-agarofuran.

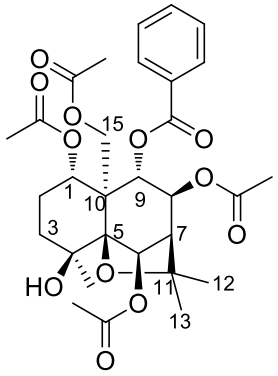

Melting point	:	220-222 ^oC
$[\alpha]^{25}_D$	:	-27.94^o (c 0.25, MeOH)
FT-IR (NaCl) υ_{max}	:	3527, 3004, 2957, 2358, 1928, 1740, 1597, 1443, 1371, 1146, 1103, 1042, 963, 871 cm^{-1}.
^{1}H NMR (500 MHz, $CDCl_3$)	:	δ [7.91 (t, *J* = 7 Hz, 2H), 7.57 (t, *J* = 7.5 Hz, 1H), 7.44 (t, *J* = 7.5 Hz, 2H), (5H-OBz-9)], 6.55 (s, 1H, H-6), 6.03 (d, *J* = 9.5 Hz, 1H, H-9), 5.68 (dd, J_1 = 9.5 Hz, J_2 = 3 Hz, 1H, H-1), 5.28 (dd, J_1 = 12.5 Hz, J_2 = 4.5 Hz, 1H, H-8), 4.84 (d, *J* = 8 Hz, 1H, H-15), 4.48 (d, *J* = 8 Hz, 1H, H-15), 2.70 (d, *J* = 0.5 Hz, 1H, OH-4), [2.47 (d, *J* = 3 Hz,

		1H), 2.39 (s, 3H), 2.13 (s, 3H), 1.88 (s, 4H), 1.70 (s, 3H), 1.65-1.64 (m, 3H), (Aliphatic CH_3, CH2 and CH protons)], [1.55 (s, 3H), 1.54 (s, 3H), 1.34 (s, 3H) (CH_3 Protons)] ppm.
^{13}C NMR (125 MHz, $CDCl_3$)	:	δ 170.5 (C, OAc-1), 169.9 (C, OAc-8), 169.8 (C, OAc-6), 169.8 (C, OAc-15), 165.6 (C, OBz-9), [133.4, 129.5, 129.4, 128.7, ((C, CH, OBz-9)], 92.4 (C-5), 84.1 (C-11), 75.3 (C-1), 75.3 (C-6), 74.0 (C-8), 70.2 (C-9), 61.1 (C-4), 60.4 (C-5), 52.2 (C-10), [50.6, 37.9, 29.7, 25.7, 24.5, 23.4, 21.4, 21.2, 20.9, 20.8 (C, CH_2, CH_3 Other aliphatic carbon)] ppm.
HR-ESIMS m/z	:	613.2260 $[M+Na]^+$ (calcd for $C_{30}H_{38}O_{12}Na$, 613.2261)

NMR spectral assignments were made on the basis of 1D, 2D NMR analysis and on comparison with the literature reports.

Crystal data for **76**: $C_{30}H_{38}O_{12}$. M = 590.60, Orthorhombic, space group P212121, a = 9.3829(3) Å, b = 11.3779(3) Å, c = 29.5068(10) Å, $\alpha = \beta = \gamma = 90°$, cell formula units Z = 4, crystal density = 1.245 mg/m^3, T = 296(2), 6284 reflections collected, [4418 reflections with I > 2\s(I)] R factor gt 0.0455 (CCDC 1812326).

6a.7.2.7. Isolation of compound 77

Figure 6a.66 represents the isolation procedure for compound **77**. It is obtained as white solid. Detailed investigation of various spectroscopic data of compound **77** revealed that it was 1α, 8β-diacetoxy-6β, 9β-dibenzoyloxy-4β-hydroxydihydro-β-agarofuran. Further evidence was made by comparing the 1D and 2D NMR data with literature [Torres-Romero *et al*., **2009**]. Structure of the isolated compound is shown below.

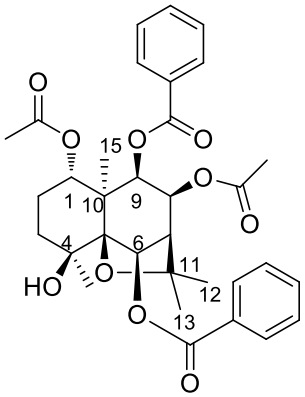

Melting point : 118-120 ^{o}C

$[\alpha]^{25}_{D}$: -11.86^{o} (c 0.25, MeOH)

FT-IR (NaCl) υ_{max} : 3553, 3064, 2949, 1738, 1599, 1451, 1370, 1275, 1236, 1177, 1108, 1040, 964, 897 cm^{-1}.

^{1}H NMR (500 MHz, $CDCl_3$) : δ [8.21 (dd, J_1 = 7 Hz, J_2 = 1.5 Hz, 2H), 8.04 (dd, J_1 = 8 Hz, J_2 = 1 Hz, 2H), 7.61-7.57 (m, 3H), 7.49-7.45 (m, 3H) (10H-OBz-6, OBz-9)], 6.00 (d, J = 5 Hz, 1H, H-9), 5.79 (s, 1H, H-6), 5.45 (dd, J_1 = 10 Hz, J_2 = 3.5 Hz, 1H, H-1), 5.17 (dd, J_1 = 12 Hz, J_2 = 4 Hz, 1H, H-8), 2.94 (s, 1H, OH-4), [2.66 (d, J = 3 Hz, 1H), 2.22 (s, 1H), 1.89 (s, 1H), 1.69-1.63 (m, 5H), 1.53 (s, 3H), 1.51 (s, 3H), 1.49 (s, 3H), 1.36 (s, 3H), 1.26 (s, 3H) (Aliphatic CH_3, CH_2 and CH protons)] ppm.

^{13}C NMR (125 MHz, $CDCl_3$) : δ 170.1(C, OAc-1), 169.8 (C, OAc-8), 165.7 (C, OBz-9), 165.4 (C, OBz-6), [133.2, 130.2, 129.8, 129.7, 129.6, 128.6, 128.6, 128.4 (C, CH, OBz-9, OBz-6)], 92.4 (C-5), 84.2 (C-11), 78.0 (C-1), 73,3 (C-6), 70.6 (C-9), 60.4 (C-4), 51.9 (C-10), [47.8, 38.6, 30.9, 29.7, 25.5, 24.0, 23.5, 23.4, 21.0, 20.9, 20.8, 14.2, 13.4 (C, CH_2, CH_3 Other aliphatic carbon)] ppm.

HR-ESIMS m/z : 617.2372 $[M+Na]^+$ (calcd for $C_{33}H_{38}O_{10}Na$, 617.2362)

NMR spectral assignments were made on the basis of 1D, 2D NMR analysis and on comparison with the literature reports.

6a.7.2.8. Isolation of compound 78

Fraction pool 28-30 was subjected to crystalize followed by the column chromatography afforded compound **78** (6 mg). From all the 1D, 2D, HRMS data and on comparison with the literature reports [Torres-Romero *et al*., **2009**], the compound was confirmed. Finally the structure was confirmed by single crystal X-ray analysis as 1α, 9β-dibenzoyloxy-4β-hydroxydihydro-β-agarofuran. Structure of the compound is shown below.

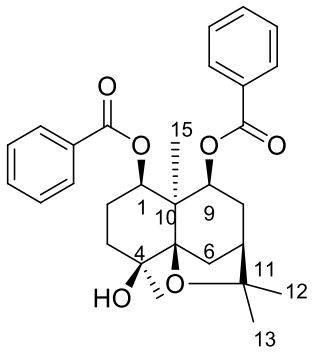

Melting point	:	170-172 ^{o}C
$[\alpha]^{25}_{D}$	:	+61.96^{o} (c 0.25, MeOH)
FT-IR (NaCl) υ_{max}	:	3543, 2933, 1974, 1916, 1716, 1596, 1453, 1386, 1281, 1172, 1107, 1021, 975, 935, 874 cm^{-1}.
^{1}H NMR (500 MHz, $CDCl_3$)	:	δ [7.82 (dd, J_1 = 9 Hz, J_2 = 1 Hz, 2H), 7.57 (dd, J_1 = 8.5 Hz, J_2 = 1 Hz, 2H), 7.48 (dd, J_1 = 7.5 Hz, J_2 = 1 Hz, 1H), 7.46-7.41 (m, 1H), 7.32 (t, J = 8 Hz, 2H), 7.24 (d, J = 8 Hz, 2H), (10H-OBz-1, OBz-9)], 5.60 (dd, J_1 = 12 Hz, J_2 = 4.5 Hz, 1H, H-1), 5.12 (d, J = 6.5 Hz, 1H, H-9), 2.98 (s, 1H, OH-4), [2.75 (bs, 1H), 2.46-2.42 (m, 1H), 2.27-2.22 (m, 1H), 2.14-2.01 (m, 2H), 1.45 (s, 3H), 1.43 (s, 3H), 1.34 (s, 3H), 1.32 (s, 3H) (Aliphatic CH_3, CH_2 and CH protons)] ppm.
^{13}C NMR (125 MHz, $CDCl_3$)	:	δ 165.6 (C, OBz-1), 165.5 (C, OBz-9), [132.8, 132.5, 130.3, 129.8, 129.6, 129.1, 127.9 (C, CH, OBz-1, OBz-9)], 90.6 (c-5), 83.6 (C-11), 74.2 (C-1), 73.5 (C-9), 70.3 (C-4), [48.3, 43.6, 37.0, 31.6, 31.2, 30.0, 24.4, 24.1,

23.8, 19.4 (C, CH_2, CH_3 Other aliphatic carbon)] ppm.

HR-ESIMS m/z : 501.2261 $[M+Na]^+$ (calcd for $C_{29}H_{34}NaO_6$, 501.2253)

NMR spectral assignments were made on the basis of 1D, 2D NMR analysis and on comparison with the literature reports.

Crystal data for **78**: $C_{29}H_{33}O_6$. M = 477.55, Orthorhombic, space group *P*212121, *a* = 8.437(10) Å, *b* = 10.012(11) Å, *c* = 30.52(3) Å, $\alpha = \beta = \gamma = 90°$, cell formula units *Z* = 4, crystal density = 1.230 mg/m^3, *T* = 302(2), 5181 reflections collected, [2521 reflections with I > 2\s(I)] R factor gt 0.0630 (CCDC 1812330).

6a.7.2.9. Isolation of compound 79

Crude Fraction Fr.A.2 was chromatographed over silica gel using 45 % ethyl acetate in hexane to give a compound **79** (6 mg) as a colourless crystal. From all the 1D, 2D, HRMS data and on comparison with the literature reports [Takaishi *et al*., **1992**], the compound was confirmed. Finally the structure was confirmed by single crystal X-ray analysis as 1*α*,2*α*,6*β*,15-tetraacetoxy-9*α*-benzoyloxy-4*β*,8*β*-dihydroxydihydro-*β*-agarofuran. Structure of the compound is shown below.

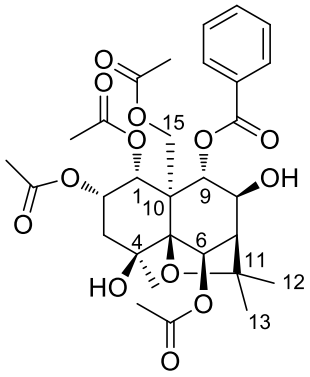

Melting point : 283-285 ^oC

$[\alpha]^{25}_D$: +11.33^o (c 0.25, MeOH)

FT-IR (NaCl) υ_{max} : 3704, 2934, 1743, 1440, 1370, 1281, 1233, 1148, 1107, 1050, 951, 869 cm^{-1}.

^{1}H NMR (500 MHz, $CDCl_3$) : δ [7.98 (t, *J* = 7 Hz, 2H), 7.60 (t, *J* = 7.5 Hz, 1H), 7.47 (t, *J* = 7.5 Hz, 2H) (5H-OBz-9)], 6.38 (s, 1H, H-6, H-9), 5.87 (d, *J* = 9.5 Hz, 1H, H-1), 5.46 (d, *J* = 3.5 Hz, 1H),

		5.33 (dd, J_1 = 6.5 Hz, J_2 = 3 Hz, 1H, H-2), 4.96 (d, J = 13.5 Hz, 1H, H-15), 4.70 (d, J = 13 Hz, 1H, H-15), 4.46 (d, J = 9 Hz, 1H, H-8), 2.80 (s, 1H, OH-4), [2.47 (d, J = 3 Hz, 1H), 2.44 (bs, 1H), 2.30 (s, 3H), 2.14 (s, 3H), 2.13-212 (m, 1H), 2.09 (s, 3H), 1.96-1.93 (m, 1H), 1.75 (s, 3H), 1.56 (s, 3H), 1.26 (s, 3H), 1.25 (s, 3H) (Aliphatic CH_3, CH_2 and CH protons)] ppm.
^{13}C NMR (125 MHz, $CDCl_3$)	:	δ 171.2 (C, OAc-2), 170.3 C, OAc-1), 170.0 (C, OAc-6), 169.6 (C, OAc-15), 166.9 (C, OBz-9), [133.7, 129.7, 129.4, 128.8 (C, CH, OBz-1, OBz-9)] 92.0 (C-5), 84.3 (C-11), [78.9, 75.8, 75.3, 74.6, 69.6, 67.8, 61.6, 60.4 (-OC), [54.2, 51.7, 42.0, 31.6, 30.9, 29.9, 25.9, 24.7, 22.7, 21.5, 21.3, 21.2, 21.1, 20.4, 14.2, 14.1 (C, CH_2, CH_3 Other aliphatic carbon)] ppm.
HR-ESIMS m/z	:	629.2230 $[M+Na]^+$ (calcd for $C_{30}H_{38}NaO_{13}$, 629.2210)

NMR spectral assignments were made on the basis of 1D, 2D NMR analysis and on comparison with the literature reports.

Crystal data for **79**: $C_{30}H_{38}O_{13}$. M = 606.60, Monoclinic, space group *P*21, a = 10.030 Å, b = 16.396 Å, c = 10.124 Å, α = 90 °, β = 105.26°, γ = 90°, cell formula units Z = 2, crystal density = 1.254 mg/m^3, T = 302(2), 5415 reflections collected, [4689 reflections with I > 2\s(I)] R factor gt 0.0894 (CCDC 1812325).

6a.7.2.10. Isolation of compound 80

Fraction pool 4-5 (FrA.4-5) was submitted to repeated column chromatography on silica gel (mesh 230-400) using 50 % ethyl acetate in hexane to yield compound 80 (30 mg). From all the 1D, 2D, HRMS data and on comparison with the literature [Carroll *et al*., **2009**], the compound was confirmed. Finally the structure was confirmed by single crystal X-ray analysis as 1*α*-acetoxy-6*β*,9*α*-dibenzoyloxy-8*α*,4*β*-dihydroxydihydro-*β*-agarofuran. Structure of the compound is shown below.

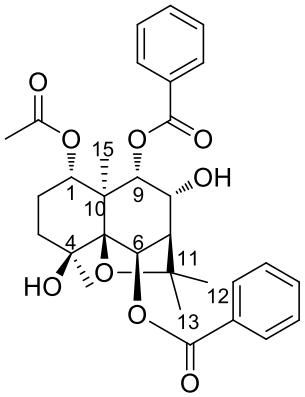

Melting point	:	210-214 ^{o}C
$[\alpha]^{25}_{D}$	:	-43.65^{o} (c 0.25, MeOH)
FT-IR (NaCl) υ_{max}	:	3532, 3062, 2947, 2361, 1924, 1722, 1597, 1450, 1371, 1277, 1174, 1112, 1066, 1033, 960, 893 cm^{-1}.
^{1}H NMR (500 MHz, $CDCl_3$)	:	δ [8.21 (d, *J* = 7.5 Hz, 2H), 8.11 (d, *J* = 7.5 Hz, 2H), 7.61-7.57 (m, 2H), 7.49-7.44 (m, 4H) (10H-OBz-6, OBz-9)], 5.53 (d, *J* = 5 Hz, 1H, H-9), 5.30 (s, 1H, H-6), 5.14 (dd, J_1 = 11.5 Hz, J_2 = 4 Hz, 1H, H-1), 4.48 (t, *J* = 4.5 Hz, 1H, H-8), 2.98 (s, 1H, OH-4), [2.61 (d, *J* = 4 Hz, 1H), 1.92-1.86 (m, 1H), 1.79-1.68 (m, 3H), 1.63 (s, 3H), 1.58 (s, 3H), 1.56 (s, 3H), 1.42 (s, 3H), 1.39 (s, 3H) (Other aliphatic CH_3, CH_2 and CH protons)] ppm.
^{13}C NMR (125 MHz, $CDCl_3$)	:	δ 170.3 (C, OAc-1), 166.0 (C, OBz-6), 165.1 (C, OBz-9), [133.6, 133.2, 130.2, 130.0, 129.8, 129.7, 128.7, 128.6, (C, CH, OBz-6, OBz-9)], 92.7 (C-5), 83.0 (C-11), 78.1 (C-1), 75.8 (C-9), 70.5 (C-6), 69.9 (C-4), 54.4 (C-8), [53.4, 49.7, 38.7, 29.7, 24.1, 23.9, 23.5, 20.9, 13,2 (C, CH_2, CH_3 Other aliphatic carbon)] ppm.
HR-ESIMS m/z	:	575.2267 $[M+Na]^+$ (calcd for $C_{31}H_{36}NaO_9$,575.2257)

NMR spectral assignments were made on the basis of 1D, 2D NMR analysis and on comparison with the literature reports.

Crystal data for **80**: $C_{31}H_{36}O_9$. M = 552.22, Monoclinic, space group *P*21, *a* = 14.637(11) Å, *b* = 13.084(9) Å, *c* = 15.817(11) Å, α = 90 °, β = 108.980(11)°, γ = 90°, cell formula units *Z* = 2, crystal density = 1.137 mg/m^3, *T* = 293(2), 12695 reflections collected, [4921 reflections with I > 2\s(I)] R factor gt 0.0759 (CCDC 1812329).

6a.7.2.11. Isolation of compound 81

Figure 6a.66 represents the isolation procedure for compound **81**. It is obtained as white solid. Detailed investigation of various spectroscopic data of compound **81** revealed that it was 1*α*,9*β*-dibenzoyloxy-6*β*-acetoxy-8*α*,4*β*-dihydroxydihydro-*β*-agarofuran. Further evidence was made by comparing the 1D and 2D NMR data with the literature reports [Gonzalez *et al*., **1993**]. Structure of the isolated compound is shown below.

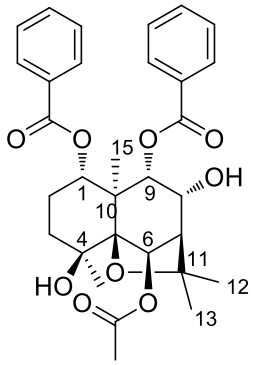

Melting point	:	221-224 °C
$[\alpha]^{25}_D$	:	-4.45° (c 0.25, MeOH)
FT-IR (NaCl) υ_{max}	:	3559, 3054, 2939, 1742, 1597, 1452, 1370, 1275, 1235, 1178, 1118, 1040, 994, 896 cm^{-1}.
^{1}H NMR (500 MHz, $CDCl_3$)	:	δ [8.26 (d, *J* = 7.5 Hz, 2H), 8.20 (d, *J* = 7.5 Hz, 2H), 7.64 (d, *J* = 7.5 Hz, 1H), 7.56 (t, *J* = 8 Hz, 3H), 7.46 (t, *J* =7.5 Hz, 2H) (10H-OBz-1, OBz-9)], 6.51 (s, 1H, H-6), 5.78 (t, *J* = 4.5 Hz, 1H, H-1), 5.62 (d, *J* = 5.5 Hz, 1H, H-9), 4.04 (q, *J* = 4 Hz, 1H, H-8), 2.93 (bs, 1H, OH-4), [2.62 (d, *J* = 4 Hz, 1H), 1.98 (s, 3H), 1.85-1.80 (m, 1H), 1.79-1.70 (m, 3H), 1.65 (s, 3H), 1.60 (s, 3H), 1.40 (s, 3H),

		1.38 (s, 3H), (Aliphatic CH_3, CH_2 and CH protons)] ppm.
^{13}C NMR (125 MHz, $CDCl_3$)	:	δ 170.6 (C, OAc-6), 166.9 (C, OBz-1), 165.8 (C, OBz-9), [133.3, 130.2, 129.9, 129.8, 129.7, 128.7, 128.6, 4 (C, CH, OBz-9, OBz-6)], 92.6 (C-5), 83.0 (C-11), 75.7 (C-1), 74.0 (C-6), 71.4 (C-9), 70.7 (C-4), 53.1 (C-8), [50.1, 38.9, 29.6, 27.8, 23.9, 23.3, 21.1, 11.6 (C, CH_2, CH_3 Other aliphatic carbon)] ppm.
HR-ESIMS m/z	:	575.2267 $[M+Na]^+$ (calcd for $C_{31}H_{36}NaO_9$, 575.2257)

NMR spectral assignments were made on the basis of 1D, 2D NMR analysis and on comparison with the literature reports.

CHAPTER 6B

Ca^{2+} Channel NMDARs inhibitory and antidiabetic activity of dihydro-*β*-agarofuran sesquiterpenoids

6b.1. Introduction

Significant focus of pharmaceutical research for the treatments of glaucoma, Alzheimer‟s disease (AD), Parkinson‟s disease (PD), and other neurodegenerative diseases (NDs) are more pertinent today. AD is the one of the most common form of dementia and a devastating neurodegenerative disorder which is considered by progressive cognitive failure [Lipton, **2006**]. Till now, the effective treatment to cure or reduce the progression of AD is limited. Early detection is therefore crucial for the diagnosis of this disease. However, the current prognosis of AD is based on clinical symptoms, the neuropsychological test, and neuroimaging which may appear several years after the pathological changes. Despite the big trouble, there is no definitive diagnosis of Alzheimer‟s disease. Detection assays have been developed to identify the biomarkers of AD which includes amyloid beta (Aβ), total tau protein, phosphorylated tau and amyloid-beta derived diffusible ligands (ADDLs) in cerebrospinal fluid (CSF) and blood. NMDA receptors have received much attention over the last few decades, due to their role in many types of neural plasticity and their involvement in excitotoxicity. There is great interest in developing clinically significant NMDA receptor antagonists that would block excitotoxic NMDARs activation, without interfering with NMDA receptor function needed for normal synaptic transmission, plasticity and memory functions.

Diabetes is a chronic disorder associated with the metabolism of carbohydrate, protein and fat owing to absolute or corresponding deficiency of insulin secretion with or without fluctuating degree of insulin resistance [Defronzo *et al*., **2015**]. According to WHO, the people with diabetes has quadrupled in the world since 1980 and its prevalence is still growing in most regions. The doubling of global prevalence from 1980 to 2014, reflecting a raise in overweight and obesity. Diabetes pervasiveness is raising mostly in low and middle

income countries. Diabetes along with higher-than-optimal blood glucose accounts for 3.7 million deaths in 2012, in which many of which could be prevented [WHO, 2016]. Throughout the past, different medicaments and drugs have been used to treat diabetes mellitus, including insulin prior to realization of its mechanism of action. A few of them has been included in the therapeutic array of medicine and some are used as combination therapy in patients with hyperglycemia in which most of them have been acquired from plants or microbes.

6b.2. NMDAR (N-methyl-D-aspartate receptors)

N-methyl-D-aspartate receptors (NMDARs) belong to the family of ionotropic glutamate receptors (iGluRs), which are critically involved in controlling synaptic plasticity and memory function. The NMDARs are composed of heterotetrameric membrane protein complexes. NMDA receptor consists of three different subunits termed GluN1-3, GluN2 and N3 subunits are encoded by four (GluN2A-D) and two (GluN3A and B) genes respectively [Monyer *et al*., **1992**]. Activation of NMDARs occurs through glycine binding site, glutamate binding site, allosteric binding site or through cationic channel especially through calcium channel. The extensive extracellular domains recognize neurotransmitter ligands and allosteric compounds and translate the binding information to regulate activity of the transmembrane ion channel. Over activation of NMDARs causes excessive influx of Ca^{2+} leading to excitotoxicity and is thought to be involved in many neurodegenerative disorders and diseases [Lipton, **2006**].

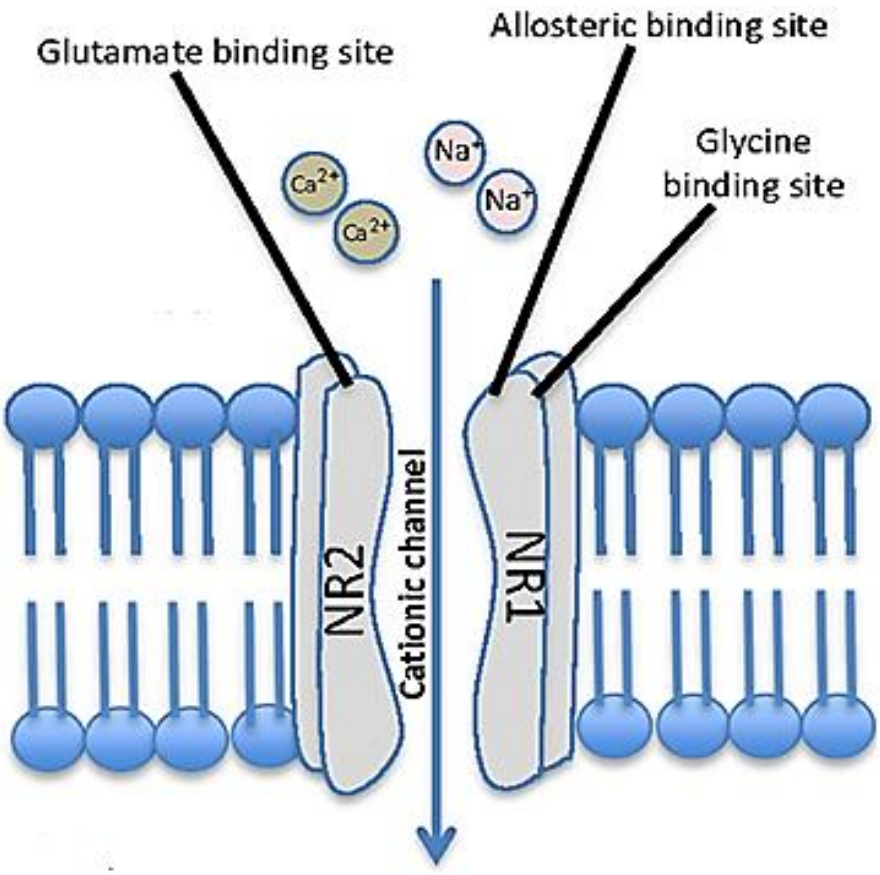

Figure 6b.1: NMDAR model illustrating important binding and modulatory sites

6b.3. Aim and scope of the present work

Celastrus paniculatus, has been used in various Indian cultural and medical traditions, such as Ayurveda and Unani. It has been used to both relax the nerves and sharpen the mental focus. *Celastrus paniculatus* is one of the plants used in 'medhyarasayanas'. The 'medhyarasayanas' are known to be beneficial to improve the intellect. Medhyarasayana drugs are used for prevention and treatment of mental disorders of all the age groups. These drugs promote the intellect (Dhi), retention power (Dhriti) and memory (Smriti). Mood disorders are known to be associated with considerable burden of disease, suicides, physical comorbidities, high economic costs, and poor quality of life. Therefore, it has become a major public health problem today. Unfortunately modern medicine based psychoactive drugs have met with limited success in treatment of various neurological and psychiatric disorders due to the multi-factorial nature of these diseases. Based on the ethnopharmacological importance of *C. paniculatus*, the NMDA receptor inhibitory activity

of isolated compounds has been carried out, which are mainly controlling the synaptic plasticity and memory function. This plant has hitherto uninvestigated for their NMDARs inhibitory potential, therefore it is timely and relevant to carry out the biological investigation. As part of our continuing search for novel antidiabetic agents of plant origin, [Ajish *et al*., **2014**; Sasikumar *et al*., **2016**], both extracts and isolated compounds were screened for their antidiabetic potential and these results are also described in this chapter.

6b.4. Effect of dihydro-*β*-agarofuran on NMDA receptor activity

In order to check the effect of compounds on NMDA receptor (NMDAR) activity, a cell-based assay system was used. The assay system works on the basis of protein-protein interaction between NMDAR and *α*-CaMKII, which was developed by the research group of Dr. R. V. Omkumar at Molecular Neurobiology Division, RGCB (US Patent Nos. **8, 304, 198**; Indian Patent No. **260367**; European Patent No. **2162742**). The plasmids coding for NMDAR subunits, GluN1, GluN2B, and α-CaMKII tagged with GFP (GFP- *α*-CaMKII) were co-transfected into HEK-293 cells and the activity of GluN2B containing NMDAR was detected upon activation of NMDAR in presence of calcium by its agonists glutamate and glycine. The activity of GluN2B containing NMDAR was detected based on the activation of GFP-α-CaMKII by Ca^{2+} influx through NMDAR and its subsequent translocation to GluN2B subunit (Figure 6b.4a).

Interaction between *α*-CaMKII and GluN2B is observed as localization spots (punctate appearance) in the endoplasmic reticulum (ER) and plasma membrane. To check the effect of compounds on NMDAR activity, the compounds at respective concentrations were added to cells. In order to determine the localization efficiency, the cells were counted using fluorescence microscope (Leica DMI 4000B inverted microscope with Leica DFC 350 FX model CCD camera) magnification at 40X. The number of green fluorescent cells with punctate appearance and the total number of green fluorescent cells were counted and the percentage of green fluorescent cells having punctate pattern was calculated as "(number of punctate cells /total number of green fluorescent cells) X 100". This number was taken as the efficiency of punctate formation or punctate cell count. For each slide, 5 or more fields were randomly selected and the average of punctate cell count for all the fields was estimated. This system provides direct data on the activity of dihydro-*β*-agarofuran against NMDAR subtype with a specific subunit (GluN2B). NMDARs are assembled early in the ER

and association of both subunits are necessary for the cell surface targeting of NMDARs (Wenthold et al., 2003). The functional NMDARs are present on the plasma membrane and allow the intracellular passage of calcium ions. At the same time, the GluN2B subunits will be present mostly in the ER. The „punctate" will be seen only when Ca^{2+} influx occur through NMDAR (Figure 6b.4a) and it was absent when NMDAR was activated in the absence of Ca^{2+} (Figure 6b.4b). In order to check the activity of dihydro-*β*-agarofuran on NMDA receptor, cells were pre-incubated with isolated compounds (50 and 100 μM) for 5 minutes and the NMDAR activity was also checked in presence of a known antagonist MK-801 (20 μM). After pre-incubation, NMDAR was activated in the presence of dihydro-*β*-agarofuran or MK-801 (with same concentrations) using the agonists of NMDAR, glutamate (100 μM), glycine (10 μM) in presence of Ca^{2+} (2 mM) for 5 minutes. The NMDAR activity was expressed in terms of localization efficiency, which was determined by counting the number of green fluorescent cells that develop punctae with respect to the total number of green fluorescent cells in that field. For each slide, five or more fields were randomly selected and were counted. NMDAR activity in the absence of dihydro-*β*-agarofuran or MK-801 was taken as the positive control.

NMDAR activity was completely blocked in the presence of 20 μM MK-801 (Figure 6b.4e), whereas, compound **78**, 1*α*, 9*β*-dibenzoyloxy-4*β*-hydroxydihydro-*β*-agarofuran showed 30 % inhibition in the NMDAR activity at 50 μM concentration. Compound **80**, 1*α*-acetoxy-6*β*, 9*β*-dibenzoyloxy-8*α*, 4*β*-dihydroxydihydro-*β*-agarofuran showed prominent NMDAR inhibition (75 %) at 50 μM concentration (Figure 6b.2, Figure 6b.3).

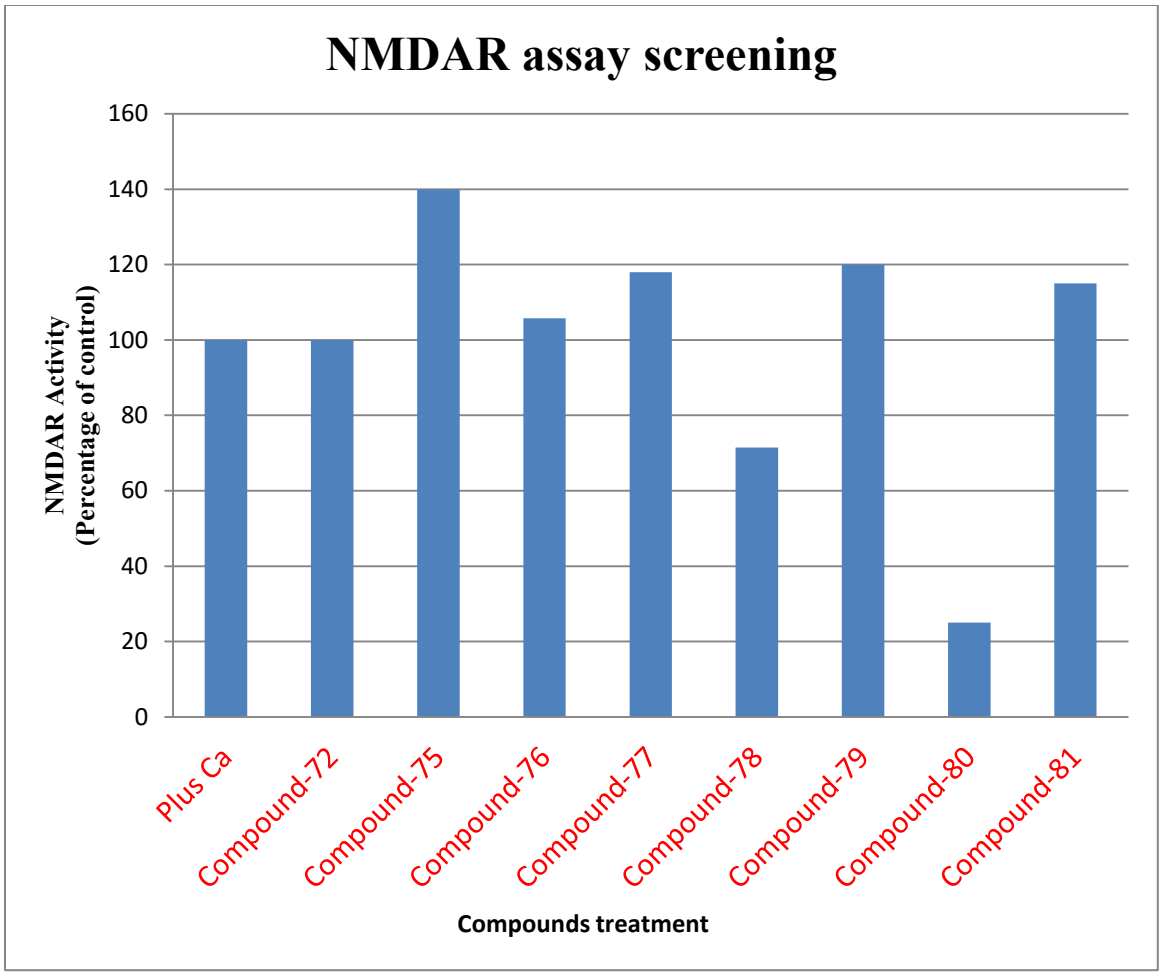

Figure 6b.2: NMDAR inhibitory activity of compounds

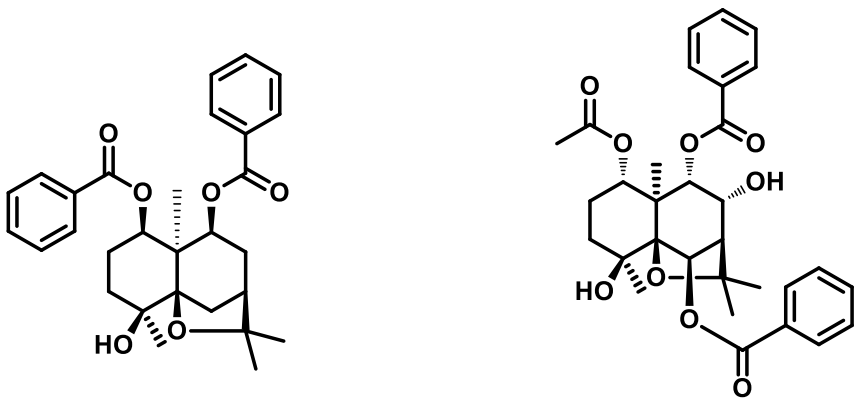

Figure 6b.3: Structure of active compounds

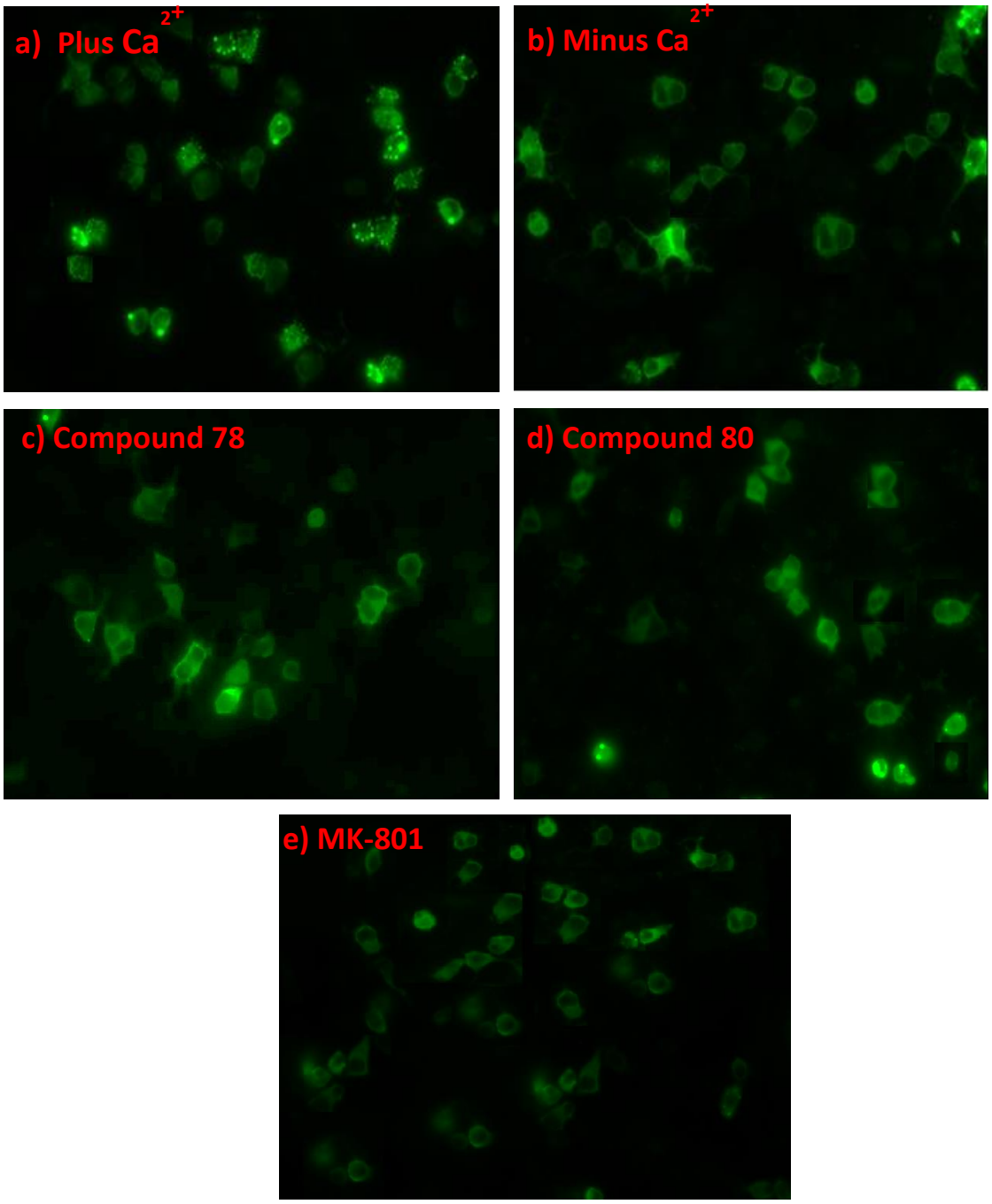

Figure 6b.4: NMDA receptor inhibitory activity: HEK-293 cells expressing GFP-α-CaMKII and GluN2B were subjected to NMDAR assay. (a) Cells which received treatment with glutamate, glycine and calcium. (b) cells which was treated with glutamate and glycine in the absence of calcium as a control. (c) Cells which received treatment with glutamate, glycine

and calcium in the presence of 50 μM compound **78**, (d) Cells which received treatment with glutamate, glycine and calcium in the presence of 50 μM compound **80**, (e) Cells which was treated with glutamate, glycine and calcium in the presence of 20 μM MK-801.

6b.5. Antidiabetic Studies

6b.5.1. Extract level antidiabetc studies of *C. paniculatus* extracts

The dried seeds of CP were subjected to successive extraction with different polar solvents such as hexane, acetone, ethanol and water at room temperature. These extracts were analysed for their inhibitory activity on *α*-glucosidase and *α*-amylase enzymes and, also for their antiglycation properties. The results showed that hexane extract effectively inhibits α-glucosidase enzyme (IC_{50} 44.44 ± 0.344 μg/mL), which is comparable to the standard acarbose tested (IC_{50} 45.37 ± 0.681 μg/mL), whereas, rest of the extracts does not show any prominent antidiabetic activity (Table 6b.1, Figure 6b.5).

Table 6b.1: Antidiabetc activity of *C. paniculatus* extracts

Extracts	***α*-glucosidase (μg/mL)**	***α*- amylase (μg/mL)**	**Antiglycation (μg/mL)**
CPH	44.44 ± 0.344	154.76 ± 0.301	337.26 ± 0.663
CPA	121.77 ± 0.511	200.08 ± 0.507	379.81 ± 0.554
CPE	171.76 ± 0.406	234.34 ± 0.230	420.58 ± 0.205
CPW	148.43 ± 0.514	249.18 ± 0.217	327.93 ± 0.571
CP Oil	149.57 ± 0.471	174.20 ± 0.256	363.53 ± 0.023
Acarbose	45.37 ± 0.681	5.53 ± 0.367	……
Ascorbic acid	……	……	48 ± 0.876

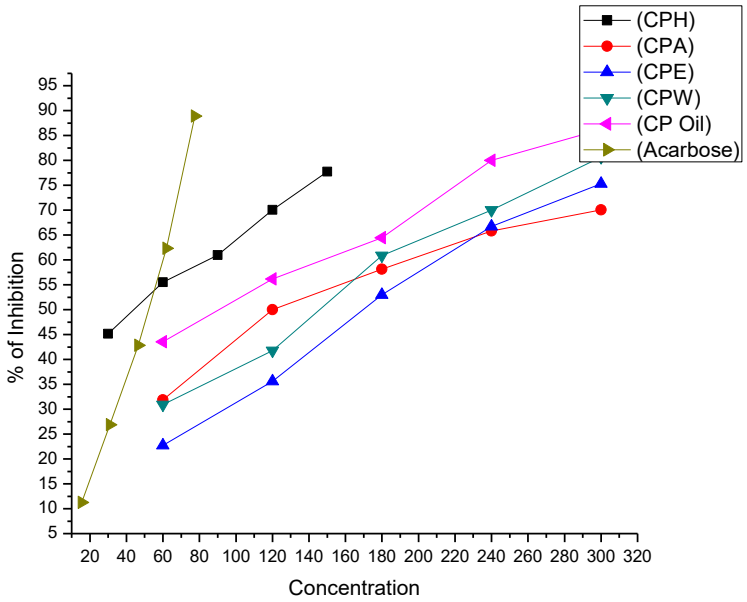

Figure 6b.5: α-Glucosidase inhibition activity of different extracts of *C. paniculatus*

6b.5.2. Antidiabetic screening of isolated compounds

In order to check the antidiabetic activity of isolated compounds (**71-81**), we examined the α-glucosidase, α-amylase inhibition and antiglycation properties of these compounds. The results obtained are summarised in table 6b.2. All the tested compounds except compound **77** showed promising α-glucosidase inhibition which is compared to the standard, acarbose. In particular, compounds **71**, **73**, **74**, **75**, **76** and **78** showed excellent α-glucosidase inhibitory activity with IC_{50} values of 39.56 ± 0.761, 35.60 ± 0.843, 36.54 ± 0.173, 44.83 ± 0.453, 42.58 ± 0.209 and 45.84 ± 0.356 µM respectively (Table 6b.2, Figure 6b.6). The compounds **71**, **73** and **74** also showed good antiglycation property with IC_{50} values of 114.27 ± 0.302, 110.61 ± 0.583 and 118.37 ± 0.372 respectively, compared to the standard ascorbic acid (Figure 6b.7). None of the compounds demonstrated promising inhibits α-amylase inhibition.

Table 6b.2: Antidiabetc activity of isolated compounds

Compound	α- Glucosidase inhibition (µM)	α-Amylase inhibition (µM)	Antiglycation (µM)
Compound **71**	39.56 ± 0.761	101.26 ± 0.401	114.27 ± 0.302
Compound **72**	51.23 ± 0.686	148.73 ± 0.478	157.40 ± 0.539
Compound **73**	35.60 ± 0.843	136.17 ± 0.583	110.61 ± 0.583

Table 6b.2 Contd…

Compound **74**	36.54 ± 0 .173	108.94 ± 0.292	118.37 ± 0.372
Compound **75**	44.83 ± 0.453	128.49 ± 0.324	139.76 ± 0.230
Compound **76**	42.58 ± 0.209	159.21 ± 0.521	144.71 ± 0.251
Compound **77**	53.67 ± 0.876	140.93 ± 0.366	143.91 ± 0.366
Compound **78**	45. 84 ± 0.356	164.72 ± 0.539	177.18 ± 0.539
Compound **79**	51.60 ± 0.767	134.42 ± 0.198	142.14 ± 0.280
Compound **80**	50.60 ± 0.766	124.73 ± 0.451	149.41 ± 0.508
Compound **81**	51.70 ± 0.403	140.05 ± 0.632	154.73 ± 0.632
Acarbose	52.87 ± 0.224	8.99 ± 0.480	…….
Ascorbic acid	…….	…….	154.63 ± 0.497

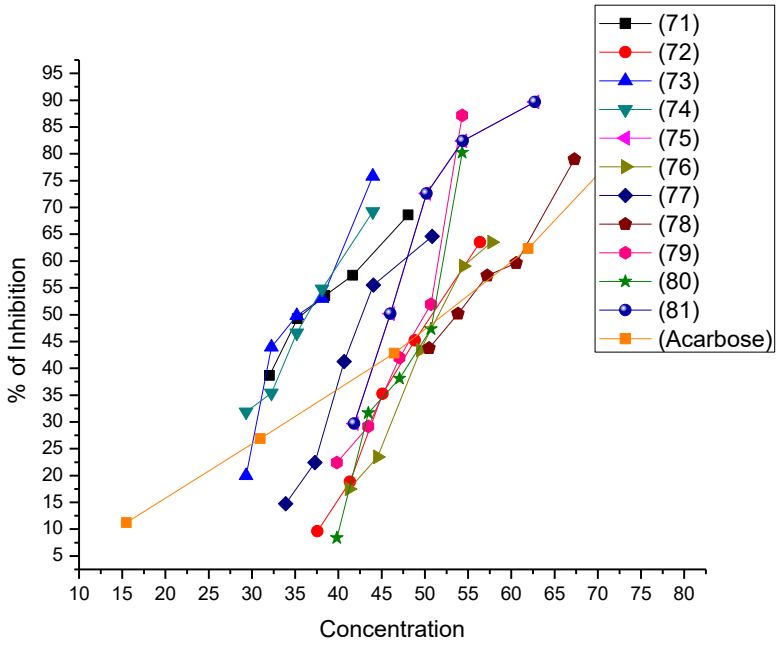

Figure 6b.6: α-Glucosidase inhibition activity of compounds

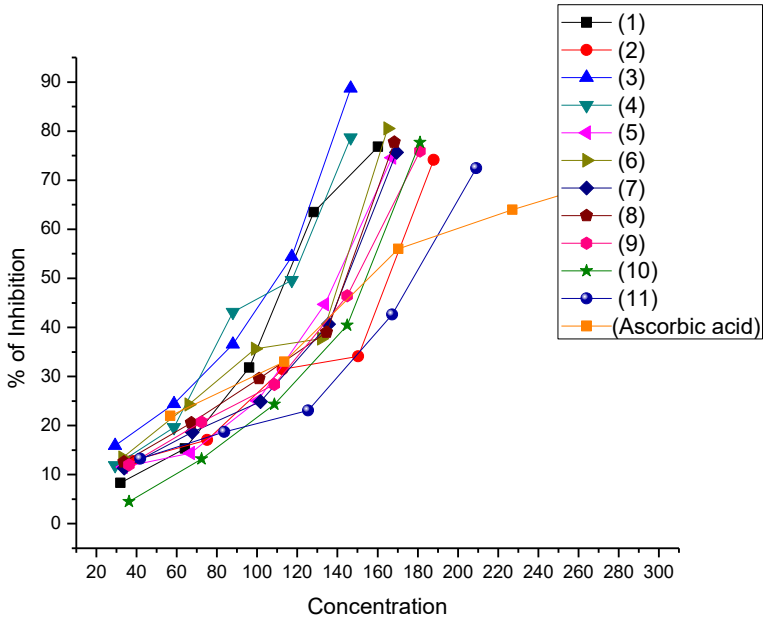

Figure 6b.7: Graph showing the % of inhibition of glycation by compounds

6b.6. Docking interaction studies of the compounds with 3A4A protein

The best conformers of the selected compounds **71**, **73**, **74**, **75**, **76** and **78** were generated by ligprep tool and used for pharmacokinetic analysis using QikProp. All of them with appreciable molecular range, especially **76** and **78** with few #stars shows the druggability of the compounds. The central nervous system toxicity (CNS) values well interpret the suitability of all the compounds with acceptable range of donor and acceptor atoms. The aqueous solubilty (QPlogS), hydrophobic component of total solvent accessible surface area (FISA) and human oral absorption percent (% HOA) predict the suitability of the selected ligands as drug with minimum deviation from Lipinski rule of five (Ro5). The interaction diagrams strongly support the suitable binding of these compounds inside the binding pocket of the protein 3A4A with lower scoring functions (D-score and G-score in kcal/mol). In **73** and **76**, the ethoxy-O forms H-bond with Ser240, while in **78** and **74**, carbonyl-O link with Ser240 and Lys156 respectively (Figure 6b.8). In **73**, there is an additional strong bond formed with Arg315, whereas in **76**, carbonyl-O forms H-bond with Hip280. As in the case of **71**, compound **75** also form a π–stacking interaction with the Hip280, but there is an additional H-bond formed between hydroxyl-H and Pro312 in **75**. All these interactions strongly favour the binding mode within the pocket of the target protein (Figure 4) and thus

we can confirm by molecular simulation approach, the druggability of these compounds as *α*-glucosidase inhibitor as proved by *in vitro* studies (Table 6b.3).

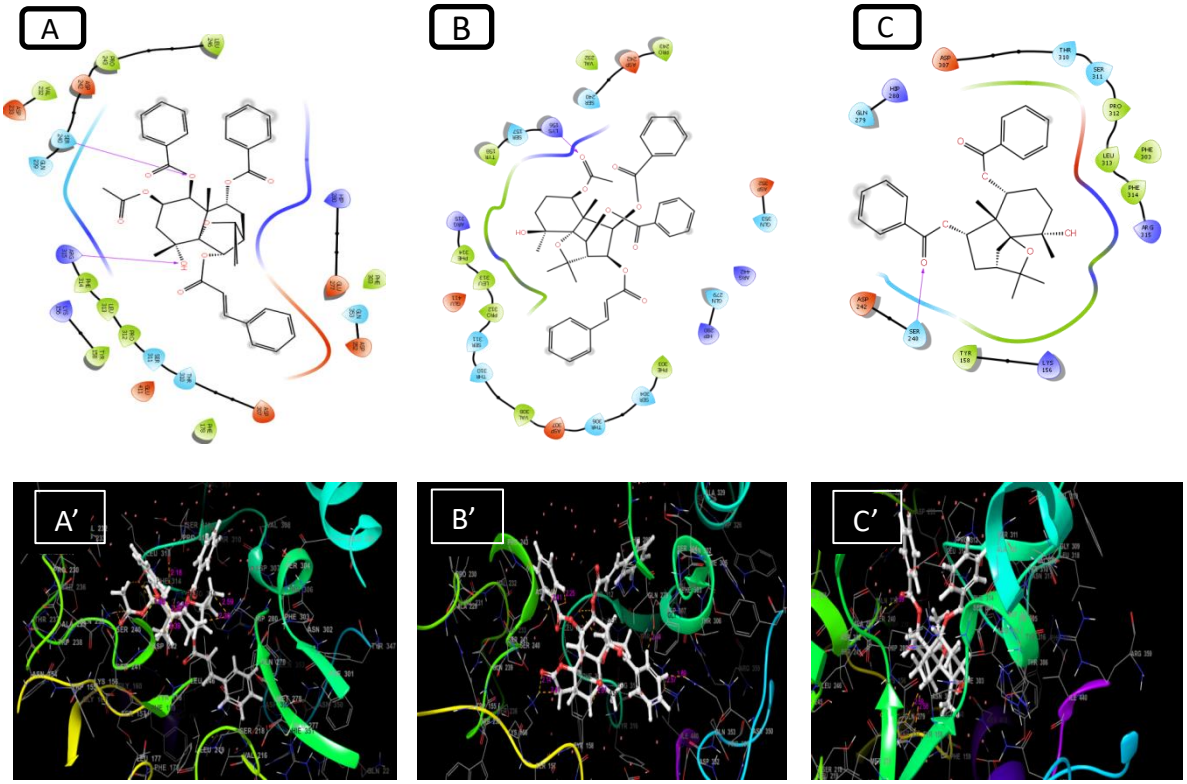

Figure 6b.8: Docking interaction studies of the compounds; (A, A‟), (B, B‟‟) and (C, C‟‟) 2D and 3D interaction diagram of compound **73**, **74** and **78** respectively with 3A4A protein.

Table 6b.3: Scoring values and selected pharmacokinetic parameters of the compounds

Compounds	D-Score	G-Score	MW	#stars	CNS	FISA	HBA	HBD	% HOA	Q PlogS	Ro5
71	-4.16	-4.16	624.729	5	-1	94.262	7.5	1	100	-8.424	2
73	-4.93	-4.93	682.766	6	-2	132.191	9.5	1	95.2	-8.54	2
74	-6.43	-6.43	682.766	6	-2	84.078	9.5	1	93.2	-8.976	2
75	-3.67	-3.67	598.691	4	0	158.954	7.5	1	100.0	-7.494	2
76	-2.83	-2.83	590.623	0	-2	77.365	11.5	1	70.5	-5.881	2
78	-5.01	-5.01	478.584	0	0	119.014	5.5	1	100.0	-6.118	1

M.W.(molecular weight):130.0 to 725.0; #stars (few stars-more drug-like): 0 to 5; CNS (central nervous system activity): -2 to +2; FISA (hydrophilic component of total solvent accessible area): 7.0 to 333.0; HBA (hydrogen bond acceptor): 2.0 to 20.0; HBD (hydrogen bond donor): 0.0 to 6.0; % HOA (percent human oral absorption): >80 % is high; QplogS

(aqueous solubility): -6.5 to 0.5; Ro5 (number of violations of Lipinski's rule of five): maximum is 4.

6b.7. Conclusion

In this chapter, we have demonstrated the Ca^{2+} channel NMDARs inhibitory activity of dihydro-*β*-agarofurans isolated from *C. paniculatus*. Among the tested compounds compound **78**, 1*α*, 9*β*-dibenzoyloxy-4*β*-hydroxydihydro-*β*-agarofuran showed 30 % inhibition in the NMDAR activity at 50 μM concentration. Whereas, compound **80**, 1*α*-acetoxy-6*β*, 9*β*-dibenzoyloxy-8*α*, 4*β*-dihydroxydihydro-*β*-agarofuran showed prominent NMDAR inhibition (75 %) at 50 μM concentration. In addition, we tested the antidiabetic potential of different extracts and isolated compounds of *Celastrus paniculatus*. All the isolated compounds showed a prominent *α*-glucosidase inhibitory activity. To the best of our knowledge, NMDAR and *α*-glucosidase inhibitory activity of dihydro-*β*-agarofuran are reported for the first time.

6b.8. Experimental session

6b.8.1. Cell culture

HEK-293 cells were maintained in a humidified cell culture incubator kept at 37 °C with 5 % CO_2 in DMEM containing 10 % FBS. After the cells attained around 80-90 % confluency in culture, cells were trypsinized using 0.05 % trypsin in PBS-EDTA solution. Trypsinized cells were seeded in 24-well culture plates for transfection.

6b.8.2. Preparation of GluN2B and GFP- α-CaMKII plasmids

The glycerol stocks of bacterial cells, containing the respective plasmids, were inoculated in Luria Bertani (LB) broth containing antibiotics (ampicillin in the case of GluN2B and kanamycin for GFP-α-CaMKII) and the bacterial cultures were incubated at 37^{o}C, overnight with rigorous shaking (~200 rpm). The bacterial cells in culture were pelleted by centrifugation at 4600 g for 15 min at 4^{o} C. The plasmids for mammalian expression were prepared using QIAGEN Midi Kit. The bacterial pellet was resuspended in 4 mL of resuspension buffer, P1, containing 50 mM Tris-Cl, pH 8.0, 10 mM EDTA and 100μg/mL RNase A for approximately 1 hour. To this solution, 4 mL of lysis buffer, P2, containing 200 mM NaOH with 1 % SDS was added, mixed thoroughly by inverting 4-6 times and incubated at room temperature for 5 mins. Next, 4 mL of neutralization buffer, P3,

containing 3.0 M potassium acetate, pH 5.0 was added, mixed gently by inverting 4-6 times, and incubated on ice for 15 minutes. After incubation, the solution was centrifuged at 20,800 g for 30 min at 4^{o}C. The supernatant containing the plasmid DNA was removed carefully and centrifuged at 20,800 g for 15 min at 4oC to get a clear solution of plasmid DNA. An anion exchange resin, DEAE coupled column (QIAGEN-tip-100), was equilibrated using 4 mL equilibration buffer QBT (750 mM NaCl, 50 mM MOPS, pH 7.0, 15 % isopropanol, 0.15 % Triton X-100) and the column was allowed to empty by gravity flow. The supernatant, obtained after centrifugation that contained the plasmid DNA, was allowed to flow through QIAGEN-tip by gravity flow. Following binding, QIAGEN-tip was washed with 2X 10 mL wash buffer QC (1.0 M NaCl, 50 mM MOPS, pH 7.0, 15 % isopropanol). The bound plasmid was eluted with 5 mL elution buffer QF (1.25 M NaCl, 50 mMTris-Cl, pH 8.5, 15 % isopropanol). The plasmid DNA, present in the elute, was precipitated using 3.5 mL isopropanol at room temperature. This solution was mixed and centrifuged at 20,800 g for 30 minutes at 4 ^{o}C. The supernatant was carefully decanted. The pellet was washed with 2 mL 70 % ethanol at room temperature at 20,800 g for 10 min. The pellet was air dried and dissolved in a suitable volume of water. The concentration of the plasmids was quantified using NanoDrop 2000 and its purity was checked on 1 % agarose gel.

6b.8.3. Transfection of plasmids into HEK-293 cells

To detect the activity of GluN2B containing NMDAR, HEK-293 cells were co-transfected with plasmids coding for GluN2B subunit of NMDAR and GFP-α-CaMKII. Co-transfection was carried out using lipofectamine (Invitrogen) according to manufacturer's protocol. For transfection, HEK-293 cells were seeded on sterile 12 mm coverslips placed in 24-well plates (~1.5 x 104 cells/well). After 18 hrs of seeding, the cells were co-transfected with the plasmids. The following solutions were prepared for transfection:

Solution A: For each transfected well, 0.15 µg of plasmid DNA for GFP-α-CaMKII and 0.35 µg each of plasmid DNA encoding subunits GluN1 and GluN2B were added to 62.5 µL Opti-MEM (Invitrogen) and were mixed well.

Solution B: For each transfected well, 2 µL lipofectamine reagent was added to 62.5 µL Opti-MEM and mixed well.

Solution A was added to Solution B, mixed gently by pipetting and incubated at room temperature for 45 minutes. After incubation, 125 µL Opti-MEM was added to the tube

containing lipid-DNA complexes. The media in each well was replaced with 250 µL of prepared solution. Cells were incubated for 5 hours at 37^{o}C in a CO_2 incubator. After 5 hours, 250 µL of Opti-MEM medium containing 20 % FBS and 20 µM MK-801 was added to stop transfection. The addition of MK-801, an NMDAR antagonist, can prevent cell death in transfected cells due to activation of NMDAR. The transfection solution was aspirated after 12 hours and 500 µL of fresh DMEM containing 10 % FBS and 20 µM MK-801 was added. The cells were further incubated at 37 ^{o}C for 24 hours.

6b.8.4. NMDAR activity dependent translocation of GFP-α-CaMKII to GluN2B

About 24 hours after transfection, cells were washed twice, first with Hank's balanced salt solution (HBSS) containing 1mM HEPES and 0.5 mM EGTA (Solution I) and then with HBSS containing 1 mM HEPES (Solution II). NMDAR was activated with its agonists, glutamate (100 µM) and glycine (10 µM), along with Ca^{2+} (2 mM) (Solution III). After 5 minutes of activation, cells were fixed with 4 % paraformaldehyde for 10-15 minutes and were washed thrice with PBS. The cover slips containing cells were mounted on a clean glass slide using glycerol:PBS (1:1) and were observed using fluorescence microscope.

6b.8.5. Antidiabetic studies

General experimental details and procedure for enzymatic antidiabetic activity studies are given in Chapter 2.

6b.8.6. Molecular docking studies

The crystal structure of isomaltase from *Saccharomyces cerevisiae* (PDB code: 3A4A) was retrieved from RCSB Protein Data Bank (PDB). It consists of a polypeptide chain with 589 amino acids and the resolution of its structure is 1.6 Å. The target was prepared for docking by Protein Preparation Wizard of Schrodinger suite 2017-2 [Sastry *et al*., **2013**] and the binding site was generated by grid preparation around the centroid of the workspace [Halgren **2007**] The prepared enzyme with three dimensional grid was used for docking against the different conformers of the ligands generated by ligprep tool, using Glide docking of Schrodinger suite [Friesner *et al*., **2004**; Halgren *et al*., **2004**]. The binding affinity was predicted and ranked based on Dock score (D-score) and Glide score (G-score) values. The adsorption, distribution, metabolism and excretion/toxicity (ADME/T) parameters for the ligands were predicted based on QikProp values (Schrödinger Release 2017-3).

Summary and Conclusion

The thesis entitled ***"Phytochemical and Biological Evaluation of Some Selected Plants from Vitaceae, Dipterocarpaceae, Moraceae and Celastraceae Family"*** embodies the results of the detailed phytochemical investigation and bioactivity studies of six medicinal plants *viz*., *Ampelocissus indica* (Vitaceae family), *Vateria indica*, *Hopea ponga* (Dipterocarpaceae family), *Artocarpus camansi, Artocarpus lakoocha* (Moraceae family) and *Celastrus paniculatus* (Celastraceae family). Moreover, nearly all the isolated molecules were subjected to biological evaluation with focus on the targets of type II diabetes mellitus, a life threatening disease.

Chapter 1 of the thesis gives a brief introduction about the importance of natural products in modern drug discovery process. The important natural products/natural product derived molecules, from various sources, which are now in clinical use for the treatment of different diseases are highlighted in this chapter. A detailed description of plant-derived compounds giving special emphasis to plant-derived antidiabetic agents is also included in this chapter.

Chapter 2 of the thesis deals with the detailed phytochemical investigation on the rare species *Ampelocissus indica*, belonging to Vitaceae family. Literature review on Vitaceae and biosynthesis of resveratrol are given in the introductory part of this chapter. Eight compounds were isolated from the rhizome of *A. indica*, *viz*., E-resveratrol (**1**), (+)-ε-viniferin (**2**), (+)-pauciflorol A (**3**), (+)-hopeaphenol (**4**), *β*-sitosterol-3-O-*β*-D-glucopyranoside (**5**), *β*-sitosterol (**6**), stigmasterol (**7**) and ethyl ferulate (**8**). Similarly, *A. indica* fruits were subjected to phytochemical investigations. Six compounds *viz*., lupeol (**9**), oleanolic acid (**10**), ursolic acid (**11**), gallic acid (**12**), 3,3'-di-O-methylellagic acid (**13**) and ellagic acid (**14**) were isolated. To the best of our knowledge, chemical constituents from *A. indica* were reported for the first time.

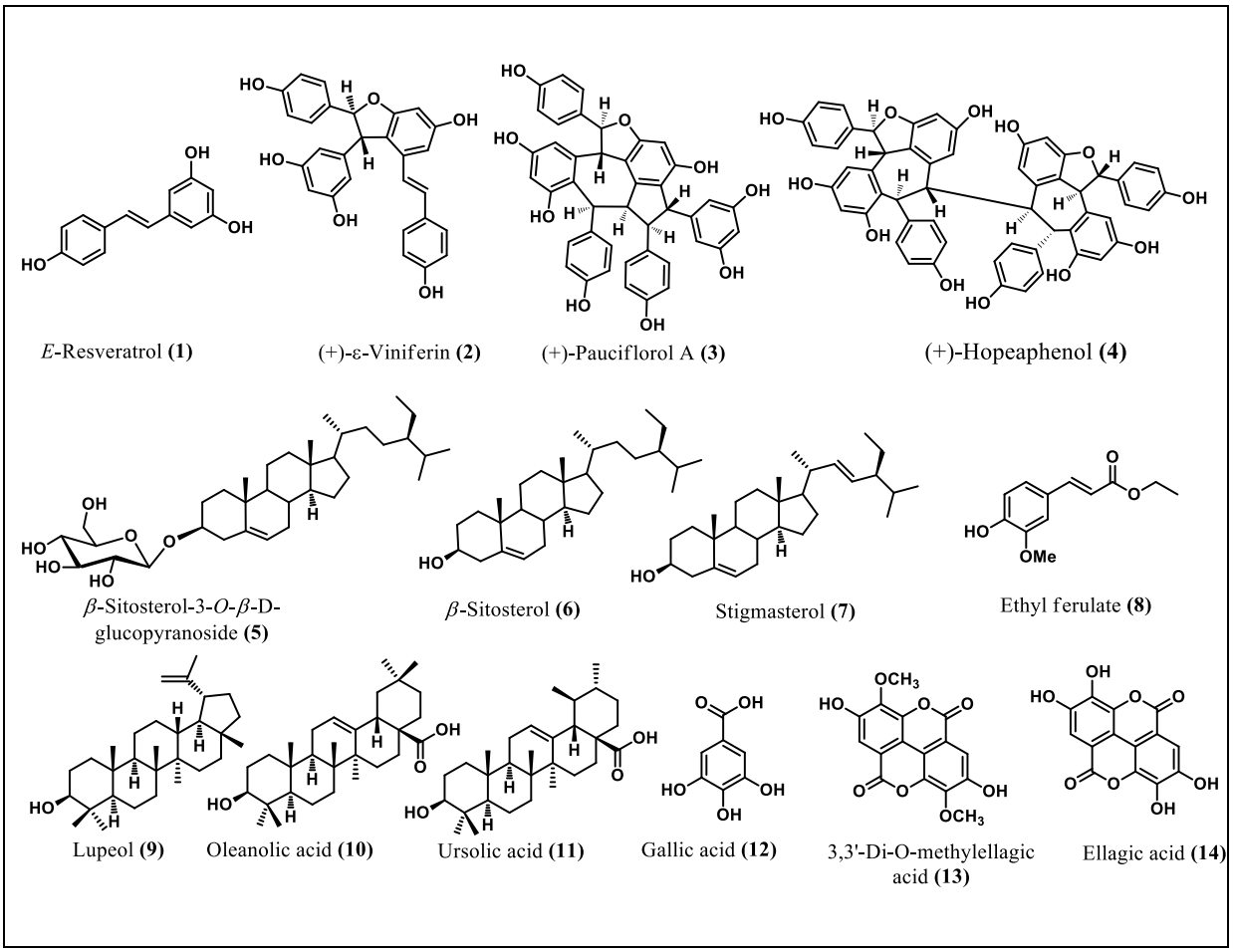

Figure 1: Structure of isolated compounds from *A. indica*

The Chapter 3 is divided into two parts. The first part (3A) deals with the isolation and structural elucidation of phytochemicals from the stem bark and seeds of *Vateria indica* (belonging to Dipterocarpaceae family). Here, a brief outline of the genus *Vateria* is given along with the detailed survey of literature on the phytochemistry of *V. indica* is described. Eight compounds have been isolated from the stem bark of *V. indica viz*., *β*-amyrin (**15**), *β*-amyrin acetate (**16**), sitoindoside I (**17**), *E*-resveratrol (**18**), (-)-ε-viniferin (**19**), (-)-hopeaphenol (**20**), vaticaphenol A (2**1**) and bergenin (**22**). Similarly, *V. indica* seeds were subjected to phytochemical investigations. Four major compounds along with fatty acids *viz*., (-)-ε-viniferin, (-)-hopeaphenol, vaticaphenol A and bergenin in high yield were isolated. In addition, the essential chemical constituents from the fatty acids were identified by GCMS analysis by matching mass spectra with spectra of reference compounds in mass spectral library of NIST and WILEY. The major fatty acids present were Palmitic acid (**27**), Linoleic

acid (**28**), Oleic acid (**29**), Stearic acid (**30**), Arachidic acid (**31**), Heneicosanoate acid (**32**). From best of our knowledge, *β*-amyrin, *β*-amyrin acetate and sitoindoside I from *V. indica* stem bark were reported for the first time. This is the first report of resveratrol oligomers from the seeds of *V. indica*.

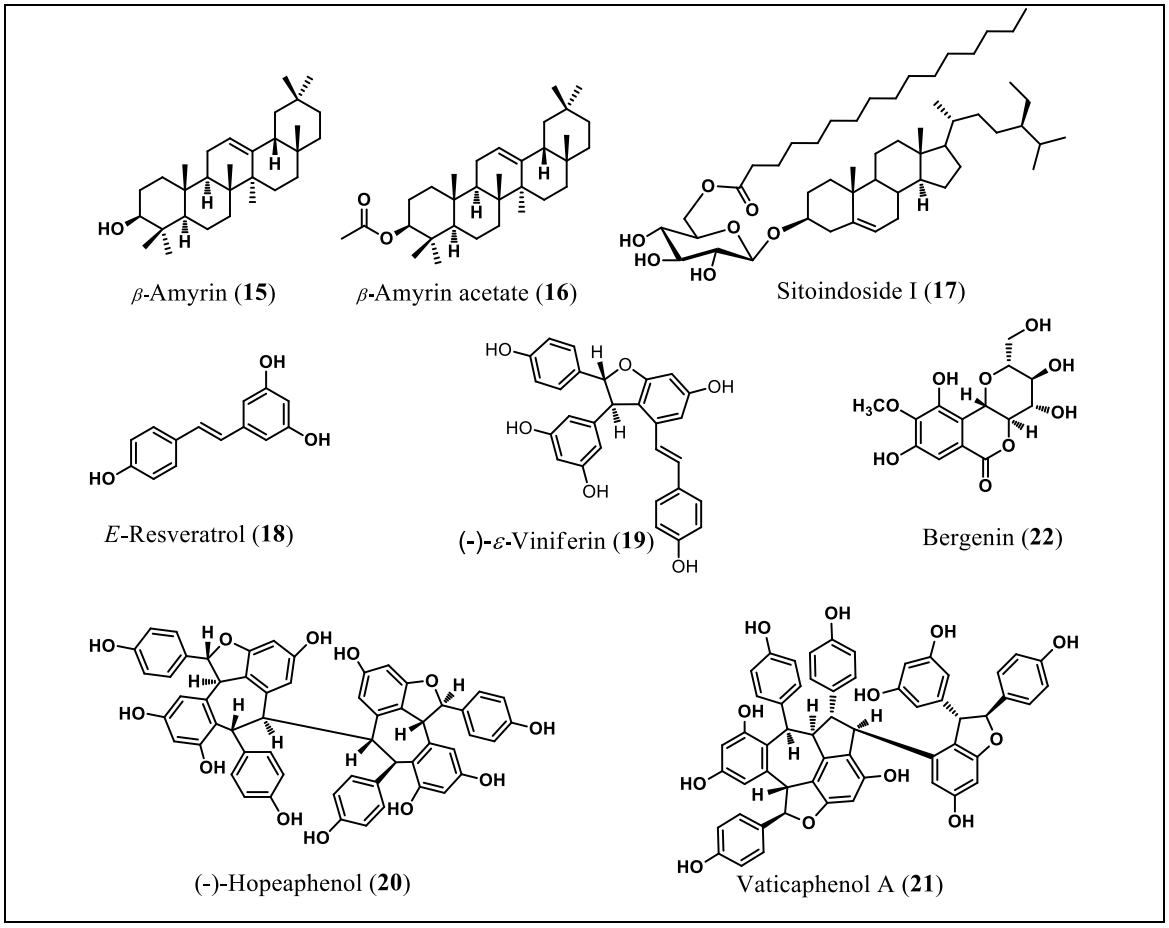

Figure 2: Structure of isolated compounds from *V. indica*

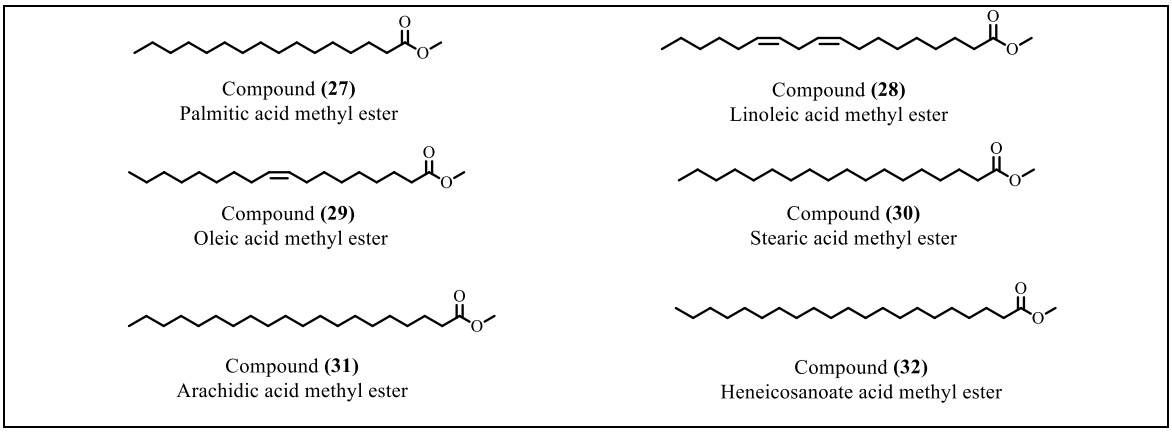

Figure 3: Structure of fatty acids from *V. indica* seeds

The second part (3B) deals with structural and antidiabetic comparison of (+) and (-)-hopeaphenols. *In vitro* results suggest that the compounds exert its antidiabetic effects through digestive enzyme inhibition and increased glucose uptake by the L6 muscle cells. These multiple modes of action increase the interest in the use of (+) and (-)-hopeaphenol as a therapeutic intervention for diabetes. In order to find out how these two molecules interact with the target proteins, molecular docking studies were carried out. The results demonstrated that both compounds effectively bind to the target proteins. To the best of our knowledge, exciting antidibetic activity of (+) and (-)-hopeaphenol are reported for the first time.

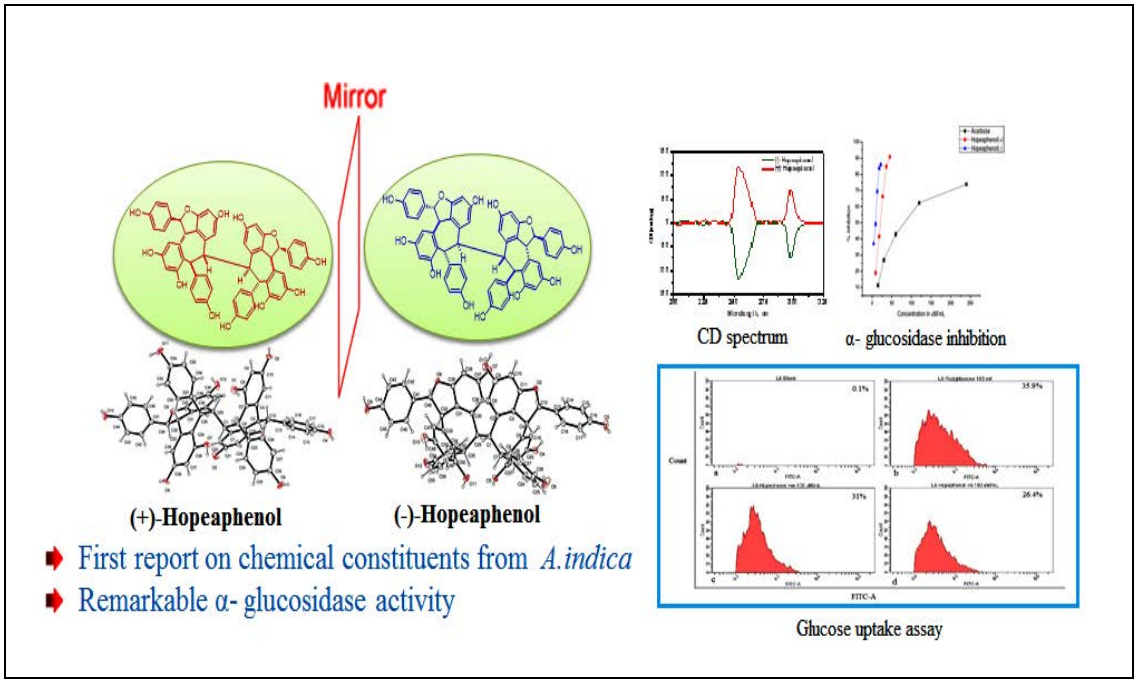

Figure 4: Structural comparison and antidibetic activity of (+) and (-)-hopeaphenol

Chapter 4 deals with the phytochemical and antidiabetic investigation of the medicinal plant *Hopea ponga*. *H. ponga* belonging to the family Dipterocarpaceae is used in several Ayurvedic preparations. Here, a brief outline of the genus *Hopea* is portrayed along with a detailed literature survey. Phytochemical investigation of the stem bark of *H. ponga* led to the identification of ten compounds *viz*., *β*-sitosterol, tetracosyl ferulate (**33**), *E*-resveratrol (**34**), (-)-*ε*-viniferin (**35**), (-)-*α*-viniferin (**36**), sitoindoside I (**37**), (-)-hopeaphenol (**38**), vaticaphenol A (**39**), *β*-sitosterol-3-*O*-*β*-D-glucopyranoside (**40**), and THPG (**41**). To the best

of our knowledge, chemical constituents from *H. ponga* and their antidiabetic activity are reported for the first time. In particular, (-)-*α*-viniferin, showed a prominent *α*-glucosidase, *α*-amylase and glycation inhibitory activities. Molecular docking studies demonstrate that the resveratrol oligomers bind effectively with the target proteins. It is also interesting to observe that both *α*-viniferin, vaticaphenol A and THPG, signifcantly increased glucose uptake in L6 cells. In addition, we have identified 13 major compounds (**42-54**) including sesquiterpenes and fatty acids from the seeds of *H. ponga*.

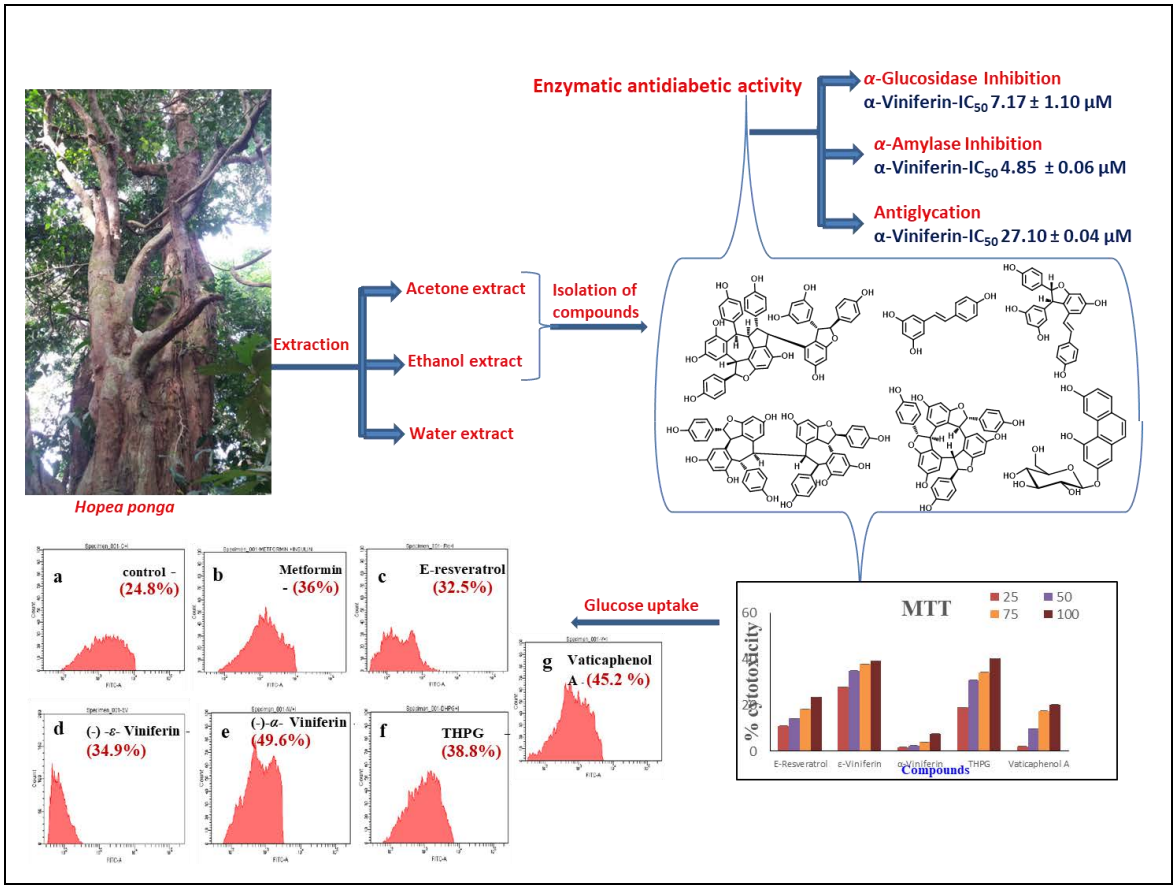

Figure 5: Structure of isolated compounds from *H. ponga* and their antidibetic activity

Chapter 5 explains the isolation of phytochemicals from the species *Artocarpus camansi and Artocarpus lakoocha* (Family: Moraceae) and evaluation of its antidiabetic potentials. In this chapter, we have successfully isolated and characterized 12 compounds from the stem bark of *A. camansi viz*., cycloartenol acetate (**55**), cycloartenol (**56**), *β*-amyrin acetate (**57**), betulinic acid (**58**), E-resveratrol (**59**), artocarpesin (**60**), artonin A (**61**),

artobiloxanthone (**62**), cycloartobiloxanthone (**63**), artoindonesianin A-3 (**64**), artonol B (**65**) and oxyresveratrol (**66**) and 4 compounds from the stem bark of *A. lakoocha viz*., morcin S (**68**) and 4-prenyl oxyresveratrol (**70**) including *E*-resveratrol and oxyresveratrol. Oxyresveratrol was also isolated in good yield from the heartwood of *A. lakoocha.* To the best of our knowledge, all the chemical constituents except triterpenoids from *A. camansi* and their antidiabetic activity are reported for the first time. In particular, *E*-resveratrol, oxyresveratrol, artobiloxanthone and artonol B, signifcantly increased glucose uptake in L6 cells.

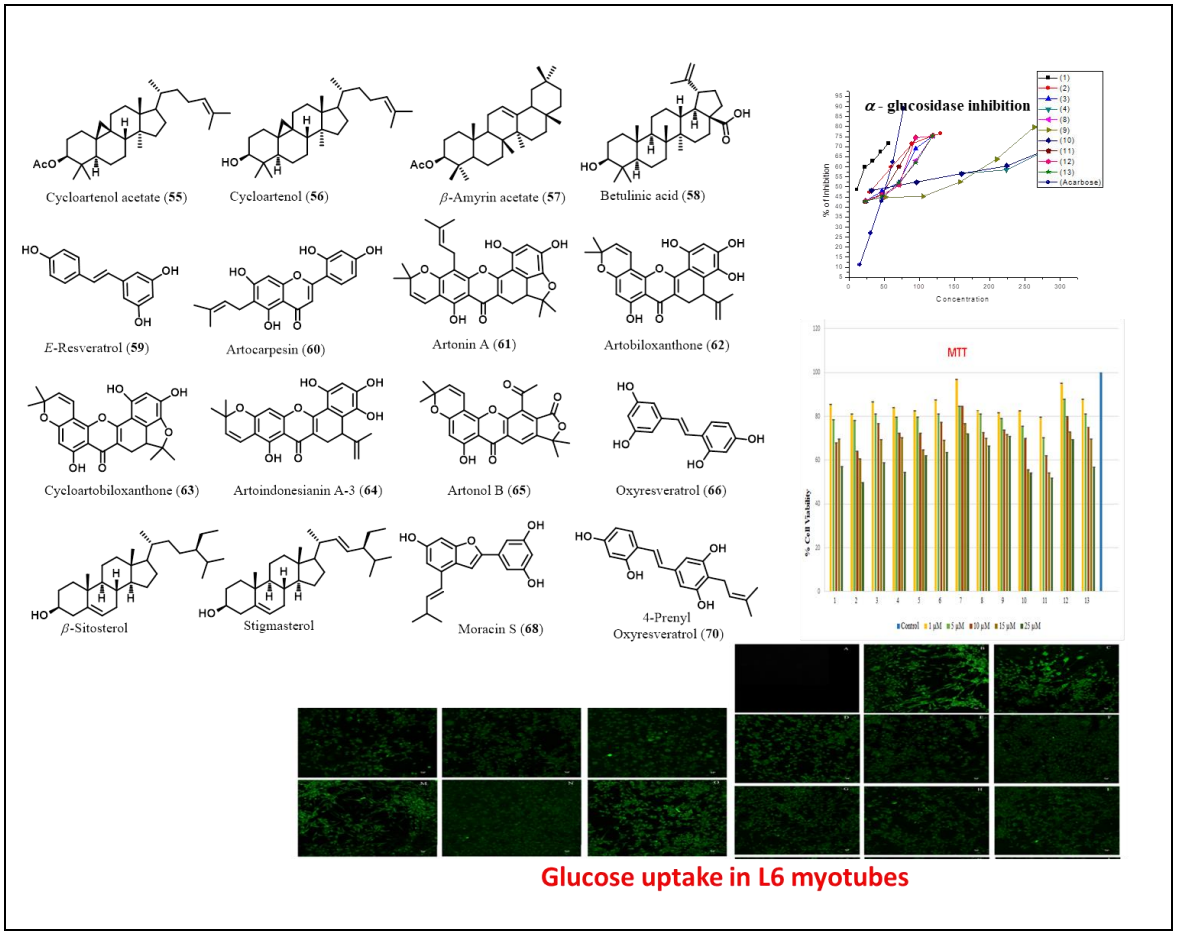

Figure 6: Structure of isolated compounds from *A. camansi* and *A. lakoocha* and their antidibetic activity

First part of chapter 6 deals with the phytochemical investigation of the seeds of *Celastrus paniculatus* (Celastraceae) leading to the identification of 11 compounds including

three novel compounds *viz*., 1α, 9β-dibenzoyloxy-6β-cinnamoyloxy-4β-hydroxydihydro-β-agarofuran (**71**), 1α,8β,15α-triacetoxy-9α-benzoyloxy-4β-hydroxydihydro-β-agarofuran (**72**) and 1α,9β-dibenzoyloxy-2β-acetoxy-6β-cinnamoyloxy-4β-hydroxyldihydro-β-agarofuran (**73**), all the isolated compounds were structurally characterized by 1D and 2D NMR spectroscopy and their stereochemistry were confirmed by single crystal X-ray studies.

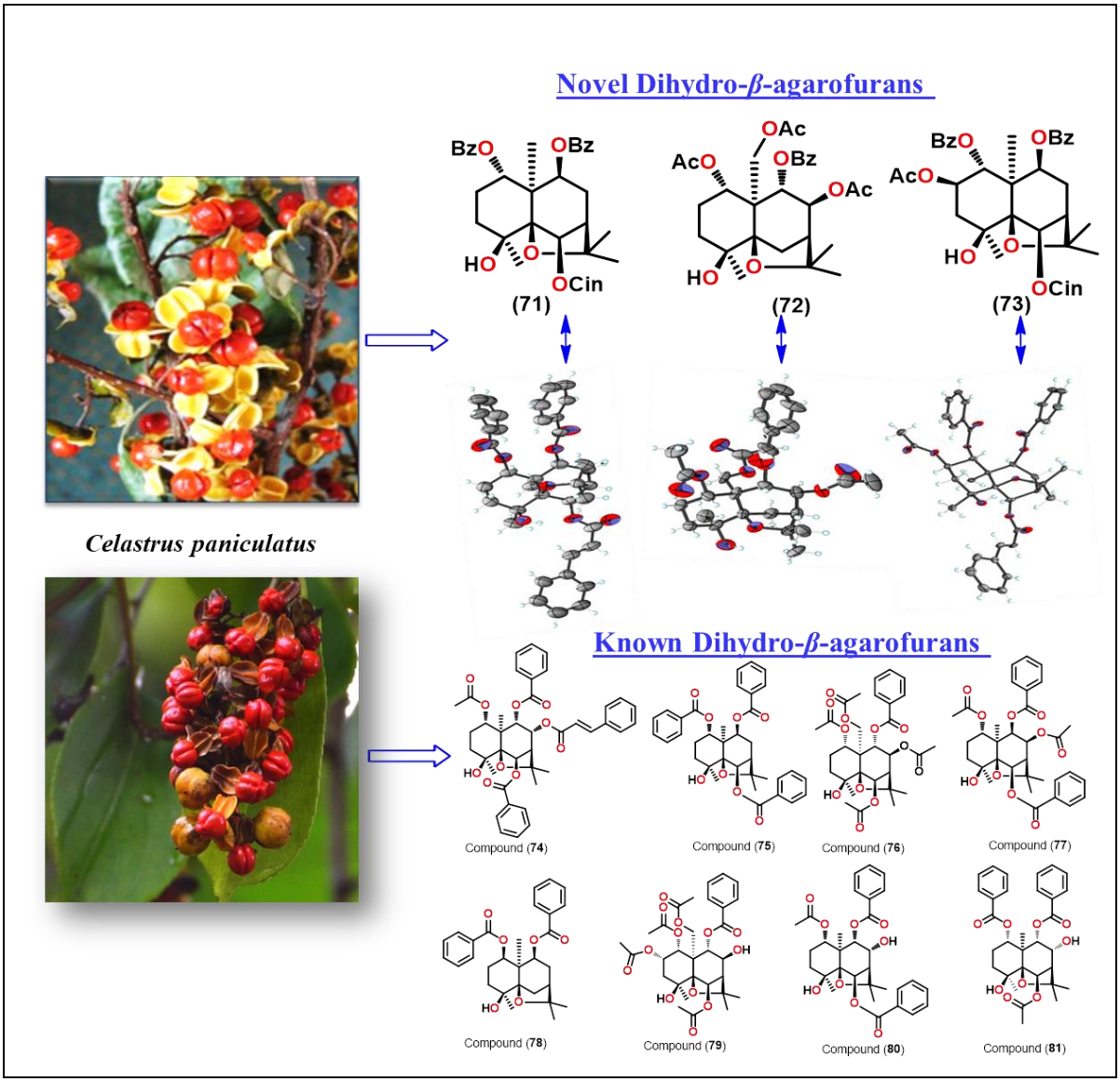

Figure 7: Structure of isolated compounds from *C. paniculatus*

Second part of chapter 6 deals with the Ca^{2+} channel NMDARs inhibitory activity of dihydro-*β*-agarofurans isolated from *C. paniculatus*. Among the tested compounds compounds **78** and **80** showed 30 and 75 % inhibition in the NMDAR activity at 50 µM concentrations respectively. In addition, we discussed the antidiabetic potential of different extracts and isolated compounds of *Celastrus paniculatus*. All the isolated compounds showed a prominent *α*-glucosidase inhibitory activity. To the best of our knowledge, NMDAR and *α*-glucosidase inhibitory activity of dihydro-*β*-agarofuran were reported for the first time.

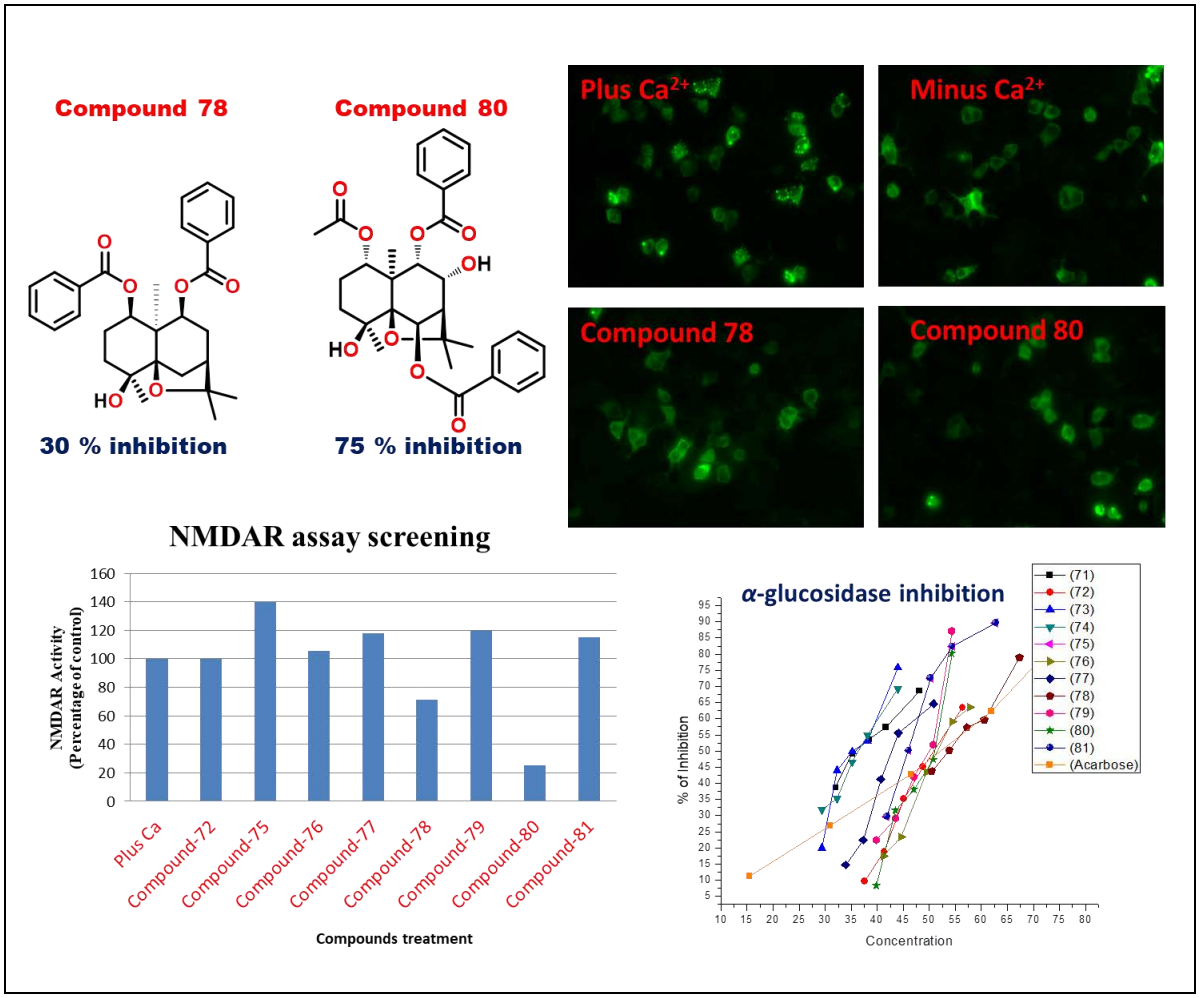

Figure 8: NMDAR and *α*-glucosidase inhibitory activity of dihydro-*β*-agarofuran

Bibliography and References

Adisakwattana, S., Lerdsuwankij, O. "Inhibitory activity of cinnamon bark species and their combination effect with acarbose against intestinal *α*-glucosidase and pancreatic *α*-amylase". *Plant Foods Hum Nutr.*, **2011**, *66*, 143–148.

Ahamad, F., Khan, R. A., Rasheed, S. "Preliminary screening of methanolic extracts of *Celastrus paniculatus* and *Tecomella undulata* for analgesic and anti-inflammatory activities". *J. Ethnopharmacol.,* **1994,** *42*, 193-198.

Aida, M., Yamaguchi, N., Hano, Y., Nomura, T. "Artonols A, B, C, D, and E, five new isoprenylated phenols from the bark *of Artocarpus communis* Forst". *Heterocycles*, **1997**, *45*, 163–175.

Aisha, F., Din, L. B., Yaacob, W. A. "Resveratrol tetramer of hopeaphenol isolated from *Shorea johorensis* (Dipterocarpaceae)". *AIP Conference Proceedings,* **2014**, *1614,* 302-308.

Ajish, K. R., Antu, K. A., Riya, M. P., Preetharani, M. R., Raghu, K. G., Dhanya, B. P., Radhakrishnan, K. V. "Studies on α-glucosidase, aldose reductase and glycation inhibitory properties of sesquiterpenes and flavonoids of *Zingiber zerumbet* Smith". *Natural Product Research,* **2015***, 29*, 947–952.

Akiyama, T., Ishida, J., Nakagawa, S., Ogawara, H., Watanabe, S., Itoh, N., Shibuya, M., Fukami, Y. "Genistein, a specific inhibitor of tyrosine-specific protein kinases". *J. Biol. Chem.,* **1987**, *262*, 5592– 5595.

Alberti, K. G., Zimmet, P. F. "Definition, diagnosis, and classification of diabetes mellitus and its complications. Part 1: diagnosis and classification of diabetes mellitus. Provisional report of a WHO consultation". *Diabetic medicine*, **1998**, *15*, 539-553.

Altman, L. J., Zito, W. Sterols and Triterpenes from the Fruit of *Artocarpus Altilis Phytochemistry*, **1976**, 15, 830-831.

Altmann, K. H., Gertsch, J. "Anticancer drugs from nature-natural products as a unique source of new microtubule-stabilizing agents". *Nat. Prod. Rep.,* **2007**, *24*, 327–357.

Alexander, H., Rolf, H., Chapter 5. ISBN, 3-7643-6081-X, Birkhauser Verlag, Basel- Boston Berlin, **2003**.

American Diabetes Association. "Diagnosis and classification of diabetes mellitus". Diabetes care. **2010,** *33*, S62-69.

Annabi, B., Lord-Dufour, S., Vézina, A., Béliveau, R. "Resveratrol targeting of carcinogen-induced brain endothelial cell inflammation biomarkers MMP-9 and COX-2 is sirt1-independent". *Drug Target Insights,* **2012**, *6*, 1–11.

Atun, S., Aznam, N., Arianingrum, R., Takaya, Y., Masatake, N. "Resveratrol derivatives from stem bark of *Hopea* and their biological activity test". *Journal of Physical Science,* **2008**, *19*, 7–21.

Baderschneider, B., Winterhalter, P. "Isolation and characterization of novel stilbene derivatives from Riesling wine". *Journal of Agricultural and Food Chemistry*, **2000**, *48*, 2681–2686.

Bai, Y., Mao, Q., Qin, J., Zheng, X., Wang, Y., Yang, K., Shen, H., Xie, L. "Resveratrol induces apoptosis and cell cycle arrest of human T24 bladder cancer cells in vitro and inhibits tumor growth in vivo". *Cancer Sci*., **2010**, *101*, 1–6.

Bailey, C.J., Turner, S.L. "Glucosamine-induced insulin resistance in L6 muscle cells". *Diabetes, Obesity and Metabolism,* **2004**, *6*, 293–298.

Balbach, A., Boarim, D. S. F. "As frutas na medicina natural. Editora Missionaria, Sao Paulo, **1992**.

Barik, B. R., Bhaumik, T., Dey, A. K., Kundu, A. B. Triterpenoids from *Artocarpus Heterophyllus*". *Phytochemistry*, **1994**, *35*, 1001-1004.

Bhattacharya, S., Sil, P. C. "Role of Plant-Derived Polyphenols in Reducing Oxidative Stress- Mediated Diabetic Complications". *Reactive Oxygen Species,* **2018**, *5*, 15–34.

Bisoli, E., Garcez, W.S., Hamerski, L., Tieppo, C. "Bioactive Pentacyclic Triterpenes from the Stems of *Combretum laxum*". *Molecules*, **2008**, *13*, 2717-2728.

Bomser, J., Singletary, K., Wallig, M. A., Smith, M. A. L. "Inhibition of TPA-induced tumor promotion in CD-1 mouse epidermis by a polyphenolic fraction from grape seeds". *Cancer Lett.,* **1999**, *135*, 151–157.

Boonphong, S., Baramee, A., Kittakoop, P., Puangsombat, P. "Antitubercular and Antiplasmodial Prenylated Flavones from the Roots of *Artocarpus altilis*". *Chiang Mai J. Sci.*, **2007**, *34*, 339–344.

Brand-Williams, W., Cuvelier, M. E., Berset, C. "Use of a Free Radical Method to Evaluate Antioxidant Activity". *LWT-Food Science and Technology,* **1995**, *30*, 25–30.

Bringmann, G., Saeb, W., Assi, L.A., Francois, G., Narayanan, A.S.S., Peters, K. "Betulinic Acid: Isolation from Triphyophyllum peltatum and Ancistrocladus heyneanus, Antimalarial Activity, and Crystal Structure of the Benzyl Ester". *Planta Medica,* **1997**, *63*, 255–257.

Buiarelli, F., Coccioli, F., Jasionowska, R., Merolle, M., Terracciano, A. "Analysis of some stilbenes in Italian wines by liquid chromatography/tandem mass spectrometry". *Rapid Commun. Mass Spectrom.,* **2007**, *21*, 2955–2964

Butler, M. S. "Natural products to drugs : natural product-derived compounds in clinical trials". *Nat. Prod. Rep*., **2008**, *25*, 475–516

Butler, M. S., "The Role of Natural Product Chemistry in Drug Discovery". *J. Nat. Prod.,* **2004**, *67*, 2141-2153.

Butler, M. S., Cooper, M. A. "Antibiotics in the clinical pipeline in 2011". *The Journal of Antibiotics*, **2011**, 64, 413–425.

Carroll, A. R., Davis, R. A., Addepalli, R., Fechner, G. A., Guymer, G. P., Forster, P. I., Quinn, R. J. "Cytotoxic agarofurans from the seeds of the Australian rainforest vine *Celastrus subspicata*". *Phytochemistry Letters,* **2009**, *2*, 163–165.

Chang, F. R., Hayashi, K., Chen, I. H., Liaw, C. C., Bastow, K. F., Nakanishi, Y., Nozaki, H., Cragg, G. M., Wu, Y. C., Lee, K. H. "Antitumor agents. 228. Five new agarofurans, reissantins A−E, and cytotoxic principles from *Reissantia buchananii"*. *J. Nat. Prod.,* **2003**, *66*, 1416-1420.

Charoenlarp, P., Radomyos, P., Harinasuta, T. "Treatment of taeniasis with Puag-Haad: a crude extract of Artocarpus lakoocha wood". *The Southeast Asian Journal of Tropical Medicine and Public Health*, **1981**, *12*, 568–570.

Chavez, H., Callo, N., Estevez-Braun, A., Ravelo, A.G., Gonzalez, A. G. "Sesquiterpene Polyol Esters from the Leaves of Maytenus macrocarpa". *J. Nat. Prod*., **1999**, *62*, 1576-1577.

Chen, Q. C., Zhang, W. Y., Jin, W., Lee, I. S., Min, B., Jung, H., Na, M., Bae, K. "Flavonoids and Isoflavonoids from Sophorae Flos Improve Glucose Uptake in vitro". Planta Med., **2010**, *76*, 79–81

Chin, Y., Balunas, M. J., Chai, H. B., Kinghorn, A. D. "Drug Discovery From Natural Sources". The AAPS Journal, **2006**, *8*, 239–253.

Chou, T. H., Chen, I. S., Sung, P. J., Peng, C. H., Shieh, P. C., Chen, J. J. "A New Dihydroagarofuranoid Sesquiterpene from Microtropis fokienensis with Antituberculosis Activity". *CHEMISTRY & BIODIVERSITY*, **2007**, *4*, 1594–1600.

Chung, M. I., Lu, C. M., Huang, P. L., Lin, C. N. "Prenylflavonoids of *Artocarpus heterophyllus*". *Phytochemistry*, **1995**, *40*, 1279-1282.

Chunquan, C., Dagang, W., Jikai, L. "Angulatueoids A-D, four Sesquiterpenes from the Seeds of *Celastrus angulatus*". *Phytochemistry*, **1992**, *31*, 2777-2780.

Coggon, P., Janes, N. F., King, F. E., King, T. J., Molyneux, R. J., Morgan, J. W. W., Sellars, K., Hopeaphenol, an Extractive of the Heartwood of *Hopea odorata* and *Balanocarpus* heimii. *J. Chem. Soc.,* **1965**, *61*, 406–409.

Coggon, P., King, T. J., Wallwork, S.C. "The Structure of Hopeaphenol". *Chem. Commun.*, **1966**, 439–440.

Coward, L., Barnes, N. C., Setchel, K. D. R., Barnes, S. "Genistein, Daidzein , and Their & Glycoside Conjugates : Antitumor Isoflavones in Soybean Foods from American and Asian Diets". *J. Agric. Food Chem.*, **1993**, *41*, 1961-1967.

Cragg, G. M., Newman, D. J. "Plants as a source of anti-cancer agents". *J. Ethnopharmacol*., **2005**, *100*, 72–79.

Dahanukar, N., Raut, R., Bhat, A. "Distribution, endemism and threat status of freshwater fishes in the Western Ghats of India". *J. Biogeogr.***, 2004**, *31,* 123–136.

Dai, J. R., Hallock, Y. F., Cardellina, J. H., Boyd, M. R. "HIV-inhibitory and cytotoxic oligostilbenes from the leaves of *Hopea malibato*". *J. Nat. Prod.,* **1998**, *61*, 351–353.

Das, M. S., Devi, G. "In vitro cytotoxicity and glucose uptake activity of fruits of *Terminalia bellirica* in Vero, L-6 and 3T3 cell lines". *Journal of Applied Pharmaceutical Science*, **2015**, *5*, 92–95.

Davis, R. A., Beattie, K. D., Xu, M., Yang, X., Yin, S., Holla, H., Healy, P. C., Sykes, M., Shelper, T., Avery, V. M., Elofsson, M., Sundin, C., Quinn, R. J. "Solving the Supply of

Resveratrol Tetramers from Papua New Guinean Rainforest Anisoptera Species That Inhibit Bacterial Type III Secretion Systems". *J. Nat. Prod.,* **2014**, *77,* 2633-2640.

De-Eknamkul, W., Potduang, B. "Biosynthesis of *β*-sitosterol and stigmasterol *in Croton sublyratus* proceeds via a mixed origin of isoprene units". *Phytochemistry*, **2003**, *62*, 389–398.

DeFronzo, R. A., Ferrannini, E., Groop, L., Henry, R. R., Herman, W. H., Holst, J. J., Hu, F. B., Kahn, C. R., Raz, I., Shulman, G. I., Simonson, D. C., Testa, M. A., Weiss, R. "Type 2 diabetes mellitus". *Nature Reviews,* Disease Primers, **2015**, *1*, 1–23.

Dhanya, R., Arun, K. B., Syama, H. P., Nisha, P., Sundaresan, A., Santhosh Kumar, T. R., Jayamurthy, P. "Rutin and quercetin enhance glucose uptake in L6 myotubes under oxidative stress induced by tertiary butyl hydrogen peroxide". *Food Chemistry,* **2014**, *158*, 546–554.

Efferth, T., Fu, Y. J., Zu, Y. G., Schwarz, G., Konkimalla, V. S., Wink, M. (2007). "Molecular target-guided tumor therapy with natural products derived from traditional Chinese medicine". *Current medicinal chemistry,* **2007**, *14* , 2024–2032.

Ehrenkranz, J. R. L., Lewis, N.G., Kahn, C. R., Roth, J. "Phlorizin : a review". *Diabetes Metab. Res. Rev.,* **2005**, *21*, 31–38.

Empl, M.T., Macke, S., Winterhalter, P., Puff, C., Lapp, S., Stoica, G., Baumg, W., Steinberg, P. "The growth of the canine glioblastoma cell line D-GBM and the canine histiocytic sarcoma cell line DH82 is inhibited by the resveratrol oligomers hopeaphenol and r2-viniferin". *Veterinary and Comparative Oncology*, **2012**, *12*, 149–159.

Evans, J. L., Goldfine, I. D., Maddux, B. A., Grodsky, G. M. "Pathways : A Unifying Hypothesis of Type 2 Diabetes". *Endocrine Reviews*, **2002**, *23*, 599–622.

Fotie, J., Bohle, D. S., Leimanis, M. L., Georges, E., Rukunga, G., Nkengfack, A. E. "Lupeol Long-Chain Fatty Acid Esters with Antimalarial Activity from *Holarrhena floribunda". J. Nat. Prod.,* **2006***, 69,* 62-67.

Friesner, R. A., Banks, J. L., Murphy, R. B., Halgren, T. A., Klicic, J. J., Mainz, D. T., Repasky, M. P., Knoll, E. H., Shelley, M., Perry, J. K., Shaw, D. E., Francis, P., Shenkin, P. S. "Glide : A New Approach for Rapid , Accurate Docking and Scoring . 1 . Method and Assessment of Docking Accuracy". *J. Med. Chem.,* **2004**, *47*, 1739-1749.

Ganesan, A. "The impact of natural products upon modern drug discovery". *Curr. Opin. Chem. Biol.,* **2008**, *12*, 306.

Gao, J. M., Wu, W. J., Zhang, J. W., Konishi, Y. "The dihydro-β-agarofuran sesquiterpenoids". *Nat. Prod. Rep.,* **2007***, 24,* 1153–1189.

Ge, H. M., Yang, W. H., Shen, Y., Jiang, N., Guo, Z. K., Luo, Q., Xu, Q., Tan, R. X. "Immunosuppressive Resveratrol Aneuploids from *Hopea chinensis". Chem. Eur. J.,* **2010**, *16*, 6338 – 6345.

Godkar, P. B., Gordon, R. K., Ravindran, A., Doctor, B. P. "*Celastrus paniculatus* seed oil and organic extracts attenuate hydrogen peroxide- and glutamate-induced injury in embryonic rat forebrain neuronal cells". *Phytomedicine,* **2006,** *13*, 29–36.

Guebailia, H. A., Chira, K., Richard, T., Mabrouk, T., Furiga, A., Merillon, J. M. "Hopeaphenol : The First Resveratrol Tetramer in Wines from North Africa". *J. Agric. Food Chem.,* **2006**, *54*, 9559−9564.

Gonzalez, A. G., Nuñez, M. P., Isabel, L., Ravelo, A. G., Jimenez, I. A. "Sesquiterpenes from *Maytenus magellanica* (Celastraceae)". *Nat. Prod. Lett.,* **1993,** *2,* 163-170.

Gonzalez-Sarr as, A., N ñe z-S nchez, M. A., Tom s-Barber n, F. A., Carlos Esp n, J. "Neuroprotective Effects of Bioavailable Polyphenol-Derived Metabolites against Oxidative Stress-Induced Cytotoxicity in Human Neuroblastoma SH-SY5Y Cells". *J. Agric. Food Chem.,* **2017**, *65*, 752−758.

Govindachari, T. R, Viswnathan, N. "The stem bark of Mappia foetida , a tree native to India, has proved to be another source significant for the isolation of camptothecin". *Phytochemistry*, **1972**, *11*, 3529-3531.

Graf, B. A., Milbury, P. E., Blumberg, J. B. "Flavonols, flavones, flavonones and human health: Epidemiological evidence". *J. Med. Chem.*, **2005**, *8*, 281-290.

Gutiérrez-Nicolás, F., Oberti, J. C., Ravelo, Á. G., Estévez-Braun, A. "β-Agarofurans and sesquiterpene pyridine alkaloids from *Maytenus spinos"a". J. Nat. Prod*., **2014**, *77,* 1853–1863.

Gutzeit, H. O., Ludwig-Muller J. "Plant Natural Products: Synthesis, Biological Functions and Practical Applications". First Edition, Wiley-VCH Verlag GmbH & Co. KGaA, **2014**.

Haefner, B. Drugs from the deep : marine natural products as drug candidates". *drug discovery today*, **2003**, *8*, 536–544.

Hakim, A. "Diversity of secondary metabolites from Genus *Artocarpus* (Moraceae)". *Bioscience*, **2010**, *2*, 146–156.

Hakim, E. H., Achmad, S. A., Juliawaty, L. D., Makmur, L., Syah, Y. M., Aimi, N., Kitajima, M., Takayama, H., Ghisalberti, E. L. "Prenylated flavonoids and related compounds of the Indonesian *Artocarpus* (Moraceae*)". J. Nat. Med.*, **2006**, *60*, 161–184.

Halgren, T. A., "Merck Molecular Force Field I. Basis, Form, Scope, Parameterization, and Performance of MMFF94". *J. Comput. Chem.,* **1996**, *17*, 490–519.

Halgren, T.A., "Merck Molecular Force Field. 111 Molecular Geometries and Vibrational Frequencies for MMFF94". *J. Comput. Chem.,* **1996**, *17*, 553–586.

Halgren, T. A., Murphy, R. B., Friesner, R. A., Beard, H. S., Frye, L.L., Pollard, W. T., Banks, J. L. "Glide : A New Approach for Rapid , Accurate Docking and Scoring. 2. Enrichment Factors in Database Screening". *J. Med. Chem.,* **2004**, *47,* 1750-1759.

Halgren, T. "New Method for Fast and Accurate Binding-site Identification and Analysis". *Chem. Biol. Drug. Des.,* **2007**, *69*, 146–148.

Hanawa, F., Tahara, S., Mizijtani, J. "Antifungal Stress Compounds From Veratrum Grandiflorum Leaves Treated With Cupric Chloride". *Phytochemistry*, **1992**, *31*, 3005-3007.

Hano, Y., Aida, M., Shiina, M., Nomura, T., Kawai, T., Ohe, H., Kagei, K. "Artonins A and B, Two New Prenylflavonoes from the Root Bark of *Artocarpus heterophyllus* Lamk". *Molecules,* **1989**, *29*, 1447-1453.

Hari, V. K. R., Sushrutha, C. K. Flora of Concern Endangered Medicinal Plants-Part I, *Vateria indica* Linn, Dipterocarpaceae–A Review". *International Journal of Research in Ayurveda & Pharmacy*, **2010,** *1*, 1–7.

He, S., Wu, B., Pan, Y., Jiang, L., "Stilbene Oligomers from *Parthenocissus laetevirens*: Isolation, Biomimetic Synthesis, Absolute Configuration, and Implication of Antioxidative Defense System in the Plant". *J. Org. Chem.,* **2008,** *73*, 5233–5241.

Heyne, K. "The Useful Indonesian Plants". Research and Development Agency The Ministry of Forestry, Jakarta, **1987,** pp. 659–703.

Hidayathulla, S., Chua, L. S., Chandrashekar, K. R., "Phytochemical Evaluation, Antioxidant And Antibacterial Activity of *Hopea Ponga* (Dennst) Mabberly Extracts". *Int. J. Pharm. Pharm. Sci.,* **2014**, *6*, 326-330.

Hlila, M. B., Mosbah, H., Majouli, K., Nejma, B., Ben, H. "Antimicrobial Activity of Scabiosa arenaria FORSSK. Extracts and Pure Compounds Using Bioguided Fractionation". *Chem. Biodiversity*, **2016**, *13*, 1262 – 1272.

Huang, C., Somwar, R., Patel, N., Niu, W., Török, D., Klip, A. "Sustained exposure of L6 myotubes to high glucose and insulin decreases insulin-stimulated GLUT4 translocation but upregulates GLUT4 activity". *Diabetes,* **2002,** *51*, 2090–2098.

Huang, K., Lin, M., Cheng, G. "Anti-inflammatory tetramers of resveratrol from the roots of Vitis amurensis and the conformations of the seven-membered ring in some oligostilbenes". *Phytochemistry*, **2001**, *58*, 357–362.

Jin, H. Z., Hwang, B. Y., Kim, H. S., Lee, J. H., Kim, Y. H., Lee, J. J., "Antiinflammatory constituents of *Celastrus orbiculatus* inhibit the NF-kB activation and NO production". *J. Nat. Prod.,* **2002**, *65*, 89-91.

Ito, J., Niwa, M. "Absolute structures of new hydroxystilbenoids vitisin C and viniferal from *Vitis vinifera* Kyohou, *Tetrahedron,* **1996**, *52*, 9991–9998.

Ito, T., Akao, Y., Yi, H., Matsumoto, K., Tanaka, T., Iinuma, M., Nozawa, Y. "Antitumor effect of resveratrol oligomers against human cancer cell lines and the molecular mechanism of apoptosis induced by vaticanol C". *Carcinogenesis*, **2003**, *24*, 1489–1497.

Ito, T., Asuda, Y. M., Be, N. A., Yama, M. O., Awa, R.S. "Chemical Constituents in the Leaves of *Vateria indica*". *Chem. Pharm. Bull.,* **2010**, *58*, 1369-1378.

Ito, T., Oyama, M., Sajiki, H., Sawa, R., Takahashi, Y. "Absolute structure of shoreaketone : a rotational isomeric resveratrol tetramer in Dipterocarpaceaeous plants". *Tetrahedron*, **2012**, *68*, 2950–2960.

Ito, T. "Structures of Oligostilbenoids in Dipterocarpaceaeous Plants and Their Biological Activities". *YAKUGAKU ZASSHI*, **2011,** *131*, 93-100.

Ito, T., Tanaka, T., Iinuma, M., Iliya, I., Nakaya, K., Ali, Z., Takahashi, Y., Sawa, R., Shirataki, Y. "New resveratrol oligomers in the stem bark of *Vatica pauciflora*". *Tetrahedron*, **2003**, *59*, 5347–5363.

Ito, T., Tanaka, T., Nakaya, K., Iinuma, M., Takahashi, Y., Naganawa, H., Ohyama, M., Nakanishi, Y., Bastow, F., Lee, K., "A new resveratrol octamer, vateriaphenol A, in *Vateria indica*". *Tetrahedron Letters*, **2001**, *42*, 5909–5912.

Jagtap, U. B., Bapat, V. A. "Artocarpus: A review of its traditional uses, phytochemistry and pharmacology". *Journal of Ethnopharmacology,* **2010**, *129*, 142–166.

Jahan, S., Gosh, T., Begum, M., Saha, B. K. "Nutritional Profile of Some Tropical Fruits in Bangladesh: Specially Anti-Oxidant Vitamins and Minerals". *Bangladesh Journal of Medical Science,* **2011**, *10*, 95-103.

Jedsadayanmata, A. "In vitro Antiglycation Activity of Arbutin". *Naresuan University Journal*, **2005**, *13*, 35-41.

Jinbo, Z., Mingan, W., Wenjun, W., Zhiqing, J., Zhaonong, H. "Insecticidal sesquiterpene pyridine alkaloids from Euonymus species". *Phytochemistry*, **2002**, *61*, 699–704.

Kapche, G. D. W. F., Fozing, C. D., Donfack, J. H., Fotso, G. W., Amadou, D., Tchana, A. N., Bezabih, M., Moundipa, P. F., Ngadjui, B. T., Abegaz, B. M. "Prenylated arylbenzofuran derivatives from *Morus mesozygia* with antioxidant activity". *Phytochemistry,* **2009,** *70*, 216–221.

Kennedy, M. L., Cortés-Selva, F., Pérez-Victoria, J. M., Jiménez, I. A., González, A.G., Muñoz, O. M., Gamarro, F., Castanys, S., Ravelo, A. G. "Chemosensitization of a multidrug-resistant Leishmania tropica line by new sesquiterpenes from *Maytenus magellanica* and *Maytenus chubutensis". J. Med. Chem*., **2001**, *44*, 4668-4676.

Keylor, M. H., Matsuura, B. S., Stephenson, C. R. J. "Chemistry and Biology of Resveratrol-Derived Natural Products. *Chemical Reviews*, **2015,** *115*, 8976–9027.

Khan, M. A., Nabi, S. G., Prakash, S., Zaman, A. "Pallidol, a resveratrol dimer from *Cissus pallida". Phytochemistry,* **1986,** *25,* 1945-1948.

Kim, N., Lee, J. O., Lee, H. J., Lee, Y. W., Kim, H. Y., Kim, S. J., Park, S. H., Lee, C. S., Ryoo, S.W., Hwang, G. S., Kim, S. O. "AMPK, a Metabolic Sensor, is involved in Isoeugenol-Induced Glucose Uptake in Muscle Cells*". J. Endocrinol.,* **2015**, *228*, 105–114.

Kim, S. E., Kim, H. S., Hong, Y. S., Kim, Y. C., Lee, J. J. "Sesquiterpene Esters from *Celastrus orbiculatus* and Their Structure - Activity Relationship on the Modulation of Multidrug Resistance". *J. Nat. Prod.,* **1999**, *62,* 697–700.

Kim, S. E., Kim, Y. H., Lee, J. J., Kim, Y. C, "A New Sesquiterpene Ester from Celastrus orbiculatus Reversing Multidrug Resistance in Cancer Cells". *J. Nat. Prod.*, **1998**, *61*, 108–111.

Kirtikar, K. R., Basu, B. D. "Indian Medicinal Plants", **2007**, *10*, 3232.

Kojima, H., Sato, N., Hatano, A., Ogura, H. "Sterol glucosides from Prunella vulgaris". *Phytochemistry*, **1990**, *29*, 2351–2355.

Kuo, Y. H., King, M. L., Chen, C. F., Chen, H. Y., Chen, C. H., Chen, K., Lee, K. H. "Two New Macrolide Sesquiterpene Pyridine Alkaloids *from Maytenus emarginata*: Emarginatine G and the Cytotoxic Emarginatine F. *J. Nat. Prod.*, **1994**, *57*, 263–269.

Kurihara, H., Kawabata, J., Ichikawa, S., Mizutania, J. "Agricultural and Biological Chemistry Oligostilbenes from *Carex pumita* Thunb. (Gyperaceae)". *Agric. Biol, Chem.,* **1990,** *54*, 1097-1099.

Lambert, C., Richard, T., Renouf, E., Bisson, J., Waffo-Téguo, P., Bordenave, L., Ollat, N., Mérillon, J.-M., Cluzet, S. "Comparative Analyses of Stilbenoids in Canes of Major *Vitis vinifera* L. Cultivars". *J. Agric. Food Chem.,* **2013***, 61*, 11392–11399.

Lan, W. C., Tzeng, C. W., Lin, C. C., Yen, F. L., Ko, H. H. "Prenylated flavonoids from *Artocarpus altilis :* Antioxidant activities and inhibitory effects on melanin production". *Phytochemistry*, **2013**, *89*, 78–88.

Langcake, P., Cornford, C. A., Pryce, R. J. "Identification of Pterostilbene as a Phytoalexin From *Vitis vinifera* Leaves". *Phytochemistry,* **1979**, *18*, 1025-1027.

Larronde, F., Richard, T., Delaunay, J., Decendit, A., Monti, J., Krisa, S., Mørillon, J. "New Stilbenoid Glucosides Isolated from *Vitis vinifera* Cell Suspension Cultures (cv.Cabernet Sauvignon)". *Letter Plant Med.,* **2005,** *71,* 888-890.

Likhitwitayawuid, K., Sritularak, B., Lipipun, V., Mathew, J., Raymond, F. "Phenolics with antiviral activity from *Millettia erythrocalyx and Artocarpus lakoocha*". *Natural Product Research,* **2005,** *19,* 177-182.

Lipton, S. A. "Paradigm shift in neuroprotection by NMDA receptor blockade : Memantine and beyond". *Nature Reviews*, **2006**, 5, 160–170.

Liu, J., Becker, H., Zapp, J., Wu, D. "Four Sesquiterpenes from the Insecticidal Plant *Celastrus angulatus*". *Phytochemistry,* **1995**, *40,* 841–846.

Lizcano, J. M., Alessi, D. R. "The insulin signalling pathway". *Current Biology,* **2002,** *12*, 236–238.

Lu, C., Lin, C. "Flavonoids and 9-Hydroxytridecyl Artocarpus from *Artocarpus heterophyllus". Phytochemistry,* **1994**, *35*, 781–783.

Luna-vázquez, F. J., Ibarra-alvarado, C., Rojas-molina, A., Rojas-molina, J. I., Rivero-cruz, F. Role of Nitric Oxide and Hydrogen Sulfide in the Vasodilator Effect of Ursolic Acid and Uvaol from Black Cherry Prunus serotina Fruits". *Molecules*, **2016**, *21*, 78.

Luo, Y., Pu, X., Luo, G., Zhou, M., Ye, Q., Liu, Y., Gu, J., Qi, H., Li, G., Zhang, G. "Nitrogen-containing dihydro-β-agarofuran derivatives from *Tripterygium wilfordii*. *J. Nat. Prod*., **2014**, *77*, 1650–1657.

Maneechai, S., De-eknamkul, W., Umehara, K., Noguchi, H. "Flavonoid and stilbenoid production in callus cultures of *Artocarpus lakoocha*". *Phytochemistry*, **2012**, *81*, 42–49.

Mattivi, F., Vrhovsek, U., Malacarne, G., Masuero, D., Zulini, L., Stefanini, M., Mose, C., Velasco, R., Guella, G. "Profiling of resveratrol oligomers, important stress metabolites, accumulating in the leaves of hybrid *Vitis vinifera* (Merzling Teroldego) genotypes infected with Plasmopara viticola". *J. Agric. Food Chem.,* **2011**, *59*, 5364–5375.

Mbaning, B. M., Lenta, B. N., Noungoue, D. T., Antheaume, C., Fongang, Y. F., Ngouela, S. A., Boyom, F. F., Rosenthal, P. J., Tsamo, E., Sewald, N., Laatsch, H. "Antiplasmodial sesquiterpenes from the seeds of *Salacia longipes* var. camerunensis". *Phytochemistry,* **2013**, *96*, 347–352.

Mcchesney, J. D., Venkataraman, S. K., Henri, J. T. "Plant natural products : Back to the future or into extinction". *Phytochemistry,* **2007**, *68*, 2015–2022.

Mccurdy, C. R., Scully, S. S. "Analgesic substances derived from natural products (natureceuticals)". *Life Sciences,* **2005**, *78*, 476–484.

Mcgarvey, D. J., Croteau, R. "Terpenoid Metabolism". *The Plant Cell*, **1995**, *7*, 1015–1026.

Mishima, S., Matsumoto, K., Futamura, Y., Araki, Y., Ito, T. "Antitumor effect of stilbenoids from Vateria indica against allografted sarcoma S-180 in animal model". *Journal of Experimental Therapeutics and Oncology,* **2003**, *3*, 283–288,

Mohidul Hasan M., Bae, H. "An Overview of Stress-Induced Resveratrol Synthesis in Grapes : Perspectives for Resveratrol-Enriched Grape products". *Molecules*, **2017**, *22*, 294.

Monyer, H., Sprengel, R., Schoepfer, R., Herb, A., Higuchi, M., Lomeli, H., Burnashev, N., Sakmann, B., Seeburg, P. H. "Heteromeric NMDA Receptors : Molecular and Functional Distinction of Subtypes". *Science,* **1992**, *256,* 1217-1220.

Morikawa, T., Chaipech, S., Matsuda, H., Hamao, M., Umeda, Y., Sato, H., Tamura, H., Kon'I, H., Ninomiya, K., Yoshikawa, M., Pongpiriyadacha, Y., Hayakawa, T., Muraoka, O. "Antidiabetogenic oligostilbenoids and 3-ethyl-4-phenyl-3,4-dihydroisocoumarins from the bark of *Shorea roxburghii*". *Bioorganic & Medicinal Chemistry,* **2012**, *20*, 832–840.

Teresa. J. P., Urones J. G., Marcos, I, S., Basabe, P., Cuadrado, J. S., Moro, R. F. "Triterpenes from *Euphorbia broteri*". *Phytochemistry*, **1987**, *26*, 1767-1776.

Mosmann, T. "Rapid Colorimetric Assay for Cellular Growth and Survival : Application to Proliferation and Cytotoxicity Assays". *Journal of lmmunological Methods*, **1983**, *65*, 55–63.

Mullard, A. "FDA drug approvals". *Nature Reviews,* **2018**, *17*, 81–85.

Muñoz-Martínez, F., Mendoza, C. R., Bazzocchi, I. L., Castanys, S., Jiménez, I. A., Gamarro, F. "Reversion of human Pgp-dependent multidrug resistance by new sesquiterpenes from *Zinowiewia costaricensis*". *J. Med. Chem.,* **2005**, *48*, 4266-4275.

Muralikrishnan, H., Chandrashekar K. R. "Regeneration of *Hopea ponga*: influence of wing loading and viability of seeds". *J. Trop. for Sci.,* **1997,** *10*, 58-65.

Myers, N., Mittermeier, R. A., Mittermeier, C. G., Fonseca, G. A. B., Kent, J. "Biodiversity hotspots for conservation priorities ". *Nature*, **2000**, *403*, 853–858.

Nadkarni, K. M. "Indian Materia Medica". *Third ed. Popular book depot, Bombay 7 and Dhootapeshwar Prakasan Ltd*. Panvel, Bombay, **1976**.

Namdaung, U., Aroonrerk, N., Suksamrarn, S., Danwisetkanjana, K., Saenboonrueng, J., Arjchomphu, W., Suksamrarn, A. "Bioactive Constituents of the Root Bark of *Artocarpus rigidus* subsp . rigidus". *Chem. Pharm. Bull.,* **2006**, *54*, 1433-1436.

Nasution, R., Barus, T., Nasution, P., Saidi, N. "Isolation and Structure Elucidation of Steroid from Leaves of *Artocarpus camansi* (Kulu) as Antidiabetic". *Int. J. Pharm. Tech. Res.,* **2014**, *6*, 1279–1285.

Nathan, D. M., Buse, J. B., Davidson, M. B., Ferrannini, E., Holman, H. R., Sherwin, R., Zinman, B. "Medical Management of Hyperglycemia in Type 2 Diabetes: A Consensus Algorithm for the Initiation and Adjustment of Therapy". *Diabetes Care*, **2009**, *32*, 193-203.

Nattrass, M., Alberti, K. G. M. M. "Biguanides". *Diabetologia,* **1978**, *14*, 71–74.

Nawwar, M. A. M., Buddrus, J., Bauer, H., Dimeric Phenolic Constituents from the Roots of *Tamarix nilotica Phytochemistry*, **1982**, *21*, 1755–1758.

Nayar, T. S., Rasiya Beegam, A., Sibi, M. "Flowering Plants of the Western Ghats, India". (2 Volumes). Palode, Thiruvananthapuram, Kerala, India: Jawaharlal Nehru Tropical Botanic Garden and Research Institute. **2014**, p.1700.

Newman, D. J., Cragg, G. M. "Natural Products As Sources of New Drugs over the 30 Years from 1981 to 2010". *J. Nat. Prod.,* **2012**, *75*, 311−335

Newman, D. J., Cragg, G. M. "Natural Products as Sources of New Drugs from 1981 to 2014". *J. Nat. Prod.,* **2016**, *79*, 629−661.

Nguyen, T. N. A., Dao, T. T., Tung, B. T., Choi, H., Kim, E., Park, J., Lim, S., Oh, W. K. "Influenza A (H1N1) neuraminidase inhibitors from *Vitis amurensis"*. *Food Chemistry*, **2011**, *124*, 437–443.

Nicolaou, K. C., Wu, T. R., Kang, Q., Chen, D. Y. "Total Synthesis of Hopeahainol A and Hopeanol". *Angew. Chem. Int. Ed.,* **2009**, *48*, 3440 –3443.

Ning, R., Lei, Y., Liu, S., Wang, H., Zhang, R., Wang, W., Zhu, Y., Zhang, H., Zhao, W. "Natural *β*-Dihydroagarofuran-Type Sesquiterpenoids as Cognition-Enhancing and Neuroprotective Agents from Medicinal Plants of the Genus *Celastrus"*. *J. Nat. Prod.,* **2015**, *78*, 2175–2186.

Omkumar, R. V., Rajeevkumar, R., Mathew Steephan, Mayadevi, M., Suma Priya, S. "Assay for detection of transient intracellular Ca^{2+}". *United States Patent*, 8, 304, 198, **2012.**

Omkumar, R. V., Rajeevkumar, R., Mathew Steephan, Mayadevi, M., Suma Priya, S. "Assay for detection of transient intracellular Ca^{2+}". *Indian Patent,* 260367, **2014.**

Omkumar, R. V., Rajeevkumar, R., Mathew Steephan, Mayadevi, M., Suma Priya, S. "Assay for detection of transient intracellular Ca^{2+}". *European Patent,* 2162742, **2015.**

Okoye, N. N., Ajaghaku, D. L., Okeke, H. N., Ilodigwe, E. E., Nworu, C. S., Okoye, F. B. C. beta-Amyrin and alpha-amyrin acetate isolated from the stem bark of *Alstonia boonei* display profound anti-inflammatory activity". *Pharm. Biol.,* **2014**, 1–9.

Osbourn, A. E., Lanzotti, V. "Plant-derived Natural Products Synthesis, Function, and Application". *Springer*, Dordrecht Heidelberg London New York, **2007.**

Oshima, Y., Ueno, J. "Ampelopsins D, E, H and cis-ampelopsin E oligostilbenes from *Ampelopsis brevipedunculata* Var. hancei roots". *Phytochemistry*, **1993**, *33*, 179-182.

Ourlad, A. G. T., Jacinto, S.D. "Cytotoxic activity of crude extracts and fractions from *Premna odorata* (Blanco), *Artocarpus camansi* (Blanco) and *Gliricidia sepium* (Jacq.) against selected human cancer cell lines". *Asian Pac. J. Trop. Biomed.,* **2015***, 5,* 1037-1041.

Paik, S. G., Blue, M. L., Fleischer, N., Shin, S. I. "Diabetes susceptibility of BALB/cBOM mice treated with STZ: inhibition by lethal irradiation and restoration by splenic lymphocytes". *Diabetes*, **1982**, *31*, 808-15.

Palanivel, R., Sweeney, G. "Regulation of fatty acid uptake and metabolism in L6 skeletal muscle cells by resistin". *FEBS Letters*, **2005**, *579*, 5049–5054.

Pandey, A., Bhatnagar, S. P. "Preliminary Phytochemical screening and antimicrobial studies on *Artocarpus lakoocha* Roxb". *Ancient Science of Life*, **2009**, *28*, 21–24.

Pandey, K. B., Rizvi, S. I. "Plant polyphenols as dietary antioxidants in human health and disease. Oxidative Medicine and Cellular Longevity". *Oxidative Medicine and Cellular Longevity*, **2009**, *2*, 270–278.

Pandeya, S. N., Kumar, R., Kumar, A., Pathak, A. K. "Antidiabetics Review on Natural Products Antidiabetics Review on Natural Products*". Research J. Pharm. and Tech*., **2010,** *3*, 300-318.

Patil, R. H., Prakash, K., Maheshwari, V. L. "Hypolipidemic effect of *Celastrus paniculatus* in experimentally induced hypercholesterolemic Wistar rats". *Ind. J. Clin. Biochem.,* **2010**, *25*, 405–410.

Pawlus, A. D., Waffo-Teguo, P., Shaver, J., Merillon, J. M. "Stilbenoid chemistry from wine and the genus *Vitis* a review*". J. Int. Sci. Vigne Vin.*, **2012,** *46,* 57-111.

Pérez-Victoria, J. M., Tincusi, B. M., Jiménez, I. A., Bazzocchi, I. L., Gupta, M. P., Castanys, S., Gamarro, F., Ravelo, A. G. "New natural sesquiterpenes as modulators of daunomycin resistance in a multidrug-resistant Leishmania tropica line". *J. Med. Chem.,* **1999**, *42*, 4388-4393.

Perry, L. M. **"**Medicinal Plants of East and South East Asia Attributed Properties and Uses". MIT, Press, Cambridge, **1980**.

Pryce, R. J., Langcake, P. "α-Viniferin: an antifungal resveratrol trimer from grapevines". *Phytochemistry*, **1977**, *16*, 1452-1456.

Rajurkar, N. S., Gaikwad, K. "Evaluation of phytochemicals, antioxidant activity and elemental content of *Adiantum capillus veneris* leaves". *J. Chem. Pharm. Res.,* **2012**, *4*, 365-374.

Ramprasath, V. R., Jones, P. J. H. "Anti-atherogenic effects of resveratrol". *European Journal of Clinical Nutrition*, **2010,** *64,* 660–668.

Reddy, S. V., Tiwari, A. K., Kumar, U. S., Rao, R. J., Rao, J. M. "Free Radical Scavenging, Enzyme Inhibitory Constituents from Antidiabetic Ayurvedic Medicinal Plant *Hydnocarpus wightiana* Blume". *Phytother. Res.,* **2005**, *19*, 277–281.

Rege, S. D., Geetha, T., Griffin, G. D., Broderick, T. L., Babu, J. R. "Neuroprotective effects of resveratrol in Alzheimer disease pathology". *Frontiers in Aging Neuroscience,* **2014**, *6*, 1–12.

Ren, Y., Yuan, C., Deng, Y., Kanagasabai, R., Ninh, T. N., Tu, V. T., Chai, H. B., Soejarto, D .D., Fuchs, J. R., Yalowich, J. C., Yu, J., Douglas Kinghorn, A. "Cytotoxic and natural killer cell stimulatory constituents of *Phyllanthus songboiensis*". *Phytochemistry,* **2015**, *111*, 132–140.

Rios, J. L., Francini, F., Schinella, G. R. "Natural Products for the Treatment of Type 2 Diabetes Mellitus". *Planta Medica*, **2015**, *81*, 975-994.

Rishton, G. M. "Natural Products as a Robust Source of New Drugs and Drug Leads : Past Successes and Present Day Issues". *The American Journal of Cardiology*, **2008,** *111*, 43-49.

Riviere, C., Pawlus, A. D., Merillon, J. M. "Natural stilbenoids : distribution in the plant kingdom and chemotaxonomic interest in Vitaceae". *Nat. Prod. Rep.,* **2012**, *29*, 1317.

Rose, P. M. B., Saranya, J., Eganathan, P., Jithin, M. M. "In vitro evaluation and comparison of antioxidant and antibacterial activities of leaf extracts of *Hopea ponga* (Dennst .) Mabberly". *International Journal of Green Pharmacy*, **2013**, 177–181.

Salguero, C. P. "A Thai Herbal Traditional Recipes for Health and Harmony". Findhorn Press, Scotland, **2003**, pp. 119.

Salonga, R. B., Hisaka, S., Nose, M. "Effect of the hot water extract of *Artocarpus camansi* leaves on 2, 4, 6-trinitrochlorobenzene (TNCB)-induced contact hypersensitivity in mice". *Biol. Pharm. Bull*., **2014**, *37*, 493-497.

Samant, J. S., Ajit Kumar, C. R., Thomas, R., Biju, C. R. "Ecology of hill streams of the Western Ghats with special reference to fish community. Annual (draft) submitted to Bombay Natural History Society". **1996**.

Santos-buelga, C., Scalbert, A. "Review Proanthocyanidins and tannin-like compounds – nature, occurrence , dietary intake and effects on nutrition and health". *J. Sci. Food. Agric,*. **2000**, *80,* 1094-1117.

Sasikumar, P., Prabha, B., Reshmitha, T. R., Veluthoor, S., Pradeep, A. K., Rohit, K. R., Dhanya, B. P., Sivan, V. V., Jithin, M. M., Kumar, N. A., Shibi, I. G., Nisha, P., Radhakrishnan, K. V. "Comparison of antidiabetic potential of (+) and (−)-hopeaphenol, a pair of enantiomers isolated from *Ampelocissus indica* (L.) and *Vateria indica* Linn., with respect to inhibition of digestive enzymes and induction of glucose uptake in L6 myotubes". *RSC Adv.,* **2016**, *6*, 77075–77082.

Sastry, G. M., Adzhigirey, M., Sherman, W. "Protein and ligand preparation : parameters, protocols, and influence on virtual screening enrichments". *J. Comput. Aided Mol. Des.,* **2013**, *27,* 221-234.

Sato, M., Fujiwara, S., Tsuchiya, H., Fujii, T. "Flavones with antibacterial activity against cariogenic bacteria". *Journal of Ethnopharmacology,* **1996**, *54*, 171-176.

Seo, E. K., Chai, H., Constant, H. L., Santisuk, T., Reutrakul, V., Beecher, C. W. W., Farnsworth, N. R., Cordell, G. A., Pezzuto, J. M., Kinghorn, A. D. "Resveratrol tetramers from *Vatica diospyroides*". *J. Org. Chem.,* **1999**, *64*, 6976-6983.

Shaheen, N., Lu, Y., Geng, P., Shao, Q., Wei, Y. "Isolation of four phenolic compounds from *Mangifera indica*. L flowers by using normal phase combined with elution extrusion

two-step high speed countercurrent chromatography". *Journal of Chromatography B*, **2017,** doi.org/10.1016/j.jchromb.2017.01.018.

Sharma, S., Misra, C. S., Arumugam, S., Roy, S., Shah, V., Davis, J. A., Shirumalla, R. K., Ray, A. "Antidiabetic Activity of Resveratrol, a known SIRT1 Activator in a Genetic Model for Type-2 Diabetes". *Phytother. Res.,* **2011,** *25*, 67–73.

Shettar, A. K., Vedamurthy, A. B. "Evaluation of in-vitro Anthelmintic Activity of *Ximenia americana*, *Hopea ponga* and *Vitex leucoxylon*". *Pharmacogn J.,* **2017**, *9,* 367-371.

Singleton, V. L., Rossi, J. A. "Colorunetry of total phenolics with phosphomolybdic-phosphotungstic acid reagents". *Amer. J. Enol. Viticult.,* **1965**, *16*, 144-58.

Snyder, S. A., Breazzano, S. P., Ross, A. G., Lin, Y., Zografos, A. L. "Total Synthesis of Diverse Carbogenic Complexity within the Resveratrol Class from a Common Building Block". *J. Am. Chem. Soc*., **2009**, *131*, 1753–1765.

Soejima, A., Wen, J. "Phylogenetic analysis of the grape family (Vitaceae) based on three chloroplast markers". *American Journal of Botany,* **2006**, *93*, 278–287.

Souza Chaves, O., Ferreira Teles, Y. C., Oliveira Monteiro, M. M., Mendes Junior, L. G., Fátima Agra, M., Andrade Braga, V., Sarmento Silva, T. M., Vanderlei de Souza, M. F. "Alkaloids and Phenolic Compounds from *Sida rhombifolia* L. (Malvaceae) and Vasorelaxant Activity of Two Indoquinoline Alkaloids". *Molecules,* **2017**, *22*, 1-9.

Spivey, A. C., Weston, M., Woodhead, S. "Celastraceae sesquiterpenoids: biological activity and synthesis". *Chem. Soc. Rev*., **2002**, *31*, 43–59.

Sritularak, B., Tantituvanont, A., Chanvorachote, P., Meksawan, K., Miyamoto, T., Kohno, Y., Likhitwitayawuid, K. "Flavonoids with free radical scavenging activity and nitric oxide inhibitory effect from the stem bark of *Artocarpus gomezianus". Journal of Medicinal Plants Research,* **2010**, *4,* 387-392.

Swami, S. B., Thakor, N. J., Haldankar, P. M., Kalse, S. B. "Jackfruit and Its Many Functional Components as Related to Human Health : A Review". *Comprehensive Reviews in Food Science and Food Safety,* **2012,** *11*, 565–576.

Syah, Y. M., Juliawaty, L.D., Achmad, S.A., Hakim, E. H., Ghisalberti, E. L. "Cytotoxic prenylated flavones from *Artocarpus champeden". J. Nat. Med.,* **2006***, 60,* 308–312.

Tagami, M., Nara,Y., Kubota, A., Sunaga, T., Maezawa, H., Fijino, H., Yamori, Y. "Morphological and functional differentiation of cultured vascular smooth-muscle cells". *Cell Tissue Res.,* **1986,** *245,* 241-246.

Takaishi, Y., Aihara, F., Tamai, S., Nakano, K., Tomimatsu, T. "Sesquiterpene Esters From *Tripterygium Wilfordii". Phyrochemistry,* **1992***, 31,* 3943- 3947.

Takaishi, Y., Tokura, K., Nocxjchi, H., Nakano, K., Murakami, K., Tomimatsu, T. Sesquiterpene Esters from *Tripterygzum Wlfordii*". *Phytochemistry*, **1991**, *30*, 1561 - 1566.

Takaishi, Y., Tamai, S., Nakano, K., Murakami, K., Tomimatsu, T. Structures of sesquiterpene polyol esters tripterygium wilfordiz Var. Regelii". *Phytochemistry*, **1991,** *30*, 3027-3031.

Takaishi, Y., Ujita, K., Tokuda, H., Nishino, H., Iwashima, A., Fujita, T. "Inhibitory effects of dihydroagarofuran sesquiterpenes on Epstein-Barr virus activation". *Cancer Letters,* **1992**, *65*, 19–26.

Takasugi, M., Munoz, L., Masamune, T., Shirata, A., Takahashi, K. "Stilbene phytoalexins from diseased mulberry". *CHEMISTRY LETTERS*, **1978**, 1241-1242.

Takaya, Y., Yan, K., Terashima, K., Ito, J., Niwa, M. "Chemical determination of the absolute structures of resveratrol dimers, ampelopsins A, B, D and F". *Tetrahedron*, **2002**, *58*, 7259–7265.

Tanaka, T., Ito, T., Nakaya, K., Iinuma, M., Riswan, S. "Oligostilbenoids in stem bark of *Vatica rassak". Phytochemistry,* **2000,** *54*, 63–69.

Tantengco, O. A .G., Jacinto, S. D. "Cytotoxic activity of crude extracts and fractions from *Premna odorata* (Blanco), *Artocarpus camansi* (Blanco) and *Gliricidia sepium* (Jacq.) against selected human cancer cell lines". *Asian Pacific Journal of Tropical Biomedicine*, **2015**, *5*, 1037–1041.

Torre, B. G. De., Albericio, F. "The Pharmaceutical Industry in 2017. An Analysis of FDA Drug Approvals from the Perspective of Molecules". *Molecules,* **2018**, *23*, 533.

Torres-romero, D., Mu, F., Jim, I. A., Gamarro, F., Bazzocchi, I. L., Salvador, E., Gonz, A. "Novel dihydro- β-agarofuran sesquiterpenes as potent modulators of human P-glycoprotein dependent multidrug resistance". *Org. Biomol. Chem.,* **2009**, *7,* 5166–5172.

Trindade, M. B., Lopes, L. S., Monteiro-moreira, A. C., Moreira, R. A., Luiza, M., Oliva, V., Beltramini, L. M. "Structural characterization of novel chitin-binding lectins from the genus *Artocarpus* and their antifungal activity". *Biochimica et Biophysica Acta,* **2006**, *1764*, 146-152.

Tsai, P. W., Castro-cruz, K. A. De, Shen, C. C., Chiou, C. T. "Chemical constituents of *Artocarpus camansi*. *Pharmacognosy Journal,* **2013,** *5*, 80–82.

Tu, Y. Q., Chen, Y. A. O. Z., Hao, J. "Sesquiterpenoids from *Celastrus paniculatus* ". *J. Nat. Prod.,* **1993**, *56*, 122–125.

Unnikrishnan, R., Anjana, R. M., Mohan, V. "Diabetes mellitus and its complications in India". *Nature Reviews Endocrinology*, **2016**, *12*, 357-370.

Uvais, S. S. M., Surendrakumar, S. "Two pyranodihydrobenzoxanthones from *Artocarpus nobilis". Phytochemistry,* **1989,** *28,* 599-605.

Venkataraman, K. "Wood phenolics in the chemotaxonomy of the Moraceae". *Phytochemistry*, **1972,** *11*, 1571-1586.

Venkateshwarlu, G., Shantha, T. R., Shiddamallayya, N., Kishore, K. R., Sridhar, B. N. "Preliminary physicochemical evaluation of sarja rasa (resin of *Vateria indica* linn .) and its traditional medicinal formulation". *International Journal of Research in Ayurveda & Pharmacy,* **2011**, *2*, 334-337.

Wagner, H., Demuth, G. "6-O-D-Apiofuranosyl)-1,6,8-Trihydroxy-3-Methyl-Anthrachingn, Ein Neues Glykobid (Franguljn 9) Aus Der Rinde Vcn Rhamnus Frangula L". *Tetrahedron Letters*, **1972**, *49*, 5013 – 5014.

Wall, M. E., Wani, M. C., Cook, C. E., Palmer, K. H., McPhail, A. I., Sim, G. A. "Plant antitumor agents. I. The isolation and structure of camptothecin, a novel alkaloidal leukemia and tumor inhibitor from camptotheca acuminate" *J. Am. Chem. Soc.,* **1966**, *88*, 3888–3890.

Watanabe, C. K. "Studies in the metabolic changes induced by administration of guanidine induced bases". *J. Biol. Chem.*, **1918**, *33*, 253-265.

Wei, B. L., Weng, J. R., Chiu, P. H., Hung, C. F., Wang, J P., Lin, C. N. "Antiinflammatory Flavonoids from *Artocarpus heterophyllus* and *Artocarpus communis". J. Agric. Food Chem.,* **2005**, *53*, 3867–3871.

Xiang, W. S., Wang, J. D., Wang, X. J., Zhang, J. "Two new components from *Gnetum pendulum". Journal of Asian Natural Products Research,* **2008**, *10*, 1081–1085.

Xiao, Z., Storms, R., Tsang, A. "A quantitative starch–iodine method for measuring alpha-amylase and glucoamylase activities". *Analytical Biochemistry*, **2006**, *351*, 146–148.

Yongqiang, T., Dagang, W., Jun, Z., Yaozu, C. "Sesquiterpene polyol esters from *Celastrus gemmatus". Phytochemistry,* **1990**, *29*, 2923–2926.

Zeng, X., Pan, X., Xu, X., Lin, J., Que, F., Tian, Y., Li, L., Liu, S. "Resveratrol Reactivates Latent HIV through Increasing Histone Acetylation and Activating Heat Shock Factor 1". *J. Agric. Food Chem.,* **2017**, *65*, 4384−4394.

Zetterström, C. E., Hasselgren, J., Salin, O., Davis, R. A., Quinn, R. J., Sundin, C., Elofsson, M. "The resveratrol tetramer (-)-hopeaphenol inhibits type III secretion in the gram-negative pathogens Yersinia pseudotuberculosis and Pseudomonas aeruginosa". *PLoS ONE*, **2013,** *8*, 1–12.

Zhang, F., Liu, J., Shi, J. S. "Anti-inflammatory activities of resveratrol in the brain : Role of resveratrol in microglial activation". *European Journal of Pharmacology*, **2010**, *636,* 1–7.

Zhang, K., Wang, Y., Chen, Y., Tu, Y., Jing, H., Huimin, H., Xiaofeng, H., Jinsong, F. "Sesquiterpenes from *Celastrus paniculatus* Subsp. Paniculatus". *Phytochemistry,* **1998**, *48,* 1067-1069.

Zhang X. Traditional medicine: its importance and protection. Protecting and promoting traditional knowledge: systems, national experiences and international dimensions. Part. **2004**, newma1: 3-6

Zheng, Z. P., Cheng, K. W., To, J. T. K., Li, H., Wang, M. "Isolation of tyrosinase inhibitors from *Artocarpus heterophyllus* and use of its extract as antibrowning agent". *Mol. Nutr. Food Res.,* **2008**, *52*, 1530–1538.

Zhu, S., Paoletti, P. "Allosteric modulators of NMDA receptors : multiple sites and mechanisms". *Current Opinion in Pharmacology*, **2015**, *20*, 14–23.

List of publications

1. Lewis Acid Catalyzed C-3 Alkylidenecyclopentenylation of Indoles: An Easy Access to Functionalized Indoles and Bisindoles" S. Sarath Chand, B. S. Sasidhar, Praveen Prakash, P. **Sasikumar, P**. Preethanuj, Florian Jaroschik, Dominique Harakat, Jean-Luc Vasse and K. V. Radhakrishnan*, RSC Adv.,* **2015**, *5*, 38075.
2. Comparison of antidiabetic potential of (+) and (-)-Hopeaphenol, a pair of enantiomers isolated from *Ampelocissus indica* (L.) and *Vateria indica* Linn, with respect to inhibition of digestive enzymes and induction of glucose uptake in L6 myotubes**" P. Sasikumar**, B. Prabha, T. R Reshmitha , Sheeba Veluthoor, Pradeepkumar, K. R Rohit, B. P Dhanya, V. V Sivan, M.M. Jithin, N. Anil Kumar, I. G. Shibi, P. Nisha and K. V. Radhakrishnan, *RSC Adv.,* **2016***, 6,* 77075–77082.
3. Phytochemical studies of an endemic and critically endangered hill banana, Musa acuminata Colla (AA) 'Karivazhai' fruit by GC-MS" , Sreejith, P. E., Linu, N. K., **Sasikumar, P**., Radhakrishnan, K. V. and M. Sabu. *Journal of Chemical and Pharmaceutical Research*, **2016**, *8*, 164-168.
4. Lewis acid promoted Regioselective Double Hydro(hetero)arylation of 6,6'-dialkyl Substituted Pentafulvene : A Facile Approach to Bisindole Derivatives, **Parameswaran Sasikumar,** Bernad Prabha, Sarngadharan Sarath Chand, Maniyamma Aswathy, Murali Madhukrishnan, Preethalayam Preethanuj, Eringathodi Suresh, Florian Jaroschik, and Kokkuvayil Vasu Radhakrishnan, *Eur. J. Org. Chem*, **2017**, *2017*, 4469–4474.
5. Lewis Acid Catalysed Activation of Zerumbone towards Sesquiterpenoid Derivatives: Sustainable Utilisation of Abundant Natural Resources towards Chemically Diverse Architectures. Dhanya, B. P., Gopalan, Greeshma, **Sasikumar Parameswaran**, Neethu S, Meenu M T, Sharathna P, John, Jubi, Sunil Varughese, Sabu. M, Dan Mathew, Kokkuvayil Vasu Radhakrishnan, *Asian J. Org. Chem.*, **2018**, *7*, 471–476.

6. Dihydro-β-agarofuran sesquiterpenoids from the seeds of *Celastrus paniculatus* Willd. and their α-glucosidase inhibitory activity, **P. Sasikumar**, P. Sharathna, B. Prabha, Sunil Varughese, N. Anil Kumar, V. V. Sivan, D. R. Sherin, E. Suresh, T. K. Manojkumar, K. V. Radhakrishnan, *Phytochemistry Letters,* **2018**, *26*, 1–8.
7. Isolation and characterization of resveratrol oligomers from the stem bark of *Hopea ponga* (Dennst.) Mabb. and their antidiabetic effect by modulation of digestive enzymes, protein glycation and glucose uptake in L6 myocytes, **P. Sasikumar**, K. Lekshmy, S. Sini, B. Prabha, N. Anil Kumar,V. V. Sivan, M. M. Jithin, P. Jayamurthy, I.G. Shibi and K. V. Radhakrishnan, *J. Ethnopharmacol.,* **2018***, under revision.*
8. Phytochemistry and antidiabetic screening of compounds from *Artocarpus camansi* and *Artocarpus lakoocha* **P. Sasikumar**, T. R Reshmitha, M. Aswathy, B. Prabha, P. Nisha and K. V. Radhakrishnan [To be submitted].
9. Investigations on Phytochemical Constituents of *Dillenia indica* and their anticancer studies **P. Sasikumar** and K. V. Radhakrishnan, [Manuscript under preparation].
10. Stereoselective functionalization of spirocyclopentadienes: Facile synthesis of highly substituted Cyclopropane P. Preethanuj, Jomy Joseph, **P. Sasikumar**, Florian Jaroschik, Dominique Harakat, Jean-Luc Vasse and K. V. Radhakrishnan [To be submitted].
11. Isolation and characterization of Oligostilbenoids from *Vatica chinensis* L. and their ameliorative effect on H_2O_2 induced oxidative stress in H9c2 cardiomyoblasts B. Prabha, T. R. Reshmitha, **P. Sasikumar**, M. Madhukrishnan, T. Sithara, P. Nisha, and K. V. Radhakrishnan, [To be submitted].

Papers Presented in International/National Conferences

1. The structural characterization of resveratrol tetramer from the bark of vateria indica , **P. Sasikumar** and K. V. Radhakrishnan, National symposium on Transcending Frontiers in Organic Chemistry, CSIR-NIIST, October 9-11, 2014 [**Poster Presentation**].

2. Isolation and Structural Characterization of (+) and (-)- Hopeaphenols from *Ampelocissus indica* and *Vateria indica* **P. Sasikumar,** Sheeba Veluthoor, K.R Rohit and K. V. Radhakrishnan, International Symposium on Phytochemisty (ISP-2015) and Prof. Dr. A. Hisham Endowment Award Ceremony, Kerala Academy of Sciences, Thiruvananthapuram [**Poster Presentation**].
3. Comparison of (+) and (-)-Hopeaphenol, a pair of enantiomers induce antidiabetic effect by digestive enzyme inhibition and glucose uptake in muscle cells, **P. Sasikumar,** P. Nisha and K. V. Radhakrishnan, XI J-NOST meeting for research scholars held at NISER, Bhubaneswar during December 14-17th, 2015 [**Poster Presentation**].
4. Hopeaphenols: α-Glucosidase inhibitors in type 2 diabetics, **P. Sasikumar,** P. Nisha and K. V. Radhakrishnan, *CTDDR-25th -28th 2016*, at CSIR-CDRI, Lucknow, Uttarpradesh [**Poster Presentation**].
5. Lewis acid catalyzed C-3alkylidenecyclopentenylation of indoles: an easy access to functionalized indoles and bisindoles **Sasikumar P**., Sarath Chand S and K. V. Radhakrishnan, CRSI-2016 at NBU, Darjeeling, West Bengal [**Poster Presentation**].
6. Isolation, characterization and biological evaluation of phytochemicals from rare, endangered and threatened (RET) species of plants of Kerala, **P. Sasikumar,** and K. V. Radhakrishnan, Prof. Dr. A. Hisham Endowment Award, 2016, Kerala Academy of Sciences, Thiruvananthapuram [**Oral Presentation**].
7. Isolation and characterization of novel dihydro-β-agarofuran sesquiterpenoids from the seeds of *Celastrus paniculatus* Willd. and their α-glucosidase inhibitory activity, **P. Sasikumar,** and K. V. Radhakrishnan, ISP-2018, an International seminar on Phytochemistry organized by Kerala academy of Sciences & Jawaharlal Nehru Tropical Botanic Garden and Research Institute, palode on 26th & 27th March 2018 [**Oral Presentation**].